

Improved Load Rating Procedures for Deteriorated Unstiffened Steel Beam Ends

Final Deliverable:

Prepared By:
Aidan Provost
Graduate Researcher
aqprovost@umass.edu

Georgios Tzortzinis, Ph.D.
Post Doctoral Researcher
georgios.tzortzinis@tu-dresden.de

Shahrukh Islam
Graduate Researcher
shahrukh@umass.edu

Simos Gerasimidis, Ph.D.
Principal Investigator
sgerasimidis@umass.edu

Sergio Breña, Ph.D.
Co-Principal Investigator
brena@umass.edu



University of Massachusetts Amherst,
130 Natural Resources Way, Amherst, MA 01003

Prepared For:
New England Transportation Consortium
January 2024

Technical Report Document Page

1. Report No. NETCR125		2. Government Accession No.		3. Recipient's Catalog No.	
4. Title and Subtitle Improved Load Rating Procedures for Deteriorated Unstiffened Steel Beam Ends				5. Report Date January 31, 2024	
				6. Performing Organization Code	
7. Author(s) Aidan Provost, George Tzortzinis, Shahrukh Islam, Simos Gerasimidis, Sergio Brena				8. Performing Organization Report No. NETCR125	
9. Performing Organization Name and Address University of Massachusetts Amherst UMass Transportation Center 130 Natural Resources Way Amherst, MA 01003				10. Work Unit No. (TRAIS)	
				11. Contract or Grant No.	
12. Sponsoring Agency Name and Address New England Transportation Consortium Maine Department of Transportation 2424 Child Street Augusta, ME 04330				13. Type of Report and Period Final Report (September 2020 to January 2024)	
				14. Sponsoring Agency Code NETC 19-3	
15. Supplementary Notes					
16. Abstract This report contains the contents of the project to enhance load rating methods for assessing corroded unstiffened beam ends for the six New England States. The first task of the project was to collect and compile inspection reports information provided by DOTs within New England. The research team was able to carefully identify trends and patterns in the data, which was used to determine the most common scenarios of corrosion encountered in bridges within New England States. Following this task, corroded bridge girder specimens were selected from existing structures to be documented and experimentally tested in the structural testing facility at UMass Amherst. The specimens were also computationally analyzed for their section loss and remaining capacity. The final goal of this project was to evaluate the load rating procedures across all of the New England States and recommend updates to the procedures based on our experimental and analytical results.					
17. Key Word Corrosion, LiDAR, 3D Scanning, web local yielding, web local buckling			18. Distribution Statement No restrictions.		
19. Security Classif. (of this report) unclassified		20. Security Classif. (of this page) unclassified		21. No. of 321	22. Price n/a

SI* (MODERN METRIC) CONVERSION FACTORS

APPROXIMATE CONVERSIONS TO SI UNITS

Symbol	When You Know	Multiply By	To Find	Symbol
LENGTH				
in	inches	25.4	millimeters	mm
ft	feet	0.305	meters	m
yd	yards	0.914	meters	m
mi	miles	1.61	kilometers	km
AREA				
in ²	square inches	645.2	square millimeters	mm ²
ft ²	square feet	0.093	square meters	m ²
yd ²	square yard	0.836	square meters	m ²
ac	acres	0.405	hectares	ha
mi ²	square miles	2.59	square kilometers	km ²
VOLUME				
fl oz	fluid ounces	29.57	milliliters	mL
gal	gallons	3.785	liters	L
ft ³	cubic feet	0.028	cubic meters	m ³
yd ³	cubic yards	0.765	cubic meters	m ³
NOTE: volumes greater than 1000 L shall be shown in m ³				
MASS				
oz	ounces	28.35	grams	g
lb	pounds	0.454	kilograms	kg
T	short tons (2000 lb)	0.907	megagrams (or "metric ton")	Mg (or "t")
TEMPERATURE (exact degrees)				
°F	Fahrenheit	5 (F-32)/9 or (F-32)/1.8	Celsius	°C
ILLUMINATION				
fc	foot-candles	10.76	lux	lx
fl	foot-Lamberts	3.426	candela/m ²	cd/m ²
FORCE and PRESSURE or STRESS				
lbf	poundforce	4.45	newtons	N
lbf/in ²	poundforce per square inch	6.89	kilopascals	kPa

APPROXIMATE CONVERSIONS FROM SI UNITS

Symbol	When You Know	Multiply By	To Find	Symbol
LENGTH				
mm	millimeters	0.039	inches	in
m	meters	3.28	feet	ft
m	meters	1.09	yards	yd
km	kilometers	0.621	miles	mi
AREA				
mm ²	square millimeters	0.0016	square inches	in ²
m ²	square meters	10.764	square feet	ft ²
m ²	square meters	1.195	square yards	yd ²
ha	hectares	2.47	acres	ac
km ²	square kilometers	0.386	square miles	mi ²
VOLUME				
mL	milliliters	0.034	fluid ounces	fl oz
L	liters	0.264	gallons	gal
m ³	cubic meters	35.314	cubic feet	ft ³
m ³	cubic meters	1.307	cubic yards	yd ³
MASS				
g	grams	0.035	ounces	oz
kg	kilograms	2.202	pounds	lb
Mg (or "t")	megagrams (or "metric ton")	1.103	short tons (2000 lb)	T
TEMPERATURE (exact degrees)				
°C	Celsius	1.8C+32	Fahrenheit	°F
ILLUMINATION				
lx	lux	0.0929	foot-candles	fc
cd/m ²	candela/m ²	0.2919	foot-Lamberts	fl
FORCE and PRESSURE or STRESS				
N	newtons	0.225	poundforce	lbf
kPa	kilopascals	0.145	poundforce per square inch	lbf/in ²

*SI is the symbol for the International System of Units. Appropriate rounding should be made to comply with Section 4 of ASTM E380.
(Revised March 2003)

A

Disclaimer

The contents of this report reflect the views of the author(s), who is responsible for the facts and the accuracy of the data presented herein. The contents do not necessarily reflect the official view or policies of the New England Transportation Consortium or the Federal Highway Administration. This report does not constitute a standard, specification, or regulation.

Table of Contents

Technical Report Document Page.....	iii
Disclaimer	vii
1. Introduction	28
2. Inspection Report Data Collection	30
2.1.1. Format of data received from the Connecticut Department of Transportation (CTDOT) Inspection reports	30
2.1.2. Format of data received from the Maine Department of Transportation (MaineDOT) Inspection reports	32
2.1.3. Format of data received from the Massachusetts Department of Transportation (MassDOT) Inspection reports	35
2.1.4. Format of data received from New Hampshire Department of Transportation (NHDOT) Inspection reports.....	38
2.1.5. Format of data received from Rhode Island Department of Transportation (RIDOT) Inspection reports	40
2.1.6. Format of data received from Vermont’s Agency of Transportation (VTrans) Inspection reports	43
2.2. Variability and Quality of Data	46
2.3. Amount of Data	51
2.4. Preliminary filtering of the data.....	51
2.5. Corrosion Patterns	52
3. Organization of Data and Post-Processing	60
3.1. Organizing Data.....	60
3.2. MATLAB script	61
3.3. Results	62
3.3.1. Connecticut.....	63
3.3.2. Maine.....	68
3.3.3. Massachusetts	68
3.3.4. New Hampshire.....	84
3.3.5. Rhode Island.....	84
3.3.6. Vermont.....	89
4. Selection of Bridges	90
4.1. Bridges Investigated	90
4.2. Beam Specimens Received.....	93

4.3.	Beam Specimen Documentation and Testing Rig.....	96
4.4.	Beams Prioritized for Testing.....	99
4.5.	Beams Selected as Untestable	99
4.5.1.	Limited Damage Criterion.....	99
4.5.2.	Extreme Damage Criterion.....	100
4.5.3.	Final comments on untestable Specimens	101
4.6.	Beam End Corrosion Documentation.....	101
4.6.1.	State Methods of Inspection	101
4.6.2.	Utilization of Existing Methods	102
4.6.3.	LiDAR and 3D Scanning Protocols.....	103
4.7.	Beam Dimensions.....	104
5.	Finite Element Modeling.....	106
6.	Laboratory Testing	109
6.1.	Specimen 1	110
6.2.	Specimen 2	111
6.3.	Specimen 3	112
6.4.	Specimen 4	113
6.5.	Specimen 5	114
6.6.	Specimen 6	115
6.7.	Specimen 7	116
6.8.	Specimen 8	117
6.9.	Specimen 9	118
6.10.	Specimen 10	119
6.11.	Specimen 11	120
6.12.	Specimen 12	121
7.	Data Results and Discussion	122
7.1.	Experimental and Finite Element Capacities.....	122
8.	Analytical Procedures by State.....	124
8.1.	CTDOT Provisions.....	124
8.2.	MassDOT Provisions, Tzortzinis Equations	125
8.3.	MaineDOT Provisions.....	126
8.4.	NHDOT Provisions	126
8.5.	RIDOT Provisions	127
8.6.	VTrans Provisions	128
8.7.	Summary	128

9.	New Rating Recommendations	132
10.	Conclusions	133
10.1.	Conclusions Corrosion Pattern Analysis	133
10.2.	Conclusions from Experiments, Simulations and Ratings	137
10.2.1.	Conclusions on Scanning and Corrosion Profiles	137
10.2.2.	Conclusions on Experiments and Simulations	137
10.2.3.	Conclusions on Ratings and Recommendations.....	138
11.	Appendix I – Detailed data and processing graphs for beam ends without a diaphragm.....	140
11.1.	Connecticut.....	140
11.1.1.	Introduction	140
11.1.2.	Pattern W1	141
11.1.3.	Pattern W2.....	152
11.1.4.	Pattern W3.....	157
11.1.5.	Pattern W4.....	162
11.1.6.	Pattern W5.....	168
11.2.	Maine.....	170
11.2.1.	Introduction	170
11.2.2.	Web Corrosion.....	170
11.2.3.	Flange Corrosion.....	171
11.2.4.	Holes.....	172
11.3.	Massachusetts.....	174
11.3.1.	Introduction	174
11.3.2.	Pattern W1	174
11.3.3.	Pattern W2.....	185
11.3.4.	Pattern W3.....	189
11.3.5.	Pattern W4.....	196
11.3.6.	Pattern W5.....	207
11.4.	New Hampshire.....	211
11.4.1.	Introduction	211
11.4.2.	Web corrosion	211
11.4.3.	Flange Corrosion.....	211
11.4.4.	Holes.....	212
11.5.	Rhode Island.....	213
11.5.1.	Introduction	213
11.5.2.	Pattern W1	215

11.5.3.	Pattern W2.....	220
11.5.4.	Pattern W3.....	221
11.5.5.	Pattern W4.....	227
11.5.6.	Pattern W5.....	231
11.6.	Vermont.....	232
11.6.1.	Introduction	232
11.6.2.	Web corrosion	232
11.6.3.	Flange corrosion	232
11.6.4.	Holes.....	233
12.	Appendix II – Detailed data and processing graphs for beam ends with a diaphragm.....	237
12.1.	Connecticut.....	237
12.1.1.	Introduction	237
12.1.2.	Pattern W1	238
12.1.3.	Pattern W3	244
12.2.	Massachusetts.....	249
12.2.1.	Introduction	249
12.2.2.	Pattern W1	249
12.2.3.	Pattern W2.....	261
12.2.4.	Pattern W3.....	267
12.2.5.	Pattern W4.....	290
12.2.6.	Pattern W5.....	300
12.3.	Rhode Island.....	303
12.3.1.	Introduction	303
12.3.2.	Pattern W1	304
12.3.3.	Pattern W3	311
13.	References	318

List of Figures

Figure 1: Sample of a report provided by CTDOT	30
Figure 2: Sketch (Left) and Photography (Right) of corrosion damage	32
Figure 3: Sample of report provided by Maine DOT	34
Figure 4 : The same beam, as was described by sketch (left) and by photograph (right). Adopted from W46010-3RY-DOT-NBI (district 5, City of Wrentham).....	36
Figure 5: Sample of report provided by MassDOT	37
Figure 6: Sample of report provided by NHDOT.....	39
Figure 7: Example of corrosion damage taken from the records of a bridge from NHDOT.....	40
Figure 8: Front page of a typical routine inspection report provided by RIDOT.....	42
Figure 9: An example of picture provided by RIDOT	43
Figure 10: Example of photo of a buckled beam found in VTrans web-portal.....	44
Figure 11: Sample of report provided by VTrans.....	45
Figure 12: Example of corrosion information (Adapted from bridge 0854, Maine).....	46
Figure 13: Example of inspection notes (Adapted from <i>BENNINGTON-BR22-19OCT2</i> , Vermont)..	46
Figure 14: Example of inspection notes (Adapted from <i>Andover 125-129</i> , New Hampshire)	46
Figure 15: Typical inspection report sketch not in scale. Adapted from N19059-101-DOT-NBI (Northampton, MA).....	47
Figure 16: Typical inspection report sketch (not to scale). Adapted from Br. #00297 (Plainfield, CT)	47
Figure 17: Typical inspection report sketch not to scale (<i>Adapted from Br. #042501, RI</i>).....	47
Figure 18: Corroded area described by only one thickness value. Adapted from W46010-3RY-DOT-NBI (Wrentham, MA)	48
Figure 19: Corroded area described by only one thickness value. Adapted from bridge 00501 (Killingly, CT).....	48
Figure 20: Corroded areas described by only one thickness value. Adapted from bridge 061901(RI)	49
Figure 21: Corroded area described by multiple thickness loss values. Sketch adopted from H08003-18J-MUN-NBI (District 2, Town of Hardwick).....	49
Figure 22: No indication of where the section loss occurs. Adapted from Br. #00297 (Plainfield, CT)	50
Figure 23: Summary of reports provided by each state.....	51
Figure 24: Bridge identification and general information isolated at the top of the spreadsheet.	60
Figure 25: Spreadsheet designed to organize corrosion data.....	61
Figure 26: To the left is P-01-005 (Massachusetts) and the right structure is 042401 (Rhode Island)	62
Figure 27: Connecticut, 02929, Route 80 Deep River	91
Figure 28. Massachusetts, 07U, Savoy.....	91
Figure 29. Maine, 3801, Jay	92
Figure 30. New Hampshire, 154/129, Newport.....	92
Figure 31. Vermont, BR3, Proctor	92
Figure 32. Vermont, BR15, Newbury	93
Figure 33. Connecticut Specimens	94
Figure 34. Massachusetts Specimens	94
Figure 35. Maine Specimens	94
Figure 36. New Hampshire Specimens	95
Figure 37. Vermont Specimens	95
Figure 38. Structural Rig Flow Chart.....	96

Figure 39. Structural Rig	98
Figure 40. Structural Rig A-‘A View	98
Figure 41. Limited Damage Steel Beams.....	100
Figure 42. Extreme Damage Criterion, Vermont Beams	100
Figure 43. Extreme Damage Criterion, New Hampshire Beams.....	101
Figure 44. Measurement Grids	103
Figure 45. REIGL VZ-2000 Terrestrial Scanner and Corroded Beam Point Cloud	103
Figure 46. Artec Leo Scanner and Sample Scan with Setup	104
Figure 47. Finite Element Model.....	107
Figure 48. CTDOT Spreadsheet Example, Adapted from CTDOT Load Rating Spreadsheet	124
Figure 49. MassDOT Equation Example for Bearing Length/Beam Depth >0.2, Adapted from MassDOT Provisions (Under Review) [47]	125
Figure 50. Maine Corroded End Capacity Estimation Example, Adapted from MaineDOT 2238 Load Rating	126
Figure 51. New Hampshire Corroded End Capacity Estimation Example, Adapted from New Hampshire Load Rating Francestown 142-160	127
Figure 52. RIDOT Spreadsheet Example, adapted from RIDOT Load Rating Spreadsheet.....	128
Figure 53. New England Beam End Capacity	129
Figure 54. Normalized New England Beam End Capacity	129
Figure 55: Web corrosion patterns distribution for beams ends without a diaphragm – CTDOT	140
Figure 56: CH1 distribution of W1 pattern for beams without a diaphragm - CTDOT	141
Figure 57: CL1 distribution of W1 pattern for beams without a diaphragm – CTDOT	142
Figure 58: Ratio of corrosion length (CL1) to corrosion height (CH1) of W1 pattern for beams without a diaphragm - CTDOT	142
Figure 59: Ratio of corrosion length (CL1) to corrosion height (CH1) for CL1 < 2.5H0 - CTDOT .	143
Figure 60: CL1 distribution for CH1 <0.3H - CTDOT	143
Figure 61: CL1 distribution for CH1 >0.9H - CTDOT	144
Figure 62: Web thickness loss distribution for pattern W1 - CTDOT	144
Figure 63: Web thickness loss distribution for CH1<0.3H and CL1<2.5H - CTDOT	145
Figure 64: Web thickness loss distribution for Ch1<0.9H and CL1<1H - CTDOT.....	145
Figure 65: Distribution of corrosion length for pattern W1 - CTDOT	146
Figure 66: Ratio between flange corrosion length for pattern W1 - CTDOT	147
Figure 67: Flange thickness Loss for pattern W1 - CTDOT	147
Figure 68: Flange thickness loss distribution for CH1<0.3 - CTDOT	148
Figure 69: Flange thickness loss distribution for CH1>0.9 - CTDOT	148
Figure 70: Extreme scenario for pattern W1 - CTDOT.....	149
Figure 71: Extreme scenario for pattern W1 - CTDOT.....	149
Figure 72: Web thickness loss for beam ends with M1 holes - CTDOT.....	150
Figure 73: Web thickness loss for beam ends with M2 holes - CTDOT.....	151
Figure 74: Web thickness loss for beam ends with M3 holes - CTDOT.....	151
Figure 75: Web thickness loss for beam ends with M4 holes - CTDOT.....	152
Figure 76: CL1 distribution for W2 pattern - CTDOT	153
Figure 77: CL2 distribution for W2 pattern - CTDOT	153
Figure 78: CH distribution for W2 pattern - CTDOT	154
Figure 79: Web thickness loss for W2 pattern - CTDOT.....	154
Figure 80: CL1 distribution for W2 pattern and CL1<0.6H - CTDOT	155
Figure 81: CL2 distribution for W2 pattern and CL1<0.6H - CTDOT	155

Figure 82: CH distribution for W2 pattern and $CL_1 < 0.6H$ - CTDOT	156
Figure 83: Web thickness loss for W2 pattern and $CL_1 < 0.6H$ - CTDOT	156
Figure 84: Extreme corrosion scenario for pattern W2 - CTDOT.....	157
Figure 85: CH2 distribution for W3 pattern - CTDOT	157
Figure 86: CL3 distribution for W3 pattern - CTDOT	158
Figure 87: CL1 distribution for W3 pattern and $CH_2 > 0.9H$ - CTDOT.....	158
Figure 88: Web thickness loss distribution for W3 pattern and $CH_2 > 0.9H$ - CTDOT	159
Figure 89: Extreme corrosion scenario for W3 pattern – CTDOT	159
Figure 90: Ratio between corrosion length in the flanges and CL3 for W3 pattern - CTDOT	160
Figure 91: Raw corrosion length in the flanges for W3 pattern - CTDOT.....	160
Figure 92: Flange thickness loss for W3 pattern - CTDOT	161
Figure 93: Flange thickness loss for W3 pattern and $CH_2 > 0.9H$ - CTDOT	161
Figure 94: CH2 distribution for W4 pattern - CTDOT	162
Figure 95: CH1 distribution for W4 pattern and $CH_2 > 0.9H$ - CTDOT	162
Figure 96: CL1 distribution for W4 pattern and $CH_2 > 0.9H$ - CTDOT.....	163
Figure 97: CL2 distribution for W4 pattern and $CH_2 > 0.9H$ - CTDOT.....	163
Figure 98: CL3 distribution for W4 pattern and $CH_2 > 0.9H$ - CTDOT.....	164
Figure 99: Web thickness loss distribution for W4 pattern and $CH_2 > 0.9H$ - CTDOT	164
Figure 100: Extreme corrosion scenario for W4 pattern - CTDOT.....	165
Figure 101: Flange thickness loss for W4 pattern - CTDOT.....	165
Figure 102: Depth of hole M1 combined with W4 pattern - CTDOT	166
Figure 103: Length of hole M1 combined with W4 pattern - CTDOT	166
Figure 104: Depth of hole M3 combined with W4 pattern - CTDOT.....	167
Figure 105: Length of hole M3 combined with W4 pattern - CTDOT	167
Figure 106: CH1 distribution of W5 pattern for beams without a diaphragm – CTDOT	168
Figure 107: CL1 distribution of W5 pattern for beams without a diaphragm – CTDOT.....	168
Figure 108: Web thickness loss distribution of W5 pattern for beams without a diaphragm – CTDOT	169
Figure 109: Extreme corrosion scenario for pattern W5 - CTDOT.....	169
Figure 110: Web thickness loss histogram from the beam ends compiled - MaineDOT.....	171
Figure 111: Bottom flange thickness loss histogram from the beam ends compiled - MaineDOT ...	171
Figure 112: Top flange thickness loss histogram from the beam ends compiled - MaineDOT	172
Figure 113: M1 web hole's height distribution of W1 web corrosion pattern for beams without a diaphragm - MaineDOT	173
Figure 114: M1 web hole's depth distribution of W1 web corrosion pattern for beams without a diaphragm - MaineDOT	173
Figure 115: Web corrosion patterns distribution for beams without a diaphragm - MassDOT	174
Figure 116: CH ₁ distribution of W1 pattern for beams without a diaphragm - MassDOT	175
Figure 117: CL ₁ distribution of W1 pattern for beams without a diaphragm - MassDOT	175
Figure 118: Ratio of corrosion length (CL ₁) to corrosion height (CH ₁) of W1 pattern for beams without a diaphragm - MassDOT	176
Figure 119: Ratio of corrosion length (CL ₁) to corrosion height (CH ₁) of W1 pattern for beams without a diaphragm (range 0-15) - MassDOT	176
Figure 120: CL1 distribution of W1 web corrosion pattern, with corrosion height up to 30% of H ₀ for beams without a diaphragm - MassDOT	177
Figure 121: Max thickness loss distribution of W1 web corrosion pattern, with corrosion height up to 30% of H ₀ for beams without a diaphragm - MassDOT	177

Figure 122: First extreme W1 web corrosion pattern, with corrosion height up to 30% of H ₀ for beams without a diaphragm - MassDOT	178
Figure 123: CL ₁ distribution of W1 web corrosion pattern with corrosion greater than 90% of H ₀ for beams without a diaphragm - MassDOT	178
Figure 124: Max thickness loss distribution of W1 web corrosion pattern with corrosion height greater than 90% of H ₀ for beams without a diaphragm - MassDOT	179
Figure 125: Second extreme W1 web corrosion pattern, with corrosion height greater than 90% of H ₀ for beams without a diaphragm - MassDOT	179
Figure 126: Third extreme W1 web corrosion pattern, with corrosion height greater than 90% of H ₀ for beams without a diaphragm - MassDOT	180
Figure 127: Ratio of flange to web corrosion length distribution of W1 web corrosion pattern with corrosion height up to 30% of H ₀ for beams without a diaphragm - MassDOT	180
Figure 128: Ratio of flange to web corrosion length distribution of W1 web corrosion pattern for extreme scenario CASE B for beams without a diaphragm - MassDOT	181
Figure 129: Ratio of flange to web corrosion length distribution of W1 web corrosion pattern for extreme scenario CASE C for beams without a diaphragm - MassDOT	181
Figure 130: Max flange thickness loss distribution of W1 web corrosion pattern with corrosion height up to 30% of H ₀ for beams without a diaphragm - MassDOT	182
Figure 131: Max flange thickness loss distribution of W1 web corrosion pattern with full height corrosion for beams without a diaphragm - MassDOT	182
Figure 132: Max thickness loss distribution for W1 web corrosion patterns and M1 hole for beams without a diaphragm - MassDOT	183
Figure 133: M1 web hole's pattern height distribution of W1 web corrosion pattern for beams without a diaphragm - MassDOT	184
Figure 134: M1 web hole's pattern length distribution of W1 web corrosion pattern for beams without a diaphragm - MassDOT	184
Figure 135: M1 extreme web hole pattern scenario of W1 web corrosion pattern, projected on W1 CASE A, for beams without a diaphragm - MassDOT	185
Figure 136: Web thickness loss distribution of W2 pattern for beams without a diaphragm - MassDOT	185
Figure 137: CH ₁ distribution of W2 pattern for beams without a diaphragm - MassDOT	186
Figure 138: CL ₁ distribution of W2 pattern for beams without a diaphragm - MassDOT	186
Figure 139: CL ₂ distribution of W2 pattern for beams without a diaphragm - MassDOT	187
Figure 140: CL ₁ distribution of W2 web corrosion pattern corroded up to 30% of H ₀ for beams without a diaphragm - MassDOT	187
Figure 141: CL ₂ distribution of W2 web corrosion pattern corroded up to 30% of H ₀ for beams without a diaphragm - MassDOT	188
Figure 142: Max thickness loss distribution of W2 web corrosion pattern corroded up to 30% of H ₀ for beams without a diaphragm - MassDOT	188
Figure 143: W1 Case A extreme web corrosion scenario projected over W2 extreme web corrosion scenario - MassDOT	189
Figure 144: CH ₂ distribution of W3 web corrosion pattern for beams without a diaphragm - MassDOT	190
Figure 145: CH ₁ distribution of W3 web corrosion pattern with full height corrosion for beams without a diaphragm - MassDOT	190
Figure 146: CH ₃ distribution of W3 web corrosion pattern with full height corrosion for beams without a diaphragm - MassDOT	191

Figure 147: CL ₁ distribution of W3 web corrosion pattern with full height corrosion for beams without a diaphragm - MassDOT	191
Figure 148: CL ₂ distribution of W3 web corrosion pattern with full height corrosion for beams without a diaphragm - MassDOT	192
Figure 149: CL ₃ distribution of W3 web corrosion pattern with full height corrosion for beams without a diaphragm - MassDOT	192
Figure 150: Max web thickness loss distribution of W3 web corrosion pattern with full height corrosion for beams without a diaphragm - MassDOT	193
Figure 151: Extreme W3 web corrosion scenario for beams without a diaphragm - MassDOT	193
Figure 152: Ratio of flange to web corrosion length distribution of W3 web corrosion pattern with full height corrosion for beams without a diaphragm - MassDOT	194
Figure 153: Max flange loss thickness distribution of W3 web corrosion pattern with full height corrosion for beams without a diaphragm - MassDOT	194
Figure 154: M1 web hole's pattern height distribution of W3 web corrosion pattern for beams without a diaphragm - MassDOT	195
Figure 155: M1 web hole's pattern length distribution of W1 web corrosion pattern for beams without a diaphragm - MassDOT	195
Figure 156: M1 extreme web hole pattern scenario of W1 web corrosion pattern, projected on W3 extreme corrosion scenario, for beams without a diaphragm - MassDOT	196
Figure 157: CH2 distribution of W4 web corrosion pattern for beams without a diaphragm - MassDOT	196
Figure 158: CH1 distribution of W4 web corrosion pattern for beams without a diaphragm - MassDOT	197
Figure 159: CL1 distribution of W4 web corrosion pattern for beams without a diaphragm - MassDOT	197
Figure 160: CL2 distribution of W4 web corrosion pattern for beams without a diaphragm - MassDOT	198
Figure 161: Max web thickness loss distribution of W4 web corrosion pattern for beams without a diaphragm - MassDOT	198
Figure 162 : CH1 distribution of W4 web corrosion pattern, with corrosion height up to 50% of H ₀ for beams without a diaphragm - MassDOT	199
Figure 163: CL1 distribution of W4 web corrosion pattern, with corrosion height up to 50% of H ₀ for beams without a diaphragm - MassDOT	199
Figure 164: CL2 distribution of W4 web corrosion pattern, with corrosion height up to 50% of H ₀ for beams without a diaphragm - MassDOT	200
Figure 165: CL3 distribution of W4 web corrosion pattern, with corrosion height up to 50% of H ₀ for beams without a diaphragm - MassDOT	200
Figure 166: Max web thickness loss distribution of W4 web corrosion pattern, with corrosion height up to 50% of H ₀ for beams without a diaphragm - MassDOT	201
Figure 167: First extreme W4 web corrosion scenario for beams without a diaphragm - MassDOT	201
Figure 168: CH1 distribution of W4 web corrosion pattern, with full height corrosion for beams without a diaphragm - MassDOT	202
Figure 169: CL1 distribution of W4 web corrosion pattern, with full height corrosion for beams without a diaphragm - MassDOT	202
Figure 170: CL2 distribution of W4 web corrosion pattern, with full height corrosion for beams without a diaphragm - MassDOT	203

Figure 171: CL3 distribution of W4 web corrosion pattern, with full height corrosion for beams without a diaphragm - MassDOT	203
Figure 172: Max web thickness loss distribution of W4 web corrosion pattern, with full height corrosion for beams without a diaphragm - MassDOT	204
Figure 173: Second extreme W4 web corrosion scenario for beams without a diaphragm - MassDOT	204
Figure 174: First extreme W4 scenario (red) projected over extreme W3 web corrosion scenario (blue) - MassDOT	205
Figure 175: Second extreme W4 scenario (red) projected over extreme W3 web corrosion scenario (blue) - MassDOT	205
Figure 176: M1 web hole's pattern height distribution of W4 web corrosion pattern for beams without a diaphragm - MassDOT	206
Figure 177: M1 web hole's pattern length distribution of W3 web corrosion pattern for beams without a diaphragm - MassDOT	207
Figure 178: Max web thickness loss distribution of W5 web corrosion pattern for beams without a diaphragm - MassDOT	207
Figure 179: CH2 distribution of W5 web corrosion pattern for beams without a diaphragm - MassDOT	208
Figure 180: Max web thickness loss distribution of W5 web corrosion pattern for beams without a diaphragm - MassDOT	208
Figure 181:Ratio of corrosion length to height of W1 web corrosion pattern for beams without a diaphragm - MassDOT	209
Figure 182: Extreme W4 web corrosion scenario for beams without a diaphragm - MassDOT	209
Figure 183: Ratio of flange to web corrosion length distribution of W5 web corrosion pattern for beams without a diaphragm - MassDOT	210
Figure 184: Max flange thickness loss distribution of W5 web corrosion pattern for beams without a diaphragm - MassDOT	210
Figure 185: Web thickness loss histogram from the beam ends compiled - NHDOT	211
Figure 186: Bottom thickness loss histogram from the beam ends compiled - NHDOT	212
Figure 187 : Top thickness loss histogram from the beam ends compiled - NHDOT	212
Figure 188: M1 web hole's height distribution of W1 web corrosion pattern for beams without a diaphragm - NHDOT	213
Figure 189: M1 web hole's length distribution of W1 web corrosion pattern for beams without a diaphragm - NHDOT	213
Figure 190 : Web corrosion patterns distribution for beams ends without diaphragm – RIDOT	214
Figure 191: CH1 distribution of W1 pattern for beams without diaphragm - RIDOT	215
Figure 192: CL1 distribution of W1 pattern for beams without a diaphragm and $CH1 < 0.5H0$ – RIDOT	215
Figure 193: Web thickness loss of W1 pattern for beams without a diaphragm, $CH1 < 0.5H0$ and $CL1 < 3H0$ – RIDOT	216
Figure 194: Extreme scenario for pattern W1 – RIDOT	216
Figure 195: Flange thickness Loss for pattern W1 – RIDOT	217
Figure 196: Flange corrosion length for pattern W1 – RIDOT	217
Figure 197: Ratio between flange corrosion length and web corrosion length for pattern W1 – RIDOT	218
Figure 198: Height of M1 holes combined with W1 pattern – RIDOT	219
Figure 199: Depth of M1 holes combined with W1 pattern – RIDOT	219

Figure 200: Height of M3 hole combined with W1 pattern – RIDOT	219
Figure 201: Depth of M3 holes combines with W1 pattern – RIDOT	220
Figure 202: Schematic representation of W2 pattern – RIDOT	221
Figure 203: CH2 distribution for W3 pattern - RIDOT.....	221
Figure 204: CH1 distribution for W3 pattern and CH2>0.9H0 - RIDOT	222
Figure 205: CH3 distribution for W3 pattern and CH2>0.9H0 - RIDOT	222
Figure 206: CL1 distribution for W3 pattern and CH2>0.9H0 - RIDOT.....	222
Figure 207: CL2 distribution for W3 pattern and CH2>0.9H0 - RIDOT.....	223
Figure 208: CL3 distribution for W3 pattern and CH2>0.9H0 - RIDOT.....	223
Figure 209: Web thickness loss distribution for W3 pattern and CH2>0.9H0 - RIDOT	223
Figure 210: Extreme corrosion case for W3 pattern - RIDOT	224
Figure 211: Flange thickness loss distribution for W3 pattern – RIDOT.....	225
Figure 212: Flange corrosion length for W3 pattern – RIDOT	225
Figure 213: ratio between flange corrosion length and web corrosion length for W3 pattern – RIDOT	225
Figure 214: Height of M3 hole combined with W3 pattern – RIDOT	226
Figure 215: Length of M3 hole combined with W3 pattern – RIDOT.....	226
Figure 216: Height of M4 holes combined with W3 pattern – RIDOT.....	226
Figure 217: Length of M3 hole combined with W3 pattern – RIDOT.....	227
Figure 218: CH2 distribution for W4 pattern – RIDOT	227
Figure 219: CH1 distribution for W4 pattern – RIDOT	228
Figure 220: CL1 distribution for W4 pattern – RIDOT	228
Figure 221: CL2 distribution for W4 pattern – RIDOT	228
Figure 222: CL3 distribution for W4 pattern – RIDOT	229
Figure 223: Web thickness loss distribution for W4 pattern – RIDOT	229
Figure 224: Flange corrosion length distribution for W4 pattern – RIDOT.....	229
Figure 225: Ratio between flange corrosion length and corrosion length for W4 pattern – RIDOT .	230
Figure 226: Flange thickness loss distribution for W4 pattern – RIDOT.....	230
Figure 227: CH1 distribution for W5 pattern – RIDOT	231
Figure 228: CL1 distribution for W5 pattern – RIDOT	231
Figure 229: Web thickness loss for W5 pattern – RIDOT	231
Figure 230: Web thickness loss histogram from the beam ends compiled - VTrans	232
Figure 231: Bottom flange thickness loss histogram from the beam ends compiled - VTrans.....	233
Figure 232: Top flange thickness loss histogram from the beam ends compiled - VTrans	233
Figure 233: M1 web hole’s height distribution beams without a diaphragm - VTrans.....	234
Figure 234: M1 web hole’s depth distribution beams without a diaphragm - VTrans.....	234
Figure 235: M3 web hole’s height distribution beams without a diaphragm - VTrans.....	235
Figure 236 : M3 web hole’s depth distribution beams without a diaphragm - VTrans.....	235
Figure 237: M4 web hole’s height distribution beams without a diaphragm - VTrans.....	236
Figure 238: M4 web hole’s depth distribution beams without a diaphragm - VTrans.....	236
Figure 239 : M4 web hole’s distance from beam edge distribution beams without a diaphragm - VTrans.....	237
Figure 240: Web corrosion patterns distribution for beams ends with a diaphragm – CTDOT.....	238
Figure 241: Distribution of corrosion height for W1 pattern – CTDOT	239
Figure 242: Corrosion length distribution for W1 pattern and CH1 <0.2H0 – CTDOT	239
Figure 243 : Corrosion length distribution for W1 pattern and CH1 >0.9H0 – CTDOT	240
Figure 244 : Web thickness loss for W1 pattern and CH1<0.2H0 – CTDOT	240

Figure 245 : Web thickness loss for W1 pattern and $CH1 > 0.9H_0$ – CTDOT	241
Figure 246: Extreme corrosion scenario (case A) for beams with a diaphragm, W1 pattern – CTDOT	241
Figure 247: Extreme corrosion scenario (case B) for beams with a diaphragm, W1 pattern – CTDOT	242
Figure 248: Comparison between extreme corrosion scenarios. Blue represents the extreme scenario for beams without diaphragm, whereas the region in red depicts extreme corrosion scenario for beams with a diaphragm – CTDOT	242
Figure 249: Comparison between extreme corrosion scenarios. Blue represents the extreme scenario for beams without diaphragm, whereas the region in red depicts extreme corrosion scenario for beams with a diaphragm – CTDOT	242
Figure 250: CH2 distribution for W3 pattern for beams with a diaphragm – CTDOT	244
Figure 251: CH1 distribution for W3 pattern for beams with a diaphragm – CTDOT	244
Figure 252: CH2 distribution for W3 pattern for beams with a diaphragm – CTDOT	245
Figure 253: CL1 distribution for W3 pattern for beams with a diaphragm – CTDOT	245
Figure 254: CL2 distribution for W3 pattern for beams with a diaphragm – CTDOT	246
Figure 255: CL3 distribution for W3 pattern for beams with a diaphragm – CTDOT	246
Figure 256: Web thickness loss distribution for W3 pattern for beams with a diaphragm – CTDOT	247
Figure 257: Extreme corrosion scenario of W3 pattern for beam ends with a diaphragm – CTDOT	248
Figure 258: Comparison between extreme corrosion scenarios. Blue represents the extreme scenario for beams without diaphragm, whereas the region in red depicts extreme corrosion scenario for beams with a diaphragm – CTDOT	248
Figure 259. Web corrosion patterns distribution for beams with a diaphragm - MassDOT	249
Figure 260. CH1 distribution of W1 web pattern for beams with a diaphragm (total 189). - MassDOT	250
Figure 261: CL1 distribution of W1 web corrosion pattern for beams with a diaphragm - MassDOT	250
Figure 262: Max thickness loss distribution of W1 web corrosion pattern for beams with a diaphragm - MassDOT	251
Figure 263: CL1 distribution of full height W1 web corrosion pattern for beams with a diaphragm - MassDOT	251
Figure 264: Max thickness loss distribution of full height W1 web corrosion pattern for beams with a diaphragm - MassDOT	252
Figure 265: Max web thickness loss distribution of W1 web corrosion pattern, with corrosion height up to 35% of H_0 , for beams with a diaphragm - MassDOT	252
Figure 266: First extreme W1 web corrosion pattern, with full height corrosion for beams with a diaphragm - MassDOT	253
Figure 267: Ratio of flange to web corrosion length distribution of W1 web corrosion pattern, with full height corrosion and up to 35% of H_0 length, for beams with a diaphragm - MassDOT	254
Figure 268: Max flange thickness loss distribution of W1 web corrosion pattern, with full height corrosion and up to 35% of H_0 length, for beams with a diaphragm - MassDOT	254
Figure 269: Max web thickness loss distribution of W1 web corrosion pattern with corrosion height up to 30% of H_0 for beams with a diaphragm - MassDOT	255
Figure 270: CL1 thickness loss distribution of W1 web corrosion pattern with corrosion height up to 30% of H_0 for beams with a diaphragm - MassDOT	255
Figure 271: Second extreme W1 web corrosion pattern, with corrosion height up to 30% of H_0 for beams with a diaphragm - MassDOT	256

Figure 272: Ratio of flange to web corrosion length distribution of W1 web corrosion pattern with corrosion height up to 30% of H_0 for beams with a diaphragm - MassDOT	256
Figure 273: Max flange thickness loss distribution of W1 web corrosion pattern with corrosion height up to 30% of H_0 for beams with a diaphragm - MassDOT	257
Figure 274: Max thickness loss distribution for W1 web corrosion patterns and M1 hole for beams with a diaphragm - MassDOT	257
Figure 275: M1 web hole's pattern height distribution of W1 web corrosion pattern for beams with a diaphragm - MassDOT	258
Figure 276: M1 web hole's pattern length distribution of W1 web corrosion pattern for beams with a diaphragm - MassDOT	258
Figure 277: CH1 distribution for beams with M1 hole and W1 web corrosion pattern and a diaphragm - MassDOT	259
Figure 278: M1 extreme web hole pattern scenario of W1 web corrosion pattern, for beams with a diaphragm - MassDOT	259
Figure 279: Max thickness loss distribution for W1 web corrosion patterns and M2 hole for beams with a diaphragm - MassDOT	260
Figure 280: M2 web hole's pattern height distribution of W1 web corrosion pattern for beams with a diaphragm - MassDOT	260
Figure 281: M2 web hole's pattern length distribution of W1 web corrosion pattern for beams with a diaphragm - MassDOT	261
Figure 282: CH1 distribution of W2 pattern for beams with a diaphragm - MassDOT	262
Figure 283: CL1 distribution of W2 pattern for beams with a diaphragm - MassDOT	262
Figure 284: CL2 distribution of W2 pattern for beams with a diaphragm - MassDOT	263
Figure 285: Web thickness loss distribution of W2 pattern for beams with a diaphragm - MassDOT	263
Figure 286: Extreme W2 web corrosion pattern for beams with a diaphragm - MassDOT	264
Figure 287: W2 extreme web corrosion scenario (with red color) projected over W1 CASE B extreme web corrosion scenario (with blue color) - MassDOT	264
Figure 288: Ratio of flange to web corrosion length distribution of W2 web corrosion pattern corrosion for beams with a diaphragm - MassDOT	265
Figure 289: Max flange loss thickness distribution of W2 web corrosion pattern for beams without a diaphragm - MassDOT	265
Figure 290: M2 web hole's pattern height distribution of W1 and W2 web corrosion patterns for beams with a diaphragm - MassDOT	266
Figure 291: M2 web hole's pattern length distribution of W1 and W2 web corrosion patterns for beams with a diaphragm - MassDOT	267
Figure 292: M2 hole pattern projected on the extreme W2 web corrosion pattern. With black color is illustrated the diaphragm that could be found with these patterns. The parameters are $a \leq 0.11$, and $b \leq 0.3$ - MassDOT	267
Figure 293: CH2 distribution of W3 web corrosion pattern for beams with a diaphragm - MassDOT	268
Figure 294: CH1 distribution of W3 web corrosion pattern for beams with a diaphragm - MassDOT	268
Figure 295: CH3 distribution of W3 web corrosion pattern for beams with a diaphragm - MassDOT	269
Figure 296: CL1 distribution of W3 web corrosion pattern for beams with a diaphragm - MassDOT	269

Figure 297: CL2 distribution of W3 web corrosion pattern for beams with a diaphragm - MassDOT	270
Figure 298: CL3 distribution of W3 web corrosion pattern for beams with a diaphragm - MassDOT	270
Figure 299: Ma web thickness loss distribution of W3 web corrosion pattern for beams with a diaphragm - MassDOT	271
Figure 300: CL1 distribution of W3 web corrosion pattern with full height corrosion for beams with a diaphragm - MassDOT	272
Figure 301: CL2 distribution of W3 web corrosion pattern with full height corrosion for beams with a diaphragm - MassDOT	272
Figure 302: CL3 distribution of W3 web corrosion pattern with full height corrosion for beams with a diaphragm - MassDOT	273
Figure 303: CH1 distribution of W3 web corrosion pattern with full height corrosion for beams with a diaphragm - MassDOT	273
Figure 304: CH3 distribution of W3 web corrosion pattern with full height corrosion for beams with a diaphragm - MassDOT	274
Figure 305: Max web thickness loss distribution of W3 web corrosion pattern with full height corrosion for beams with a diaphragm - MassDOT	274
Figure 306: CL1 distribution of W3 web corrosion pattern with full height corrosion and deteriorated length up to 60% of H_0 for beams with a diaphragm - MassDOT	275
Figure 307: CH1 distribution of W3 web corrosion pattern with full height corrosion and deteriorated length up to 60% of H_0 for beams with a diaphragm - MassDOT	275
Figure 308: CH3 distribution of W3 web corrosion pattern with full height corrosion and deteriorated length up to 60% of H_0 for beams with diaphragm a - MassDOT	276
Figure 309: CL2 distribution of W3 web corrosion pattern with full height corrosion and deteriorated length up to 60% of H_0 for beams with a diaphragm - MassDOT	276
Figure 310: Max web thickness loss distribution, of W3 web corrosion pattern, with full height corrosion and deteriorated length up to 60% of H_0 for beams with a diaphragm - MassDOT	277
Figure 311: Ratio of flange to web corrosion length distribution, of W3 web corrosion pattern, with full height corrosion and deteriorated length up to 60% of H_0 for beams with a diaphragm - MassDOT	277
Figure 312: Max flange loss thickness distribution, for beams with W3 web corrosion pattern, with full height corrosion, deteriorated length up to 60% of H_0 and with a diaphragm - MassDOT	278
Figure 313: First extreme flange and W3 web corrosion scenario for beams with a diaphragm. - MassDOT	278
Figure 314: CH1 distribution of W3 web corrosion pattern, with full height corrosion and deteriorated length up to 230% of H_0 , for beams with a diaphragm - MassDOT	279
Figure 315: CH3 distribution of W3 web corrosion pattern, with full height corrosion and deteriorated length up to 230% of H_0 , for beams with a diaphragm - MassDOT	279
Figure 316: CL1 distribution of W3 web corrosion pattern, with full height corrosion and deteriorated length up to 230% of H_0 , for beams with a diaphragm - MassDOT	280
Figure 317: Max web thickness loss distribution, of W3 web corrosion pattern, with full height corrosion and deteriorated length up to 230% of H_0 , for beams with a diaphragm - MassDOT	280
Figure 318: Ratio of flange to web corrosion length distribution, of W3 web corrosion pattern, with full height corrosion and deteriorated length up to 230% of H_0 for beams with a diaphragm - MassDOT	281

Figure 319: Max flange loss thickness distribution, for beams with W3 web corrosion pattern, with full height corrosion, deteriorated length up to 230% of H_0 and with a diaphragm - MassDOT	281
Figure 320: Second extreme flange and W3 web corrosion scenario for beams with a diaphragm - MassDOT	282
Figure 321: CL1 distribution of W3 web corrosion pattern, with corrosion height up to 50% of H_0 , for beams with a diaphragm - MassDOT	282
Figure 322: CL2 distribution of W3 web corrosion pattern, with corrosion height up to 50% of H_0 , for beams with a diaphragm - MassDOT	283
Figure 323: CL3 distribution of W3 web corrosion pattern, with corrosion height up to 50% of H_0 , for beams with a diaphragm - MassDOT	283
Figure 324: CH1 distribution of W3 web corrosion pattern, with corrosion height up to 50% of H_0 , for beams with a diaphragm - MassDOT	284
Figure 325: CH2 distribution of W3 web corrosion pattern, with corrosion height up to 50% of H_0 , for beams with a diaphragm - MassDOT	284
Figure 326: CH3 distribution of W3 web corrosion pattern, with corrosion height up to 50% of H_0 , for beams with a diaphragm - MassDOT	285
Figure 327: Max web thickness loss distribution of W3 web corrosion pattern, with corrosion height up to 50% of H_0 , for beams with a diaphragm - MassDOT	285
Figure 328: Ratio of flange to web corrosion length distribution, of W3 web corrosion pattern, with corrosion height up to 50% of H_0 , for beams with a diaphragm - MassDOT	286
Figure 329: Max flange loss thickness distribution, for beams with W3 web corrosion pattern, with corrosion height up to 50% of H_0 , for beams with a diaphragm - MassDOT	286
Figure 330: Third extreme flange and W3 web corrosion scenario for beams with a diaphragm - MassDOT	287
Figure 331: M1 web hole's pattern height distribution of W3 web corrosion pattern for beams with a diaphragm - MassDOT	288
Figure 332: M1 web hole's pattern length distribution of W3 web corrosion pattern for beams with a diaphragm - MassDOT	288
Figure 333: M1 web hole's ratio length to height distribution of W3 web corrosion pattern for beams with a diaphragm - MassDOT	288
Figure 334: Max corrosion height distribution of W3 pattern with M1 hole, for beams with a diaphragm - MassDOT	289
Figure 335: M1 hole pattern projected on the second extreme W3 web corrosion pattern scenario. With black color is illustrated the diaphragm that could be found with these patterns - MassDOT ..	289
Figure 336: CH1 distribution of W4 web corrosion pattern for beams with a diaphragm - MassDOT	290
Figure 337: CH2 distribution of W4 web corrosion pattern for beams with a diaphragm - MassDOT	291
Figure 338: Max web thickness loss distribution of W4 web corrosion pattern for beams with a diaphragm - MassDOT	291
Figure 339: CL1 distribution of W4 web corrosion pattern for beams with a diaphragm - MassDOT	291
Figure 340: CL2 distribution of W4 web corrosion pattern for beams with a diaphragm - MassDOT	292
Figure 341: CL3 distribution of W4 web corrosion pattern for beams with a diaphragm - MassDOT	292

Figure 342: CH1 distribution of W4 web corrosion pattern with full height corrosion for beams with a diaphragm - MassDOT	293
Figure 343: CL1 distribution of W4 web corrosion pattern with full height corrosion for beams with a diaphragm - MassDOT	293
Figure 344: CL2 distribution of W4 web corrosion pattern with full height corrosion for beams with a diaphragm - MassDOT	294
Figure 345: CL3 distribution of W4 web corrosion pattern with full height corrosion for beams with a diaphragm - MassDOT	294
Figure 346: Max web thickness loss distribution of W4 web corrosion pattern with full height corrosion for beams with a diaphragm - MassDOT	295
Figure 347: First extreme W4 web corrosion scenario for beams with a diaphragm - MassDOT	295
Figure 348: CH1 distribution of W4 web corrosion pattern, with corrosion height up to 40% of H_0 , for beams with a diaphragm - MassDOT	296
Figure 349: CL1 distribution of W4 web corrosion pattern, with corrosion height up to 40% of H_0 , for beams with a diaphragm - MassDOT	296
Figure 350: CL3 distribution of W4 web corrosion pattern, with corrosion height up to 40% of H_0 , for beams with a diaphragm - MassDOT	297
Figure 351: CL2 distribution of W4 web corrosion pattern, with corrosion height up to 40% of H_0 , for beams with a diaphragm - MassDOT	297
Figure 352: Max web thickness loss distribution of W4 web corrosion pattern, with corrosion height up to 40% of H_0 , for beams with a diaphragm - MassDOT	298
Figure 353: Second extreme W4 web corrosion scenario for beams with a diaphragm - MassDOT	298
Figure 354: M2 web hole's pattern height distribution of W3 and W4 web corrosion pattern for beams with a diaphragm - MassDOT	299
Figure 355: M2 web hole's pattern length distribution of W3 and W4 web corrosion pattern for beams with a diaphragm - MassDOT	299
Figure 356: Extreme M2 hole pattern scenario projected on second extreme W4 web corrosion scenario for beams with a diaphragm - MassDOT	300
Figure 357: CH1 distribution of W5 web corrosion pattern for beams with a diaphragm - MassDOT	300
Figure 358: CL1 distribution of W4 web corrosion pattern for beams with a diaphragm - MassDOT	301
Figure 359: Max web thickness loss distribution of W5 web corrosion pattern for beams with a diaphragm - MassDOT	301
Figure 360: Max flange thickness loss of beams with W5 web corrosion pattern for beams with a diaphragm - MassDOT	302
Figure 361: Ratio of flange to web corrosion length distribution, of W5 web corrosion pattern for beams with a diaphragm - MassDOT	302
Figure 362: Extreme W5 web corrosion scenario for beams with a diaphragm - MassDOT	303
Figure 363: Web corrosion patterns distribution for beams ends with a diaphragm – RIDOT	304
Figure 364: CH1 distribution for beams with diaphragm and W1 corrosion pattern – RIDOT	305
Figure 365: CL1 distribution for beams with diaphragm and W1 corrosion pattern – RIDOT	305
Figure 366: Web thickness loss distribution for beams with diaphragm and W1 corrosion pattern – RIDOT	306
Figure 367: Extreme corrosion case of W1 pattern for beams with a diaphragm – RIDOT	306

Figure 368: Comparison between extreme corrosion scenarios. Blue represents the extreme scenario for beams without diaphragm, whereas the region in red depicts extreme corrosion scenario for beams with a diaphragm – RIDOT	307
Figure 369: Flange corrosion length for beam ends with diaphragm for W1 pattern – RIDOT	307
Figure 370: Ratio between flange corrosion length and web corrosion length for W1 pattern – RIDOT	308
Figure 371: Flange thickness loss distribution for W1 pattern – RIDOT.....	308
Figure 372: Height of M1 holes combined with W1 pattern – RIDOT.....	309
Figure 373: Depth of M1 holes combined with W1 pattern – RIDOT.....	310
Figure 374: Height of M3 holes combined with W1 pattern – RIDOT.....	310
Figure 375: Depth of M3 holes combined with W1 pattern – RIDOT.....	311
Figure 376: CH2 distribution for W3 pattern – RIDOT	311
Figure 377: CH1 distribution for W3 pattern – RIDOT	312
Figure 378: CH3 distribution for W3 pattern – RIDOT	312
Figure 379: CL1 distribution for W3 pattern – RIDOT	313
Figure 380: CL2 distribution for W3 pattern – RIDOT	313
Figure 381: CL3 distribution for W3 pattern – RIDOT	314
Figure 382: Web thickness loss distribution for W3 pattern – RIDOT.....	315
Figure 383: Flange corrosion length for W3 pattern – RIDOT	315
Figure 384: Ratio between flange corrosion length and web corrosion length for W3 pattern – RIDOT	316
Figure 385: Flange thickness loss distribution for W3 pattern – RIDOT.....	316

List of Tables

Table 1: Project Tasks	28
Table 2: Preliminary Sorting of Inspection reports	52
Table 3: Web corrosion pattern W1	53
Table 4: Web corrosion pattern W2	54
Table 5: Web corrosion pattern W3	54
Table 6: Web corrosion pattern W4	55
Table 7: Web corrosion pattern W5	55
Table 8: Web corrosion pattern W6.	56
Table 9: Web hole pattern M1	57
Table 10: Web hole pattern M2.....	57
Table 11: Web hole pattern M3.....	58
Table 12: Web hole pattern M4.....	58
Table 13: Beam end categorization metrics for beam ends without a diaphragm system.....	63
Table 14: Beam end categorization metrics for beam ends with a diaphragm system.....	63
Table 15: Dominant cases for beams without a diaphragm system.....	64
Table 16: Dominant cases for beams with diaphragm	64
Table 17: Final corrosion patterns for W1 and W2 without holes (beam ends without diaphragm) - CTDOT.....	65
Table 18 : Final corrosion patterns for W3 and W4 without holes (beam ends without diaphragm) - CTDOT.....	66
Table 19: Final corrosion patterns for W5 without holes (beam ends without diaphragm) - CTDOT. 66	
Table 20: Final corrosion patterns for W1 and W2 without holes (beam ends with diaphragm) - CTDOT.....	67
Table 21: Final corrosion patterns for W3 and W4 without holes (beam ends with diaphragm) - CTDOT.....	68
Table 22: Beam end categorization metrics for beam ends without a diaphragm system.....	69
Table 23 : Beam end categorization metrics or beam ends with a diaphragm system	69
Table 24: Distribution of beam ends according to district	69
Table 25: Metrics for beam ends with a diaphragm after the merging.....	70
Table 26: Metrics for beam ends without a diaphragm after the merging.....	70
Table 27: Final corrosion patterns for W1 and W2 without holes (beam ends without a diaphragm) - MassDOT	72
Table 28: Final corrosion patterns for W1 and W2 with holes (beam ends without a diaphragm) - MassDOT	73
Table 29: Final corrosion patterns for W3 and W4 without holes (beam ends without a diaphragm) - MassDOT	73
Table 30: Final corrosion patterns for W3 and W4 with holes (beam ends without a diaphragm) - MassDOT	75
Table 31: Final corrosion patterns for W5 without holes (beam ends without a diaphragm) - MassDOT	75
Table 32: Final corrosion patterns for W1 and W2 without holes (beam ends with a diaphragm) - MassDOT	77
Table 33: Final corrosion patterns for W1 and W2 with holes (beam ends with a diaphragm) - MassDOT	79

Table 34: Final corrosion patterns for W1 and W2 with holes (beam ends with a diaphragm) - MassDOT	79
Table 35: Final corrosion patterns for W3 and W4 without holes (beam ends with a diaphragm) - MassDOT	80
Table 36: Final corrosion patterns for W3 and W4 with holes (beam ends with a diaphragm) - MassDOT	82
Table 37: Final corrosion patterns for W3 and W4 with holes (beam ends with a diaphragm) - MassDOT	82
Table 38: Final corrosion patterns for W5 with holes (beam ends with a diaphragm) - MassDOT	84
Table 39: Beam end categorization metrics for beam ends without a diaphragm	85
Table 40: Beam end categorization metrics for beam ends with a diaphragm	85
Table 41: Dominant cases for beams without a diaphragm	85
Table 42: Dominant cases for beams with a diaphragm	86
Table 43: Final corrosion patterns for W1 and W2 without holes (beam ends without a diaphragm) - RIDOT	87
Table 44: Final corrosion patterns for W3 and W4 without holes (beam ends without a diaphragm) - RIDOT	88
Table 45 : Final corrosion patterns for W1 and W2 without holes (beam ends with a diaphragm) - RIDOT	89
Table 46: Beams Received by State	93
Table 47. Beam Specimen Measurements	105
Table 48. Specimen 1 Corrosion Profile	110
Table 49. Specimen 1 Experimental Results	110
Table 50. Specimen 2 Corrosion Profile	111
Table 51. Specimen 2 Experimental Results	111
Table 52. Specimen 3 Corrosion Profile	112
Table 53. Specimen 3 Experimental Results	112
Table 54. Specimen 4 Corrosion Profile	113
Table 55. Specimen 4 Experimental Results	113
Table 56. Specimen 5 Corrosion Profile	114
Table 57. Specimen 5 Experimental Results	114
Table 58. Specimen 6 Corrosion Profile	115
Table 59. Specimen 6 Experimental Results	115
Table 60. Specimen 7 Corrosion Profile	116
Table 61. Specimen 7 Experimental Results	116
Table 62. Specimen 8 Corrosion Profile	117
Table 63. Specimen 8 Experimental Results	117
Table 64. Specimen 9 Corrosion Profile	118
Table 65. Specimen 9 Experimental Results	118
Table 66. Specimen 10 Corrosion Profile	119
Table 67. Specimen 10 Experimental Results	119
Table 68. Specimen 11 Corrosion Profile	120
Table 69. Specimen 11 Experimental Results	120
Table 70. Specimen 12 Corrosion Profile	121
Table 71. Specimen 12 Experimental Results	121
Table 72. Summarized Experimental and Finite Element Capacities	122
Table 73. Experimental Capacity Evaluation by State	131

Table 74. Experimental Capacity Evaluation, Percent Difference from Experiment.....	131
Table 75: Summary of extreme scenarios of W1 pattern - CTDOT.....	149
Table 76: Holes and patterns for beams without a diaphragm - CTDOT.....	150
Table 77: Hole appearances for beams without a diaphragm - MassDOT.....	183
Table 78: Hole appearances for beams- MassDOT.....	206
Table 79: Holes and patterns for beams without a diaphragm – RIDOT	218
Table 80: Holes for beams ends from VTrans.....	233
Table 81: Holes and patterns for beams ends with diaphragm from CTDOT.....	243
Table 82: Dimensions of holes of pattern W3 for beam ends with a diaphragm – CTDOT	243
Table 83: Holes for beams with a diaphragm – MassDOT	265
Table 84: Holes and patterns for beams ends with diaphragm from RIDOT	309
Table 85: Dimensions of M4 hole combined with W3 pattern – RIDOT	317

1. Introduction

While transportation systems serve most of the nations' population, ASCE [1] points out that 7.5% of the bridges in the U.S. are structurally deficient. In absolute terms, this means that roughly 46,000 bridges in the U.S. need constant attention and/or repairs. This number is only expected to grow in the coming years, as our nation's infrastructure continues to age and deteriorate. New England is home to 10,155 steel bridges, 7,344 of which are labelled as "Fair" or "Poor" via the InfoBridge database [46].

When considering steel bridges, corrosion represents a major source of deterioration particularly in coastal regions or in areas where de-icing chemicals are used and may result in the loss of serviceability of affected bridges. Corrosion can occur anywhere on the steel bridge beams, but the area of interest for this study is the beam end. Beam ends are critical to the structural system, as damage to them significantly reduces the capacity of the whole beam. In extreme cases, corrosion can lead to the failure or closing of a bridge. For this reason, determining an estimate of remaining capacity via laboratory tests of the beams and structural system is a crucial task. Conducting these tests ultimately help us understand and assure the safety of other bridge systems. Additionally, corrosion can often cause irregular patterns, thus causing more challenges in the construction of models that predict the remaining capacity of damaged beams ([2]-[45],[54],[55],[57],[58]).

Corrosion is a pressing issue for steel bridges in the New England region specifically. With harsh precipitation and winter temperatures, chemical use is necessary for de-icing roads and bridge structures. As a result of this process, inspectors have been observing increasing corrosion due to de-icing chemicals and water. This project aims to develop tools which can more accurately estimate the remaining capacity of corroded beams in the New England region than those currently available to engineers. To achieve this, the project was divided into six tasks, summarized in Table 1:

Table 1: Project tasks

Task #	Description of work
Task 1	Identify common unstiffened beam-end corrosion topologies
Task 2	Review of existing structures
Task 3	Laboratory testing
Task 4	Calculate and validate/update the new load rating procedures
Task 5	Draft final report, Technology Transfer tool box
Task 6	Final report

This report exclusively covers tasks one through four and stands as the final task (Task 6) in this project. In general, the first task was to collect and compile the inspection reports information provided by state Departments of Transportation (DOTs) of the New England region. Using this data, the most common shapes and locations of corrosion were identified in bridge beam ends. This allowed the research team to select bridge candidates

with beam specimens of interest to be delivered and tested at the University of Massachusetts Amherst. Upon arrival, these specimens were measured, classified on testability, and inventoried. A total of fifty-two beams were received from five of the six New England States. Of the beams received, twelve beams were tested as a part of this project. Beam specimens were then measured and scanned to evaluate section loss and for input data for Finite Element Simulation via the research team's protocol. Following damage evaluation, the specimens were experimentally tested for their remaining capacity. Finally, the capacities of the corroded ends were estimated using each state's load rating procedures which allowed the research team to make recommendations and update or validate current procedures.

2. Inspection Report Data Collection

The database available for this project was provided all state DOTs from the New England region. As each state has its own method of reporting data, the specific inspection report processes of each state are discussed in the following section. It is important to note in this data collection process that the project focuses on the corrosion of beam ends whose bridge superstructures National Bridge Inventory (NBI) ratings were less than or equal to 5.

2.1.1. Format of data received from the Connecticut Department of Transportation (CTDOT) Inspection reports

According to the CTDOT Bridge Manual [23], there are two types of inspection reports for bridge structures in the State of Connecticut: (i) Routine inspections and (ii) In-depth inspections. Routine inspections are conducted on a biennial basis and aim to identify critical problems or deficiencies so corrections can be made before the structure presents hazards to the public.

For this project, only routine inspections were provided and considered to evaluate corrosion patterns and damage in the bridge beams. Figure 1 depicts an example of a report from CTDOT.

Form: BRI-19, Rev. 2/15 Inspection type: Routine Inspection Date: 5/21/2019 Inspected by: Infrastructure Engineers	Bridge No 05158	Town: WASHINGTON Carried: TUNNEL ROAD Crossed: SHEPAUG RIVER Inventory Route: Non-NHS
---	------------------------	--

STRUCTURE INVENTORY & APPRAISAL

<p style="text-align: center; margin: 0;">INSPECTION</p> <p>Structurally Deficient <input checked="" type="checkbox"/> Functionally Obsolete <input type="checkbox"/></p> <p>Sufficiency Rating <input type="text" value="56.6"/></p> <p>(90) Inspection Date <input type="text" value="05/21/2019"/> (91) Frequency <input type="text" value="24"/></p> <p>Indepth Insp <input type="text" value="No"/> Proposed next Indepth Year <input type="text"/></p> <p>Deck Survey Date <input type="text"/> Class <input type="text" value="01"/></p> <p>Access <input type="text" value="22 - 30-40 ft.reach required"/> Flagman <input type="text" value="0"/></p> <table border="1" style="width: 100%; border-collapse: collapse; margin-top: 5px;"> <thead> <tr> <th style="width: 20%;">Fracture</th> <th style="width: 20%;">Frequency</th> <th style="width: 20%;">Date</th> <th style="width: 40%;">Type</th> </tr> </thead> <tbody> <tr> <td>Underwater</td> <td><input type="text"/></td> <td><input type="text"/></td> <td><input type="text"/></td> </tr> <tr> <td>Special</td> <td><input type="text"/></td> <td><input type="text"/></td> <td><input type="text"/></td> </tr> </tbody> </table>	Fracture	Frequency	Date	Type	Underwater	<input type="text"/>	<input type="text"/>	<input type="text"/>	Special	<input type="text"/>	<input type="text"/>	<input type="text"/>	<p style="text-align: center; margin: 0;">STRUCTURE TYPE & MATERIALS</p> <p>(43) Structure Type, Main</p> <p>A) Material <input type="text" value="3 - Steel"/></p> <p>B) Design Type <input type="text" value="02 - Stringer/Multi-beam or Girder"/></p> <p>(44) Structure Type, Approach</p> <p>A) Material <input type="text" value="0 - Other"/></p> <p>B) Design Type <input type="text" value="00 - Other"/></p> <p>(45) Number of Spans, Main Unit <input type="text" value="003"/></p> <p>(46) Number of Approach Spans <input type="text" value="0000"/></p> <p>(107) Deck Structure Type <input type="text" value="1 - Concrete Cast-in-Place"/></p> <p>(108) Wearing Surface/Protection Systems</p> <p>A) Type of Wearing Surface <input type="text" value="6 - Bituminous"/></p> <p>B) Type of Membrane <input type="text" value="0 - None"/></p> <p>C) Type of Deck Protection <input type="text" value="0 - None"/></p> <p>Substructure</p> <p>A) Material <input type="text" value="2 - CONCRETE"/></p> <p>B) Design Type <input type="text" value="2 - STUB ABUTMENT"/></p> <p>Paint</p> <p>Type <input type="text" value="3 - Non-Lead Paint"/></p> <p>Year <input type="text" value="1956"/></p> <p>Comment <input type="text" value="Based on visual inspection."/></p>
Fracture	Frequency	Date	Type										
Underwater	<input type="text"/>	<input type="text"/>	<input type="text"/>										
Special	<input type="text"/>	<input type="text"/>	<input type="text"/>										
<p style="text-align: center; margin: 0;">IDENTIFICATION</p> <p>Bridge Name <input type="text" value="05158"/></p> <p>Town Code - Name <input type="text" value="79720 - WASHINGTON"/></p> <p>(5) Inventory Route</p> <p>(A) Record Type <input on"="" structure"="" the="" type="text" value="1 - Route carried "/></p> <p>(B) Signing Prefix <input type="text" value="5 - CITY STREET"/></p> <p>(C) Level of Service <input type="text" value="0 - NONE OF THE BELOW"/></p> <p>(D) Route Number. <input type="text" value="00000"/></p> <p>(E) Dir Suffix <input type="text" value="0 - NOT APPLICABLE"/></p> <p>(6A) Featured Intersected <input type="text" value="SHEPAUG RIVER"/></p> <p>(6B) Critical Facility Indicator <input type="text"/></p> <p>(7) Facility Carried <input type="text" value="TUNNEL ROAD"/></p> <p>(9) Location <input type="text" value="100 FT S OF CHURCH HILL R"/></p> <p>(11) Mile Post <input type="text" value="0"/> Miles</p> <p>(16) Latitude <input type="text" value="41"/> Deg. <input type="text" value="37"/> Min. <input type="text" value="18.26"/> Sec.</p> <p>(17) Longitude <input type="text" value="-73"/> Deg. <input type="text" value="19"/> Min. <input type="text" value="32.62"/> Sec.</p> <p>(98) Border Bridge</p> <p>(A) State Code <input type="text"/> (B) Percent Responsibility <input type="text"/> %</p> <p>(C) Border Town Name <input type="text"/></p> <p>(99) Border Bridge Structure No. <input type="text"/></p>	<p style="text-align: center; margin: 0;">GEOMETRIC DATA</p> <p>(48) Length of Maximum Span <input type="text" value="36"/> ft.</p> <p>(49) Structure Length <input type="text" value="112"/> ft.</p> <p>(50) Curb or Sidewalk Widths</p> <p>A) Left <input type="text" value="0"/> ft. <input type="text" value="9"/> in. B) Right <input type="text" value="0"/> ft. <input type="text" value="9"/> in.</p> <p>(51) Bridge Roadway Width Curb to Curb <input type="text" value="22"/> ft. <input type="text" value="0"/> in.</p> <p>(52) Deck Width, Out to Out <input type="text" value="25"/> ft. <input type="text" value="6"/> in.</p> <p>(32) Approach Roadway Width <input type="text" value="24"/> ft.</p>												

Figure 1: Sample of report provided by CTDOT

Routine inspection reports, in general, are divided into the 11 following sections:

1. Report cover
2. Table of contents
3. Report title page
4. Location map
5. Structure inventory and appraisal (BRI-19)
6. Inventory routes under structure (BRI-25)
7. Inspection Data (BRI-18)
8. National bridge elements
9. Fracture critical data (BRI-12)
10. Sketches
11. Pictures

The first three sections present general information about the report and the bridge structure (e.g., identification number, date of report, company responsible for the inspection report). The “*Location map*” section describes the bridge location, including its latitude and longitude. The “*Structure inventory and appraisal (BRI-19)*” section presents a summary of the NBI ratings, which are imperative to scope of this work. The section “*Inventory routes under structure (BRI-25)*” summarizes information about the route under the bridge. It is important to note that in case the structure is above water, this section is not considered or presented in the inspection report.

The section “*Inspection data (BRI-18)*” denotes specific details and data from the field inspection. This section is of major interest to the project because many reports include comments about the condition of the structure, field measurements, bridge component conditions, and often the corresponding NBI ratings.

The table depicted in section “*National bridge elements*” is required by Federal Highway Administration (FHWA) [24]. For this reason, all reports present a similar table. Such a table summarizes the condition of several components of the bridge.

The section “*Fracture critical data (BRI-12)*” aims to report all fractures encountered in the bridge. Finally, the sections “*Sketches*” and “*Pictures*” report visual information, which complements the notes presented in the “*Inspection data*” section. It is worthwhile pointing out that all pictures are labeled. Often, inspection notes reference pictures so a reader or inspector can fully understand what is being described in the notes.

Much of the corrosion information gathered to meet the goals of this task was found by compiling the notes of inspection data, sketches, and the pictures. Figure 2 below depicts a corrosion scenario described by a sketch and by a photograph presented in an inspection report from the State of Connecticut.

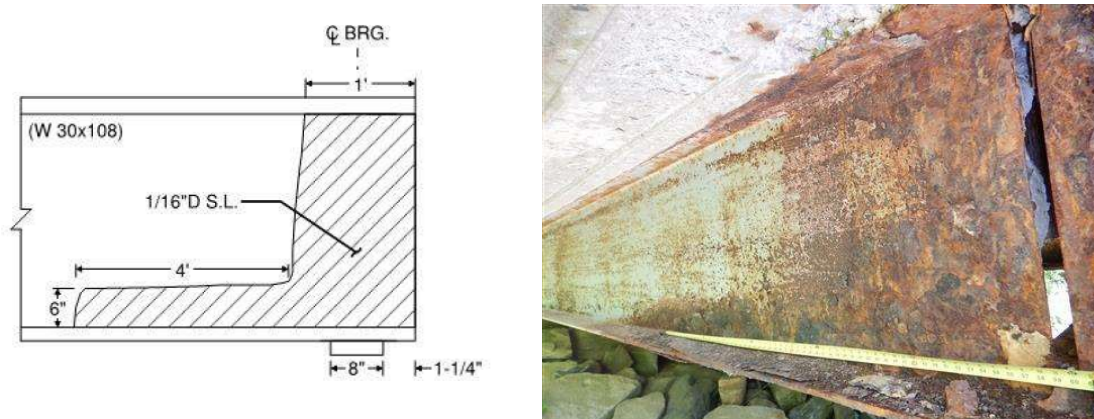


Figure 2: Sketch (Left) and Photography (Right) of corrosion damage

2.1.2. Format of data received from the Maine Department of Transportation (MaineDOT) Inspection reports

Similarly to the State of Connecticut, there are four types of reports collected from the State of Maine (MaineDOT): (i) Routine inspections, (ii) Special inspections, (iii) Underwater inspections, and (iv) Fracture critical inspections. The routine inspections are conducted on a regular basis, special inspections are conducted on demand, and underwater inspections are often conducted on a 60-month cycle. Fracture critical inspections are conducted on a 24-month cycle.

The inspection reports from MaineDOT are, in general, organized into the following five sections:

1. Report cover
2. National bridge inventory
3. Inspection notes report
4. Element inspection
5. Photos

The “*report cover*” provides general information about the bridge structure and the report. For instance, name and ID of the bridge, as well as the type of inspection can be found in this section. In the section “*National bridge inventory*”, shown in Figure 3, the report summarizes the NBI ratings for several items of the bridge. These ratings are of interest to the evaluation of corrosion patterns and severity of damage.

The section “*Element inspection*” consists of a table which summarizes the condition of several components of the bridge and is required by FHWA. The “*Inspection notes report*” section provides comments and field measurements based on the inspection. Lastly, the section “*Photos*” depicts several photographic records of the bridge under inspection.

Unfortunately, not all reports include field measurements. This can cause difficulty in the assessment of the impact caused by corrosion. Additionally, the photographs documented include labels but are not referenced in the field notes, which poses a challenge in identifying each part of the structure.

With the goal of increasing the available corrosion damage data for the project, the load ratings were provided by the MaineDOT. Via the load rating data, more information about corrosion is provided and were ultimately used to determine the beam type of each bridge. It was feasible to estimate the section loss in bridge beams by compiling information from the documents provided by MaineDOT.

National Bridge Inventory

Status: 1 - SD

Bridge Name: KENNEDY

Sufficiency Rating: 49.1

Inspections	
(90) INSPECTION DATE	& (91) DESIGNATED INSPECTION FREQUENCY
	24 04/18/2019
(92) CRITICAL FEATURE INSPECTION	& (93) CFI DATE
(92A) FRACTURE CRITICAL DETAIL	N
(92B) UNDERWATER INSPECTION	N
(92C) OTHER SPECIAL INSPECTION	N

Identification	
(1) STATE CODE	231 - Maine
(8) STRUCTURE NUMBER	0394
(5) INVENTORY ROUTE	
(5A) RECORD TYPE	1: Route carried "on" the structure
(5B) ROUTE SIGNING PREFIX	5 - CITY STREET
(5C) DESIGNATED LEVEL OF SERVICE	0 - None
(5) INVENTORY ROUTE	0
(5) INVENTORY ROUTE	0 - NOT APPLICABLE
(2) HIGHWAY AGENCY DISTRICT	03 - Western
(3) COUNTY CODE	007 Franklin
(4) PLACE CODE	81300
(6) FEATURES INTERSECTED	HOUGHTON BROOK
(7) FACILITY CARRIED	TEMPLE RD
(9) LOCATION	0.8 MI E RTE 156
(11) MILEPOINT	1.300
(12) BASE HIGHWAY NETWORK	Inventory Route is not on the Base Network
(13) LRS INVENTORY ROUTE, SUBROUTE	
(13A) LRS INVENTORY ROUTE	0000701105
(13B) SUBROUTE NUMBER	00
(16) LATITUDE	44.70501
(17) LONGITUDE	-70.39612
(98A) BORDER BRIDGE CODE	
(98B) PERCENT RESPONSIBILITY	0
(99) BORDER BRIDGE STRUCT NO.	

Structure Type and Material	
(43) STRUCTURE TYPE, MAIN	
(43A) KIND OF MATERIAL/DESIGN	3 - Steel
(43B) TYPE OF DESIGN/CONSTR	02 - Stringer/Multi-beam or Girder
(44) STRUCTURE TYPE, APPROACH SPANS	
(44A) KIND OF MATERIAL/DESIGN	0 - Other
(44B) TYPE OF DESIGN/CONSTRUCTION	00 - Other
(45) NUMBER OF SPANS IN MAIN UNIT	1
(46) NUMBER OF APPROACH SPANS	0
(107) DECK STRUCTURE TYPE	8 - Wood or Timber
(108) WEARING SURFACE/PROTECTIVE SYSTEMS	
(108A) WEARING SURFACE	7 - Wood or Timber
(108B) DECK MEMBRANE	0 - None
(108C) DECK PROTECTION	0 - None

Age of Service	
(27) YEAR BUILT	1990
(106) YEAR RECONSTRUCTED	2010
(42) TYPE OF SERVICE	
(42A) TYPE OF SERVICE ON BRIDGE	1 - Highway
(42B) TYPE OF SERVICE UNDER BRIDGE	5 - Waterway
(28) LANES	
(28A) LANES ON THE STRUCTURE	01
(28B) LANES UNDER THE STRUCTURE	00
(29) AVERAGE DAILY TRAFFIC	64
(30) YEAR OF AVERAGE DAILY TRAFFIC	2016
(109) AVERAGE DAILY TRUCK TRAFFIC	5
(19) BYPASS DETOUR LENGTH	100

Figure 3: Sample of report provided by MaineDOT

2.1.3. Format of data received from the Massachusetts Department of Transportation (MassDOT) Inspection reports

The inspection reports from MassDOT can be subdivided in twelve types and the information is taken from the MassDOT Bridge Inspection Handbook [48]:

- i. Routine: This report aims to provide information on the overall condition of the bridge.
- ii. Special member: This report provides information regarding a specific element of the bridge.
- iii. Combination of routine and special member: This report culminates information on the overall condition of the bridge and specific elements.
- iv. Closed/Rehabilitation: This report has a primary focus on the traffic safety of a closed bridge.
- v. Other: This report primarily focuses on documenting special events (for example floods or repairs).
- vi. Underwater: This report documents the conditions of the bed of the water feature and the bridge structure. This report type has three types of its own: routine, special member, low clearance
- vii. Freeze-Thaw: This report documents the conditions of the exposed concrete
- viii. Fracture Critical: This report documents fracture critical members and elements of the structure and their condition
- ix. Initial Inspection: This report is to document after a structure is built or rehabilitated or being added to the bridge inventory. It includes the inspection of elements and records the “as-built” structure.
- x. Damage Inspection: This report documents the structure after an incident to inspect, record the resulting damage, and how it may impact other parts of the structure
- xi. Divers Activity Report: Provides observations and remarks on the structure underwater and what was conducted in the dive/inspection
- xii. Element Level Inspection: This report is of the bridge elements in the structure (National Bridge Elements, Bridge Management Elements, Agency Developed Elements)

Although the reports from MassDOT are not formally divided into different sections, each inspection report follows the same structure:

1. NBI Ratings
2. Inspection notes
3. Photos
4. National Bridge Element inspection

The first section, “NBI ratings” displays the ratings of several NBI items and general information about the bridge. This includes but is not limited to the structure’s name, location, structural system, and deck type. Figure 5 depicts the first page of a MassDOT bridge inspection report.

The “inspection notes” section consists of written information about the elements of the bridge structure. Often, imperative information and measurements, such as corrosion

data, can be found in this section. Additionally, this section contains details regarding bridge elements and defects that were detected during the inspection.

The “Photos” section contains several pictures from the bridge inspection, which often include a detailed description. Additionally, the inspection notes reference the photographs often, aiming to illustrate what is being described by text. The combination of sketches, photos and inspection notes represent the major source of corrosion data. Figure 4 depicts an example of a sketch and a picture illustrating corrosion damage taken from the records of MassDOT.

Finally, the last section, “National Bridge Element inspection”, presents the table requested by FHWA [24].



**Figure 4 : The same beam, as was described by sketch (left) and by photograph (right).
Adopted from W46010-3RY-DOT-NBI (district 5, City of Wrentham)**

2-DIST 05	B.I.N. AF0	STRUCTURES INSPECTION FIELD REPORT	BR. DEPT. NO. K-01-010
ROUTINE INSPECTION			
CITY/TOWN KINGSTON		8-STRUCTURE NO. K01010-AF0-DOT-NBI	11-Kilo. POINT 028.871
07-FACILITY CARRIED ST 3 PILGRIM HWY		MEMORIAL NAME/LOCAL NAME GRAND ARMY	41-STATUS A:OPEN
06-FEATURES INTERSECTED HWY LANDING RD		26-FUNCTIONAL CLASS Freeway/Expressway	90-ROUTINE INSP. DATE FEB 19, 2016
43-STRUCTURE TYPE 402 : Steel continuous Stringer/Girder		22-OWNER State Highway Agency	27-YR BUILT 1955
107-DECK TYPE 1 : Concrete Cast-in-Place		21-MAINTAINER State Highway Agency	106-YR REBUILT 1979
		WEATHER SUNNY	YR REHAB'D (NON 106) 0000
		TEMP (air) 4°C	DIST BRIDGE INSPECTION ENGINEER G. Simpson
		TEAM LEADER W. Ferry	
		TEAM MEMBERS M. SILVIA, M. MARSHALL	

<table border="1" style="width:100%; border-collapse: collapse;"> <tr> <td style="text-align:center;">ITEM 58</td> <td style="text-align:center;">6</td> <td style="text-align:right;">DEF</td> </tr> <tr> <td colspan="3">DECK</td> </tr> <tr><td>1.Wearing surface</td><td style="text-align:center;">7</td><td style="text-align:center;">-</td></tr> <tr><td>2.Deck Condition</td><td style="text-align:center;">6</td><td style="text-align:center;">-</td></tr> <tr><td>3.Stay in place forms</td><td style="text-align:center;">6</td><td style="text-align:center;">-</td></tr> <tr><td>4.Curbs</td><td style="text-align:center;">N</td><td style="text-align:center;">-</td></tr> <tr><td>5.Median</td><td style="text-align:center;">H</td><td style="text-align:center;">-</td></tr> <tr><td>6.Sidewalks</td><td style="text-align:center;">N</td><td style="text-align:center;">-</td></tr> <tr><td>7.Parapets</td><td style="text-align:center;">7</td><td style="text-align:center;">-</td></tr> <tr><td>8.Railing</td><td style="text-align:center;">N</td><td style="text-align:center;">-</td></tr> <tr><td>9.Anti Missile Fence</td><td style="text-align:center;">N</td><td style="text-align:center;">-</td></tr> <tr><td>10.Drainage System</td><td style="text-align:center;">N</td><td style="text-align:center;">-</td></tr> <tr><td>11.Lighting Standards</td><td style="text-align:center;">N</td><td style="text-align:center;">-</td></tr> <tr><td>12.Utilities</td><td style="text-align:center;">N</td><td style="text-align:center;">-</td></tr> <tr><td>13.Deck Joints</td><td style="text-align:center;">4</td><td style="text-align:center;">S-A</td></tr> <tr><td>14.</td><td style="text-align:center;">N</td><td style="text-align:center;">-</td></tr> <tr><td>15.</td><td style="text-align:center;">N</td><td style="text-align:center;">-</td></tr> <tr><td>16.</td><td style="text-align:center;">N</td><td style="text-align:center;">-</td></tr> <tr> <td colspan="3">CURB REVEAL (In millimeters)</td> </tr> <tr> <td></td> <td style="text-align:center;">E N</td> <td style="text-align:center;">W N</td> </tr> <tr> <td colspan="3">APPROACHES</td> </tr> <tr> <td>a. Appr. pavement condition</td> <td style="text-align:center;">7</td> <td style="text-align:center;">-</td> </tr> <tr> <td>b. Appr. Roadway Settlement</td> <td style="text-align:center;">7</td> <td style="text-align:center;">-</td> </tr> <tr> <td>c. Appr. Sidewalk Settlement</td> <td style="text-align:center;">N</td> <td style="text-align:center;">-</td> </tr> <tr> <td>d.</td> <td style="text-align:center;">N</td> <td style="text-align:center;">-</td> </tr> <tr> <td colspan="3">OVERHEAD SIGNS (Attached to bridge) (Y/N)</td> </tr> <tr> <td></td> <td style="text-align:center;">N</td> <td style="text-align:center;">-</td> </tr> <tr> <td colspan="3">DEF</td> </tr> <tr> <td>a. Condition of Welds</td> <td style="text-align:center;">N</td> <td style="text-align:center;">-</td> </tr> <tr> <td>b. Condition of Bolts</td> <td style="text-align:center;">N</td> <td style="text-align:center;">-</td> </tr> <tr> <td>c. Condition of Signs</td> <td style="text-align:center;">N</td> <td style="text-align:center;">-</td> </tr> </table>	ITEM 58	6	DEF	DECK			1.Wearing surface	7	-	2.Deck Condition	6	-	3.Stay in place forms	6	-	4.Curbs	N	-	5.Median	H	-	6.Sidewalks	N	-	7.Parapets	7	-	8.Railing	N	-	9.Anti Missile Fence	N	-	10.Drainage System	N	-	11.Lighting Standards	N	-	12.Utilities	N	-	13.Deck Joints	4	S-A	14.	N	-	15.	N	-	16.	N	-	CURB REVEAL (In millimeters)				E N	W N	APPROACHES			a. Appr. pavement condition	7	-	b. Appr. Roadway Settlement	7	-	c. Appr. Sidewalk Settlement	N	-	d.	N	-	OVERHEAD SIGNS (Attached to bridge) (Y/N)				N	-	DEF			a. Condition of Welds	N	-	b. Condition of Bolts	N	-	c. Condition of Signs	N	-	<table border="1" style="width:100%; border-collapse: collapse;"> <tr> <td style="text-align:center;">ITEM 59</td> <td style="text-align:center;">5</td> <td style="text-align:right;">DEF</td> </tr> <tr> <td colspan="3">SUPERSTRUCTURE</td> </tr> <tr><td>1.Stringers</td><td style="text-align:center;">N</td><td style="text-align:center;">-</td></tr> <tr><td>2.Floorbeams</td><td style="text-align:center;">N</td><td style="text-align:center;">-</td></tr> <tr><td>3.Floor System Bracing</td><td style="text-align:center;">N</td><td style="text-align:center;">-</td></tr> <tr><td>4.Girders or Beams</td><td style="text-align:center;">5</td><td style="text-align:center;">S-P</td></tr> <tr><td>5.Trusses - General</td><td style="text-align:center;">N</td><td style="text-align:center;">-</td></tr> <tr><td> a. Upper Chords</td><td style="text-align:center;">N</td><td style="text-align:center;">-</td></tr> <tr><td> b. Lower Chords</td><td style="text-align:center;">N</td><td style="text-align:center;">-</td></tr> <tr><td> c. Web Members</td><td style="text-align:center;">N</td><td style="text-align:center;">-</td></tr> <tr><td> d. Lateral Bracing</td><td style="text-align:center;">N</td><td style="text-align:center;">-</td></tr> <tr><td> e. Sway Bracings</td><td style="text-align:center;">N</td><td style="text-align:center;">-</td></tr> <tr><td> f. Portals</td><td style="text-align:center;">N</td><td style="text-align:center;">-</td></tr> <tr><td> g. End Posts</td><td style="text-align:center;">N</td><td style="text-align:center;">-</td></tr> <tr><td>6.Pin & Hangers</td><td style="text-align:center;">N</td><td style="text-align:center;">-</td></tr> <tr><td>7.Conn Plt's, Gussets & Angles</td><td style="text-align:center;">7</td><td style="text-align:center;">-</td></tr> <tr><td>8.Cover Plates</td><td style="text-align:center;">N</td><td style="text-align:center;">-</td></tr> <tr><td>9.Bearing Devices</td><td style="text-align:center;">6</td><td style="text-align:center;">M-P</td></tr> <tr><td>10.Diaphragms/Cross Frames</td><td style="text-align:center;">7</td><td style="text-align:center;">-</td></tr> <tr><td>11.Rivets & Bolts</td><td style="text-align:center;">7</td><td style="text-align:center;">-</td></tr> <tr><td>12.Welds</td><td style="text-align:center;">7</td><td style="text-align:center;">-</td></tr> <tr><td>13.Member Alignment</td><td style="text-align:center;">6</td><td style="text-align:center;">-</td></tr> <tr><td>14.Paint/Coating</td><td style="text-align:center;">4</td><td style="text-align:center;">S-A</td></tr> <tr><td>15.</td><td style="text-align:center;">N</td><td style="text-align:center;">-</td></tr> <tr> <td colspan="3">Year Painted 1979</td> </tr> <tr> <td colspan="3">COLLISION DAMAGE: Please explain None <input checked="" type="checkbox"/> Minor () Moderate () Severe ()</td> </tr> <tr> <td colspan="3">LOAD DEFLECTION: Please explain None () Minor (<input checked="" type="checkbox"/>) Moderate () Severe ()</td> </tr> <tr> <td colspan="3">LOAD VIBRATION: Please explain None () Minor (<input checked="" type="checkbox"/>) Moderate () Severe ()</td> </tr> <tr> <td colspan="3">Any Fracture Critical Member: (Y/N) N</td> </tr> <tr> <td colspan="3">Any Cracks: (Y/N) N</td> </tr> </table>	ITEM 59	5	DEF	SUPERSTRUCTURE			1.Stringers	N	-	2.Floorbeams	N	-	3.Floor System Bracing	N	-	4.Girders or Beams	5	S-P	5.Trusses - General	N	-	a. Upper Chords	N	-	b. Lower Chords	N	-	c. Web Members	N	-	d. Lateral Bracing	N	-	e. Sway Bracings	N	-	f. Portals	N	-	g. End Posts	N	-	6.Pin & Hangers	N	-	7.Conn Plt's, Gussets & Angles	7	-	8.Cover Plates	N	-	9.Bearing Devices	6	M-P	10.Diaphragms/Cross Frames	7	-	11.Rivets & Bolts	7	-	12.Welds	7	-	13.Member Alignment	6	-	14.Paint/Coating	4	S-A	15.	N	-	Year Painted 1979			COLLISION DAMAGE: Please explain None <input checked="" type="checkbox"/> Minor () Moderate () Severe ()			LOAD DEFLECTION: Please explain None () Minor (<input checked="" type="checkbox"/>) Moderate () Severe ()			LOAD VIBRATION: Please explain None () Minor (<input checked="" type="checkbox"/>) Moderate () Severe ()			Any Fracture Critical Member: (Y/N) N			Any Cracks: (Y/N) N			<table border="1" style="width:100%; border-collapse: collapse;"> <tr> <td style="text-align:center;">ITEM 60</td> <td style="text-align:center;">7</td> <td style="text-align:right;">DEF</td> </tr> <tr> <td colspan="3">SUBSTRUCTURE</td> </tr> <tr> <td colspan="3">1. Abutments</td> </tr> <tr> <td></td> <td style="text-align:center;">Dive</td> <td style="text-align:center;">Cur</td> </tr> <tr> <td>a. Pedestals</td> <td style="text-align:center;">N</td> <td style="text-align:center;">N</td> </tr> <tr> <td>b. Bridge Seats</td> <td style="text-align:center;">N</td> <td style="text-align:center;">7</td> </tr> <tr> <td>c. Backwalls</td> <td style="text-align:center;">N</td> <td style="text-align:center;">6</td> </tr> <tr> <td>d. Breastwalls</td> <td style="text-align:center;">N</td> <td style="text-align:center;">7</td> </tr> <tr> <td>e. Wingwalls</td> <td style="text-align:center;">N</td> <td style="text-align:center;">7</td> </tr> <tr> <td>f. Slope Paving/Rip-Rap</td> <td style="text-align:center;">N</td> <td style="text-align:center;">6</td> </tr> <tr> <td>g. Pointing</td> <td style="text-align:center;">N</td> <td style="text-align:center;">N</td> </tr> <tr> <td>h. Footings</td> <td style="text-align:center;">N</td> <td style="text-align:center;">H</td> </tr> <tr> <td>i. Piles</td> <td style="text-align:center;">N</td> <td style="text-align:center;">H</td> </tr> <tr> <td>j. Scour</td> <td style="text-align:center;">N</td> <td style="text-align:center;">N</td> </tr> <tr> <td>k. Settlement</td> <td style="text-align:center;">N</td> <td style="text-align:center;">7</td> </tr> <tr> <td>l.</td> <td style="text-align:center;">N</td> <td style="text-align:center;">N</td> </tr> <tr> <td>m.</td> <td style="text-align:center;">N</td> <td style="text-align:center;">N</td> </tr> <tr> <td colspan="3">2. Piers or Bents</td> </tr> <tr> <td></td> <td style="text-align:center;">Dive</td> <td style="text-align:center;">Cur</td> </tr> <tr> <td>a. Pedestals</td> <td style="text-align:center;">N</td> <td style="text-align:center;">N</td> </tr> <tr> <td>b. Caps</td> <td style="text-align:center;">N</td> <td style="text-align:center;">7</td> </tr> <tr> <td>c. Columns</td> <td style="text-align:center;">N</td> <td style="text-align:center;">7</td> </tr> <tr> <td>d. Stems/Webs/Pierwalls</td> <td style="text-align:center;">N</td> <td style="text-align:center;">N</td> </tr> <tr> <td>e. Pointing</td> <td style="text-align:center;">N</td> <td style="text-align:center;">N</td> </tr> <tr> <td>f. Footing</td> <td style="text-align:center;">N</td> <td style="text-align:center;">H</td> </tr> <tr> <td>g. Piles</td> <td style="text-align:center;">N</td> <td style="text-align:center;">H</td> </tr> <tr> <td>h. Scour</td> <td style="text-align:center;">N</td> <td style="text-align:center;">N</td> </tr> <tr> <td>i. Settlement</td> <td style="text-align:center;">N</td> <td style="text-align:center;">7</td> </tr> <tr> <td>j.</td> <td style="text-align:center;">N</td> <td style="text-align:center;">N</td> </tr> <tr> <td>k.</td> <td style="text-align:center;">N</td> <td style="text-align:center;">N</td> </tr> <tr> <td colspan="3">3. Pile Bents</td> </tr> <tr> <td>a. Pile Caps</td> <td style="text-align:center;">N</td> <td style="text-align:center;">N</td> </tr> <tr> <td>b. Piles</td> <td style="text-align:center;">N</td> <td style="text-align:center;">N</td> </tr> <tr> <td>c. Diagonal Bracing</td> <td style="text-align:center;">N</td> <td style="text-align:center;">N</td> </tr> <tr> <td>d. Horizontal Bracing</td> <td style="text-align:center;">N</td> <td style="text-align:center;">N</td> </tr> <tr> <td>e. Fasteners</td> <td style="text-align:center;">N</td> <td style="text-align:center;">N</td> </tr> <tr> <td colspan="3">UNDERMINING (Y/N) If YES please explain N</td> </tr> <tr> <td colspan="3">COLLISION DAMAGE: None <input checked="" type="checkbox"/> Minor () Moderate () Severe ()</td> </tr> <tr> <td colspan="3">SCOUR: Please explain None <input checked="" type="checkbox"/> Minor () Moderate () Severe ()</td> </tr> <tr> <td>I-60 (Dive Report):</td> <td style="text-align:center;">N</td> <td>I-60 (This Report): 7</td> </tr> <tr> <td colspan="3">93B-U/W (DIVE) Insp 00/00/0000</td> </tr> </table>	ITEM 60	7	DEF	SUBSTRUCTURE			1. Abutments				Dive	Cur	a. Pedestals	N	N	b. Bridge Seats	N	7	c. Backwalls	N	6	d. Breastwalls	N	7	e. Wingwalls	N	7	f. Slope Paving/Rip-Rap	N	6	g. Pointing	N	N	h. Footings	N	H	i. Piles	N	H	j. Scour	N	N	k. Settlement	N	7	l.	N	N	m.	N	N	2. Piers or Bents				Dive	Cur	a. Pedestals	N	N	b. Caps	N	7	c. Columns	N	7	d. Stems/Webs/Pierwalls	N	N	e. Pointing	N	N	f. Footing	N	H	g. Piles	N	H	h. Scour	N	N	i. Settlement	N	7	j.	N	N	k.	N	N	3. Pile Bents			a. Pile Caps	N	N	b. Piles	N	N	c. Diagonal Bracing	N	N	d. Horizontal Bracing	N	N	e. Fasteners	N	N	UNDERMINING (Y/N) If YES please explain N			COLLISION DAMAGE: None <input checked="" type="checkbox"/> Minor () Moderate () Severe ()			SCOUR: Please explain None <input checked="" type="checkbox"/> Minor () Moderate () Severe ()			I-60 (Dive Report):	N	I-60 (This Report): 7	93B-U/W (DIVE) Insp 00/00/0000		
ITEM 58	6	DEF																																																																																																																																																																																																																																																																																																																		
DECK																																																																																																																																																																																																																																																																																																																				
1.Wearing surface	7	-																																																																																																																																																																																																																																																																																																																		
2.Deck Condition	6	-																																																																																																																																																																																																																																																																																																																		
3.Stay in place forms	6	-																																																																																																																																																																																																																																																																																																																		
4.Curbs	N	-																																																																																																																																																																																																																																																																																																																		
5.Median	H	-																																																																																																																																																																																																																																																																																																																		
6.Sidewalks	N	-																																																																																																																																																																																																																																																																																																																		
7.Parapets	7	-																																																																																																																																																																																																																																																																																																																		
8.Railing	N	-																																																																																																																																																																																																																																																																																																																		
9.Anti Missile Fence	N	-																																																																																																																																																																																																																																																																																																																		
10.Drainage System	N	-																																																																																																																																																																																																																																																																																																																		
11.Lighting Standards	N	-																																																																																																																																																																																																																																																																																																																		
12.Utilities	N	-																																																																																																																																																																																																																																																																																																																		
13.Deck Joints	4	S-A																																																																																																																																																																																																																																																																																																																		
14.	N	-																																																																																																																																																																																																																																																																																																																		
15.	N	-																																																																																																																																																																																																																																																																																																																		
16.	N	-																																																																																																																																																																																																																																																																																																																		
CURB REVEAL (In millimeters)																																																																																																																																																																																																																																																																																																																				
	E N	W N																																																																																																																																																																																																																																																																																																																		
APPROACHES																																																																																																																																																																																																																																																																																																																				
a. Appr. pavement condition	7	-																																																																																																																																																																																																																																																																																																																		
b. Appr. Roadway Settlement	7	-																																																																																																																																																																																																																																																																																																																		
c. Appr. Sidewalk Settlement	N	-																																																																																																																																																																																																																																																																																																																		
d.	N	-																																																																																																																																																																																																																																																																																																																		
OVERHEAD SIGNS (Attached to bridge) (Y/N)																																																																																																																																																																																																																																																																																																																				
	N	-																																																																																																																																																																																																																																																																																																																		
DEF																																																																																																																																																																																																																																																																																																																				
a. Condition of Welds	N	-																																																																																																																																																																																																																																																																																																																		
b. Condition of Bolts	N	-																																																																																																																																																																																																																																																																																																																		
c. Condition of Signs	N	-																																																																																																																																																																																																																																																																																																																		
ITEM 59	5	DEF																																																																																																																																																																																																																																																																																																																		
SUPERSTRUCTURE																																																																																																																																																																																																																																																																																																																				
1.Stringers	N	-																																																																																																																																																																																																																																																																																																																		
2.Floorbeams	N	-																																																																																																																																																																																																																																																																																																																		
3.Floor System Bracing	N	-																																																																																																																																																																																																																																																																																																																		
4.Girders or Beams	5	S-P																																																																																																																																																																																																																																																																																																																		
5.Trusses - General	N	-																																																																																																																																																																																																																																																																																																																		
a. Upper Chords	N	-																																																																																																																																																																																																																																																																																																																		
b. Lower Chords	N	-																																																																																																																																																																																																																																																																																																																		
c. Web Members	N	-																																																																																																																																																																																																																																																																																																																		
d. Lateral Bracing	N	-																																																																																																																																																																																																																																																																																																																		
e. Sway Bracings	N	-																																																																																																																																																																																																																																																																																																																		
f. Portals	N	-																																																																																																																																																																																																																																																																																																																		
g. End Posts	N	-																																																																																																																																																																																																																																																																																																																		
6.Pin & Hangers	N	-																																																																																																																																																																																																																																																																																																																		
7.Conn Plt's, Gussets & Angles	7	-																																																																																																																																																																																																																																																																																																																		
8.Cover Plates	N	-																																																																																																																																																																																																																																																																																																																		
9.Bearing Devices	6	M-P																																																																																																																																																																																																																																																																																																																		
10.Diaphragms/Cross Frames	7	-																																																																																																																																																																																																																																																																																																																		
11.Rivets & Bolts	7	-																																																																																																																																																																																																																																																																																																																		
12.Welds	7	-																																																																																																																																																																																																																																																																																																																		
13.Member Alignment	6	-																																																																																																																																																																																																																																																																																																																		
14.Paint/Coating	4	S-A																																																																																																																																																																																																																																																																																																																		
15.	N	-																																																																																																																																																																																																																																																																																																																		
Year Painted 1979																																																																																																																																																																																																																																																																																																																				
COLLISION DAMAGE: Please explain None <input checked="" type="checkbox"/> Minor () Moderate () Severe ()																																																																																																																																																																																																																																																																																																																				
LOAD DEFLECTION: Please explain None () Minor (<input checked="" type="checkbox"/>) Moderate () Severe ()																																																																																																																																																																																																																																																																																																																				
LOAD VIBRATION: Please explain None () Minor (<input checked="" type="checkbox"/>) Moderate () Severe ()																																																																																																																																																																																																																																																																																																																				
Any Fracture Critical Member: (Y/N) N																																																																																																																																																																																																																																																																																																																				
Any Cracks: (Y/N) N																																																																																																																																																																																																																																																																																																																				
ITEM 60	7	DEF																																																																																																																																																																																																																																																																																																																		
SUBSTRUCTURE																																																																																																																																																																																																																																																																																																																				
1. Abutments																																																																																																																																																																																																																																																																																																																				
	Dive	Cur																																																																																																																																																																																																																																																																																																																		
a. Pedestals	N	N																																																																																																																																																																																																																																																																																																																		
b. Bridge Seats	N	7																																																																																																																																																																																																																																																																																																																		
c. Backwalls	N	6																																																																																																																																																																																																																																																																																																																		
d. Breastwalls	N	7																																																																																																																																																																																																																																																																																																																		
e. Wingwalls	N	7																																																																																																																																																																																																																																																																																																																		
f. Slope Paving/Rip-Rap	N	6																																																																																																																																																																																																																																																																																																																		
g. Pointing	N	N																																																																																																																																																																																																																																																																																																																		
h. Footings	N	H																																																																																																																																																																																																																																																																																																																		
i. Piles	N	H																																																																																																																																																																																																																																																																																																																		
j. Scour	N	N																																																																																																																																																																																																																																																																																																																		
k. Settlement	N	7																																																																																																																																																																																																																																																																																																																		
l.	N	N																																																																																																																																																																																																																																																																																																																		
m.	N	N																																																																																																																																																																																																																																																																																																																		
2. Piers or Bents																																																																																																																																																																																																																																																																																																																				
	Dive	Cur																																																																																																																																																																																																																																																																																																																		
a. Pedestals	N	N																																																																																																																																																																																																																																																																																																																		
b. Caps	N	7																																																																																																																																																																																																																																																																																																																		
c. Columns	N	7																																																																																																																																																																																																																																																																																																																		
d. Stems/Webs/Pierwalls	N	N																																																																																																																																																																																																																																																																																																																		
e. Pointing	N	N																																																																																																																																																																																																																																																																																																																		
f. Footing	N	H																																																																																																																																																																																																																																																																																																																		
g. Piles	N	H																																																																																																																																																																																																																																																																																																																		
h. Scour	N	N																																																																																																																																																																																																																																																																																																																		
i. Settlement	N	7																																																																																																																																																																																																																																																																																																																		
j.	N	N																																																																																																																																																																																																																																																																																																																		
k.	N	N																																																																																																																																																																																																																																																																																																																		
3. Pile Bents																																																																																																																																																																																																																																																																																																																				
a. Pile Caps	N	N																																																																																																																																																																																																																																																																																																																		
b. Piles	N	N																																																																																																																																																																																																																																																																																																																		
c. Diagonal Bracing	N	N																																																																																																																																																																																																																																																																																																																		
d. Horizontal Bracing	N	N																																																																																																																																																																																																																																																																																																																		
e. Fasteners	N	N																																																																																																																																																																																																																																																																																																																		
UNDERMINING (Y/N) If YES please explain N																																																																																																																																																																																																																																																																																																																				
COLLISION DAMAGE: None <input checked="" type="checkbox"/> Minor () Moderate () Severe ()																																																																																																																																																																																																																																																																																																																				
SCOUR: Please explain None <input checked="" type="checkbox"/> Minor () Moderate () Severe ()																																																																																																																																																																																																																																																																																																																				
I-60 (Dive Report):	N	I-60 (This Report): 7																																																																																																																																																																																																																																																																																																																		
93B-U/W (DIVE) Insp 00/00/0000																																																																																																																																																																																																																																																																																																																				

X=UNKNOWN N=NOT APPLICABLE H=HIDDEN/INACCESSIBLE R=REMOVED

RTN/17-96

Figure 5: Sample of report provided by MassDOT

2.1.4. Format of data received from New Hampshire Department of Transportation (NHDOT) Inspection reports

The NHDOT Bridge Inspection Manual [25] divides their inspections and reports into 7 types:

- i. Routine inspections (Regular inspection or National Bridge Inspection Standards, NBIS, inspection): Conducted to compare the current condition of the bridge with the previously documented condition.
- ii. Inventory inspections: Consists of the first inspection performed on the bridge. It aims to collect information regarding size, location, structural and functional conditions.
- iii. In-Depth inspections: Provides detailed reports, using hands-on techniques. In-depth reports can be requested for specific parts of the structure.
- iv. Fracture Critical Member inspections: Utilizes hands-on techniques with non-destructive tests to provide detailed reports regarding fracture critical members.
- v. Special inspections: Used to evaluate load posted bridges, inspect bridges that are out of service, monitor suspected or known deficiencies, or assess bridge or bridge members following a natural or manmade emergency.
- vi. Underwater (Diving) inspections: Utilized to determine the condition of the portions of the bridge which cannot be inspected visually.
- vii. Damage inspections: Aims to check whether the bridge is safe to remain open after damaged was caused by environmental effects and/or human actions.

Although there are no formal sections in the reports from NHDOT, all the reports have the same layout with 5 sections as follows:

1. Report cover
2. Element details
3. Bridge and inspection notes
4. Inspection history

The section “report cover” comprises two pages and contain all the general information about the bridge. All information pertaining to identification (for instance, NBI number of the bridge), the NBI condition of elements, dimensions and structure type can be found in this section. Figure 6 depicts an excerpt of a report cover from NHDOT.

Bridge Inspection Report

NBI Structure Number: 004401700013500

Chester 170/135

Date of Inspection: 11/10/2020
 Date Report Sent: 12/29/2020
 Owner: Municipality
 Bridge Inspection Group: D-Team
 Bridge Maintenance Crew: OTHER

HANSON ROAD
 over
EXETER RIVER

Recommended Postings:

Weight: **E-2**

Weight Sign OK

SIGNS IN PLACE. 11/10/20

Width: **Not Required**

Width Sign OK

Primary Height Sign Recommendation: *None*
 Optional Centerline Height Sign Rec: *None*

Clearances: Over: 99.99
 (Feet) Under: 0.00
 Route: 99.99

Height Sign OK

Condition:

Red List Status: Municipal Redlist
 Deck: 4 Poor
 Superstructure: 5 Fair
 Substructure: 5 Fair
 Culvert: N/A (NBI)
 Sufficiency Rating: 49.5 %

Bridge Rail: Substandard
 Rail Transition: Substandard
 Bridge Approach Rail: Substandard
 Approach Rail Ends: Substandard

Structure Type and Materials:

Number of Main Spans: 1
 Number of Approach Spans: 0

Main Span Material and Design Type
 Steel/Stringer/Girder

NH Bridge Type: IB-C (I Beams w/ Concrete Deck)
 Deck Type: Concrete-Cast-in-Place
 Wearing Surface: Bituminous
 Membrane: Unknown
 Deck Protection: None
 Curb Reveal: Not Measured
 Plan Location: unknown
 Total Bridge Length: 31.0 ft
 Right Curb/Sidewalk Width: 0.0 ft
 Total Bridge Width: 28.0 ft
 Median: No median
 Bridge Skew: 0.00 °
 Year Built/Rebuilt: 1932

Bridge Dimensions:

Length Maximum Span: 26.0 ft
 Left Curb/Sidewalk Width: 0.0 ft
 Width Curb to Curb: 26.0 ft
 Approach Roadway Width: 22.0 ft
 (W/Shoulders)

Figure 6: Sample of report provided by NHDOT

The “element details” section contains a table where the elements of the bridge are discussed individually. Corrosion data can most often be found in this section of the report. It is imperative to note that there is great variability among reports pertaining to the data presented in this table. For example, not all bridge reports present the same items in the table. More specifically to the scope of this project, there are reports which contain corrosion information while others do not.

The “Element states” section presents the table required by FHWA [24]. This table summarizes the condition of several bridge components. The section “Bridge and inspection notes” describes the observed flaws found during present and past inspections in the bridge structure.

Lastly, the section “Inspection history” includes a table depicting the history of the NBI rating of bridge elements. This does not include every bridge element. This table is helpful in identifying the condition in time for given bridge elements. Additionally, this table can give insight into repairs done on a given bridge component.

It is crucial to note that a “photos” section was not provided in the reports but was reported in a separate file by NHDOT. Every photograph was labeled, but they are often not referenced in the text. While photos from the inspections are provided, no sketches regarding corrosion damage are found on the photographic records. Figure 7 depicts an example of corrosion damage taken from the records of a bridge from NHDOT.

Monday, November 13, 2017
BEAM #8 ON SOUTH END
1/2" REMAINING ON
BOTTOM FLANGE EIGHT
FEET IN LENGTH LIGHT
SECTION LOSS. MRL



D210 17

Figure 7: Example of corrosion damage taken from the records of a bridge from NHDOT

2.1.5. Format of data received from Rhode Island Department of Transportation (RIDOT) Inspection reports

According to the RIDOT Bridge Inspection Manual [26], the RIDOT conducts 8 types of inspections and reports:

- i. Inventory: Consists of the first inspection of the bridge, right after it is entered into the bridge file. The purpose of such a report is to provide the required inventory information of the original structure type, size, location as well as to document its structural and functional conditions.
- ii. Routine: Conducted in a time interval no greater than 24 months and serves to assess if all service requirements are satisfied.
- iii. Damage: Consists of an unscheduled inspection which evaluates the structural damage caused to the bridge by environmental effects and/or human actions.
- iv. In-depth: Provides detailed assessment of the condition of the bridge or bridge elements.

- v. Fracture critical: Details the condition of fracture critical members, i.e., members under tension which fracture could cause the structure to collapse partially or entirely.
- vi. Underwater: Used to determine the condition of the underwater portion of the bridge substructure and the surrounding channel.
- vii. Interim (Special) and miscellaneous: Conducted either in bridges which can no longer support the minimum live loads, closed bridges, or bridges which have gone through a flood event or bridges located on a public roadway that has suspected or known deterioration on one or more of its members.
- viii. Non-NBI inspections: Aim to classify the non-NBI bridge into a similar type of bridge presented in the NBI. Once the classification is done, the NBI procedure for the classified type of bridge must be used.

While the sections of the reports are not explicitly denoted, RIDOT follows a structured template. To clearly discuss the reports, the following 5 sections are considered:

1. Identification, structure inventory and appraisal
2. Bridge notes
3. Inspection notes
4. Element inspection
5. Element notes

The “Identification, structure inventory and appraisal” section consists of the first and second pages of the reports. Here, general information about the bridge is reported (e.g., identification and location) and several NBI items discussing many bridge elements are summarized. Additionally, the reports from RIDOT discuss and present the historical records of some NBI ratings. Figure 8 depicts the first page of a report provided by RIDOT.

In the section “Bridge notes”, many details about the procedure during the inspection was provided. This includes but is not limited to the equipment required, whether local police were present, and the labeling or layout of the bridge beams. In the section “Inspection notes”, one can find general information about the crew responsible for the inspection, the temperature, and additional comments about NBI ratings.



RIDOT Bridge Inspection Report

035701
Pontiac Ave RR

Inspected By: WSP-STEERE
Inspector: DAVE LOWELL
Inspection Date: 11/18/2019

Bridge Condition **Fair**

<p>IDENTIFICATION</p> <p>Bridge ID: 035701 NBI Number: Pontiac Ave RR Structure Name: Pontiac Ave RR Location (9): 1.1 Mi S of JCT RI 37 Carries (7): PONTIAC AV Type of Service (42A): 5 Highway-pedestrian Feature Crossed (6): PONTIAC BRANCH RR Type of Service (42B): 2 Railroad Placecode (4): Cranston County (3): Providence State (1): 44 Rhode Island Station: NBI Region (2): District 4 Latitude (16): 41.7431274 Longitude (17): -71.4574361 Owner (22): 01 State Highway Agency Custodian (21): 01 State Highway Agency</p> <table border="1" style="width: 100%; border-collapse: collapse;"> <tr> <td style="width: 30%;">Year Built (27): 1975</td> <td>Border State: Not Applicable (P)</td> </tr> <tr> <td>Year Recon (106):</td> <td>Border Number:</td> </tr> <tr> <td>Historical (37): 5 Not eligible for NRHP</td> <td>% Responsibility:</td> </tr> </table>	Year Built (27): 1975	Border State: Not Applicable (P)	Year Recon (106):	Border Number:	Historical (37): 5 Not eligible for NRHP	% Responsibility:	<p>INSPECTION</p> <p>Date of Routine Inspection (90): 11/18/2019 Frequency (91): 24 Next Inspection: 11/18/2021</p> <table border="1" style="width: 100%; border-collapse: collapse;"> <thead> <tr> <th>Inspection Type</th> <th>Freq (92)</th> <th>Last Insp (93)</th> <th>Next Insp</th> </tr> </thead> <tbody> <tr> <td>Element</td> <td>24</td> <td>11/18/2019</td> <td>11/18/2021</td> </tr> <tr> <td>Fracture Critical (A)</td> <td></td> <td>1/1/1901</td> <td>1/1/1901</td> </tr> <tr> <td>Underwater (B)</td> <td></td> <td>1/1/1901</td> <td>1/1/1901</td> </tr> <tr> <td>Special Insp (C)</td> <td></td> <td>1/1/1901</td> <td>1/1/1901</td> </tr> </tbody> </table> <p>LOAD RATING AND POSTING</p> <p>Posting Status (41): A Open, no restriction Posting % (70): 5 At/Above Legal Loads Rating Date: 4/16/2014 Design Load (31): 5 MS 18 (HS 20) Opr Method (63): 3 LRFR Load & Res. Fact Opr Rating (64): 79.00 Tons Inv Method (65): 3 LRFR Load & Res. Fact Inv Rating (66): 61.00 Tons</p>	Inspection Type	Freq (92)	Last Insp (93)	Next Insp	Element	24	11/18/2019	11/18/2021	Fracture Critical (A)		1/1/1901	1/1/1901	Underwater (B)		1/1/1901	1/1/1901	Special Insp (C)		1/1/1901	1/1/1901
Year Built (27): 1975	Border State: Not Applicable (P)																										
Year Recon (106):	Border Number:																										
Historical (37): 5 Not eligible for NRHP	% Responsibility:																										
Inspection Type	Freq (92)	Last Insp (93)	Next Insp																								
Element	24	11/18/2019	11/18/2021																								
Fracture Critical (A)		1/1/1901	1/1/1901																								
Underwater (B)		1/1/1901	1/1/1901																								
Special Insp (C)		1/1/1901	1/1/1901																								

<p>DECK GEOMETRY</p> <p>Deck Geometry (68): 9 Above Desirable Crit Deck Area: 5,022.00 Deck Type (107): 1 Concrete-Cast-in-Place Wearing Surface (108A): 6 Bituminous Membrane (108B): 1 Built-up Deck Protection (108C): None O. to O. Width (52): 62.00 Curb / Sidewalk Width L (50A): 5.00 Curb / Sidewalk Width R (50B): 5.00 Median (33): 0 No median</p>	<p>DECK CONDITION</p> <p>Deck Rating (58): 6 Satisfactory Bridge Rail (36A): 1 Meets Standards Transition (36B): 1 Meets Standards Approach Rail (36C): 0 Substandard Approach Rail Ends (36D): 1 Meets Standards</p>
--	--

<p>SUPERSTRUCTURE GEOMETRY</p> <p># of Main Spans (45): 1 # of Approach Spans (46): 0 Main Material (43 A): 3 Steel Main Design (43 B): 02 Stringer/Girder Max Span Length (48): 74.95 Structure Length (49): 81.00 NBIS Length (37): Long Enough Temp Structure (103): Not Applicable (P) Skew (34): 30 Structure Flared (35): 0 No flare Parallel Structure (101): No bridge exists Approach Alignment (72): 8 Equal Desirable Crit</p>	<p>SUPERSTRUCTURE CONDITION</p> <p>Superstructure Rating (59): 5 Fair Structure Evaluation (67): 5 Above Min Tolerable</p>
--	--

Figure 8: Front page of a typical routine inspection report provided by RIDOT

The section “Element inspection” presents the table required by FHWA [24], which summarizes the condition of several components of the bridge. Lastly, in the section “Element notes”, detailed information and field measurements for distinct elements of the bridge are provided. In general, the corrosion damage and information are found in this section.

While the RIDOT reports do not present a section containing photos, all reports provided are accompanied with photographic records. The photographs are labeled with comments and measurements provided, as depicted in Figure 9. For some reports and bridges, more documentation on corrosion damage was provided. Among the outstanding documents, section loss calculations and corrosion damage sketches were provided.

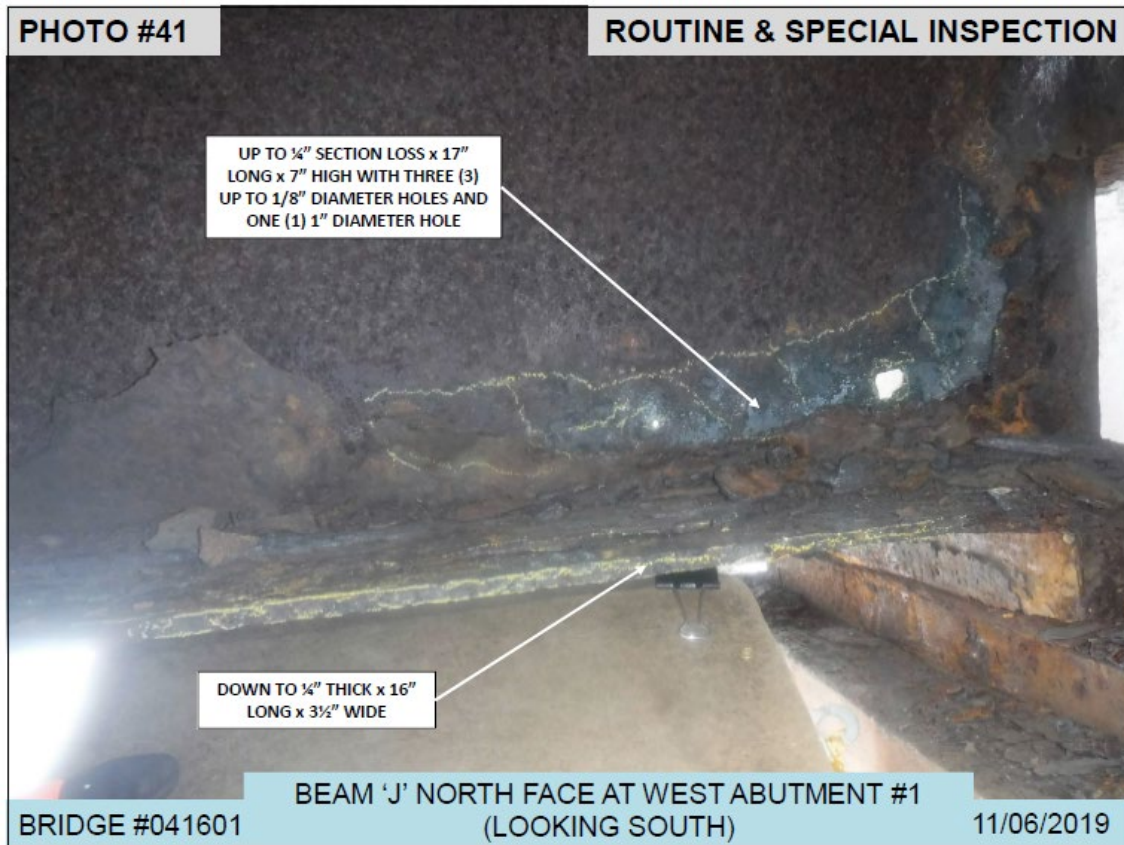


Figure 9: An example of picture provided by RIDOT

2.1.6. Format of data received from Vermont’s Agency of Transportation (VTrans) Inspection reports

The VTrans Bridge Inspection Manual [27] indicates the existence of three types of reports:

- i. Routine inspections: Conducted on a regular basis by VTrans.
- ii. Special inspections: Required in situations when special equipment is needed during inspections.
- iii. Underwater inspections: Aim to check the underwater elements of the bridge and the condition of foundations.

The inspection reports from VTrans consist of a table which sections are, in general, the elements of the bridge that are to be analyzed. The reports are organized in the following seven sections:

1. Approach
2. Deck
3. Superstructure

4. Substructure
5. Piers
6. Channel
7. Summary

VTrans bridge inspection reports do not contain a cover but present general information about the bridge and the inspection report. This is given in a header on the first page of the report. Figure 11 depicts an example of a first page of a VTrans report.

The section “Approach” contains information about the condition of the settlement, erosion on abutments, and the condition of the rails. The section following “Approach” is denoted as “Deck”, where information about the asphalt, joints and drains can be found.

The next section refers to the “Superstructure”. Most of the information regarding corrosion can be found in this section, making it crucial to this project. Additionally, this section often contains comments on the condition of the floor beams, and the painting of the beams.

The following section is the “Substructure” and discusses its elements, such as abutments and wingwalls. The last two element sections of the report discuss the condition of the “Piers” and “Channels” of the bridge structure. Lastly, there is a “Summary” section in which an overview about the bridge is provided along with NBI ratings.

The reports do not depict photographic records, as this type of data can be found for all bridges in the VTrans web-portal. Not all pictures are labeled, and the text does not often reference the photographs. No sketches regarding corrosion are provided along with the photographs or the inspection reports. Figure 10 depicts an example of photo which can be found in VTrans web-portal.



Figure 10: Example of photo of a buckled beam found in VTrans web-portal

State of Vermont Bridge Inspection Form

Date: 04/20/20  Route: C3081 Bridge #: 42 District: 7
 Town: Barnet Bridge Type: Single Span Rolled Beam
 Crossing: South Peacham Brook Inspectors: MJK MJ

Approach ~

Rail: Galv. Standard Steel Beam <input type="button" value="v"/> and Type <input type="button" value="v"/> Condition <input type="button" value="v"/>
Posts: Galv. Standard Steel I Beam <input type="button" value="v"/> and Type <input type="button" value="v"/> Condition <input type="button" value="v"/> Some areas of impact damage with couple post are twisted and bent back
Settlement: Minor <input type="button" value="v"/>
Erosion: Minor <input type="button" value="v"/>

Deck ~

Wearing Surface: Asphalt <input type="button" value="v"/> Condition <input type="button" value="v"/> Other - <input type="button" value="v"/> Litter with cracking and potholes with 10" +/- of cover of asphalt and gravel
Curb: Concrete <input type="button" value="v"/> Condition <input type="button" value="v"/> Pavement is flush with top of curbing so unable to view facing
Sidewalks: N/A <input type="button" value="v"/>
Rail: Galv. Standard Steel Beam <input type="button" value="v"/> and Type <input type="button" value="v"/> Condition <input type="button" value="v"/> Galv beam retrofitted years ago with heavy duty C channels 2 tier.
Posts: A588 Standard Steel I Beam <input type="button" value="v"/> and Type <input type="button" value="v"/> Condition <input type="button" value="v"/> Heavy duty I beams attach to longitudinal I beams that have heavy rusting and holes through webbing in places. Downstream side post and rail pushed back

Figure 11: Sample of report provided by VTrans

2.2. Variability and Quality of Data

A first observation from all the inspection reports is that there is variability among the reports from different states in terms of the quantity of information provided and the structure of how information is reported. This finding is expected, as different states have been inspecting bridges differently and according to their needs and goals. It should be noted however, that with this variability, the reports from all states still meet the minimum requirements of NBI reporting.

The most noticeable differences between the inspection reports can be found when we consider the following two groups: MaineDOT, NHDOT and VTrans in Group 1 and RIDOT, MassDOT and CTDOT in Group 2. The Northern New England States (Group 1) have inspection reports which rarely provide sketches where the Southern New England States (Group 2) often provide sketches and photographs. Another related important note is that several reports from Group 1, in which corrosion information is provided in a generic form, are the result of a visual inspection. For this reason, there are no detailed measurements or thickness losses provided in the report. It is imperative to note that the methods of Group 2 were developed over time and had performed inspection methods much like those of Group 1 in the past. For example, CTDOT has required sketches since around 2001 while other states do not require sketches. Figure 12, Figure 13 and Figure 14 depict examples of corrosion information provided by the DOTs of the Northern States (Group 1).

Superstructure **NBI Item 59: 5**
 Downstream exterior girder has steel delamination of top flange and light section loss near web.
 7 of 10 girders in good condition with paint which is generally intact. The other 3 have paint freckling and flaking. Noticeable light section loss at web/flange interface scattered along girders. All bearings have major to complete paint loss with moderate surface rust.

Figure 12: Example of corrosion information (Adapted from bridge 0854, Maine)

Stringers: Rolled Beams and < > Varying amounts of rust scale throughout out. The exterior beams and abutment 1 beam end of beam 4 have heavy rust scale. The fascia beams have significant section loss and small perforations could soon occur. The upstream fascia beam has a small area in the web near abutment 2 w/ 1" perforations.

Figure 13: Example of inspection notes (Adapted from BENNINGTON-BR22-19OCT2, Vermont)

107	Steel Open Girder/Beam	I-BEAMS
		LIGHT SECTION LOSS AT ENDS OF BEAMS.
L 515	Steel Protective Coating	PAINT PEELING IN AREAS.
L 1000	Corrosion	LIGHT SECTION LOSS AT ENDS OF BEAMS.

Figure 14: Example of inspection notes (Adapted from Andover 125-129, New Hampshire)

The generic description of corrosion data and the lack of cross referencing to the pictures pose a challenge for the compilation and identification of corrosion patterns and the condition of the beams.

While there is visual inspection, many reports from the Southern New England States (Group 2) provide sketches regarding corrosion information. It is important to note that many of these sketches are not to scale and are depicted in Figures 15, Figure 16 and Figure 17.

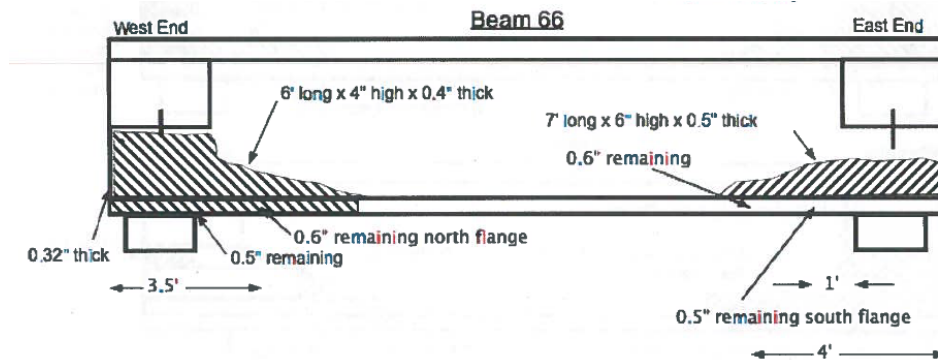


Figure 15: Typical inspection report sketch not in scale. Adapted from N19059-101-DOT-NBI (Northampton, MA)

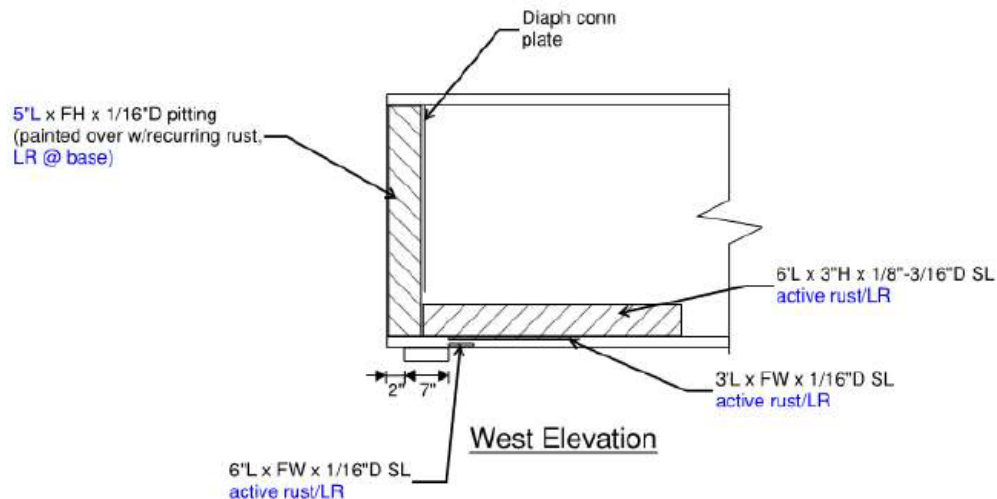


Figure 16: Typical inspection report sketch (not to scale). Adapted from Br. #00297 (Plainfield, CT)

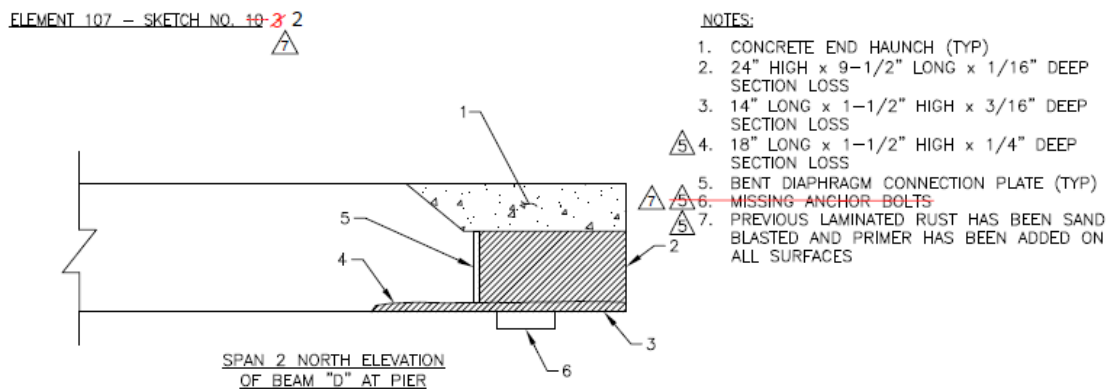


Figure 17: Typical inspection report sketch not to scale (Adapted from Br. #042501, RI)

The reports from all states that contain information about corrosion most often include a single data point of web thickness measurement. This is a gross simplification of the corrosion region since it is likely that web thickness will vary within a corroded region of the beam. The corrosion damage is considered uniform within the corroded region, and the given measurement is assumed to be the maximum thickness loss. The sparsity of thickness measurements is critical to note and consider here, as the average thickness of the beam is an important parameter of capacity load equations. Figure 18, Figure 19, and Figure 20 show the variation in how some of the New England States report this critical section loss parameter. The inspection reports from Massachusetts, Connecticut, and Rhode Island are where diagrams like these can be found.

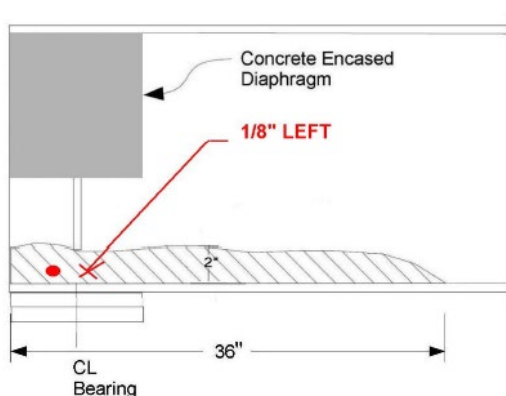


Figure 18: Corroded area described by only one thickness value. Adapted from W46010-3RY-DOT-NBI (Wrentham, MA)

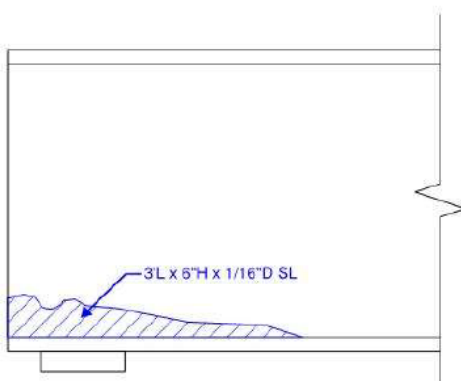


Figure 19: Corroded area described by only one thickness value. Adapted from bridge 00501 (Killingly, CT)

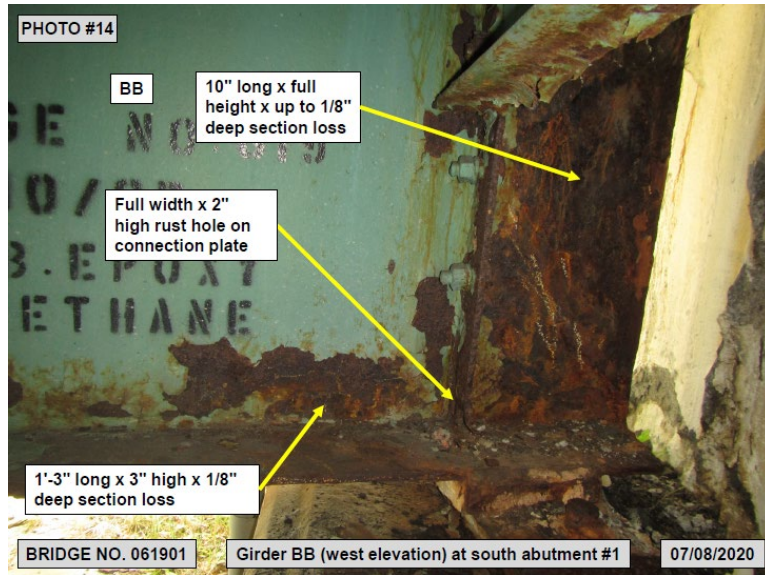


Figure 20: Corroded areas described by only one thickness value. Adapted from bridge 061901(RI)

There are also cases, where multiple thickness measurements are provided in an effort of the inspector to provide higher accuracy, as shown in Figure 21. It is worthwhile to note that the thickness measurement and its variation throughout the corroded region are important parameters needed when assessing the load capacity of the beams.

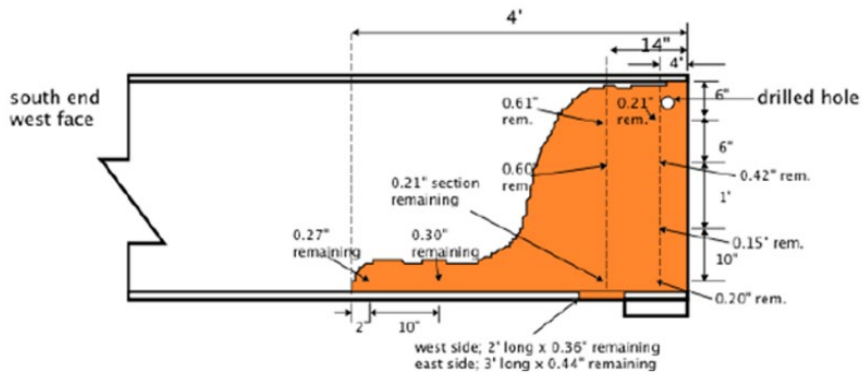


Figure 21: Corroded area described by multiple thickness loss values. Sketch adopted from H08003-18J-MUN-NBI (District 2, Town of Hardwick, MA)

There are sketches that provide an interval of section loss over a particular area. While this interval is depicted in a given area, they do not often indicate where the maximum and minimum loss occurs, as depicted in Figure 22.

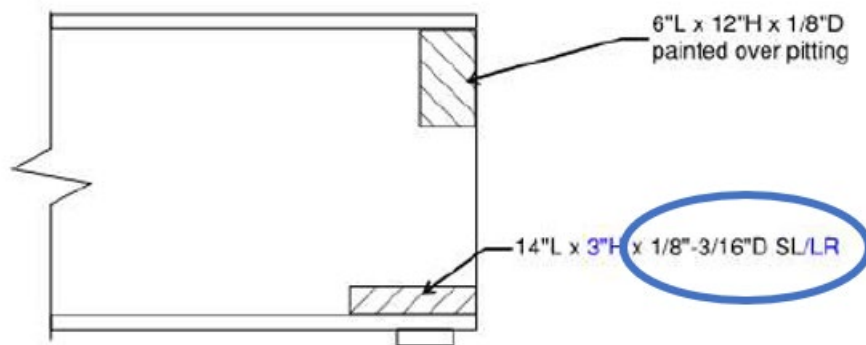


Figure 22: No indication of where the section loss occurs. Adapted from Br. #00297 (Plainfield, CT)

While they provide incredible insight to the beam end condition, sketches are often not enough to accurately describe corroded beam ends. For this reason, it is important that a report depicts a coherent combination of sketches, photographs, and written descriptions regarding the phenomenon. In some cases, there are times where reporting is not accurate, i.e., when the description and the sketches/pictures do not match. Additionally, some pictures do not have labels nor captions, which hinders the understanding of the records. This usually happens to simplify and to generalize a condition. An example of this could be that the area of section loss is described as a rectangle, but the real pictures depict another pattern. In many cases, this simplification is used for 100% material loss, leading to overestimation of the phenomenon.

As a general note, the reports typically from the Northern New England States (Group 1), lack information regarding the type of beams used in the construction of the bridge structure. This information is imperative to this work, as it provides a basis to understand the current conditions of the beams being analyzed relative to a control point or, original data.

2.3. Amount of Data

Figure 23 presents the amount of inspection reports each state in the New England region provided for this research work. In summary, our team received a total of 553 inspection reports. However, some reports were from the same bridge in a different time or inspection interval. As a result, our team was able to create a database of 515 total bridges across the six New England States.

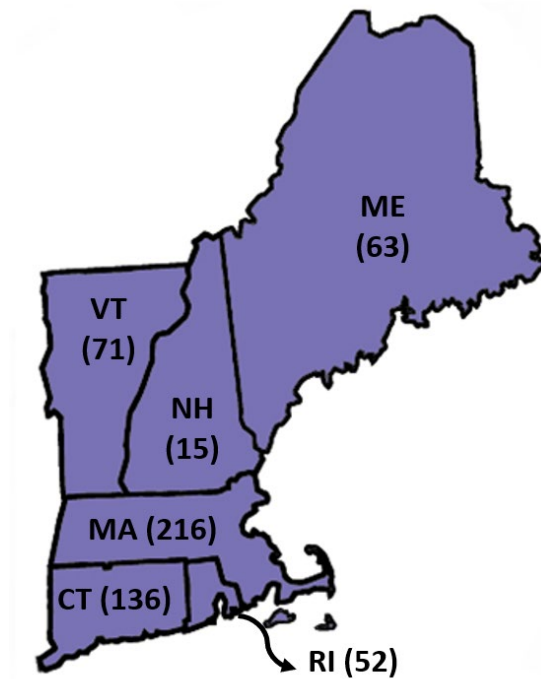


Figure 23: Summary of reports provided by each state

2.4. Preliminary filtering of the data

As discussed above, not all the provided reports were used in the final bridge database of this research work. Some of them included but were not limited to reports describing other types of bridges (e.g., concrete bridges) and reports in which no corrosion information was provided. These bridges and reports could not be used in the database generated because they are out of the scope of the current work. As a result of this, the inspection reports needed to be sorted and compiled. Table 2 summarizes the number of reports used to create the current database.

Table 2: Preliminary sorting of inspection reports

State	All	Summarized	Stiffeners	Previous Reports (In time)	No data/No corrosion/Other type of damage	Other type of bridge	Too corroded
Connecticut	136	55	83	1	18	5	--
Maine	63	32	7	1	31	--	--
Massachusetts	216	93	30	33	36	23	1
New Hampshire	15	13	--	--	2	--	--
Rhode Island	52	13	37	--	8	1	--
Vermont	71	19	0	3	48	1	--
Total	553	225	157	38	143	30	1

Table 2 includes the detailed numbers of the reports used from each state. The first column shows the number of all reports provided from each state. The second column details how many reports were summarized and effectively contributed to our database. The third column isolates inspection reports of bridges with stiffened beams; these reports were disregarded due to this type of beam being out of the scope of this project. The fourth column of Table 2 identifies reports which describe the evolution of the corrosion phenomenon in time. For example, many of the reports describe the same bridge at different time intervals. Although it is important to observe the evolution of corrosion, and possibly develop prediction tools, these reports were removed from post-processing as only the current (latest) condition of these bridges was accounted for. The fifth column of Table 2 shows the inspection reports which did not provide corrosion. There was a single report, which described a bridge with extreme corrosion, which the research team decided should be removed from further post-processing.

As a result, from the 553 reports provided by the states, 225 reports were summarized. From the summarized reports, our team was able to obtain data for 1,723 beam ends. The amount of information collected is considered a rich source of data, from which the research team can draw conclusions regarding deterioration of unstiffened beam ends due to corrosion.

2.5. Corrosion Patterns

Building on a recently completed research project in MA, the research team identified six primary web corrosion patterns and four web hole patterns to classify the damage in bridge beam ends. These patterns were generated based on the most common types of corrosion identified in the beam ends of the reports provided by MassDOT, as discussed in [28].

In this project, the corrosion patterns identified previously were used. The existing patterns allowed our team to describe more than 95% of the new data available in the reports for this project. With this large percentage of beams that could be described by existing patterns, our team decided that no new corrosion type needed to be created. This observation is not surprising because the source of corrosion in all states is similar: salt-laden water leaking through bridge expansion joints located at beam ends.

The goal of creating the corrosion patterns is to simplify and classify the extensive data available. This type of corrosion classification allowed our team to describe and group cases that were similar. As a result, we were able to summarize the data into Excel spreadsheets and efficiently extract conclusions from the data available via MATLAB. Furthermore, this classification allowed building analytical models that included the most common corrosion patterns to conduct parametric analyses of beams containing these patterns.

Table 3 through Table 8 describe the web corrosion patterns. These tables provide a label for the pattern, a diagram, a real inspection report example, and a brief description.

Table 3: Web corrosion pattern W1

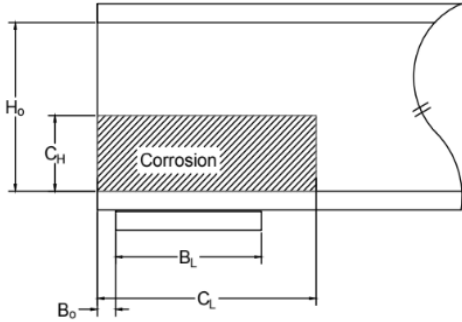
Pattern name	Pattern shape	Example from an inspection report
W1		 <p data-bbox="940 1079 1433 1171">Adopted from H-23-011-1UQ-DOT-NBI (District 3, Town of Hopkinton)</p>
	<p data-bbox="384 1211 1437 1391">Short description: W1 is a rectangular shape corrosion pattern which appears at the beam end above the bearing. The dimensions of the damaged area are C_H for the depth of the damaged area and C_L for the length. B_L is the bearing width and B_o is the length of the free end of the beam beyond the bearing. The photograph on the right shows a case of W1 for which the C_H is equal to the depth of the beam web H_o.</p>	

Table 4: Web corrosion pattern W2

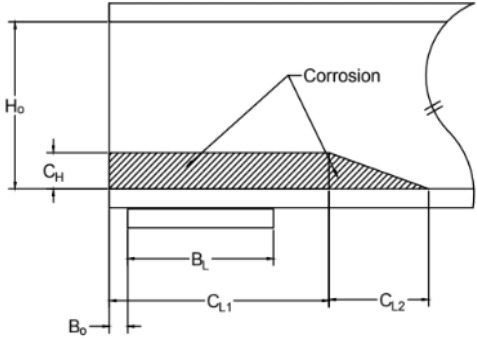
Pattern name	Pattern shape	Indicative example from an inspection report
W2		 <p data-bbox="930 741 1417 831">Adopted from N-06-015-3WR-DOT-NBI (District 5, Town of New Bedford)</p>
<p>Short description: W2 is similar to W1 with the addition of a triangular shaped corrosion area at the end of the rectangular shape. For W2, C_H is the depth of the damaged area, while C_{L1} is the length of the rectangular part of the corrosion. C_{L2} is the length of the triangular damage. B_L is the bearing width and B_0 is the length of the free end of the beam beyond the bearing. The photograph on the right shows a typical case of W2.</p>		

Table 5: Web corrosion pattern W3

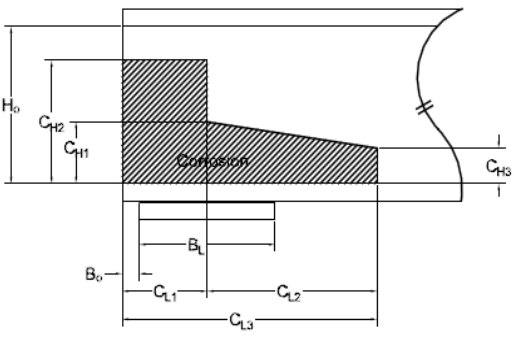
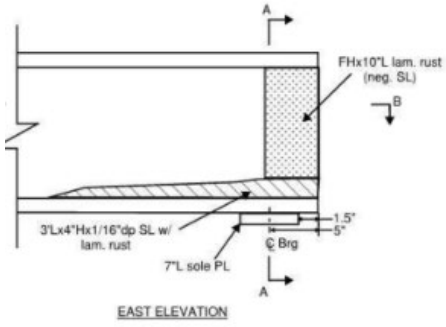
Pattern name	Pattern shape	Indicative example from an inspection report
W3		 <p data-bbox="930 1682 1417 1809">Adapted from Bridge 00162, Girder G1, Span 2, Pier 2 West Haven, Connecticut</p>
<p>Short description: W3 is a more complex shape than W1 and W2. It can be described by the three areas as shown at the sketch above (left). For W3, the depth of the corroded area is described using C_{H1}, C_{H2} and C_{H3}. Similarly, C_{L1} and C_{L2} are used to provide the length of the corroded area. B_L is the bearing width and B_0 is the length of the free end of the beam beyond the bearing. The photograph on the right shows a typical case of W3.</p>		

Table 6: Web corrosion pattern W4

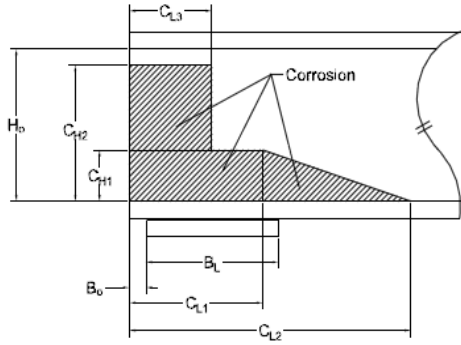
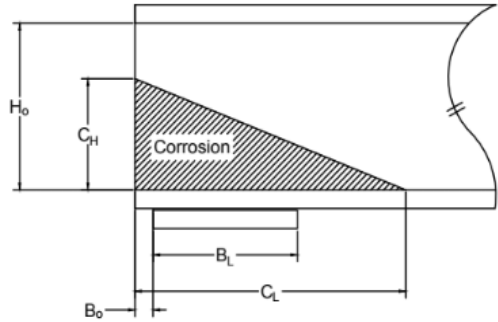
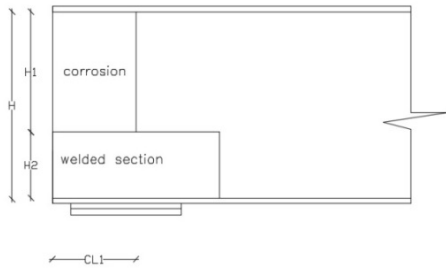
Pattern name	Pattern shape	Indicative example from an inspection report
W4		 <p>Adapted from Bridge 042401, Girder C, Abutment 2 New London Ave, Rhode Island</p>
<p>Short description: W4 is a slight modification of W3 to include the bottom left rectangular shape. The depth of the corroded area is described using C_{H1} and C_{H2}. Similarly, C_{L1}, C_{L2} and C_{L3} are used to provide the length of the corroded area. B_L is the bearing width and B_0 is the length of the free end of the beam beyond the bearing. The photograph on the right shows a typical case of W4.</p>		

Table 7: Web corrosion pattern W5

Pattern name	Pattern shape	Indicative example from an inspection report
W5		 <p>Adapted from W-05-024-0T4-MUN-NBI (District 2, Town of Ware)</p>
<p>Short description: W5 is a simple triangular shape corroded area described by C_H which is the height of the triangle and C_L which is the length of the triangle. B_L is the bearing</p>		

width and B_o is the length of the free end of the beam beyond the bearing. The photograph on the right shows a typical case of W5.

Table 8: Web corrosion pattern W6.

Pattern name	Pattern shape	Indicative example from an inspection report
<p>W6</p>		 <p>Adapted from N-19-064-10C-DOT-NBI (District 2, City of Northampton, Massachusetts)</p>
	<p>Short description: W6 is a rare case but it is included here for the sake of completeness. It involves a plate at the bottom side of the web. The corrosion extends above the repaired section as shown in the graph above (left). For this case, H_1 is the height of the corroded area, C_{L1} is the length of the corroded area, and H_2 is the height of the repair plate. The photograph on the right shows a typical case of W6.</p>	

Much like the web corrosion patterns, no new web hole corrosion patterns were created as the existing patterns described more than 95% of the beam ends. Table 9 through Table 12 depict the web hole corrosion patterns considered. These tables provide a label for the pattern, a diagram, a real inspection report example, and a brief description.

Table 9: Web hole pattern M1

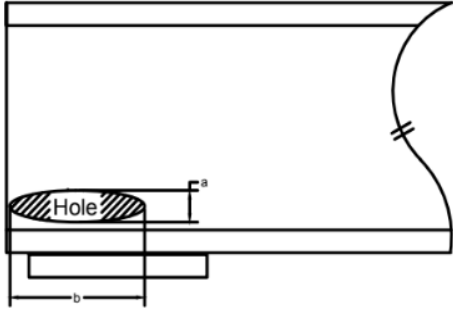
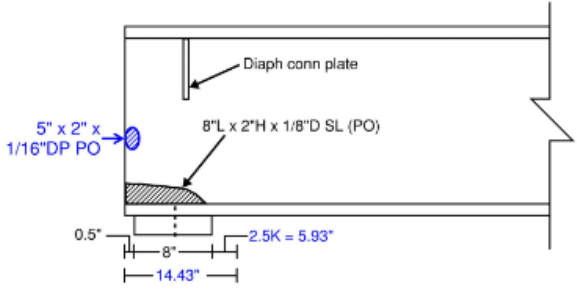
Pattern name	Hole shape	Indicative example from an inspection report
M1		 <p style="text-align: center;">G2 WEST ELEVATION</p> <p style="text-align: center;">Adapted from Bridge 00636, Girder 2, Span 2, Pier 2 Middletown, Connecticut</p>
<p>Short description: M1 is a case where a hole appears at the lower part of the web and extends longitudinally over the bearing. For this case, a is the height of the hole and b is the length of the hole. The photograph on the right shows a typical case of M1.</p>		

Table 10: Web hole pattern M2

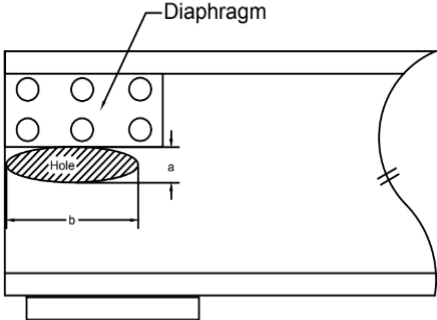
Pattern name	Hole shape	Indicative example from an inspection report
M2		 <p style="text-align: center;">Adapted from S-24-017-14K-DOT-634 (District 2, City of Springfield, Massachusetts)</p>
<p>Short description: M2 is a case where the beams have a diaphragm and the hole appears just below the diaphragm. For this case, a is the height of the hole and b is the length of the hole. The photograph on the right shows a typical case of M2.</p>		

Table 11: Web hole pattern M3

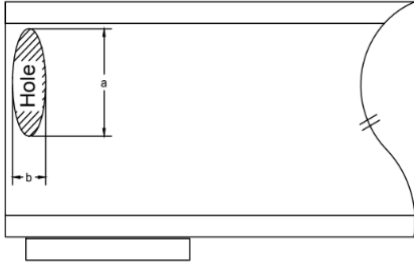
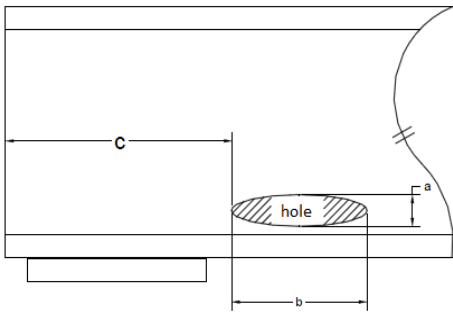
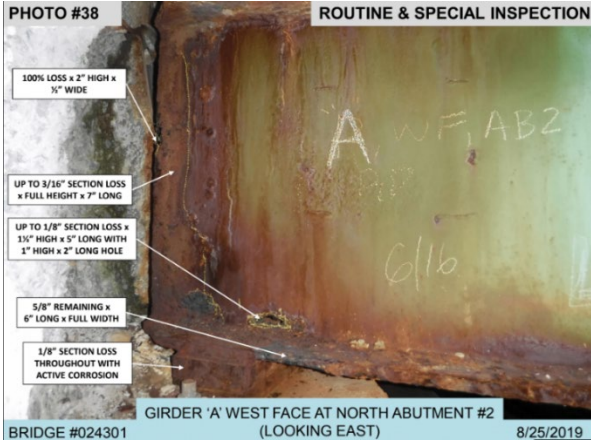
Pattern name	Hole shape	Indicative example from an inspection report
M3		 <p>Adapted from F-04-017-23N-DOT-634 (District 3, City of Fitchburg, Massachusetts)</p>
<p>Short description: M3 is a case where a hole appears at the top part of the beam. For this case, a is the height of the hole and b is the length of the hole. The photograph on the right shows a typical case of M3.</p>		

Table 12: Web hole pattern M4

Pattern name	Hole shape	Indicative example from an inspection report
M4		 <p>Adapted from Bridge 024301, Girder A West Face, North Abutment 2 Lafayette RR, Rhode Island</p> <p>Short description: M4 is a case where a hole appears away from the bearing at the lower part of the beam. For this case, a is the height of the hole, b is the length of the hole, and c is the distance of the end of the hole from the end of the beam. The photograph on the right shows a typical case of M4.</p>

It is worthwhile mentioning that the beam ends usually present a combination of corrosion web patterns and web hole patterns. Additionally, the same beam end can present more than a single web hole pattern. The three following combinations of web hole patterns were considered in this project: M1+M2, M1+M3, and M2+M4.

Flange Corrosion

The reports from each state often describe the flange corrosion by measuring only the length of the phenomenon and the thickness loss. As a result, there is the underlying assumption that corrosion is uniform across the width of the flanges. Although this is a rough assumption, this is recurring when dealing with corrosion. For instance, a similar assumption is made when the thickness loss is uniform in the corroded area.

Therefore, to summarize the flange corrosion, no pattern was created. Instead, the length and thickness loss were recorded. In case the report did not show any information regarding flange corrosion, no corrosion was considered in the flanges.

3. Organization of Data and Post-Processing

3.1. Organizing Data

To work with the extensive amount of available data, the corrosion information from the reports was organized into Excel spreadsheets. The usage of Excel allows one to easily organize the phenomenon by using the parameters defined for each corrosion pattern. Once the data was organized, our team was able to run a MATLAB code which provides efficiency in post-processing the data available in the reports.

Figure 24 depicts the top of the spreadsheet, which includes general information for the bridge, such as name, location, construction year, and so on.

Identification	columns:	5	Item 59 Condition:	5		
Bridge:	N-19-062-106 (n-s)	Area:	NORTHAMPTON	Construction:	1965	
				Location:	42°19'58.84"N 72°37'16.72"W	
Girders:	30WF99		Stringers:	concrete	Spans:	
					4	
No of corroded beams:	4	At both ends:	0	Type	composite	
				fy:		
6	Beam type	30WF99	30WF99	30WF99	30WF99	same_end
7	Web cor. Type:	W1	W3	W3	W1	0
8	CL1 (%H):	127.16%	42.38%	42.38%	42.38%	

Figure 24: Bridge identification and general information isolated at the top of the spreadsheet

Every bridge is described by a sheet in an Excel file. This allows for many bridges to be placed into a single file. Each corroded beam end is described by a single column with cells which contain general information regarding the beams. This allowed the team to compile each beam end from a given bridge into one sheet. Thus, in a single Excel file we were able to gather all the beam ends from each bridge from every state. However, to maintain organization and to avoid errors, our team decided to separate Excel files by state. Excel files varied between Group 1 and Group 2 and was dependent on the amount of corrosion data that was presented for a given beam end.

By describing each corroded beam end within a column, we accurately consider each unique beam end case. Figure 25 depicts the whole column in which the corrosion data of each beam end is summarized.

The first section of the spreadsheet describes the web corrosion pattern (lines 7-13 in Figure 25). The first field that must be filled concerns the beam type, (shaded area A, in Figure 25). Then, in part B (lines 8-13 and 18-20) the corrosion shape is described using one of the six defined corrosion patterns, the corresponding dimensions are normalized with the height H_0 , where $H_0 = H - 2t_f$, and the web thickness loss is reported as well, where H is the depth of the beam and t_f the flange thickness.

The second part of the spreadsheet involves the hole patterns. In Part C, if a web hole exists, it is classified according to the hole patterns discussed earlier in the report. In case hole dimensions are given, they are normalized the same way as web corrosion lengths. In Part D, the diaphragm and signs of buckling are reported with “yes” or “no”.

	A	B	C	D	E	F	G	H	I
1	Identification	columns:		5	Item 59 Condition:	5			
2	Bridge:	N-19-062-106 (n-s)	Area:	NORTHAMPTON	Construction:	1965	Location:	42°19'58.84"N 72°37'16.72"W	
3	Girders:	30WF99			Stringers:	concrete	Spans:	4	
4	No of corroded beams:		at both ends:	0	Type	composite	fy:		
5	Beam ID (Insp. report):	Beam29	Beam 36 N	Beam 42	Beam 43	Beam 43			
6	Beam type	30WF99	30WF99	30WF99	30WF99	same_end			
7	Web cor. Type:	W1	W3	W3	W1	0			
8	CL1 (%H):	127.16%	42.38%	42.38%	42.38%				
9	CL2 (%H):		148.35%	148.35%					
10	CL3 (%H):								
11	CH1 (%H):	14.12%	14.12%	14.12%	14.12%				
12	CH2 (%H):		28.25%	28.25%					
13	CH3 (%H):		14.12%	14.12%					
14	Hole pattern:	No	No	No	No	No			
15	a(%H):								
16	b(%H):								
17	c(%H):								
18	Max thickness loss (no holes):	0.0%	48.00%	48.00%	38.0%	0%			
19	Min. thickness loss:	0%	15.00%	10.00%	0.00%	0.00%			
20	Thickness loss/ distance:								
21	Diaphragm:	No	No	No	No	No			
22	Signs of buckling:	No	No	No	No	No			
23	Flange corrosion:								
24	Top flange	No	No	No	No	No			
25	Corrosion length (%H):								
26	Max thickness loss (%):								
27	Min thickness loss (%):								
28	Cf/Ct top								
29	Thickness loss/ distance:								
30	Flange hole:								
31	Location(%H):								
32	Hole's length:								
33	Bottom flange	Yes	Yes	Yes	Yes	Yes			
34	Corrosion length (%H): Cf b	3.53%	135.64%	135.64%	135.64%	135.64%			
35	Max thickness loss (%):	56.71%	25.00%	25.00%	7.00%	24.00%			
36	Min thickness loss (%):	0%	20.00%	9.00%	0.00%	0.00%			
37	Cf>Ct bottom	2.78%	71.12%	71.12%	302.06%	0.00%			
38	Thickness loss/ distance:								
39	Flange hole:								
40	Location:								
41	Hole's length(in):								
42	Support type:	Plates	Plates	Plates	Plates	Plates			
43	Bearing length (%H):	42.38%	42.38%	42.38%	42.38%	42.38%			
44	B (in)	n.d.	n.d.	n.d.	n.d.	n.d.			
45	Bearing corrosion:	yes	yes	yes	yes	yes			
46	Bearing deformation:	n.d.	n.d.	n.d.	n.d.	n.d.			
47	Previous repairs:	no	no	no	no	no			

Figure 25: Spreadsheet designed to organize corrosion data

Part E is dedicated to flange corrosion identification. The corrosion length and the thickness loss are reported. It is critical to note that thickness loss considers both sides of a given beam end and its corrosion. Additionally, in a case with a hole present, its position and length are reported. Finally, in Part F, the condition of the bearing is described, if any information is available.

3.2. MATLAB script

Once all the available data was organized into Excel spreadsheets, we could assume that the information from all beam ends is stored in the same shape. Using this information, a MATLAB script was created to post-process the data stored in the spreadsheets.

The MATLAB script used in this project was first developed in [28, 44] and was updated to be utilized here. Upon running, the code looks for the existence of diaphragm in the beam ends. Further, the code accounted for the patterns of each beam end stores the parameters written in the spreadsheet into MATLAB matrices. From this, our team could assess the maximum length, maximum height, etc., for each pattern.

3.3. Results

Following the post-processing of the data from the reports provided, our team could determine, for instance, the most common patterns, or the extreme cases of corrosion. Some of the states studied in this project have a significantly greater amount of recorded beam-ends than others. Additionally, in some cases, it was not possible to determine the corrosion pattern from every state. In response to this, results were presented by state, rather than as a region. This was adopted to avoid bias in the results and to provide useful data by state.

Additionally, with the division of results by states, the results were further divided into two categories; to address structures that had diaphragms and structures that did not. It is imperative to distinguish that a structure was considered to have “diaphragms” for either concrete diaphragms or for cases in which the connection plate of the metallic diaphragm occupied a significant area of the web, as depicted in Figure 26.



Figure 26: To the left is P-01-005 (Massachusetts) and the right structure is 042401 (Rhode Island)

3.3.1. Connecticut

3.3.1.1. General Metrics

Following the methodology explained above, our research team was able to compile information of 369 beams ends without diaphragms from the reports provided by CTDOT. It is important to note that beam ends without corrosion are not considered in this count. To help with the understating of the behavior of corrosion and extract more meaningful results, patterns W1 and W2 were grouped, as well as patterns W3 and W4. By doing this, the research team was able to easily distinguish the relevant web corrosion patterns and relevant hole patterns. Table 13 and Table 14 depict the results obtained by grouping the corrosion patterns of beams with and without diaphragm.

Table 13: Beam end categorization metrics for beam ends without a diaphragm system

	Number	No Hole	M1	M2	M3	M4	M1 and M2	M1 and M3	M2 and M4
W1 and W2	243	236	3	0	2	3	0	1	0
W3 and W4	50	45	3	0	2	0	0	1	0
W5	26	26	0	0	0	0	0	0	0
W6	2	2	0	0	0	0	0	0	0
Total	321	309	6	0	4	3	0	2	0

Table 14: Beam end categorization metrics for beam ends with a diaphragm system

	Number	No Hole	M1	M2	M3	M4	M1 and M2	M1 and M3	M2 and M4
W1 and W2	36	33	1	1	0	0	0	0	0
W3 and W4	10	9	1	0	0	0	0	0	0
W5	2	2	0	0	0	0	0	0	0
W6	0	0	0	0	0	0	0	0	0
Total	48	44	2	1	0	0	0	0	0

3.3.1.2. Final Corrosion patterns

From the data shown above, it becomes clear that the majority of beam end deterioration does not include holes. Additionally, it is also clear that the W1, W2, W3 and W4 patterns are present in a large majority of the beam ends. It is important to note that although patterns W1 and W2 and W3 and W4 were grouped together, these patterns were separately analyzed. Further results of isolated patterns can be found in the Appendix section of this report.

Based on Table 13 and Table 14, the research group was able to determine the most dominant cases of corrosion, which are shaded in green in Table 15 and Table 16. On the other hand, cases shaded in red were disregarded, as they were very sparse in number.

Table 15: Dominant cases for beams without a diaphragm system

	Number	No Hole	M1	M2	M3	M4	M1 and M2	M1 and M3	M2 and M4
W1 and W2	243	236	3	0	2	3	0	1	0
W3 and W4	50	45	3	0	2	0	0	1	0
W5	26	26	0	0	0	0	0	0	0
W6	2	2	0	0	0	0	0	0	0
Total	321	309	6	0	4	3	0	2	0

Table 16: Dominant cases for beams with a diaphragm

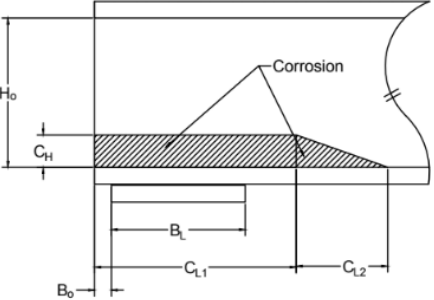
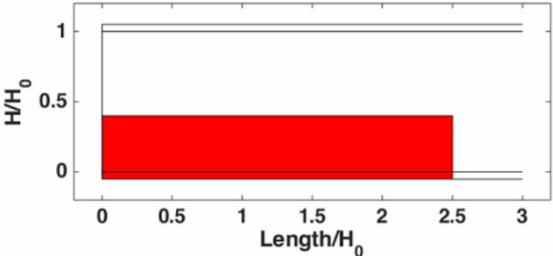
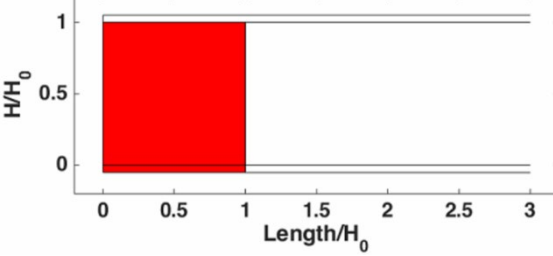
	Number	No Hole	M1	M2	M3	M4	M1 and M2	M1 and M3	M2 and M4
W1 and W2	36	33	1	1	0	0	0	0	0
W3 and W4	10	9	1	0	0	0	0	0	0
W5	2	2	0	0	0	0	0	0	0
W6	0	0	0	0	0	0	0	0	0
Total	48	44	2	1	0	0	0	0	0

3.3.1.3. Beams ends without a diaphragm system

3.3.1.3.1. W1 and W2

Based on the 317 appearances of W1 and W2 without a diaphragm system, our team was able to determine the most common cases regarding web and flange corrosion for both patterns and the most common interaction between the parameters of a pattern. Table 17, Table 18, and Table 19 depict the most common trends observed in the compiled data. The graphs which allowed the team to observe these behaviors are found in the Appendices of this report.

Table 17: Final corrosion patterns for W1 and W2 without holes (beam ends without a diaphragm) - CTDOT

Auxiliary Sketch	
	
Description	Pattern W1
<p>Case A</p> $0 < CH_1 < 0.4H_0, 0 < CL_1 < 2.5H_0$ $0 < \frac{t_{loss}}{t_{web}} \leq 0.4$ $1 \leq \frac{C_f}{C_l} \leq 3, \text{ with } 0.1 \leq \frac{t_{loss}}{t_{flange}} \leq 0.7$	
<p>Case B</p> $0 < CH_1 < 1H_0, 0 < CL_1 < 1H_0$ $0 < \frac{t_{loss}}{t_{web}} \leq 0.4$ $1 \leq \frac{C_f}{C_l} \leq 2.5, \text{ with}$ $\frac{t_{loss}}{t_{flange}} \text{ taking values of } 0.2, 0.4, 0.6, 1$	

3.3.1.3.2. W3 and W4

Table 18 : Final corrosion patterns for W3 and W4 without holes (beam ends without a diaphragm) - CTDOT

Auxiliary Sketch	
Description	Pattern W3
<p>Case A $0 < CH_1 < 0.4H_0, 0 < CH_2 < 1H_0, 0 < CH_3 < 0.4H_0, 0 < CL_1 < 1H_0, 0 < CL_2 < 1.5H_0, 0 < CL_3 < 2.5H_0$ $0 < \frac{t_{loss}}{t_{web}} \leq 0.4$ $0 < \frac{C_f}{H_0} \leq 0.4, \text{ with } 0 < \frac{t_{loss}}{t_{flange}} \leq 0.4$</p>	

3.3.1.3.3. W5

Table 19: Final corrosion patterns for W5 without holes (beam ends without a diaphragm) - CTDOT

Auxiliary Sketch	
Description	Pattern W5
<p>Case A $0 < CH_1 < 0.2H_0, 0.4H_0 < CL_1 < 1.5H_0$ $0.1 \leq \frac{t_{loss}}{t_{web}} \leq 0.5$ $0 < \frac{C_f}{H_0} \leq 1.5, \text{ with } 0 < \frac{t_{loss}}{t_{flange}} \leq 0.4$</p>	

3.3.1.4. Beam ends with a diaphragm system

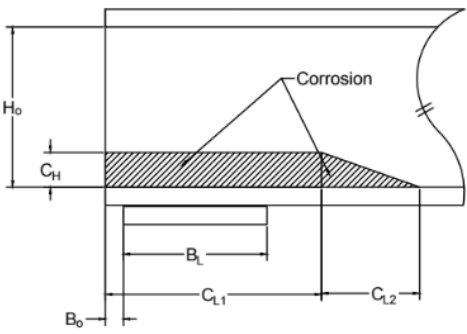
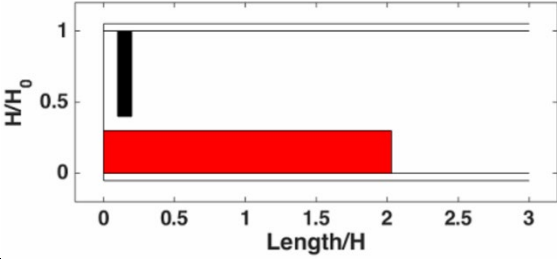
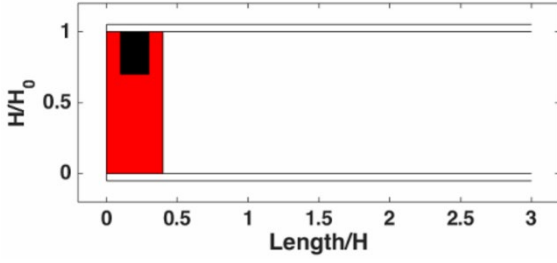
3.3.1.4.1. W1 and W2

The goal of this section of the report is to describe the interaction between the parameters of the corrosion patterns. To meet this goal, the main trends in patterns W1 and W2 were observed. As commented in the previous sections, patterns W1 and W2 were grouped, as W1 can be expressed from W2 pattern if CL2 is zero.

The existence of the diaphragm makes the understanding of the corrosion problem more difficult, due to the inability to predict the diaphragms' location placement. For this reason, in this section, only observed cases of corrosion are plotted.

From the results, it was observed that beam ends with a diaphragm have two main trends. It was found that in both cases, CL2 is equal to 0. Additionally, the corrosion height was found either to be the full height or up to 40% of H0, as depicted in Table 20.

Table 20: Final corrosion patterns for W1 and W2 without holes (beam ends with a diaphragm) - CTDOT

Auxiliary Sketch	
	
<p>Description</p> <p>Case A (Report 01807, CT, Span 1, G4, Pier 1) $0.1H_0 < CH_1 < 0.3H_0, 0 < CL_1 < 2.5H_0$ $0 < \frac{t_{loss}}{t_{web}} \leq 0.3$ $1 \leq \frac{c_f}{c_l} \leq 3, \text{ with } 0.1 \leq \frac{t_{loss}}{t_{flange}} \leq 0.4$</p>	<p>Pattern W1</p> 
<p>Case B (01732, CT, Span 3, G6, Pier 2) $0 < CH_1 < 1H_0, 0.2H_0 < CL_1 < 0.4H_0$ $0.2 \leq \frac{t_{loss}}{t_{web}} \leq 0.4$ $0 < \frac{c_f}{c_l} \leq 1, \text{ with}$ $\frac{t_{loss}}{t_{flange}}$ takes values of 0.2, 0.4</p>	

3.3.1.4.2. W3 and W4

Table 21: Final corrosion patterns for W3 and W4 without holes (beam ends with a diaphragm)
- CTDOT

Auxiliary Sketch	
<p>Description</p> <p>Case A (00281, CT, Span 2, G1, Pier 2, East EI)</p> $0 < CH_1 < 0.2H_0, 0 < CH_2 < 1H_0, 0 < CH_3 < 0.2H_0, 0.2H_0 < CL_1 < 0.4H_0, 0 < CL_2 < 2H_0, 0.5H_0 < CL_3 < 2.5H_0$ $0.1 \leq \frac{t_{loss}}{t_{web}} \leq 0.3$ $0 < \frac{c_f}{H_0} \leq 1, \text{ with } 0 < \frac{t_{loss}}{t_{flange}} \leq 0.2$	<p>Pattern W3</p>

3.3.2. Maine

As discussed in the previous sections, the bridge inspection reports did not provide enough documentation to allow the research team to match the corrosion patterns to the existing beams. For this reason, it was not possible to account for the most common corrosion topologies. The results the research team was able to obtain from the documentation provided by MaineDOT can be found in the Appendix section of this report.

3.3.3. Massachusetts

3.3.3.1. General Metrics

Following the two stage post-processing described above, the 808 beam ends were categorized to all the patterns. It must be mentioned that out of the 808, 69 beam ends had no corrosion. Therefore, from this point on there will be 739 beam ends as the total number in the following tables. At this stage, it was decided to group some of the patterns together: W1 with W2, W3 with W4. A further distinction between beam ends with and without diaphragm was also realized. The categorization metrics are shown in Table 22 and Table 23 for all the 739 beam ends.

Table 22: Beam end categorization metrics for beam ends without a diaphragm system**Beam ends without a diaphragm**

	Number	No Hole	M1	M2	M3	M4	M1 and M2	M1 and M3	M2 and M4
W1 and W2	171	154	13	1	3	0	0	3	0
W3 and W4	96	78	14	0	3	1	0	4	0
W5	17	13	3	1	0	0	0	0	0
W6	2	2	0	0	0	0	0	0	0
Total	286	247	30	2	6	1	0	7	0

Table 23 : Beam end categorization metrics or beam ends with a diaphragm system**Beam ends with a diaphragm**

	Number	No Hole	M1	M2	M3	M4	M1 and M2	M1 and M3	M2 and M4
W1 and W2	268	235	13	13	5	2	1	0	0
W3 and W4	176	125	35	8	6	2	9	4	1
W5	9	9	0	0	0	0	0	0	0
W6	0	0	0	0	0	0	0	0	0
Total	453	369	48	21	11	4	10	4	1

From the data shown above, it becomes clear that most of the beam end deterioration does not include holes. In addition, it is also very clear that many beam ends belong to W1, W2, W3 and W4 patterns. Table 24 shows the same categorization according to different districts.

Table 24: Distribution of beam ends according to district

	Total	District 1	District 2	District 3	District 4	District 5
W1	380	2	79	31	9	259
W2	59	4	4	0	2	49
W3	216	7	60	72	20	57

W4	56	1	7	4	0	44
W5	26	3	4	3	0	16
W6	2	0	2	0	0	0

3.3.3.2. Final Corrosion patterns

As mentioned above, the pattern W1 is merged with W2 and pattern W3 is merged with W4. W1 can be expressed from W2 pattern if CL_2 is set to zero. This allowed us to group W1 and W2 into one case which can be carried through the post-processing; there are 3 extreme scenarios identified. It is imperative to note that both the W1 and W2 patterns were examined separately.

Similarly, W3 and W4 can be expressed as a W3 pattern with $Cl_3(W4)=Cl_1$ and $C_{H1}=C_{H3}$. Based on this merge, the cases which were selected as “more dominant” are shown in green in the following two tables. The cases which have a red shade were disregarded as they were very few. In total, the green cases consist of the 91% of all the cases of corroded beam ends which is considered an adequate threshold. The data were divided in 2 main categories, beams ends with diaphragm and without. The dimensions of the pattern are normalized with the height H_0 , where $H_0 = H - 2t_f$. It should be mentioned that the final corrosion patterns for the top flange are considered intact, because only at 19 out of 732 beam ends top flange deterioration was reported.

Table 25: Metrics for beam ends with a diaphragm after the merging

Beam ends with a diaphragm

	Frequency	No Hole	M1	M2	M3	M4	M1 and M2	M1 and M3	M2 and M4
W1 and W2	268	235	13	13	5	2	1	0	0
W3 and W4	176	125	35	8	6	2	9	4	1
W5	9	9	0	0	0	0	0	0	0
W6	0	0	0	0	0	0	0	0	0
Total	453	369	48	21	11	4	10	4	1

Table 26: Metrics for beam ends without a diaphragm after the merging

Beam ends without a diaphragm

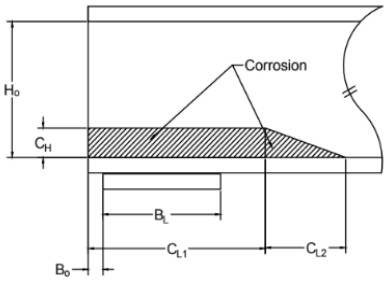
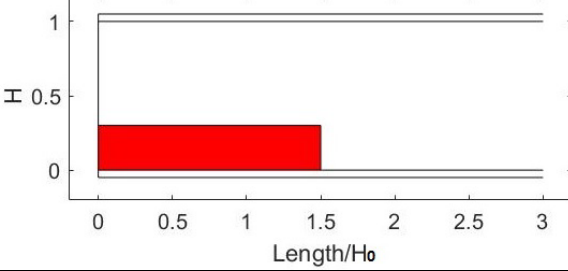
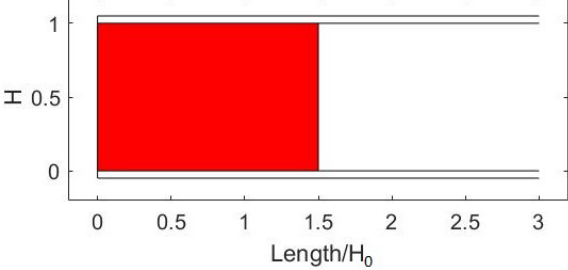
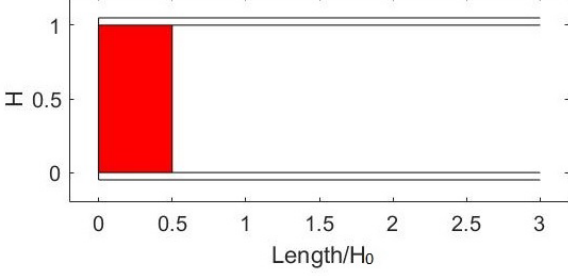
	Frequency	No Hole	M1	M2	M3	M4	M1 and M2	M1 and M3	M2 and M4
--	-----------	---------	----	----	----	----	-----------	-----------	-----------

W1 and W2	171	154	13	1	3	0	0	3	0
W3 and W4	96	78	14	0	3	1	0	4	0
W5	17	13	3	1	0	0	0	0	0
W6	2	2	0	0	0	0	0	0	0
Total	286	247	30	2	6	1	0	7	0

3.3.3.3. Beam ends without a diaphragm system

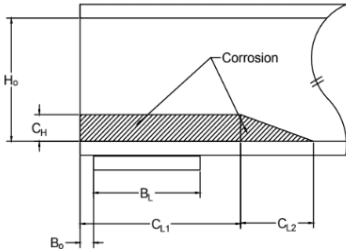
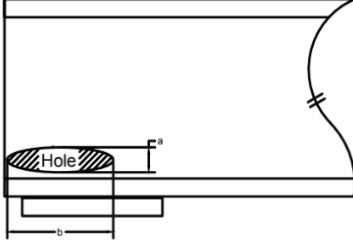
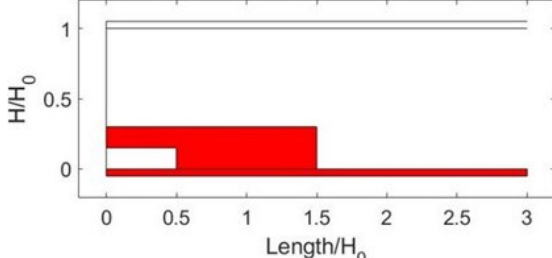
3.3.3.3.1. W1 and W2

Table 27: Final corrosion patterns for W1 and W2 without holes (beam ends without a diaphragm) - MassDOT

Description	W1 and W2 pattern
<p>Helpful sketch</p> 	
<p>Case A: $0 < CH_1 \leq 0.3H_o$, $0 < CL_1 \leq 1.5H_o$ and $\frac{t_{loss}}{t_{web}}$ takes values of {0.2, 0.4, 0.6, 0.8} $1 \leq \frac{C_f}{C_l} \leq 2$, with $\frac{t_{loss}}{t_{flange}}$ taking values of {0.2, 0.4, 0.6, 0.8}</p>	
<p>Case B: $CH_1 = H_o$, $0 < CL_1 \leq 1.5H_o$ and $\frac{t_{loss}}{t_{web}}$ takes values of {0.2, 0.8} $1 \leq \frac{C_f}{C_l} \leq 2$, with $\frac{t_{loss}}{t_{flange}}$ taking values of {0.45, 0.65}</p>	
<p>Case C: $CH_1 = H_o$, $0 < CL_1 \leq 0.5H_o$ and $\frac{t_{loss}}{t_{web}}$ takes values {0.2, 0.8} $1 \leq \frac{C_f}{C_l} \leq 2$, with $\frac{t_{loss}}{t_{flange}}$ taking values of {0.45, 0.65}</p>	

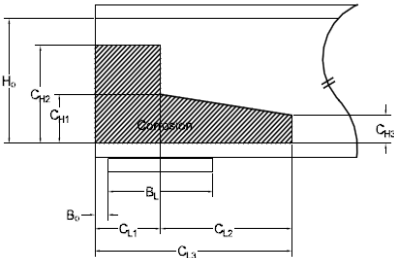
3.3.3.3.2. M1 hole pattern

Table 28: Final corrosion patterns for W1 and W2 with holes (beam ends without a diaphragm) - MassDOT

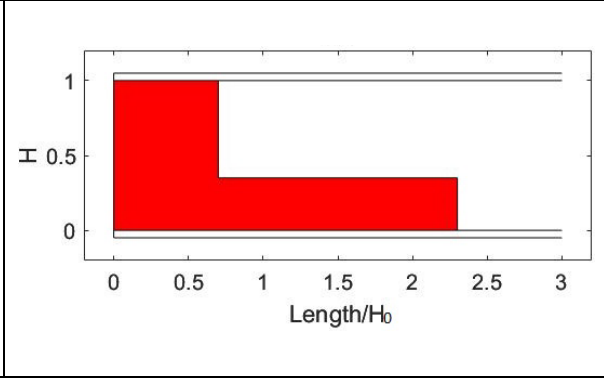
Description	W1 and W2 pattern
<p data-bbox="432 398 539 465">Helpful sketches</p> 	
<p data-bbox="240 813 707 880">The extreme scenario is projected on the W1 and W2 Case C:</p> <p data-bbox="240 880 746 947">The extreme hole scenario was found on W2, with $a=0.15$ and $b=0.5$.</p>	

3.3.3.3.3. W3 and W4

Table 29: Final corrosion patterns for W3 and W4 without holes (beam ends without a diaphragm) - MassDOT

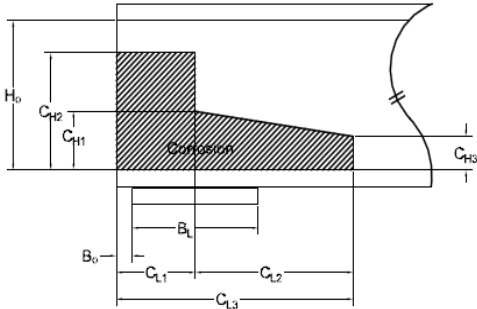
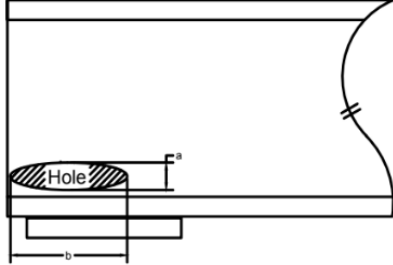
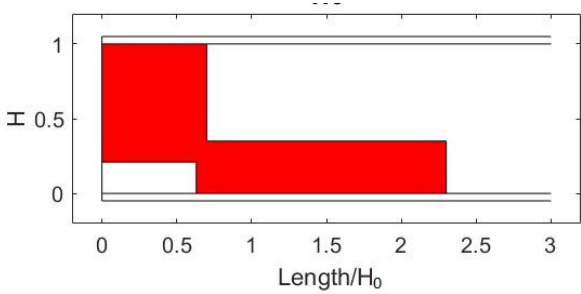
Description	W3 and W4 pattern
<p data-bbox="432 1364 523 1431">Helpful sketch</p> 	

The extreme scenario is:
 $0 < CH_1 \leq 0.35H_o$, $0 < CH_3 \leq 0.35H_o$
 $0.05H_o < CL_1 \leq 0.7H_o$, $0.5H_o < CL_3 \leq 2.3H_o$
 $\frac{t_{loss}}{t_{web}}$ taking values of {0.1,0.2,0.3,0.4,0.5,0.6,0.7,0.8}
 $\frac{C_f}{C_{L3}} = 1$, with
 $\frac{t_{loss}}{t_{flange}}$ taking values of {0.4, 0.6, 0.8}



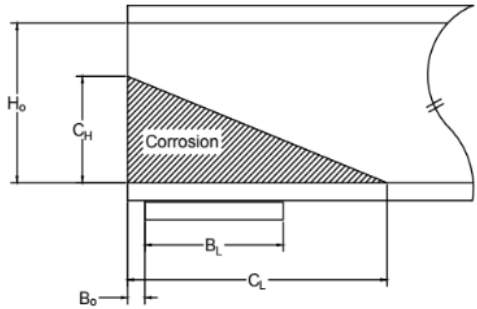
3.3.3.3.4. M1 hole pattern

Table 30: Final corrosion patterns for W3 and W4 with holes (beam ends without a diaphragm) - MassDOT

Description	W3 and W4 pattern
<p>Helpful sketches</p> 	
<p>The extreme scenario is: Holes seem to be mainly thin and long across the web, with the extreme case $a=0.21H_0$ and $b=0.63H_0$.</p>	

3.3.3.3.5. W5

Table 31: Final corrosion patterns for W5 without holes (beam ends without a diaphragm) - MassDOT

Description	W5 pattern
<p>Helpful sketch</p> 	

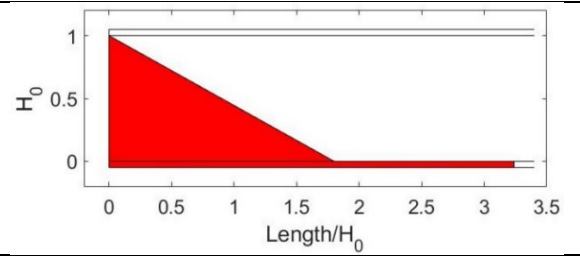
The extreme scenario is:

$$0.15H_o \leq CH_1 \leq 1H_o, \quad 0 < CL_1 \leq 0.35H_o$$

$$\frac{t_{loss}}{t_{web}} \text{ takes values of } \{0.2, 0.5\}, \quad 1 \leq \frac{c_f}{c_{L3}} \leq$$

1.8, with

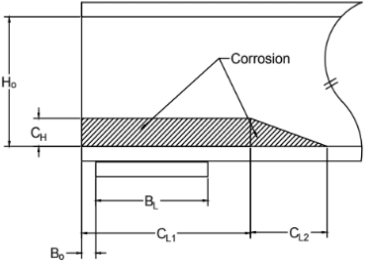
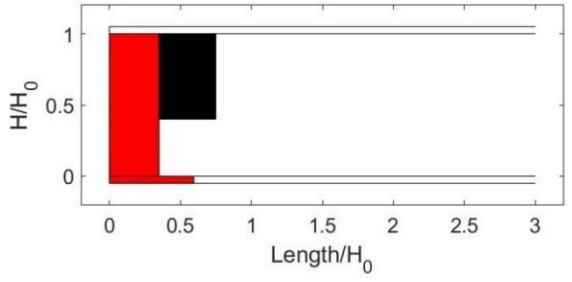
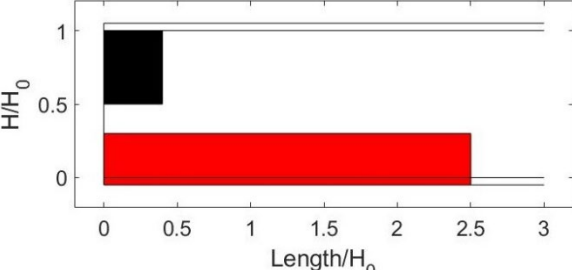
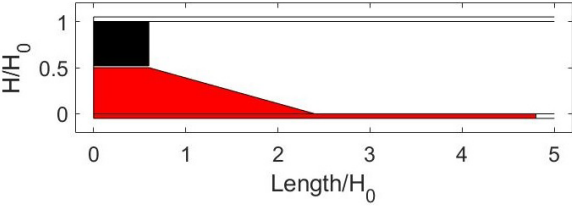
$$\frac{t_{loss}}{t_{flange}} \text{ taking values of } \{0.1, 0.8\}$$



3.3.3.4. Beam ends with a diaphragm

3.3.3.4.1. W1 and W2

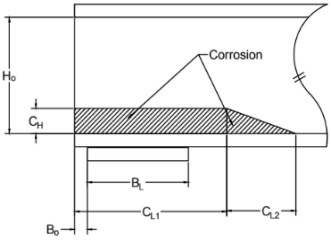
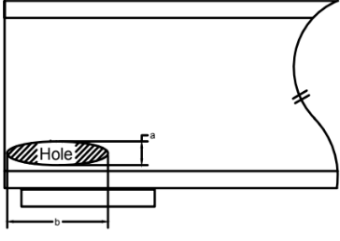
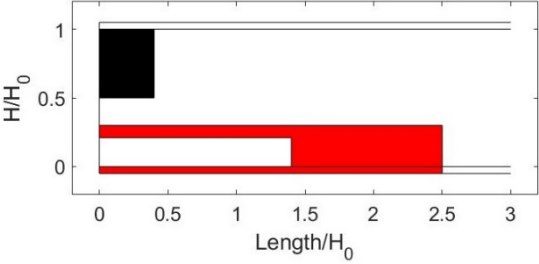
Table 32: Final corrosion patterns for W1 and W2 without holes (beam ends with a diaphragm) - MassDOT

Description	W1 and W2 pattern
<p>Helpful sketch</p> 	
<p>Case A: $0 < CL_1 \leq 0.35H_0$, $\frac{t_{loss}}{t_{web}}$ taking values of {0.2,0.4,0.6,0.8} Flange: $0.15 < \frac{t_{loss}}{t_{flange}} \leq 0.45$, $1 \leq \frac{Cf}{Cl} \leq 1.7$</p>	
<p>Case B: $0 < CL_1 \leq 2.5H_0$, $\frac{t_{loss}}{t_{web}}$ taking values of {0.2,0.4,0.6,0.8} Flange: $0 \leq \frac{Cf}{Cl} \leq 1$, $\frac{t_{loss}}{t_{flange}}$ taking values of {0.2,0.4,0.6,0.8}</p>	
<p>Case C: $0 < CH_1 \leq 0.5H_0$, $0 < CL_1 \leq 0.6H_0$ $0 < CL_2 \leq 1.8H_0$, $\frac{t_{loss}}{t_{web}}$ taking values of {0.2,0.4,0.6,0.8} $1 < \frac{Cf}{Cl} \leq 2$, $\frac{t_{loss}}{t_{flange}}$ taking values of {0.2,0.4,0.6,0.8}</p>	

Case A is the first extreme corrosion scenario in the web and flange, with full height corrosion and length up to 35% of H_0 . The corroded area is often located before the diaphragm, which is illustrated with black in the figures of this report. Case B is the second extreme corrosion scenario in the web and flange. The corroded area extends longitudinally in the web above the flange. Case C is the third extreme corrosion scenario in the web and flange.

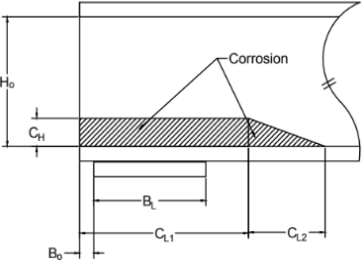
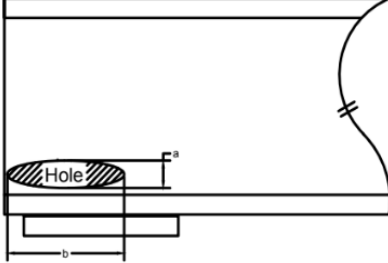
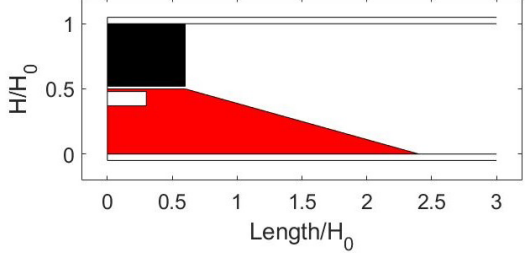
3.3.3.4.2. M1 Holes

Table 33: Final corrosion patterns for W1 and W2 with holes (beam ends with a diaphragm) - MassDOT

Description	W1 and W2 pattern
<p data-bbox="276 517 379 584">Helpful sketches</p> 	
<p data-bbox="240 719 783 887">M1 holes were equally distributed between web corrosion scenarios CASE A and CASE B, with maximum length $1.4H_0$ and height $0.21H_0$. M2 mainly appeared in the third scenario.</p>	

3.3.3.4.3. M2 Holes

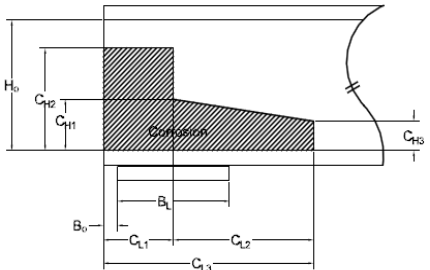
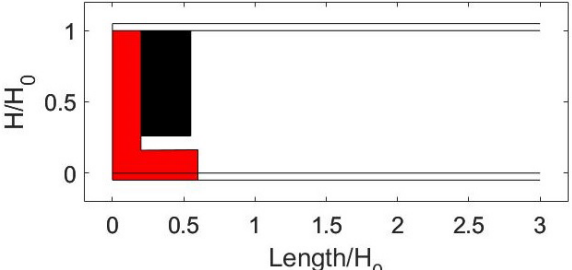
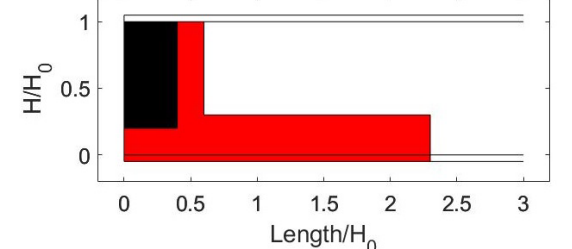
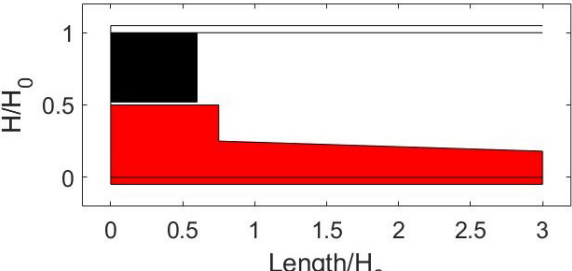
Table 34: Final corrosion patterns for W1 and W2 with holes (beam ends with a diaphragm) - MassDOT

Description	W1 and W2 pattern
<p data-bbox="448 1216 555 1283">Helpful sketches</p> 	
<p data-bbox="240 1715 778 1850">M2 hole pattern projected on the extreme third web corrosion pattern. With black color the diaphragm is illustrated in a possible configuration, with $a \leq 0.11$, and $b \leq 0.3$.</p>	

3.3.3.4.4. W3 and W4

As discussed earlier in the report, W3 and W4 were merged for analysis. However, in this case, both patterns were examined separately, and three extreme scenarios were identified. It was noticed that extreme scenarios of W3 are the most critical. Following this, two main trends were found: a) full height corrosion, or b) corrosion up to 30% of H_0 .

Table 35: Final corrosion patterns for W3 and W4 without holes (beam ends with a diaphragm) - MassDOT

Description	W3 and W4 pattern
<p>Helpful sketch</p> 	
<p>Case A: $0.25H_0 < CL_3 \leq 0.6H_0$, $0.1H_0 < CL_1 \leq 0.2H_0$ $0.06H_0 < CH_1 = CH_3 \leq 0.16H_0$, $\frac{t_{loss}}{t_{web}}$ takes values of {0.4,0.6} $\frac{Cf}{Cl} = 1.2$ and $\frac{t_{loss}}{t_{flange}}$ takes values of {0.3, 0.6}</p>	
<p>Case B: $0.6H_0 < CL_3 \leq 2.3H_0$, $0.2 < CL_1 \leq 0.6H_0$ $0.05 < CH_1 = CH_3 \leq 0.30H_0$, $\frac{t_{loss}}{t_{web}}$ takes values of {0.4,0.6,0.8}, $\frac{Cf}{Cl} = 1$ and, $\frac{t_{loss}}{t_{flange}}$ takes the value of {0.65}</p>	
<p>Case C: $0.5H_0 < CL_3 \leq 3H_0$, $0.1H_0 < CL_1 \leq 0.75H_0$ $0.05H_0 < CH_1 \leq 0.25H_0$, $0.05H_0 < CH_3 \leq 0.18H_0$, $\frac{t_{loss}}{t_{web}}$ takes values of {0.4,0.6,0.8} $\frac{Cf}{Cl} = 1$ and $\frac{t_{loss}}{t_{flange}}$ takes values of {0.3, 0.6, 0.8}</p>	

3.3.3.4.5. M1 Holes

Table 36: Final corrosion patterns for W3 and W4 with holes (beam ends with a diaphragm) - MassDOT

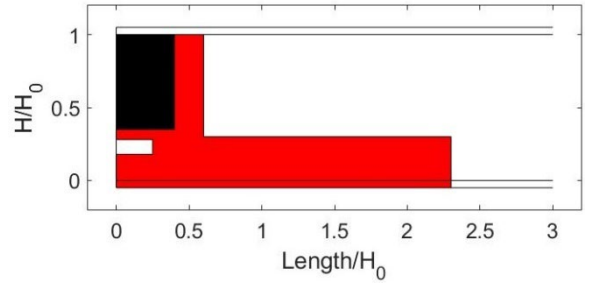
Description	W3 and W4 pattern
<p data-bbox="427 398 539 465">Helpful sketches</p>	
<p data-bbox="239 833 746 1102">Holes appeared mainly with a full height corroded web and they seem to be mainly thin and long across the web. Most of the cases have ratio of hole's length to height up to 6, and length up to 50% of H_0. Thus, for the extreme hole scenario, hole's height is considered as 0.083.</p> <p data-bbox="239 1124 678 1191">For W4, M1 hole appears as pit hole (0.0044 x 0.0044).</p>	

3.3.3.4.6. M2 Holes

Table 37: Final corrosion patterns for W3 and W4 with holes (beam ends with a diaphragm) - MassDOT

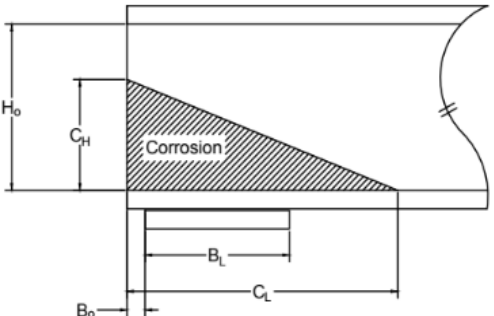
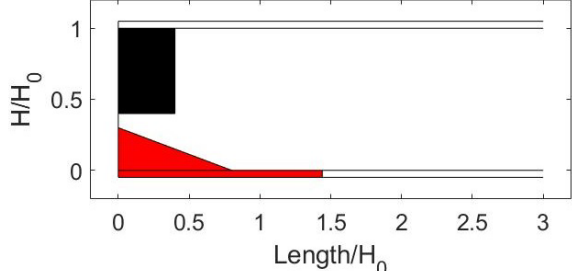
Description	W3 and W4 pattern
<p data-bbox="427 1458 539 1525">Helpful sketches</p>	

M2 holes were examined together for both patterns W3 and W4 because there were found only 7 times. The extreme hole scenario with $a \leq 0.1$ and $b \leq 0.25$ is projected on the Case B extreme web corrosion scenario.



3.3.3.4.7. W5

Table 38: Final corrosion patterns for W5 with holes (beam ends with a diaphragm) - MassDOT

Description	W5 pattern
<p>Helpful sketch</p> 	
<p>$0.3H_0 \leq CL_1 \leq 0.85H_0$, $0.15H_0 < CH_1 \leq 0.30H_0$</p> <p>$\frac{t_{loss}}{t_{web}}$ takes the value {0.35}</p> <p>$\frac{t_{loss}}{t_{flange}}$ takes the values {0.3,0.6,0.8} with C_f taking the values of {1, 1.6}</p> <p>C_l</p>	

3.3.4. New Hampshire

As described earlier, the bridge inspection reports from the state of New Hampshire did not provide enough documentation to allow the research team to match corrosion patterns to current damage in the beams of the bridge structures. For this reason, it was not possible to account for the most common corrosion topologies. The results the research team were able to obtain from the documentation provided by NHDOT can be found in the Appendix of this report.

3.3.5. Rhode Island

3.3.5.1. General Metrics

Following the methodology explained above, the research team was able to compile information on 88 beam ends from the inspection reports provided by RIDOT. It is important to note that beam ends without corrosion are not considered in this count. To ease the understanding of the behavior of corrosion and extract more meaningful results, patterns W1 and W2 were grouped, as well as patterns W3 and W4. With these groupings, the research team was able to easily distinguish the relevant web corrosion patterns and relevant hole patterns present in the bridge structures for the state of Rhode Island. Table 39 and Table 40 depict the results obtained by grouping the corrosion patterns of beams with and without a diaphragm.

Table 39: Beam end categorization metrics for beam ends without a diaphragm

	Frequency	No Hole	M1	M2	M3	M4	M1 and M2	M1 and M3	M2 and M4
W1 and W2	26	24	2	0	0	0	0	0	0
W3 and W4	21	19	0	0	1	1	0	0	0
W5	4	4	0	0	0	0	0	0	0
W6	0	0	0	0	0	0	0	0	0
Total	51	47	2	0	1	1	0	0	0

Table 40: Beam end categorization metrics for beam ends with a diaphragm

	Frequency	No Hole	M1	M2	M3	M4	M1 and M2	M1 and M3	M2 and M4
W1 and W2	28	25	2	0	1	0	0	0	0
W3 and W4	9	8	0	0	0	1	0	0	0
W5	0	0	0	0	0	0	0	0	0
W6	0	0	0	0	0	0	0	0	0
Total	37	33	2	0	1	1	0	0	0

3.3.5.2. Final Corrosion patterns

From the data shown above, it becomes clear that most of the beam end deterioration does not include holes. In addition, it is also very clear that most of the beam ends belong to W1, W2, W3 and W4 patterns. It is worthwhile pointing out that although patterns W1 and W2 and W3 and W4 were grouped together, these patterns were separately analyzed. Besides that, the results of isolated patterns can be found in the appendix.

Based on Table 39 and Table 40, the research group was able to determine the most dominant cases, which are shaded in green in Table 41 and Table 42. On the other hand, cases shaded in red were disregarded, as they were very few.

Table 41: Dominant cases for beams without a diaphragm

	Number	No Hole	M1	M2	M3	M4	M1 and M2	M1 and M3	M2 and M4
W1 and W2	26	24	2	0	0	0	0	0	0
W3 and W4	21	19	0	0	1	1	0	0	0
W5	4	4	0	0	0	0	0	0	0
W6	0	0	0	0	0	0	0	0	0
Total	51	47	2	0	1	1	0	0	0

Table 42: Dominant cases for beams with a diaphragm

	Number	No Hole	M1	M2	M3	M4	M1 and M2	M1 and M3	M2 and M4
W1 and W2	28	25	2	0	1	0	0	0	0
W3 and W4	9	8	0	0	0	1	0	0	0
W5	0	0	0	0	0	0	0	0	0
W6	0	0	0	0	0	0	0	0	0
Total	37	33	2	0	1	1	0	0	0

3.3.5.3. Beams ends without a diaphragm

3.3.5.3.1. W1 and W2

Based on the 49 appearances of the W1 and W2 patterns without a diaphragm, our team was able to determine the most common cases regarding web and flange corrosion for each, and the most common interaction between the parameters of a pattern. Table 43, Table 44 and Table 45 depict the most common trends observed in the compiled data. The graphs which allowed one to observe these behaviors can be found in the Appendix of this report.

Table 43: Final corrosion patterns for W1 and W2 without holes (beam ends without a diaphragm) - RIDOT

Auxiliary Sketch	
Description	Pattern W1
<p>Case A</p> $0 < CH_1 < 0.5H_0, 0 < CL_1 < 3H_0$ $0 < \frac{t_{loss}}{t_{web}} \leq 0.3$ $1 \leq \frac{c_f}{c_l} \leq 3, \text{ with } 0.2 \leq \frac{t_{loss}}{t_{flange}} \leq 0.7$	
<p>Case B</p> <p>Extreme Scenario (085901, RI, GE, West)</p> $0 < CH_1 < 0.5H_0, 0 < CL_1 < 9.2H_0$ $0 < \frac{t_{loss}}{t_{web}} \leq 0.3$ $0 < \frac{c_f}{c_l} \leq 6.4, \text{ with}$ $\frac{t_{loss}}{t_{flange}} \text{ taking values of } \{0.2\}$	

3.3.5.3.2. W3 and W4

Table 44: Final corrosion patterns for W3 and W4 without holes (beam ends without a diaphragm) - RIDOT

Auxiliary Sketch	
Description	Pattern W3
<p>Case A</p> $0 < CH_1 < 0.6H_0,$ $CH_2 \text{ take the value of } \{1H_0\}, 0.5H_0 < CH_3 < 2.5H_0, 0 < CL_1 < 0.5H_0, 0.3H_0 < CL_2 < 2H_0, 0.5H_0 < CL_3 < 2.5H_0$ $0 < \frac{t_{loss}}{t_{web}} \leq 0.5$ $0 < \frac{c_f}{H_0} \leq 2, \text{ with } 0 < \frac{t_{loss}}{t_{flange}} \leq 0.6$	

3.3.5.4. Beams ends with a diaphragm

3.3.5.4.1. W1 and W2

The goal of this section was to understand the interaction between the parameters of the corrosion patterns. To do this, the main trends in patterns W1 and W2 were observed. As discussed in the previous sections, patterns W1 and W2 were grouped. Our team was able to generate W1 from W2, i.e., W1 can be expressed from the W2 pattern if CL2 is zero.

Additionally, the existence of the diaphragm makes the understanding of the problem harder, as one is not able to predict where the diaphragm will be placed. For this reason, in this section, only observed cases of corrosion were plotted.

**Table 45 : Final corrosion patterns for W1 and W2 without holes (beam ends with a diaphragm)
- RIDOT**

Auxiliary Sketch	
Description	Pattern W1
<p>Case A (Report 01807, CT, Span 1, G4, Pier 1) $0 < CH_1 < 0.2H_0$, $0.3H_0 < CL_1 < 2.5H_0$ $0.1 \leq \frac{t_{loss}}{t_{web}} \leq 0.3$ $0.3 \leq \frac{c_f}{c_t} \leq 3$, with $0.1 \leq \frac{t_{loss}}{t_{flange}} \leq 0.3$</p>	
<p>Case B Extreme Scenario (042801, RI, P2, Gk, S3) $0 < CH_1 < 1H_0$, $0 < CL_1 < 0.6H_0$ $0.1 \leq \frac{t_{loss}}{t_{web}} \leq 0.7$</p>	

3.3.6. Vermont

As discussed earlier in the report, the bridge inspection reports did not provide enough documentation to allow the research team to match the corrosion patterns. For this reason, it was not possible to account for the most common corrosion topologies. The results the research team were able to obtain from the documentation provided by VTrans can be found in the Appendix of this report.

4. Selection of Bridges

4.1. Bridges Investigated

As stated above, our team received a total of 553 inspection reports from the six New England States. Among these 553 reports, there were structures with multiple inspection reports. This resulted in a final structure database of 515 total bridges across the six New England States. From the 553 reports studied, 225 reports were compiled and summarized for beam end corrosion data. This allowed our team to gather data for 1,723 beam ends as part of the corrosion topology study, from which we selected structures with corroded beam end candidates of interest. While there were several structures which were of interest to the research team, there were many factors that influenced the research team's ability to receive all of the specimens. Many of these factors were dependent on timing, as structures may be scheduled for demolition and the timelines may change; the bridge had to be demolished or scheduled for demolition within the project timeline to ensure the team received the specimens. Other factors that affected the team's receiving of the beams were directly related to the viability of beam specimens post demolition; there were situations where beams were destroyed due to their excessive damage and resulting fragility in the demolition process.

At the beginning of the project, the discussion between states to arrange potential beam specimen deliveries was on a bi-weekly to monthly basis. This part of the task was to discuss our structures of interest with constant and clear communication between all of the New England States. This was crucial as bridge beam specimens are the cornerstone of the project and their quantity is directly dependent on when or if a bridge structure is demolished or replaced. Once a structure begins undergoing the demolition process, the transport and receiving of a given structure's beam specimens becomes very fast paced as storing these components can take up a large amount of space and transporting them can be expensive. Additionally, the research team wanted to receive as many of the beam ends as possible to ensure a great representation across beam types, corrosion topologies, and across all the New England States.

The following structures were determined to be viable candidates through the corrosion topology studies and were structures scheduled for demolition within the project timeline. Figures 27 through 32 show the in-place structures before demolition.



Figure 27: Connecticut, 02929, Route 80 Deep River



Figure 28. Massachusetts, 07U, Savoy



Figure 29. Maine, 3801, Jay

<p>✕</p> <p>Newport 154/129</p> <p>SAND HILL ROAD over BROOK</p> <p>POSTED: No Posting Required.</p> <p>Owner: Municipality, Bridge Type: IB-BP, Year Built: 1984, Rebuilt: 0 No. Main Spans: 1, No. App. Spans: 0, Total Bridge Length: 27 feet, Tier: 5 Condition - Deck: 3, Super: 2, Sub: 5</p>	
--	--

Figure 30. New Hampshire, 154/129, Newport



Figure 31. Vermont, BR3, Proctor



Figure 32. Vermont, BR15, Newbury

4.2. Beam Specimens Received

Fortunately, five out of the six states were able to provide the research team specimens for section loss analysis and for testing. These beam specimens were stored on site at the Brack Structural Testing Facility at The University of Massachusetts Amherst. The number of beams received by state can be found in Table 46 below along with the specimens present on site in Figures 33 through 37.

Table 46: Beams Received by State

State	Beams Received
Connecticut	3
Maine	10
Vermont	16
Massachusetts	11
New Hampshire	12
Rhode Island	0
Total	52



Figure 33. Connecticut Specimens



Figure 34. Massachusetts Specimens



Figure 35. Maine Specimens



Figure 36. New Hampshire Specimens



Figure 37. Vermont Specimens

It is important here to note the ages of the structures because of their differences in corrosion, their beam types, but most importantly their material composition. The Connecticut bridge was constructed in 1916; the beams that were received were from a different structure and added on as a rehabilitation. The bridge in Jay, Maine was constructed in 1941. The New Hampshire structure we received beam specimens from was constructed in 1984. Finally, the Proctor and Newbury Vermont bridges were constructed in 1936 and 1946 respectively.

As the project progressed the research team also made site visits to many bridges to investigate beam end conditions and to see if there were specimens of interest for testing. The team performed 3D scans on site for each of these visits to see the damage on the desired beam ends. These site visits were very beneficial on a multitude of scales. For a few states, the site visits gave more insight into the damage present on the structure, helped with the documentation for their records, and even assisted in pushing for repair on structures. Other site visits were for the team to decide if beam specimens would be viable for testing. Two of these occurred in Massachusetts where the research team went on site to photograph and scan the corroded beam ends to document the corrosion. For

these cases, the beams ultimately were not chosen for testing due to their similarity to previous tests or their excessive damage.

4.3. Beam Specimen Documentation and Testing Rig

For the specimens that were received by the New England States, many reports included the steel beam shapes of the beam specimens being received by the University of Massachusetts Amherst. If they were not included in the inspection reports, the information was given by the individual states. This documentation was done as a baseline check of the beam specimens being delivered but also for the researchers to check against with their own laboratory measurements.

Once delivered to the university, the research team took measurements to compare to the documentation provided by the states. This was a check performed as there are instances where the beams on a bridge structure do not match the as-built drawing callouts. Additionally, these initial measurements were important for selecting the correct arrangement of the structural testing rig. The outline of this process can be found in the flowchart in Figure 38 below.

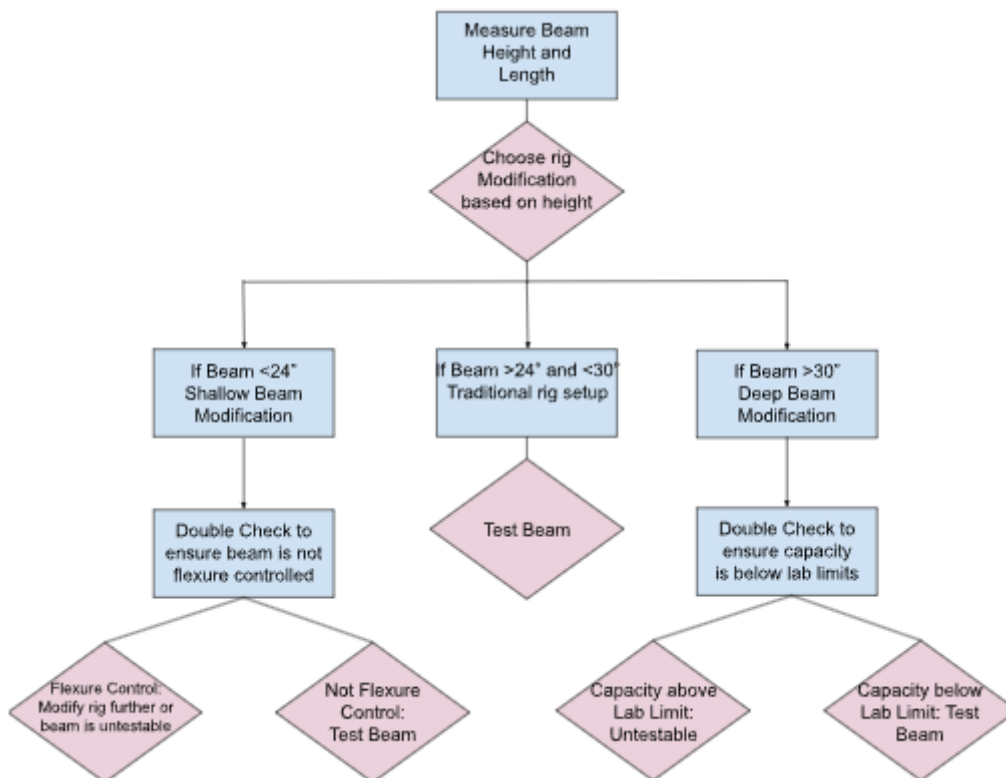


Figure 38. Structural Rig Flow Chart

The outcome of the flow chart above would determine if the original structural testing rig needed modification. The original rig components were designed for the corroded beam

ends project conducted by Tzortzinis in [28]. In this project, the corroded specimens were loaded from the top of the beam specimen [28]. This rig was then modified which allowed for a higher loading to be applied via direct loading/shear application. Corroded beams specimens are loaded from the bottom at the corroded end. This is to ensure that a shear failure mode and the true capacity of the end is reached and that undesirable failure modes, such as flexure, are avoided. Additionally, there are C-channels which were welded to threaded rods connected to W12x40s which stand vertically along the length of the beam. These C-channels have an attached low friction plastic attached to the outside of their webs. Ultimately, these channels face the beam with the plastic almost touching the edge of the top flange. This is to ensure bracing to prevent lateral torsional buckling modes and the beam from dangerously falling out of the testing rig while also allowing for ease of vertical movement for the beam specimen. The back support was a steel plate that rested on the 100 kip load cell. Both the crossbeam and the corroded end were grouted on the flange, this was to ensure continuity in the loading process and a flat, leveled loading surface as to not introduce eccentricity. A key component that was utilized in the first two experiments was a roller support under the corroded end, courtesy of MassDOT. For the modifications made for the larger beam specimens from Maine (experiments three through twelve), the roller had to be removed. The corroded end in experiments three through twelve sat directly on the load beam above the hydraulic rams. The hydraulic rams had caps that allowed for movement to mimic a roller when the MassDOT roller was not utilized. Below the beam specimen, two linear string potentiometers were used for displacement measuring in the loading process, one located close to the area of loading, and one located below the crossbeam. A rack of six linear rod potentiometers was also utilized in the experiments. This rack was placed so the potentiometers could measure the out of plane web displacement along the height of the web throughout the loading process until buckling occurred. The base rig used for this project is shown below in Figure 39 and Figure 40.

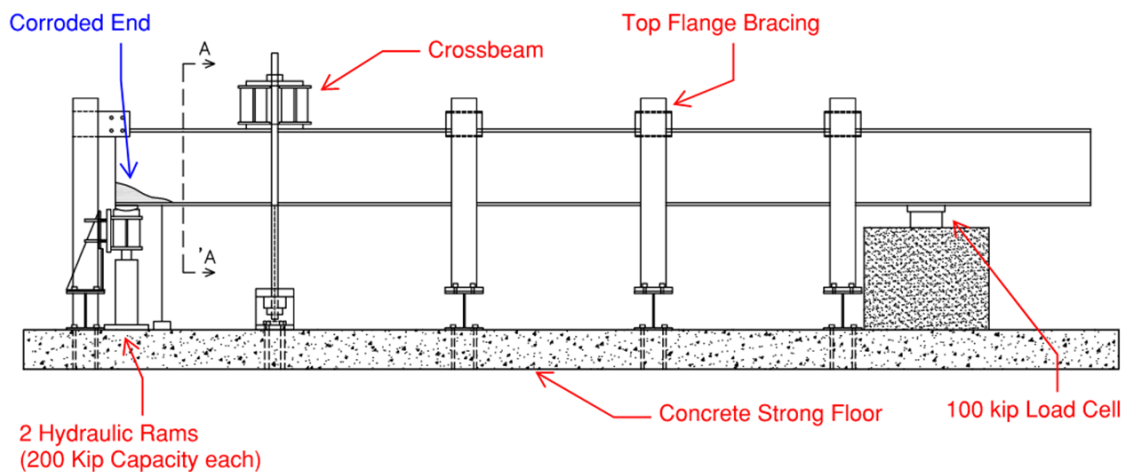


Figure 39. Structural Rig

The load beam above the hydraulic rams is a W10x77 with 4-1/2"x1/2" stiffener plates. The crossbeam is composed of two W12x58 with three 12"x18"x1-1/2" plates on the top and bottom and 4"x 1/4" plates used for stiffeners. There are two threaded rods connecting the crossbeam to anchor blocks in the strong floor. The anchor blocks are composed of a 16"x12"x2-1/2" top plate, a 16"x12"x1-1/2" bottom plate, 1-1/2" thick side plates.

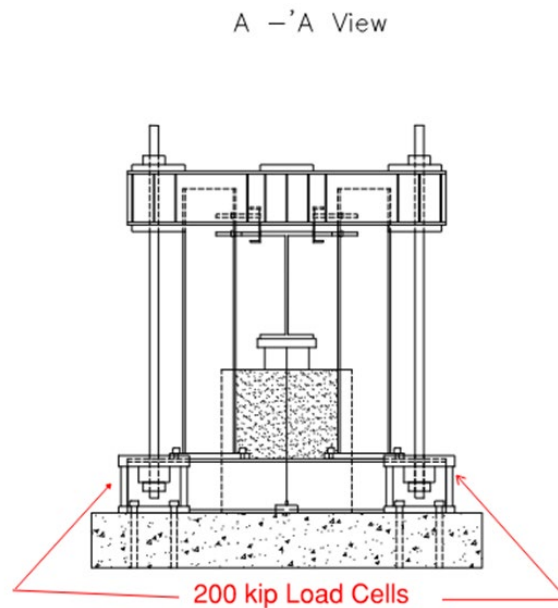


Figure 40. Structural Rig A-A View

The following instrumentation was used during the experiments for recording data:

- 6: 3.937 inch Linear Rod Potentiometers (TR-0100 by Novotechnik)
- 2: 10 inch Linear Motion Transducer String Potentiometers (Ametek P-10A)
- 2: 200 kip Omega Load Cells at Crossbeam (Omega LC8400-213-200k)
- 1: 100 kip Load Cell at Back of Beam (Lebow 3176-100k)
- 1: 10 kip Pressure Transducer (THE Honeywell)

4.4. Beams Prioritized for Testing

Beams that were visually viable for testing moved into the next phase of the process. This phase would include removing bearing plates if present on the beam and removing rust and paint on the web specifically at the tested beam end. This allowed the researchers to analyse the true section loss exhibited on the corroded end.

Each beam specimen was cleaned on the web of the specimen to remove rust, paint, and other debris. Additional cleaning with a hammer or paint chipping tool was needed in some cases to remove pack rust. The descaling was performed by the researchers and maintenance crews from the University of Massachusetts Amherst. The tools utilized and descaling processes were thoroughly investigated and overseen by the Environmental Health and Safety office of the University of Massachusetts Amherst. Appropriate personal protection equipment (PPE) was worn when operating the machinery which included a PAPR Respirator and shield, safety goggles, gloves, and proper protective footwear and clothing. The main tool used for descaling was a Model 40 DESCO Needle gun with a Dominator 6-gallon ULPA Filter vacuum. This equipment used pressurized air to push steel needles onto the surface of an object to clean off the debris. The DESCO was regularly checked for bag cleaning and, when in operation, for a specific operating pressure set on the attached air compressor to make sure the tool was used in the ideal range for cleaning and not too high as to induce tool damage.

4.5. Beams Selected as Untestable

There were several beams received from different states in our inventory that could not be tested. It was our goal to limit the number of beams that had to be discarded and deemed untestable. The main two criteria that lead to a beam being flagged as untestable were due to limited damage or extreme damage. These two criteria are explained at length below.

4.5.1. Limited Damage Criterion

Beams that were flagged with the limited damage criterion were done via visual inspection. The beams that fell under this labelling exhibited little to no damage at the end. This would mean that the team may observe a different failure mode of the beam rather than a beam end failure. Thus, the beam end capacity would not accurately be captured. Additionally, the beams that we received that had limited beam end deterioration were often too strong, having a capacity too large to induce failure with our current equipment.



Figure 41. Limited Damage Steel Beams

4.5.2. Extreme Damage Criterion

Beams that were flagged with the extreme damage criterion were done via visual inspection. The beams that fell under this labelling exhibited excessive damage at the end. In many of these cases, the beams under this criterion could not be properly placed into the testing rig and were too damaged to accurately estimate residual capacity. This damage could have been due purely to environmental conditions, but in the case of Figure 42, the extreme corrosion was present then the beam end was destroyed in the demolition process. There are many other beam specimens that the research team investigated where one beam had two corroded ends. There are instances where one corroded end was deemed untestable, but the specimen was kept to test the other end which was deemed testable via our protocol. This was the case for many of the New Hampshire beam specimens received and pictured in Figure 43.

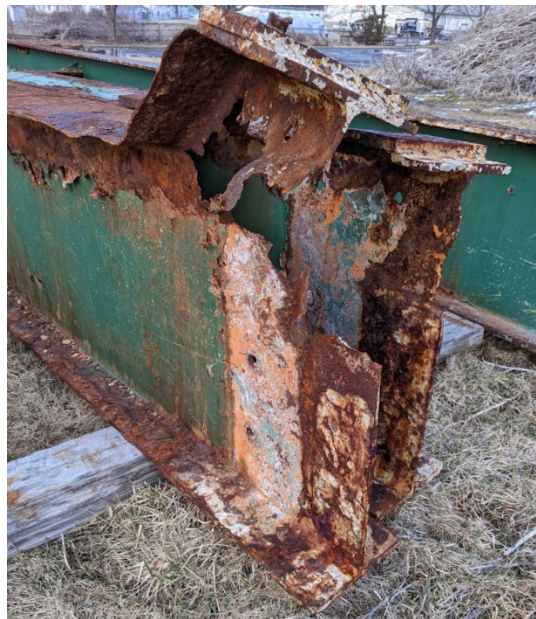


Figure 42. Extreme Damage Criterion, Vermont Beams



Figure 43. Extreme Damage Criterion, New Hampshire Beams

4.5.3. Final comments on untestable Specimens

It is important to note that these two criteria were originally established for a way to prioritize testing but ended up being used as a method for discarding the beams. It was the goal of the team to test all of the beams received. The beams chosen to be shipped to the University of Massachusetts were selected via the inspection reports. Since many of the inspection reports across the New England States vary in their documentation of deterioration, there were cases where the deterioration amounts and locations were not known to the research team until their arrival on site. The team then carried out rigorous calculations and inspection of the beams in question before ultimately deciding they were untestable. Additionally, it is important to note that there were many beams with significant damage present on many structures that were severely damaged in their removal. After receiving these beams, it was determined through inspection and long discussion that they were untestable via the extreme damage criterion.

4.6. Beam End Corrosion Documentation

4.6.1. State Methods of Inspection

As part of the project communications, the research team met with each of the state's departments of transportation to discuss the current state of practice regarding each state's methods. It was a major goal of the team to test current inspection methods, understand the challenges of inspectors, and introduce new methods for evaluating section loss on bridge girders.

A major topic of discussion was the challenges that are faced by bridge inspection teams. The main challenges that were the most prominent and immediately brought to our attention by the state departments of transportation were accessibility, debris/obstructions on or around the structure and its components, and measurement accuracy. As stated throughout, the major goal of this project was to evaluate current capacity evaluations among all the New England States, with the heaviest focus on the actual evaluation

equations. While this was still the focus, the research team felt it necessary to investigate solutions to challenges that inspectors have on site to fully encapsulate the goal.

The states that the team was able to meet with shared that their current methods of inspection heavily depend upon a combination of visual inspection and tools such as an ultrasonic thickness gauge, slide callipers, straight edges, and/or levels. With these tools comes great hurdles for inspectors due to measurement limitations, inaccuracy, and accessibility. For measuring web thickness in particular, ultrasonic thickness gauges and slide callipers are often used but are limited to one point measurement at a time, a need for an extremely clean measurement surface, and for the tools to be placed directly on points of interest. These tools make it very difficult to evaluate the entire corrosion profile and to measure major corrosion conditions like pitting.

Knowing the major challenges inspectors face with accessibility and current measurement tools, the team took the opportunity to utilize advanced technology and methods for section loss evaluation. Along with the use of the current tools listed above, the research team utilized 3D scanning technologies to evaluate the section loss of a corroded end. This section is dedicated to showing the culmination of section loss evaluation performed throughout the project.

4.6.2. Utilization of Existing Methods

For the first six experiments, the research team utilized the PocketMIKE ultrasonic thickness gauge for thickness measurements on the corroded end [50]. This tool, or an equivalent ultrasonic thickness d-meter, is typically utilized by inspectors for an on-site bridge inspection of corroded ends when a thickness reading is necessary. Following the cleaning of the corroded end, the team devised a grid on the web for measurements to be taken. This grid was constructed by attaching chicken wire via magnets and spray painting over it. While it is typical to take one or a few thickness measurements in the field, many of which are at the discretion of the inspector based on visual inspection rather than a prescribed location. The researchers took very thorough measurements, particularly at the base of the web where capacity is governed. A figure depicting this measurement grid can be seen below in Figure 44. The team found the PocketMIKE's reliability and accuracy very challenging even in a laboratory environment which prevented the team from getting accurate measurements in pitted regions. The use of LiDAR and 3D Scanning however, was able to accurately measure this phenomenon and the entire section loss observed at the beam end.



Figure 44. Measurement Grids

4.6.3. LiDAR and 3D Scanning Protocols

Experiments one through six were scanned using the RIEGL VZ2000 terrestrial LiDAR scanner [52, 53]. Because the terrestrial scanner remains stationary during the scanning process, the team had to utilize target points to align multiple scans. For the terrestrial scanner, target points were placed around the beam specimen in the lab. For these targets, the research team utilized a checkerboard pattern that could be easily placed around the beam specimen. Along with these reference points, the team could use points already present around the Brack Structural Testing Facility, such as a corner point on the steel testing rig. The alignment of point clouds followed the protocol that was devised by the research team and utilized methods of Tzortzinis in [29]. Using the open-source platform CloudCompare [51], these point clouds were aligned using the references above. Once aligned, the two sides of the corroded web can be compared, and a distance measurement can be calculated. Utilizing this data and codes designed by our research team in MATLAB, contour maps depicting the section loss of the beam end can be created. These contour maps were cross checked with measurements taken by the Pocket Mike ultrasonic thickness gauge to ensure an accurate representation of the corroded end [50]. The finalized contour was used as a representation of the section loss and was ultimately incorporated into the finite element simulations of the experiments via Python in the finite element analysis program ABAQUS [49].

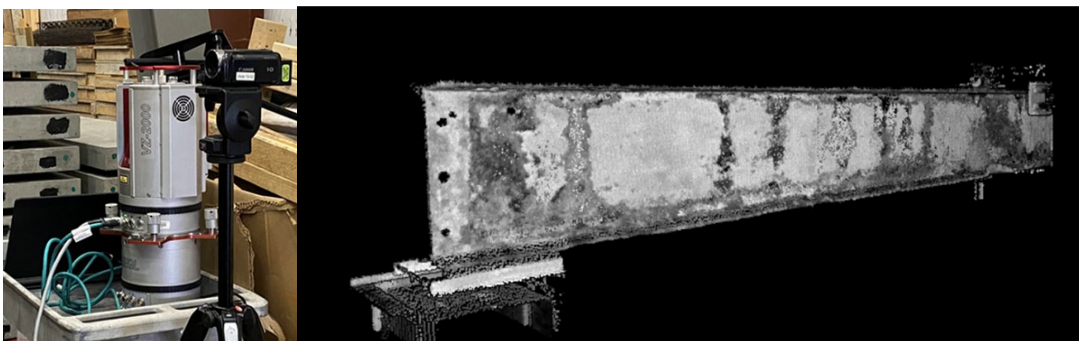


Figure 45. REIGL VZ-2000 Terrestrial Scanner and Corroded Beam Point Cloud

Experiments seven through twelve were scanned using the Artec LEO 3D Scanner. With this technology, target surfaces, lettering, magnetic spheres, were primarily used along with supplemental target checkerboards and lettering. Unlike the RIEGL Scanner, the Artec LEO encourages constant movement, and its small size allowed the research team to capture multiple types of scans. This included the two-sided scan like the RIEGL had done but also what the team refers to as “closed loop scans”, where both sides of the beam specimen are captured without the need of alignment. If scans were performed using a multiple scan, two-sided method, the team utilized its created methods of alignment using point picking and the auto-alignment features of Artec Studio [52]. The Artec Leo scanner with a sample scan using the sphere targets can be seen in Figure 46.



Figure 46. Artec Leo Scanner and sample scan with setup

4.7. Beam Dimensions

Each specimen had to be measured, particularly the corroded web. Using the provisions generated by Tzortzinis for MassDOT in [47], the average web thickness in the corroded region and the initial out of plane web deviation was determined. For the corroded web region, the average thickness was taken from point cloud data. Out of plane web deviation is very difficult to measure in practice; the research team utilized a combination of straight edges, calliper measurements, and laser levels to evaluate this measurement. This measurement was classified into the closest parameter for web deviation (i.e. 0.1, 0.5, or $1 t_{web}$). Additionally, the average thickness of the bottom flange was found via handheld measurement tools and point cloud measurements. These measurements can be found for each specimen in Table 47.

Table 47. Beam Specimen Measurements

State and Number (Experiment)	Average Web Thickness in CL x 4 inch area at base of web (MA Provisions)	Intact Web Thickness (Inches)	Average Thickness of bottom flange at corroded end (Inches)	Intact average flange Thickness (Inches)	Web Deviation (.1t_web, .5t_web, or 1t_web)	Beam Depth (inches)
CT 1 (Exp1)	0.43	0.51	0.54	0.765	0.5	20
CT 2 (Exp 2)	0.38	0.42	0.46	0.68	0.5	24
ME 1 (Exp 3)	0.46	0.58	0.73	0.88	0.1	33
ME 2 (Exp 4)	0.55	0.58	0.61	0.88	0.1	33
ME 3 (Exp 5)	0.51	0.58	0.68	0.88	0.1	33
ME 4 (Exp 6)	0.48	0.58	0.69	0.88	0.1	33
ME 5 (Exp 7)	0.45	0.58	0.62	0.88	0.1	33
ME 6 (Exp 8)	0.52	0.58	0.62	0.88	0.1	33
ME 7 (Exp 9)	0.50	0.58	0.71	0.88	0.1	33
ME 8 (Exp 10)	0.55	0.58	0.78	0.88	0.1	33
ME 9 (Exp 11)	0.56	0.58	0.71	0.88	0.1	33
ME 10 (Exp 12)	0.50	0.58	0.73	0.88	0.1	33

5. Finite Element Modeling

For each of the twelve experiments, finite element models were created to replicate the experiments performed in the laboratory testing portion of the project. The research team developed finite element models in correlation with work conducted by Tzortzinis in previous MassDOT projects on corroded ends [28]. The program used to model each of the beam specimens was ABAQUS. Each corrosion profile contour was created in MATLAB and was imported using in-house codes via Microsoft Excel and Python. The beam measurements used to create the model were based on lab measurements, inspection reports, and engineering judgement.

The beam components were all created using shell elements. These shell elements would be assigned thickness values pertaining to the thickness of the beam section, such as flange thickness and web thickness. For corroded sections, the levels of the corrosion contour maps would be used as the thickness inputs. All of the shell thicknesses use a middle surface assignment to avoid any possible unexpected problems with eccentric loading or displacement. Each model was composed of S3 and S4R shell elements to accommodate the nonuniformity of the corrosion patterns present at the beam end. These elements are typical shell elements, S3 is a three sided shell element while the S4R is a four sided shell element. The team performed mesh convergence for models of this type previously through models made in [28, 29].

The same material properties were assumed across all twelve experiments and simulations performed on the beam specimens. Based on the age of the structure and the beam type, the research team decided to use the steel properties found by Tzortzinis in [28]. The web was considered to be steel with a yield stress of 46 ksi and an ultimate stress of 64 ksi. The material properties for the flanges were considered to be steel with a yield stress of 38 ksi and an ultimate stress of 63.9 ksi. Both materials were assumed to be elastic with linear hardening.

The beam model contained several boundary conditions which pertained and were used to simulate the real conditions within the laboratory experiments. The back reaction was assumed to be a “pinned” reaction and the crossbeam and threaded rods were modeled as a spring. The spring stiffness was assumed to be 593.855 kip/in as a baseline from experiments conducted by Tzortzinis in [29] but was then tailored and fine-tuned (reduced or increased) based on experimental results if necessary. For the loaded end, the boundary conditions were selected to simulate a “roller” as the team felt it was the best representation of the roller support provided by MassDOT and could also simulate the load beam which was free to behave as a roller support when the MassDOT support was not used. Finally, the lateral torsional buckling supports were applied as constraints directly on the beam’s top flange in the locations for which they were present in the laboratory experiment. Additionally, it is important to note that experiments three through twelve all had plates attached as a bracing system for the bridge, these bolted/riveted plates were not considered in the simulation or the capacity estimation process as they were not attached to the flanges of the beam, spanned most of the web but not the entirety, and did not lie within the lengths for which average thickness was taken. While the plates’ presence here could influence the stiffness of the system, they would not add capacity to

the corroded end. A diagram of the finite element simulation model can be found in Figure 47.

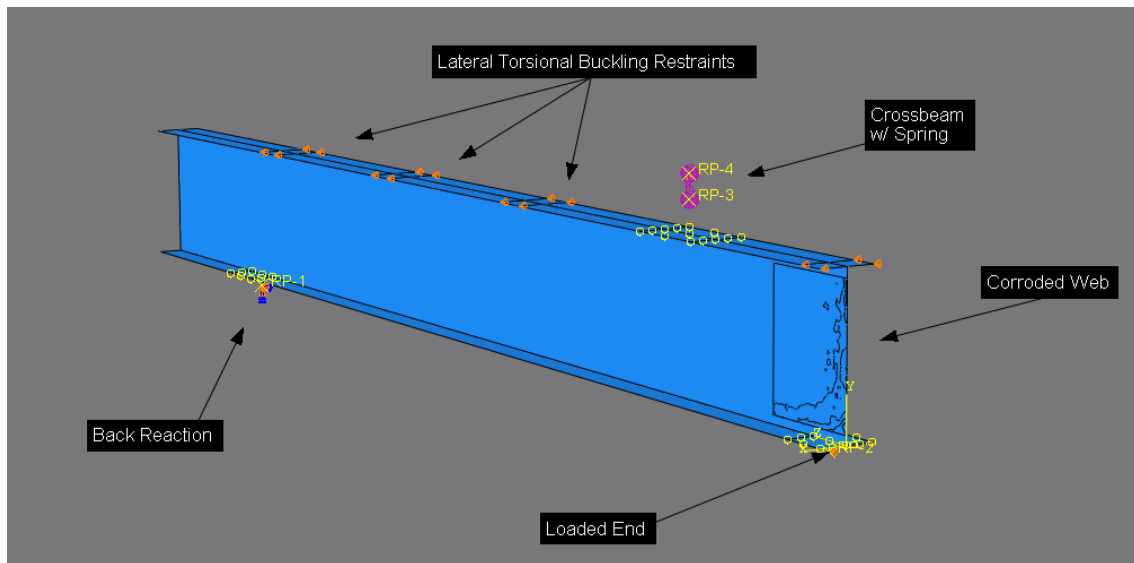


Figure 47. Finite Element Model

Each specimen had an eigenvalue analysis performed where the team could analyze the potential failure modes and what would be entered into the static model as an initial imperfection. The eigenmode chosen for this imperfection was based on two features: the failure mode of the beam and the measured initial web deviation of the beam. This initial web deviation was measured in accordance with Tzortzinis and MassDOT in [28,47]. The research team utilized a combination of straightedges, laser levels, and caliper measurements to accurately estimate the initial web deviation, or initial imperfection, present on the beam. This estimation and measurement ultimately guided the team as to what mode and how much deviation was implemented into the static analysis.

The static analysis was a two-step process, the first for the application of self-weight and the weight of the crossbeam, and the second for the loading to induce beam end buckling. The self-weight for each beam was assumed based on inspection reports, lab measurements of the beam geometry, and engineering judgement. A load for the crossbeam was also applied in this step. In the second step where the beam end was loaded until failure, a vertical displacement was applied to a reference point below the corroded end. This point was connected to the entire bearing surface below the corroded end, so the model distributed load in the same way as the laboratory tests.

There were many key assumptions made in the modelling of the beam specimens. The first key piece of the model is the contour maps used to describe the corrosion profile present on the beam. Contour maps have been used by the research team in previous projects with MassDOT to describe the remaining thickness of corroded ends; with this there is an assumption that each level of the remaining thickness contour map takes a particular value of “thickness” based on the bounds of the contour. Other key assumptions that were made in the modelling process were averaging flange thicknesses for beams that have varying thicknesses and averaging the corroded thickness of the flange in the area of the bearing. The intact flange measurements were based on lab measurements and

beam manual dimensions where the corroded flange sections were based on lab measurements and point cloud measurements.

The finite element models still require some fine-tuning adjustments, but the current models are considered for this report. The final versions of these models will be included and documented in papers outside of this report.

6. Laboratory Testing

All of the loading experiments were conducted in the Brack Structural Testing Facility at the University of Massachusetts Amherst. Each beam was checked and selected for testing based on the criteria highlighted in Section 4.5. Each specimen was loaded in the testing rig shown in Section 4.3 of this report. This testing rig would be modified based on the size and damage of each of the beams. To avoid multiple modifications, specimens with similar size and from the same bridge were tested in order. Planning and executing testing using this strategy was to limit the delay between tests to ensure the team could test as many specimens as possible in the project timeline.

In each of the twelve experiments conducted in this project, failure in the form of beam end web buckling was achieved through either web yielding or web crippling. This was expected via preliminary predictions of the research team and based on previous work done by Tzortzinis et. al. in the MassDOT project conducted in a similar way here at the University of Massachusetts Amherst [28]. Overall, the project's experiments were a success as the desired failure and true remaining capacity of the corroded end was achieved and captured.

The following section contains the details of each beam specimen tested. In total, twelve experiments were conducted, two beams from the state of Connecticut and ten from the state of Maine. Photos of the beams prior to testing were taken on each side of the corroded end. The section loss evaluation via 3D scanning is represented here by corrosion contour maps. For experimental results, there are photographs of the final buckled shape of the beam after load testing. Each specimen was loaded until beam end failure occurred in the specimen. It is important to note that the difference in results between the two linear string potentiometers placed below the beam specimen was used in calculating the displacement curve of the experiment and finite element analysis. The load-displacement curves for the experiments and the corresponding finite element simulations are present for each of the twelve specimens tested within this project.

6.1. Specimen 1

Specimen 1 was assumed to be a 20” deep American Standard from the 02929 bridge on Route 80 in Deep River, Connecticut. This beam type was assumed based on the structural drawings, our own in-lab measurements, and engineering judgment. The beam was used as an addition in efforts to rehabilitate the structure. It came from another structure before being placed on the 02929 bridge. The section loss profile was created using the RIEGL VZ-2000. This profile can be found in Table 48. The section loss profile was one that the research team had not observed before and had a semi-circular profile with heavy corrosion at mid-height. The corrosion length was taken to be 3 inches. The experimental capacity of the corroded end was 129.8 kips. The experimental and finite element load-displacement curves can be found in Table 49.

Table 48. Specimen 1 Corrosion Profile

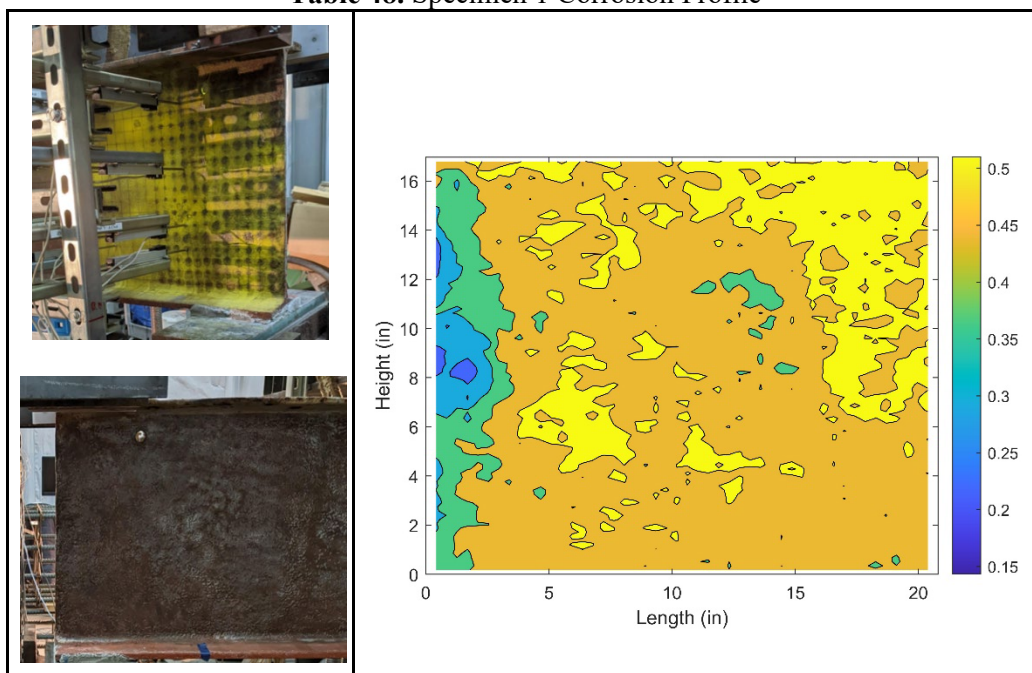
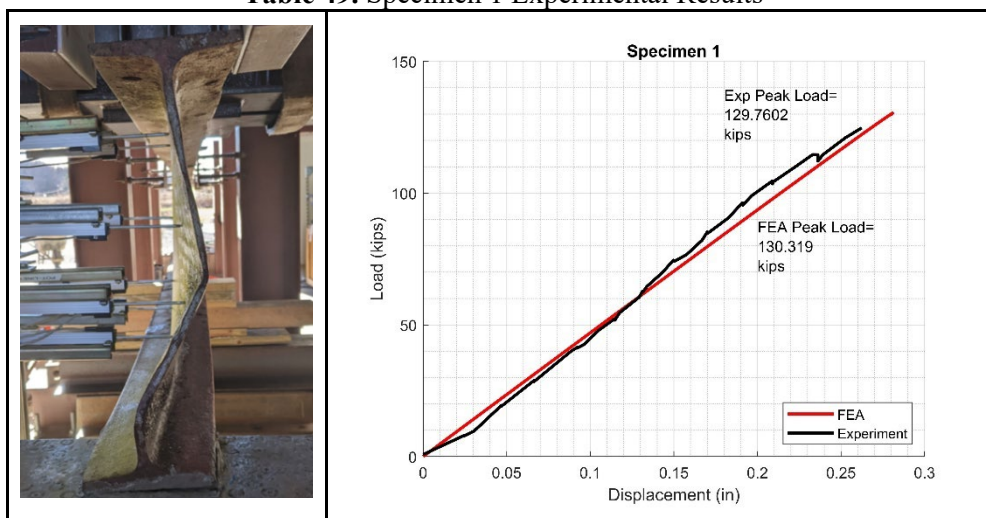


Table 49. Specimen 1 Experimental Results



6.2. Specimen 2

Specimen 2 was assumed to be a 24” deep CB 241-19 from the 02929 bridge on Route 80 in Deep River, Connecticut. This beam type was assumed based on the structural drawings, our own in-lab measurements, and engineering judgment. The beam was used as an addition in efforts to rehabilitate the structure. It came from another structure before being placed on the 02929 bridge. The section loss profile shown in Table 50 was created using the RIEGL VZ-2000. The corrosion length was taken to be 11.8 inches. The experimental capacity of the corroded end was 113.3 kips. One can observe in the experimental loading a sudden jump down in displacement at around 90 kips applied, this is likely due to settling in the system during a loading pause and slipping of the string potentiometers which were hooked below the specimen. The experimental and finite element load-displacement curves can be found in Table 51.

Table 50. Specimen 2 Corrosion Profile

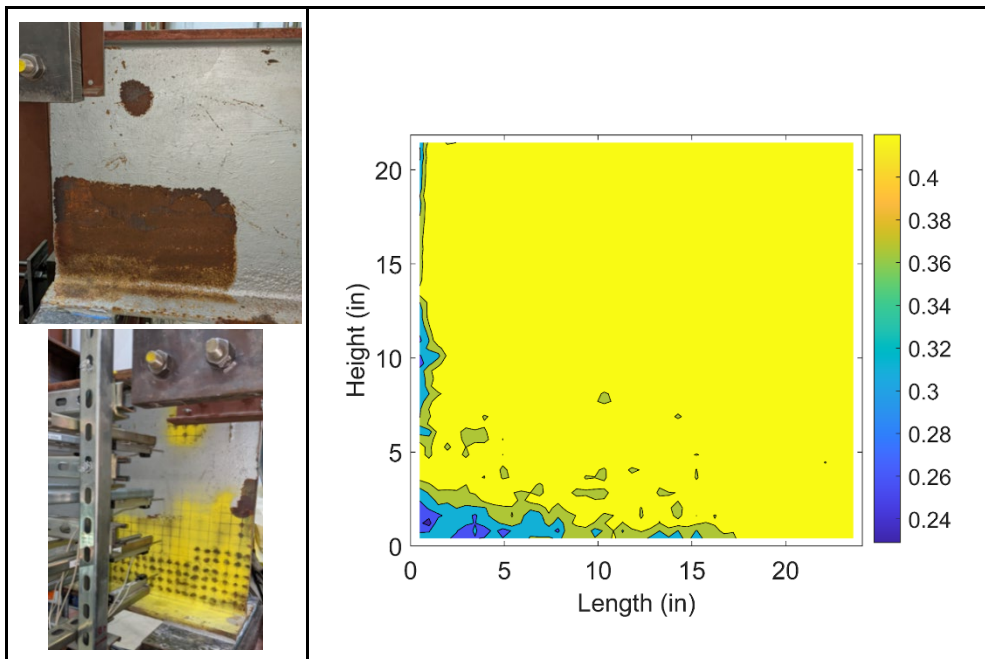
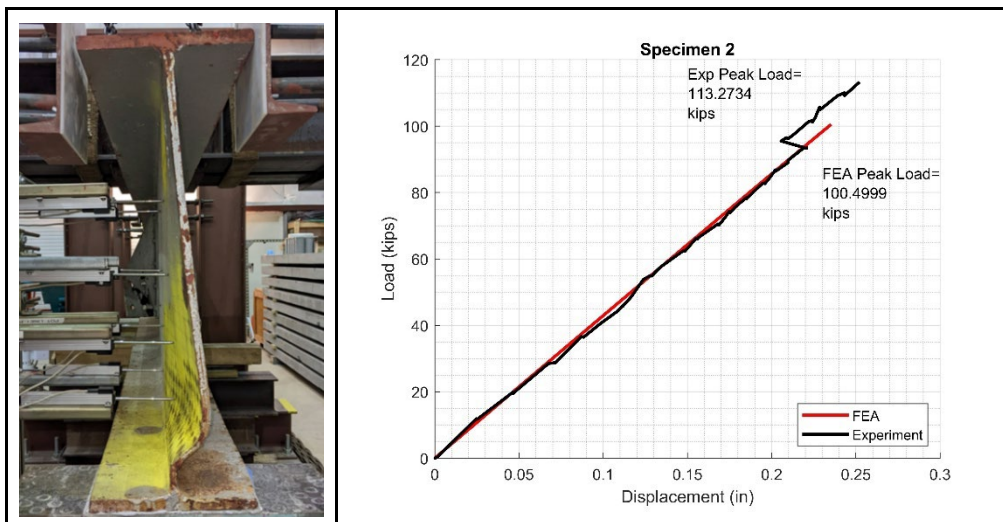


Table 51. Specimen 2 Experimental Results



6.3. Specimen 3

Specimen 3 was assumed to be a B33x132 from the 3801 bridge in Jay, Maine. This beam type was assumed based on the structural drawings, our own in-lab measurements, and engineering judgment. The section loss profile shown in Table 52 was created using the RIEGL VZ-2000. The corrosion length was taken to be 13.315 inches. The experimental capacity of the corroded end was 199.8 kips. The experimental and finite element load-displacement curves can be found in Table 53.

Table 52. Specimen 3 Corrosion Profile

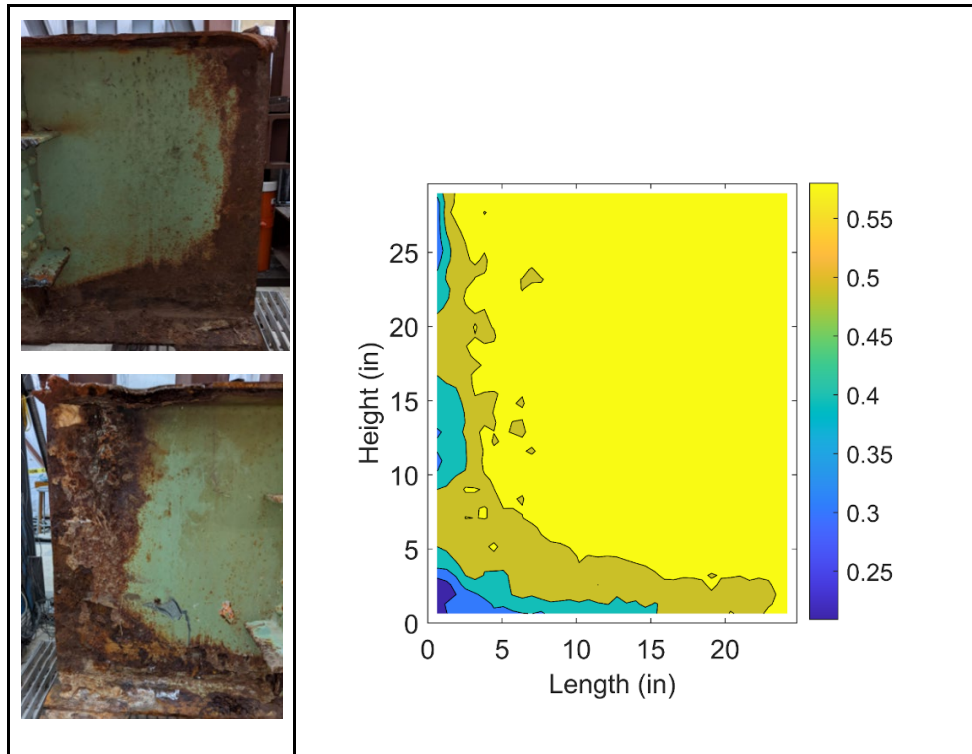
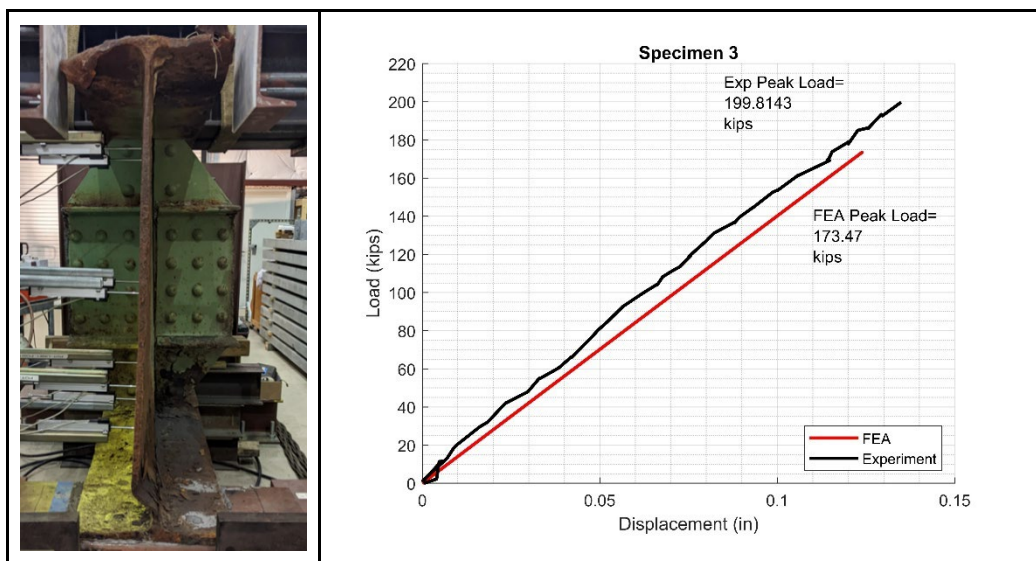


Table 53. Specimen 3 Experimental Results



6.4. Specimen 4

Specimen 4 was assumed to be a B33x132 from the 3801 bridge in Jay, Maine. This beam type was assumed based on the structural drawings, our own in-lab measurements, and engineering judgment. The section loss profile shown in Table 54 was created using the RIEGL VZ-2000. The corrosion length was taken to be 13.315 inches. The experimental capacity of the corroded end was 284.5 kips. The experimental and finite element load-displacement curves can be found in Table 55.

Table 54. Specimen 4 Corrosion Profile

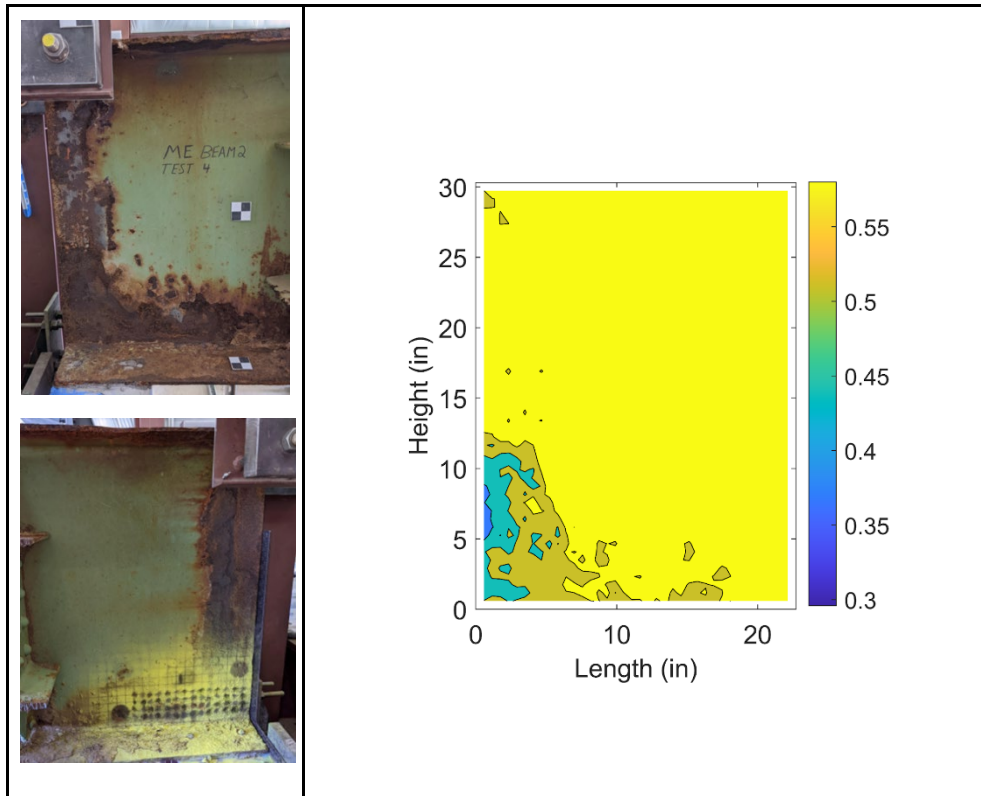
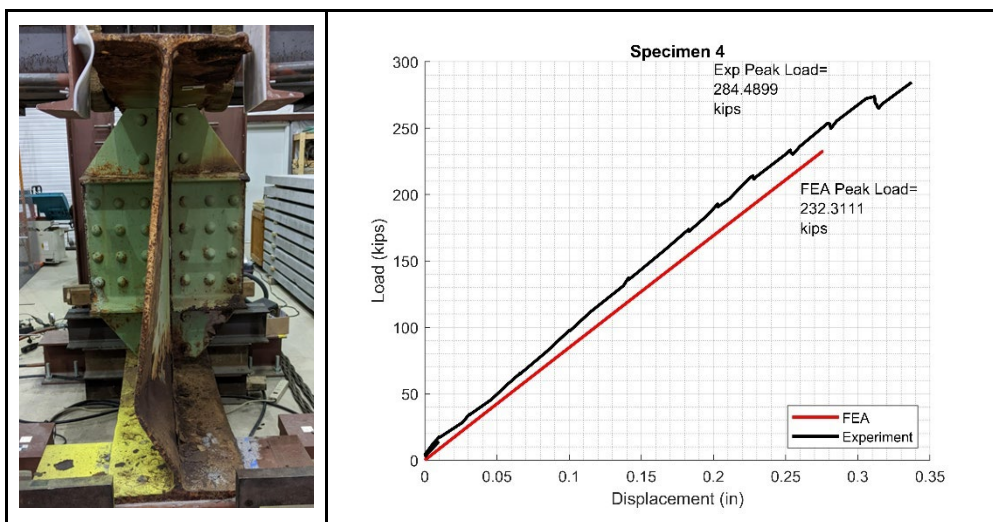


Table 55. Specimen 4 Experimental Results



6.5. Specimen 5

Specimen 5 was assumed to be a B33x132 from the 3801 bridge in Jay, Maine. This beam type was assumed based on the structural drawings, our own in-lab measurements, and engineering judgment. The section loss profile shown in Table 56 was created using the RIEGL VZ-2000. The corrosion length was taken to be 11 inches. The experimental capacity of the corroded end was 224.1 kips. The experimental and finite element load-displacement curves can be found in Table 57.

Table 56. Specimen 5 Corrosion Profile

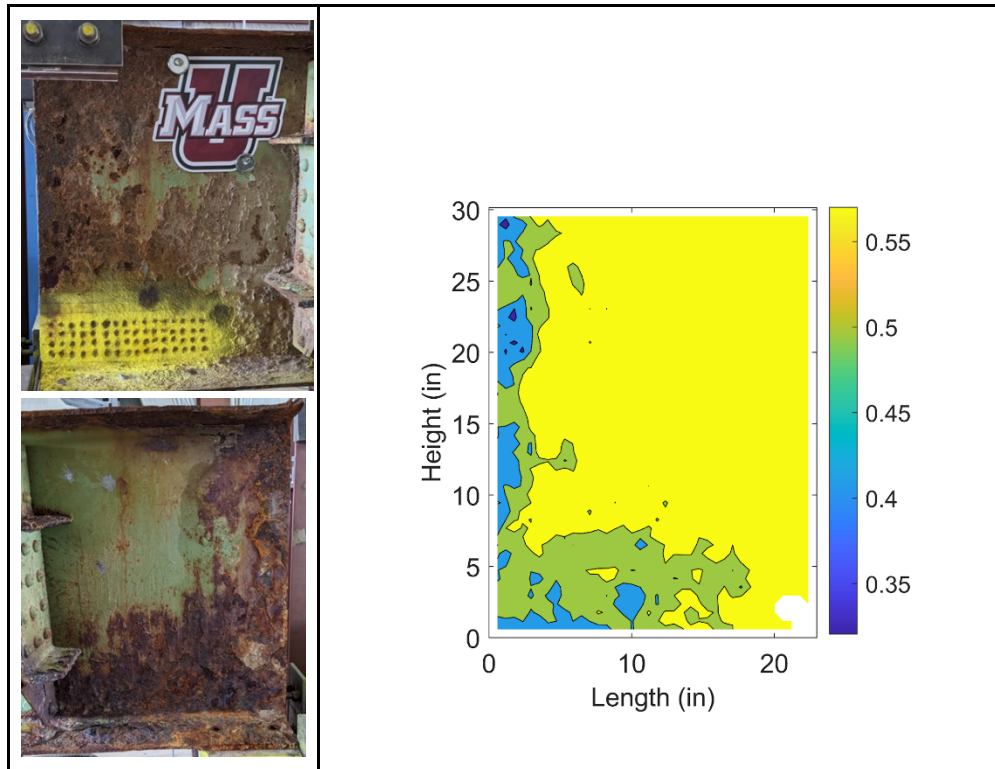
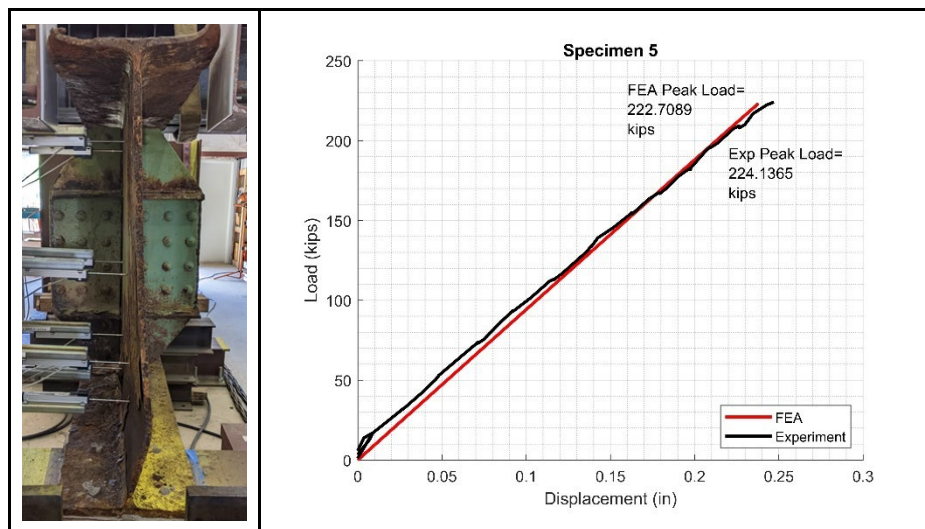


Table 57. Specimen 5 Experimental Results



6.6. Specimen 6

Specimen 6 was assumed to be a B33x132 from the 3801 bridge in Jay, Maine. This beam type was assumed based on the structural drawings, our own in-lab measurements, and engineering judgment. The section loss profile shown in Table 58 was created using the RIEGL VZ-2000. The corrosion length was taken to be 12 inches. The experimental capacity of the corroded end was 211.1 kips. One can observe in the experimental loading a sudden jump down in displacement at around 10 kips applied, this is likely due to settling in the system during an initial loading pause. The experimental and finite element load-displacement curves can be found in Table 59.

Table 58. Specimen 6 Corrosion Profile

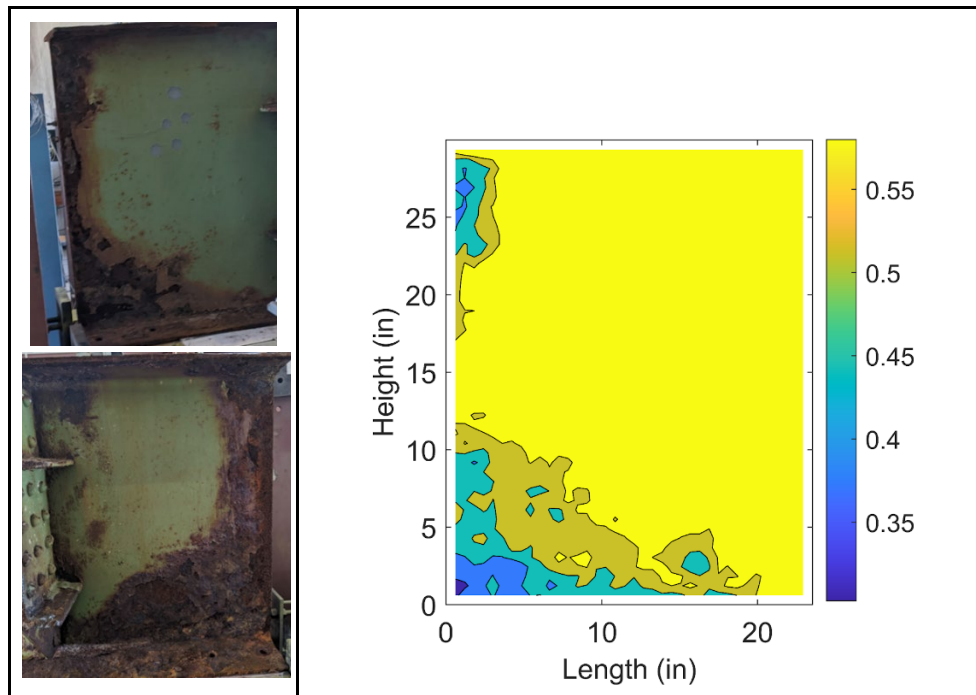
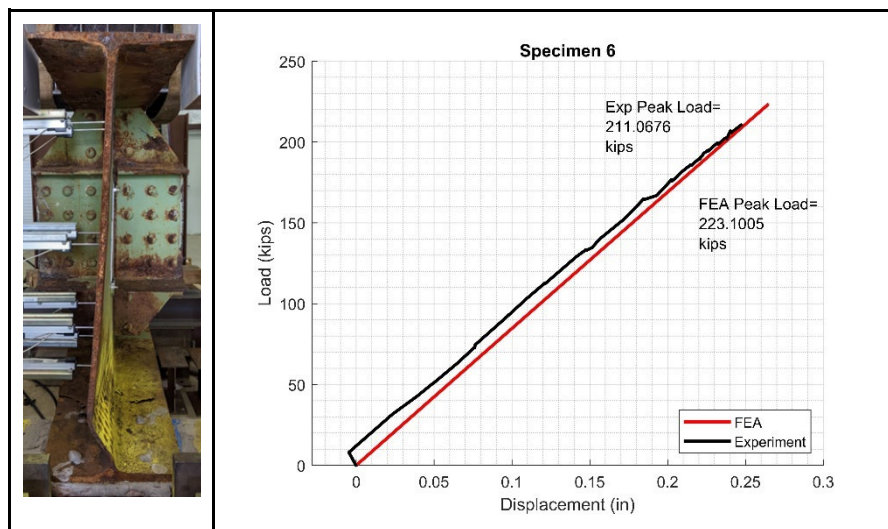


Table 59. Specimen 6 Experimental Results



6.7. Specimen 7

Specimen 7 was assumed to be a B33x132 from the 3801 bridge in Jay, Maine. This beam type was assumed based on the structural drawings, our own in-lab measurements, and engineering judgment. The section loss profile shown in Table 60 was created using the Artec Leo. The corrosion length was taken to be 13.315 inches. The experimental capacity of the corroded end was 230.1 kips. The experimental and finite element load-displacement curves can be found in Table 61.

Table 60. Specimen 7 Corrosion Profile

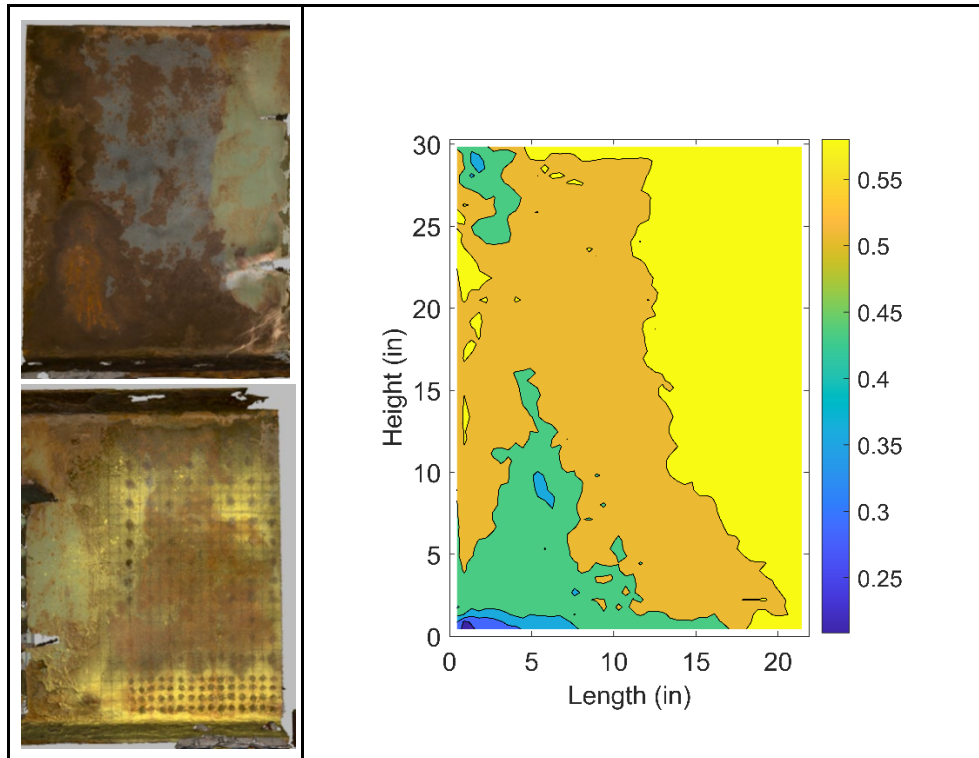
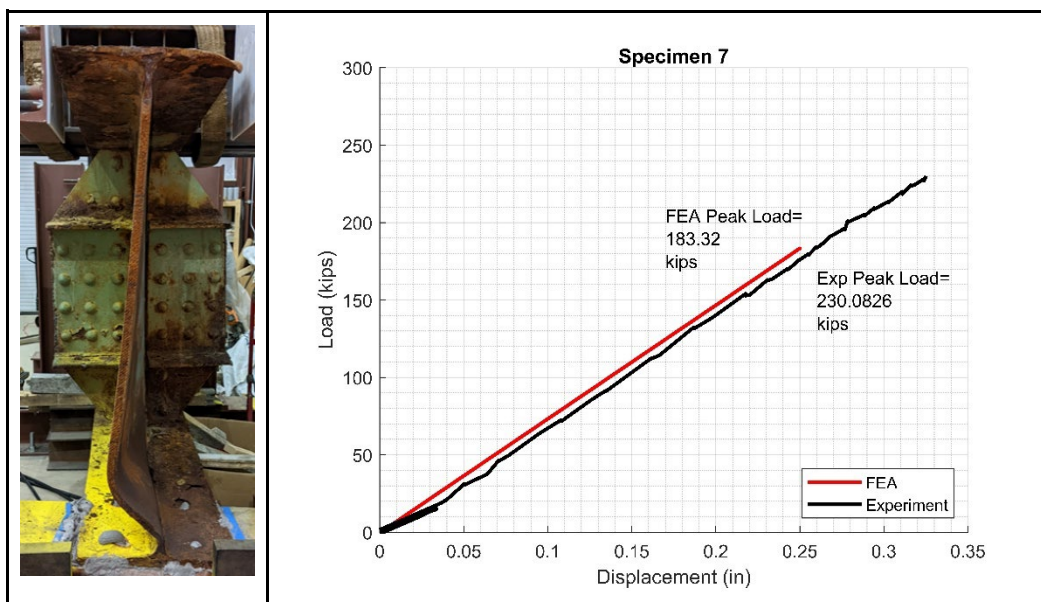


Table 61. Specimen 7 Experimental Results



6.8. Specimen 8

Specimen 8 was assumed to be a B33x132 from the 3801 bridge in Jay, Maine. This beam type was assumed based on the structural drawings, our own in-lab measurements, and engineering judgment. The section loss profile shown in Table 62 was created using the Artec Leo. The corrosion length was taken to be 11.39 inches. The experimental capacity of the corroded end was 253.2 kips. The experimental and finite element load-displacement curves can be found in Table 63.

Table 62. Specimen 8 Corrosion Profile

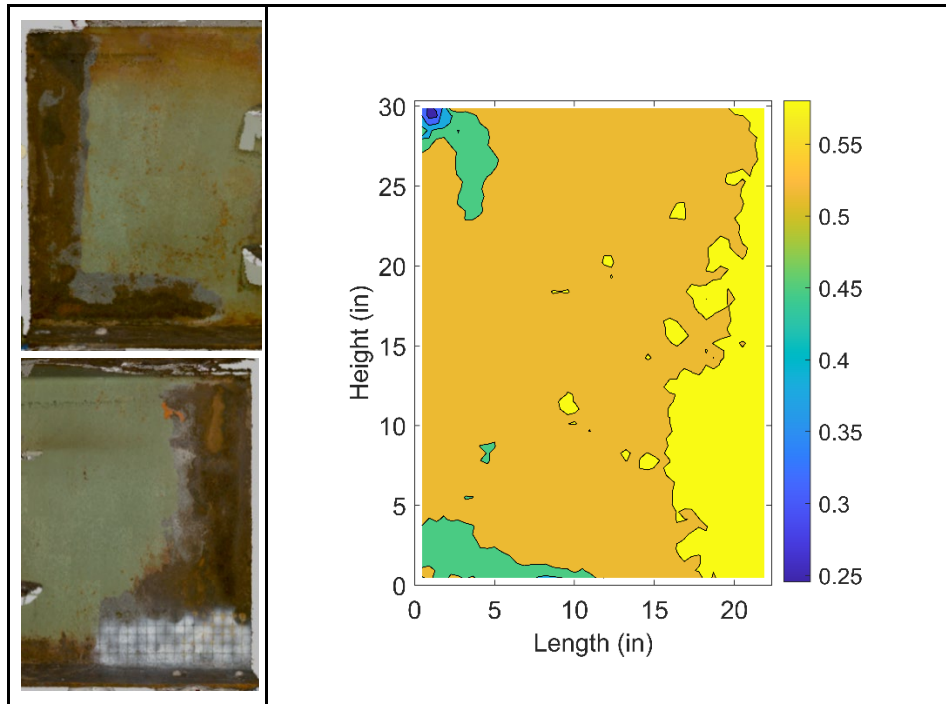
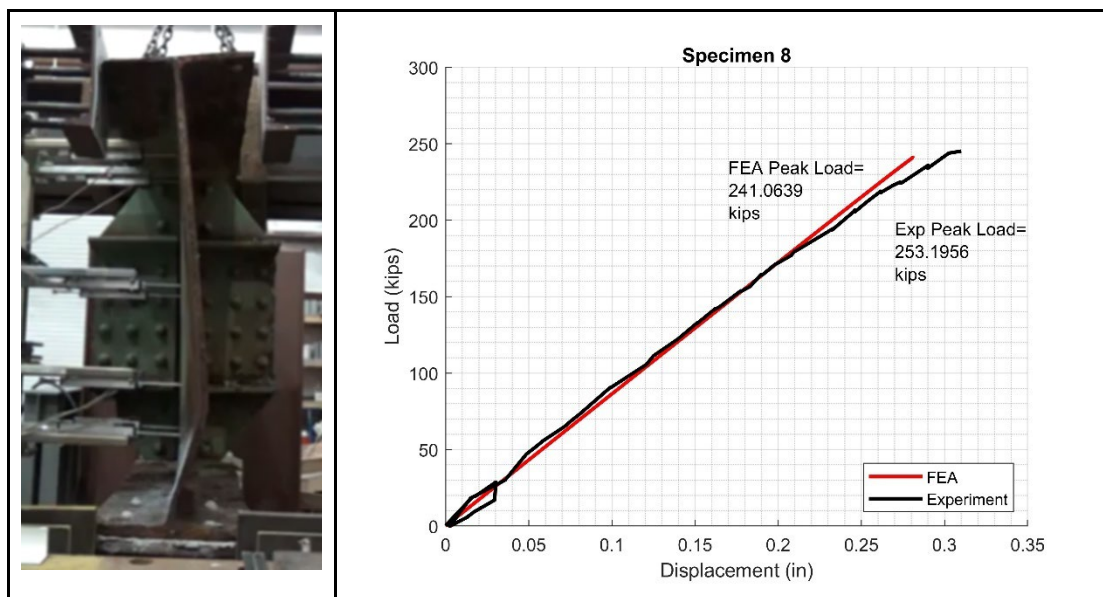


Table 63. Specimen 8 Experimental Results



6.9. Specimen 9

Specimen 9 was assumed to be a B33x132 from the 3801 bridge in Jay, Maine. This beam type was assumed based on the structural drawings, our own in-lab measurements, and engineering judgment. The section loss profile shown in Table 64 was created using the Artec Leo. The corrosion length was taken to be 13.315 inches. The experimental capacity of the corroded end was 257.3 kips. The experimental and finite element load-displacement curves can be found in Table 65.

Table 64. Specimen 9 Corrosion Profile

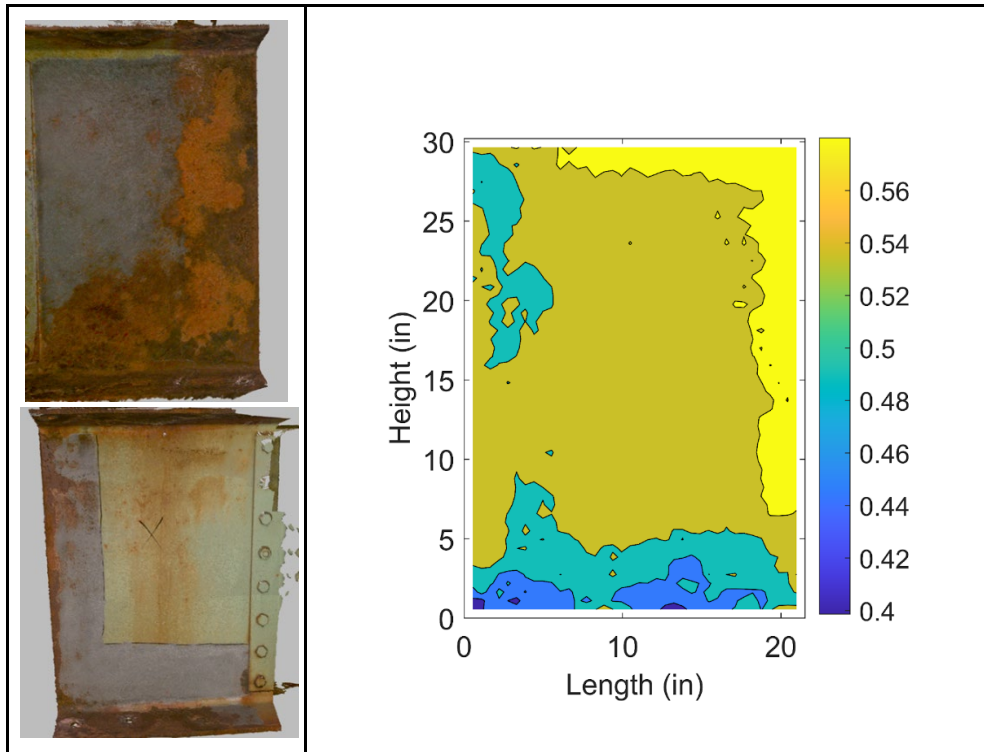
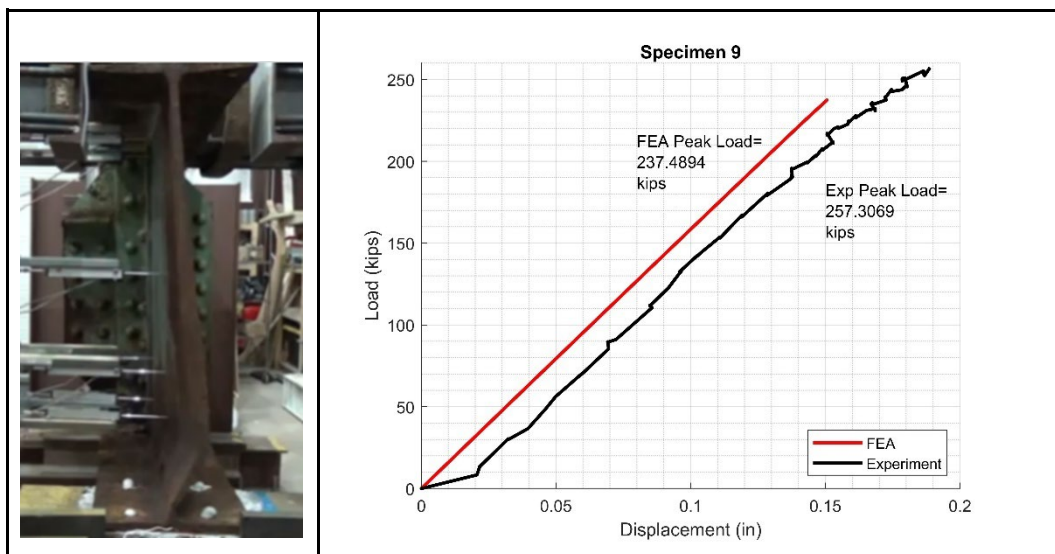


Table 65. Specimen 9 Experimental Results



6.10. Specimen 10

Specimen 10 was assumed to be a B33x132 from the 3801 bridge in Jay, Maine. This beam type was assumed based on the structural drawings, our own in-lab measurements, and engineering judgment. The section loss profile shown in Table 66 was created using the Artec Leo. The corrosion length was taken to be 13.315 inches. The experimental capacity of the corroded end was 297.6 kips. The experimental and finite element load-displacement curves can be found in Table 67.

Table 66. Specimen 10 Corrosion Profile

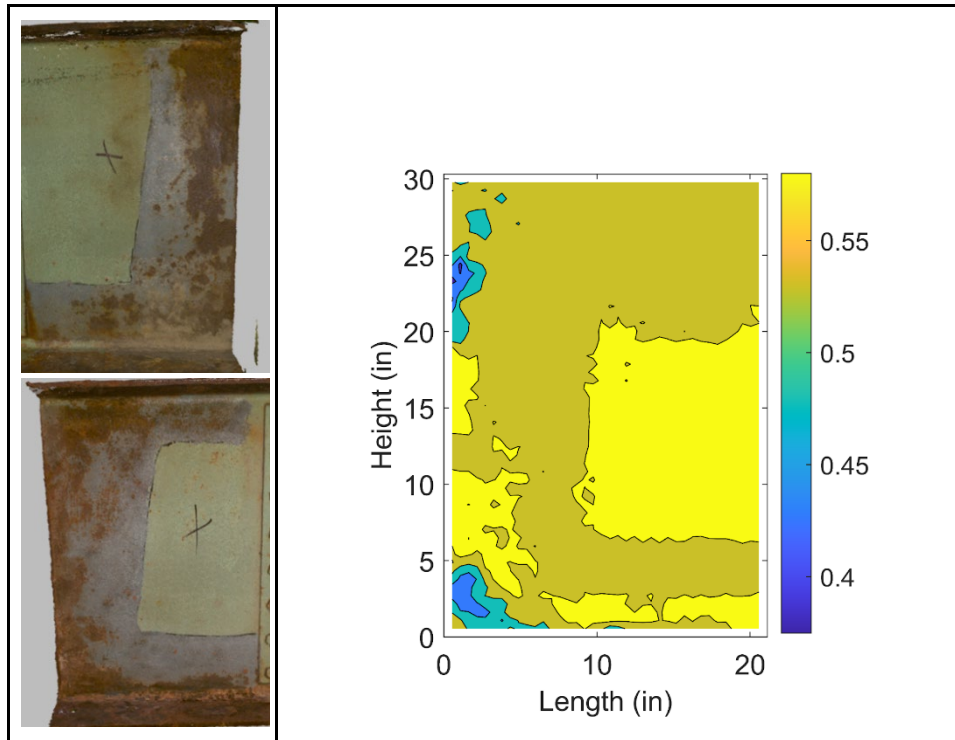
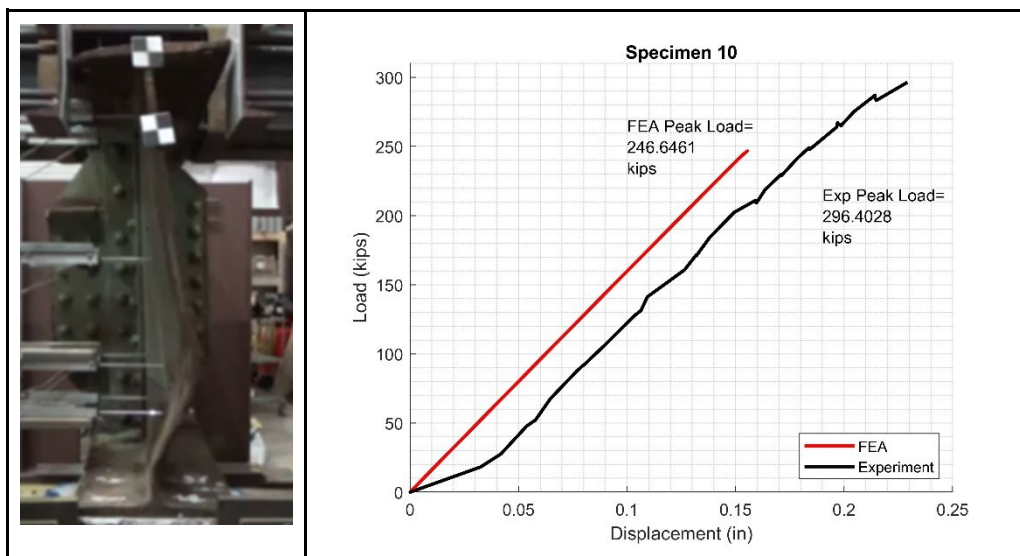


Table 67. Specimen 10 Experimental Results



6.11. Specimen 11

Specimen 11 was assumed to be a B33x132 from the 3801 bridge in Jay, Maine. This beam type was assumed based on the structural drawings, our own in-lab measurements, and engineering judgment. The section loss profile shown in Table 68 was created using the Artec Leo. It is important to note there was a calibration error that occurred in one of the linear string potentiometers for displacement measurements, so this specimen only considers displacement closest to the crossbeam and not the difference between the two linear displacement measurements. The experimental capacity of the corroded end was 267.1 kips. The experimental and finite element load-displacement curves can be found in Table 69.

Table 68. Specimen 11 Corrosion Profile

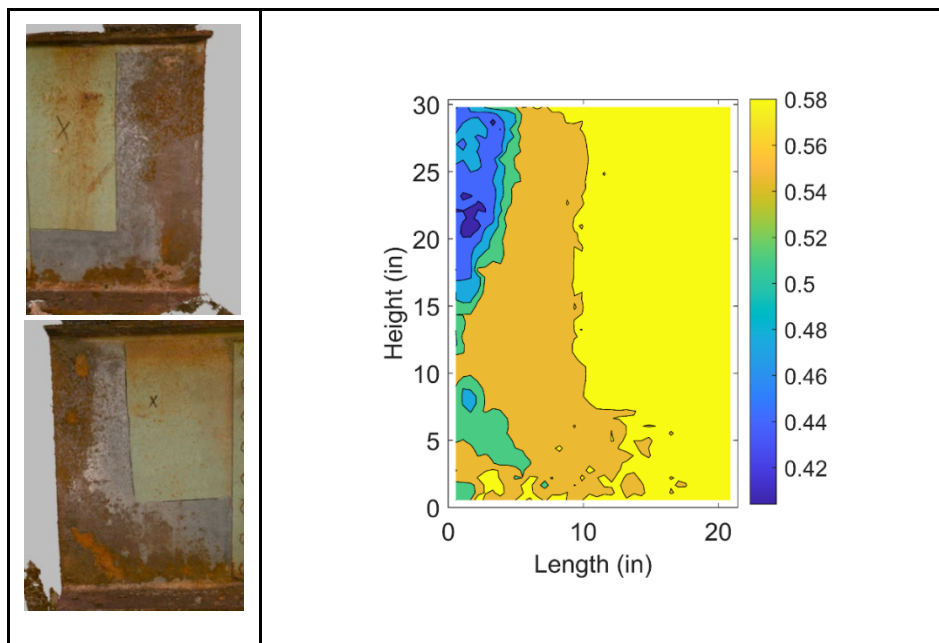
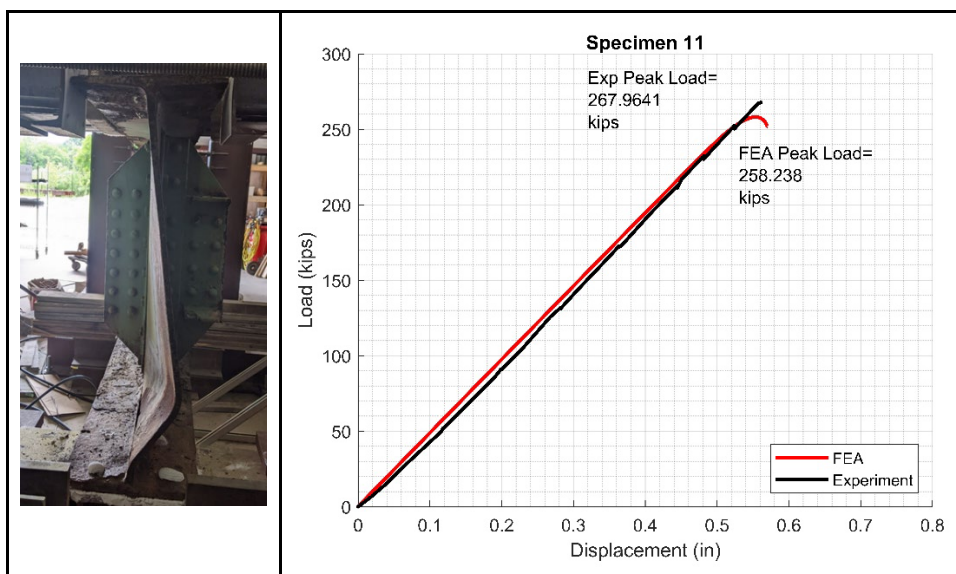


Table 69. Specimen 11 Experimental Results



6.12. Specimen 12

Specimen 12 was assumed to be a B33x132 from the 3801 bridge in Jay, Maine. This beam type was assumed based on the structural drawings, our own in-lab measurements, and engineering judgment. The section loss profile was created using the Artec Leo and can be found in Table 70. The corrosion length was taken to be 13.315 inches. The experimental capacity of the corroded end was 232.3 kips. The experimental and finite element load-displacement curves can be found in Table 71. It is important to note there was a calibration error that occurred in one of the linear string potentiometers for displacement measurements, so this specimen only considers displacement closest to the beam end and not the difference between the two linear displacement measurements.

Table 70. Specimen 12 Corrosion Profile

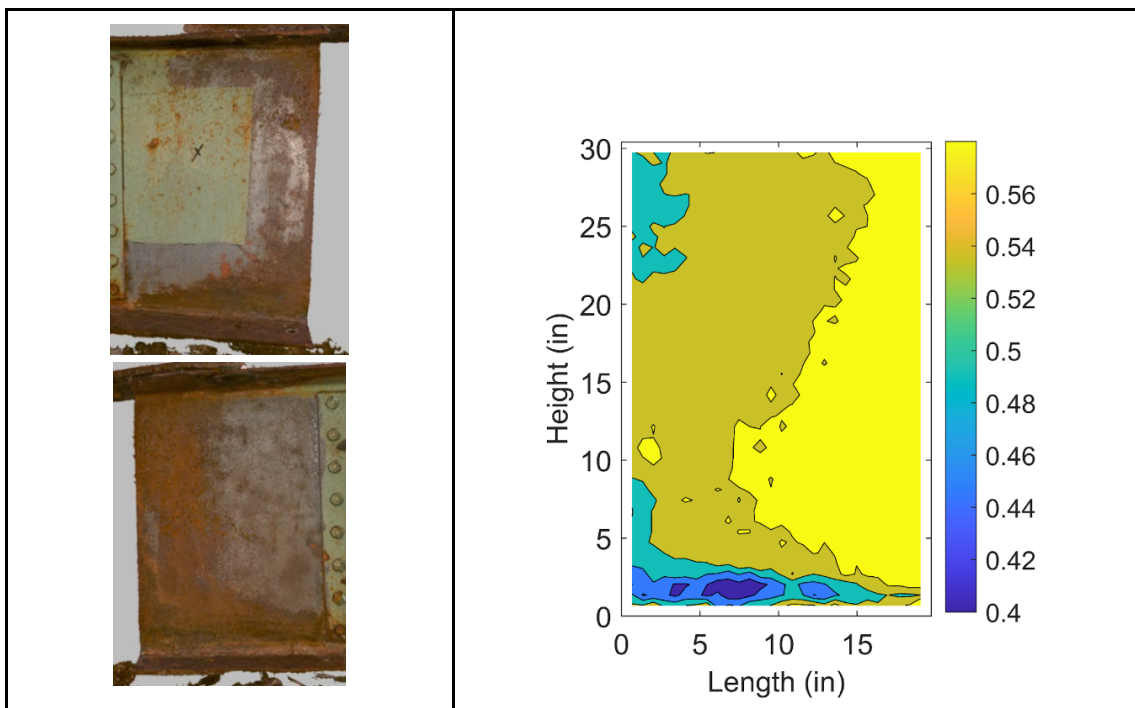
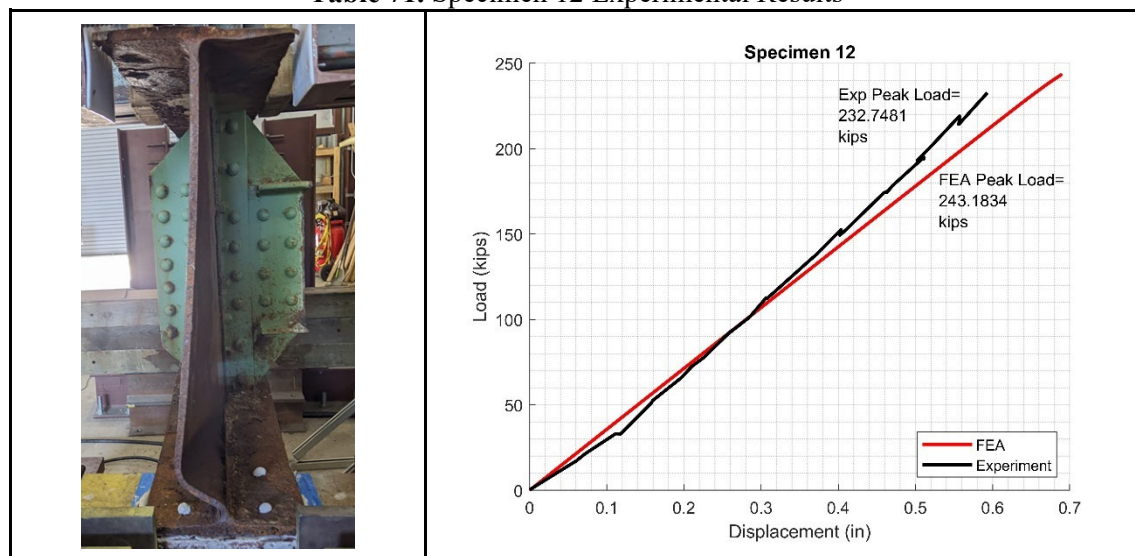


Table 71. Specimen 12 Experimental Results



7. Data Results and Discussion

7.1. Experimental and Finite Element Capacities

All the peak loads achieved in the experiments and finite element simulations can be found in Table 72. Buckling failure at the corroded end was achieved in each experiment and was achieved in the finite element simulations. There are many cases where the peak loads achieved in the finite element analyses were reasonably close to the predicted and the resulting capacities found in the experiments. There were some discrepancies between the experimental and simulated results particularly at the beginning of the loading process; the team attributes this to being from the settlement and closing of any gaps in the system, particularly between supports. Following the onset of loading, one can see from the graphs that the stiffnesses of both the experimental and simulation systems aligned reasonably well with one another. We have found that material properties, most importantly the yield stress, likely contributes to a simulated underprediction of the experimental capacity. The research team found, based on all the assumptions made in the modelling process, that the resulting finite element peak loads were sufficient and credible.

Table 72. Summarized Experimental and Finite Element Capacities

State and Number (Experiment)	Yield Assumed (ksi)	Peak Experimental Loads (kips)	Peak Finite Element Analysis Loads (kips)	Percent Error
CT 1 (Exp1)	46	129.76	130.32	0.43 %
CT 2 (Exp 2)	46	113.27	100.50	12.71 %
ME 1 (Exp 3)	46	199.81	173.47	15.18 %
ME 2 (Exp 4)	46	284.48	232.31	22.46 %
ME 3 (Exp 5)	46	224.14	222.71	0.64 %
ME 4 (Exp 6)	46	211.06	223.10	5.40 %
ME 5 (Exp 7)	46	230.08	183.32	25.51 %
ME 6 (Exp 8)	46	253.196	241.06	5.03 %
ME 7 (Exp 9)	46	257.31	237.49	8.35 %
ME 8 (Exp 10)	46	296.4	246.65	20.17 %
ME 9 (Exp 11)	46	267.96	258.24	4.17 %
ME 10 (Exp 12)	46	232.32	243.18	4.47 %

It is important to note the other factors that could contribute to error in the case of experimental and finite element results. A major source of error in the experimental process was minor equipment errors in the experimental rig. There were cases in the experiments where string pots to measure the vertical displacement of the beam were dislodged from the beam specimen or reached their minimum length due to excessive displacement. Additionally, there were occasions where the data acquisition readings could have been skewed due to voltage and power issues due to outputs from the sensors.

The major source of error in the scanning process was due to beam cleaning. The beam specimens had to be cleaned rigorously but there were occasions where some very hard pack rust or minor surface level rust could not be removed. This can ultimately introduce minor error via scanning results and ultimately predictions and finite element results.

An additional source of error that could arise in the scanning process was in scan alignment. While closed-loop scanning can be utilized in the lab environment, it is often not as common in the field. For two-sided scanning, the minor errors from alignment can be heavily mitigated by visual and numerical inspection in cloud compare, or even thickness checkpoints found with other equipment such as an ultrasonic thickness gauge or slide calliper. Even considering these possible sources of error, the scanning methods of the research team provide data with higher accuracy than tools like the ultrasonic thickness gauge and can provide an entire corrosion profile as opposed to a point-by-point measurement or visual inspection method.

8. Analytical Procedures by State

To evaluate the analytical procedures of each New England state, the research team maintained strong communication with each of the departments of transportation. The team met with many of the New England States to investigate typical inspection and documentation methods for bridge structural evaluations. These meetings gave good insight into what is used to evaluate the capacity of individual components and ultimately load rate the entire structure. From here, the research team investigated the capacity estimation and load rating procedures provided by each state to compare them directly to the experiments conducted throughout the project. The equations and calculations of interest include each state's methods for determining the remaining capacity of a corroded end via the web local yielding and web local crippling failure criteria.

8.1.. CTDOT Provisions

The Connecticut provisions for evaluating the remaining capacity of corroded beam ends were provided via an Excel spreadsheet. In this spreadsheet, each beam specimen was entered with their baseline dimensions. Section losses were then applied to those base dimensions based on what was observed and calculated by the research team. Because this tool is used by CTDOT, there were no fundamental modifications made to the spreadsheet and the team used it as an inspector would but only with a focus on the unstiffened parameters. The equations used are in accordance with the BDS and MBE provisions, for unstiffened webs this is Appendix D6.5 of BDS specifically. The research team only considered the unfactored capacities as the results would be compared to other state procedures and the real experimental tests. An example of the spreadsheet pages used from CTDOT are found in Figure 48 below.

Beam End Identification			System		Condition		Member Properties (kip, in)										Section Loss (%)			Code
Span	Member	Support	ψ_c	ψ_e	E	F_{yw}	D	t_w	t_f	K	L_{cw}	N	SL_w	SL_f	SL_e	Override				
1	ct1	1	1	1	29000	36	20	0.51	0.765	1.629	3.5	7	7.84%	29.67%	13.93%					
2	ct2	2	1	1	29000	36	24	0.42	0.68	1.263	3.5	7	9.62%	20.24%	10.89%					
3	me1	3	1	1	29000	36	33.15	0.58	0.88	1.808	5	10	20.48%	16.75%	8.15%					
4	me2	4	1	1	29000	36	33.15	0.58	0.88	1.808	5	10	4.83%	30.48%	14.83%					
5	me3	5	1	1	29000	36	33.15	0.58	0.88	1.808	5	10	10.03%	22.50%	10.50%					
6	me4	6	1	1	29000	36	33.15	0.58	0.88	1.808	5	10	14.71%	21.70%	10.56%					
7	me5	7	1	1	29000	36	33.15	0.58	0.88	1.808	5	10	13.78%	29.20%	14.21%					
8	me6	8	1	1	29000	36	33.15	0.58	0.88	1.808	5	10	8.02%	29.43%	14.33%					
9	me7	9	1	1	29000	36	33.15	0.58	0.88	1.808	5	10	14.53%	19.77%	9.62%					
10	me8	10	1	1	29000	36	33.15	0.58	0.88	1.808	5	10	4.81%	11.82%	5.75%					
11	me9	11	1	1	29000	36	33.15	0.58	0.88	1.808	5	10	2.22%	19.05%	9.27%					
12	me10	12	1	1	29000	36	33.15	0.58	0.88	1.808	5	10	11.36%	17.11%	8.33%					

6.3.1.2 Unstiffened Webs

For section loss to the unstiffened webs of flexural members near the supports – The effects of web local yielding and web local crippling shall be evaluated at the strength limit state according to the provisions of *BDS Appendix D6.5*.

For section loss at the critical section of the web just above the bottom flange, the distance, k, from the bottom of the bottom flange to the top of the bottom flange-web fillet shall be taken as the thickness of the bottom flange. This assumes that the fillet is corroded completely.

6.3.1.2.1 Effective Section

The length of beam beyond the back face of the bearing may be relied upon for support up to a distance, 2.5k, but not greater than the distance from the back face of the bearing to the end of the beam.

This provision effectively removes the BDS provision that the concentrated load shall be greater than the depth of the member from the end of the beam to use *BDS Eq. D6.5.2-2*. Note that the intention of removing the aforementioned BDS provisions is to accept a greater level of risk.

Figure 48. CTDOT Spreadsheet and Provisions Example, Adapted from CTDOT Load Rating Spreadsheet [56]

8.2. MassDOT Provisions, Tzortzinis Equations

The Massachusetts provisions for evaluating the remaining capacity of corroded beam ends were provided via the most current provisions under review for the MassDOT Bridge Manual [47]. These provisions revised the MassDOT procedures and introduced the consideration of the web deviation parameter and the Corrosion Length (CL) parameter. The out of plane web deviation parameter was measured in the laboratory and determines the given parameters utilized for the web crippling equation. The larger the initial web imperfection, the lower the capacity. The CL parameter is bounded from half of the bearing length ($N/2$) to $N+md$, the bearing length plus the beam depth multiplied by a parameter “m” which is dependent on web deviation. Additionally, the t_{ave} parameter is the average thickness taken within this $N+md$ length. The research team only considered the unfactored capacities as the results would be compared to other state procedures and the real experimental tests. An example of the equations used by for the MassDOT capacity estimations can be found in Figure 49 below.

$$t_{ave} = \frac{(N + m d - H) * t_w}{(N + m d)}$$

Where:

t_{ave}	=	average remaining web thickness (in.)
N	=	bearing length (in.)
m	=	factor specified in Table 7.2.9-1
d	=	beam depth (in.)
H	=	total length of hole(s) along length used for capacity within (N + m d) (in.)
t_w	=	remaining web thickness (in.)

Table 7.2.9-1: Values of Factor (m) - for Average Web Thickness Calculation

	Imperfection Amplitude (i)*		
	$i > 0.5 t_{web}$	$0.5 t_{web} \geq i > 0.1 t_{web}$	$i \leq 0.1 t_{web}$
$N/d > 0.2$	0.2	0.2	0.1
$N/d \leq 0.2$	0.1	0.1	0.0

*Values shall not be interpolated

For beam end reactions when $N/d > 0.2$

$$R_{n,(2)} = \left(a \sqrt{EF_y t_f} t_{ave}^{1.5} + b^{\frac{(0.33d)}{N}} \left(\frac{4(N-H)}{d} - 0.2 \right) \sqrt{\frac{EF_y t_f}{t_{ave}^{1.5}}} t_{ave}^3 \right) \left(\frac{CL}{N + m d} \right)^{0.15}$$

Table 7.2.9-2: Factors for Calculating $R_{n,(2)}$ when $N/d > 0.2$

	Imperfection Amplitude (i)*		
	$i > 0.5 t_{web}$	$0.5 t_{web} \geq i > 0.1 t_{web}$	$i \leq 0.1 t_{web}$
a	0.37	0.32	0.57
b	0.17	0.50	0.23

In *Values shall not be interpolated

Figure 49. MassDOT Equation Example for Bearing Length/Beam Depth > 0.2 , Photographs from MassDOT Bridge Manual (under review) [47]

8.3. MaineDOT Provisions

The Maine provisions for evaluating the remaining capacity of corroded beam ends were provided via their Load Rating Guidelines and a Load Rating Example. The specific provisions used are AASHTO LRFD [30-31]. For context, a key parameter here is d_b which refers to depth of the web. The research team only considered the unfactored capacities as the results would be compared to other state procedures and the real experimental tests. The average thickness of the web for the yielding calculation is done over the length $2.5k+N$, where N is the bearing length and k is length of the web toe fillet plus the flange thickness. There was a different parameter utilized called h_{sl} in the load rating examples and provisions that calculated the average thickness based on the height of the section loss; the team discussed with Maine inspectors, and it was decided to not use this parameter. Therefore, the team assumed the average web thickness for crippling is taken over the bearing length N . An example of the equations used by MaineDOT for capacity estimations can be found in Figure 50.

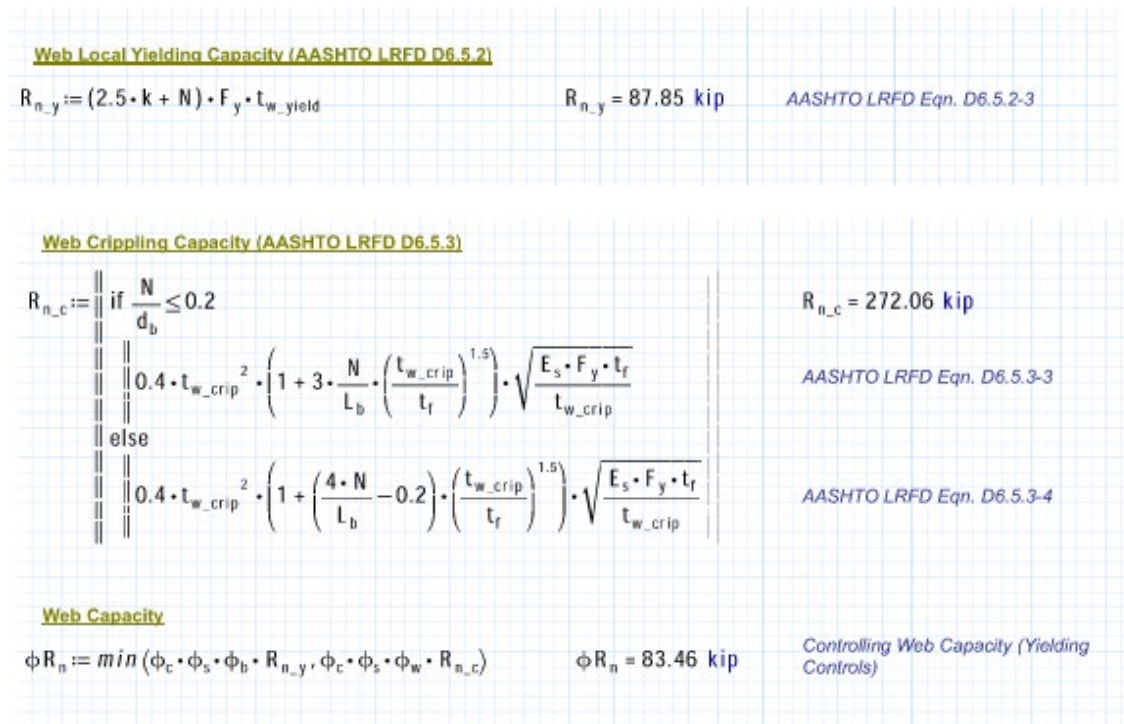


Figure 50. Maine Corroded End Capacity Estimation Example, Adapted from MaineDOT 2238 Load Rating [31]

8.4. NHDOT Provisions

The New Hampshire provisions for evaluating the remaining capacity of corroded beam ends were provided via their Load Rating Guidelines and a Load Rating Example. The specific provisions used are AASHTO LRFD [30]. The main difference between New Hampshire and Maine’s use of this provision is the use of full beam depth versus web depth. You will notice New Hampshire uses the full beam depth here as opposed to Maine’s utilization of d_b . The average thickness of the web for the yielding calculation is

done over the length $2.5k+N$, where N is the bearing length and k is length of the web toe fillet plus the flange thickness. The average web thickness for crippling was assumed to be taken over the bearing length N based on what was stated in the examples and provisions. The research team only considered the unfactored capacities as the results would be compared to other state procedures and the real experimental tests. An example of the equations used by NHDOT [25] for capacity estimations can be found in Figure 51.

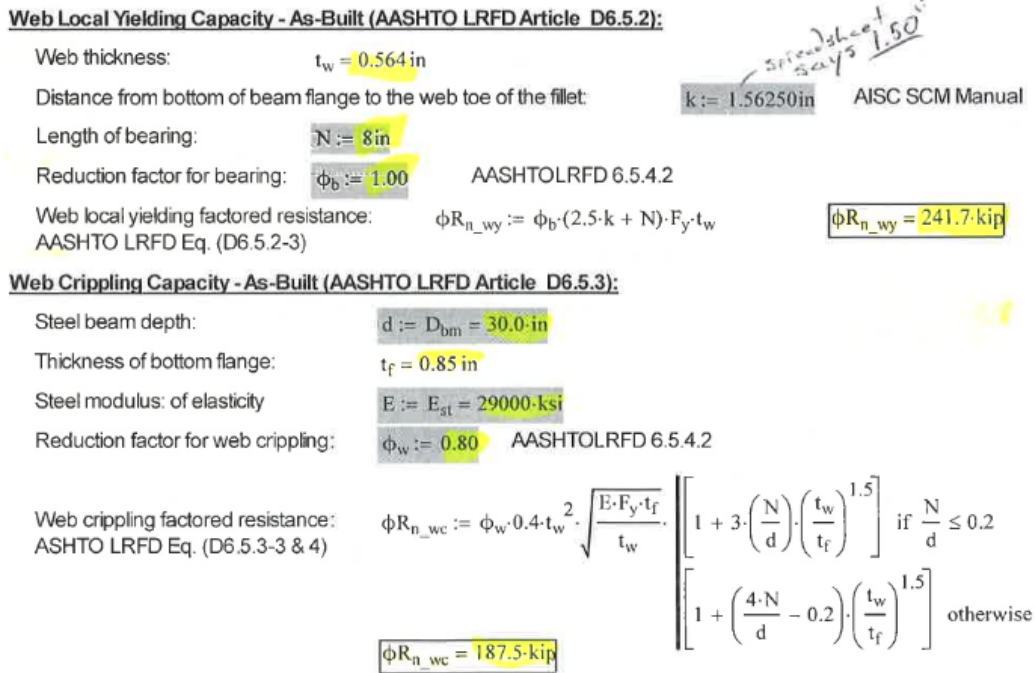


Figure 51. New Hampshire Corroded End Capacity Estimation Example, Adapted from New Hampshire Load Rating Frankestown 142-160 [25]

8.5. RIDOT Provisions

The Rhode Island provisions for evaluating the remaining capacity of corroded beam ends were provided via an Excel spreadsheet. In this spreadsheet, each beam specimen was entered with their baseline dimensions. Section losses were then applied to those base dimensions based on what was observed and calculated by the research team. Because this tool is used by RIDOT, there were no fundamental modifications made to the spreadsheet and the team used it as a load rater would but only with a focus on the unstiffened parameters. The RIDOT spreadsheet provided extensive documentation and figures for guidance in the process that were imbedded in the spreadsheet. The average thickness of the web for the yielding calculation is done over the length $2.5k+N$, where N is the bearing length and k is length of the web toe fillet plus the flange thickness. The average web thickness for crippling is taken over the bearing length N . Additionally, there was a provision for interior-pier reactions as well as concentrated loads applied away from the end at a distance of the beam depth (d) or greater. For uniformity and because both sets of beams tested were from single-span structures, this provision was assumed to be negligible. The research team only considered the unfactored capacities as the

results would be compared to other state procedures and the real experimental tests. An example of the spreadsheet pages used from RIDOT [26] are found in Figure 52.

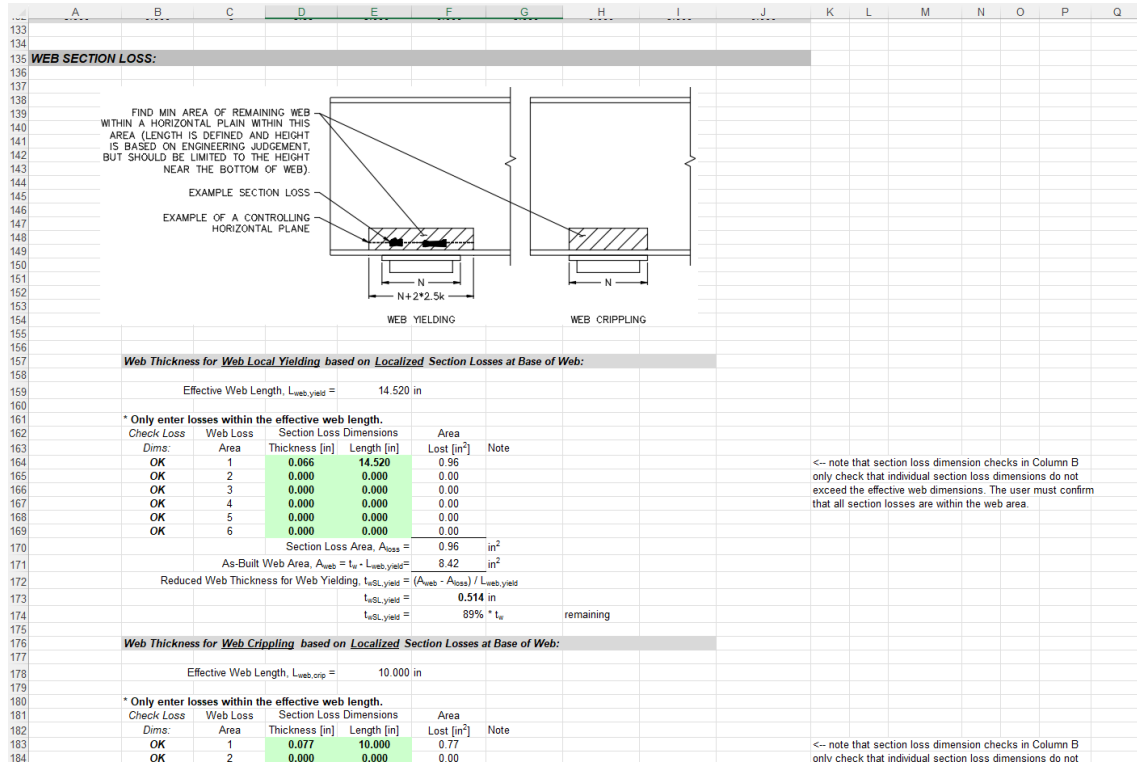


Figure 52. RIDOT Spreadsheet Example, adapted from RIDOT Load Rating Spreadsheet [26]

8.6. VTrans Provisions

The procedures to evaluate corroded ends from the state of Vermont are done per the MBE provisions via 6A.6.5 Effects of deterioration on Load Rating [27]. Along with this, field measurements are taken and there is visual inspection conducted to evaluate loss in the girders. The team did not receive the procedures by the draft of this work and therefore did not test the capacity evaluation methods at this time.

8.7. Summary

With all of the provisions provided by each state, the research team was able to compile and use each method of capacity estimation for each specimen tested in the project. It is very important to note that the data used in each of the capacity estimations for the section loss was estimated using the results of the LiDAR and 3D Scanning technologies. This allowed for more precise estimations in the evaluation for peak load. Current inspection methods often depend on visual inspection and/or hand tools such as callipers or ultrasonic thickness gauges that estimate thickness one point at a time. Because of this, the ranges for capacity estimation can be far wider spread in real field inspections than the evaluations performed by the research team.

The capacity evaluation using each state’s provisions was conducted on each specimen and compiled into graphs shown in Figure 53 and Figure 54. Figure 53 shows the true capacity found in the experiment with the corresponding predictions from the state provisions. Figure 54 shows the same capacity and predictions normalized to the experimental capacity. The summarized values pictured in Figure 53 along with the peak loads from the Finite Element Simulations can be found in Table 73. The summarized percent differences between the evaluation methods and the experimental peak loads can be found in Table 74.

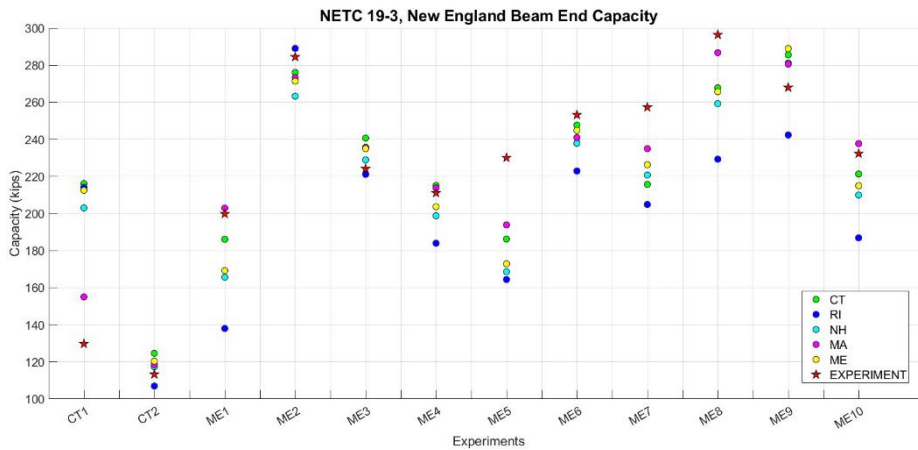


Figure 53. New England Beam End Capacity

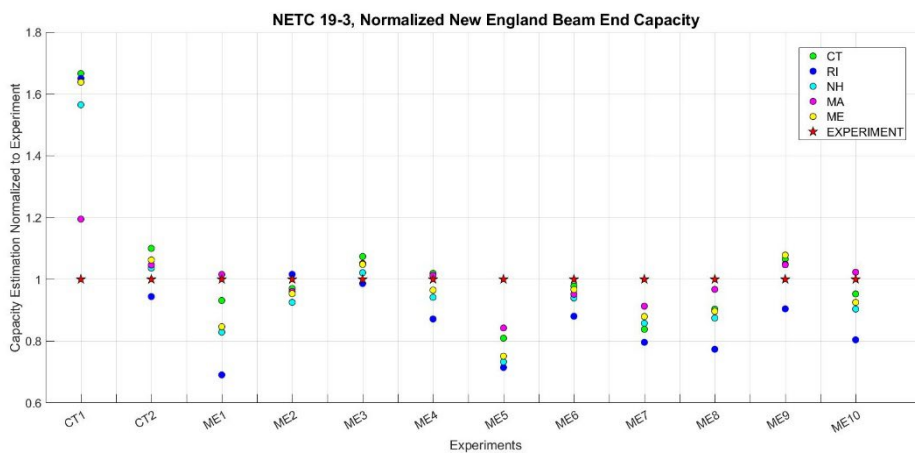


Figure 54. Normalized New England Beam End Capacity

There are several critical observations that can be drawn from the beam end capacity provision comparison. In most cases, the prediction for every state is conservative or a close estimation, however there are cases that this is not true (CT1, CT2, ME3, ME9).

The research team found that, across all the experiments, the Massachusetts guidelines were the most all-encompassing evaluation of the beam end [47]. These provisions incorporate the parameter *CL* and the influence of web deviation imperfections. They are closer to the experimental capacity in seven of the twelve experiments. And for the cases that they are not, they are second or third best in four cases, with a margin of about 1%-2.5% to the best prediction in these cases. The worst performance of the MassDOT provisions compared to the other states’ guidelines was in Experiment 5 with a margin of

approximately 3.7% from the best prediction. It is important to note that the MassDOT guidelines are also the only ones that can capture the CT1 experimental load with relative success due to the selection of the corrosion length and the resulting load reduction and weight of the average thickness. For CT1 specifically, the corrosion length was chosen as 3.5 inches because of the limited section loss along the length of the beam end and because CL has a lower limit of half of the bearing length. The selection of corrosion length, as stated in the provisions above, is based on engineering judgement and can be easily chosen based on the scanning results via contour mapping.

Table 73. Experimental Capacity Evaluation by State (kips)

	Exp	MA	ME	CT	NH	RI	VT
CT 1 (Exp1)	129.76	155.04	212.55	216.18	203.04	214.14	NA
CT 2 (Exp 2)	113.27	118.51	120.37	124.61	117.38	106.96	NA
ME 1 (Exp 3)	199.81	202.96	169.19	186.13	165.68	138.00	NA
ME 2 (Exp 4)	284.48	273.29	271.37	276.06	263.31	289.06	NA
ME 3 (Exp 5)	224.14	235.71	235.00	240.69	228.93	221.15	NA
ME 4 (Exp 6)	211.06	213.79	203.70	215.15	198.80	183.99	NA
ME 5 (Exp 7)	230.08	193.87	172.87	186.26	168.65	164.44	NA
ME 6 (Exp 8)	253.20	240.96	244.85	247.67	237.93	222.94	NA
ME 7 (Exp 9)	257.31	234.98	226.33	215.71	220.75	204.88	NA
ME 8 (Exp 10)	297.62	286.77	265.75	267.81	259.27	229.33	NA
ME 9 (Exp 11)	267.14	288.95	285.59	281.12	242.36	271.05	NA
ME 10 (Exp 12)	232.32	237.7	215.01	221.36	209.98	186.88	NA

Table 74. Experimental Capacity Evaluation, Percent Error from Experiment

	MA	ME	CT	NH	RI	VT
CT 1 (Exp1)	16.31 %	38.95 %	39.98 %	36.09 %	39.40 %	NA
CT 2 (Exp 2)	4.42 %	5.90 %	9.10 %	3.50 %	5.90 %	NA
ME 1 (Exp 3)	1.55 %	18.10 %	7.35 %	20.60 %	44.79 %	NA
ME 2 (Exp 4)	4.09 %	4.83 %	3.05 %	8.04 %	1.58 %	NA
ME 3 (Exp 5)	4.91 %	4.62 %	6.88 %	2.09 %	1.35 %	NA
ME 4 (Exp 6)	1.28 %	3.61 %	1.90 %	6.17 %	14.71 %	NA
ME 5 (Exp 7)	18.68 %	33.09 %	23.53 %	36.42 %	39.92 %	NA
ME 6 (Exp 8)	5.08 %	3.41 %	2.23 %	6.42 %	13.57 %	NA
ME 7 (Exp 9)	9.50 %	13.69 %	19.29 %	16.56 %	25.59 %	NA
ME 8 (Exp 10)	3.78 %	11.99 %	11.13 %	14.79 %	29.78 %	NA
ME 9 (Exp 11)	7.55 %	6.46 %	4.97 %	10.22 %	1.44 %	NA
ME 10 (Exp 12)	2.26 %	8.05 %	4.95 %	10.64 %	24.32 %	NA

Note: Green Indicates the lowest Percent difference for the capacity evaluation method for the given specimen

9. New Rating Recommendations

Following the analysis and comparison of each of the New England States' analytical procedures for evaluating beam end corrosion, the team observed that many of the results found match or are conservative in predicting the remaining capacity of the corroded end. By utilizing our LiDAR and 3D Scanning technologies, the team was able to capture high detailed data that accurately represents section loss in the beam specimen. By utilizing this data with the current provisions of each state, the team found that the length of corrosion and ultimately the average remaining web thickness was critical in accurately estimating the remaining capacity, as has been observed previously in MassDOT Report 19-008, September 2019 [28].

The first recommendation made by the research team is to utilize advanced technologies such as 3D scanning to monitor and evaluate section loss on steel beam ends due to corrosion. It is clear from prior work done by Tzortzinis in [29] and the protocols created by the research team that 3D scanning provides vast opportunity in accurately identifying areas of significant section loss, classifying corrosion topologies, and assisting greatly in the capacity evaluation of a corroded beam end.

As stated in Section 8.2, the CL parameter defines the corrosion length for which the average thickness is taken. This corrosion length is bounded from $N/2$ to $N+md$, the bearing length plus the beam depth multiplied by a parameter "m" which is dependent on web deviation. In the crippling capacity equations of [47], if the length of corrosion is not taken to be the full $N+md$ length, then a knockdown of the capacity takes place to account for the influence of the average thickness via the factor $(CL/N+md)^{0.15}$ found in the equation of Figure 49 via the MassDOT Bridge Manual (under review) [47]. Web deviation imperfections create major knockdowns in remaining capacity and have proven to have great influence on the beam webs. With the web of the beam behaving much like a column, the larger the initial out of plane deformation, the larger the influence in reducing the buckling capacity. The parameter CL provides a limit and range to where the average thickness of the end can be estimated. This parameter allows the inspector to quantify the average web thickness but also utilize engineering judgement in measuring and estimating the length over which the major section loss occurs. Finally, alongside the encompassing provisions, it is clear that the performance and accuracy of the equations is quite high and consistent across different beam types and section loss quantities. This can be best seen in Section 7, Figure 53 and Figure 54 as well as Table 73 and Table 74.

10. Conclusions

10.1. Conclusions Corrosion Pattern Analysis

In the first task of the project, our team analyzed 225 reports from six states in the New England region; Connecticut, Rhode Island, Maine, New Hampshire, Vermont, and Massachusetts. This allowed for the analysis of 1,723 total beam ends across all the states. The most important finding that we found through this analysis was the vast presence of the W1 corrosion pattern across the beam ends of the New England States. While this was the most important finding in this task, there were many trends our team noticed among reporting and beam end conditions upon analysis of the state inspection reports.

Several trends were found after compiling, summarizing, and post processing data obtained from the states of the New England region. These trends reflect several important components of this project and the goal of this work overall. Reflecting on the tasks of the project and this report, our team observed these trends to be categorized by two types, the way states report the inspection of a bridge structure and the corrosion patterns observed in those bridge structures via the inspection reports.

Inspection Report Comparisons Among New England States

When considering the reporting methods of each state, our team concluded that subdividing the New England region was helpful to the post-processing of data. As discussed in the report, the state's departments of transportation were placed into two groups:

- MaineDOT, NHDOT and VTrans in Group 1 and
- RIDOT, MassDOT and CTDOT in Group 2.

It is important to note that inspection reports where no data could be gathered were not included in the finalized conclusions, data, and graphs of this report.

The trends found in terms of inspection reports can be summarized as follows:

- The most common trend found in the methods of inspection were that the Northern New England States (Group 1) have inspection reports which rarely provide sketches where the Southern New England States (Group 2) often provide sketches and photographs. It is again important to note that the methods of Group 2 were developed over time and had performed inspection methods much like those of Group 1 in the past.
- An additional trend that was identified was the span of years in which many of these bridge structures were built. There were trends identified at a state and regional level. It is important to note here that there was only one report in our finalized compilation from Vermont which indicated the year a single bridge was built (1991). The majority of bridges our team analyzed in the New England region were built between 1928 and 1978. We then separated this information by state. For Connecticut, many bridges were built between 1955 and 1970. Regarding Massachusetts, most of the bridges were built between 1947 and 1969. For the state of Maine, our team found that many bridges were built between 1928 and 1991. Regarding Rhode Island, we found that all of the bridges analyzed were

built between 1935 and 1975. For the state of New Hampshire, most of the bridges analyzed were built between 1920 and 1994. This information is imperative in order to identify the grade of steel and the beam dimensions used for the steel beams used in construction.

- Another common trend found in several reports from Group 1 is the way corrosion is reported. In many reports from the states in Group 1, corrosion information is provided in a generic form, which results from a visual inspection. No finite measurements and thickness losses were reported. Some conclusions our team was able to draw from these reporting trends were that while reporting and documenting corrosion varies from state to state, there tended to be general uniformity among the report structures. This allowed our team to compile the reports more efficiently.

Corrosion Phenomenon Comparisons Among New England States

At a general level, the results of post-processing data analysis for the inspection reports can be divided into two groups as discussed above. While the results in previous sections of this report focus on the presentation of the reports by each New England state, this information ultimately determines the corrosion pattern results. In the case of Group 1, MaineDOT, NHDOT and VTrans, the reports provided do not present sufficient documentation to create common corrosion patterns for their states. This documentation primarily refers to sketches or dimensional measurements, which is likely not provided due to inspections being visually conducted.

This allowed our research team to further isolate results of the states of the New England region who had sufficient documentation to allow for the creation of common corrosion patterns found by state. These states departments of transportation were in Group 2, which included RIDOT, MassDOT, and CTDOT. Upon isolating the states that provided enough information, each state had patterns generated specific to the data gathered from their reports. These patterns included the several types of corrosion shapes and damage discussed earlier in this report. Additionally, the patterns considered structures with and without diaphragms as part of the structural system. It can be observed that the presence of a diaphragm changes the corrosion patterns observed and is considered a separate pattern from structures without diaphragms.

There are several conclusions that can be drawn from the data analyzed by Massachusetts, Rhode Island, and Connecticut when a diaphragm system is present. Each state has its most prominent corrosion pattern found in the reports:

- For Massachusetts, the most common corrosion pattern was the W1 corrosion pattern closely followed by the W3 corrosion pattern. Regarding the state of Rhode Island, the most common corrosion pattern was W1. For the state of Connecticut, the most common corrosion pattern was W1 corrosion.
- It can be seen from the states which corrosion patterns could be generated for bridges with diaphragms present, that the W1 corrosion pattern is the most prevalent.
- Across all patterns and states with a diaphragm present, it was found that the thickness loss had great range from no thickness loss to complete thickness loss.
- The most prominent range for thickness loss was around 18% to 55% across all states and corrosion patterns for structures with diaphragms.

- In addition to the corrosion shapes, there were also holes observed in the beam end specimens with a diaphragm present from the different states. Among the data from Connecticut, Massachusetts, and Rhode Island, it was found that the M1 hole corrosion pattern was the most common.
- The following conclusions discuss the corrosion measurement parameters, shapes, and the trends found. It is worth noting again that this section only applies to Connecticut, Massachusetts, and Rhode Island where corrosion parameters and patterns could be identified and generated.
 - Our team discovered that among beams with a diaphragm system that the W1 pattern has parameters that followed a very interesting trend; the CH height parameter had many cases varying from minimal height corrosion to half height corrosion. Additionally, our team saw that in the Connecticut and Massachusetts specimens specifically, full height corrosion showed a strong presence. This is very different from the CH height parameter for beams without a diaphragm, which had many cases varying from minimal height corrosion to half height corrosion. Via the parameter graphics created for the CL parameters in Massachusetts and Rhode Island, it appeared that many of the beam ends had smaller ranges for corrosion length when compared to beam ends without a diaphragm system present. This is particularly interesting because the W1 corrosion pattern was the most prominent corrosion pattern identified in the analysis.
 - Another interesting trend our team found in the analysis was in the parameters of the W3 corrosion pattern. Our team found that the most intriguing of the parameters here were the CH2 height parameter and the CL3 length parameter. These parameters represent the largest height and length in the W3 corrosion pattern, respectively. In the case of beams with a diaphragm present, the CH2 parameter often equaled full height corrosion. Regarding the CL3 parameter for the W3 case with a diaphragm system, the length had large variation. Our team observed extreme cases in which CL3 was approximately 500% of the web height in Massachusetts. Among Connecticut and Rhode Island, there were cases that reached around 250% and 300% of web height, respectively.

There are several conclusions that can be drawn from the data analyzed by Massachusetts, Rhode Island, and Connecticut when no diaphragm system is present. Each state has its most prominent corrosion pattern found in the reports:

- For Massachusetts, the most common corrosion pattern was W1 corrosion. The state of Rhode Island had W1 as its most common corrosion pattern but also had several W3 corrosion patterns present throughout the bridge specimens. Regarding Connecticut, the most common corrosion pattern was W1 corrosion.
- It can be seen from the states for which corrosion patterns could be generated for bridges without diaphragms present, that the W1 corrosion pattern is the most common.
- Across all patterns and states without a diaphragm present, it was found that the web thickness loss had great range from no thickness loss to complete thickness loss. The most prominent range for thickness loss was around 18% to 50% across all states and corrosion patterns.

- Similar to the structures with a diaphragm, there were also holes observed in the beam end specimens without a diaphragm present from the different states. From the data analyzed and compiled from Massachusetts, Rhode Island, and Connecticut, it was found that the M1 hole corrosion pattern was the most prevalent.
- The following conclusions discuss the corrosion measurement parameters, shapes, and the trends found. It is worth noting again that this section only applies to Connecticut, Massachusetts, and Rhode Island where corrosion parameters and patterns could be identified and generated.
 - Our team discovered that among beams without a diaphragm system that the W1 pattern, the most prominent pattern, has parameters that followed a very interesting trend; the CH height parameter was often less than half of the height of a given beam. This was true across Rhode Island, Connecticut, and Massachusetts. While this was true for the height, the length parameter CL varied from minimal length corrosion to a length corrosion of approximately 300% the height of the web. Among Rhode Island, Connecticut, and Massachusetts, the corrosion length maximum was greater than the full web height. This is particularly interesting because the W1 corrosion pattern was the most prominent corrosion pattern identified in the analysis.
 - An interesting trend our team found in the analysis was in the parameters of the W3 corrosion pattern. As discussed above, our team found that the most intriguing of the parameters here were the CH2 height parameter and the CL3 length parameter. These parameters represent the largest height and length in the W3 corrosion pattern, respectively. In the case of beams with a diaphragm present, the CH2 parameter often equaled full height corrosion. A critical note here is that this was also the case when a diaphragm is present, as described above. Similar to cases with a diaphragm, the CL3 parameter for the cases of W3 without a diaphragm system had large variation in the length. Our team observed extreme cases in which CL3 had extreme cases in Connecticut and Massachusetts. These were approximately 300% and 225% of web height, respectively. The interesting part of both the height and length measurements for the W3 corrosion patterns was the similarity regardless of if a diaphragm is present.

The comparison of these corrosion patterns may suggest that many similarities arise among the parameters of given corrosion patterns throughout the states of New England.

Connection with laboratory testing and rating recommendations

These findings are crucial to our work on this project for several reasons. Recognizing corrosion patterns and thickness losses across the beams of several states allowed our team to sort and generate data for the next part of this project. Once the damage done by corrosion to beam end specimens can be identified and understood, the goal then becomes finding the remaining beam capacity. Based on the common corrosion patterns and thickness loss measurements, the remaining capacity of the beams can be found.

The main conclusions that can be drawn from the analyses conducted and discussed throughout this report is that corrosion patterns can be generated to classify the damage exhibited throughout the inspection reports and bridges of the New England States. There

are clear trends identified of the phenomenon across all of the states. These trends are helpful in identifying types of damage and will ultimately contribute to finding the remaining capacity of a beam and the overall bridge structure.

Within this work, there were limitations in the main corrosion patterns our team was able to identify for each state. If a bridge inspection was conducted and corrosion is reported qualitatively, measurement parameters become difficult to establish. This limitation ultimately means that corrosion patterns cannot be generated. Another limitation of the work is the amount of data that can be received and used for the project. This could be lack of information presented in the inspection reports, minimal inspection reports to process, and the overall validity of the beams via the scope of the project.

10.2. Conclusions from Experiments, Simulations and Ratings

Utilizing the rigorous analysis of the beam ends performed in the first task of the project, the research team was able to select bridges and individual ends of interest for testing at the Brack Structural Testing facility at The University of Massachusetts Amherst. Each beam that was tested had to be documented thoroughly for section loss. The team utilized in-house 3D scanning protocols for this process which were then used to evaluate the current methods of each New England state and to create finite element simulations. Each of these specimens were then load tested for their remaining capacity. Finally, each beam end specimen was evaluated using the procedures for capacity estimation of corroded ends by state and compared to the experimental peak loads achieved.

10.2.1. Conclusions on Scanning and Corrosion Profiles

There are several major conclusions we can draw from our evaluation of corrosion via 3D scanning.

- Beams from the same bridge exhibit similar corrosion profiles. This was observed in the first task of the project when the team analyzed inspection reports across all the New England States but can also be seen in each of the Maine beam specimens that were tested in experiments three through twelve. While the section loss itself varied, the shapes mainly resembled that of the W3 or W4 classification.
- Scanning provides a fast method to evaluate section loss for corroded beam ends. To document the corroded end or even the isolated area at the base of the corroded web using current practices takes several hours. Scanning the beam end takes minutes to perform and can be post processed quickly using in-house algorithms.
- Scanning allows for vast data and provides the entire profile of a corroded end. While an ultrasonic thickness gauge and slide caliper were used for measurements throughout the course of this project, the scanning provides an all-inclusive evaluation of the section loss on the corroded end which includes corrosion profiles, exorbitant section loss data, and damage that cannot be read by other tools accurately such as severe pitting.

10.2.2. Conclusions on Experiments and Simulations

The team was able to draw many conclusions regarding the experiments conducted throughout this project.

- Each experiment was conducted and successfully captured the corroded end capacity. It was imperative to capture the beam end's capacity and not to capture flexure or any other failure in other parts of the beam. Buckling failure was successfully achieved in each beam end experiment.
- Buckling primarily occurred in the base or lower 50% of the web height and was localized. In a few of the laboratory experiments conducted, such as experiment one, buckling was induced at mid-height. This is likely due to the heaviest section loss being present at the mid-height of the web. While this was the observation, the team found that this capacity can still be estimated accurately via the provisions by Tzortzinis [47].
- The web deviation parameter was very similar across many of the experiments, the first two beams were of different shape and from the state of Connecticut. These two beams had around a $0.5t_{web}$ deviation. The Maine beams in experiments three through twelve were all from the same structure and had approximately $0.1t_{web}$ deviation present in each specimen. Beam specimens from the same bridge exhibited similar corrosion patterns and similar web deviation.
- The finite element models created to replicate the experimental results were able to capture the peak loads well and replicate the buckling shape. The largest difference in peak load observed was by about 15% and is likely due to modelling assumptions made in the finite element portion of this report.

10.2.3. Conclusions on Ratings and Recommendations

Following corrosion classification and experimental testing conducted throughout the project, the research team was able to draw the following conclusions about the capacity evaluations by state and the recommendations for capacity estimation.

- The Massachusetts provisions updated by Tzortzinis in [47] are the most accurate predictions of the actual capacity of the corroded beam ends overall. While there were cases where other state's provisions were closer to predicting the corroded beam end capacity, the Massachusetts provisions consistently perform with higher fidelity.
- The provisions incorporated in [47] consider key features such as a capacity reduction for a weighted thickness based on the CL parameter and for an increased amount of initial web deviation. This provides a more comprehensive evaluation of the beam end and provides a more accurate representation of section loss and geometric imperfection than other evaluation methods.
- While all of the state provisions perform quite well regarding the experimental predictions, it is imperative to note that this is largely in part because of the scanning data, which provides a vast data field of thicknesses that allow for high quality capacity estimation. Visual inspection and handheld tools for point measurements will cause more uncertainty and inaccuracy in capacity estimation and may cause gross over or under estimations in the capacity estimation process.

The limitations of this work are mainly concerning the time of the project. There were several challenges that took place due to laboratory delays such as access to move beam

specimens, cleaning beam specimens, and rig modifications that had to be made to accommodate the specimen for each test. With more time, the research team would have performed more experiments as a part of this phase and tested the material properties of the beam specimens. The research team will continue to conduct experiments, document section loss via scanning, update the finite element models, and conduct material tests. These results will be documented outside of this current project report.

11. Appendix I – Detailed data and processing graphs for beam ends without a diaphragm

11.1. Connecticut

11.1.1. Introduction

As discussed in previous sections, the data was divided by state as the number of beams ends was significantly different from one state to the other. Thus, to not introduce bias in the results, all states were individually analyzed. Beyond this, the beam ends were divided into two sub-groups: ends with diaphragm and the ends without diaphragms. In this section, all information and graphs presented focus on beams ends without diaphragms from the state of Connecticut.

Figure 55 depicts the frequency of patterns obtained for beam ends without diaphragm from the reports provided by CTDOT.

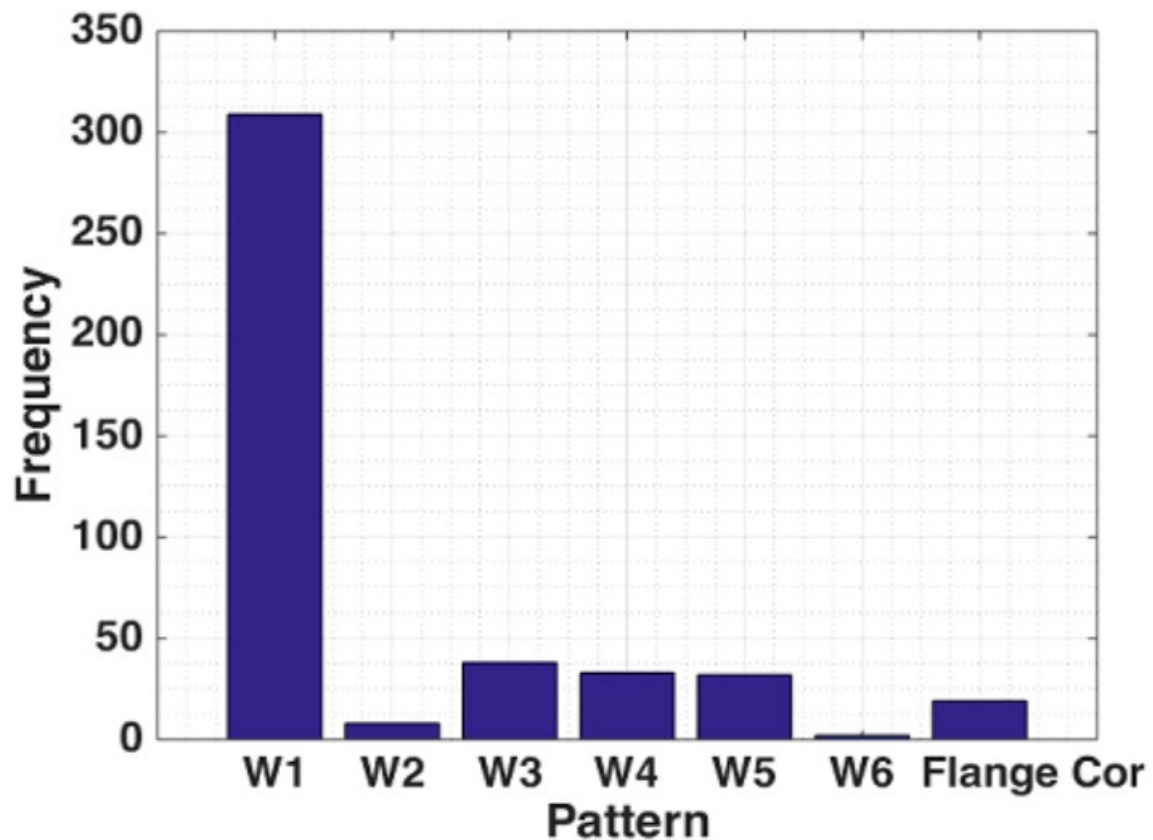


Figure 55: Web corrosion patterns distribution for beams ends without a diaphragm – CTDOT

It is worthwhile pointing out that the characteristic dimensions of the patterns - i.e., CH1, CH2, CH3, CL1, CL2, CL3 - were normalized with the web height, H_0 , where $H_0 = H - 2 t_f$.

11.1.2. Pattern W1

11.1.2.1. Web corrosion

The distribution of CH_1 for this pattern is depicted in Figure 56. From Figure 56 two dominant trends can be seen: (i) full height corrosion, or (ii) corrosion up to 40% of the web, which can be written as:

$$0 < CH_1 \leq 0.4H \text{ and } 0.9H \leq CH_1 \leq 1H$$

The parameters for the corrosion patterns can be found with corresponding diagrams in Section 1.5 *Corrosion Patterns* of this report.

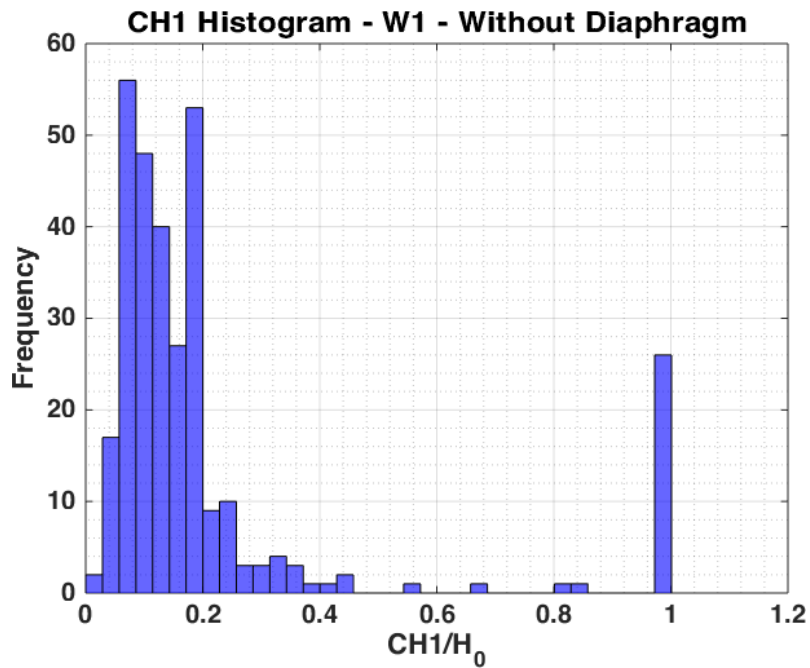


Figure 56: CH_1 distribution of W1 pattern for beams without a diaphragm - CTDOT

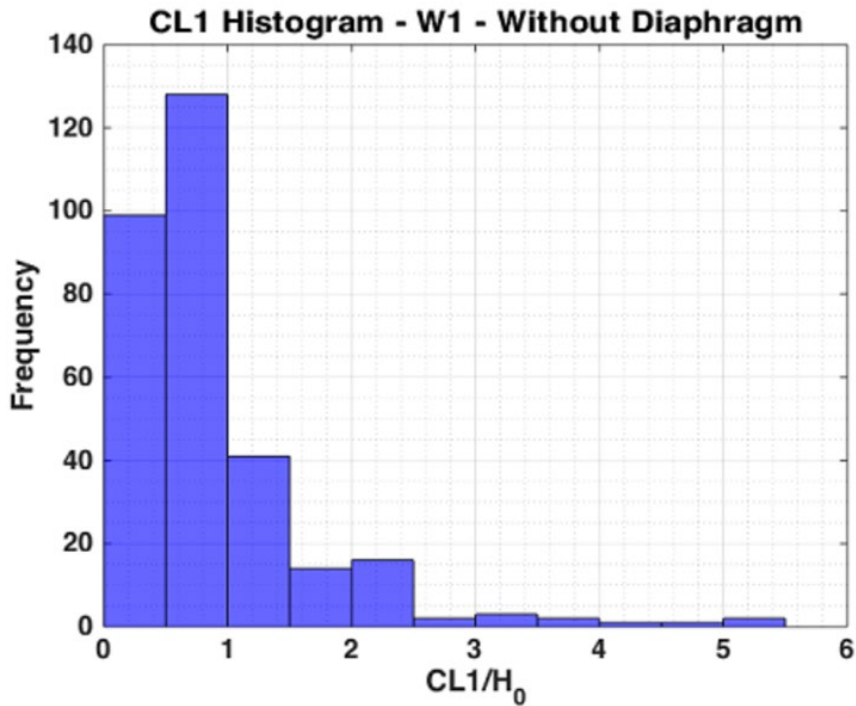


Figure 57: CL1 distribution of W1 pattern for beams without a diaphragm – CTDOT

Upon investigation of Figure 57, no major trend could be found. While no dominant trend could be seen, it is reasonable to state that the corrosion present for W1 is dominated by values smaller than 2.5H₀.

Aiming to compare the length and height of corrosion, Figure 58 depicts the ratio between the length and height of corrosion. It is possible to observe that the length is usually several times greater than the height.

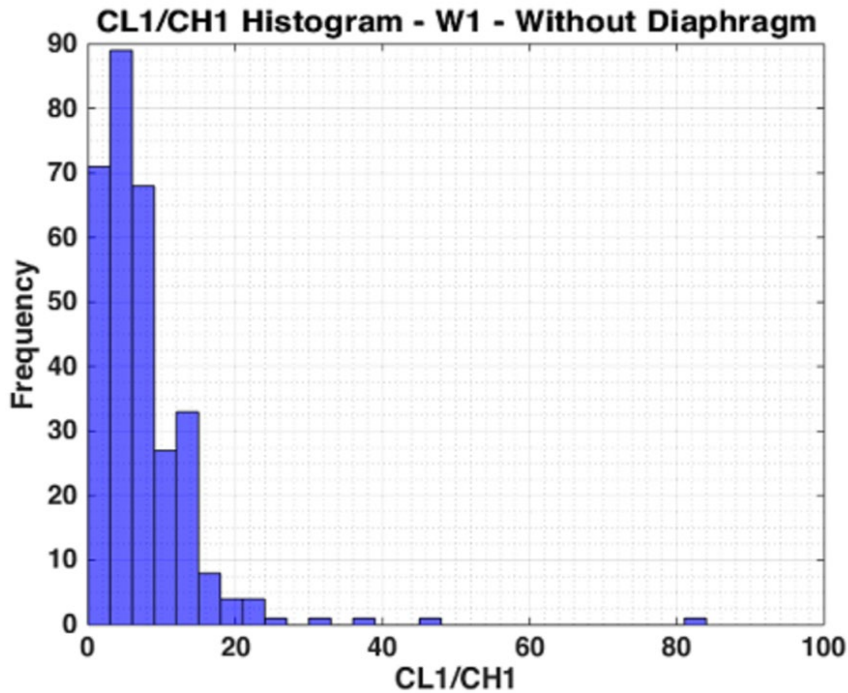


Figure 58: Ratio of corrosion length (CL1) to corrosion height (CH1) of W1 pattern for beams without a diaphragm - CTDOT

As many lengths are less than $2.5H$, our team was able to check the ratio for beams ends where $CL1 < 2.5H$. The resulting histogram is depicted in Figure 59.

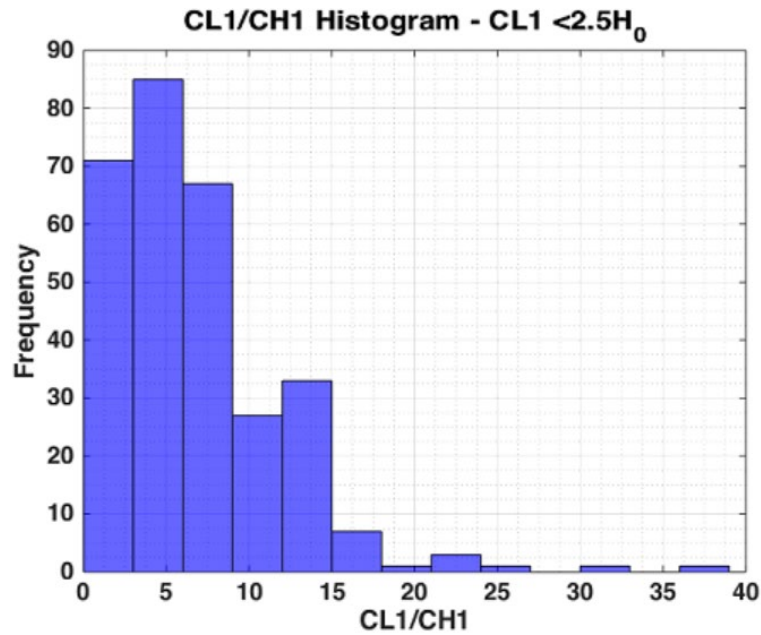


Figure 59: Ratio of corrosion length (CL1) to corrosion height (CH1) for $CL1 < 2.5H_0$ - CTDOT

Beyond this, to deepen the understanding regarding the interaction between CH1 and CL1, our team could isolate trends depicted in the CH1 distribution. As a result, our team could plot the length of corrosion for $CH1 < 0.3H_0$. Figure 60 depicts the final distribution of CL1 for this case.

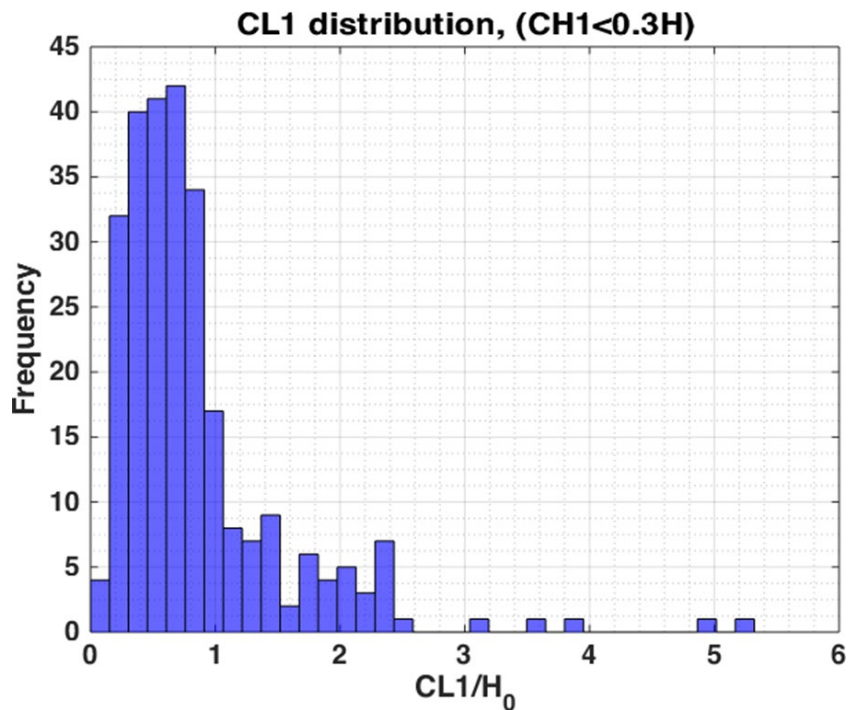


Figure 60: CL1 distribution for $CH1 < 0.3H$ - CTDOT

A similar study to the $CH1 < 0.3H0$ case, our team conducted a study on the case where $CH1 > 0.9H$. Figure 61 below depicts the final distribution for this case.

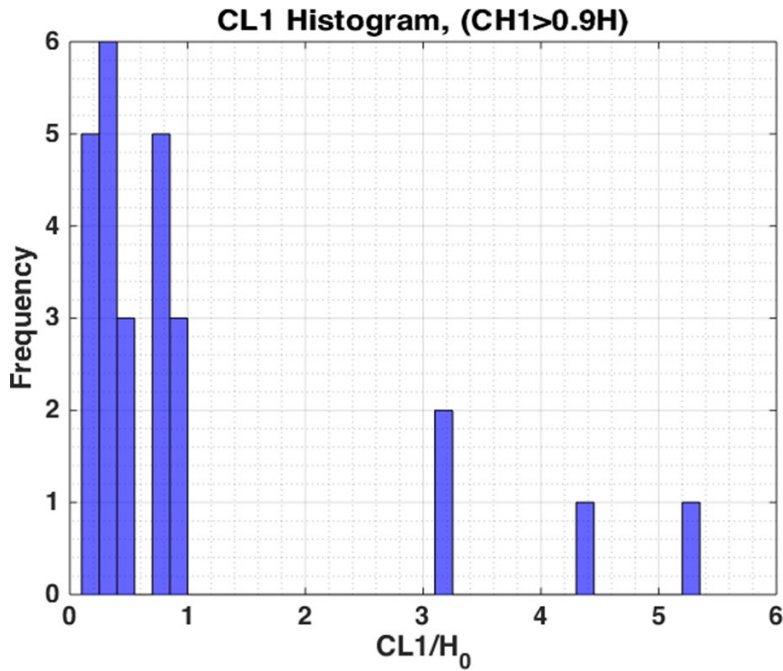


Figure 61: CL1 distribution for $CH1 > 0.9H$ - CTDOT

When comparing Figure 60 to Figure 61, it is apparent that when the corrosion height is large, the corrosion length is often smaller. On the other hand, for small heights of corrosion, the corrosion length tends to be greater than the corrosion height.

Figure 62 depicts the distribution of web thickness loss for pattern W1. It is noticeable that much of the thickness loss for the W1 case is no greater than 50%.

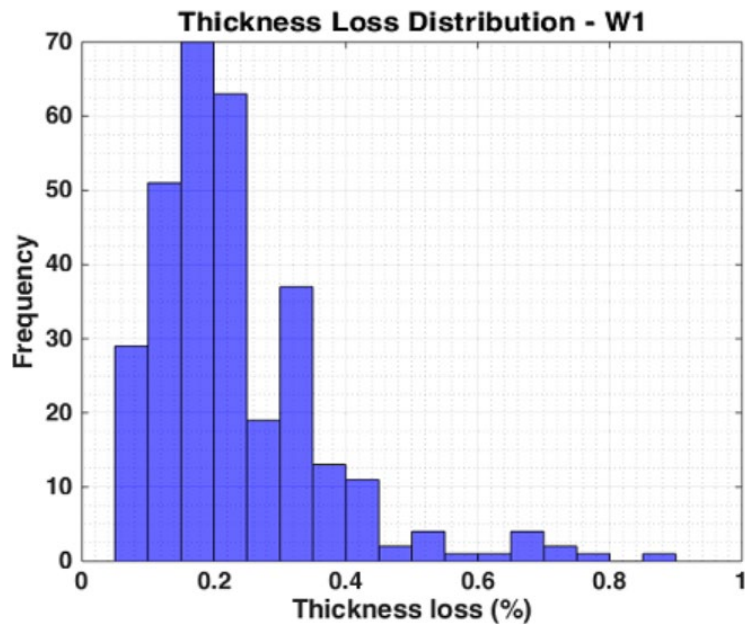


Figure 62: Web thickness loss distribution for pattern W1 - CTDOT

Similar to the analysis conducted for corrosion length, our team was able to study the thickness loss for the two main trends detected previously. The resulting distributions are depicted in the Figure 63 and Figure 64.

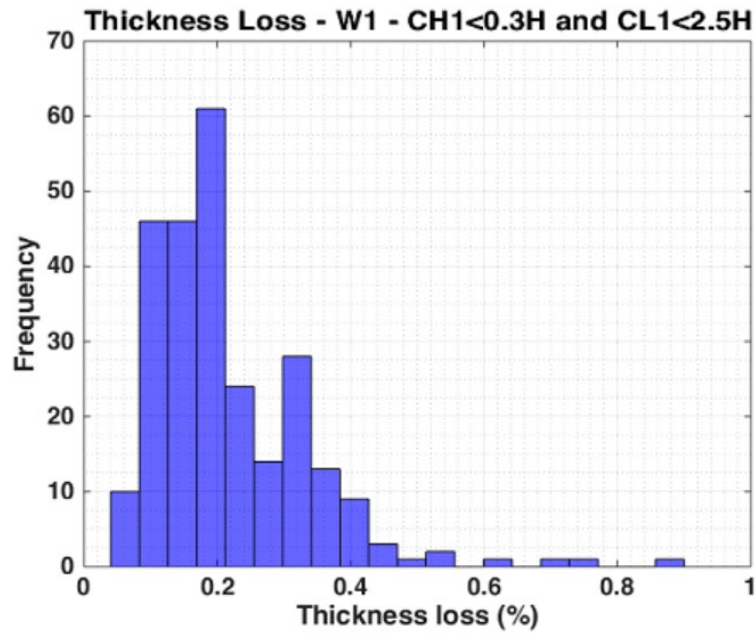


Figure 63: Web thickness loss distribution for CH1<0.3H and CL1<2.5H - CTDOT

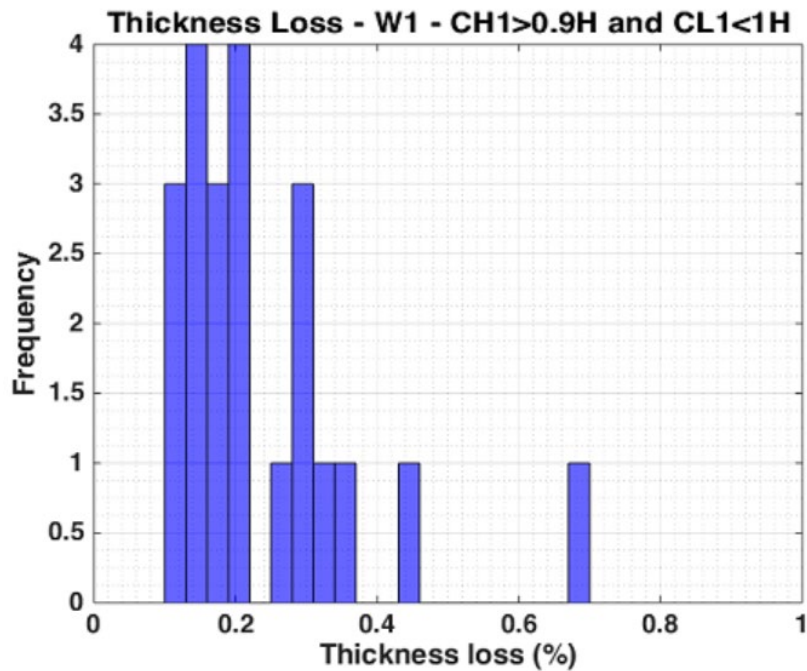


Figure 64: Web thickness loss distribution for Ch1<0.9H and CL1<1H - CTDOT

11.1.2.2. Flange corrosion

Figure 65 depicts the length of corrosion in the flanges. It is worthwhile in recognizing that there is significantly less information regarding flange corrosion.

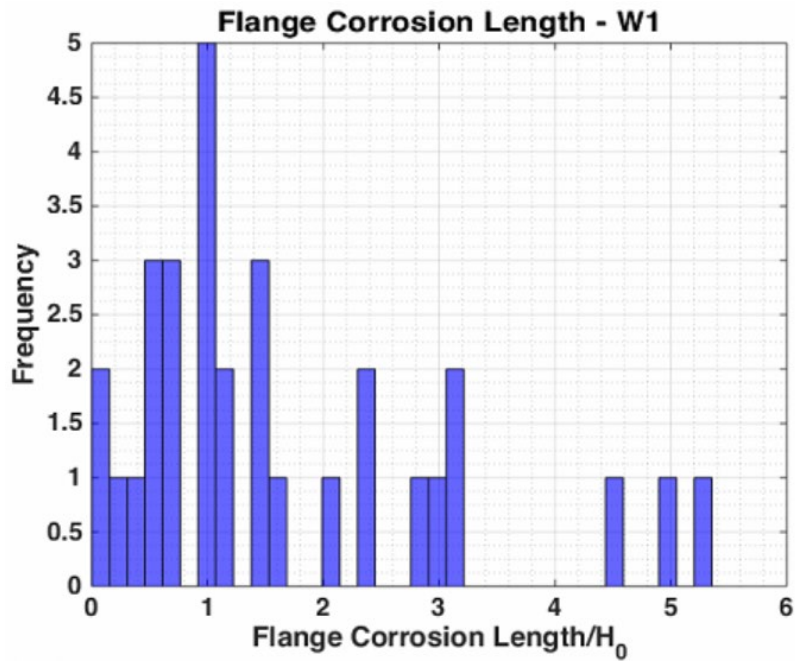


Figure 65: Distribution of corrosion length for pattern W1 - CTDOT

To compare the length of corrosion in the flanges with the length of corrosion in the web, Figure 66 was created. Here, the graph depicts the ratio of C_f/C_l , where C_f is the length of corrosion in the flanges and C_l is the web length corrosion.

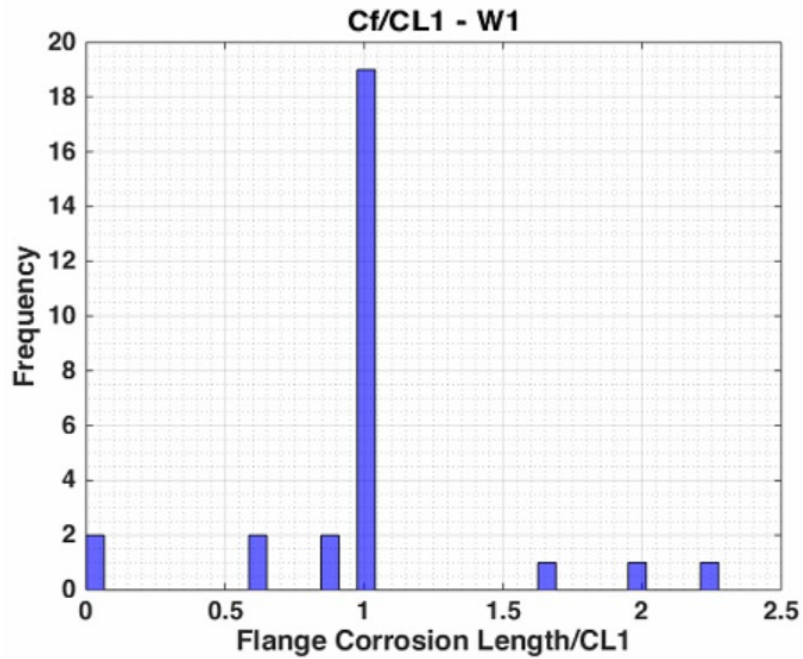


Figure 66: Ratio between flange corrosion length for pattern W1 - CTDOT

From Figure 66, it was valid to assume that the length of corrosion is the same for both web and flange. Therefore, for trends previously identified, our team assumed that the length of corrosion in the flange was equal to the corrosion in the web.

Regarding the thickness loss of the flanges, the research team was able to plot the distribution depicted in Figure 67.

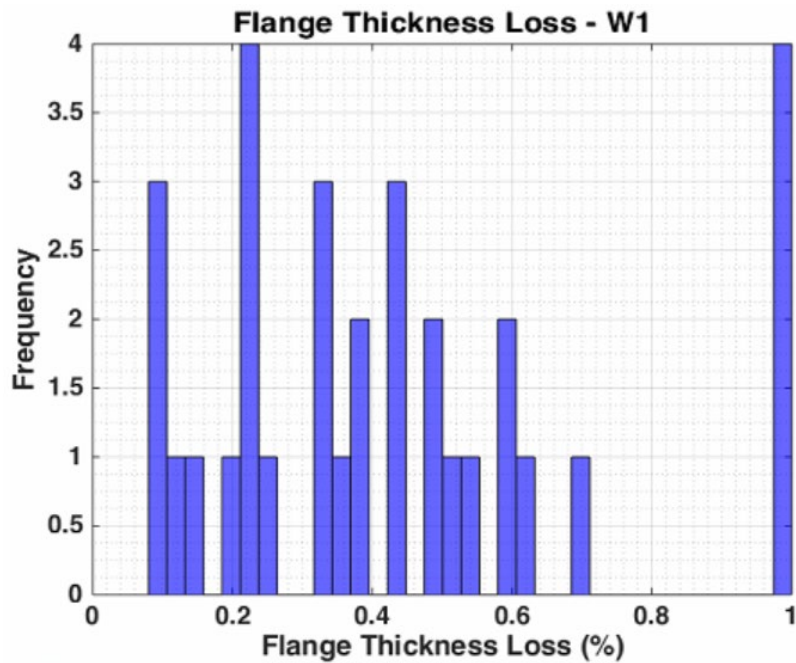


Figure 67: Flange thickness Loss for pattern W1 - CTDOT

Similarly, our team was able to isolate the thickness loss for either trends found previously, as depicted in Figure 68 and Figure 69.

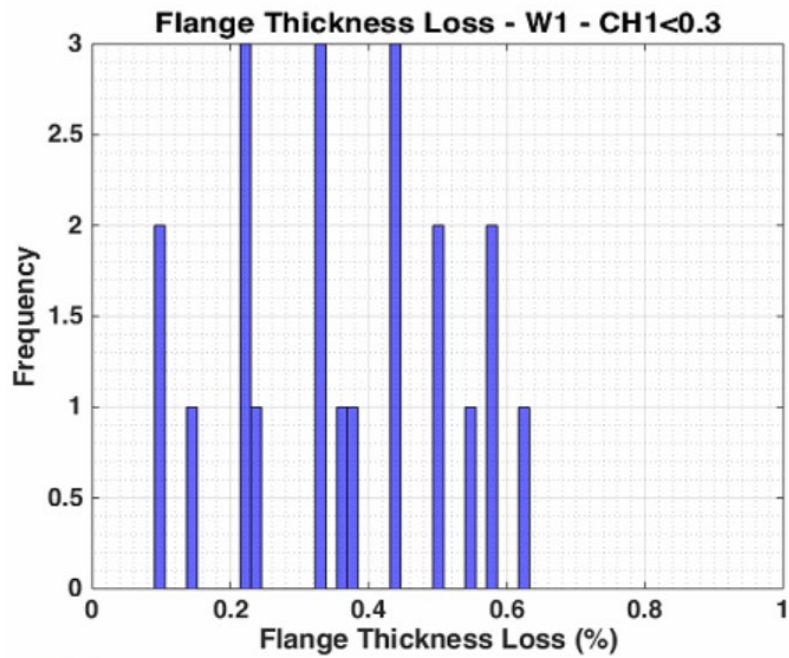


Figure 68: Flange thickness loss distribution for CH1<0.3 - CTDOT

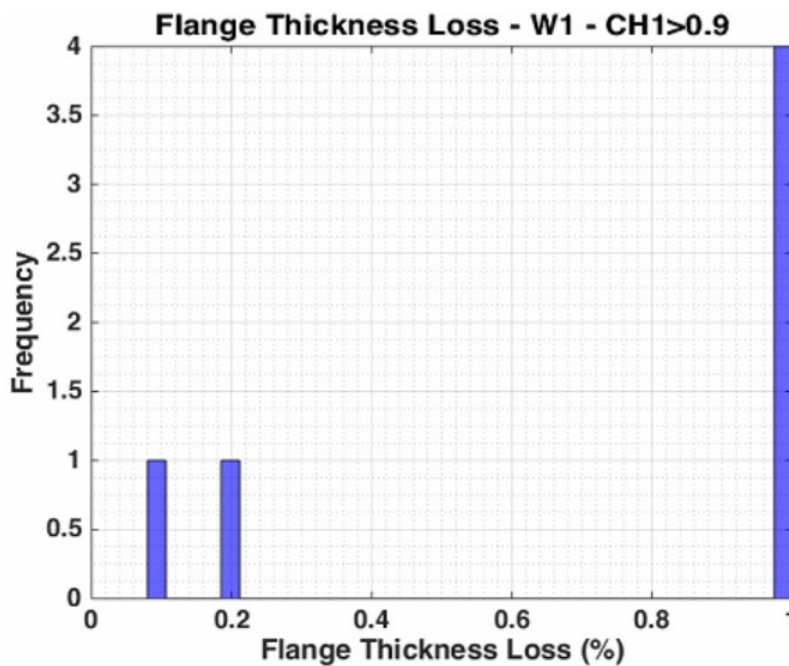


Figure 69: Flange thickness loss distribution for CH1>0.9 - CTDOT

For beam ends which CH1 is less than 0.3H, the thickness loss on the flanges tended to be small. This was different for cases which CH1 is greater than 0.9H, which resulted in a thickness loss of almost 100%. This allowed our team to assume the beams described by W1 patterns present the two patterns described in Table 75.

Table 75: Summary of extreme scenarios of W1 pattern - CTDOT

#	Pattern	CH1	CL1	tloss/tweb	Cf	tloss/tflange
1	W1	(0,0.4]	(0,2.5]	(0, 0.5]	(0,2.5]	[0.1,0.6]
2	W1	1	(0,1]	(0,0.4]	(0,1]	[0.9, 1]

Based on Table 75, our team was able to plot the extreme corrosion scenarios for pattern W1.

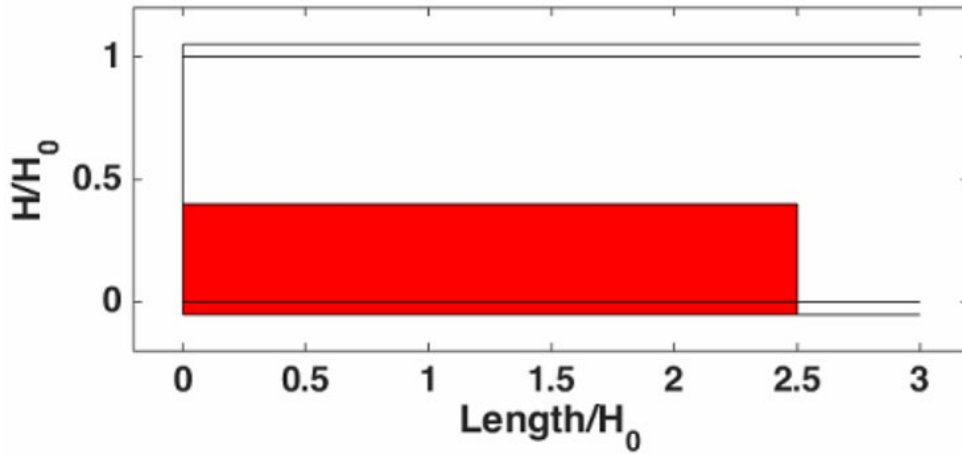


Figure 70: Extreme scenario for pattern W1 - CTDOT

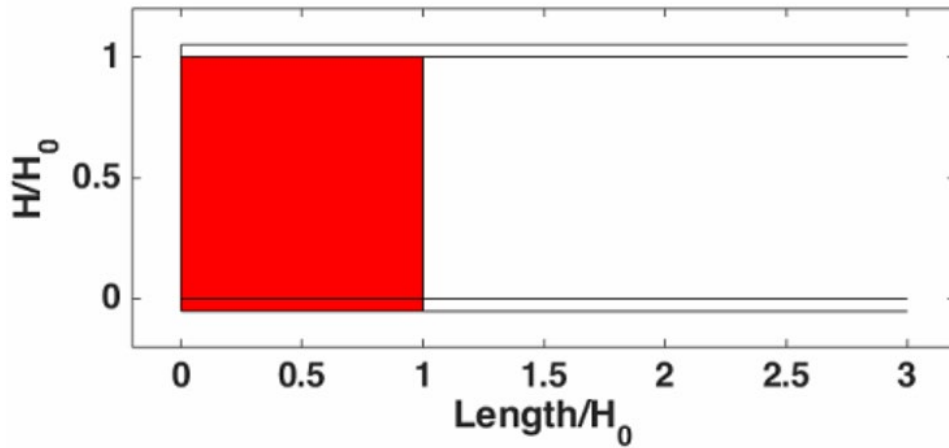


Figure 71: Extreme scenario for pattern W1 - CTDOT

11.1.2.3. Holes

The frequency of hole appearance is portrayed in Table 76.

Table 76: Holes and patterns for beams without a diaphragm - CTDOT

	Number	No Hole	M1	M2	M3	M4	M1 and M2	M1 and M3	M2 and M4
W1	309	290	3	1	2	2	0	1	0
W2	6	5	0	0	0	1	0	0	0
W3	38	35	1	0	1	0	0	1	0
W4	33	30	2	0	1	0	0	0	0
W5	34	34	0	0	0	0	0	0	0
W6	2	2	0	0	0	0	0	0	0

It is imperative to acknowledge that corrosion holes are frequently reported just in the notes of these reports. This means that, although more holes have been reported in the provided reports, not all corrosion holes had dimensions or pictures. For this reason, they were not able to be accounted for in our database.

The web thickness loss distribution for beam ends with M1 holes is:

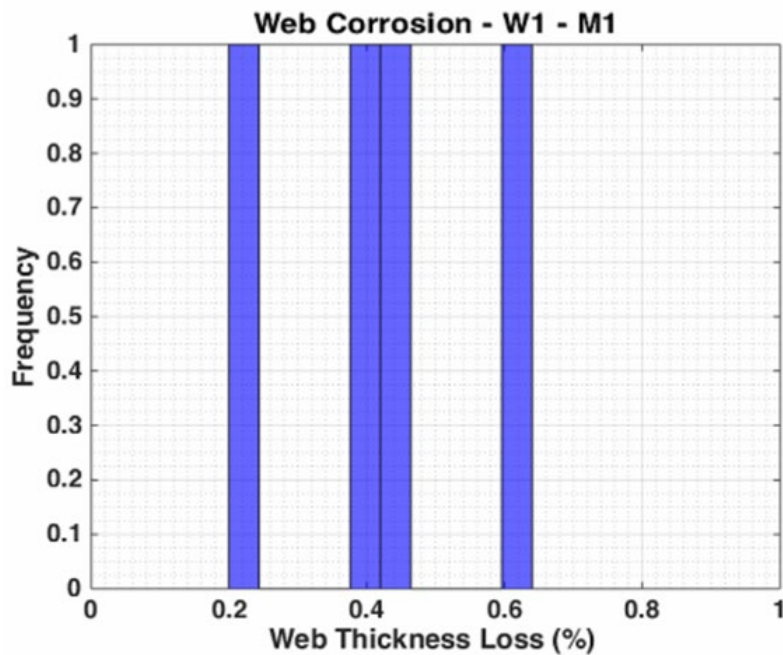


Figure 72: Web thickness loss for beam ends with M1 holes - CTDOT

The web thickness loss distribution for beam ends with M2 holes is:

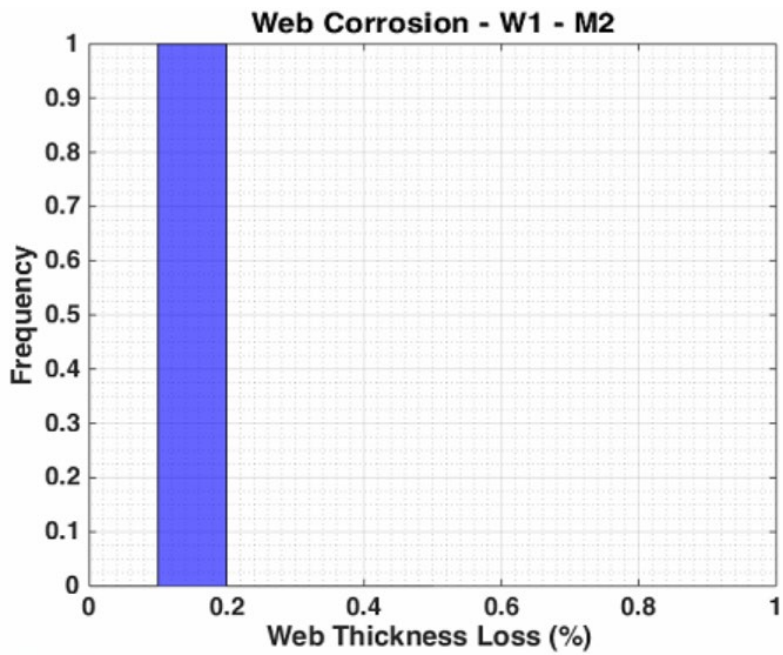


Figure 73: Web thickness loss for beam ends with M2 holes - CTDOT

The web thickness loss distribution for beam ends with M3 holes is:

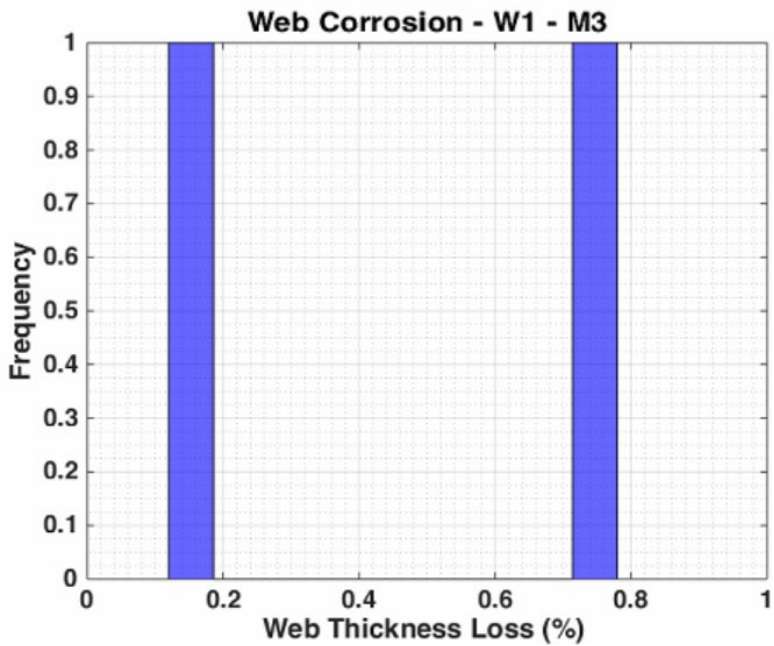


Figure 74: Web thickness loss for beam ends with M3 holes - CTDOT

The web thickness loss distribution for beam ends with M4 holes is:

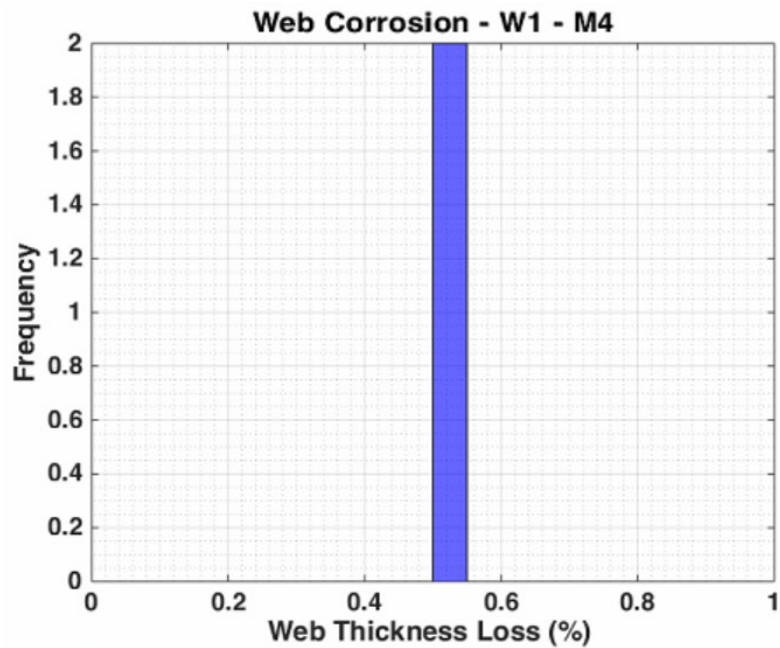


Figure 75: Web thickness loss for beam ends with M4 holes - CTDOT

From Figure 72, Figure 73, Figure 74, and Figure 75 is not possible to determine the thickness in which the holes will appear. While this is a clear observation, the figures hint that corrosion holes can appear even for cases in which the thickness loss is not extreme. As a result of this, and due to the small amount of data regarding corrosion holes, it is not possible to define any trend or try to make any prediction of what causes the holes to appear.

11.1.3. Pattern W2

11.1.3.1. Web corrosion

The W2 corrosion pattern was observed only six times throughout the reports from the state of Connecticut. In a similar way to how W1 was recorded, the measurements for the W2 pattern provided in the reports were normalized by H0. Figure 76, Figure 77 and Figure 78 depict the distribution of the parameters of pattern W2. The parameters for the corrosion patterns can be found with corresponding diagrams in Section 1.5 *Corrosion Patterns* of this report.

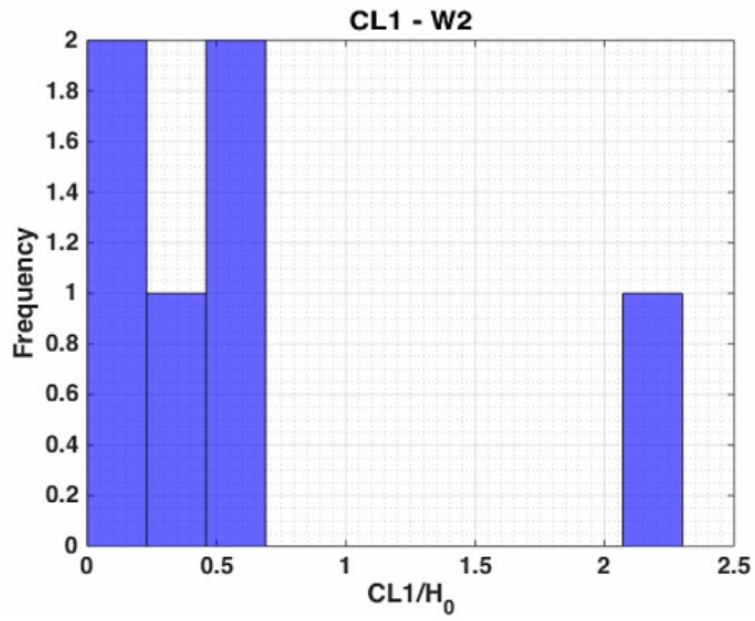


Figure 76: CL1 distribution for W2 pattern - CTDOT

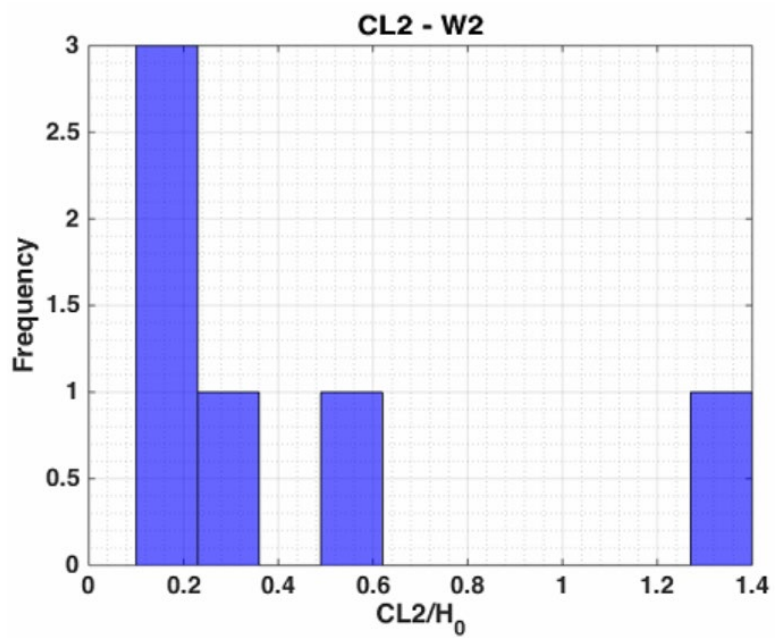


Figure 77: CL2 distribution for W2 pattern - CTDOT

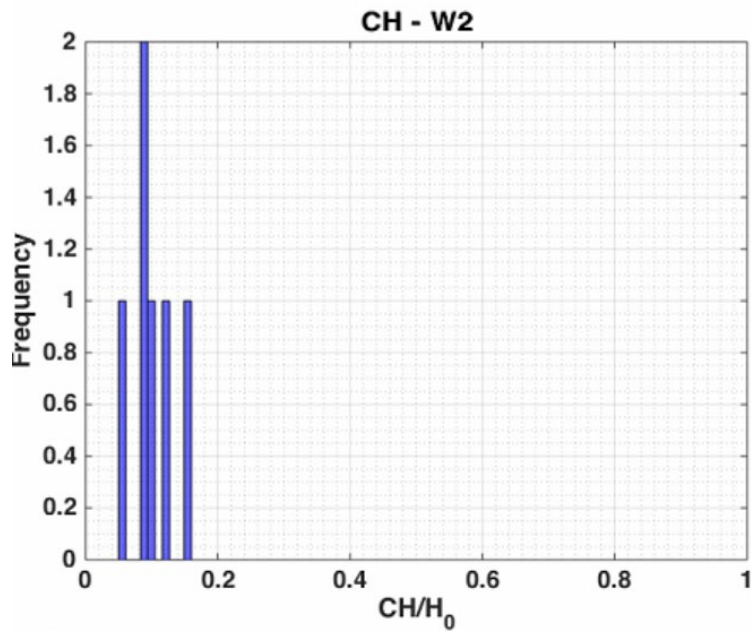


Figure 78: CH distribution for W2 pattern - CTDOT

The distribution of web thickness loss depicted in Figure 79.

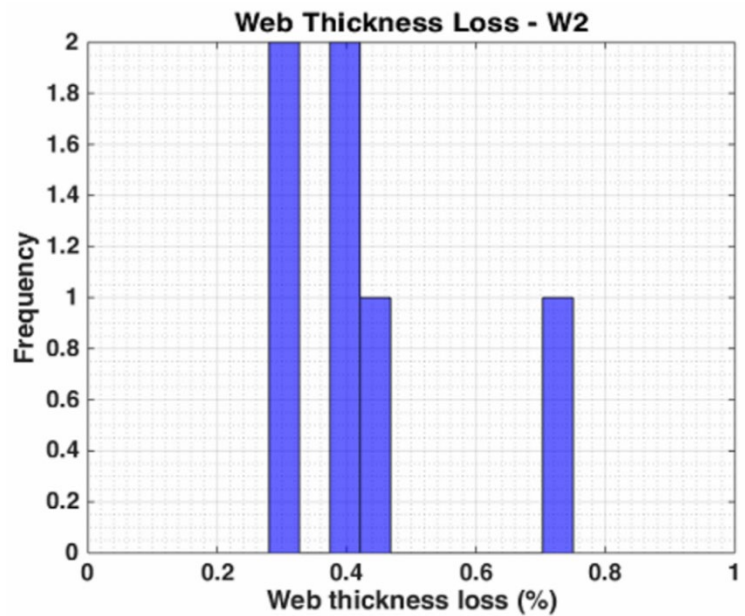


Figure 79: Web thickness loss for W2 pattern - CTDOT

From Figure 76, there is a trend present regarding CL1, as $CL1 < 0.6H0$ for most of the beam ends reported. This allowed our team to analyze the behavior of the other parameters given that $CL1 < 0.6H0$.

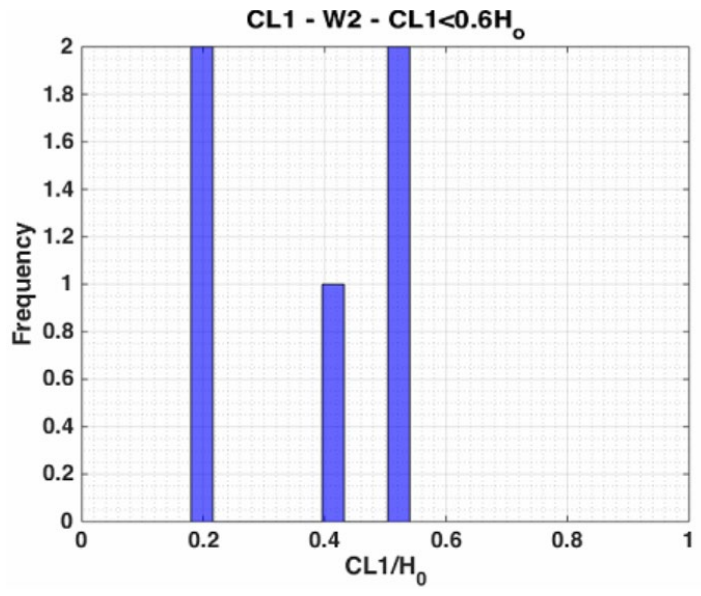


Figure 80: CL1 distribution for W2 pattern and CL1<0.6H - CTDOT

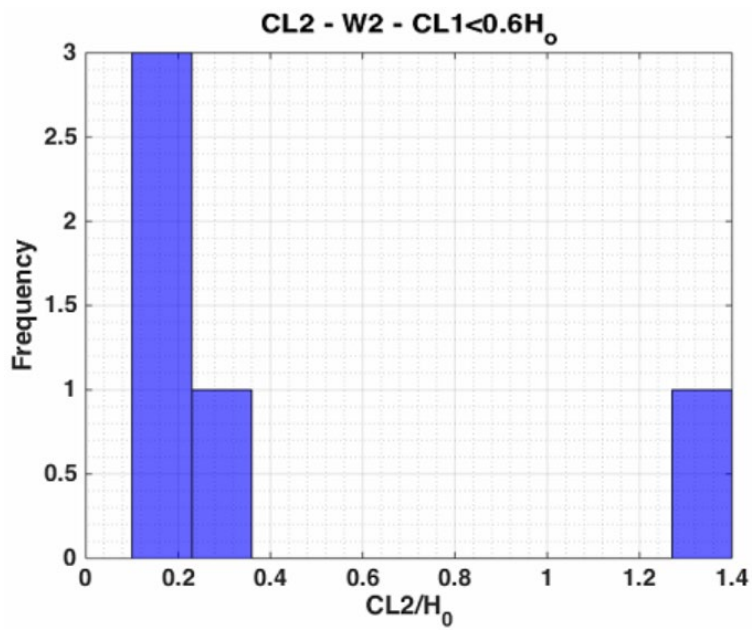


Figure 81: CL2 distribution for W2 pattern and CL1<0.6H - CTDOT

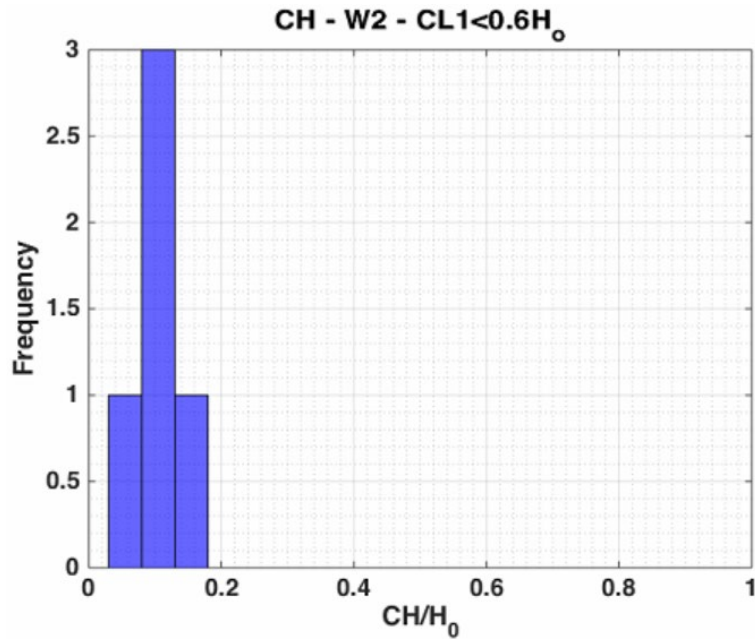


Figure 82: CH distribution for W2 pattern and CL1<0.6H - CTDOT

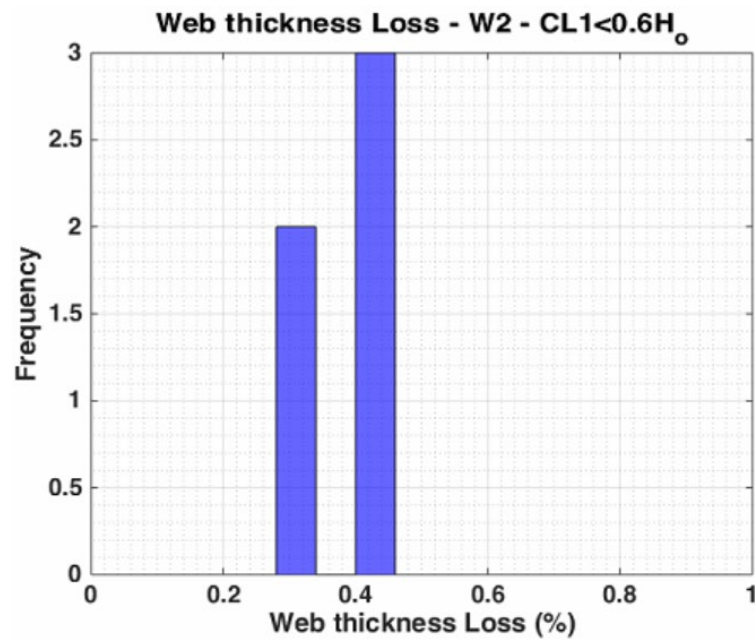


Figure 83: Web thickness loss for W2 pattern and CL1<0.6H - CTDOT

Therefore, it is valid to assume that $0 < CL_1 \leq 0.6 H_0$, $0.1H_0 \leq CL_2 \leq 0.4H_0$, $0 < CH \leq 0.2H_0$ and $0.3 \leq \frac{t_{loss}}{t_{web}} \leq 0.45$. The extreme scenario for W2 is depicted in Figure 84.

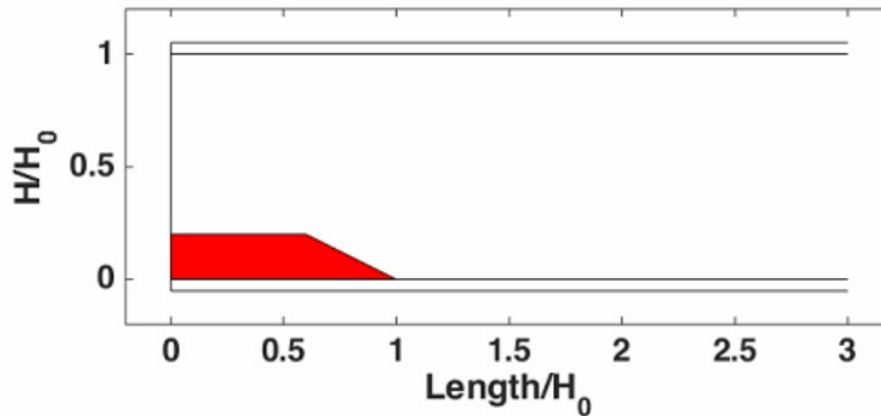


Figure 84: Extreme corrosion scenario for pattern W2 - CTDOT

11.1.3.2. Flange corrosion

It was not possible to perform flange corrosion analysis for pattern W2 as no information about corrosion in the flanges was provided for the beam ends identified with a W2 corrosion pattern.

11.1.3.3. Holes

Only a single hole was reported for this pattern. The topology of the recorded hole is an M4 corrosion hole pattern. The dimensions for the given hole are: $a = 0.18$, $b = 1.42$, and $c = 1.36$.

11.1.4. Pattern W3

11.1.4.1. Web corrosion

The analysis began by studying the distribution of CH2, depicted in Figure 85. The parameters for the corrosion patterns can be found with corresponding diagrams in Section 1.5 *Corrosion Patterns* of this report.

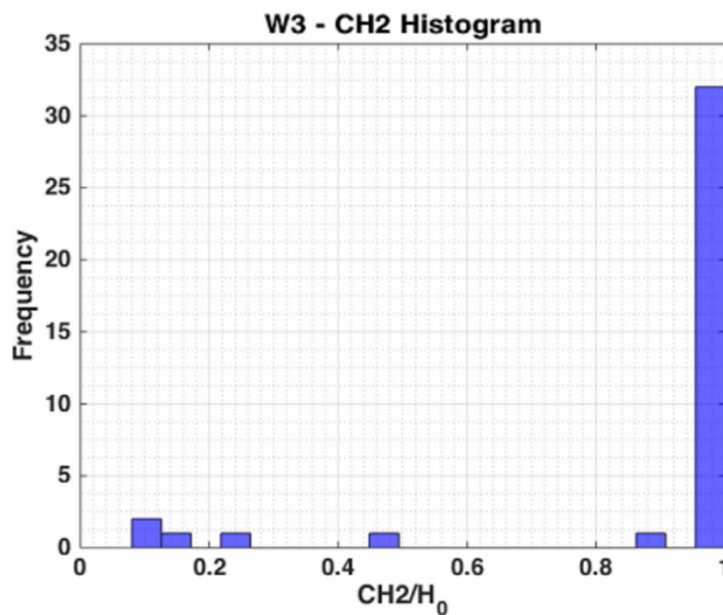


Figure 85: CH2 distribution for W3 pattern - CTDOT

A single trend for when $CH_2 > 0.9H_0$ is clearly observed in Figure 85. Given that $CH_2 > 0.9H_0$, our team could plot the distribution of the other parameters of the corrosion pattern given that $CH_2 > 0.9H_0$. This is shown in the following figures.

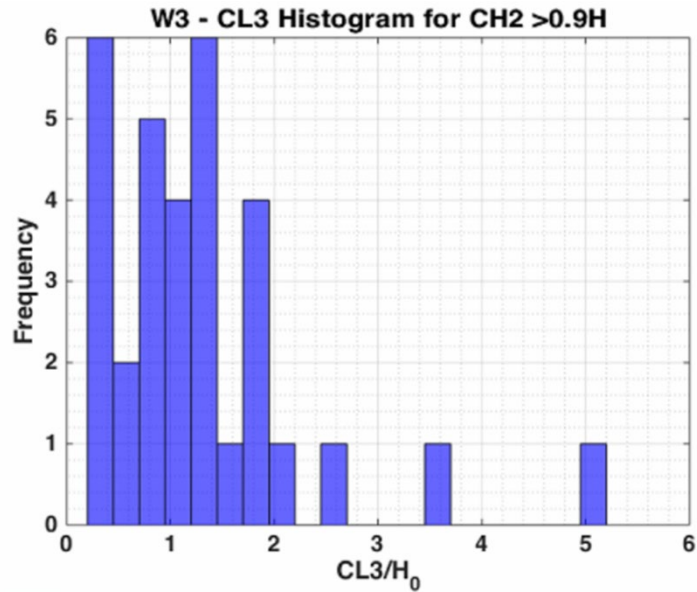


Figure 86: CL3 distribution for W3 pattern - CTDOT

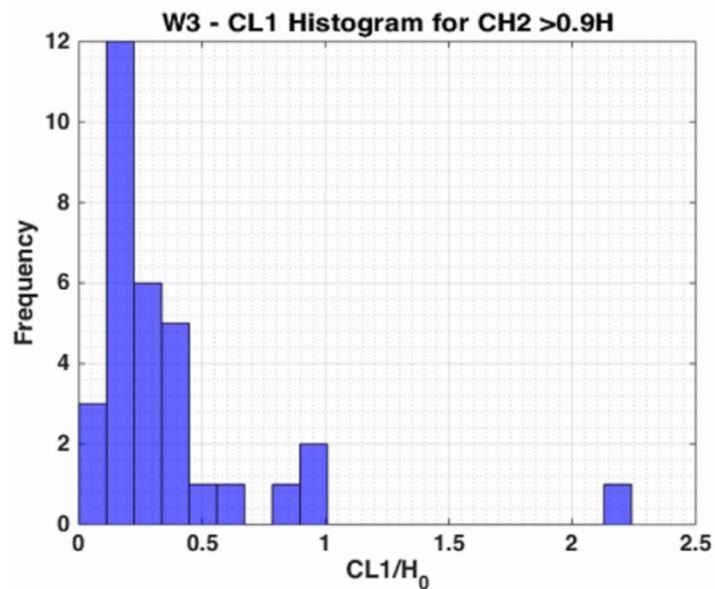


Figure 87: CL1 distribution for W3 pattern and $CH_2 > 0.9H$ - CTDOT

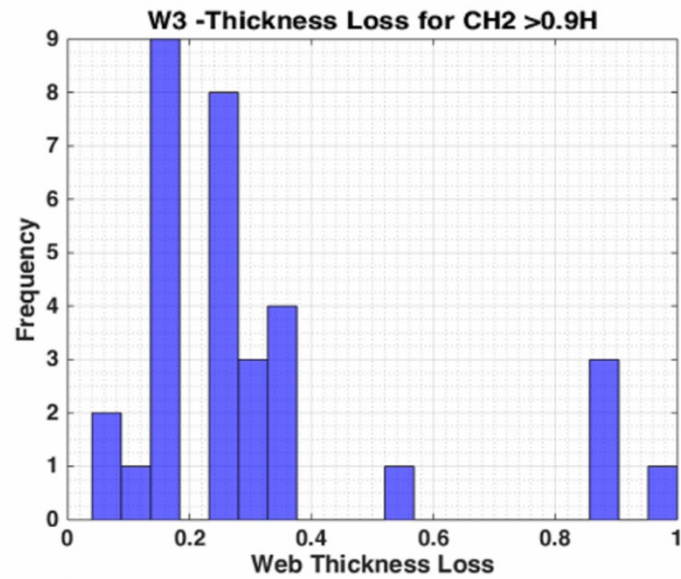


Figure 88: Web thickness loss distribution for W3 pattern and CH2>0.9H - CTDOT

From the last figures, our team was able to conclude that:

$$\begin{aligned}
 0 < CH_1 &\leq 0.4H_0 \\
 0.9H_0 &\leq CH_2 \leq 1H_0 \\
 0 < CH_3 &\leq 0.4H_0 \\
 0 < CL_1 &\leq 1H_0 \\
 0 < CL_2 &\leq 1.5H_0 \\
 0 < CL_3 &\leq 2.5H_0 \\
 0 < \frac{t_{loss}}{t_{web}} &\leq 0.4
 \end{aligned}$$

This resulted in the extreme scenario for pattern W3:

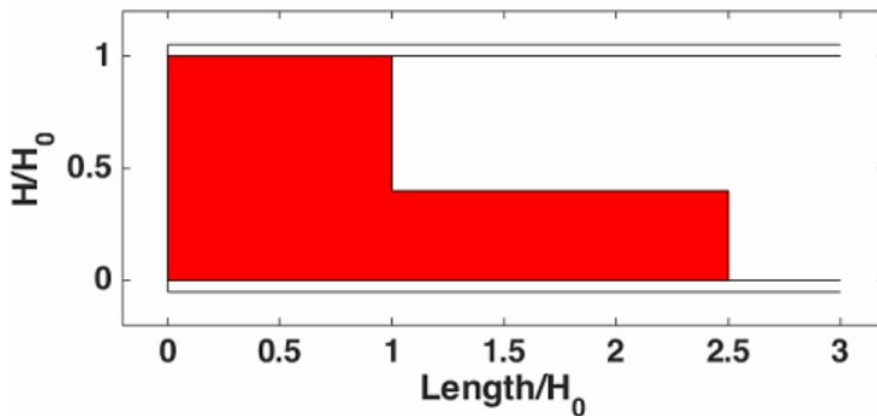


Figure 89: Extreme corrosion scenario for W3 pattern – CTDOT

11.1.4.2. Flange corrosion

The ratio between the length of corrosion in the flanges and the total corroded length (CL3) is depicted in Figure 90. Figure 91 depicts the raw corrosion length in the flange.

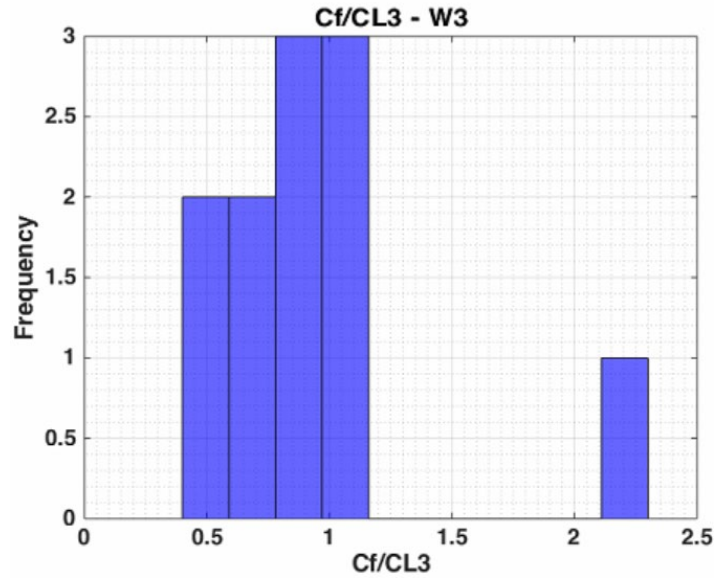


Figure 90: Ratio between corrosion length in the flanges and CL3 for W3 pattern - CTDOT

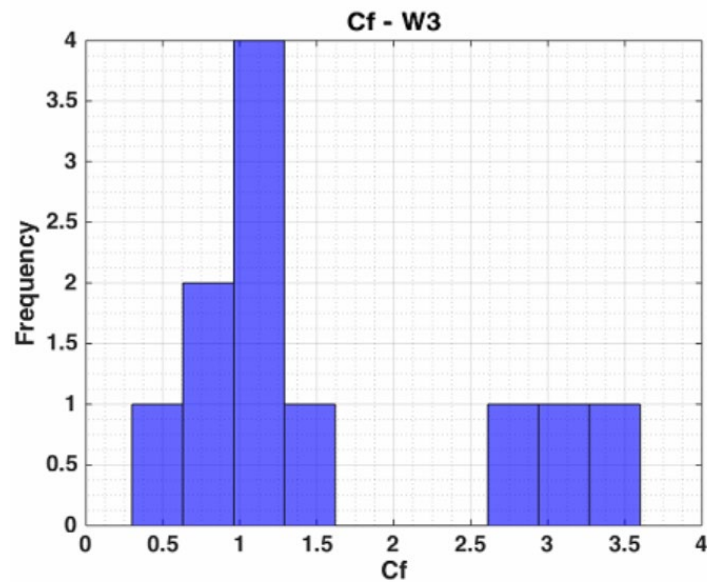


Figure 91: Raw corrosion length in the flanges for W3 pattern - CTDOT

Figure 92 depicts the distribution of the thickness loss in the flanges. Similar to the previous sections, our team could assess the distribution of thickness loss for $CH_2 > 0.9$. This case is depicted on Figure 93.

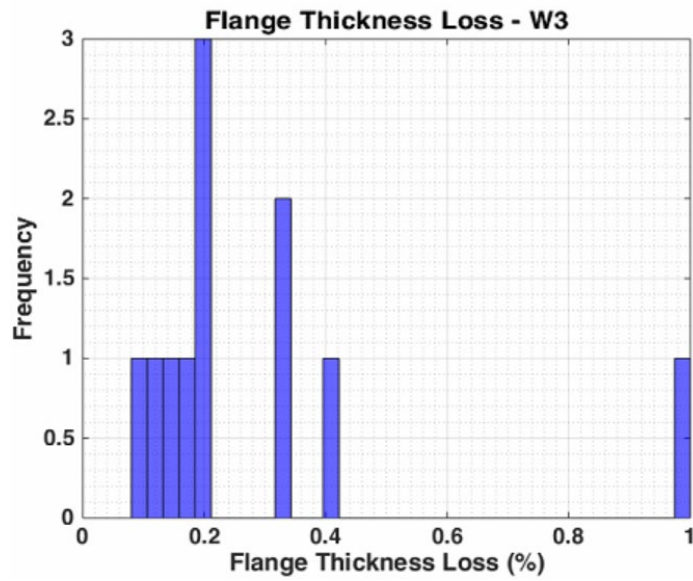


Figure 92: Flange thickness loss for W3 pattern - CTDOT

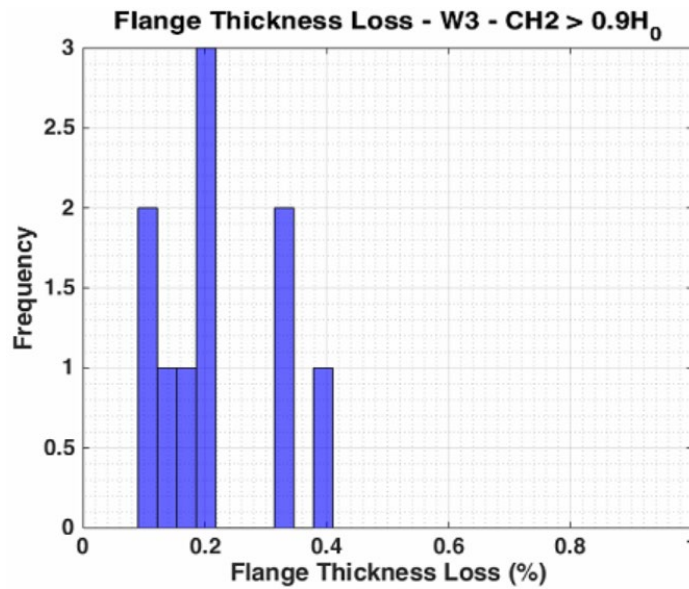


Figure 93: Flange thickness loss for W3 pattern and CH2>0.9H - CTDOT

As a result, for the case of CH2>0.9H0, our team assumed that $0.1 < \frac{t_{loss}}{t_{flange}} < 0.4$.

11.1.4.3. Holes

Only four corrosion holes were observed in the reports provided by CTDOT. Additionally, two of the holes were observed in the same beam end. Due to the limited amount of information, the research team was not able to draw conclusions or trends from the information provided.

11.1.5. Pattern W4

11.1.5.1. Web Corrosion

Like the other studies conducted, this study started by analyzing CH2, depicted in Figure 94. The parameters for the corrosion patterns can be found with corresponding diagrams in Section 1.5 *Corrosion Patterns* of this report.

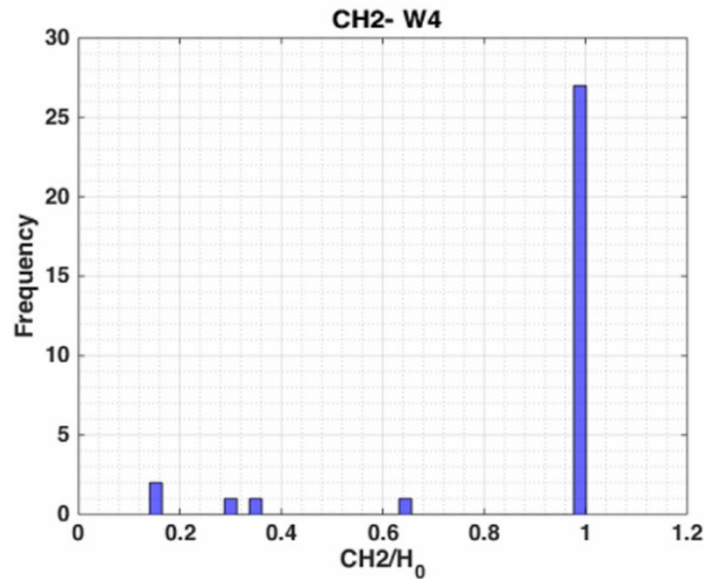


Figure 94: CH2 distribution for W4 pattern - CTDOT

Figure 94 clearly depicts that CH2 is equal to 1 for most beam ends reported. Using this information, our team was able to further analyze the other parameters for CH2>0.9H0. The following figures depict the behavior of the other parameters for CH2>0.9H0.

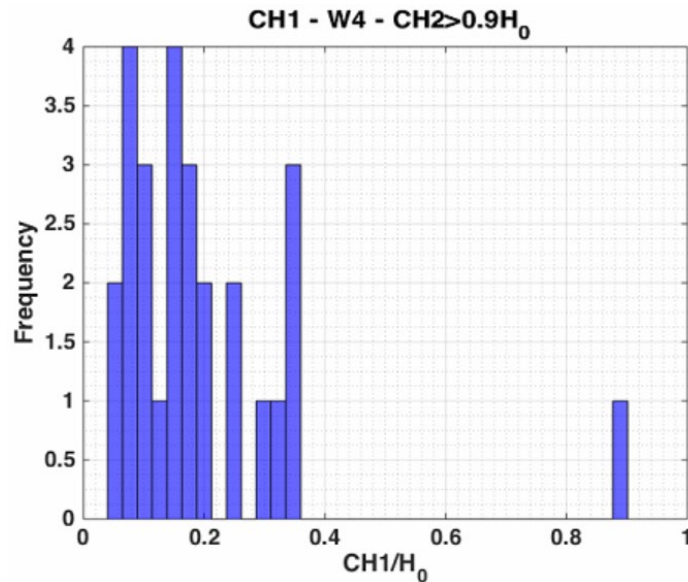


Figure 95: CH1 distribution for W4 pattern and CH2>0.9H - CTDOT

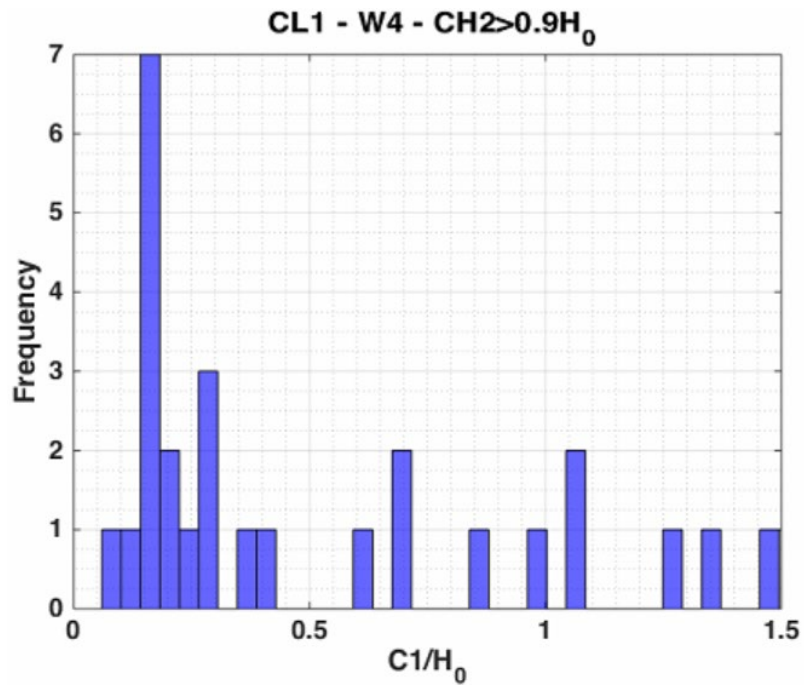


Figure 96: CL1 distribution for W4 pattern and CH2>0.9H - CTDOT

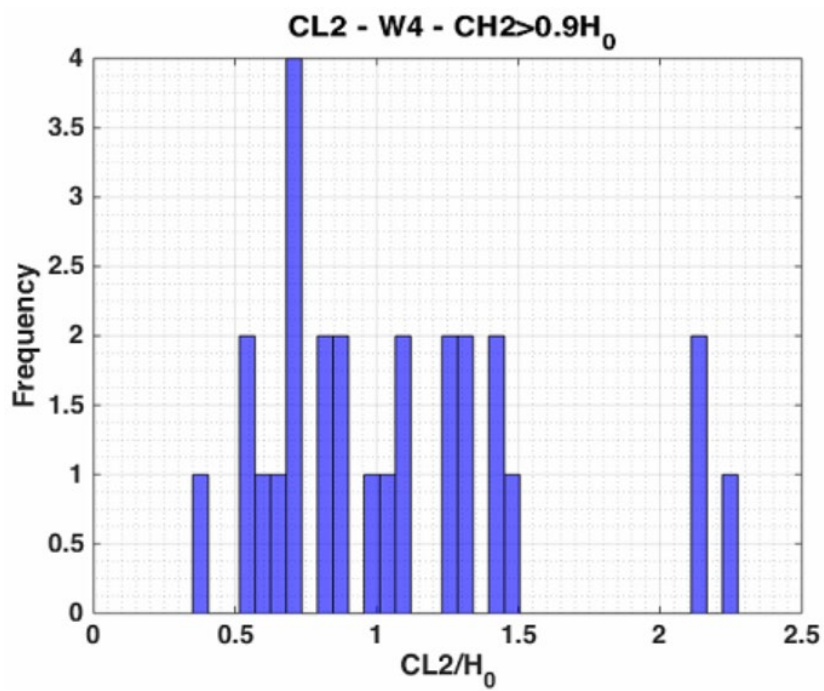


Figure 97: CL2 distribution for W4 pattern and CH2>0.9H - CTDOT

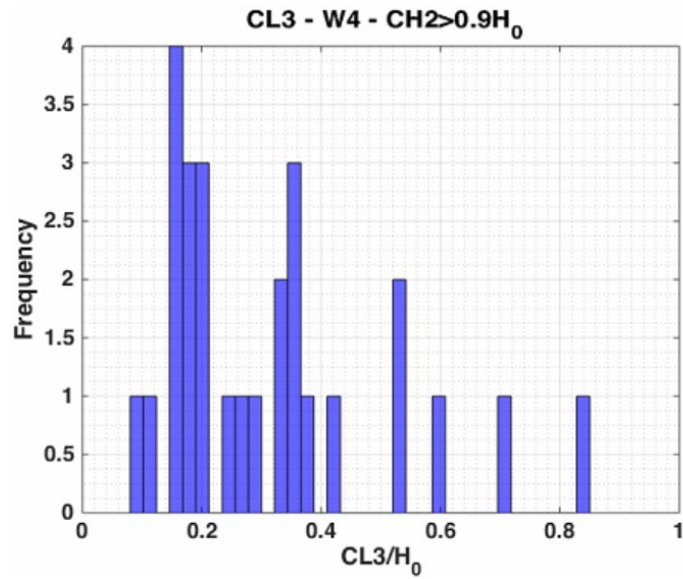


Figure 98: CL3 distribution for W4 pattern and CH₂>0.9H - CTDOT

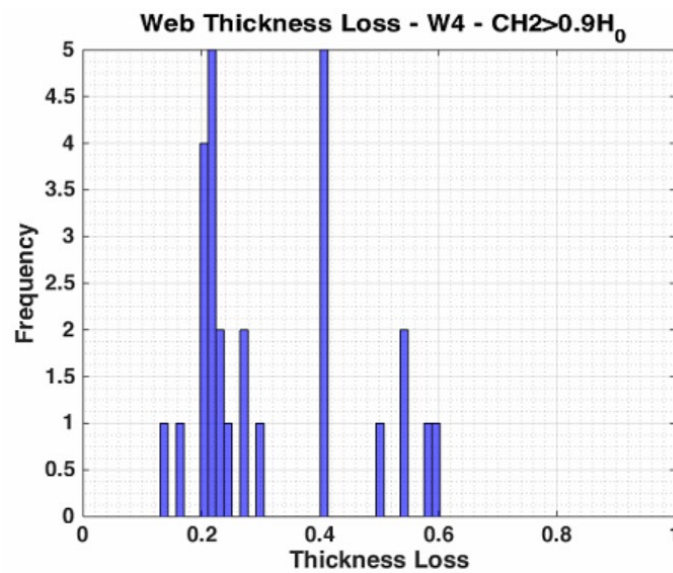


Figure 99: Web thickness loss distribution for W4 pattern and CH₂>0.9H - CTDOT

From these figures, our team was able to conclude that:

$$\begin{aligned}
 0 < CH_1 &\leq 0.4H_0 \\
 0.9H_0 &\leq CH_2 \leq 1H_0 \\
 0 < CL_1 &\leq 1H_0 \\
 0.5H_0 < CL_2 &\leq 1.5H_0 \\
 0.1H_0 < CL_3 &\leq 0.5H_0 \\
 0.1 \leq \frac{t_{loss}}{t_{web}} &\leq 0.6
 \end{aligned}$$

Thus, the extreme scenario for pattern W4 is:

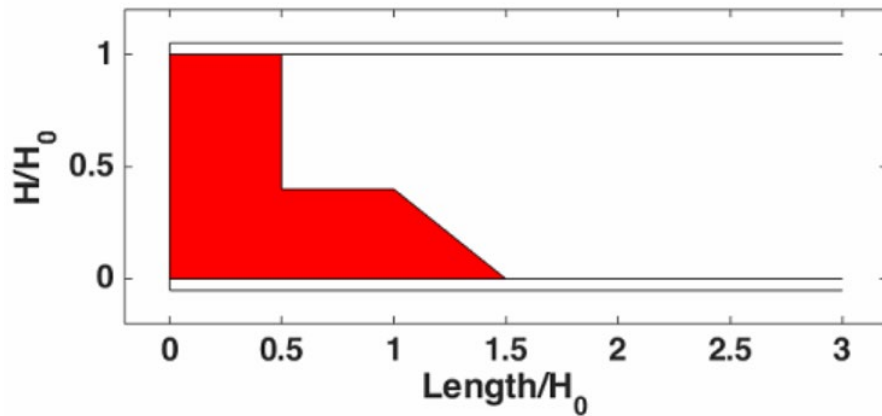


Figure 100: Extreme corrosion scenario for W4 pattern - CTDOT

11.1.5.2. Flange Corrosion

The information regarding flange corrosion combined with the W4 corrosion pattern was rarely observed in the reports analyzed from CTDOT. For this reason, the research team was not able to draw any conclusion nor trends from the available data. The histogram of the two observed flange corrosion scenarios can be found in Figure 101.

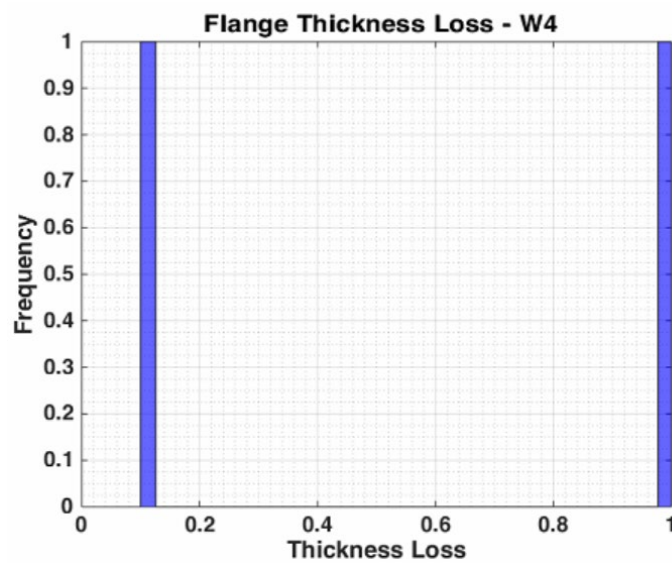


Figure 101: Flange thickness loss for W4 pattern - CTDOT

11.1.5.3. Holes

For the corrosion combination of W4 with holes, only three holes were observed with the W4 pattern. It is important to note that the data here is not enough in order to draw conclusions via the histograms in Figure 102, Figure 103, Figure 104, and Figure 105. These depict the dimensions of the holes observed.

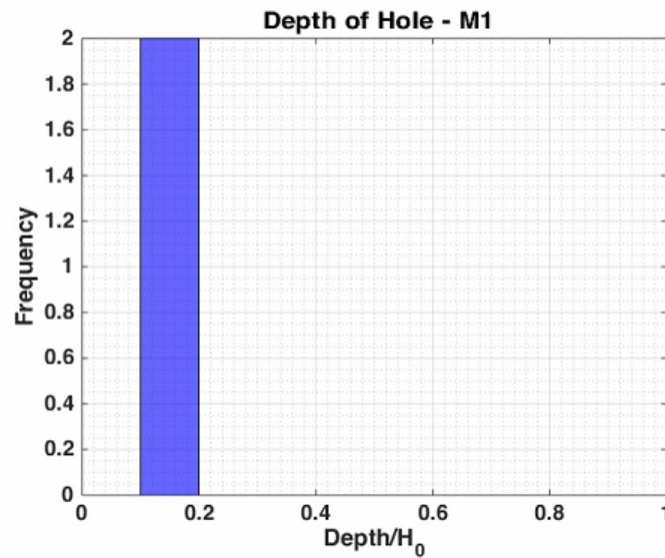


Figure 102: Depth of hole M1 combined with W4 pattern - CTDOT

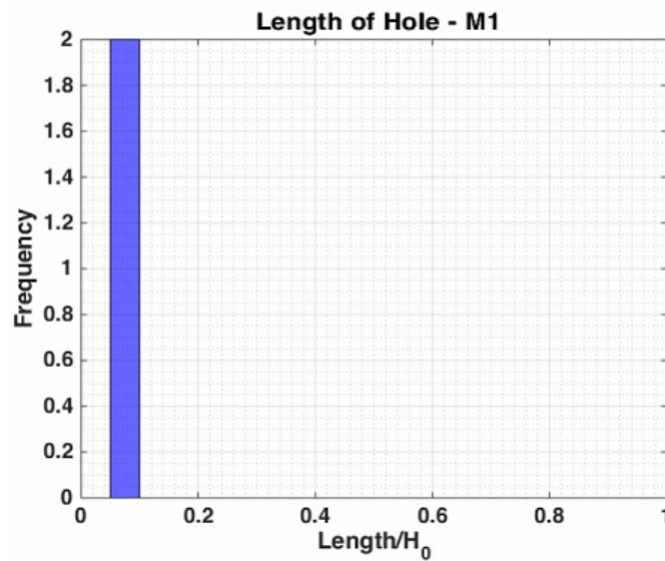


Figure 103: Length of hole M1 combined with W4 pattern - CTDOT

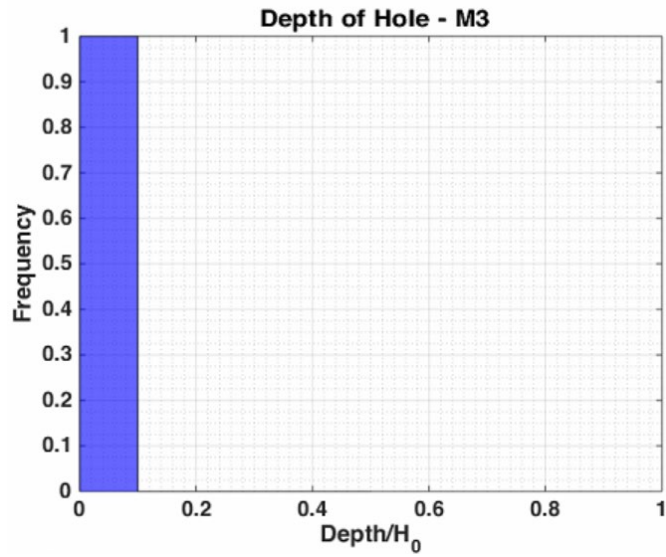


Figure 104: Depth of hole M3 combined with W4 pattern - CTDOT

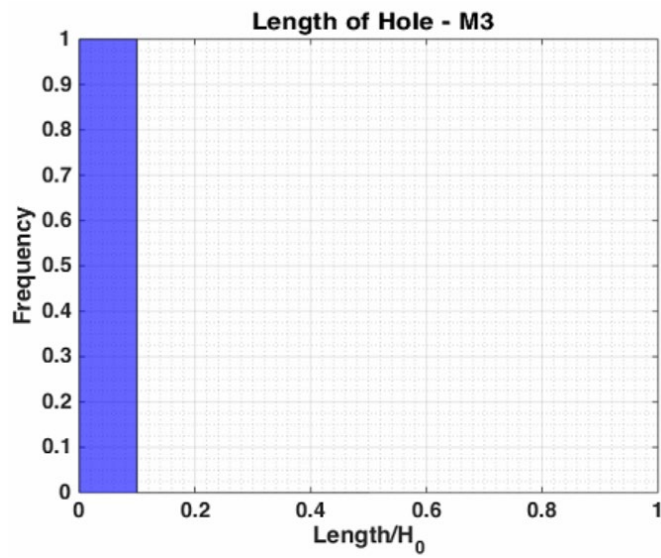


Figure 105: Length of hole M3 combined with W4 pattern - CTDOT

11.1.6. Pattern W5

11.1.6.1. Web corrosion

The study began by analyzing the height of corrosion. Figure 106 depicts the distribution of CH1 for pattern W5. The parameters for the corrosion patterns can be found with corresponding diagrams in Section 1.5 *Corrosion Patterns* of this report.

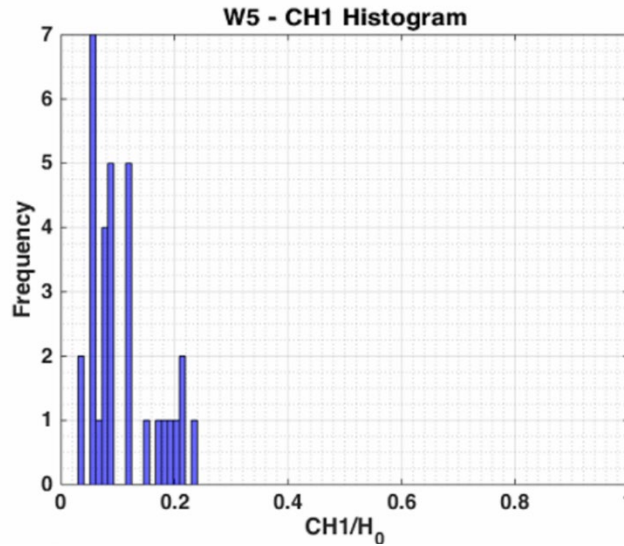


Figure 106: CH1 distribution of W5 pattern for beams without a diaphragm – CTDOT

Figure 106 clearly depicts that CH1 tends to be smaller than 0.2H0. This means that when analyzing the behavior of CL1 for when CH1 < 0.2H0, we found:

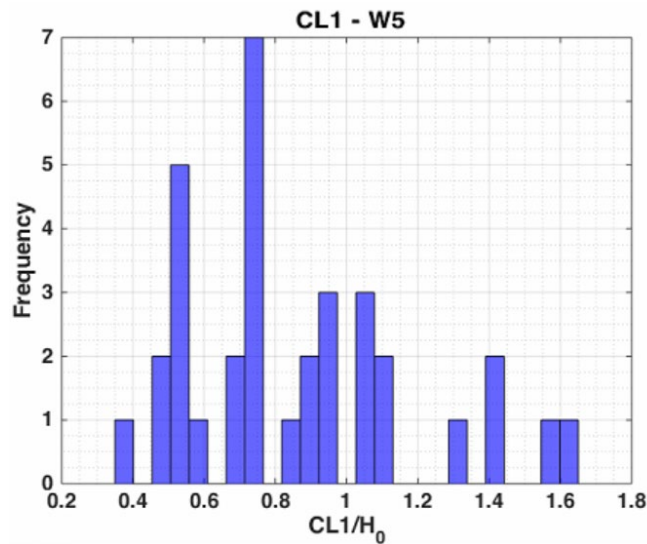


Figure 107: CL1 distribution of W5 pattern for beams without a diaphragm – CTDOT

Figure 108 depicts the web thickness loss for $CH_2 > 0.9H_0$:

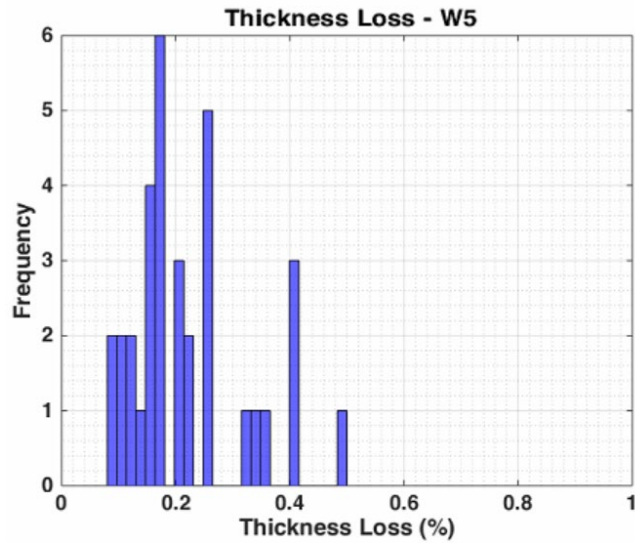


Figure 108: Web thickness loss distribution of W5 pattern for beams without a diaphragm – CTDOT

From the last figures, our team concluded that:

$$0 < CH_1 \leq 0.2H_0$$

$$0.4H_0 \leq CL_1 \leq 1.5H_0$$

$$0.1 \leq \frac{t_{loss}}{t_{web}} \leq 0.5$$

The extreme scenario for W5 pattern is:

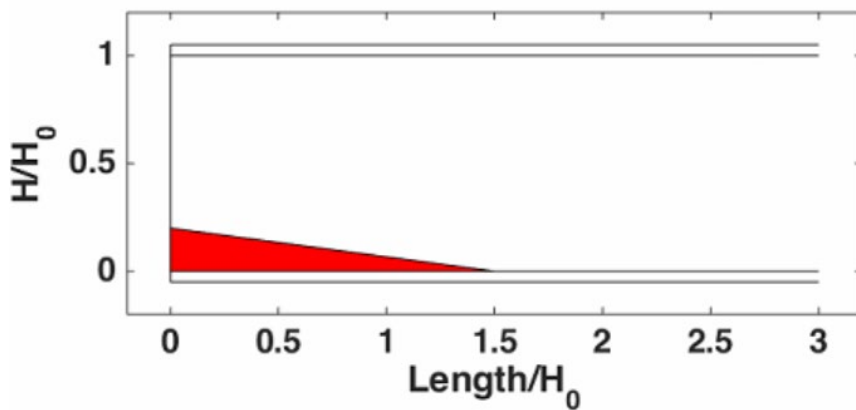


Figure 109: Extreme corrosion scenario for pattern W5 - CTDOT

11.1.6.2. Flange corrosion

Data regarding flange corrosion was very limited in the reports analyzed. Only two beam ends had a combination of the W5 corrosion pattern and flange corrosion. For this reason, the research team was not able to draw conclusion regarding flange corrosion.

11.1.6.3. Holes

No hole corrosion patterns combined with the W5 corrosion pattern were observed in the bridge inspection reports provided by CTDOT.

11.2. Maine

11.2.1. Introduction

As discussed in previous sections, the reports from Maine DOT do not provided specific information regarding corrosion. Due to the absence of measurements, photographic records and sketches, the research team was not able to identify the corrosion patterns from the inspection reports provided.

While this was the case, the reports often reported information regarding thickness loss in the flanges and webs. It is worthwhile pointing out, however, that the information presented in the reports usually does not refer to a specific beam of the bridge. For these cases, the research team opted to store the information as if it referred to a single beam of the bridge, instead of assuming it a common feature for all the beams of the bridge. This means that several of the bridge inspection reports compiled by the research team comprise the information of a single beam.

The results are presented state by state as the amount of beam ends varies considerably from one state to the other. From the reports provided by MaineDOT, the research team was able to compile 39 beam ends. It is important to note that none of the beam ends reported presented diaphragms.

11.2.2. Web Corrosion

Most of the reports presented information regarding web thickness loss. The information is provided without specifically referring to a beam. Figure 110 depicts the histogram of web thickness loss for the beams ends provided by MaineDOT.

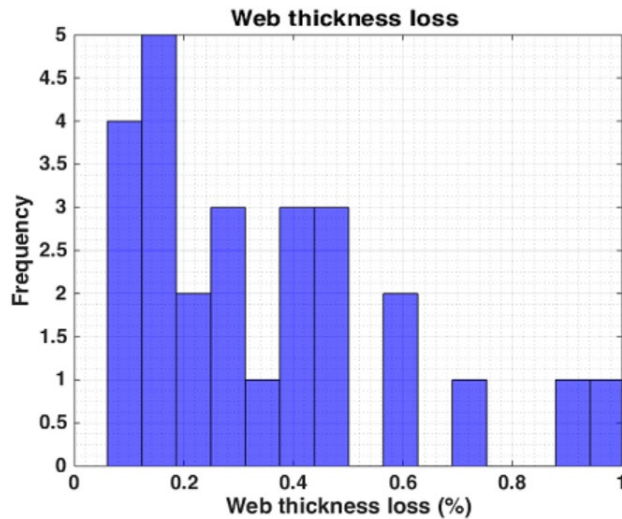


Figure 110: Web thickness loss histogram from the beam ends compiled - MaineDOT

The research team was not able to gather information regarding corrosion length or corrosion height from the reports provided by MaineDOT. These parameters would be beneficial to have as they assist the team in developing common corrosion patterns and shapes.

11.2.3. Flange Corrosion

Most of the reports that contained information regarding the web thickness loss also included information regarding flange thickness loss. More precisely, 29 out of the 39 beam ends compiled presented information regarding corrosion in the flanges. Figure 111 and Figure 112 depict the flange thickness loss for the bottom and top flanges, respectively.

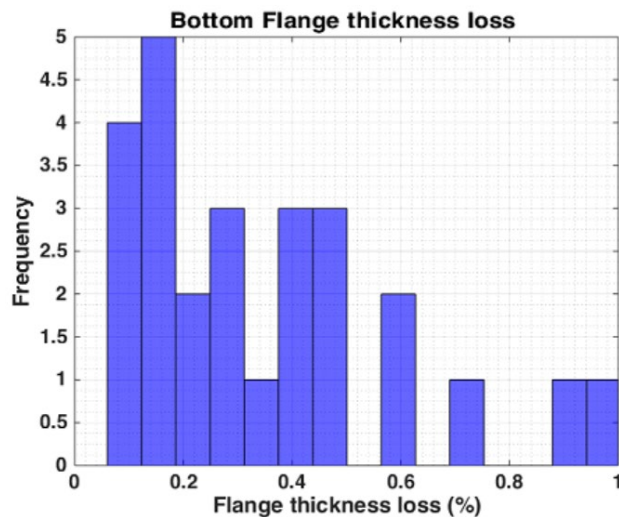


Figure 111: Bottom flange thickness loss histogram from the beam ends compiled - MaineDOT

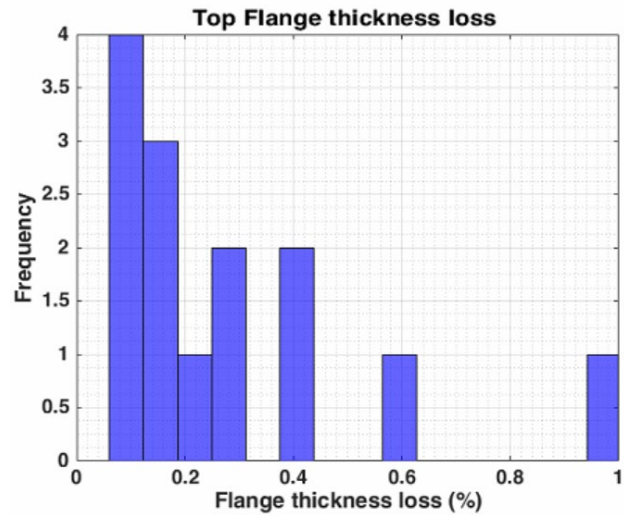


Figure 112: Top flange thickness loss histogram from the beam ends compiled - MaineDOT

The comparison between Figure 111 and Figure 112 clearly shows that the thickness loss of top flanges is smaller than the thickness loss of the bottom flanges. This is likely a result of how ice and water flow to the bottom flanges.

11.2.4. Holes

The holes documented in the inspection reports provided by MaineDOT always have measurements and dimensions. From the reports provided by MaineDOT, the research team was able to identify five holes among the beam ends. All the holes reported by the bridge inspection reports had pictures that clearly depicted the holes, allowing the research team to classify the beam end into a topology.

All five holes observed in the reports are M1. Additionally, Figure 113 and Figure 114 depict the dimensions of the holes observed in the bridge inspection reports from MaineDOT.

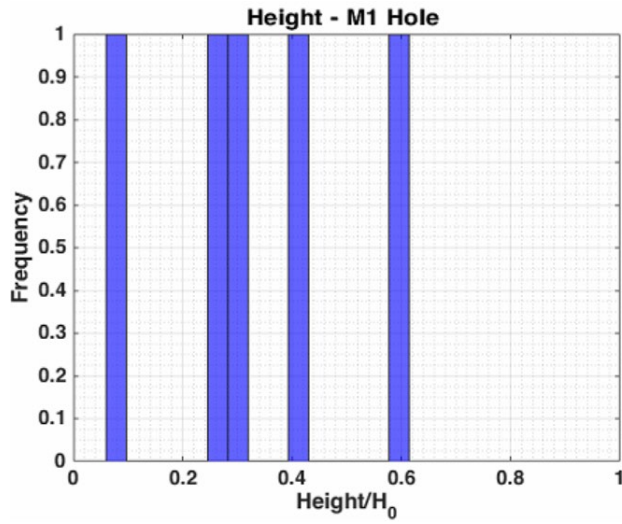


Figure 113: M1 web hole's height distribution of W1 web corrosion pattern for beams without a diaphragm - MaineDOT

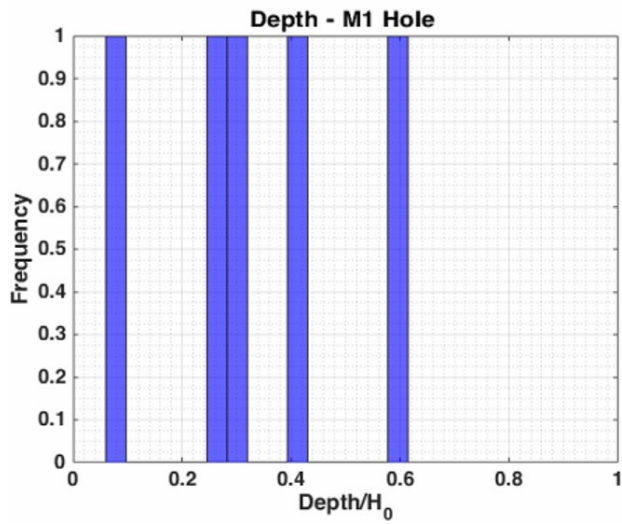


Figure 114: M1 web hole's depth distribution of W1 web corrosion pattern for beams without a diaphragm - MaineDOT

11.3. Massachusetts

11.3.1. Introduction

The data for Massachusetts was divided in two main categories, beams ends with a diaphragm and without a diaphragm. All the graphs in this part of the document represent the second case. Figure 115 contains the frequency of each of the defined corrosion patterns (the total amount of times each pattern appears in the reports).

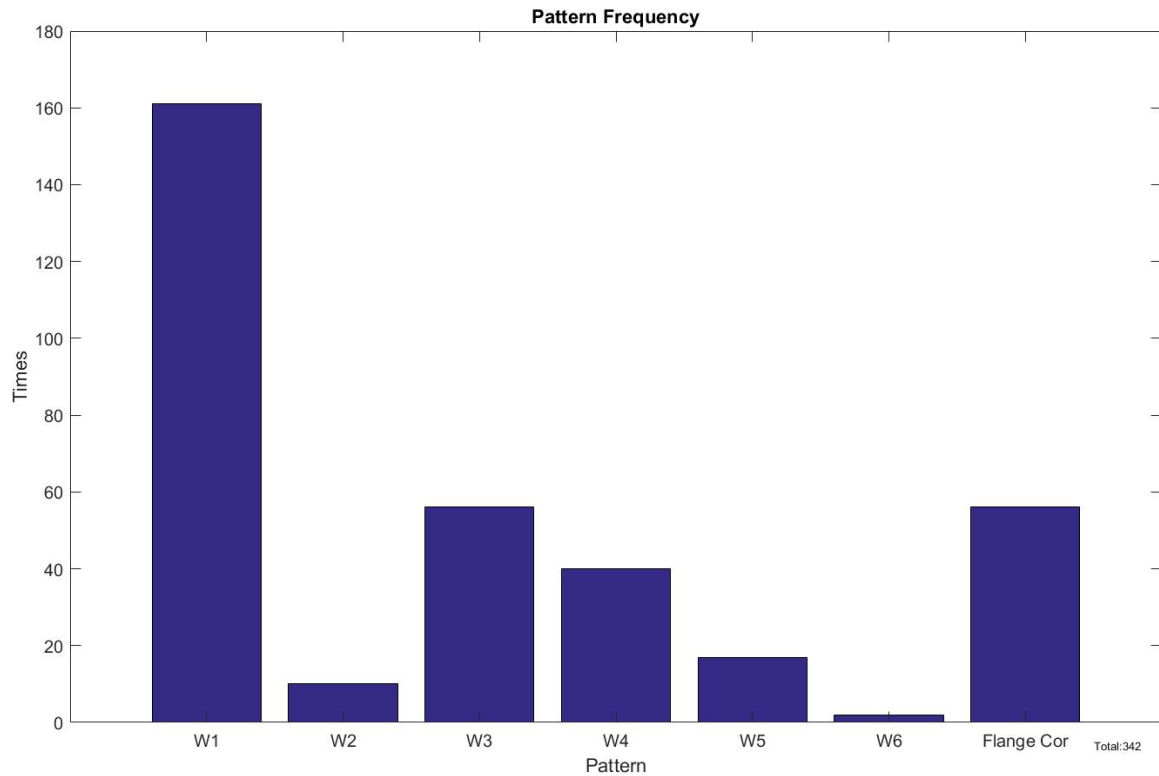


Figure 115: Web corrosion patterns distribution for beams without a diaphragm - MassDOT

For each web corrosion pattern, we have normalized the characteristic dimensions (CH_1 , CH_2 , CH_3 , CL_1 , CL_2 , CL_3) with the height H_0 , where $H_0 = H - 2t_f$.

11.3.2. Pattern W1

11.3.2.1. Web Corrosion

The distribution of CH_1 is shown in Figure 116. From this histogram, 2 main trends are noticed: either a) full height corrosion, or b) corrosion up to 30% of H_0 . The parameters for the corrosion patterns can be found with corresponding diagrams in Section 1.5 *Corrosion Patterns* of this report.

$$0 < CH_1 \leq 0.3H \text{ and } 0.9H \leq CH_1 \leq H$$

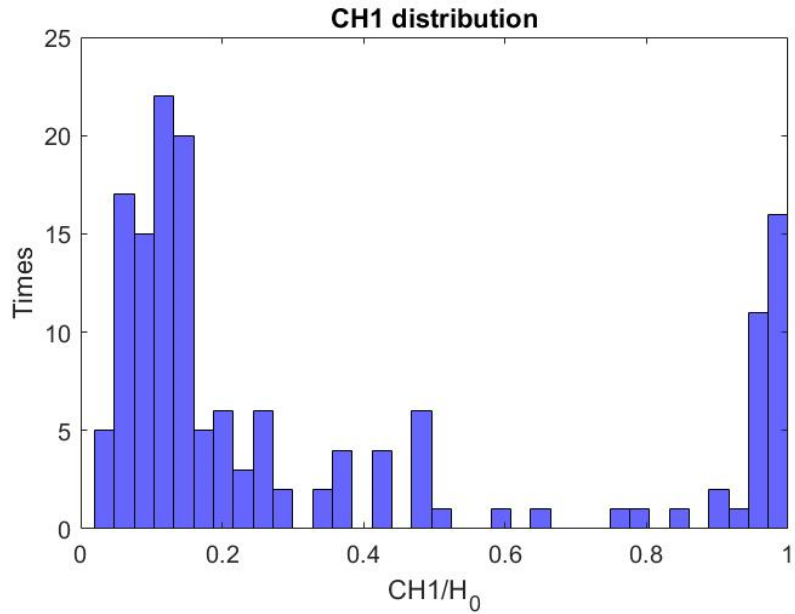


Figure 116: CH₁ distribution of W1 pattern for beams without a diaphragm - MassDOT

Similarly, the CL₁ distribution is shown in Figure 117. From this histogram, it is valid to say that most of the web corrosion length is up to 1.5 times the H₀.

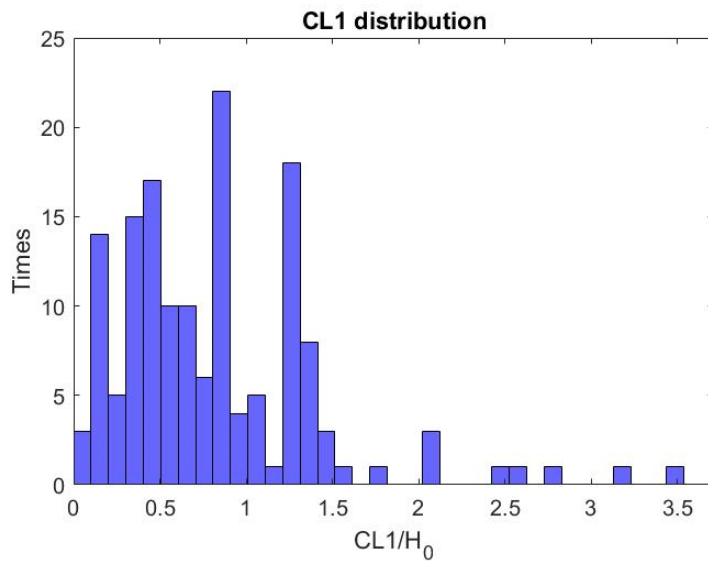


Figure 117: CL₁ distribution of W1 pattern for beams without a diaphragm - MassDOT

Figure 118 shows the ratio of CL₁/CH₁ which indicates that in general, the length of the corroded area is bigger than its height. Figure 119 focuses on the range 0-15 for the same distribution.

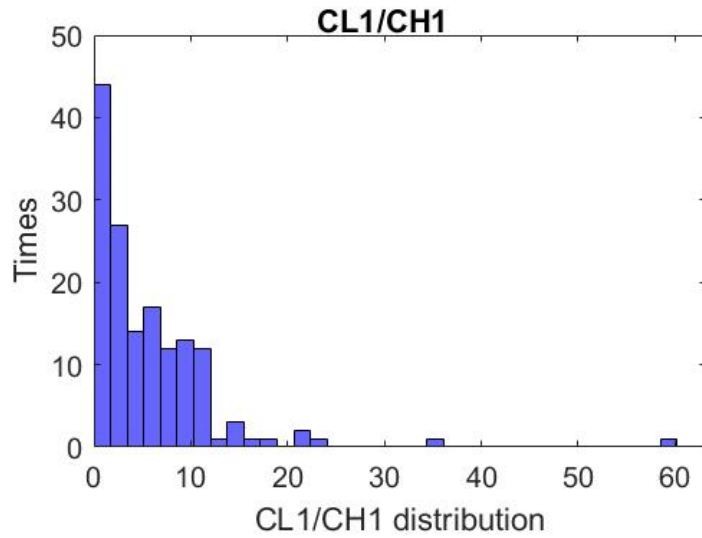


Figure 118: Ratio of corrosion length (CL_1) to corrosion height (CH_1) of W1 pattern for beams without a diaphragm - MassDOT

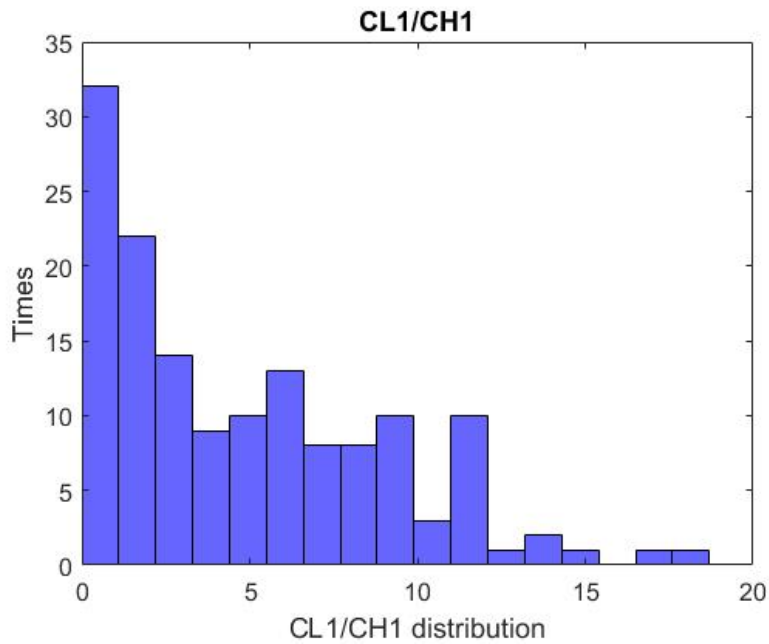


Figure 119: Ratio of corrosion length (CL_1) to corrosion height (CH_1) of W1 pattern for beams without a diaphragm (range 0-15) - MassDOT

As an additional step, the corrosion length and the web thickness loss distribution for each of the two cases of CH_1 were plotted, a) for $CH_1 < 0.3H_0$ (Figure 120) and b) for $CH_1 > 0.9H_0$ (Figure 121).

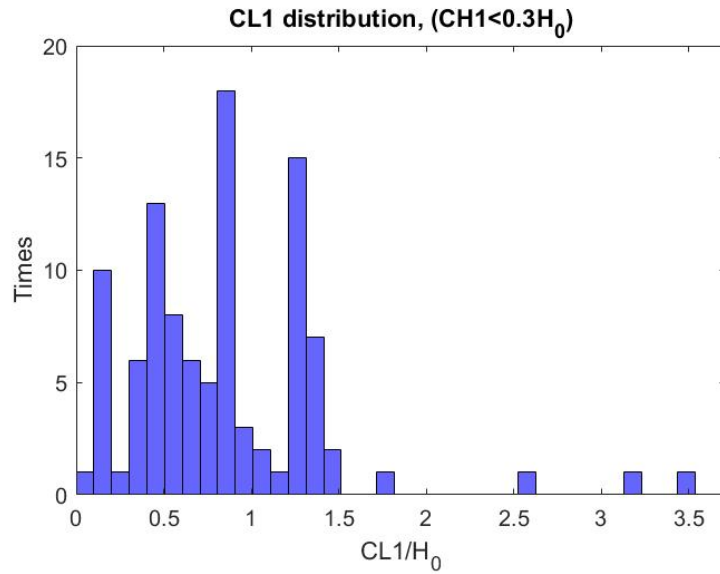


Figure 120: CL1 distribution of W1 web corrosion pattern, with corrosion height up to 30% of H₀ for beams without a diaphragm - MassDOT

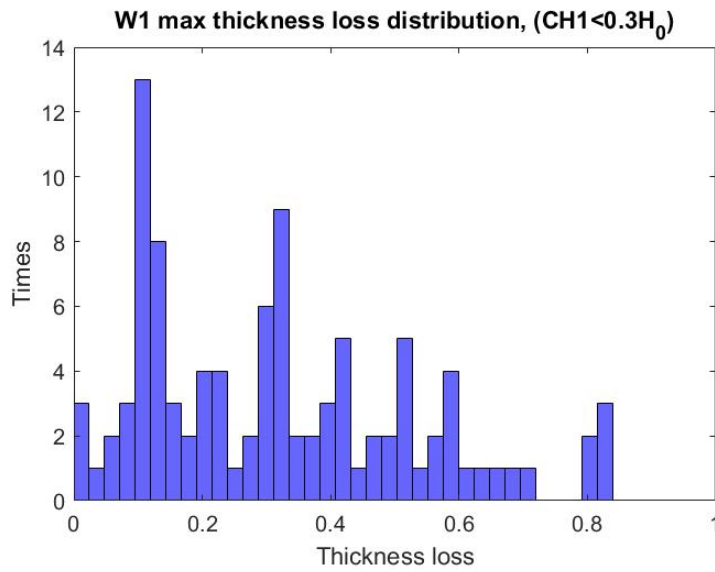


Figure 121: Max thickness loss distribution of W1 web corrosion pattern, with corrosion height up to 30% of H₀ for beams without a diaphragm - MassDOT

Based on Figure 121, we can define as extreme case the following, which covers 103 out of the 161 beam ends that demonstrate a W1 corrosion pattern without diaphragms:

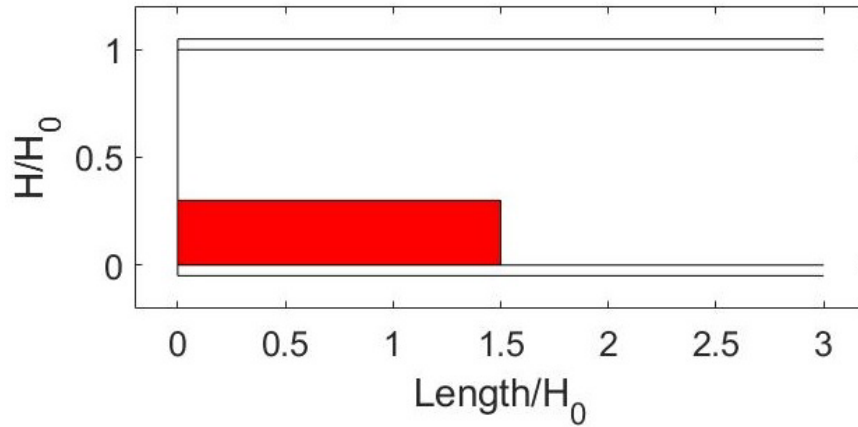


Figure 122: First extreme W1 web corrosion pattern, with corrosion height up to 30% of H0 for beams without a diaphragm - MassDOT

Based on Figure 122, the values for the web thickness loss are: $\frac{t_{loss}}{t_{web}}$ take values of {0.2,0.4,0.6,0.8}

Figure 123 shows the distribution of CL1 for the case when $CH_1 > 0.9H_0$.

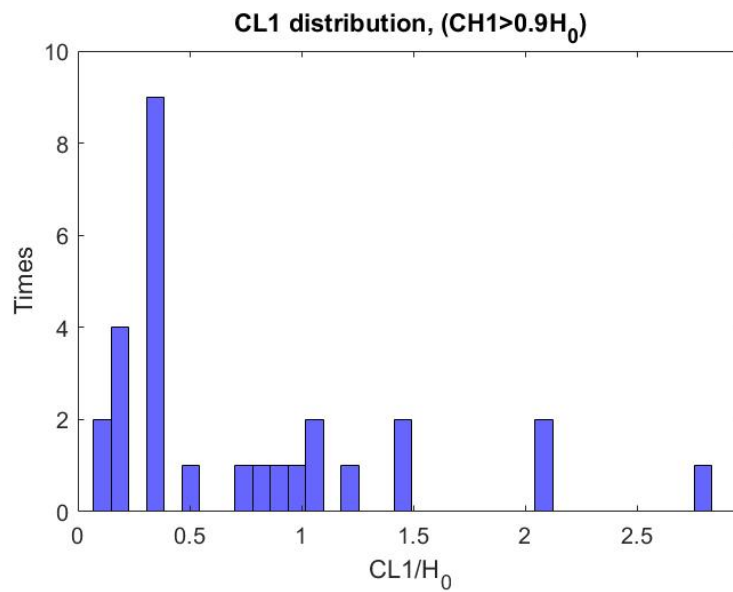


Figure 123: CL1 distribution of W1 web corrosion pattern with corrosion greater than 90% of H0 for beams without a diaphragm - MassDOT

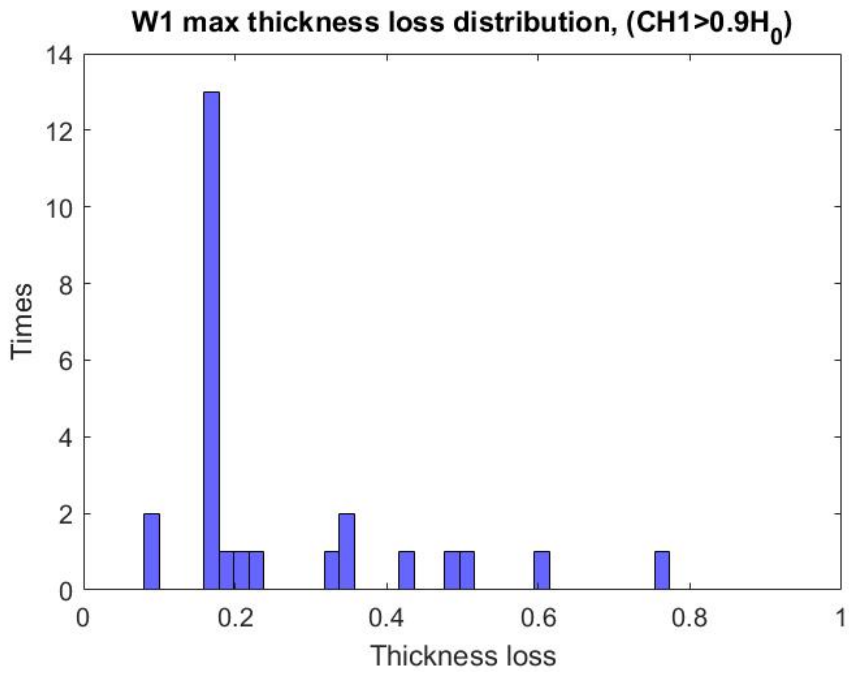


Figure 124: Max thickness loss distribution of W1 web corrosion pattern with corrosion height greater than 90% of H_0 for beams without a diaphragm - MassDOT

Figure 124 shows the maximum thickness loss distribution for the same groups of beams. Therefore, for the full height corrosion ($>0.9H_0$), two different cases are identified as shown in Figure 125 and Figure 126.

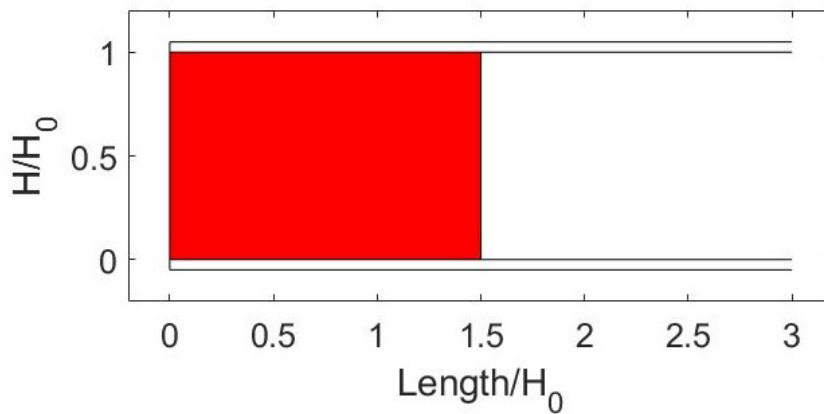


Figure 125: Second extreme W1 web corrosion pattern, with corrosion height greater than 90% of H_0 for beams without a diaphragm - MassDOT

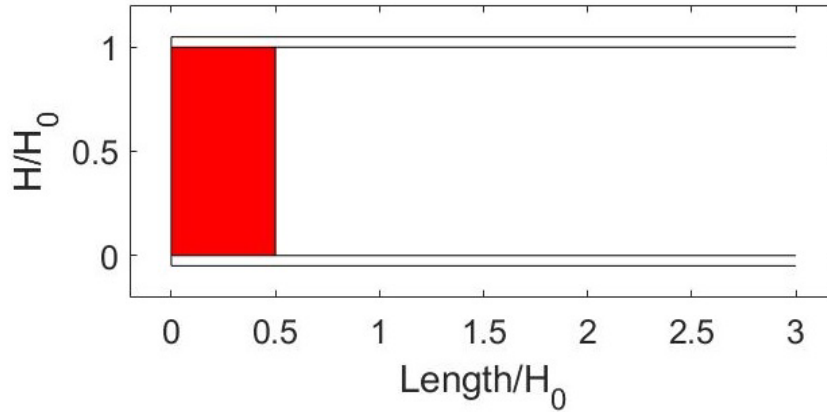


Figure 126: Third extreme W1 web corrosion pattern, with corrosion height greater than 90% of H_0 for beams without a diaphragm - MassDOT

From Figure 124 we can conclude that the web thickness loss for this case is:

$\frac{t_{loss}}{t_{web}}$ takes values of {0.2,0.8}

11.3.2.2. Flange Corrosion

For each of the three cases (Figure 122, Figure 125, Figure 126) the ratio of the length of the corroded flange over the length of the corroded web was plotted (figure Figure 127, Figure 128, Figure 129).

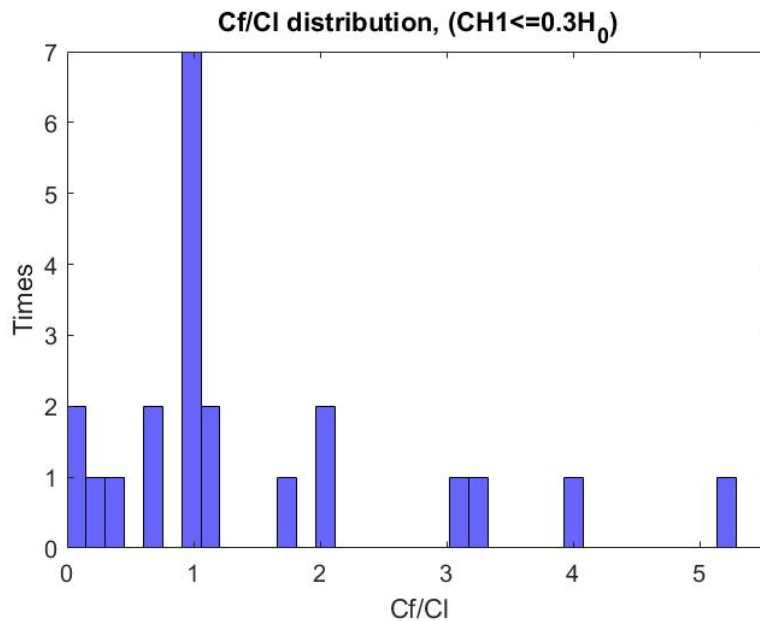


Figure 127: Ratio of flange to web corrosion length distribution of W1 web corrosion pattern with corrosion height up to 30% of H_0 for beams without a diaphragm - MassDOT

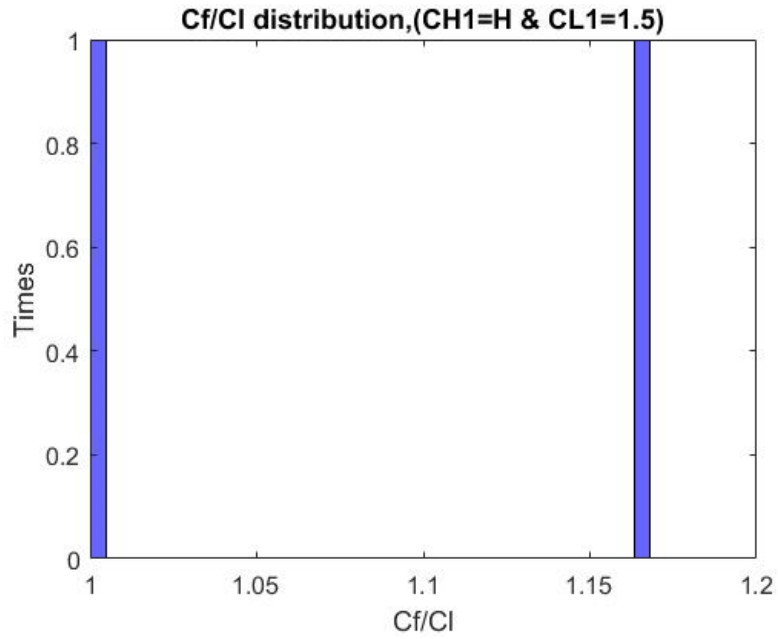


Figure 128: Ratio of flange to web corrosion length distribution of W1 web corrosion pattern for extreme scenario CASE B for beams without a diaphragm - MassDOT

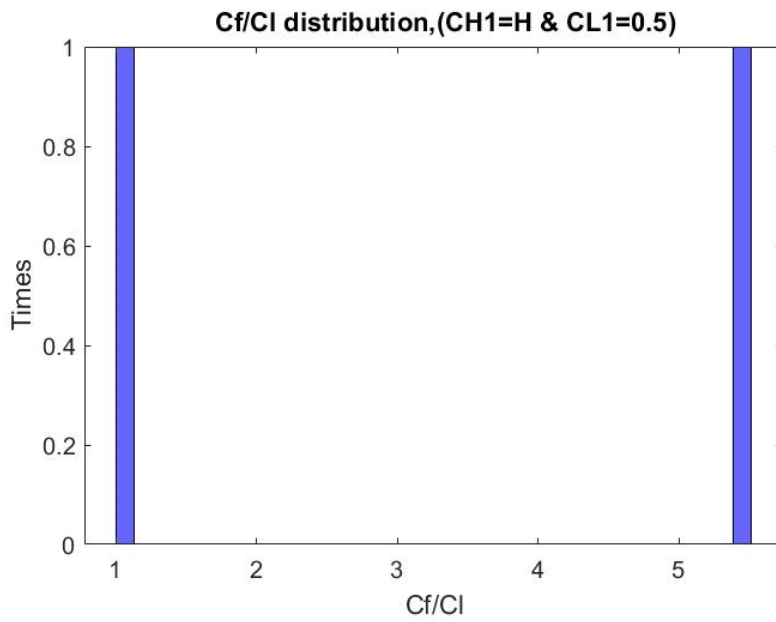


Figure 129: Ratio of flange to web corrosion length distribution of W1 web corrosion pattern for extreme scenario CASE C for beams without a diaphragm - MassDOT

The flange thickness loss is plotted in Figure 130:

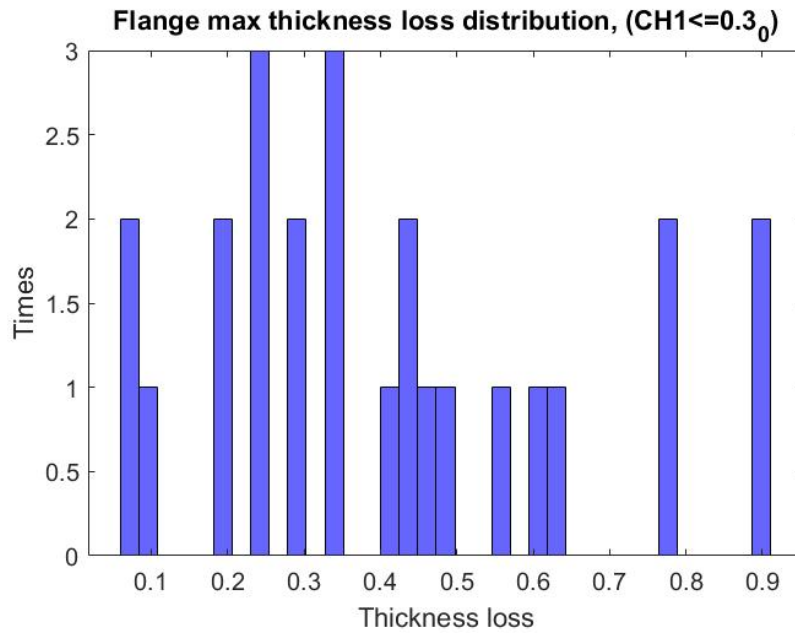


Figure 130: Max flange thickness loss distribution of W1 web corrosion pattern with corrosion height up to 30% of H₀ for beams without a diaphragm - MassDOT

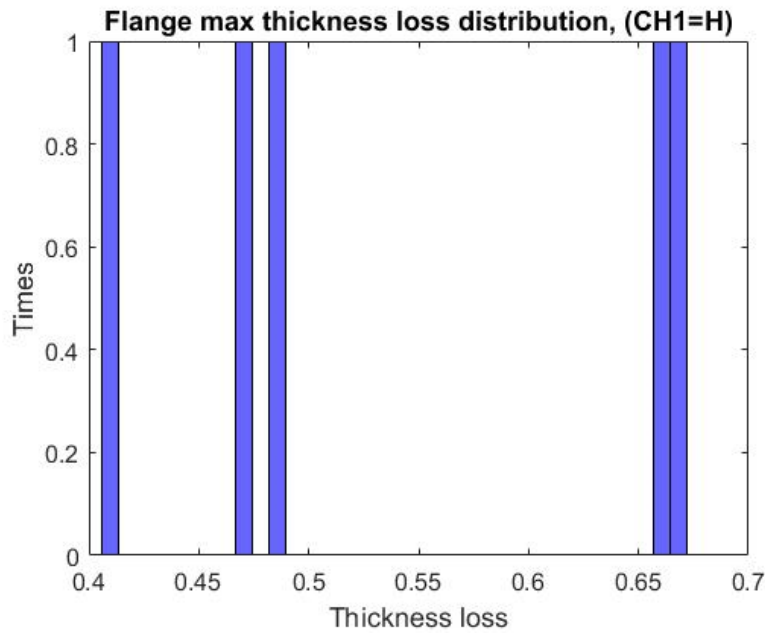


Figure 131: Max flange thickness loss distribution of W1 web corrosion pattern with full height corrosion for beams without a diaphragm - MassDOT

Thus, for Case A: $\frac{t_{loss}}{t_{flange}}$ takes values of {0.2,0.4,0.6,0.8} (Figure 130) and for Cases B and

C: $\frac{t_{loss}}{t_{flange}}$ takes values of {0.45,0.65} (Figure 131).

For all cases $1 \leq \frac{c_f}{c_l} \leq 2$ (Figure 127, Figure 128, Figure 129).

11.3.2.3. Holes

The frequency of hole appearance is shown in Table 77.

Table 77: Hole appearances for beams without a diaphragm - MassDOT

	Number	No hole	M1	M2	M3	M4	M12	M13	M24
W1	161	146	9	1	3	0	0	2	0
W2	10	8	2	0	0	0	0	0	0
W3	56	44	7	0	3	1	0	1	0
W4	40	347	4	0	0	0	0	2	0
W5	17	13	3	1	0	0	0	0	0
W6	2	2	0	0	0	0	0	0	0

According to the table, the W1 pattern is combined 9 times with the M1 hole pattern (not all cases provide data). The web thickness loss at these cases is given as shown in Figure 132:

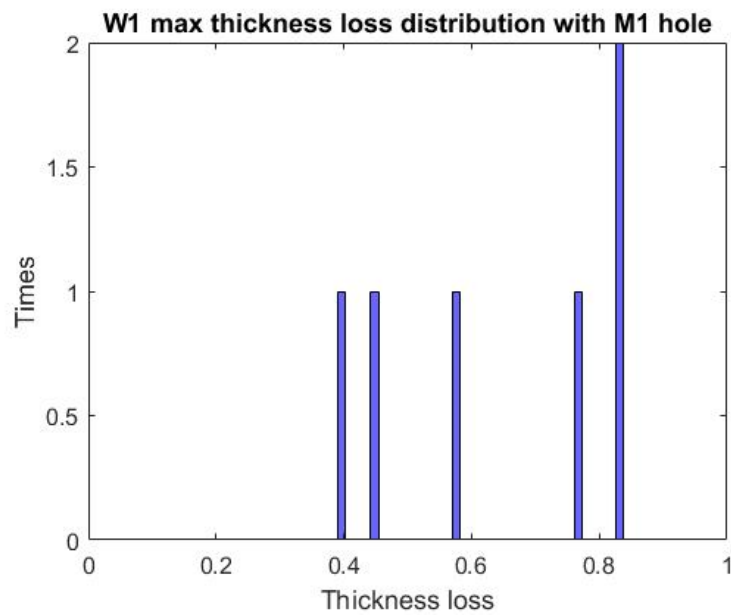


Figure 132: Max thickness loss distribution for W1 web corrosion patterns and M1 hole for beams without a diaphragm - MassDOT

Thus, we could say that the holes appear when the web thickness loss exceeds 40%. The distribution of the holes dimensions is shown below:

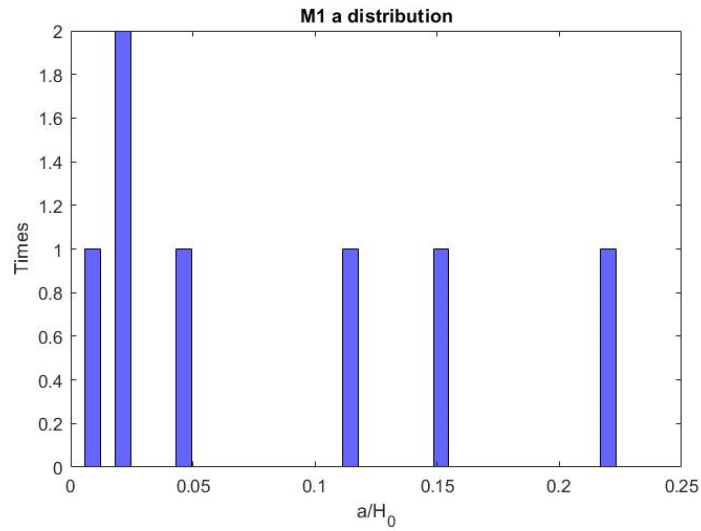


Figure 133: M1 web hole's pattern height distribution of W1 web corrosion pattern for beams without a diaphragm - MassDOT

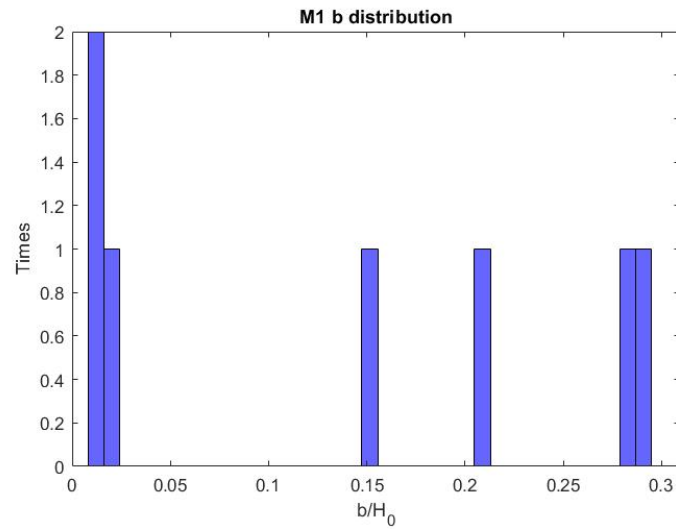


Figure 134: M1 web hole's pattern length distribution of W1 web corrosion pattern for beams without a diaphragm - MassDOT

Observing Figure 133 and Figure 134, our team decided that M1 appears in the form of pit holes (very small dimensions) or in a rectangular shape with the long side parallel to flange. Due to the small number of the available data for the holes, dimensions are not investigated for each case A, B, C separately.

The extreme scenario, projected on the W1 corrosion pattern Case C with $a=0.22H$ and $b=0.3H_0$ is presented below:

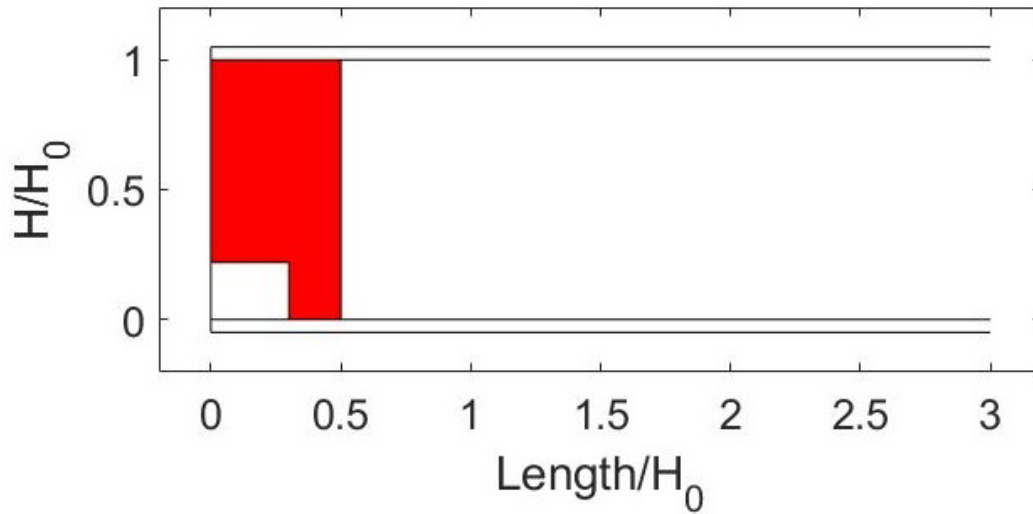


Figure 135: M1 extreme web hole pattern scenario of W1 web corrosion pattern, projected on W1 CASE A, for beams without a diaphragm - MassDOT

11.3.3. Pattern W2

11.3.3.1. Web corrosion

The W2 pattern was observed in total only 10 times. Similar to the W1 pattern, the distributions of all normalized dimensions and web thickness loss were plotted. The parameters for the corrosion patterns can be found with corresponding diagrams in Section 1.5 *Corrosion Patterns* of this report.

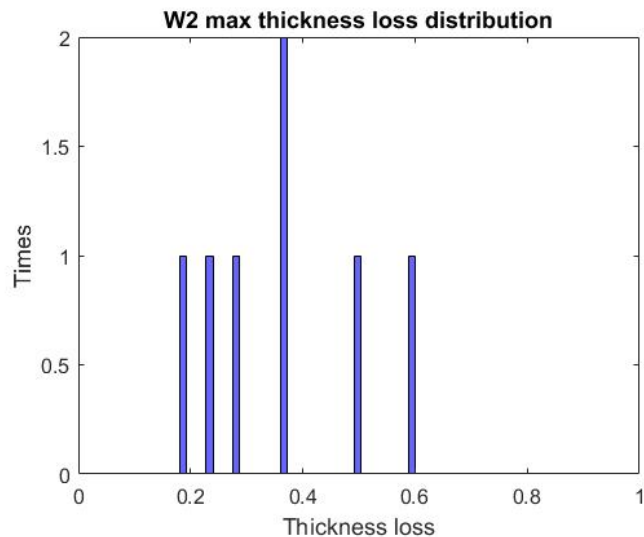


Figure 136: Web thickness loss distribution of W2 pattern for beams without a diaphragm - MassDOT

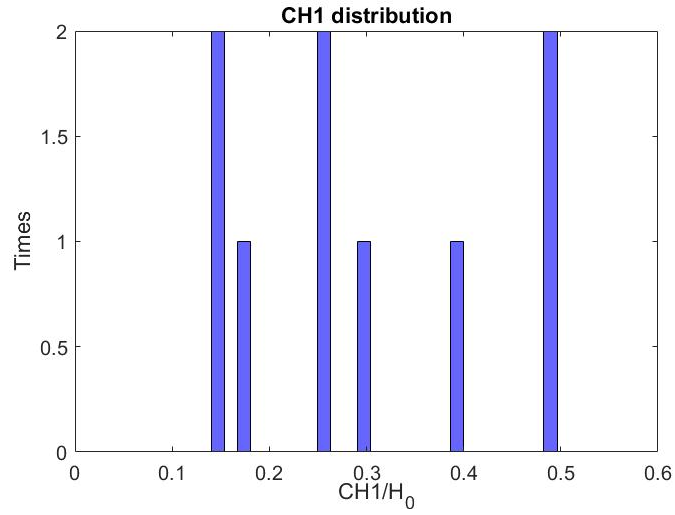


Figure 137: CH₁ distribution of W2 pattern for beams without a diaphragm - MassDOT

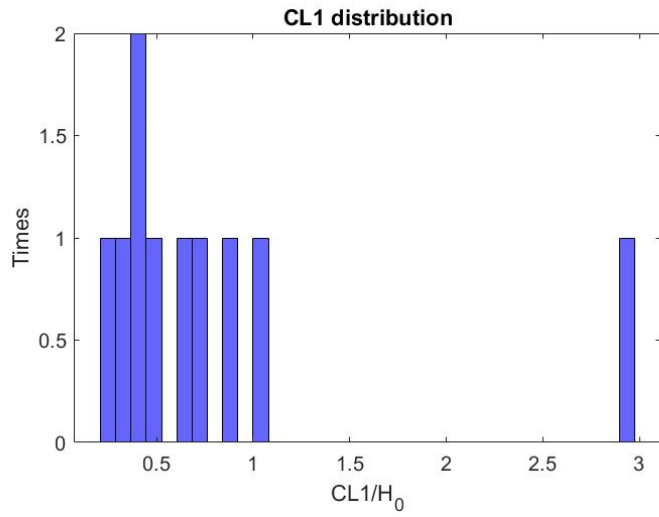


Figure 138: CL₁ distribution of W2 pattern for beams without a diaphragm - MassDOT

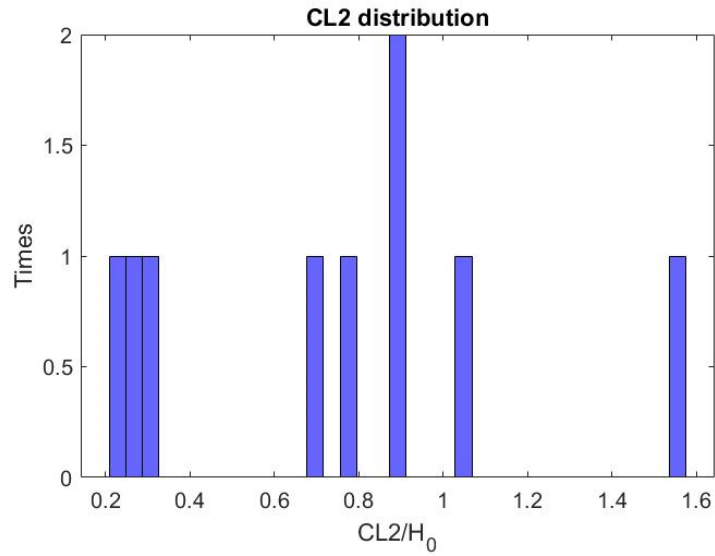


Figure 139: CL₂ distribution of W2 pattern for beams without a diaphragm - MassDOT

From Figure 137, for 6 out of 9 cases, the corrosion height is up to 0.3 H. For these cases, the web corrosion height, length and web thickness loss are presented below:

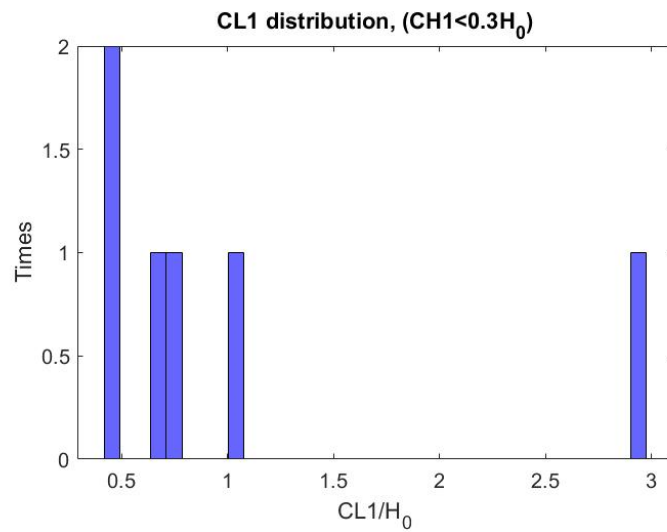


Figure 140: CL₁ distribution of W2 web corrosion pattern corroded up to 30% of H₀ for beams without a diaphragm - MassDOT

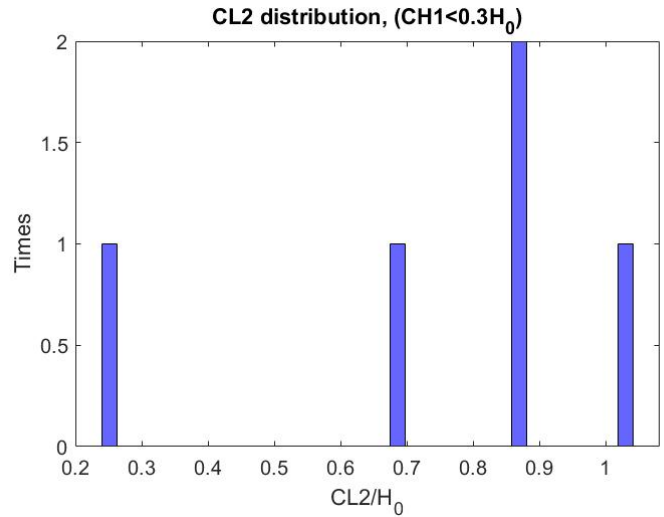


Figure 141: CL2 distribution of W2 web corrosion pattern corroded up to 30% of H0 for beams without a diaphragm - MassDOT

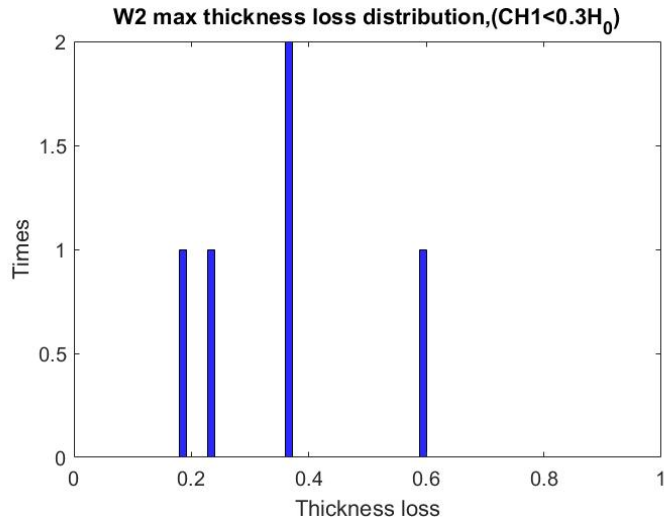


Figure 142: Max thickness loss distribution of W2 web corrosion pattern corroded up to 30% of H0 for beams without a diaphragm - MassDOT

From Figure 138 and Figure 139: $0.5 < CL_1 \leq 1.1H$, $0.25 < CL_2 \leq 1.2H$, where the extreme scenario is illustrated as:

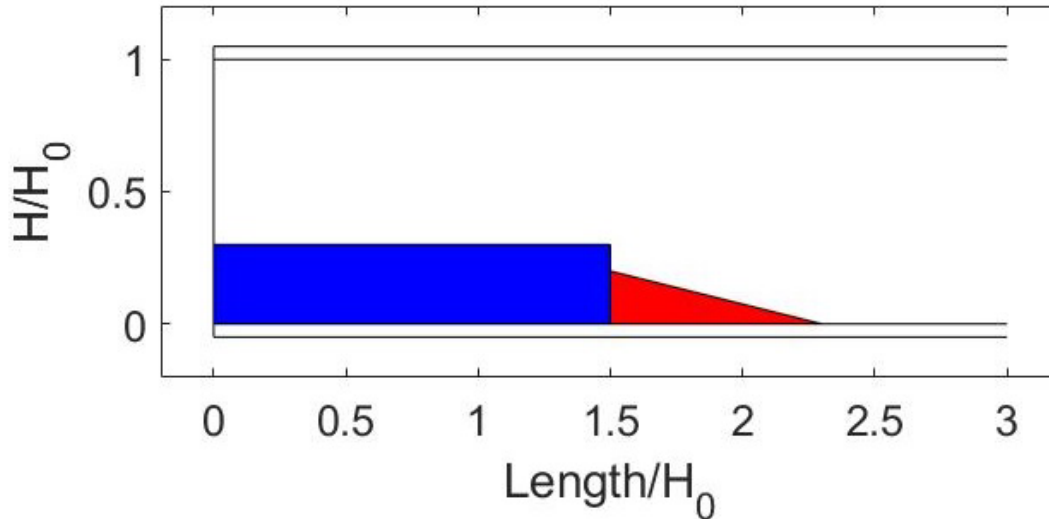


Figure 143: W1 Case A extreme web corrosion scenario projected over W2 extreme web corrosion scenario - MassDOT

The blue area indicates the Case A of W1 pattern, and with red the extreme W2 pattern scenario. Since the rest of W2 cases fit in the blue shadowed area, W1 case A can be merged with W2. According to Figure 136 the thickness loss for W2 is in the Case A-W1 range.

11.3.3.2. Flange corrosion

There was no analysis conducted on flange corrosion since the worst scenario is included in the W1 corrosion scenario.

11.3.3.3. Holes

In W2 pattern the M1 hole appears twice with dimensions $a_1=b_1=0.05$ and $a_2=0.15$ and $b_2=0.5$ which exceeds the W1 and M1 combination max hole length.

11.3.4. Pattern W3

11.3.4.1. Web Corrosion

The parameters for the corrosion patterns can be found with corresponding diagrams in Section 1.5 *Corrosion Patterns* of this report. The data analysis started with the CH2 distribution:

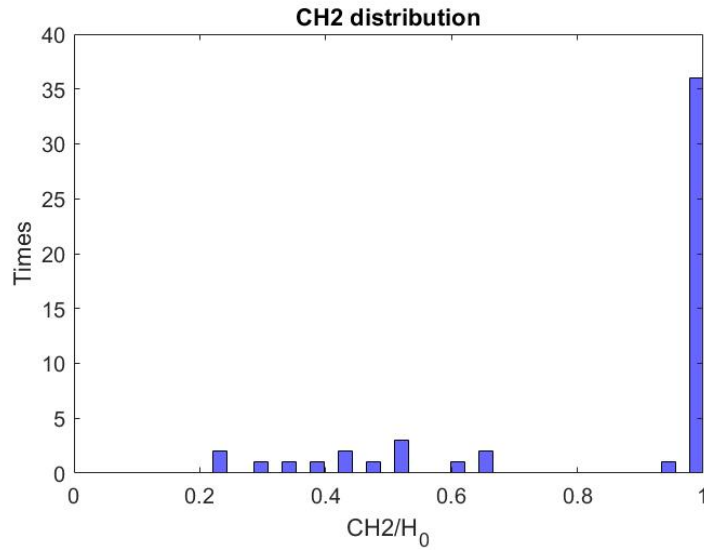


Figure 144: CH₂ distribution of W3 web corrosion pattern for beams without a diaphragm - MassDOT

From Figure 144, it is obvious that the dominant scenario is the full height corroded web case. For CH₂=H₀ the dimension and thickness distributions are presented.

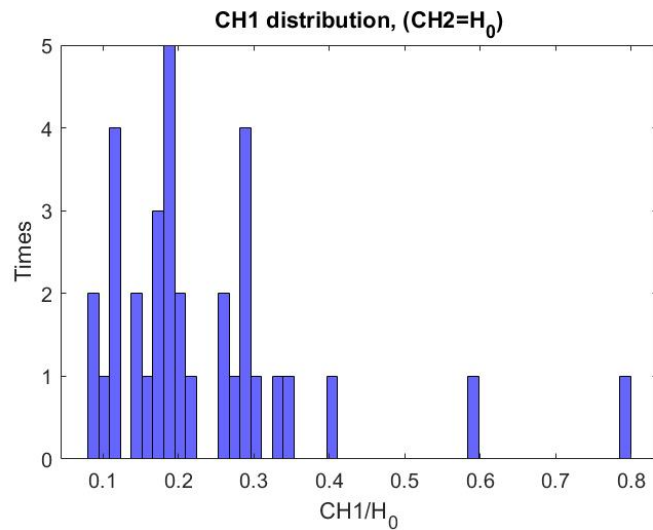


Figure 145: CH₁ distribution of W3 web corrosion pattern with full height corrosion for beams without a diaphragm - MassDOT

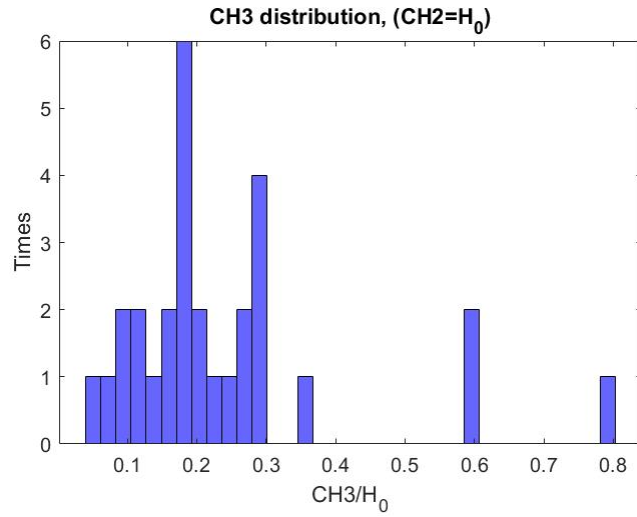


Figure 146: CH₃ distribution of W3 web corrosion pattern with full height corrosion for beams without a diaphragm - MassDOT

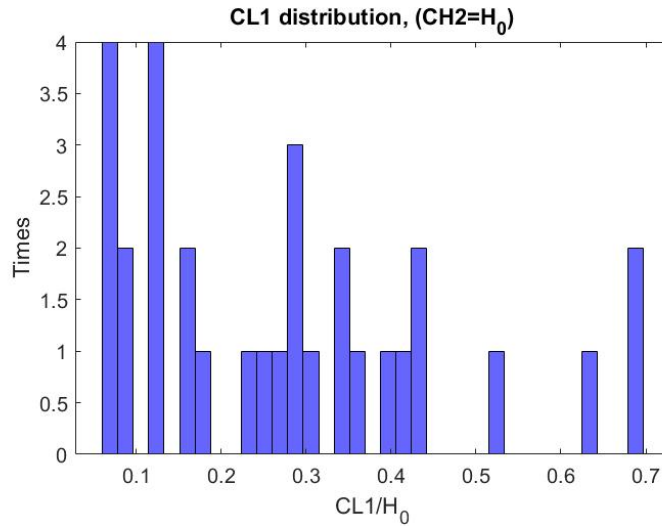


Figure 147: CL1 distribution of W3 web corrosion pattern with full height corrosion for beams without a diaphragm - MassDOT

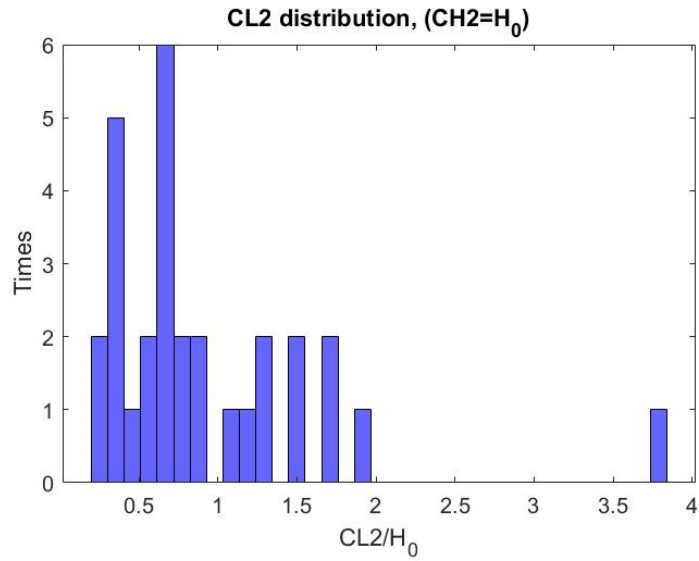


Figure 148: CL₂ distribution of W3 web corrosion pattern with full height corrosion for beams without a diaphragm - MassDOT

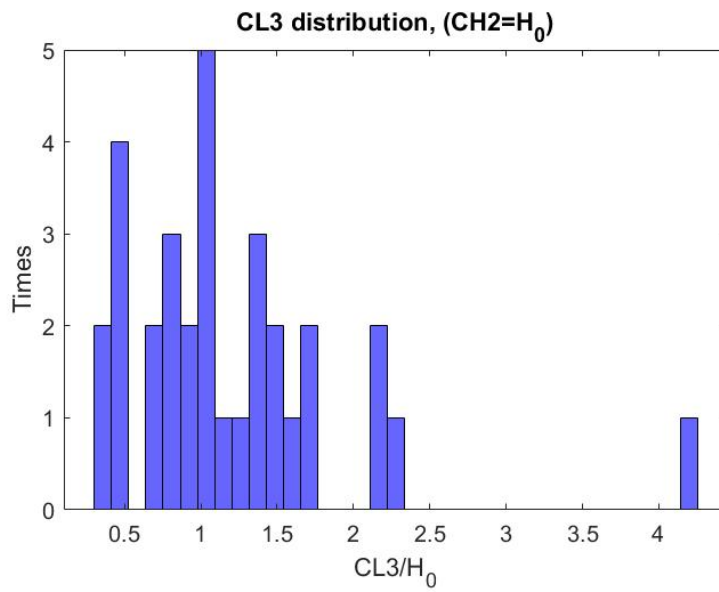


Figure 149: CL₃ distribution of W3 web corrosion pattern with full height corrosion for beams without a diaphragm - MassDOT

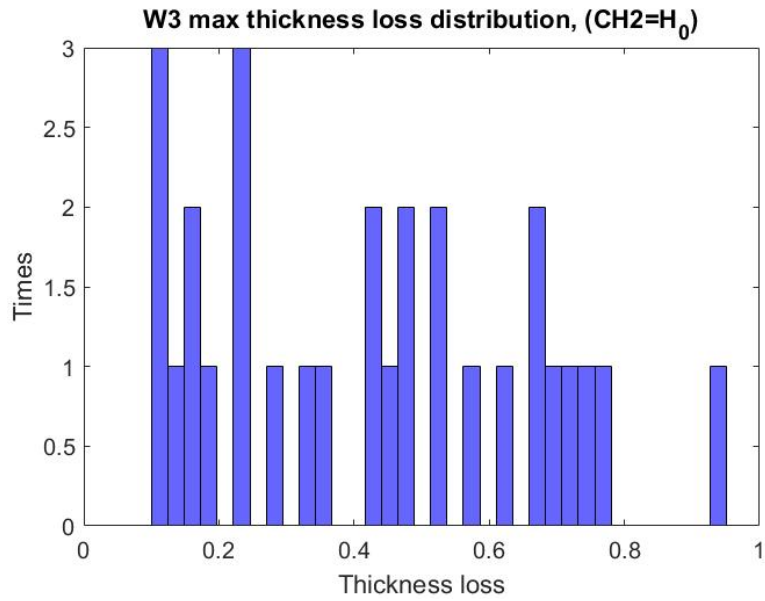


Figure 150: Max web thickness loss distribution of W3 web corrosion pattern with full height corrosion for beams without a diaphragm - MassDOT

From the last figures we can conclude that:

$$0 < CH_1 \leq 0.35$$

$$0 < CH_3 \leq 0.35$$

$$0.05 < CL_1 \leq 0.7$$

$$0.5 < CL_3 \leq 2.3$$

$$\frac{t_{loss}}{t_{web}} \text{ takes values of } \{0.1, 0.2, 0.3, 0.4, 0.5, 0.6, 0.7, 0.8\}$$

And therefore, the extreme scenario is:

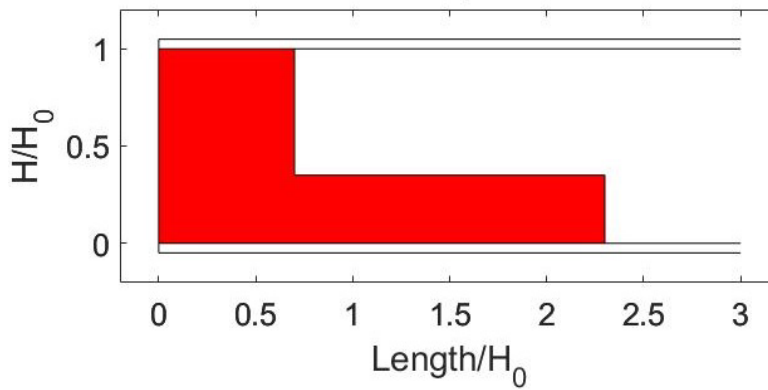


Figure 151: Extreme W3 web corrosion scenario for beams without a diaphragm - MassDOT

11.3.4.2. Flange Corrosion

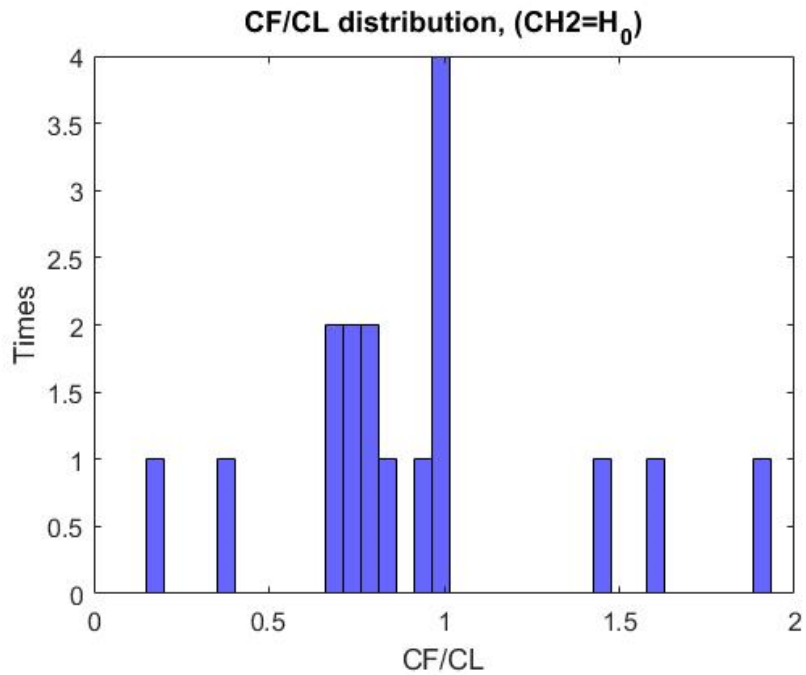


Figure 152: Ratio of flange to web corrosion length distribution of W3 web corrosion pattern with full height corrosion for beams without a diaphragm - MassDOT

Based on Figure 152, the parameter CF is considered equal to parameter CL.

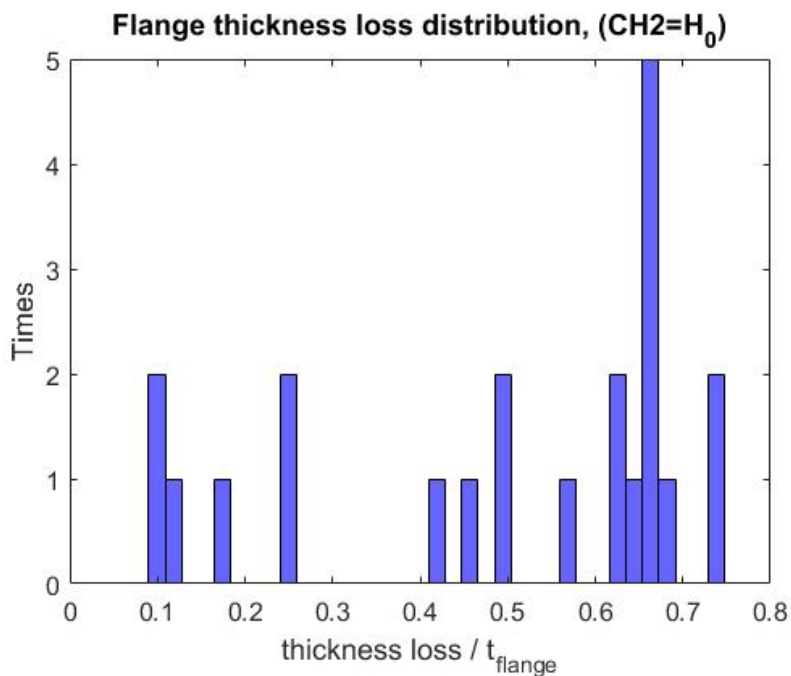


Figure 153: Max flange loss thickness distribution of W3 web corrosion pattern with full height corrosion for beams without a diaphragm - MassDOT

$$\frac{t_{loss}}{t_{flange}} \text{ takes values of } \{0.4, 0.6, 0.8\}$$

11.3.4.3. Holes

Holes dimensions distribution:

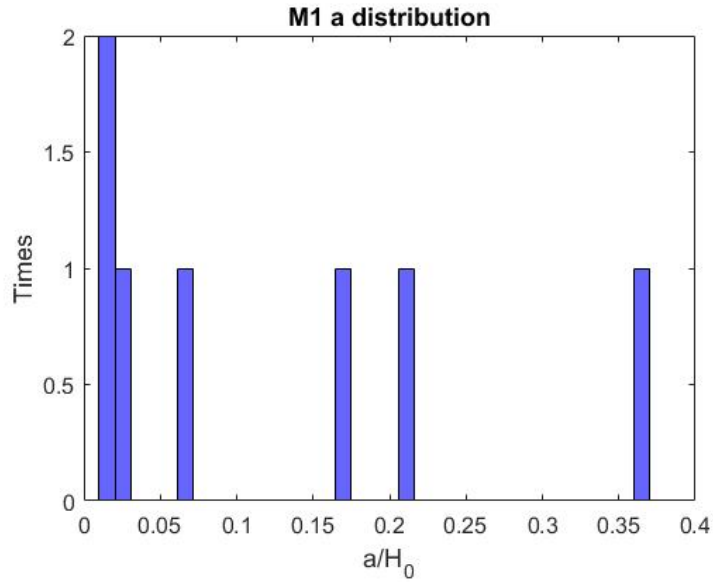


Figure 154: M1 web hole's pattern height distribution of W3 web corrosion pattern for beams without a diaphragm - MassDOT

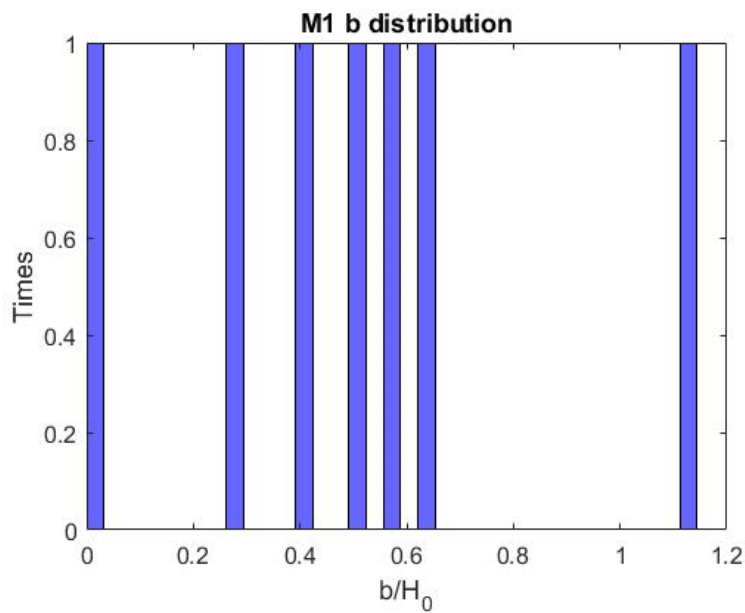


Figure 155: M1 web hole's pattern length distribution of W1 web corrosion pattern for beams without a diaphragm - MassDOT

The extreme corrosion hole scenario with parameters $a=0.21$ and $b=0.63$ are presented below. This extreme case is projected on the W3 pattern corroded area:

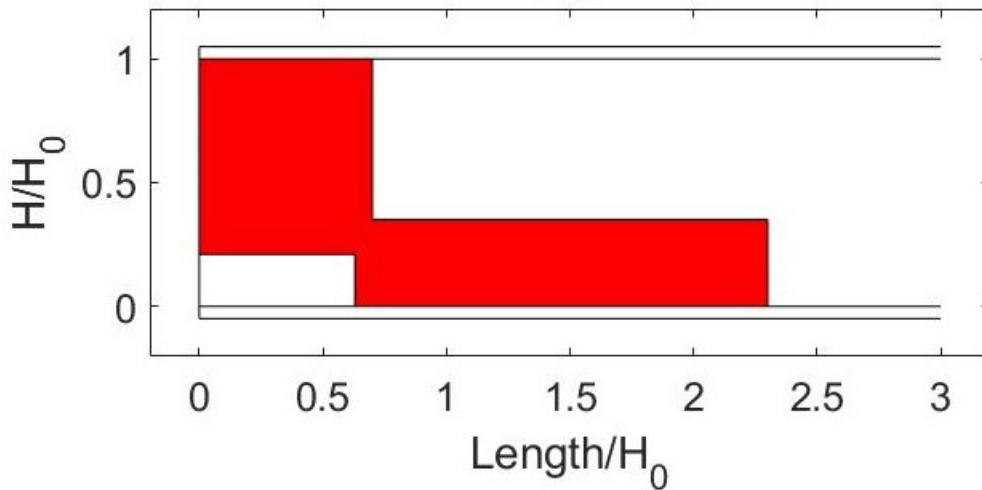


Figure 156: M1 extreme web hole pattern scenario of W1 web corrosion pattern, projected on W3 extreme corrosion scenario, for beams without a diaphragm - MassDOT

11.3.5. Pattern W4

11.3.5.1. Web Corrosion

The thickness loss, as well as the distribution of all normalized dimensions are plotted in the following figures. The parameters for the corrosion patterns can be found with corresponding diagrams in Section 1.5 *Corrosion Patterns* of this report.

This is a bar chart that plots Times (0 to 5) vs CH1/H_0 from 0 to .8

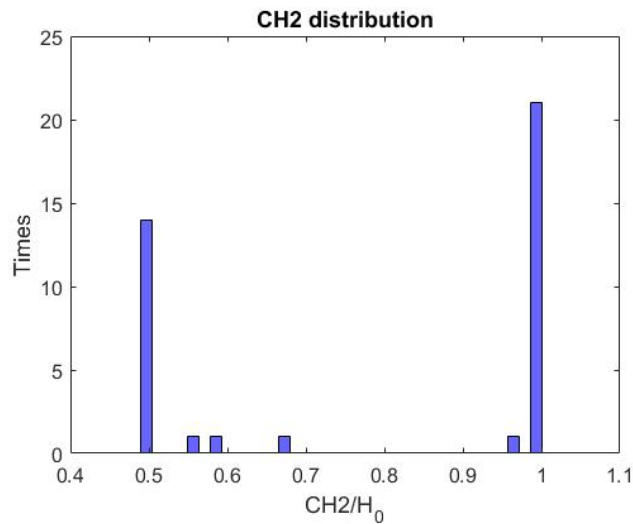


Figure 157: CH2 distribution of W4 web corrosion pattern for beams without a diaphragm - MassDOT

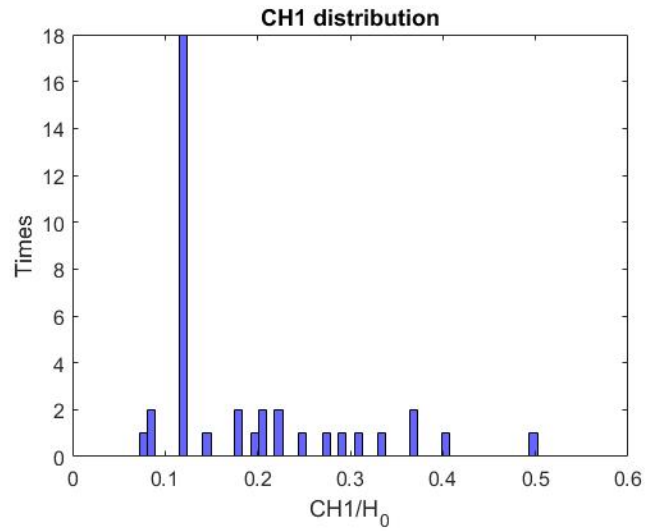


Figure 158: CH1 distribution of W4 web corrosion pattern for beams without a diaphragm - MassDOT

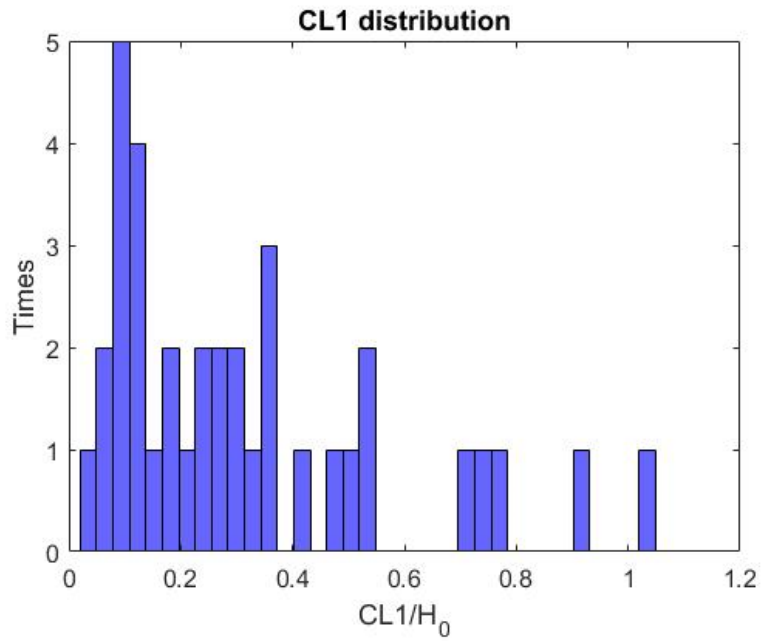


Figure 159: CL1 distribution of W4 web corrosion pattern for beams without a diaphragm - MassDOT

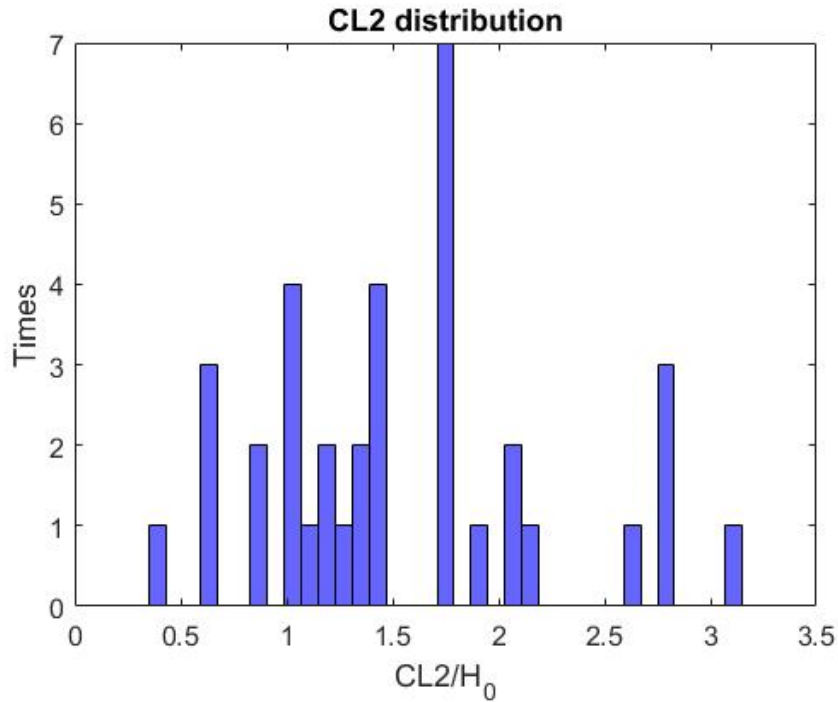


Figure 160: CL2 distribution of W4 web corrosion pattern for beams without a diaphragm - MassDOT

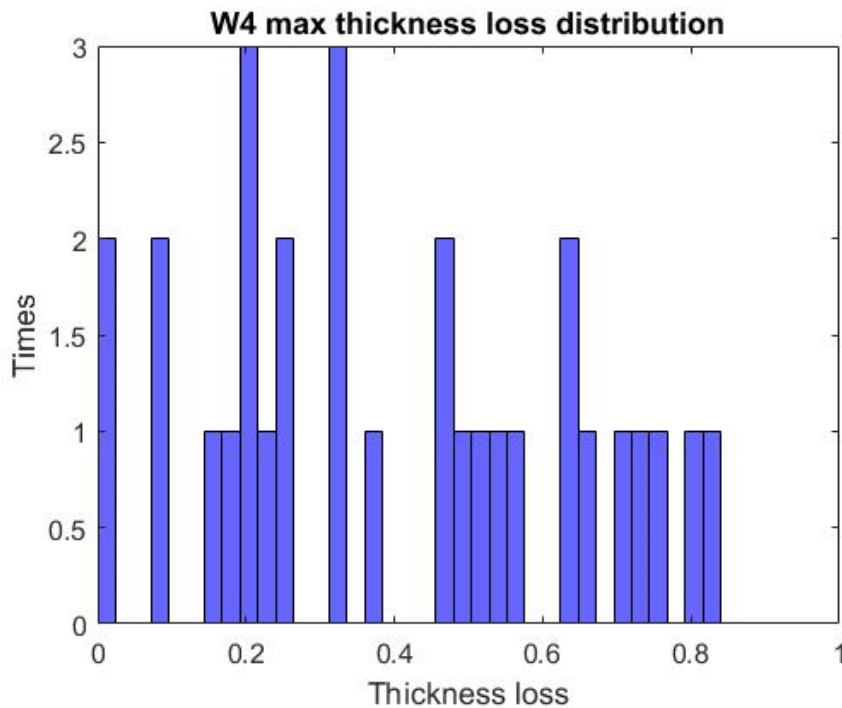


Figure 161: Max web thickness loss distribution of W4 web corrosion pattern for beams without a diaphragm - MassDOT

From the CH2 histogram (Figure 157), two main trends were noticed: either a) full height corrosion, or b) corrosion up to 50% of H_0 . As an additional step, the corrosion dimensions (CH1, CL1, CL2, CL3) and the web thickness loss distribution for each of the two cases of CH1 were plotted, a) for $CH1=0.5H_0$ and b) for $CH1=H_0$.

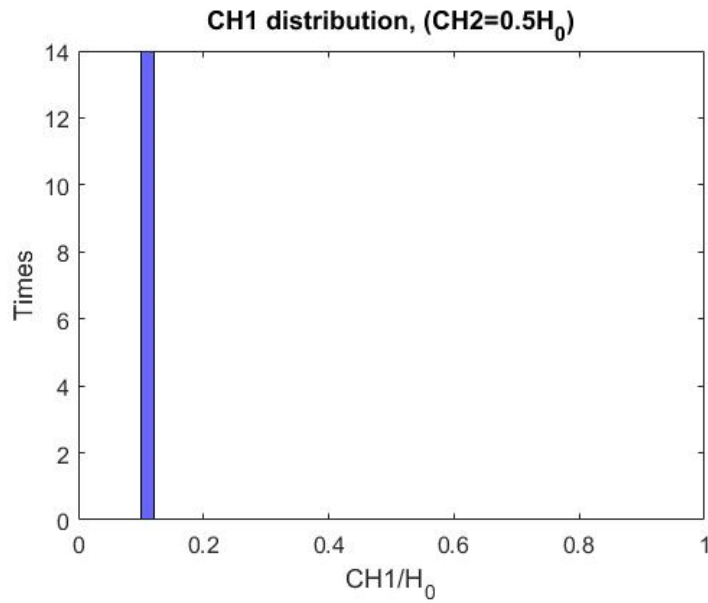


Figure 162 : CH1 distribution of W4 web corrosion pattern, with corrosion height up to 50% of H₀ for beams without a diaphragm - MassDOT

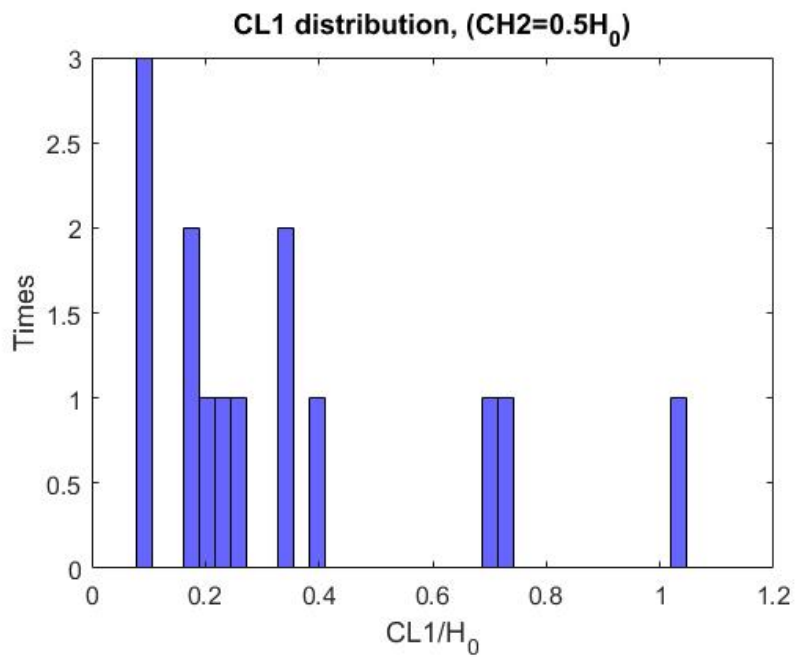


Figure 163: CL1 distribution of W4 web corrosion pattern, with corrosion height up to 50% of H₀ for beams without a diaphragm - MassDOT

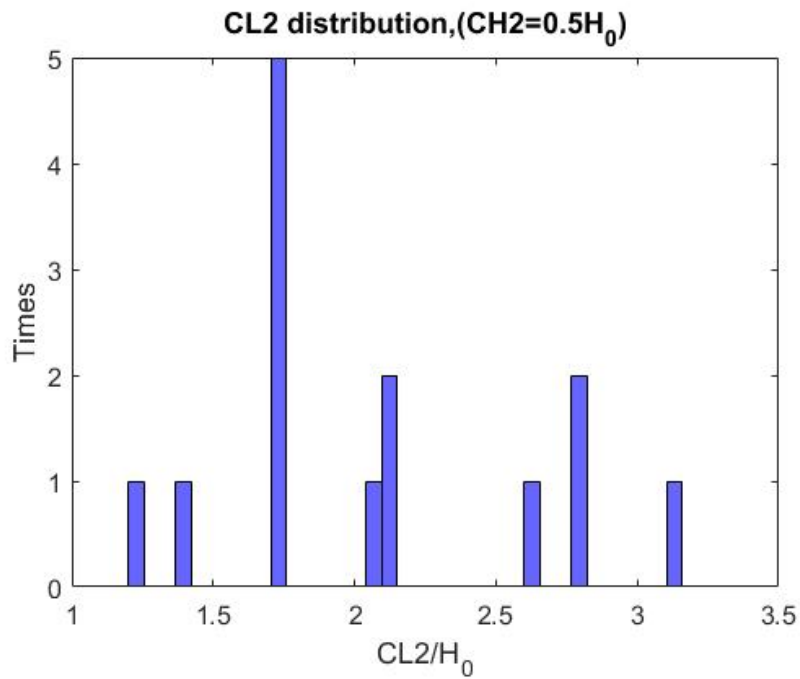


Figure 164: CL2 distribution of W4 web corrosion pattern, with corrosion height up to 50% of H₀ for beams without a diaphragm - MassDOT

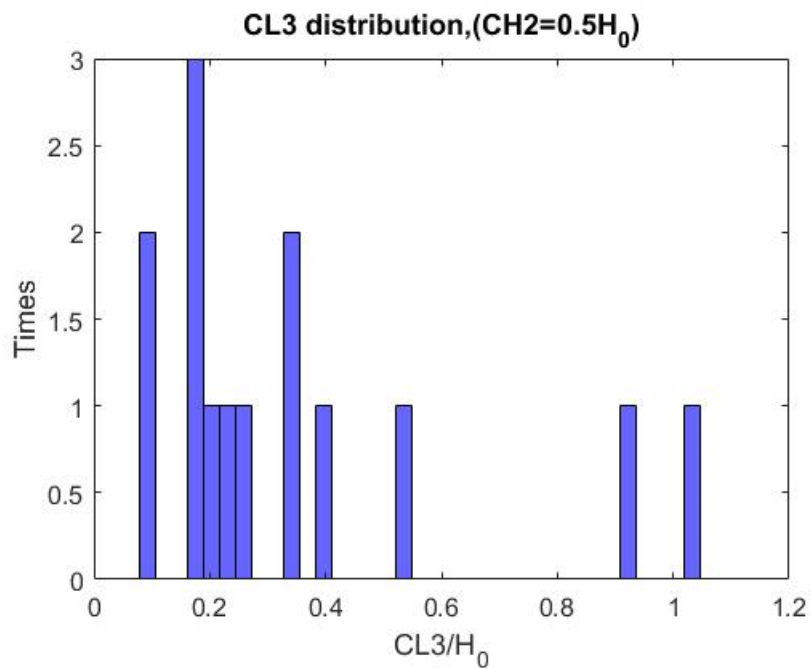


Figure 165: CL3 distribution of W4 web corrosion pattern, with corrosion height up to 50% of H₀ for beams without a diaphragm - MassDOT

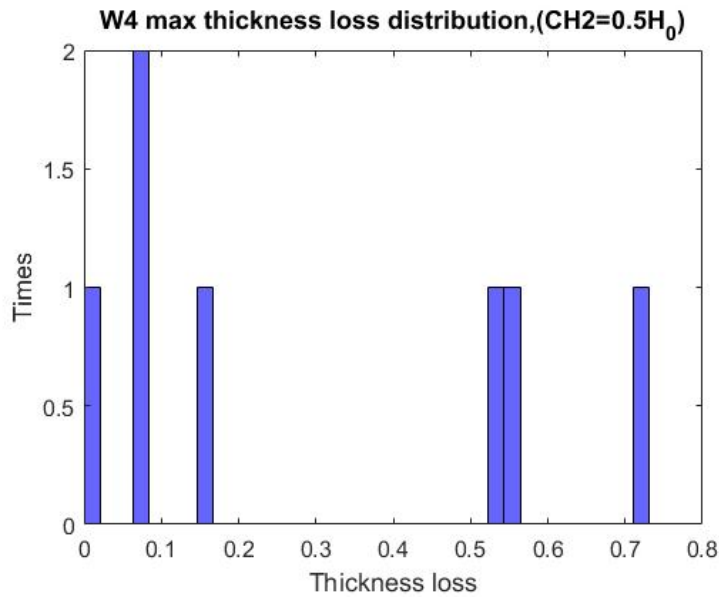


Figure 166: Max web thickness loss distribution of W4 web corrosion pattern, with corrosion height up to 50% of H_0 for beams without a diaphragm - MassDOT

Based on Figure 162, Figure 163, Figure 164, Figure 165, Figure 166:

$$CH_1 = 0.12H_0$$

$$1.2H_0 \leq CL_2 \leq 3.2H_0$$

$$0.2H_0 \leq CL_1 \cong CL_3 \leq 0.4H_0$$

$$\frac{t_{loss}}{t_{web}} \text{ takes values of } \{0.05, 0.15, 0.55, 0.75\}$$

The extreme scenario is:

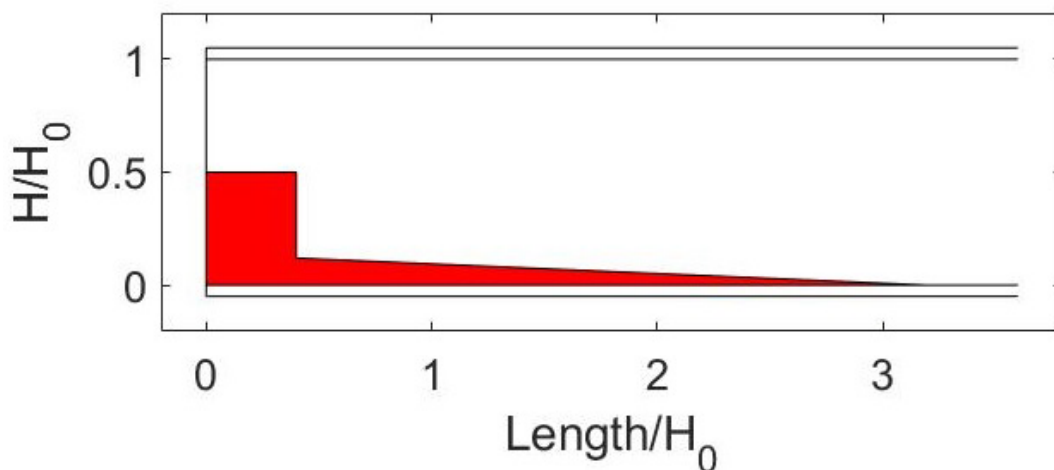


Figure 167: First extreme W4 web corrosion scenario for beams without a diaphragm - MassDOT

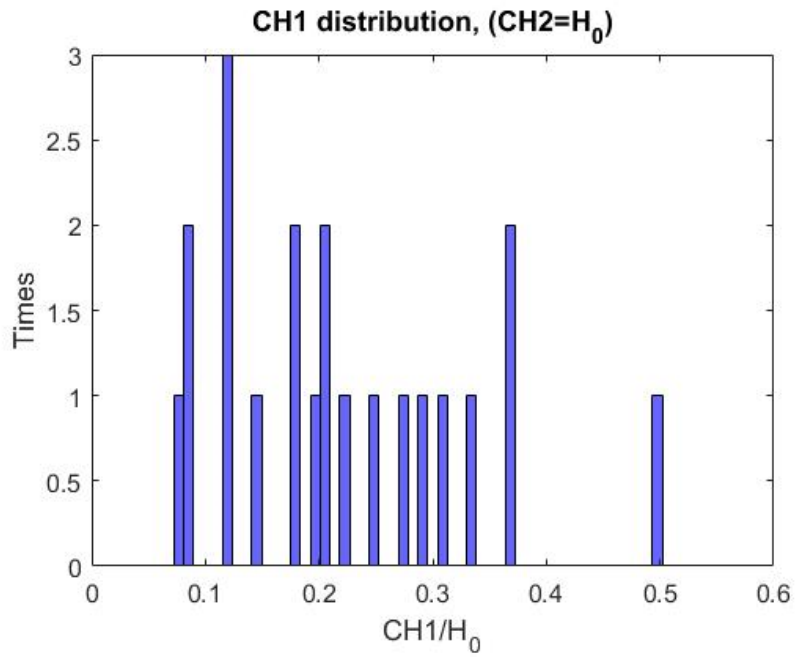


Figure 168: CH1 distribution of W4 web corrosion pattern, with full height corrosion for beams without a diaphragm - MassDOT

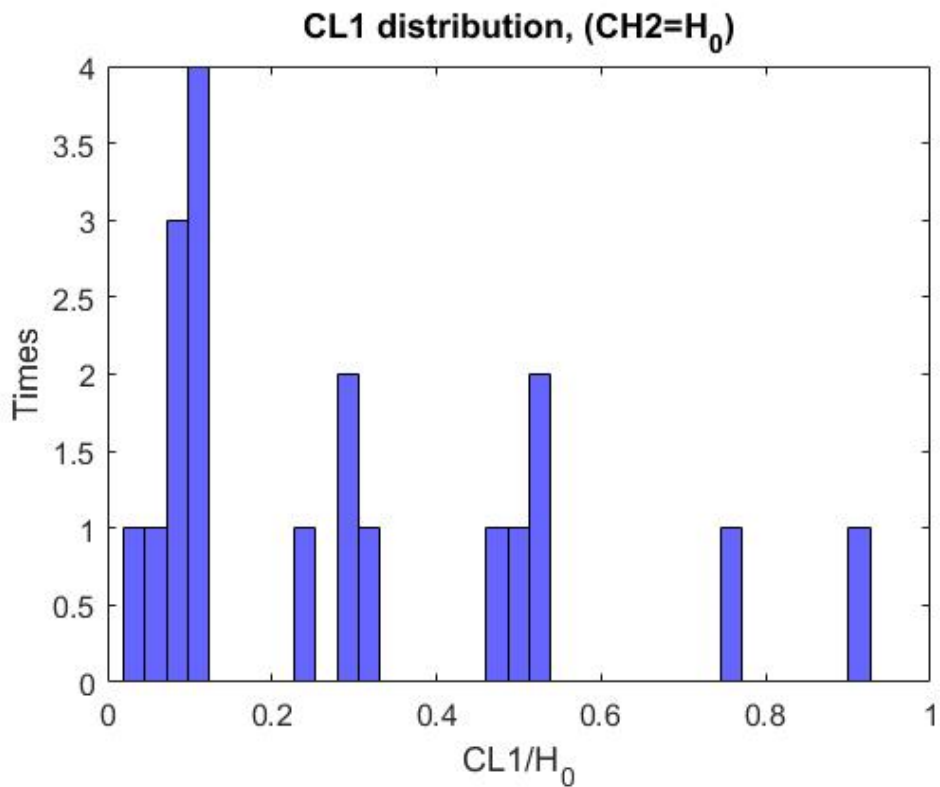


Figure 169: CL1 distribution of W4 web corrosion pattern, with full height corrosion for beams without a diaphragm - MassDOT

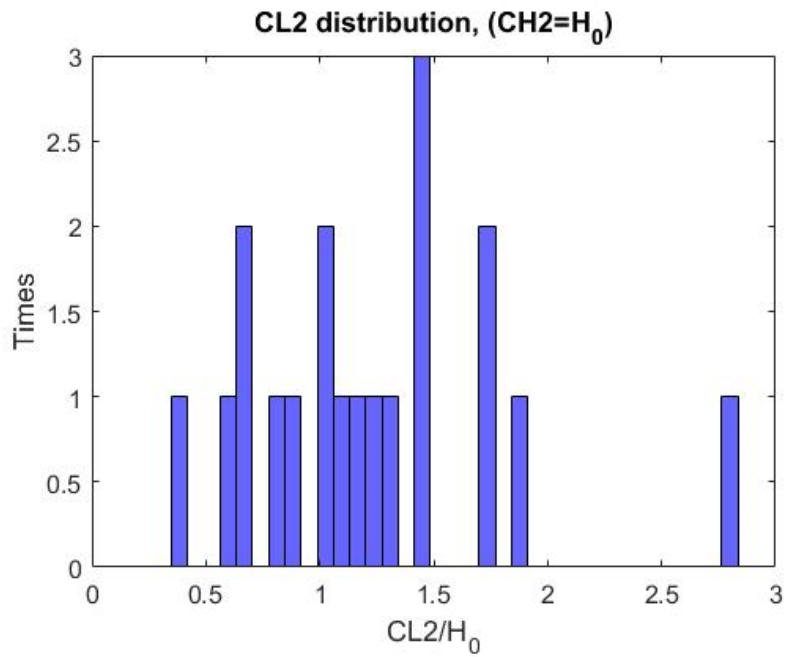


Figure 170: CL2 distribution of W4 web corrosion pattern, with full height corrosion for beams without a diaphragm - MassDOT

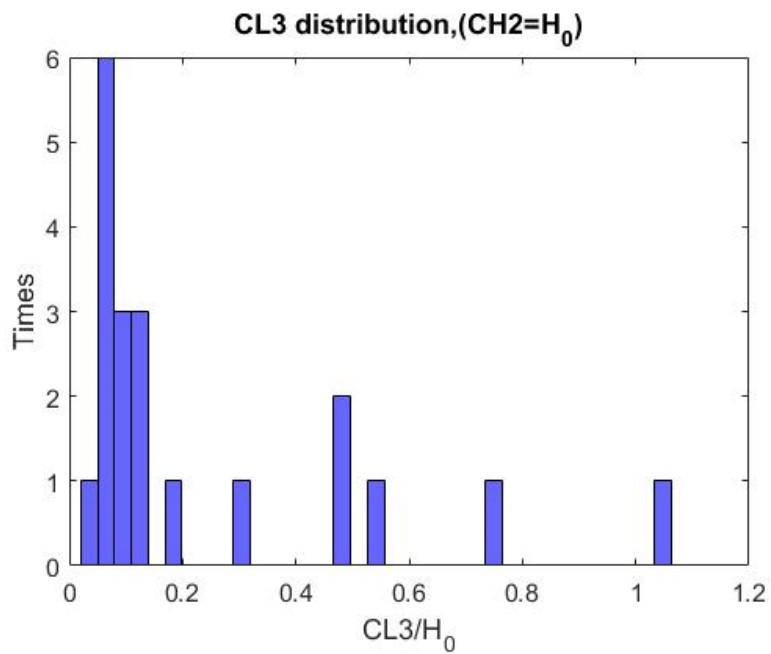


Figure 171: CL3 distribution of W4 web corrosion pattern, with full height corrosion for beams without a diaphragm - MassDOT

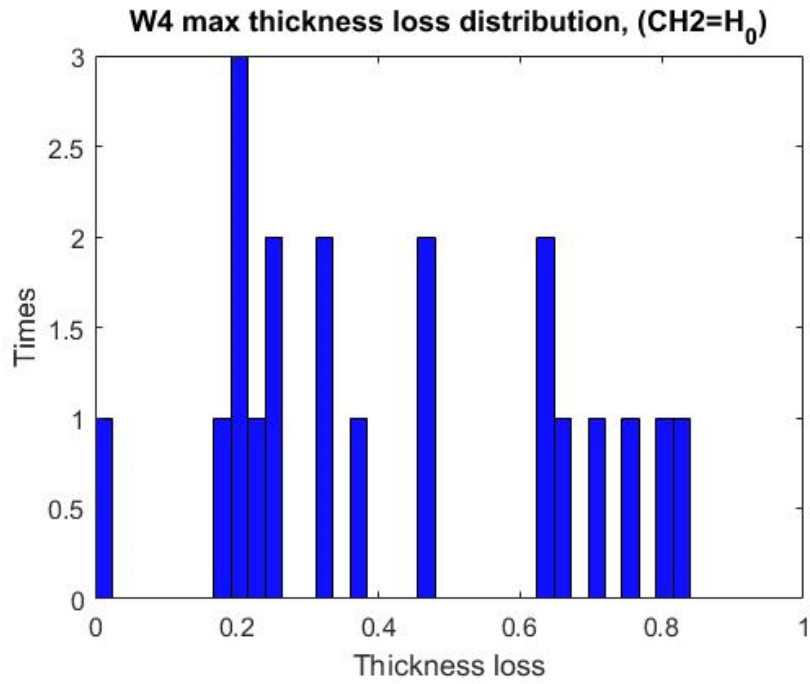


Figure 172: Max web thickness loss distribution of W4 web corrosion pattern, with full height corrosion for beams without a diaphragm - MassDOT

For the full height corrosion:

$$0.1H_0 \leq CH_1 \leq 0.5H_0$$

$$0 < CL_1 \leq 0.9H_0$$

$$0.5H_0 \leq CL_2 \leq 1.8H_0$$

$$0 < CL_3 \leq 0.2H_0$$

with thickness loss:

$$\frac{t_{loss}}{t_{web}} \text{ takes values of } \{0.2, 0.4, 0.6, 0.8\}$$

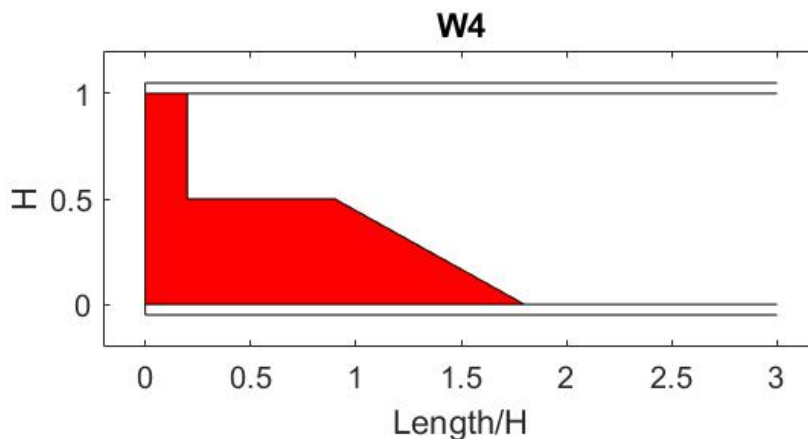


Figure 173: Second extreme W4 web corrosion scenario for beams without a diaphragm - MassDOT

The two W4 extreme scenarios are now projected over the extreme W3 scenario (blue colour):

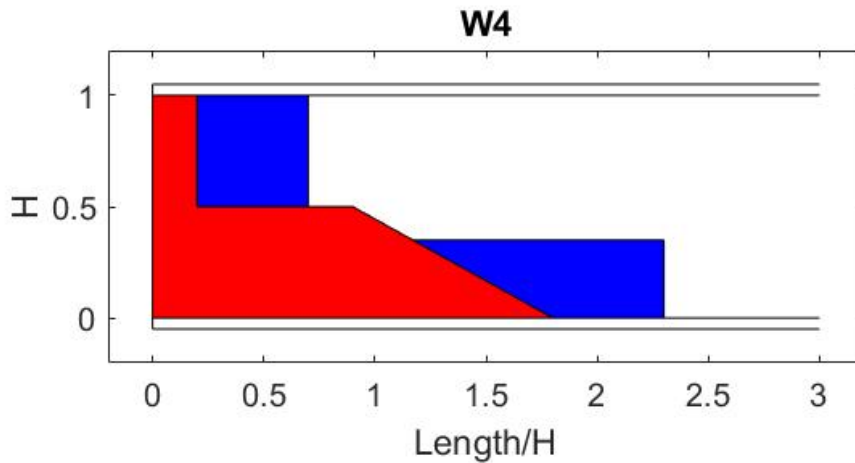


Figure 174: First extreme W4 scenario (red) projected over extreme W3 web corrosion scenario (blue) - MassDOT

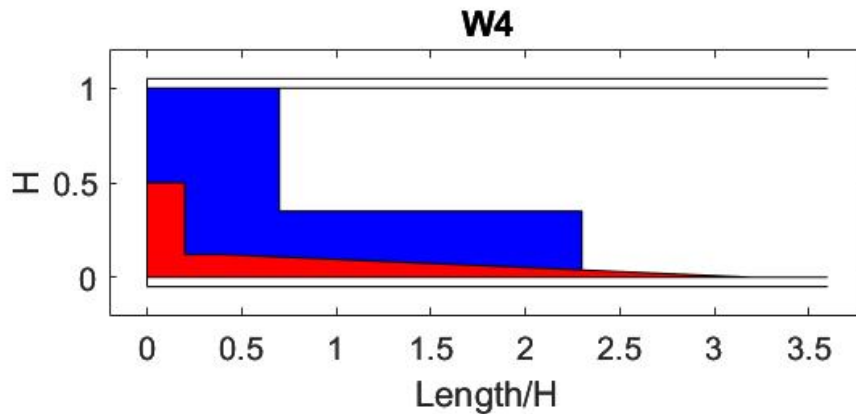


Figure 175: Second extreme W4 scenario (red) projected over extreme W3 web corrosion scenario (blue) - MassDOT

Considering the way W3 and W4 have been defined, W3 can be expressed by W4 if we set $W4CL1=W4CL3$ and $W4CH3 \neq 0$. Figure 174 and Figure 175 demonstrate that W3 includes the extreme W4 scenarios, thus W3 and W4 could be merged to one pattern.

11.3.5.2. Flange Corrosion

There is no analysis of flange corrosion and the generation of a separate flange corrosion pattern since the worst scenario was included in the W3 corrosion scenario.

11.3.5.3. Holes

Table 78: Hole appearances for beams- MassDOT

	Number	No hole	M1	M2	M3	M4	M12	M13	M24
W1	161	146	9	1	3	0	0	2	0
W2	10	8	2	0	0	0	0	0	0
W3	56	44	7	0	3	1	0	1	0
W4	40	347	4	0	0	0	0	2	0
W5	17	13	3	1	0	0	0	0	0
W6	2	2	0	0	0	0	0	0	0

According to the table, the W4 pattern is combined four times with the M1 hole pattern. The available data are not enough to extract conclusions about the web thickness loss at these cases. The corrosion holes dimension distribution can be seen in the figures below:

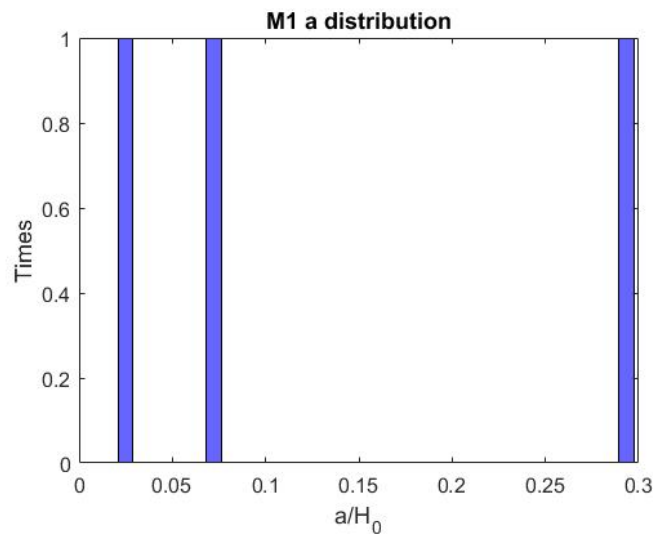


Figure 176: M1 web hole's pattern height distribution of W4 web corrosion pattern for beams without a diaphragm - MassDOT

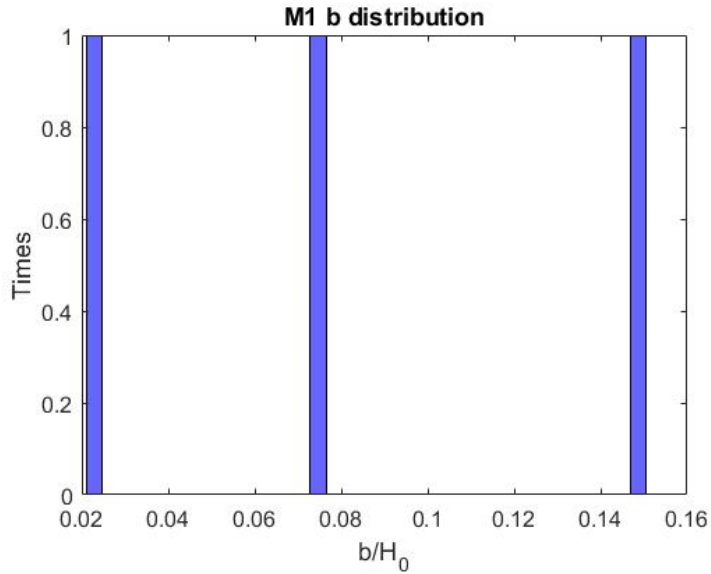


Figure 177: M1 web hole's pattern length distribution of W3 web corrosion pattern for beams without a diaphragm - MassDOT

The extreme hole corrosion cases belong in the range of the W3 pattern with M1 pattern holes (Figure 156).

11.3.6. Pattern W5

11.3.6.1. Web corrosion

Across the inspection reports, the W5 corrosion pattern was observed in total only 17 times. The parameters for the corrosion patterns can be found with corresponding diagrams in Section 1.5 *Corrosion Patterns* of this report. The normalized dimensions and the web thickness loss for the W5 pattern are presented below:

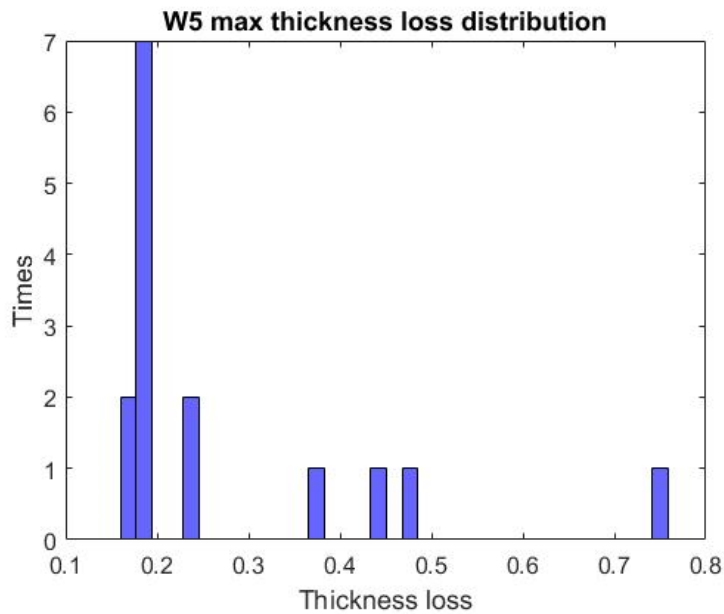


Figure 178. Max web thickness loss distribution of W5 web corrosion pattern for beams without a diaphragm - MassDOT

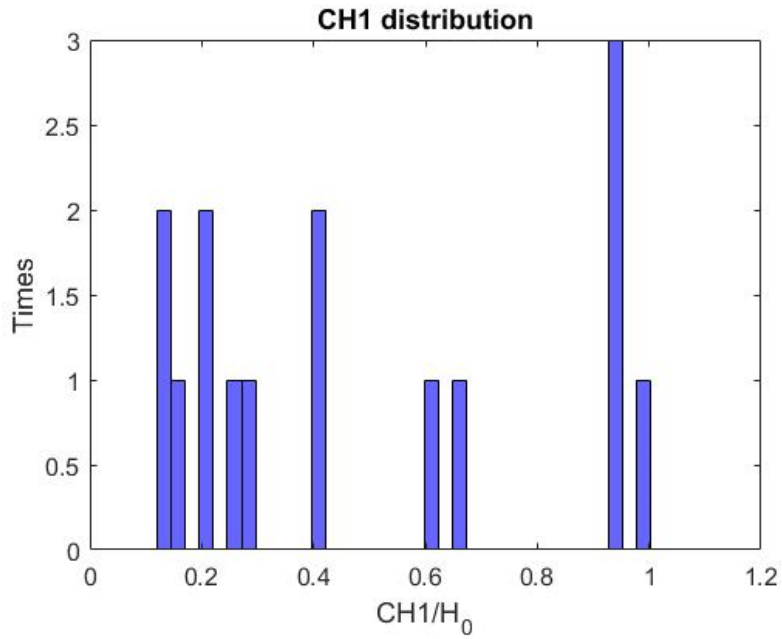


Figure 179: CH2 distribution of W5 web corrosion pattern for beams without a diaphragm - MassDOT

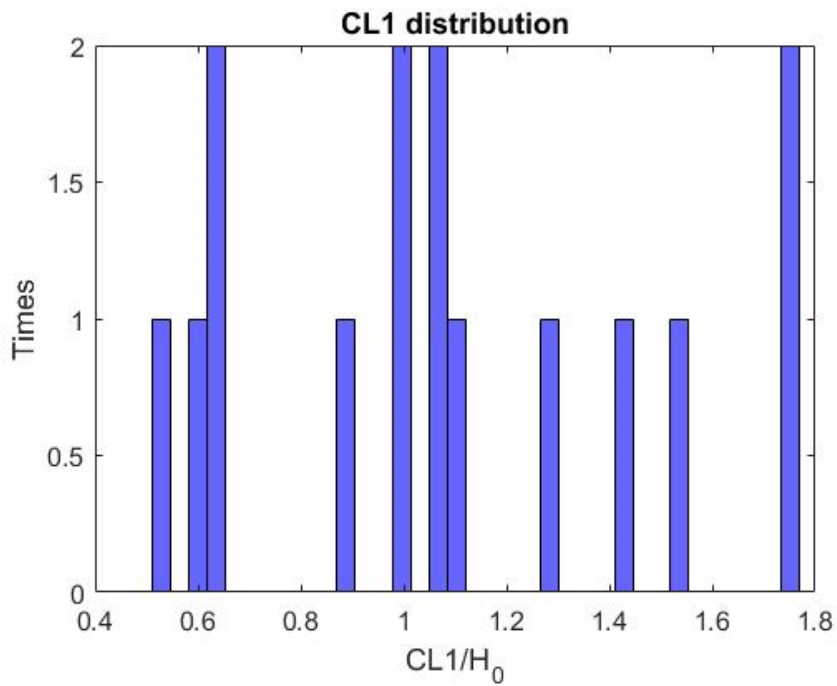


Figure 180: Max web thickness loss distribution of W5 web corrosion pattern for beams without a diaphragm - MassDOT

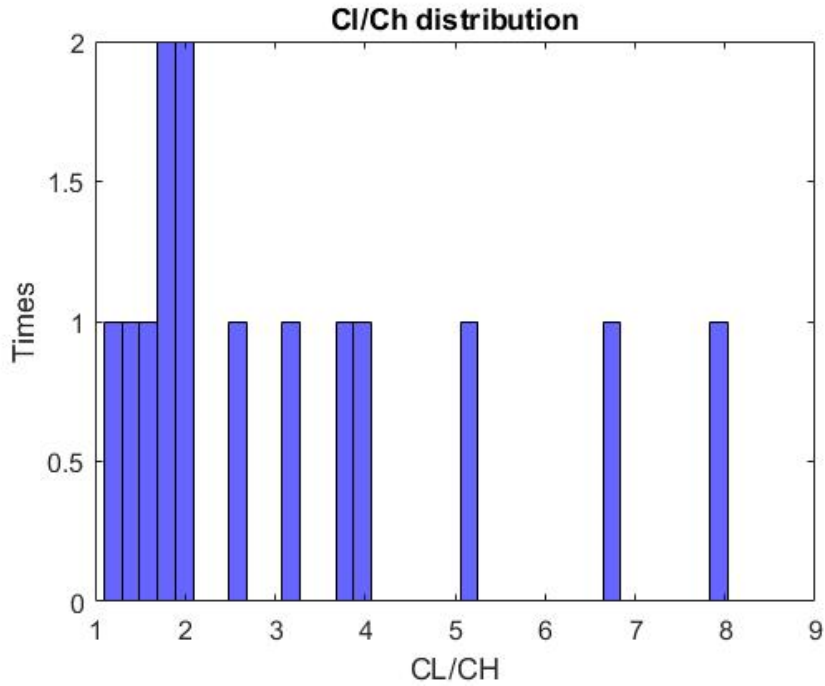


Figure 181:Ratio of corrosion length to height of W1 web corrosion pattern for beams without a diaphragm - MassDOT

From Figure 179, our team described the following: $0.15H_0 \leq CH_1 \leq H_0$

From Figure 180, our team described: $0.5H_0 \leq CH_1 \leq 1.8H_0$, with thickness loss: $\frac{t_{loss}}{t_{web}}$ that takes values of {0.2,0.5}

The extreme case:

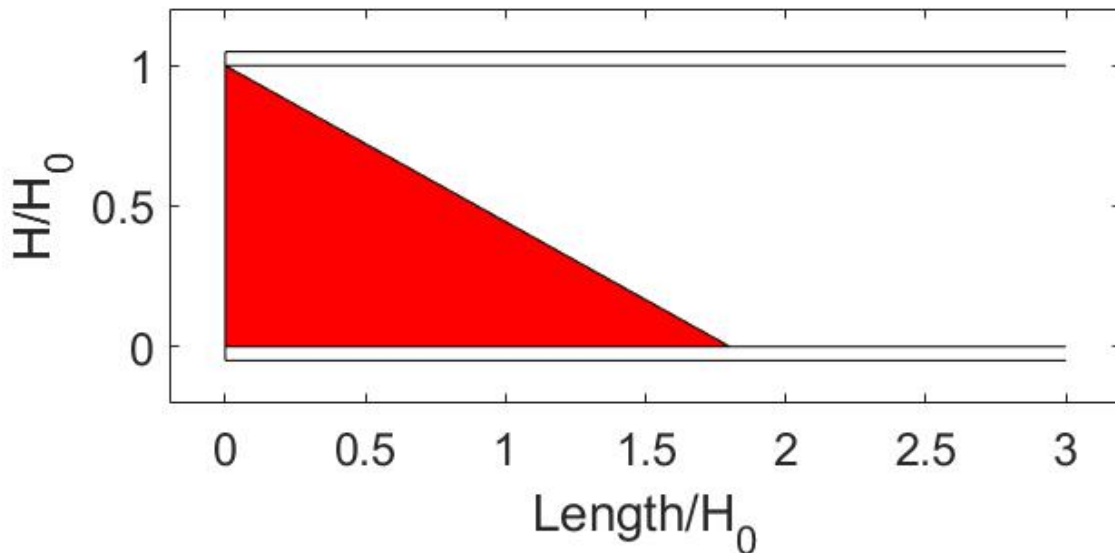


Figure 182: Extreme W4 web corrosion scenario for beams without a diaphragm - MassDOT

According to Figure 181 the tested cases should have a ratio $1 \leq \frac{CL}{CH} \leq 4$.

11.3.6.2. Flange corrosion

Our team plotted the ratio of the length of the corroded flange over the length of the corroded web in the following figure.

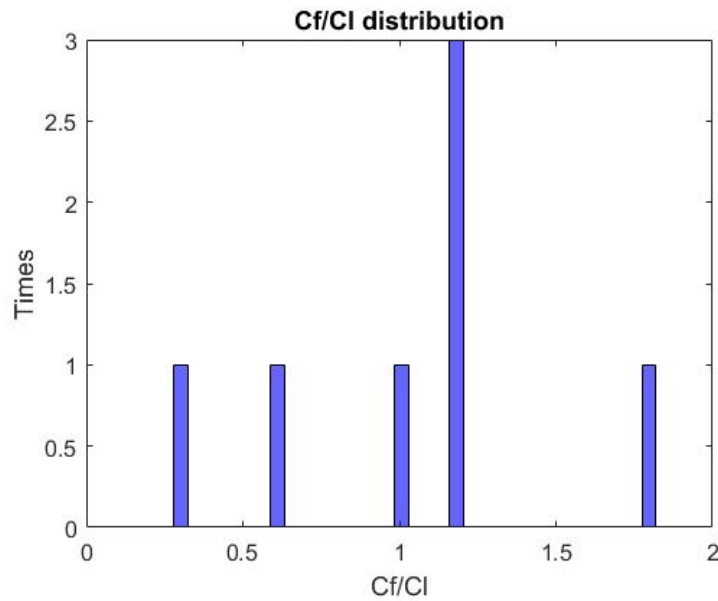


Figure 183: Ratio of flange to web corrosion length distribution of W5 web corrosion pattern for beams without a diaphragm - MassDOT

Thus, our team stated the following: $1 \leq \frac{C_f}{C_l} \leq 1.8$

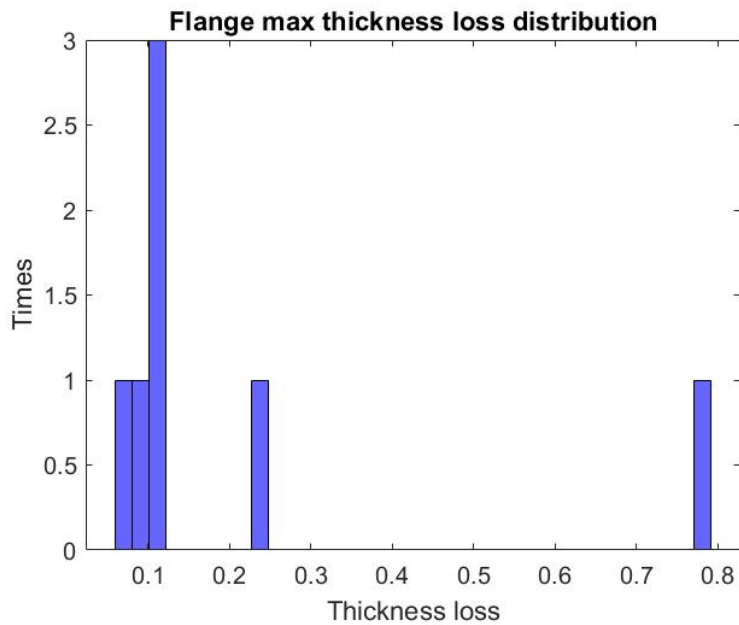


Figure 184: Max flange thickness loss distribution of W5 web corrosion pattern for beams without a diaphragm - MassDOT

11.3.6.3. Holes

There are very few cases found in the inspection reports with corrosion holes. To have an accurate data set, more data is necessary. As a result, and for validity, these cases were disregarded.

11.4. New Hampshire

11.4.1. Introduction

Similar to the inspection reports from MaineDOT, the reports provided by NHDOT do not provide the dimensions of the corroded areas of the beams. Additionally, the corrosion information provided for web and flange thickness loss are clearly linked to the beams.

Altogether, the research team was able to compile 13 out of the 15 reports provided by NHDOT. From the compiled reports, the research team was able to gather corrosion information of exactly 41 beam ends. Most of the information consists of the thickness loss of flanges and webs. It is worthwhile mentioning that none of the beam ends had diaphragms.

11.4.2. Web corrosion

The inspection reports do not always provide information regarding web thickness loss. More precisely, only 20% of the reports provided such information. Figure 185 depicts the histogram of the web thickness loss reported in the bridge inspection reports from NHDOT.

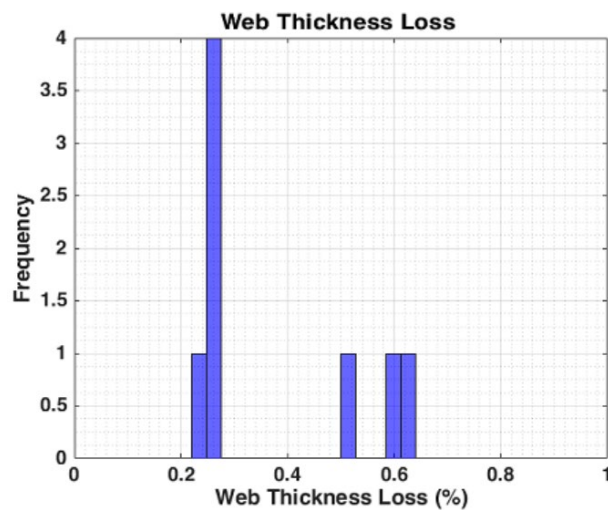


Figure 185: Web thickness loss histogram from the beam ends compiled - NHDOT

As discussed above, the research team was not able to gather information regarding corrosion length or corrosion height from the reports provided by NHDOT. This meant that our team could not create corrosion patterns for the bridge beams we analyzed via NHDOT's inspection reports.

11.4.3. Flange Corrosion

Many inspection reports provided by NHDOT had information regarding flange corrosion. Specifically, 36 out of the 40 compiled beam ends had information of flange corrosion either on the top flange or on the bottom flange. Figure 186 and Figure 187 depict the histogram of corrosion obtained for the bottom and top flanges, respectively.

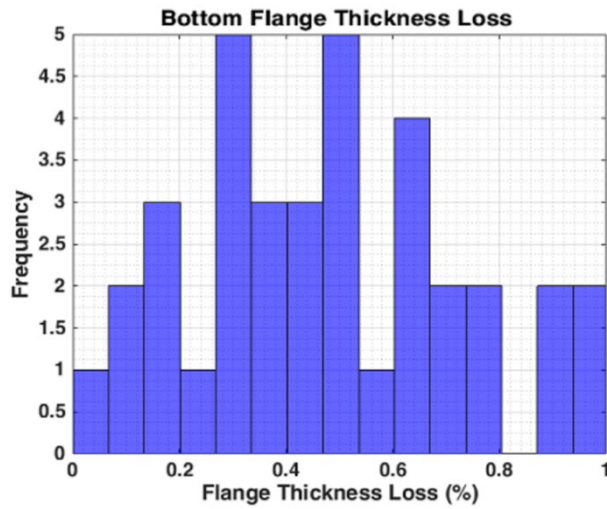


Figure 186: Bottom thickness loss histogram from the beam ends compiled - NHDOT

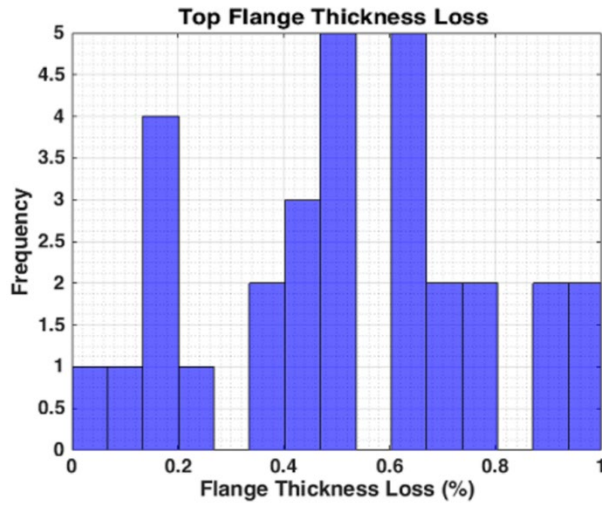


Figure 187 : Top thickness loss histogram from the beam ends compiled - NHDOT

11.4.4. Holes

Only two holes were observed in the inspection reports provided by NHDOT. Additionally, both holes were reported with photographs. The dimensions of the holes are described by the plots in Figure 188 and Figure 189.

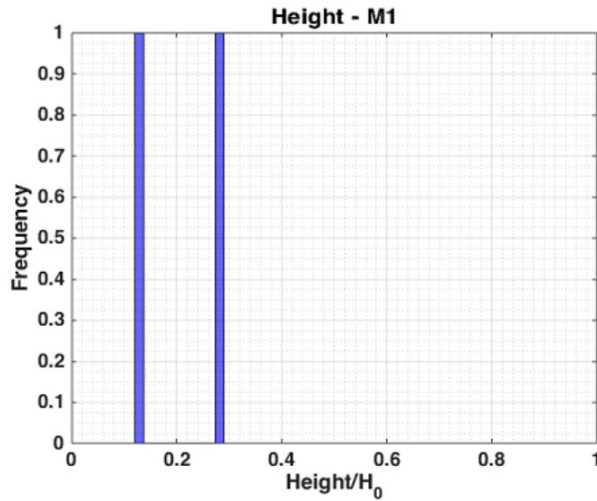


Figure 188: M1 web hole’s height distribution of W1 web corrosion pattern for beams without a diaphragm - NHDOT

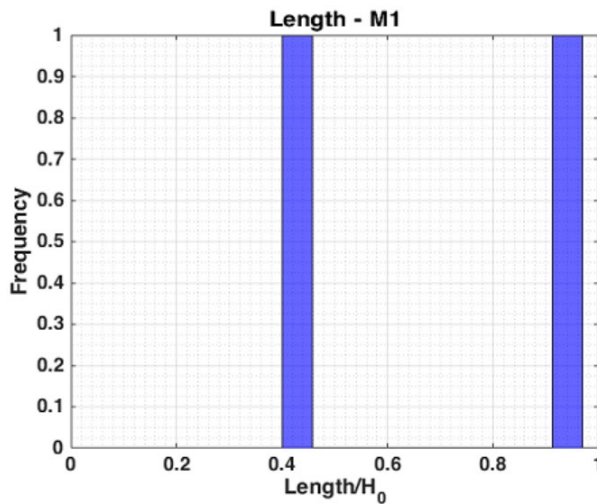


Figure 189: M1 web hole’s length distribution of W1 web corrosion pattern for beams without a diaphragm - NHDOT

11.5. Rhode Island

11.5.1. Introduction

As discussed in the previous sections, the results are presented for each state individually as the amount of beam ends vary significantly from one state to the other. In addition to dividing data by state, the beam ends were also divided into two subgroups. The beam ends without a diaphragm system and the beam ends with a diaphragm system.

From the reports provided by RIDOT, the research team was able to gather corrosion information of 89 beam ends without a diaphragm. Figure 190 depicts the frequency of corrosion patterns for beam ends without a diaphragm.

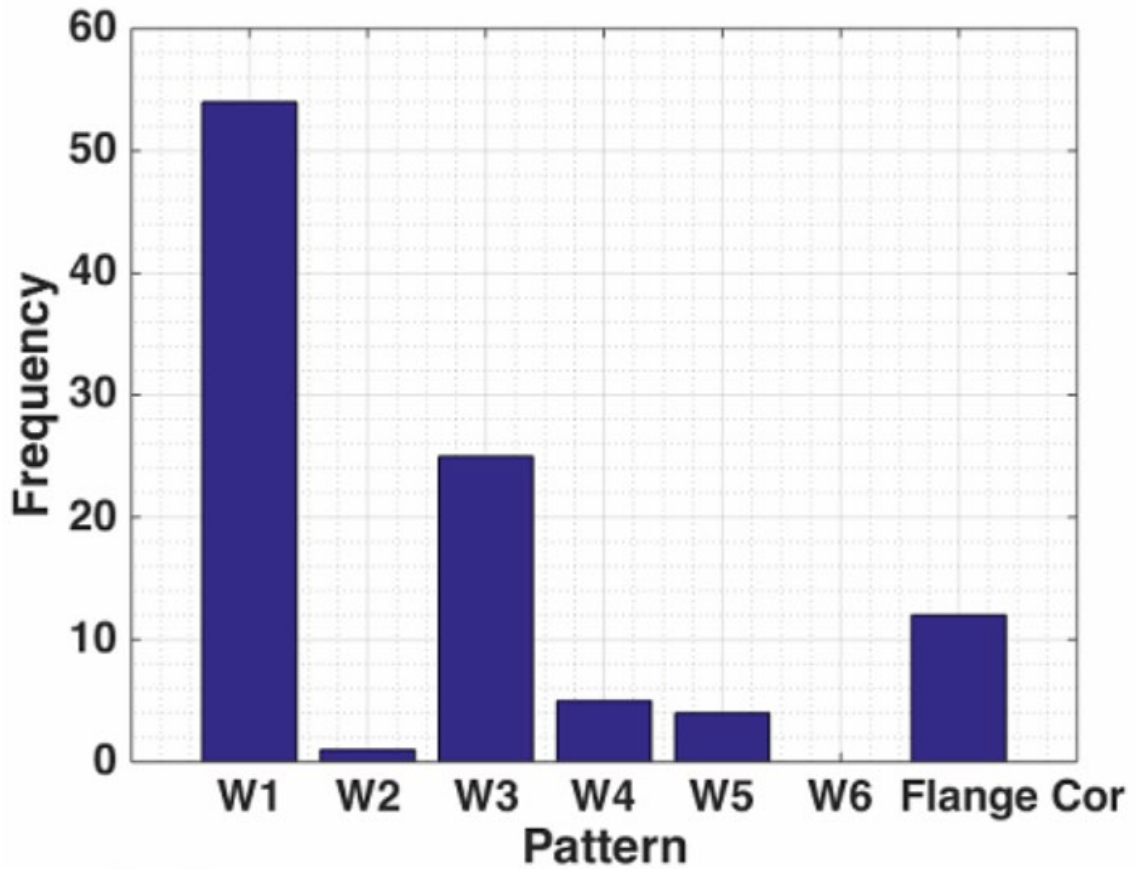


Figure 190 : Web corrosion patterns distribution for beams ends without diaphragm – RIDOT

11.5.2. Pattern W1

11.5.2.1. Web corrosion

The parameters for the corrosion patterns can be found with corresponding diagrams in Section 1.5 *Corrosion Patterns* of this report. The study starts by analyzing the height of corrosion for pattern W1, depicted in Figure 191.

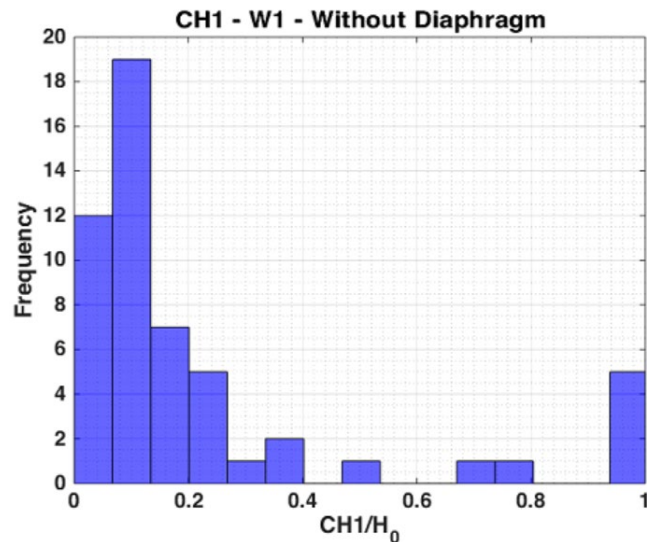


Figure 191: CH1 distribution of W1 pattern for beams without diaphragm - RIDOT

From Figure 191 is possible to observe that most of the beam ends have $CH_1 < 0.5$. Our team was able to isolate the beams which present $CH_1 < 0.5$. By doing this, we expected to understand the interaction between the parameters of the corrosion pattern W1. Additionally, our team expected to detect a pattern from which there is opportunity to determine an extreme scenario.

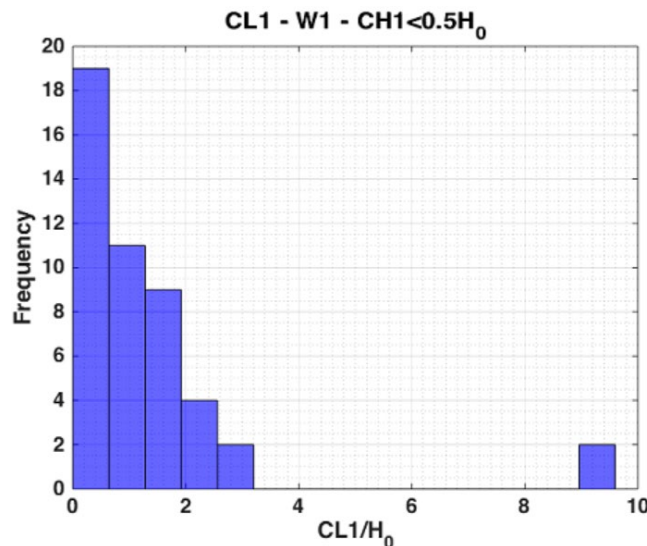


Figure 192: CL1 distribution of W1 pattern for beams without a diaphragm and $CH_1 < 0.5H_0$ - RIDOT

Figure 192 clearly depicts a trend, which is $CL_1 < 3$. Therefore, our team assumed that:

$$0 < CH_1 \leq 0.5H_0$$

$$0 < CL_1 \leq 3H_0$$

Figure 193 depicts the web thickness loss for the case $CH_1 < 0.5H_0$ and $CL_1 < 3$.

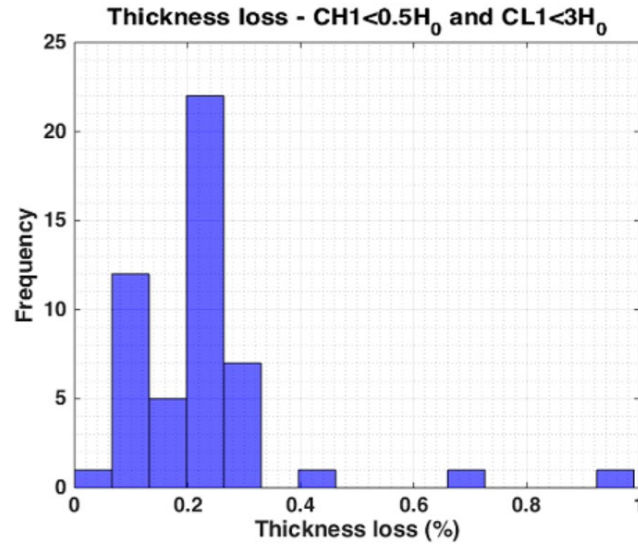


Figure 193: Web thickness loss of W1 pattern for beams without a diaphragm, $CH_1 < 0.5H_0$ and $CL_1 < 3H_0$ – RIDOT

Figure 193 depicts that the thickness loss clusters between 0% until 30%. That, is:

$$0 < \frac{t_{web}}{t_{loss}} \leq 0.3$$

By gathering the intervals determined from Figure 191, Figure 192 and Figure 193, our team was able to determine the extreme case of corrosion for pattern W1. A schematic illustration of this extreme case of corrosion is depicted in Figure 194.

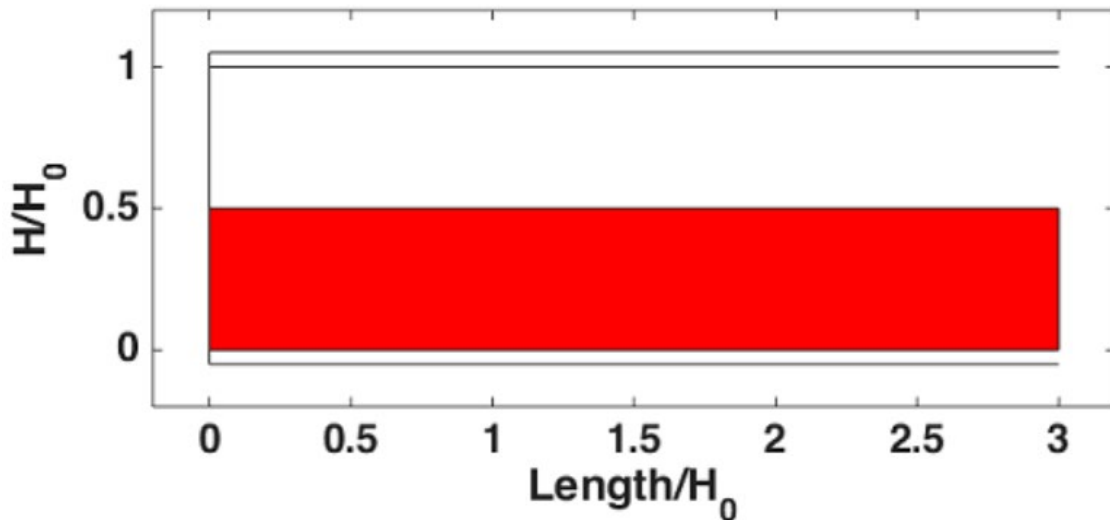


Figure 194: Extreme scenario for pattern W1 – RIDOT

11.5.2.2. Flange corrosion

The research team was able to record flange corrosion information for only 12 beam ends from the reports provided by RIDOT. Half of the recorded measurements are combined with pattern W1.

Due to the limited quantities of beams with flange corrosion, the team was not able to detect any trend regarding flange corrosion from the recorded data. Figure 195, Figure 196 and Figure 197 depict the statistics the research team was able to extract from the available data.

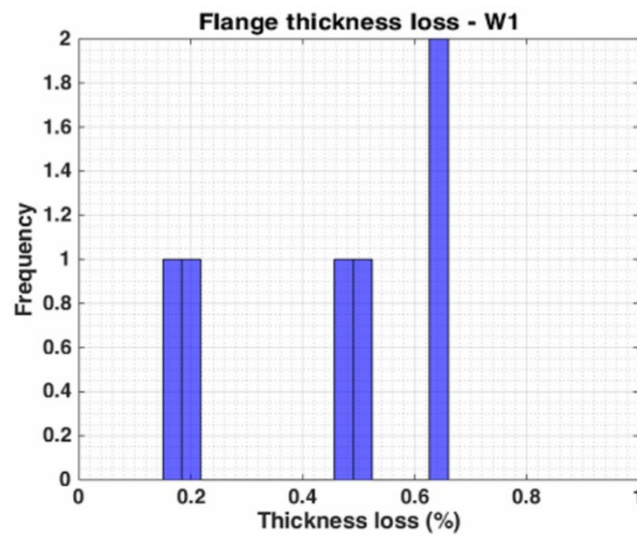


Figure 195: Flange thickness Loss for pattern W1 – RIDOT

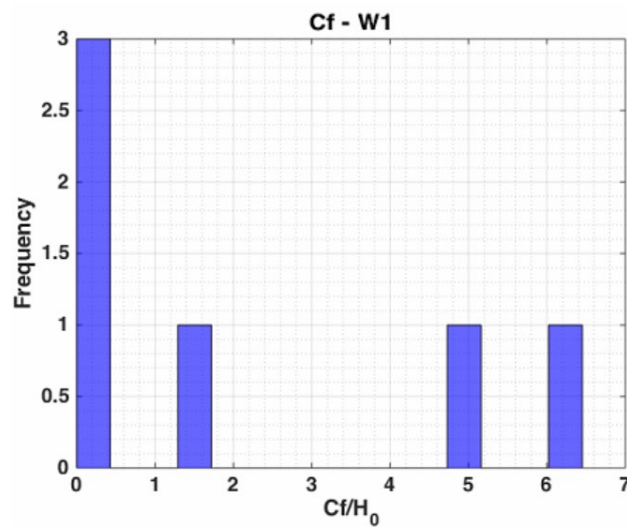


Figure 196: Flange corrosion length for pattern W1 – RIDOT

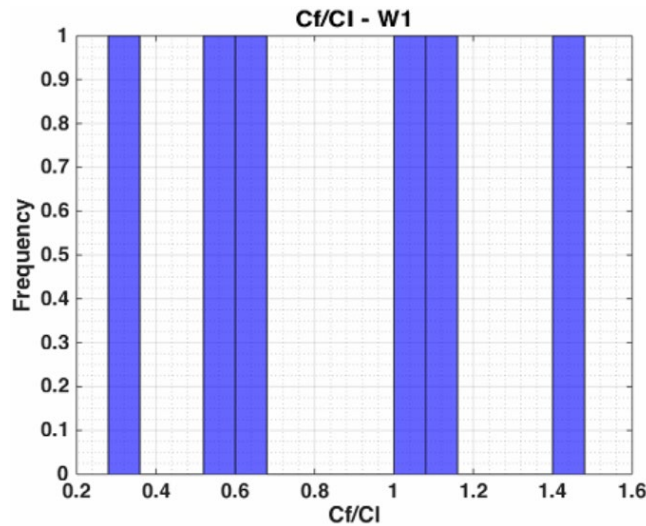


Figure 197: Ratio between flange corrosion length and web corrosion length for pattern W1 – RIDOT

11.5.2.3. Holes

Table 79: Holes and patterns for beams without a diaphragm – RIDOT portrays the frequency of corrosion patterns and holes that the research team was able to record from the bridge inspection reports provided by RIDOT.

Table 79: Holes and patterns for beams without a diaphragm – RIDOT

	Number	No Hole	M 1	M 2	M 3	M 4	M1 and M2	M1 and M3	M2 and M4
W1	54	49	4	0	1	0	0	0	0
W2	1	1	0	0	0	0	0	0	0
W3	25	21	0	0	1	2	0	0	0
W4	5	5	0	0	0	0	0	0	0
W5	4	4	0	0	0	0	0	0	0
W6	0	0	0	0	0	0	0	0	0

Therefore, only 5 holes were reported and were combined with the W1 corrosion pattern. Unfortunately, no trend was detected by the research team. Figure 198, Figure 199, Figure 200 and Figure 201 depicts the dimensions of the recorded corrosion holes.

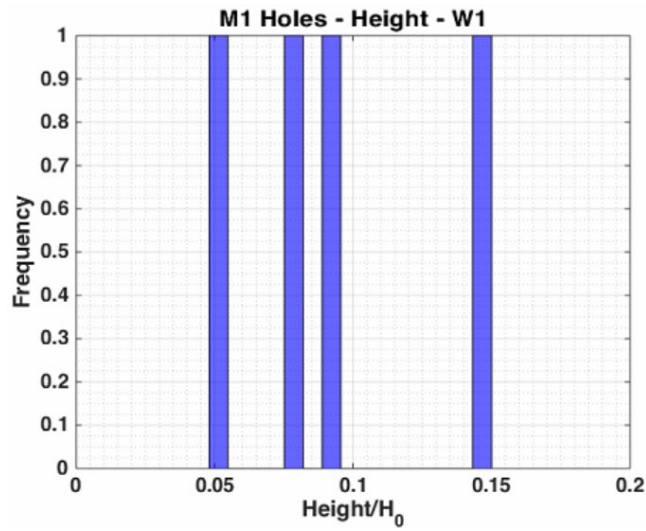


Figure 198: Height of M1 holes combined with W1 pattern – RIDOT

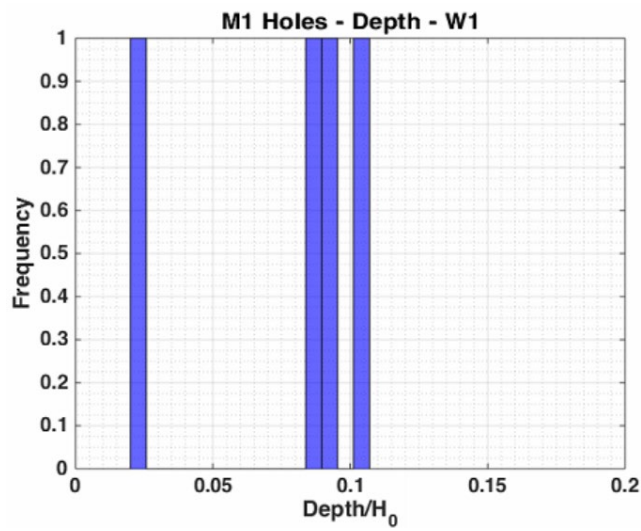


Figure 199: Depth of M1 holes combined with W1 pattern – RIDOT

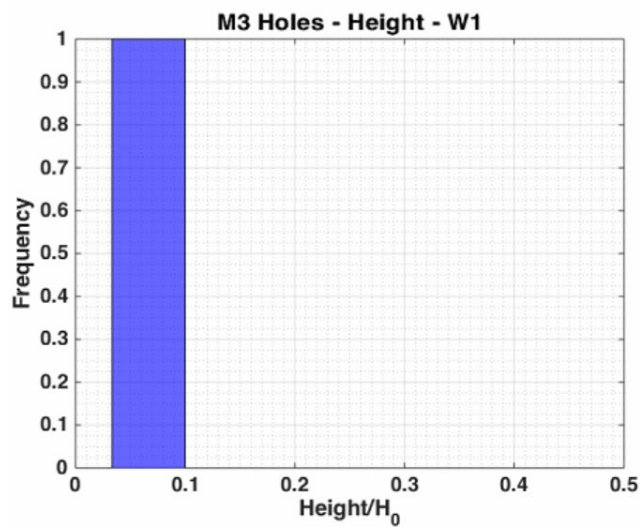


Figure 200: Height of M3 hole combined with W1 pattern – RIDOT

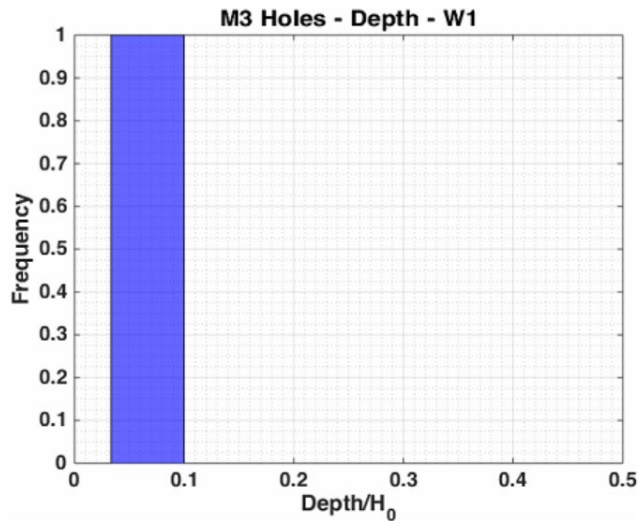


Figure 201: Depth of M3 holes combines with W1 pattern – RIDOT

11.5.3. Pattern W2

11.5.3.1. Web Corrosion

Just a single case of the W2 corrosion pattern was recorded. Therefore, it was not possible to study trends from the available data. The parameters for the corrosion patterns can be found with corresponding diagrams in Section 1.5 *Corrosion Patterns* of this report.

The dimensions of the recorded W2 case are:

$$\frac{CH_1}{H_0} = 11\%$$

$$\frac{CL_1}{H_0} = 26.2\%$$

$$\frac{CL_2}{H_0} = 16.6\%$$

$$\frac{t_{loss}}{t_{web}} = 24.4\%$$

Figure 202 depicts a schematic sketch of the recorded W2 case.

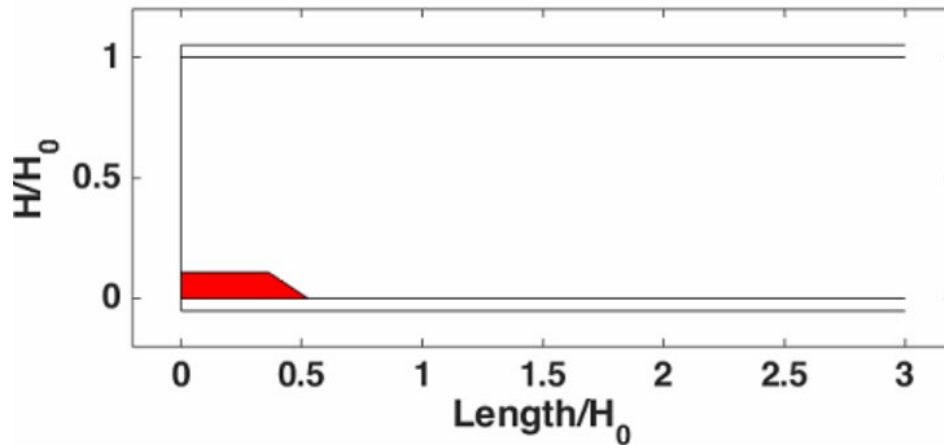


Figure 202: Schematic representation of W2 pattern – RIDOT

11.5.3.2. Flange Corrosion

There was no flange corrosion analyzed or recorded for this case.

11.5.3.3. Holes

There were no holes analyzed, recorded, or combined with this case.

11.5.4. Pattern W3

11.5.4.1. Web Corrosion

Similar to the other cases, the study of W3 corrosion pattern begins by the analysis of the total corrosion height, characterized by parameters CH2 of pattern W3. The parameters for the corrosion patterns can be found with corresponding diagrams in Section 1.5 *Corrosion Patterns* of this report. Figure 203 depicts the resulting distribution of CH2 for beams ends without diaphragm.

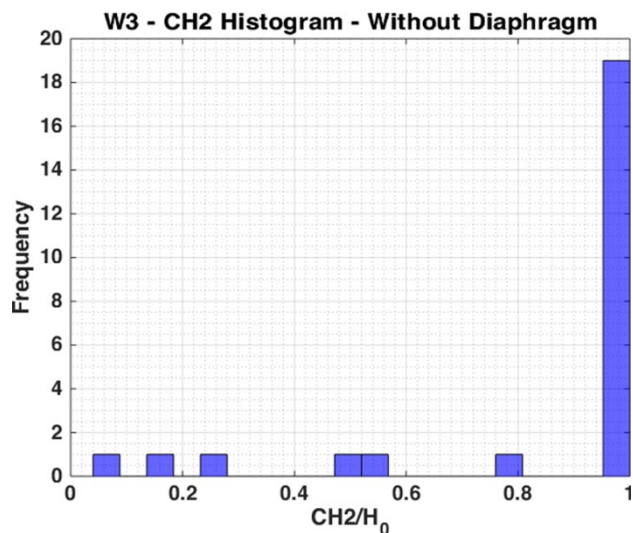


Figure 203: CH2 distribution for W3 pattern - RIDOT

Figure 203 depicts the clear trend that $CH_2 > 0.9H_0$. Therefore, one is able to obtain the distribution of the other parameters given that $Ch_2 > 0.9H_0$. Figures Figure 204, Figure 205,

Figure 206, Figure 207 and Figure 208 depict the behavior of the other parameters given that $CH2 > 0.9H0$.

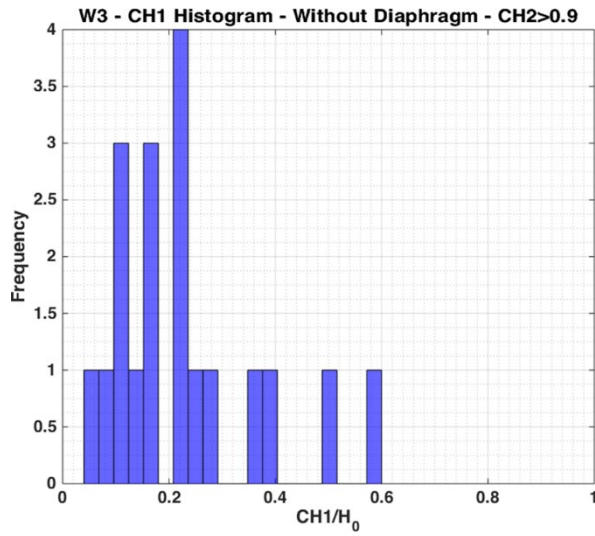


Figure 204: CH1 distribution for W3 pattern and $CH2 > 0.9H0$ - RIDOT

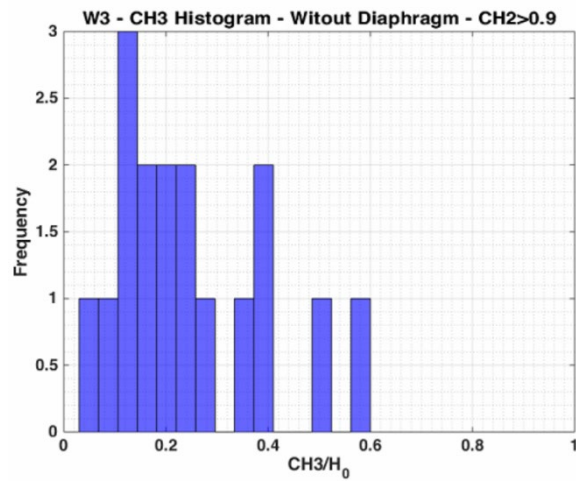


Figure 205: CH3 distribution for W3 pattern and $CH2 > 0.9H0$ - RIDOT

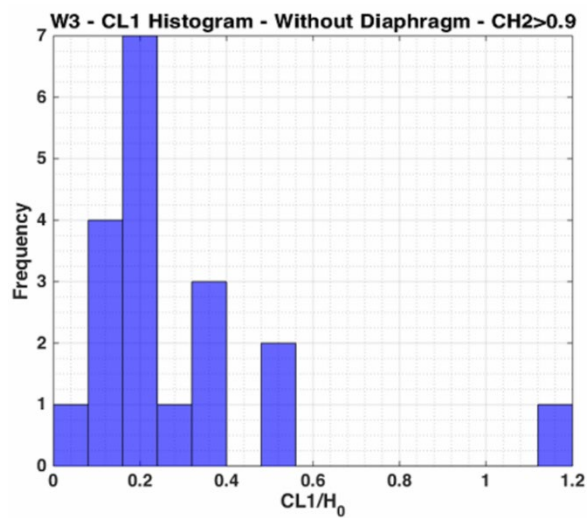


Figure 206: CL1 distribution for W3 pattern and $CH2 > 0.9H0$ - RIDOT

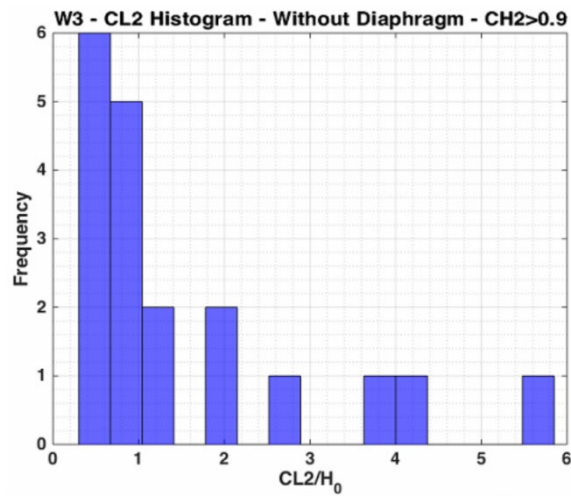


Figure 207: CL2 distribution for W3 pattern and CH2>0.9H0 - RIDOT

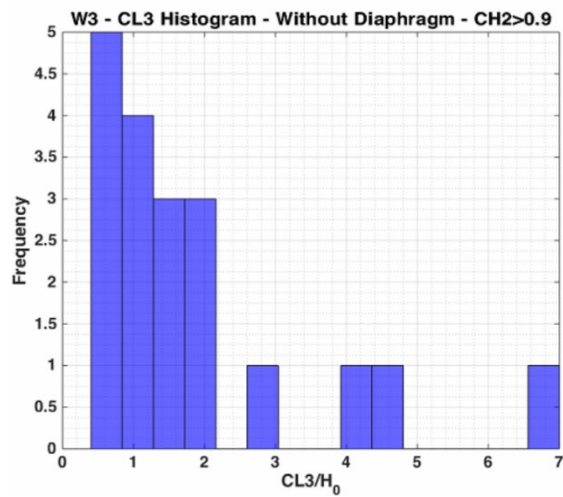


Figure 208: CL3 distribution for W3 pattern and CH2>0.9H0 - RIDOT

Figure 209 depicts the web thickness loss for the W3 corrosion pattern.

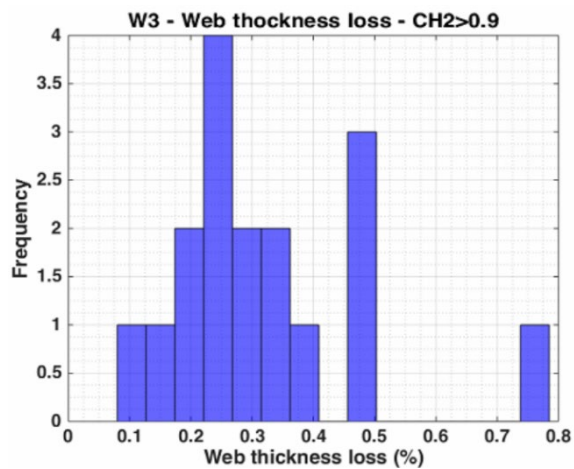


Figure 209: Web thickness loss distribution for W3 pattern and CH2>0.9H0 - RIDOT

From the previous figures, our team was able to determine the intervals for the W3 corrosion patterns, which can be written as:

$$0 \leq CH_1 \leq 0.4H_0$$

$$0.9H_0 \leq CH_2 \leq 1H_0$$

$$0 \leq CH_3 \leq 0.4H_0$$

$$0 \leq CL_1 \leq 0.5H_0$$

$$0 \leq CL_2 \leq 2.5H_0$$

$$0.5H_0 \leq CL_3 \leq 3H_0$$

$$0.1 \leq \frac{t_{loss}}{t_{web}} \leq 0.5$$

Figure 210 depicts a schematic representation of the extreme corrosion case for W3 corrosion pattern.

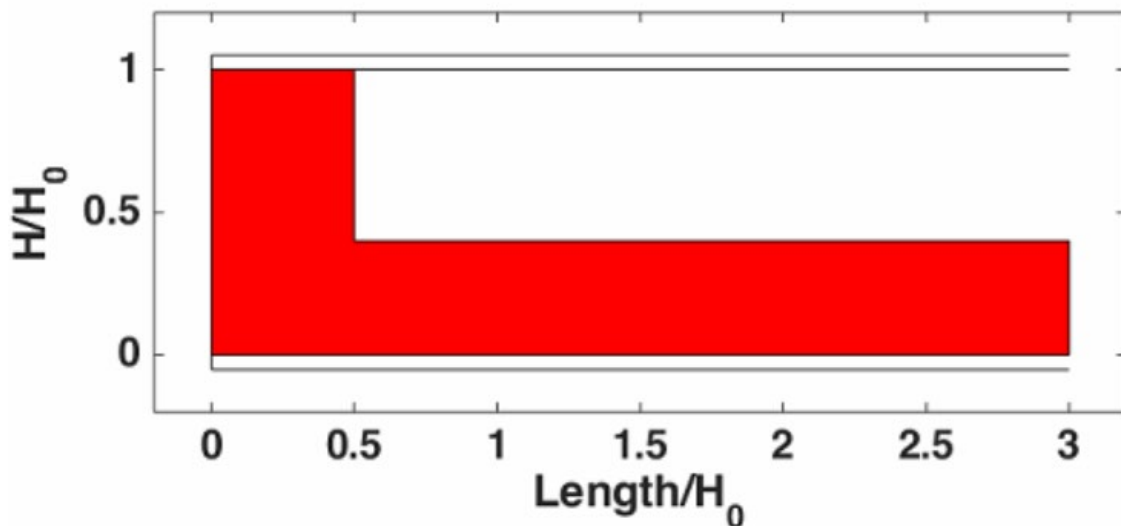


Figure 210: Extreme corrosion case for W3 pattern - RIDOT

11.5.4.2. Flange Corrosion

From the bridge inspection reports, the research team was able to record 4 cases of flange corrosion combined with the pattern W3. No trend was detected by the research team regarding the flange thickness loss. Figures Figure 211, Figure 212 and Figure 213 depict the statistics that the research team was able to obtain from the bridge inspection reports.

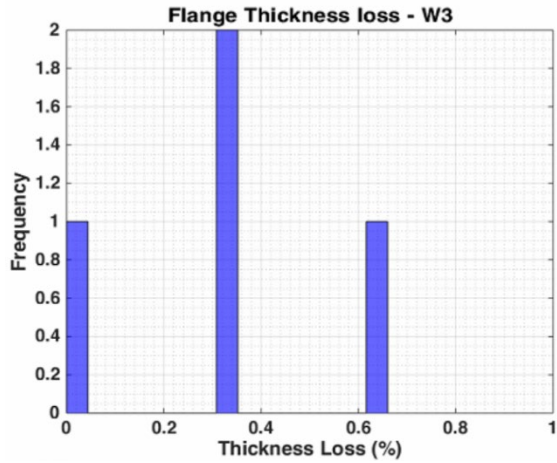


Figure 211: Flange thickness loss distribution for W3 pattern – RIDOT

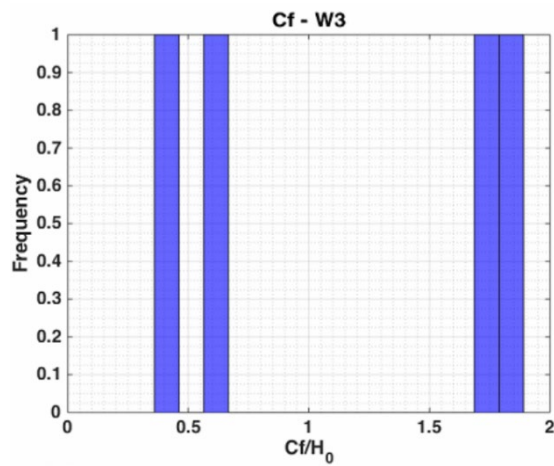


Figure 212: Flange corrosion length for W3 pattern – RIDOT

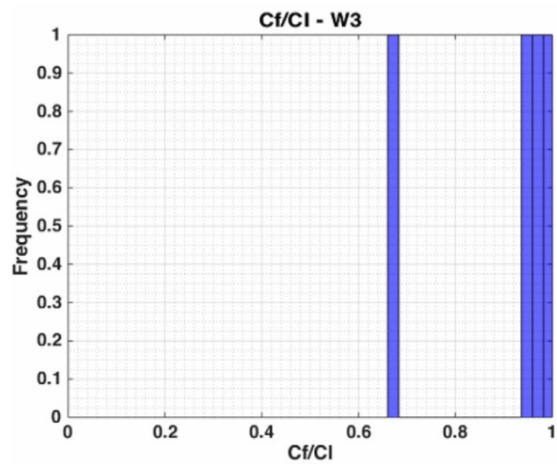


Figure 213: ratio between flange corrosion length and web corrosion length for W3 pattern – RIDOT

It is worth noting that, although no trend was depicted, it is possible to observe that the behavior of the corrosion of the flanges is similar to the corrosion of the web. That is, the length of corroded flange is close to the total length of web corrosion.

11.5.4.3. Holes

From the bridge inspection reports provided by RIDOT, the research team was able to record only 3 holes combined with the W3 corrosion pattern, as portrayed in Figures 186, 187, 188, and 189. As not all three holes belong to the same topology, the research team was not able to identify trends in the data.

Figure 214, Figure 215, Figure 216 and Figure 217 depict the dimensions of the recorded holes.

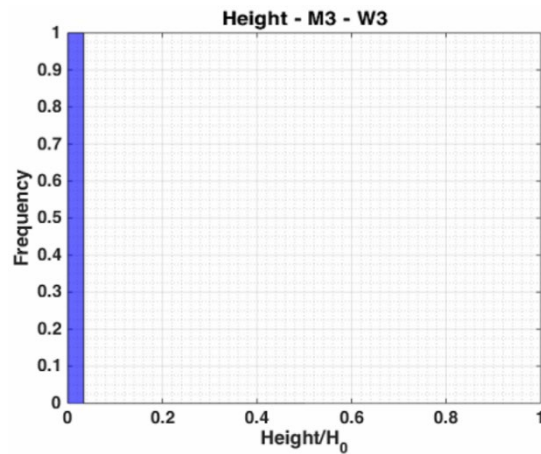


Figure 214: Height of M3 hole combined with W3 pattern – RIDOT

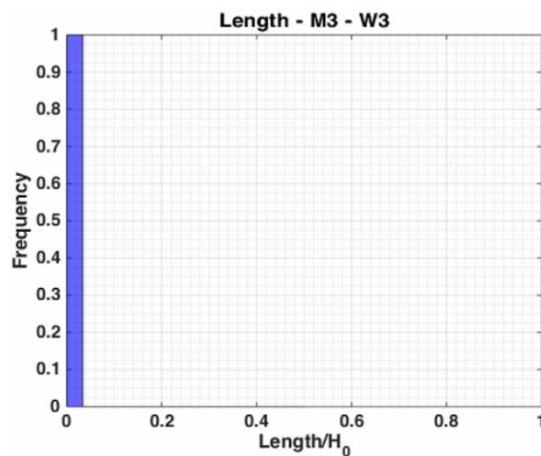


Figure 215: Length of M3 hole combined with W3 pattern – RIDOT

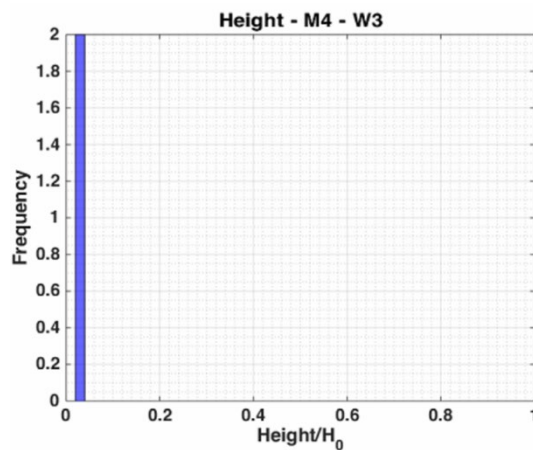


Figure 216: Height of M4 holes combined with W3 pattern – RIDOT

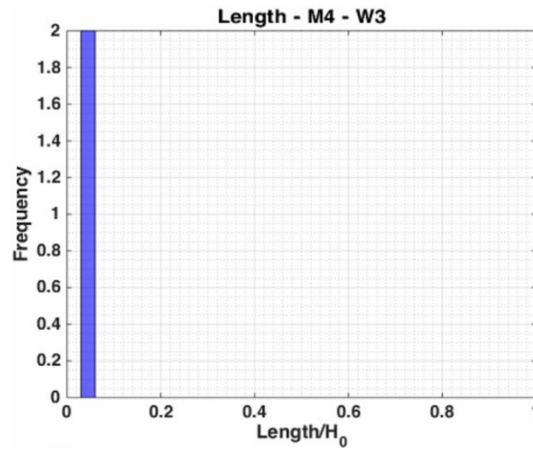


Figure 217: Length of M3 hole combined with W3 pattern – RIDOT

11.5.5. Pattern W4

11.5.5.1. Web Corrosion

Figure 218 depicts the distribution of CH2 of pattern W4. Figure 218 clearly depicts the trend of $CH2 > 0.9H_0$. The research team was not able to detect trends as the other parameters of W4 pattern are scattered, which limited our research team in detecting trends. The parameters for the corrosion patterns can be found with corresponding diagrams in Section 1.5 *Corrosion Patterns* of this report. Figure 219, Figure 220, Figure 221 and Figure 222 depict the distribution of the other parameters recorded from the bridge inspection reports.

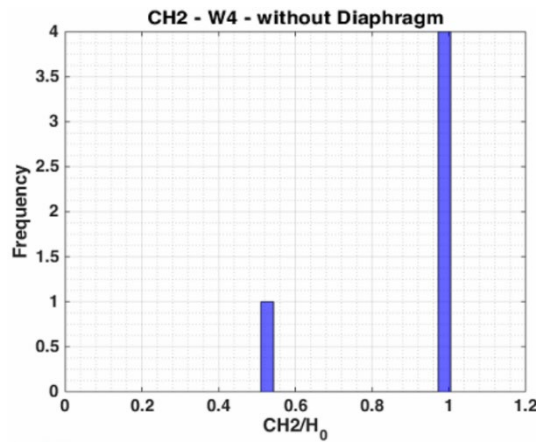


Figure 218: CH2 distribution for W4 pattern – RIDOT

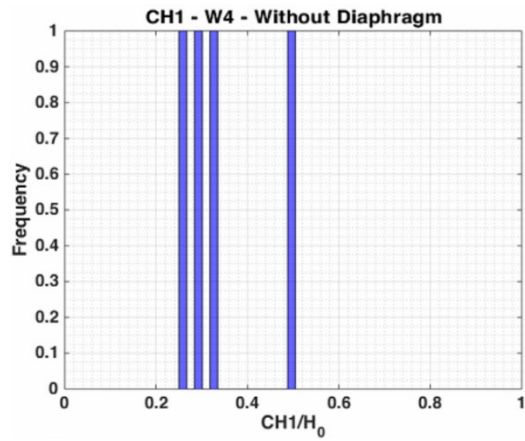


Figure 219: CH1 distribution for W4 pattern – RIDOT

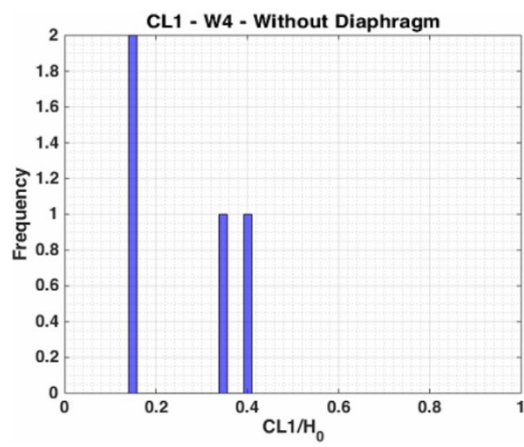


Figure 220: CL1 distribution for W4 pattern – RIDOT

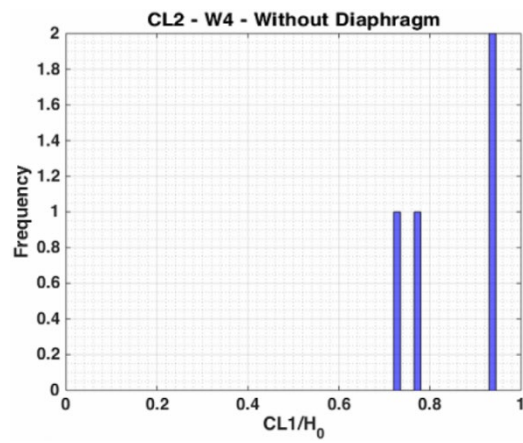


Figure 221: CL2 distribution for W4 pattern – RIDOT

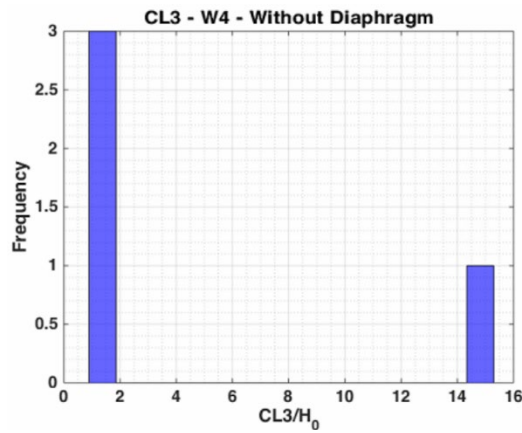


Figure 222: CL3 distribution for W4 pattern – RIDOT

Figure 223 depicts the web thickness loss of the W4 corrosion pattern.

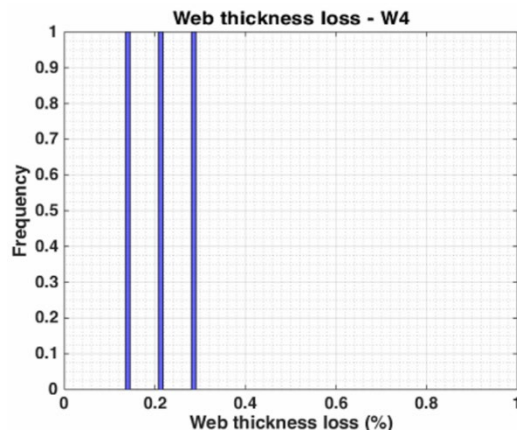


Figure 223: Web thickness loss distribution for W4 pattern – RIDOT

11.5.5.2. Flange Corrosion

From the bridge inspection reports, the research team was able to record just two measurements of flange corrosion combined with the W4 corrosion pattern. As two recorded pattern instances are not enough to define trends, Figure 224, Figure 225, and Figure 226 depict the measurements provided by the inspection reports.

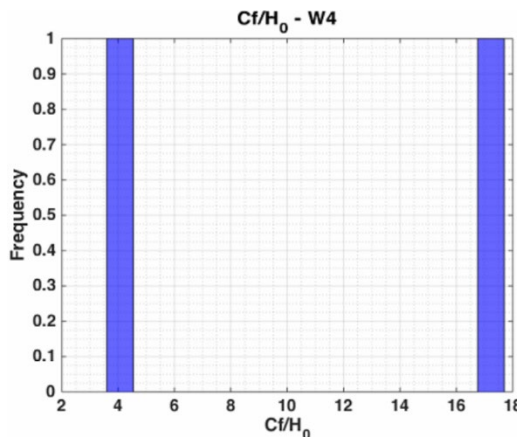


Figure 224: Flange corrosion length distribution for W4 pattern – RIDOT

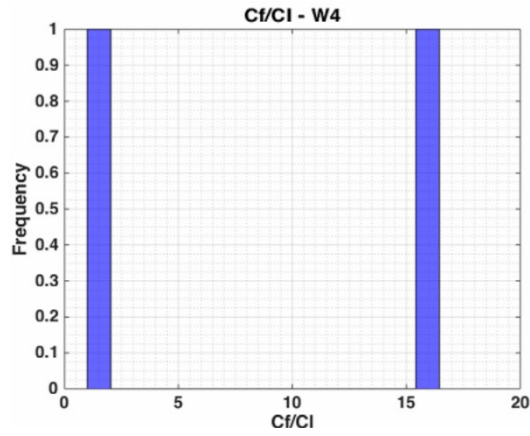


Figure 225: Ratio between flange corrosion length and corrosion length for W4 pattern – RIDOT

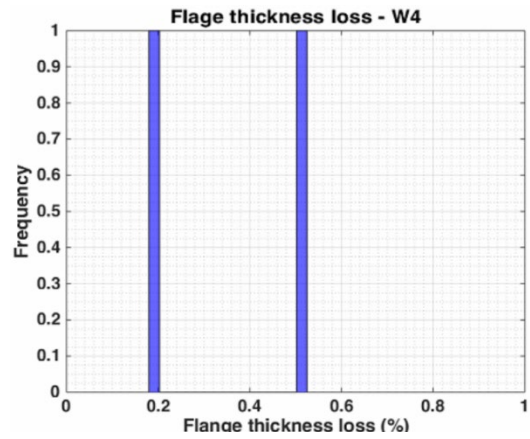


Figure 226: Flange thickness loss distribution for W4 pattern – RIDOT

11.5.5.3. Holes

No holes were reported in this section which combined with the W4 corrosion pattern.

11.5.6. Pattern W5

11.5.6.1. Web corrosion

The research team was able to record data from 4 cases of the W5 corrosion pattern. The parameters for the corrosion patterns can be found with corresponding diagrams in Section 1.5 *Corrosion Patterns* of this report. As the amount of data recorded was not enough to detect any trends, Figure 227 and Figure 228 depict only the histogram of the parameters.

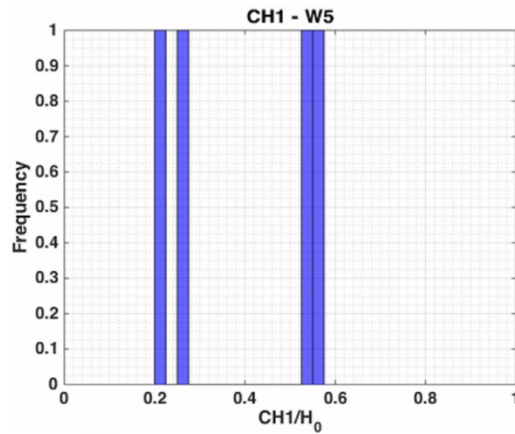


Figure 227: CH1 distribution for W5 pattern – RIDOT

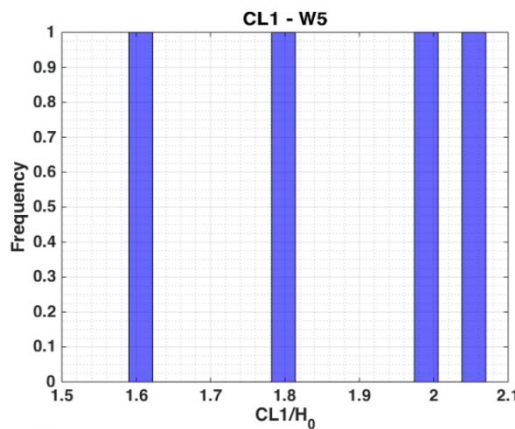


Figure 228: CL1 distribution for W5 pattern – RIDOT

Figure 229 depicts the web thickness loss for the W5 corrosion pattern.

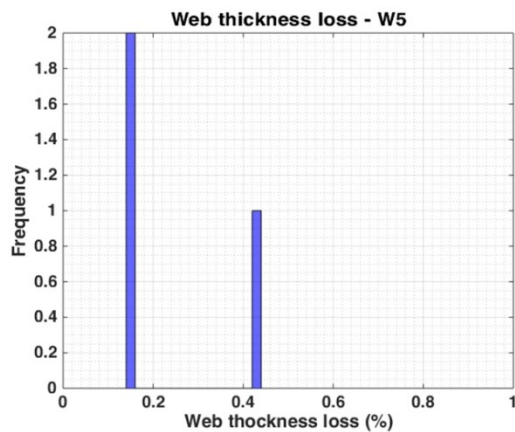


Figure 229: Web thickness loss for W5 pattern – RIDOT

11.5.6.2. Flange corrosion

No flange corrosion information was reported combined with the W5 corrosion pattern.

11.5.6.3. Holes

No holes were reported combined with the W5 corrosion pattern.

11.6. Vermont

11.6.1. Introduction

The research team was able to find corrosion information in only 15 out of approximately 70 reports provided by VTrans. From the compiled reports, we were able to gather information for 36 beams ends. Similar to the reports from MaineDOT and NHDOT, the reports from VTrans do not present the measurements of the corroded area. Therefore, only information regarding web and flange thickness loss were collected. Additionally, this means that corrosion patterns were not created due to the lack of parameters. It is also imperative to note that the reports did not clearly link the corrosion information to a specific beam. Aiming to treat the reports from all states equally, the information was compiled as if it referred to a single beam.

11.6.2. Web corrosion

As stated above, the absence of sketches and labels on the pictures hampered the research team to classify the corrosion topology. For this reason, the only information regarding web corrosion that the research team was able to obtain from the VTrans bridge inspection reports was the web thickness loss. Figure 230 depicts the histogram of web thickness loss obtained from the data provided by VTrans reports.

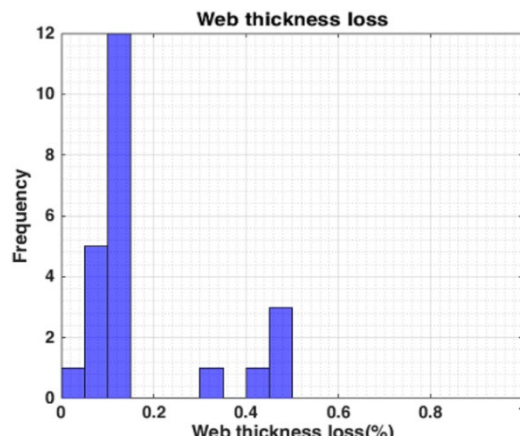


Figure 230: Web thickness loss histogram from the beam ends compiled - VTrans

11.6.3. Flange corrosion

Similar to the reports from MaineDOT and NHDOT, the reports from VTrans often present information regarding the thickness loss in the flanges. Figures Figure 231 and Figure 232 depict the thickness loss for bottom and top flanges, respectively.

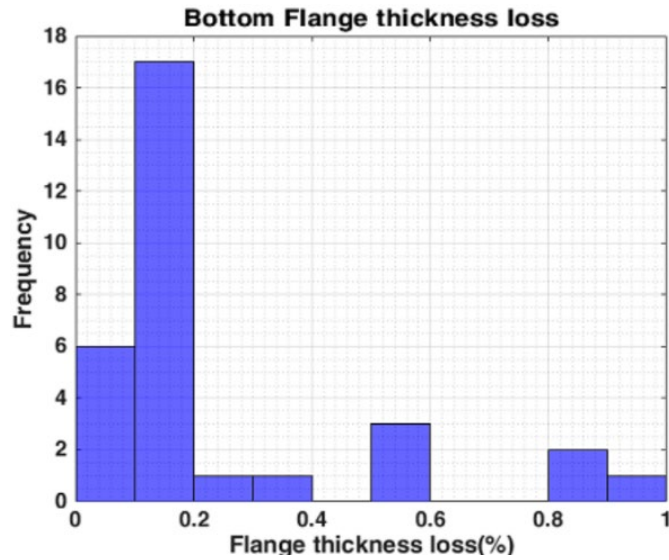


Figure 231: Bottom flange thickness loss histogram from the beam ends compiled - VTrans

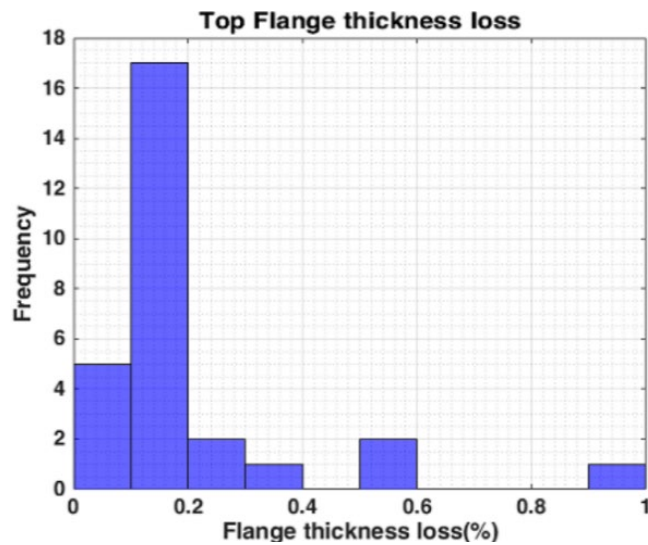


Figure 232: Top flange thickness loss histogram from the beam ends compiled - VTrans

11.6.4. Holes

Although a relatively small amount of beam ends was compiled, a significant number of holes were observed in the data. 11 holes were observed in the documents provided by VTrans. Table 52 denotes the topologies of the observed holes.

Table 80: Holes for beams ends from VTrans

Topology	# of reported holes
M1	5
M2	0
M3	2
M4	2
M1+M3	1

M1+M2	0
M2+M4	0

The dimensions of the holes are depicted in Figure 233, Figure 234, Figure 235, Figure 236, Figure 237, Figure 238, and Figure 239.

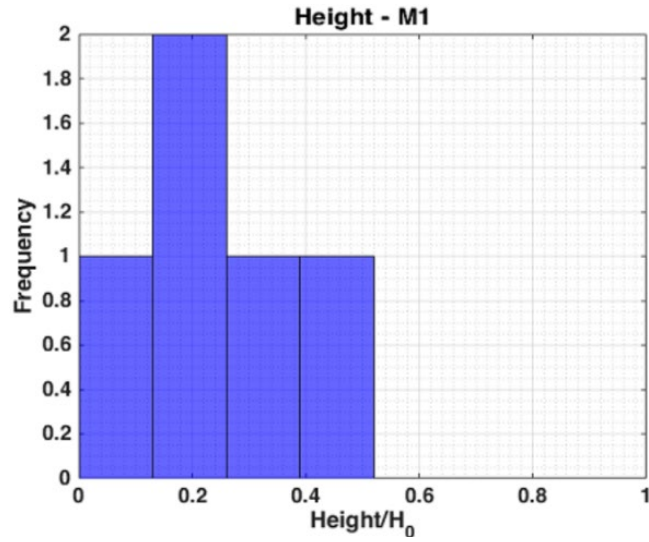


Figure 233: M1 web hole's height distribution beams without a diaphragm - VTrans

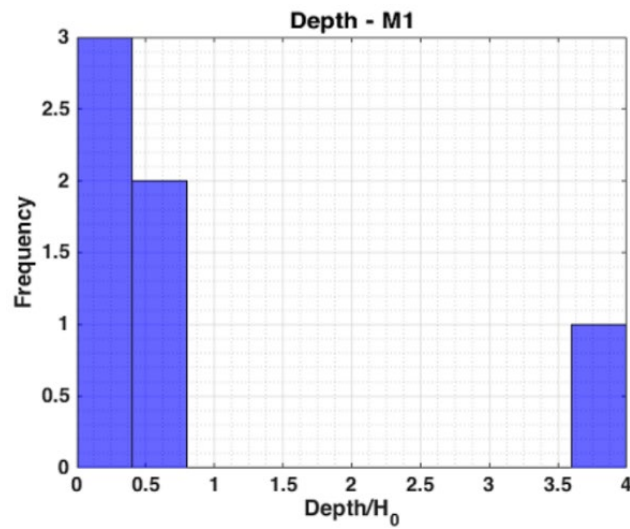


Figure 234: M1 web hole's depth distribution beams without a diaphragm - VTrans

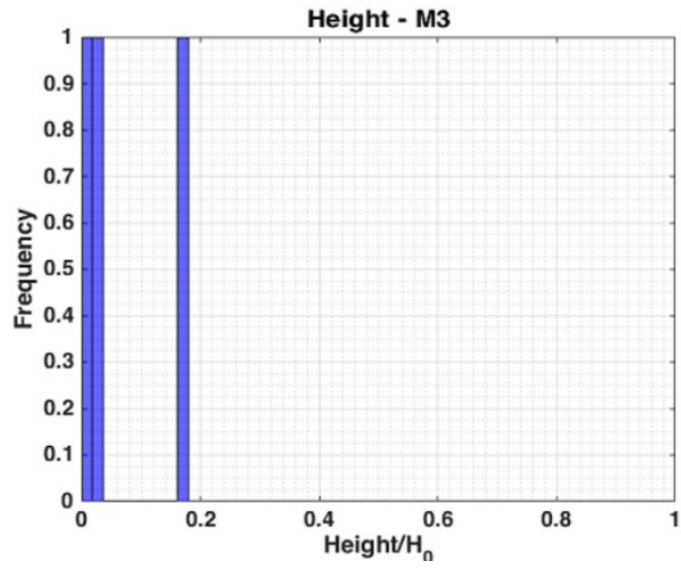


Figure 235: M3 web hole's height distribution beams without a diaphragm - VTrans

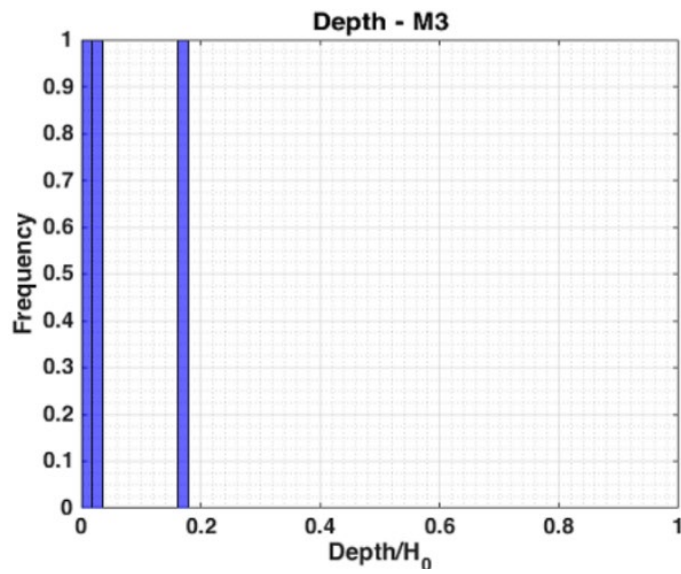


Figure 236 : M3 web hole's depth distribution beams without a diaphragm - VTrans

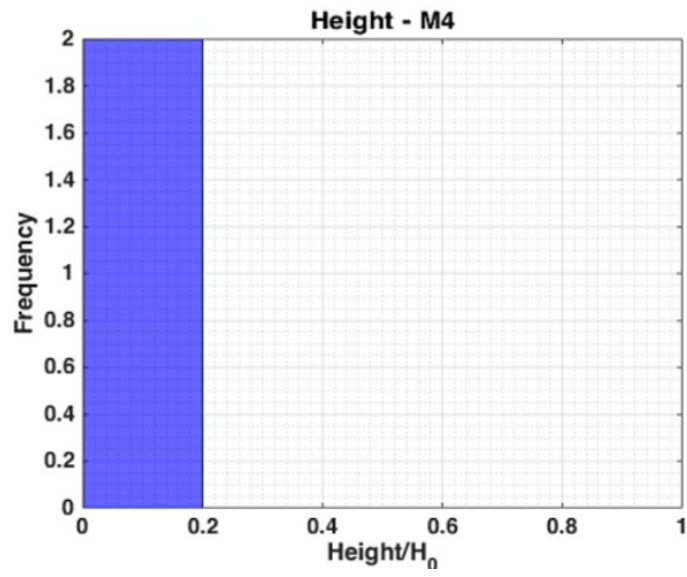


Figure 237: M4 web hole's height distribution beams without a diaphragm - VTrans

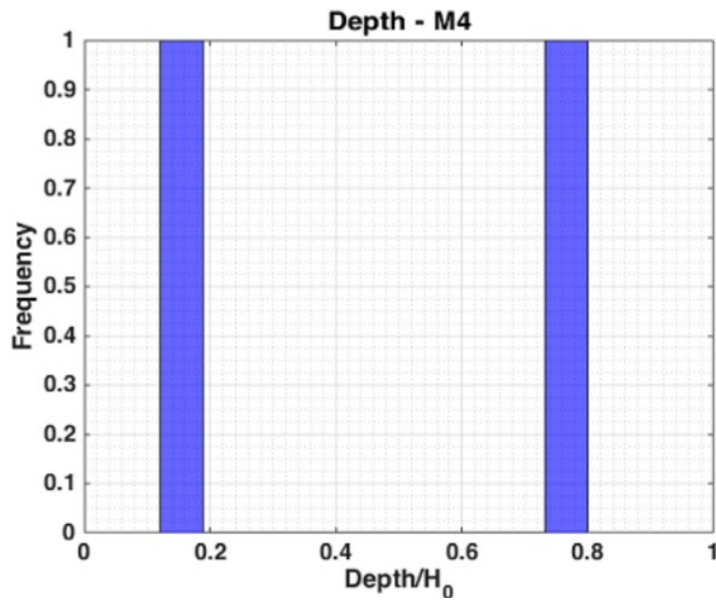


Figure 238: M4 web hole's depth distribution beams without a diaphragm - VTrans

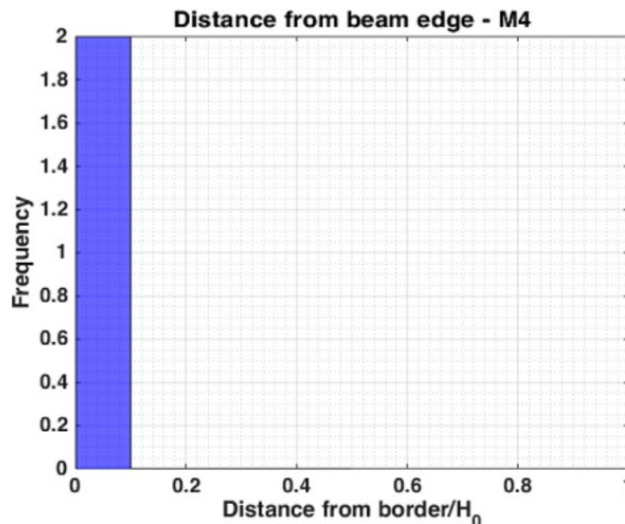


Figure 239 : M4 web hole's distance from beam edge distribution beams without a diaphragm - VTrans

12. Appendix II – Detailed data and processing graphs for beam ends with a diaphragm

12.1. Connecticut

12.1.1. Introduction

As commented in the previous sections, the data was divided by state as the number of beams ends were significantly different from one state to the other. Thus, to not introduce bias in the results, all states were individually analyzed. Following this initial grouping of the data, beam ends were divided into two sub-groups: the ones with diaphragm and the ones without. In this section all information and graphs presented regard the beams ends with a diaphragm system from Connecticut.

Figure 240 depicts the frequency of patterns obtained for beam ends with a diaphragm from the reports provided by CTDOT.

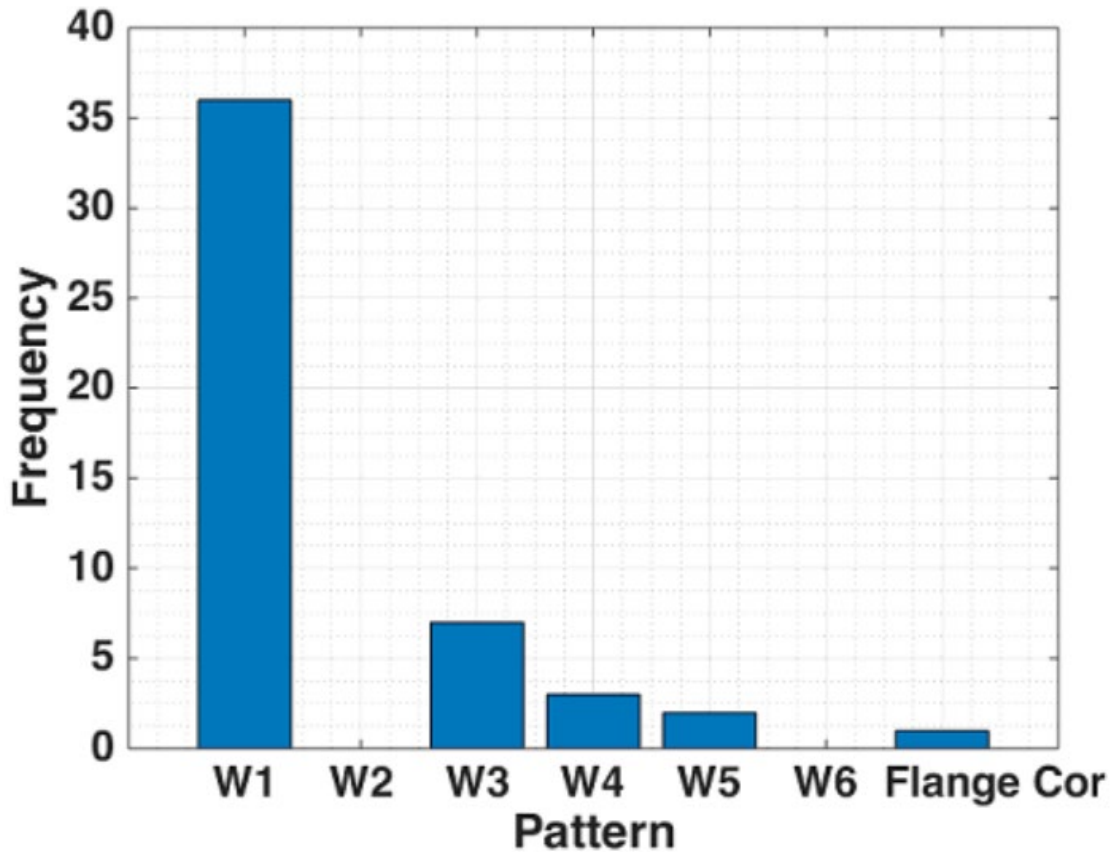


Figure 240: Web corrosion patterns distribution for beams ends with a diaphragm – CTDOT

Similar to all other cases, the dimensions CH1, CH2, CH3, CL1, CL2, CL3 are always normalized by H_0 , where $H_0 = H - 2t_f$.

12.1.2. Pattern W1

12.1.2.1. Web corrosion

The study began with the analysis of the distribution of the corrosion height, depicted in Figure 241. The parameters for the corrosion patterns can be found with corresponding diagrams in Section 1.5 *Corrosion Patterns* of this report.

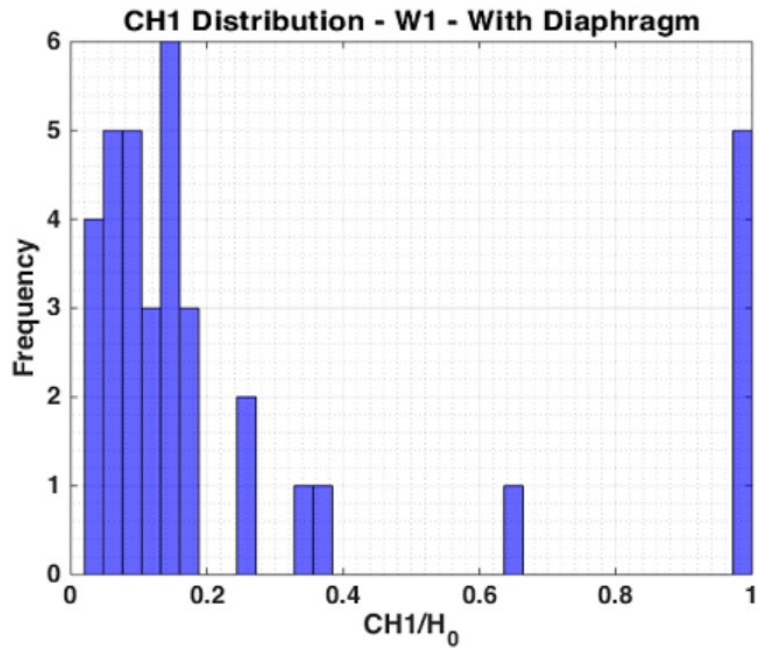


Figure 241: Distribution of corrosion height for W1 pattern – CTDOT

Our team discovered that, similar to the beams without a diaphragm, two trends are noticeable: (i) $CH1 < 0.2H_0$, (ii) $CH1 > 0.9H_0$.

Figure 242 depicts the length of corrosion for $CH1 < 0.2H_0$, whereas Figure 243 depicts the length corrosion distribution for $CH1 > 0.9H_0$.

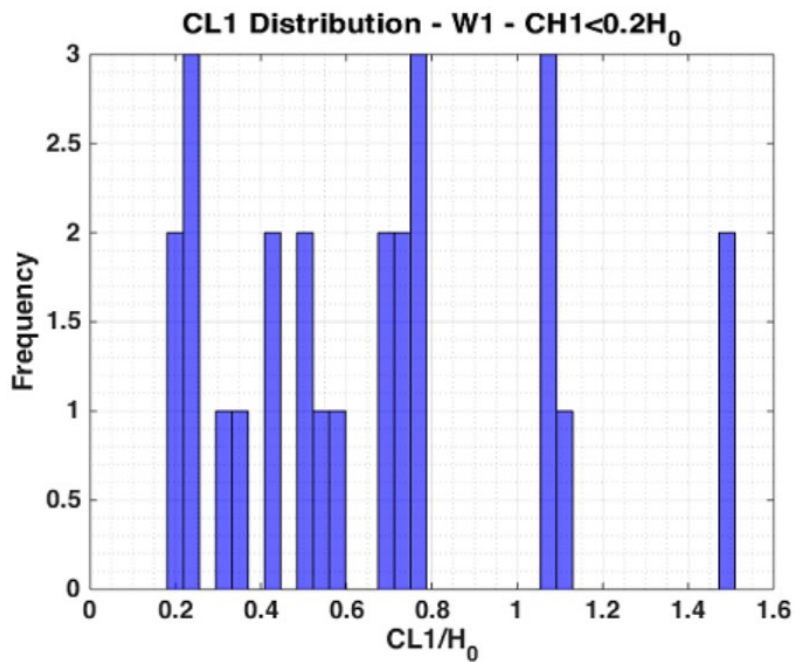


Figure 242: Corrosion length distribution for W1 pattern and $CH1 < 0.2H_0$ – CTDOT

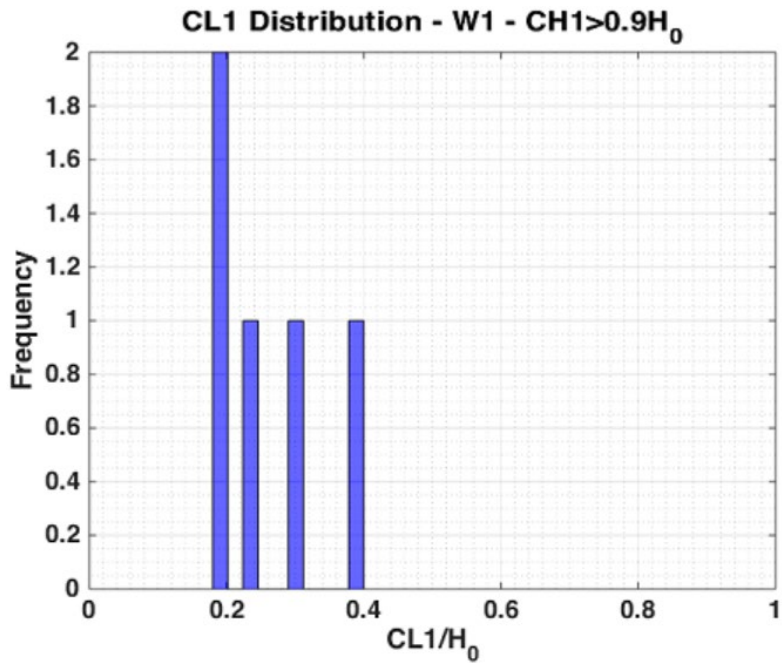


Figure 243 : Corrosion length distribution for W1 pattern and CH1 > 0.9H0 – CTDOT

Figure 244 and Figure 245 depict the web thickness loss for CH1 < 0.2H0 and CH1 > 0.9H0, respectively.

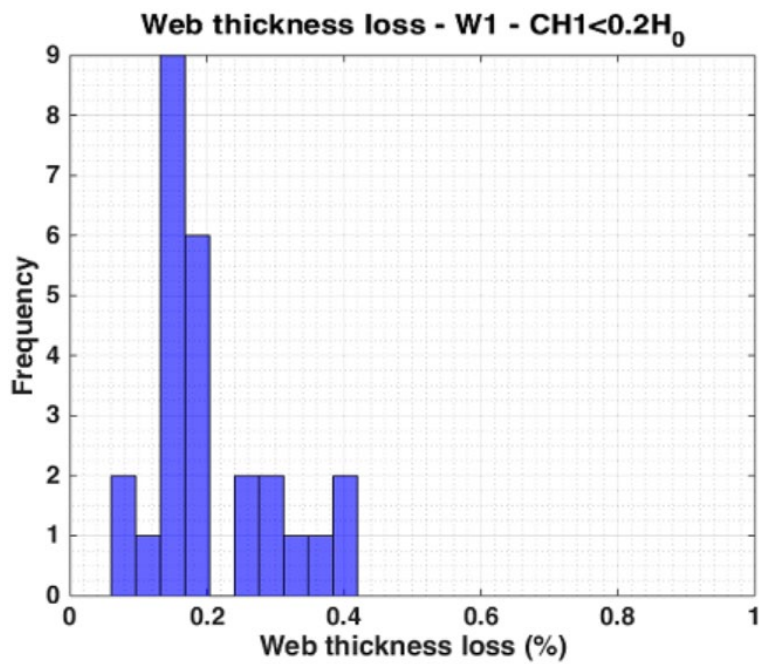


Figure 244 : Web thickness loss for W1 pattern and CH1 < 0.2H0 – CTDOT

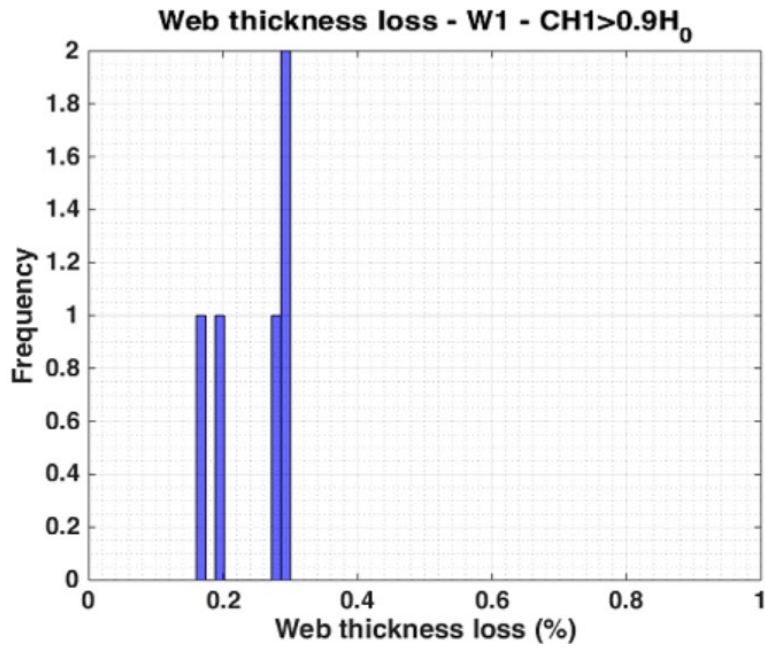


Figure 245 : Web thickness loss for W1 pattern and $CH1 > 0.9H_0$ – CTDOT

Therefore, from the last figures, our team was able to define the following two corrosion cases:

Case A {■($0 < CH1 \leq 0.2H_0 @ 0.2H_0 \leq CL1 \leq 1.1H_0 @ 0.1 \leq t_{loss}/t_{web} \leq 0.4$)}

Case B {■($0.9H_0 \leq CH1 \leq 1H_0 @ 0.2H_0 \leq CL1 \leq 0.4H_0 @ 0.1 \leq t_{loss}/t_{web} \leq 0.3$)}

Figure 246 and Figure 247 depict Case A and B.

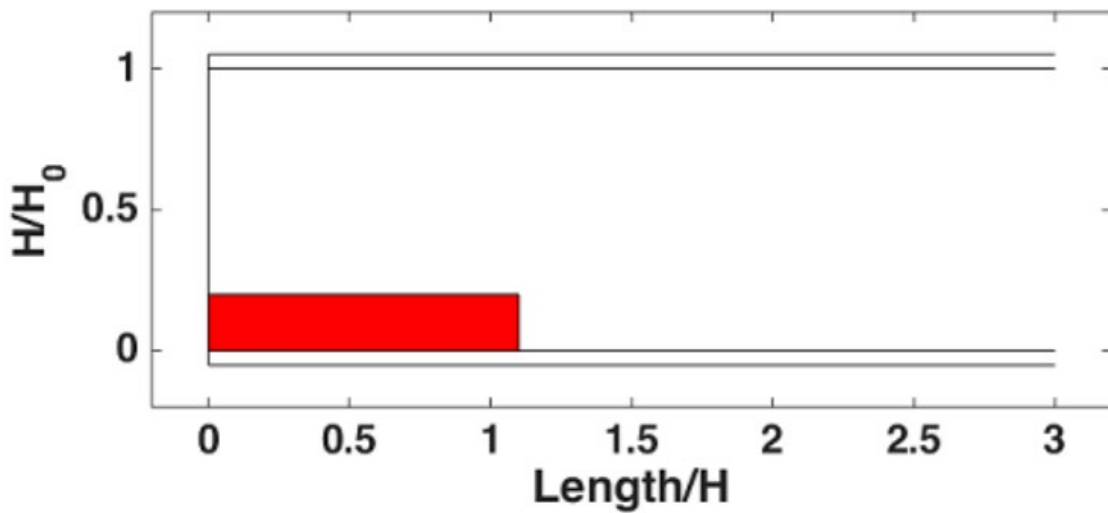


Figure 246: Extreme corrosion scenario (case A) for beams with a diaphragm, W1 pattern – CTDOT

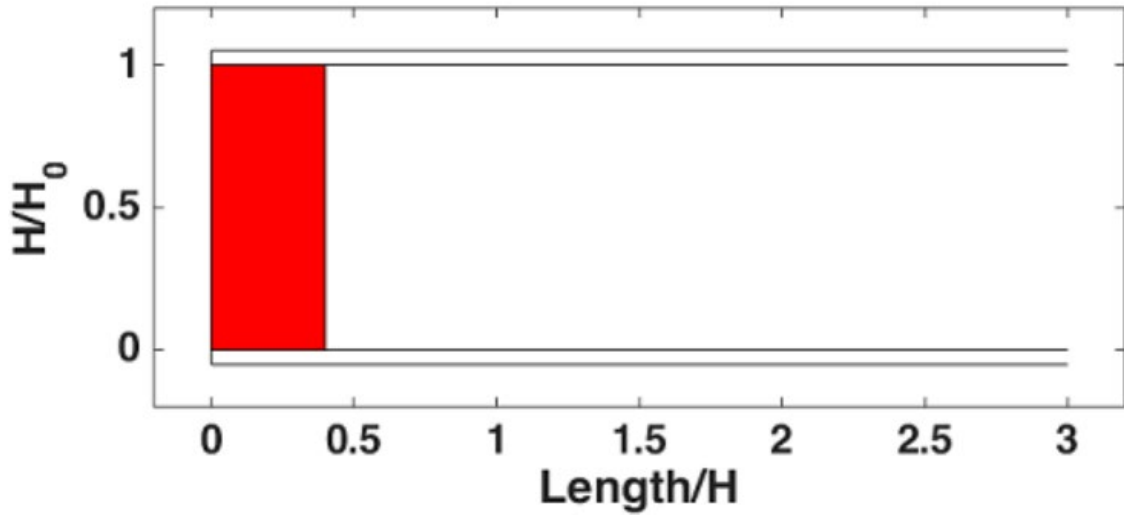


Figure 247: Extreme corrosion scenario (case B) for beams with a diaphragm, W1 pattern – CTDOT

Figure 248 and Figure 249 depict the overlapping of extreme corrosion cases for beams with and without a diaphragm system.

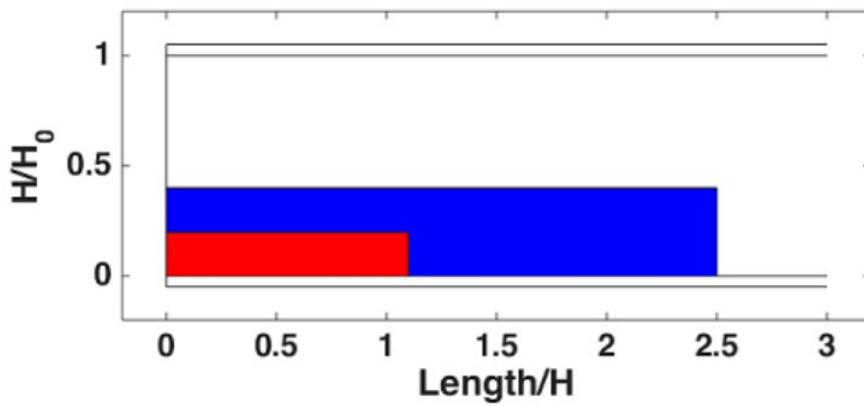


Figure 248: Comparison between extreme corrosion scenarios. Blue represents the extreme scenario for beams without diaphragm, whereas the region in red depicts extreme corrosion scenario for beams with a diaphragm – CTDOT

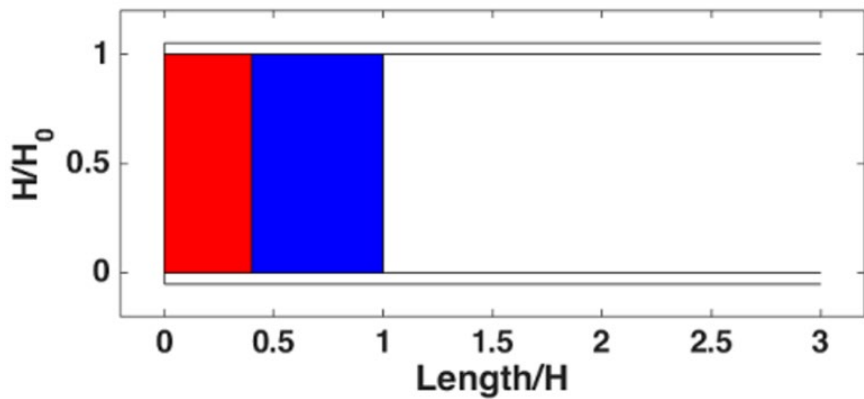


Figure 249: Comparison between extreme corrosion scenarios. Blue represents the extreme scenario for beams without diaphragm, whereas the region in red depicts extreme corrosion scenario for beams with a diaphragm – CTDOT

12.1.2.2. Flange corrosion

The research team was not able to collect information regarding flange corrosion for beam ends with a diaphragm system. For this reason, we were not able to study the flange corrosion of beams ends with a diaphragm from Connecticut.

12.1.2.3. Holes

Table 81 presents the frequency of holes and patterns found for beams ends with diaphragm.

Table 81: Holes and patterns for beams ends with diaphragm from CTDOT

	Number	No Hole	M 1	M 2	M 3	M 4	M1 and M2	M1 and M3	M2 and M4
W1	36	34	1	1	0	0	0	0	0
W2	0	0	0	0	0	0	0	0	0
W3	7	7	0	0	0	0	0	0	0
W4	3	2	1	0	0	0	0	0	0
W5	2	2	0	0	0	0	0	0	0
W6	0	0	0	0	0	0	0	0	0

According to Table 53, only two holes were observed combined with the W1 corrosion pattern. The small amount of data available meant that the research could not draw conclusions. The dimensions of the holes are:

Table 82: Dimensions of holes of pattern W3 for beam ends with a diaphragm – CTDOT

Hole topology	Length	Deep
M1	17.7%	17.7%
M2	24%	24%

12.1.3. Pattern W3

12.1.3.1. Web corrosion

Although just seven cases of the W3 corrosion pattern combined with diaphragms were recorded, all cases presented corrosion height equal to the height of the web, as depicted in Figure 250. The parameters for the corrosion patterns can be found with corresponding diagrams in Section 1.5 *Corrosion Patterns* of this report.

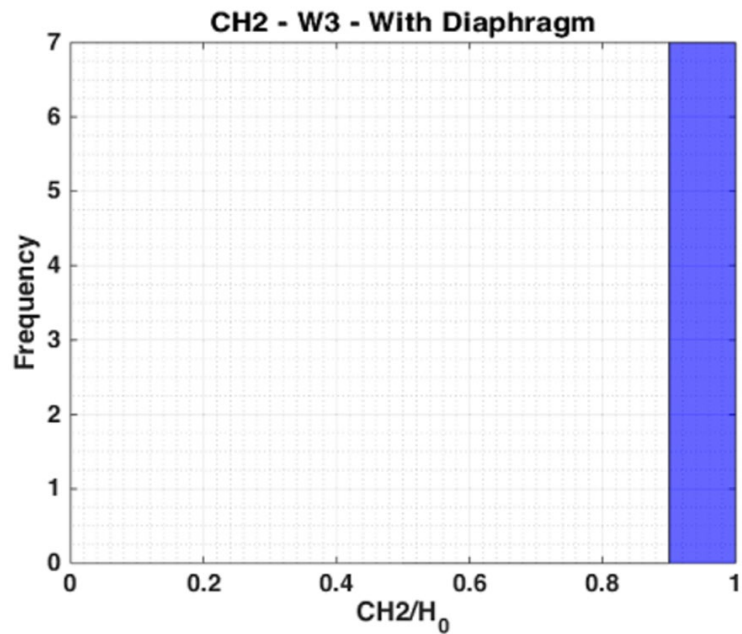


Figure 250: CH2 distribution for W3 pattern for beams with a diaphragm – CTDOT

The other parameters of the W3 corrosion pattern are plotted in Figure 251, Figure 252, Figure 253, Figure 254 and Figure 255.

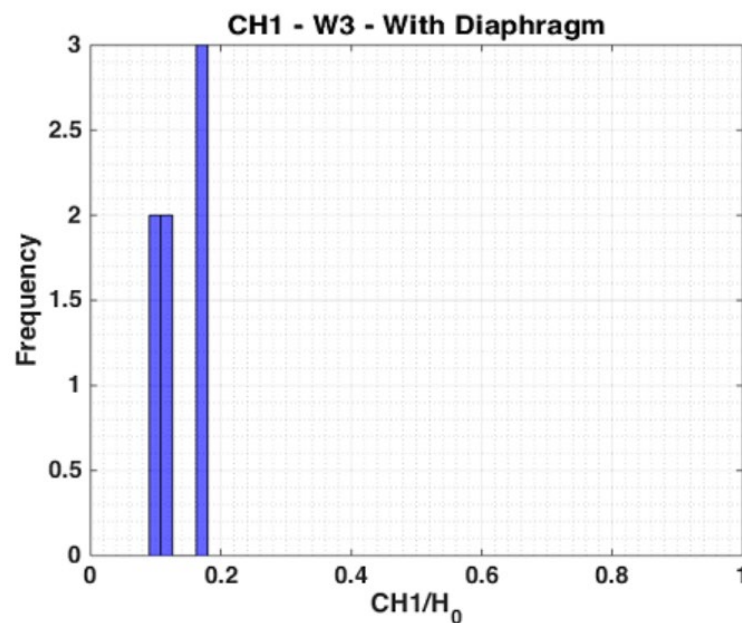


Figure 251: CH1 distribution for W3 pattern for beams with a diaphragm – CTDOT

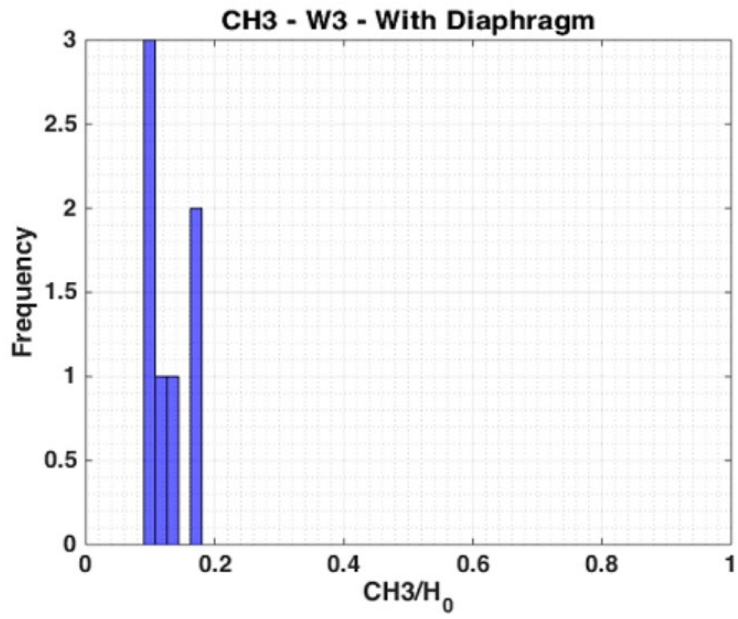


Figure 252: CH2 distribution for W3 pattern for beams with a diaphragm – CTDOT

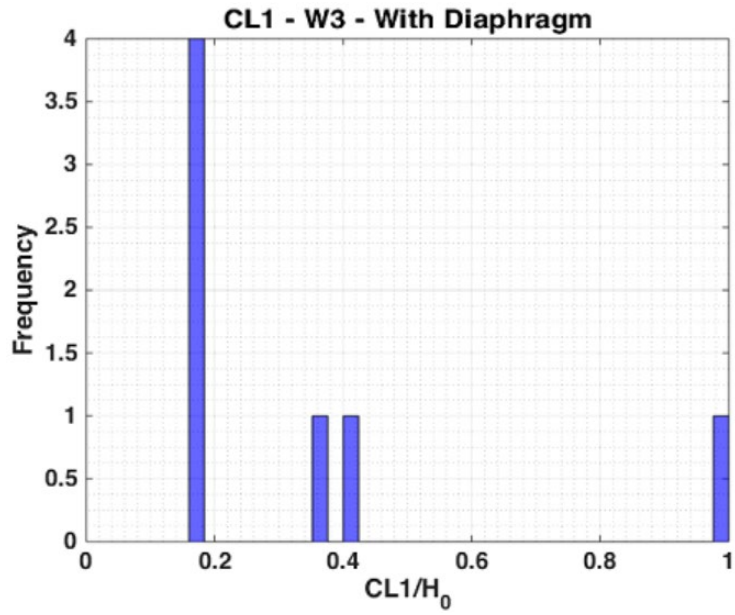


Figure 253: CL1 distribution for W3 pattern for beams with a diaphragm – CTDOT

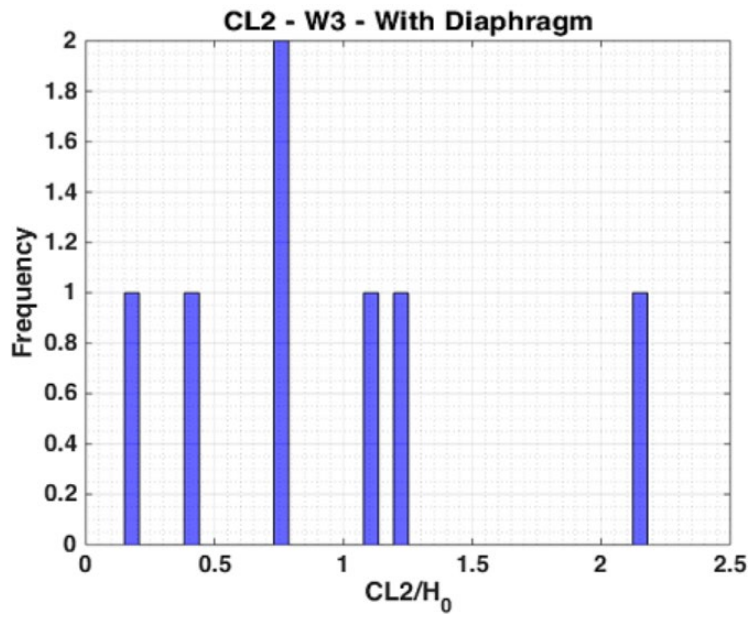


Figure 254: CL2 distribution for W3 pattern for beams with a diaphragm – CTDOT

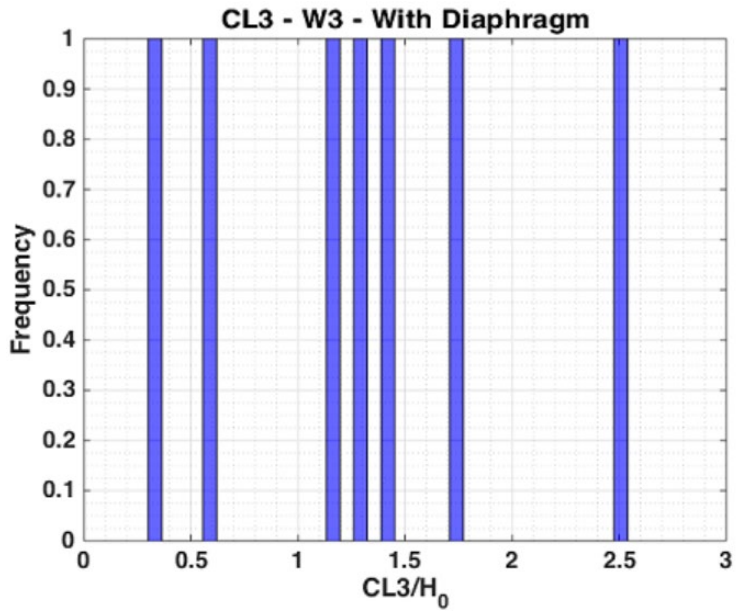


Figure 255: CL3 distribution for W3 pattern for beams with a diaphragm – CTDOT

Figure 256 depicts the web thickness loss distribution for pattern W3.

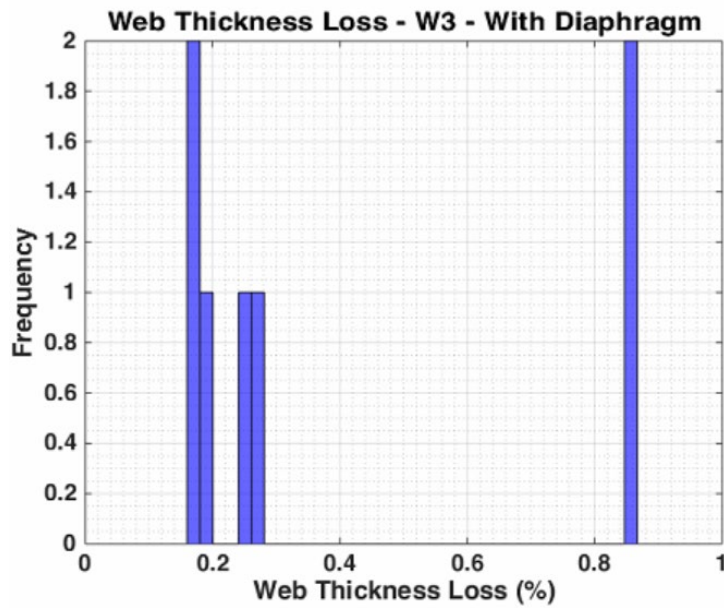


Figure 256: Web thickness loss distribution for W3 pattern for beams with a diaphragm – CTDOT

Therefore, from the last figures, our team was able to determine the intervals of the W3 corrosion pattern for beams ends with diaphragms.

$$0.1H_0 \leq CH_1 \leq 0.2H_0$$

CH_2 takes the value of {1}

$$0.1H_0 \leq CH_3 \leq 0.2H_0$$

$$0.2H_0 \leq CL_1 \leq 0.4H_0$$

$$0.4H_0 \leq CL_2 \leq 2.2H_0$$

$$0.4H_0 \leq CL_3 \leq 2.5H_0$$

$$\frac{t_{loss}}{t_{web}} \text{ takes the values of } \{0.2, 0.25, 0.85\}$$

Figure 257 depicts the extreme case of the W3 corrosion pattern for beam ends with a diaphragm system.

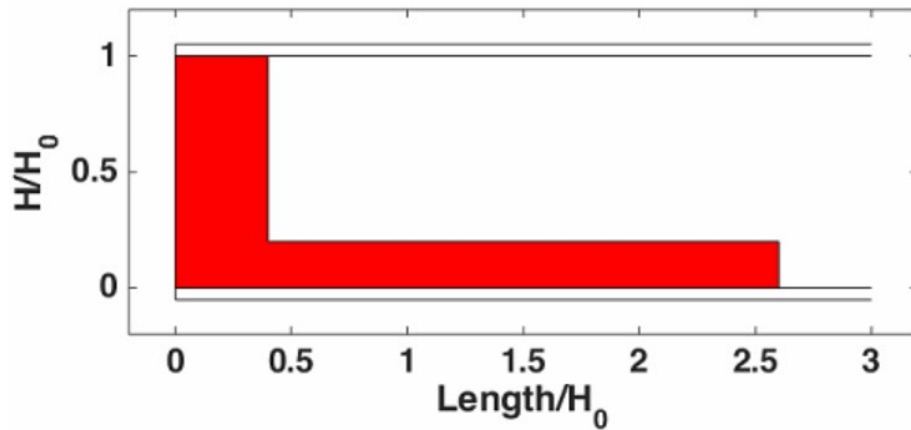


Figure 257: Extreme corrosion scenario of W3 pattern for beam ends with a diaphragm – CTDOT

Figure 258 displays the comparison between the corrosion for beam ends with and without a diaphragm system.

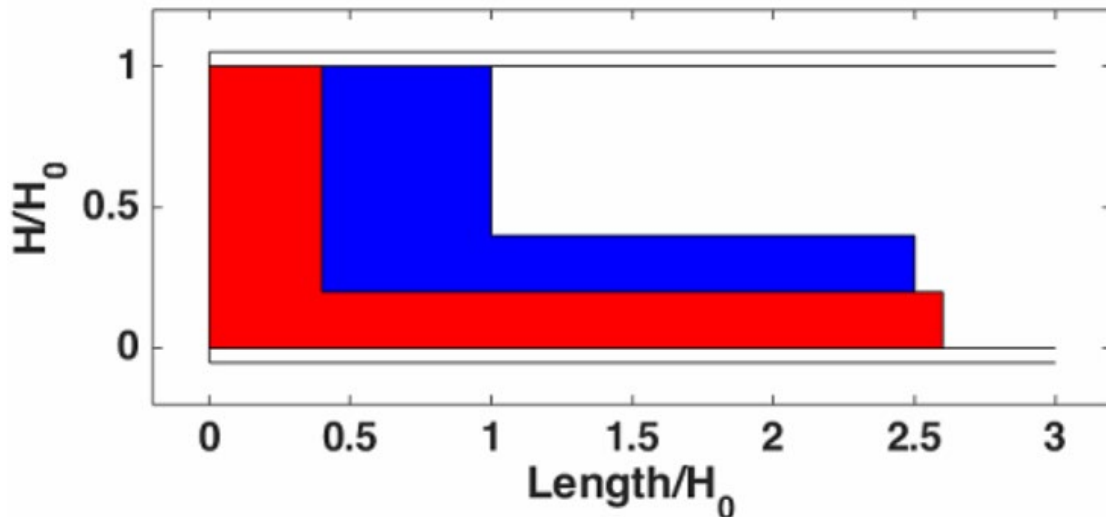


Figure 258: Comparison between extreme corrosion scenarios. Blue represents the extreme scenario for beams without diaphragm, whereas the region in red depicts extreme corrosion scenario for beams with a diaphragm – CTDOT

12.1.3.2. Flange corrosion

No information regarding flange corrosion combined with the W3 corrosion patterns for beam ends with a diaphragm were found in the reports provided by CTDOT.

12.1.3.3. Holes

As displayed in Table 53 , no holes were found combined with the W3 corrosion patterns in beam ends with a diaphragm.

12.2. Massachusetts

12.2.1. Introduction

The data was divided into two main categories, beams ends with a diaphragm system and beam ends without a diaphragm system. All the graphs in this part of the document represent the first case. The histogram below contains the frequency of each of the defined corrosion patterns (the total amount of times each pattern appears in the reports).

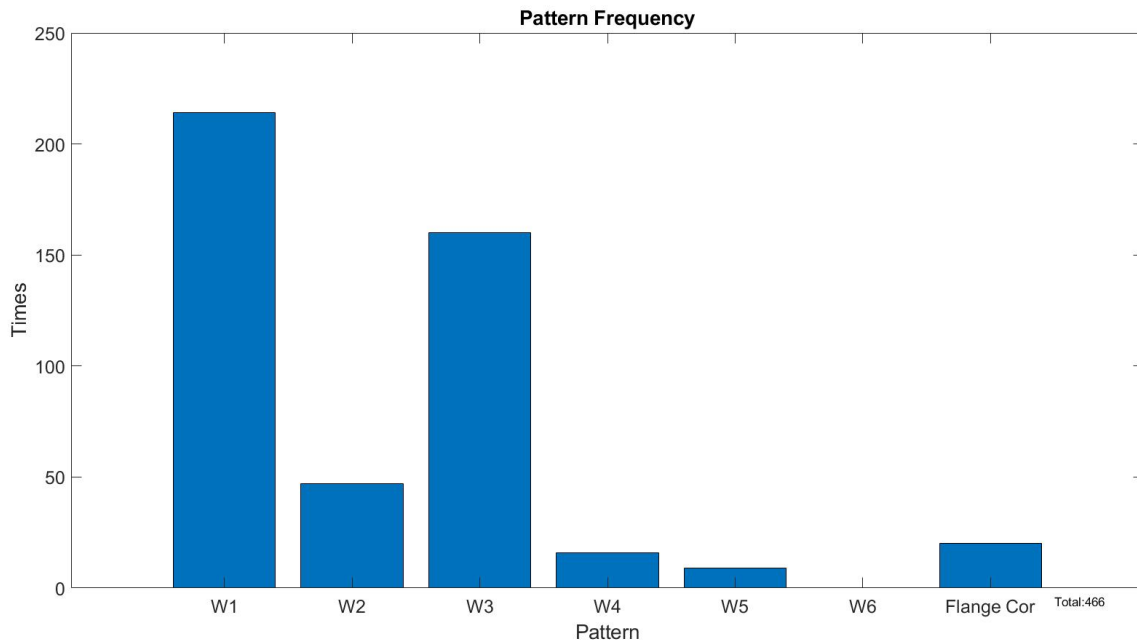


Figure 259. Web corrosion patterns distribution for beams with a diaphragm - MassDOT

For each web corrosion pattern, we have normalized the characteristic dimensions (CH1, CH2, CH3, CL1, CL2, CL3) with the height H_0 , where $H_0 = H - 2t_f$.

12.2.2. Pattern W1

12.2.2.1. Web Corrosion

The parameters for the corrosion patterns can be found with corresponding diagrams in Section 1.5 *Corrosion Patterns* of this report.

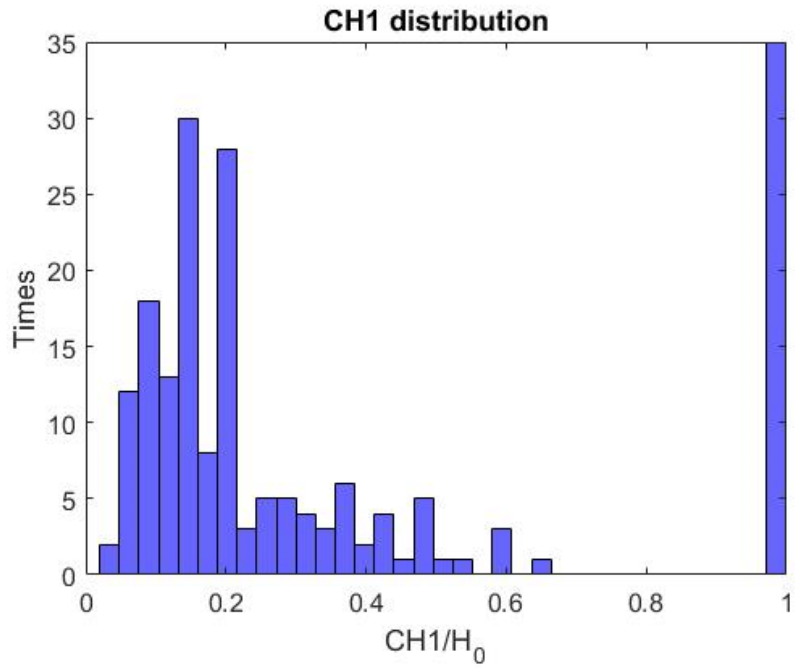


Figure 260. CH1 distribution of W1 web pattern for beams with a diaphragm (total 189). - MassDOT

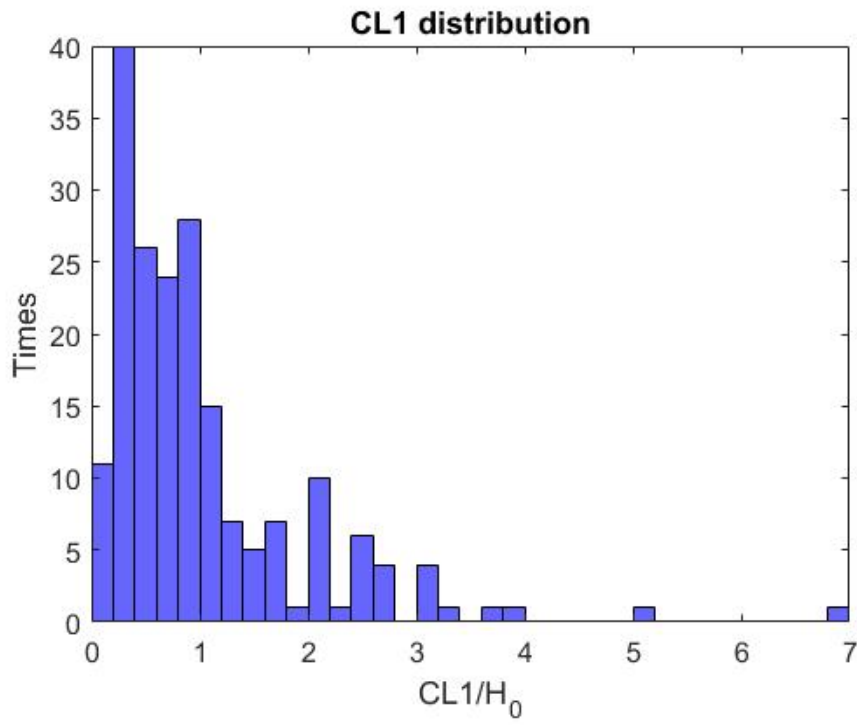


Figure 261: CL1 distribution of W1 web corrosion pattern for beams with a diaphragm - MassDOT

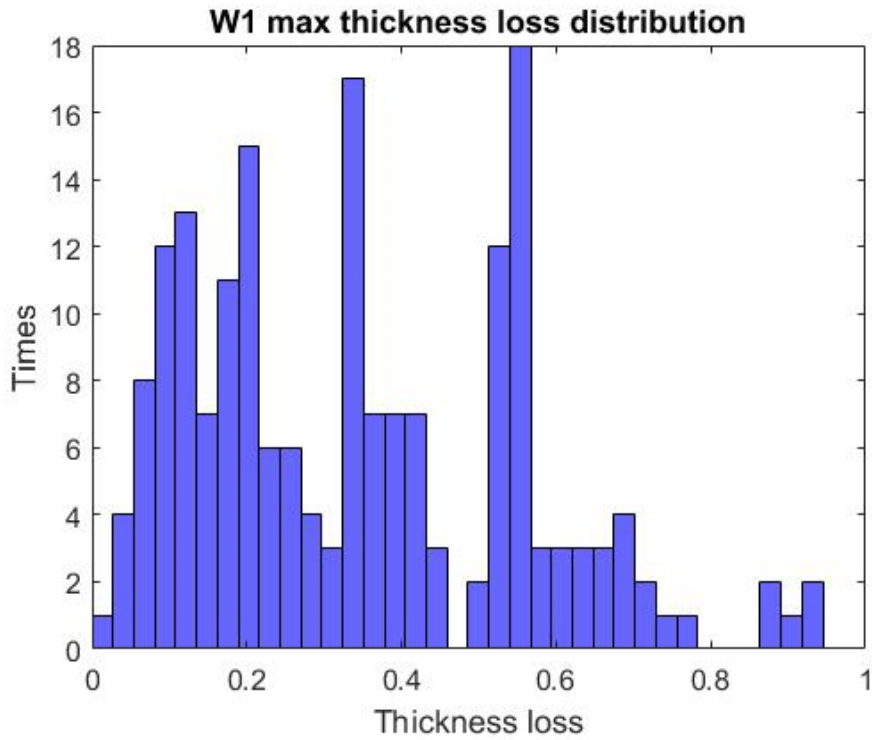


Figure 262: Max thickness loss distribution of W1 web corrosion pattern for beams with a diaphragm - MassDOT

From the CH1 histogram, two main trends are noticed, which cover almost the 85% of cases (158 out of 189): either a) full height corrosion, or b) corrosion up to 30% of H_0 .

$$CH_1 = H_0 \text{ or } 0 < CH_1 \leq 0.3H_0$$

For full height:

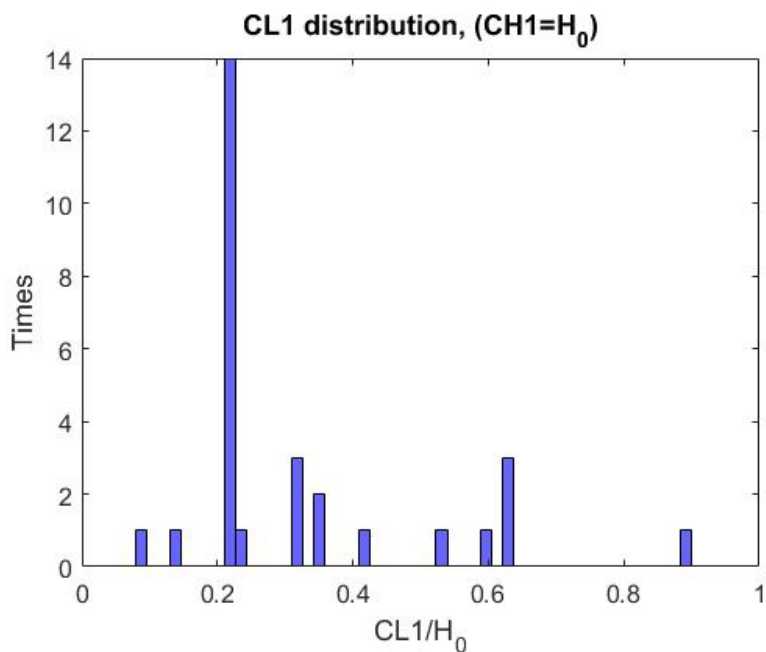


Figure 263: CL1 distribution of full height W1 web corrosion pattern for beams with a diaphragm - MassDOT

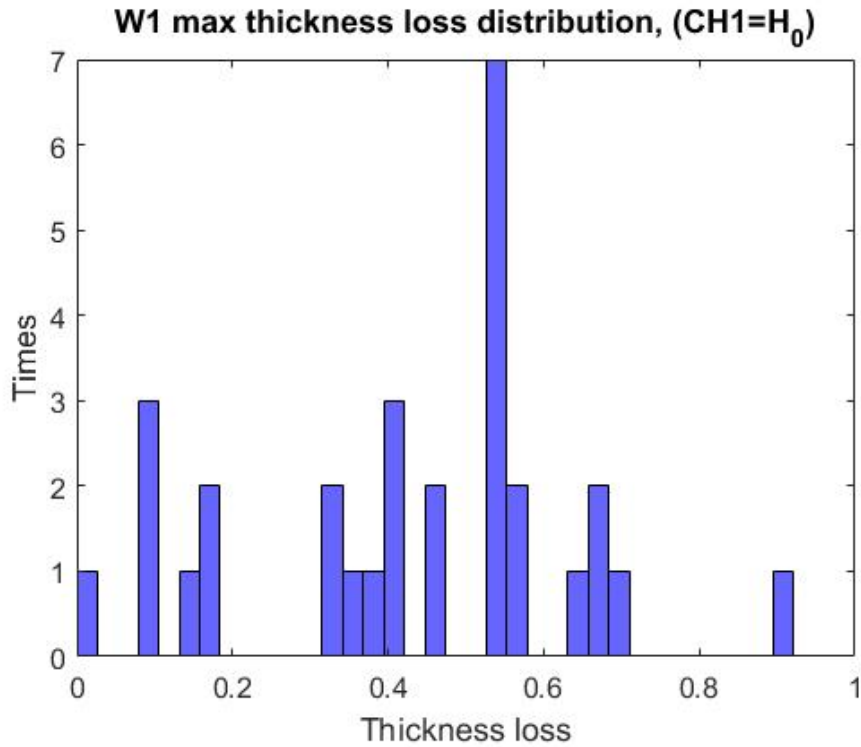
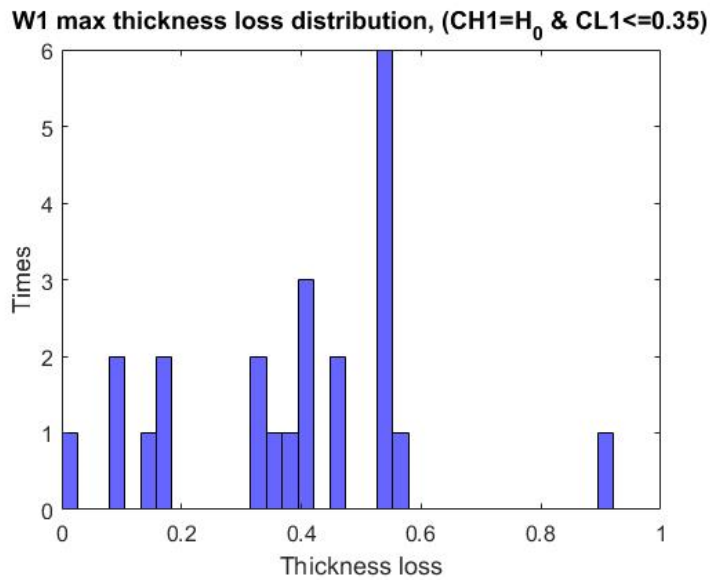


Figure 264: Max thickness loss distribution of full height W1 web corrosion pattern for beams with a diaphragm - MassDOT

By observing the figure for full height corrosion and $CL \leq 0.35H$, we saw:



(8)

Figure 265: Max web thickness loss distribution of W1 web corrosion pattern, with corrosion height up to 35% of H₀, for beams with a diaphragm - MassDOT

For the full height corrosion case, one case is identified: **CASE A**

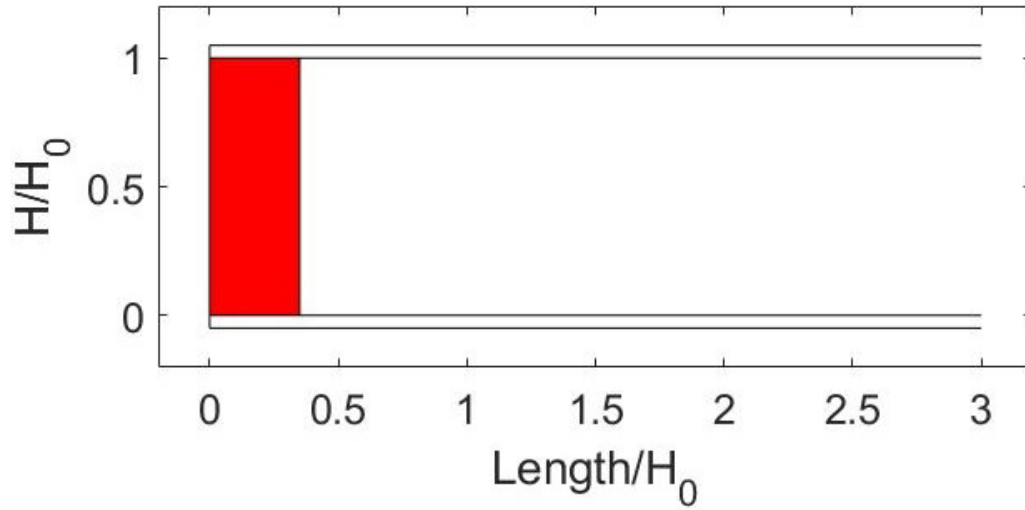


Figure 266: First extreme W1 web corrosion pattern, with full height corrosion for beams with a diaphragm - MassDOT

With web thickness loss $\frac{t_{\text{loss}}}{t_{\text{web}}}$ takes values of $\{0.2, 0.4, 0.6\}$ (Figure 86)

12.2.2.2. Flange Corrosion for Case A

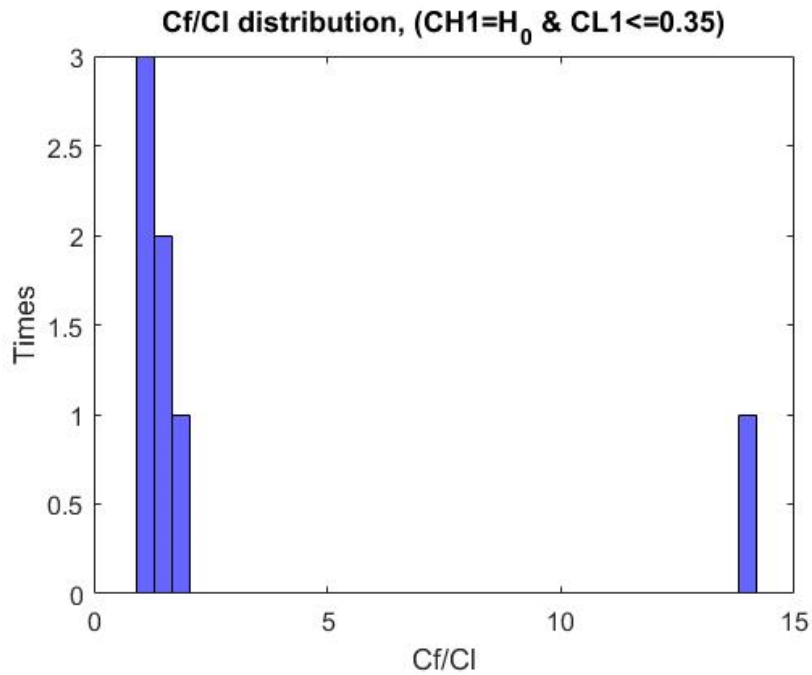


Figure 267: Ratio of flange to web corrosion length distribution of W1 web corrosion pattern, with full height corrosion and up to 35% of H_0 length, for beams with a diaphragm - MassDOT

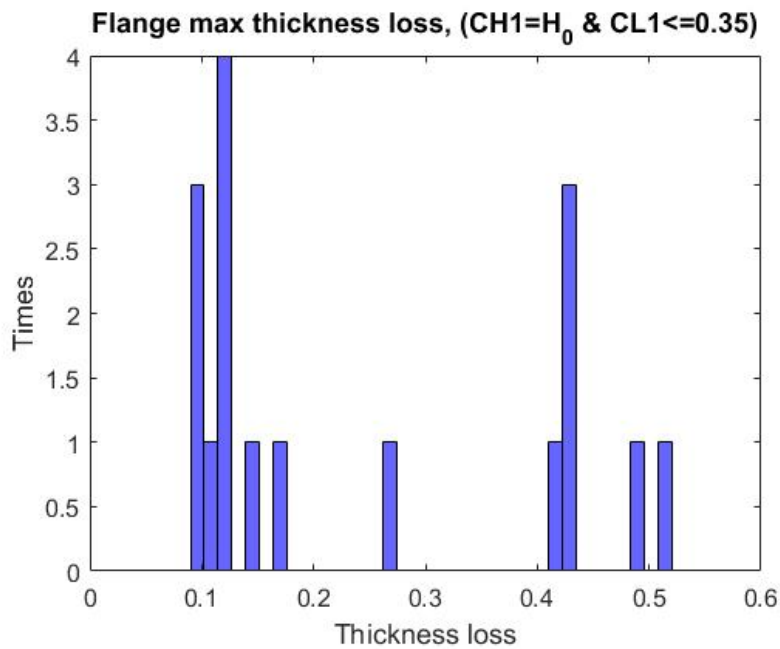


Figure 268: Max flange thickness loss distribution of W1 web corrosion pattern, with full height corrosion and up to 35% of H_0 length, for beams with a diaphragm - MassDOT

Thus, for case A: $\frac{t_{loss}}{t_{flange}}$ takes values of {0.15,0.45} (Figure 268). The ratio of the length of the corroded flange over the length of the corroded web $1 \leq \frac{C_f}{C_l} \leq 1.7$

For $0 < CH_1 \leq 0.3$

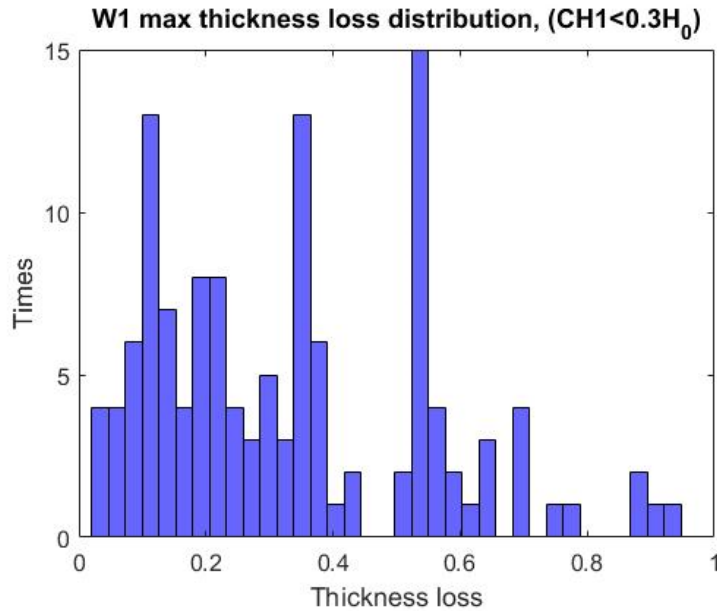


Figure 269: Max web thickness loss distribution of W1 web corrosion pattern with corrosion height up to 30% of H_0 for beams with a diaphragm - MassDOT

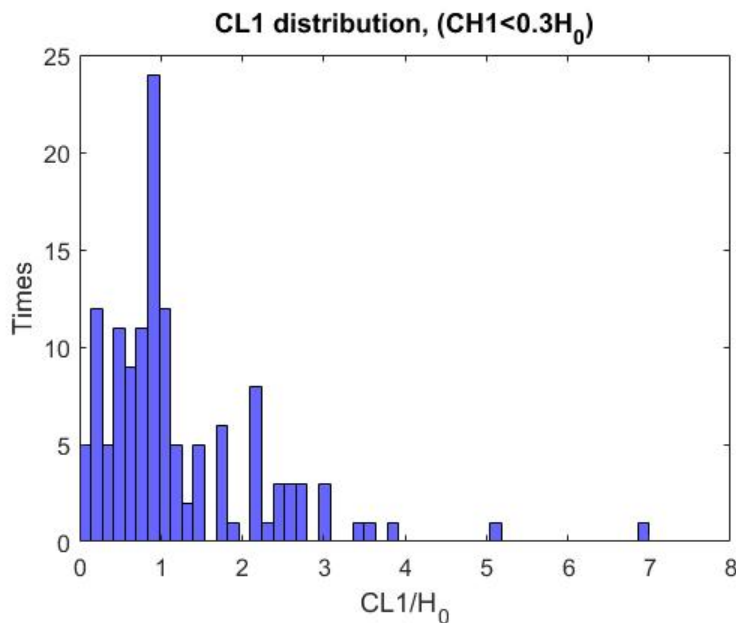


Figure 270: CL1 thickness loss distribution of W1 web corrosion pattern with corrosion height up to 30% of H_0 for beams with a diaphragm - MassDOT

From Figure 270, $0 < CL_1 \leq 2.5$ with web thickness loss $\frac{t_{loss}}{t_{web}}$ takes values of {0.2,0.4,0.6,0.8}.

CASE B

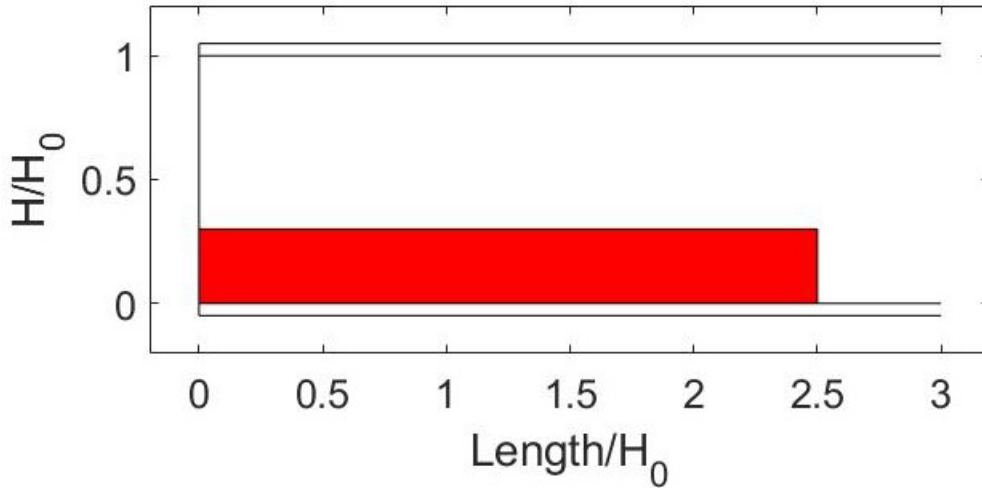


Figure 271: Second extreme W1 web corrosion pattern, with corrosion height up to 30% of H_0 for beams with a diaphragm - MassDOT

For Case B: $\frac{t_{loss}}{t_{flange}}$ takes values of {0.2,0.4,0.6,0.8} (Figure 269). The ratio of the length of the corroded flange over the length of the corroded web $0 < \frac{c_f}{c_l} \leq 1$ (Figure 267).

12.2.2.3. Flange Corrosion for Case B

For $CH_1 < 0.3H_0$

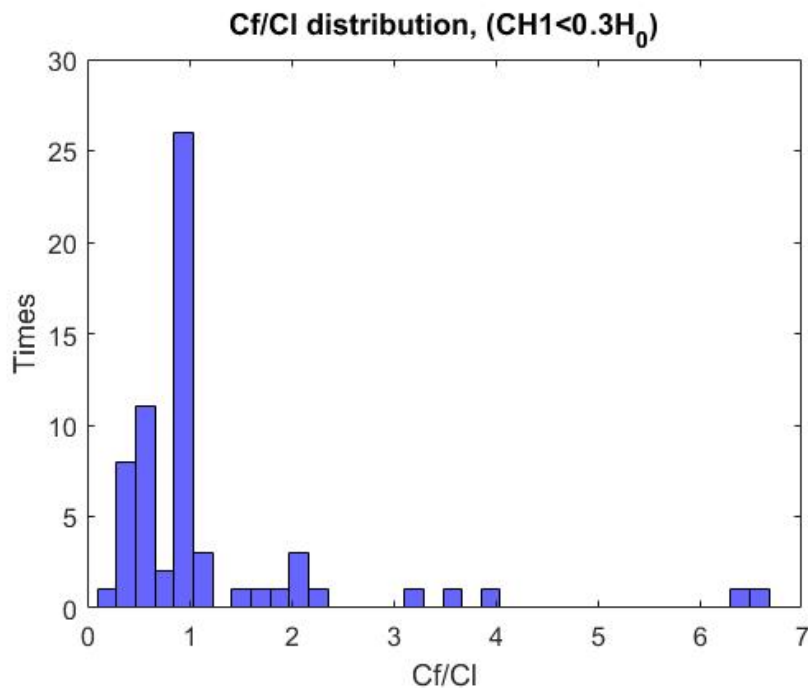


Figure 272: Ratio of flange to web corrosion length distribution of W1 web corrosion pattern with corrosion height up to 30% of H_0 for beams with a diaphragm - MassDOT

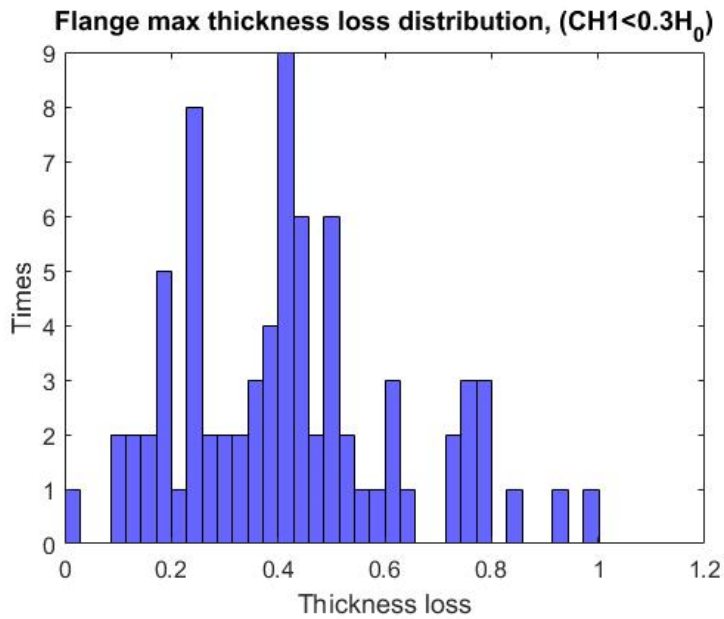


Figure 273: Max flange thickness loss distribution of W1 web corrosion pattern with corrosion height up to 30% of H_0 for beams with a diaphragm - MassDOT

12.2.2.4. Holes

The W1 corrosion pattern is combined 11 times with the M1 hole corrosion pattern. The web thickness loss, holes dimensions, and corrosion height at these cases are given as:

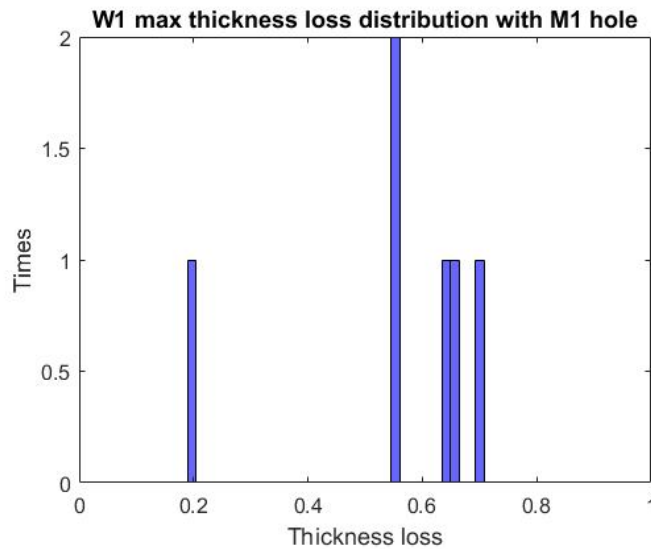


Figure 274. Max thickness loss distribution for W1 web corrosion patterns and M1 hole for beams with a diaphragm - MassDOT

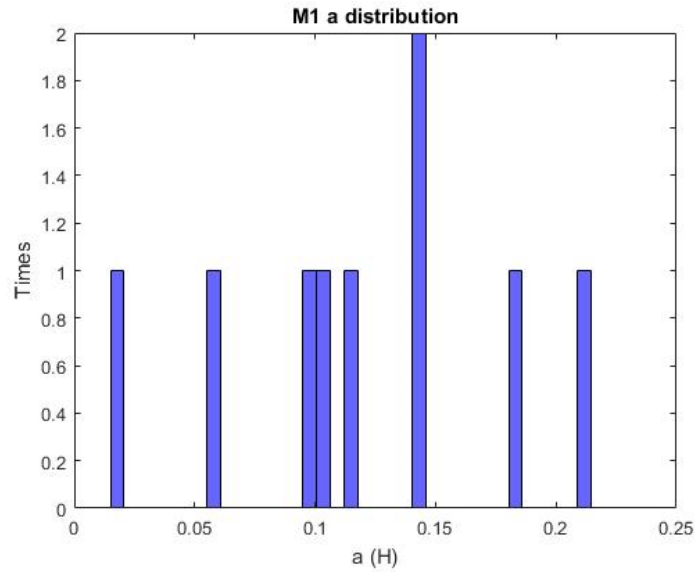


Figure 275: M1 web hole's pattern height distribution of W1 web corrosion pattern for beams with a diaphragm - MassDOT

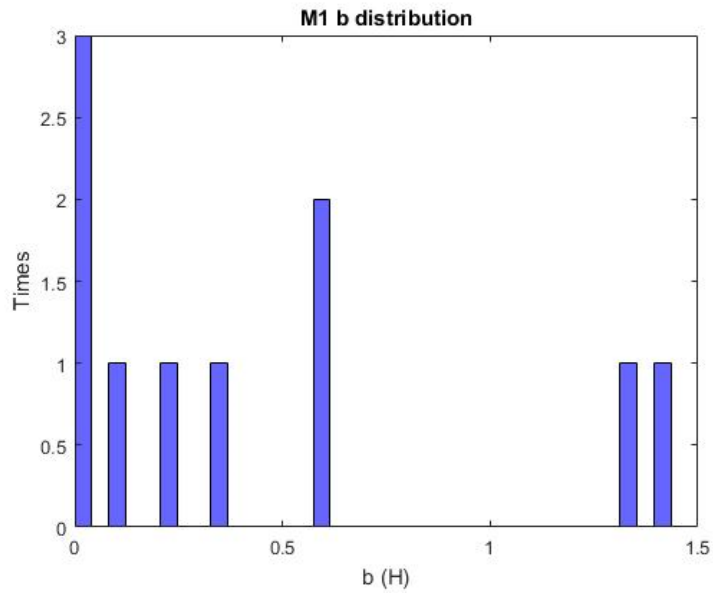


Figure 276: M1 web hole's pattern length distribution of W1 web corrosion pattern for beams with a diaphragm - MassDOT

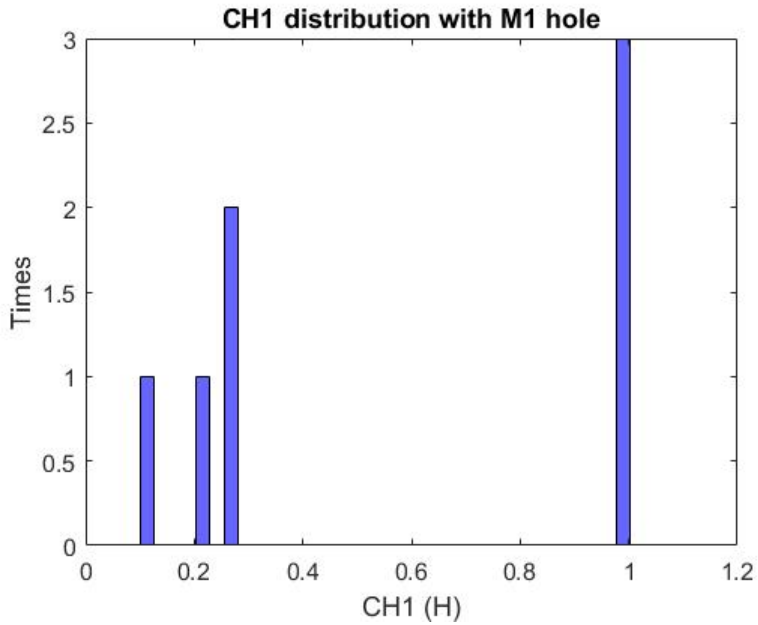


Figure 277: CH1 distribution for beams with M1 hole and W1 web corrosion pattern and a diaphragm - MassDOT

From Figure 277, we can conclude that holes are equally distributed between web corrosion scenarios CASE A and CASE B. It is worth mentioning that there are two cases of long holes that are parallel to flange holes (Figure 276). The two longest holes ($1.3H_0$ and $1.4H_0$) are also the corrosion holes with the highest height (0.18 and 0.21) respectively. As a result, an extreme hole case is considered the following (projected on Case B web corrosion scenario):

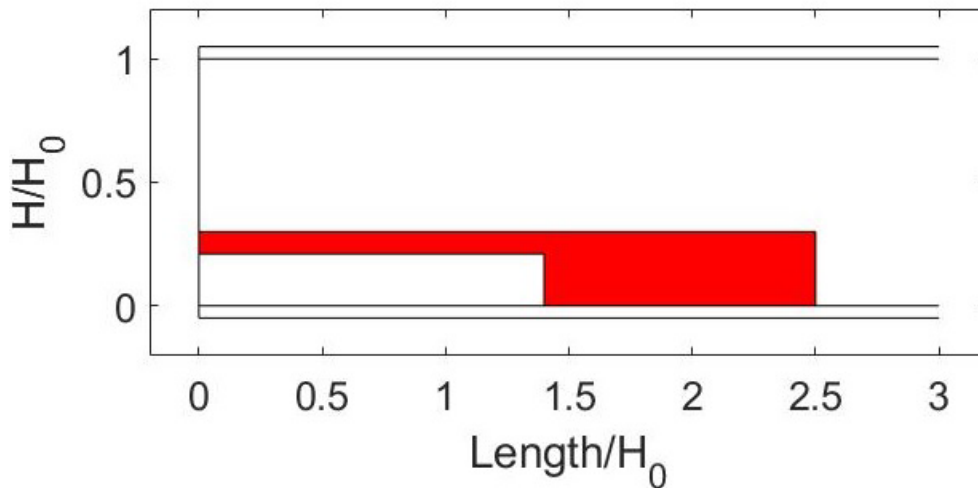


Figure 278: M1 extreme web hole pattern scenario of W1 web corrosion pattern, for beams with a diaphragm - MassDOT

There are also 4 cases of the M2 corrosion hole pattern. The web thickness loss, holes dimensions, and corrosion height at these cases are given as:

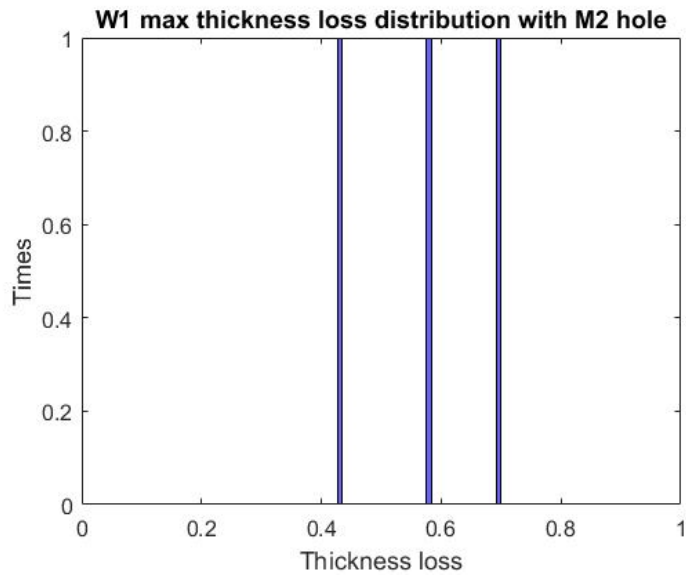


Figure 279. Max thickness loss distribution for W1 web corrosion patterns and M2 hole for beams with a diaphragm - MassDOT

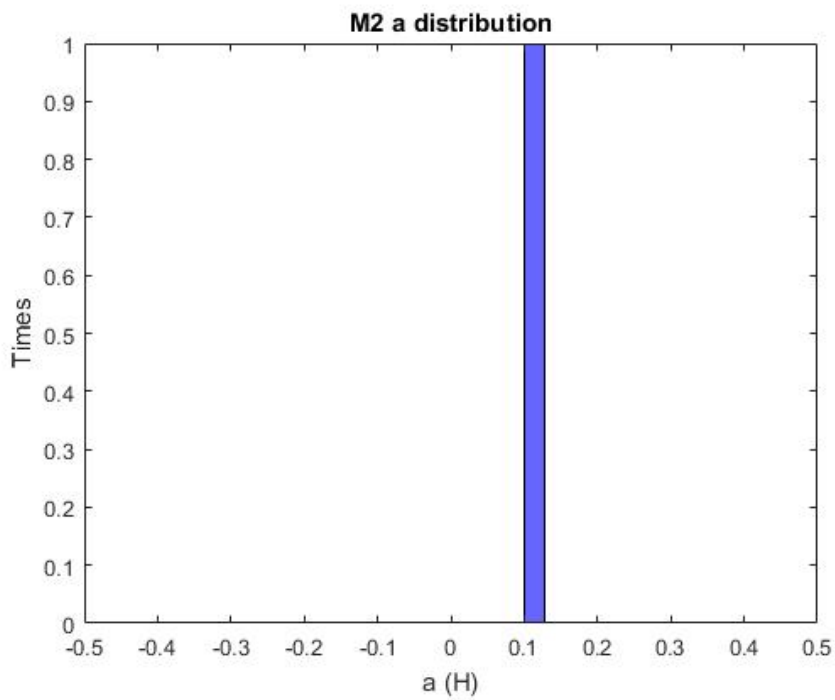


Figure 280: M2 web hole's pattern height distribution of W1 web corrosion pattern for beams with a diaphragm - MassDOT

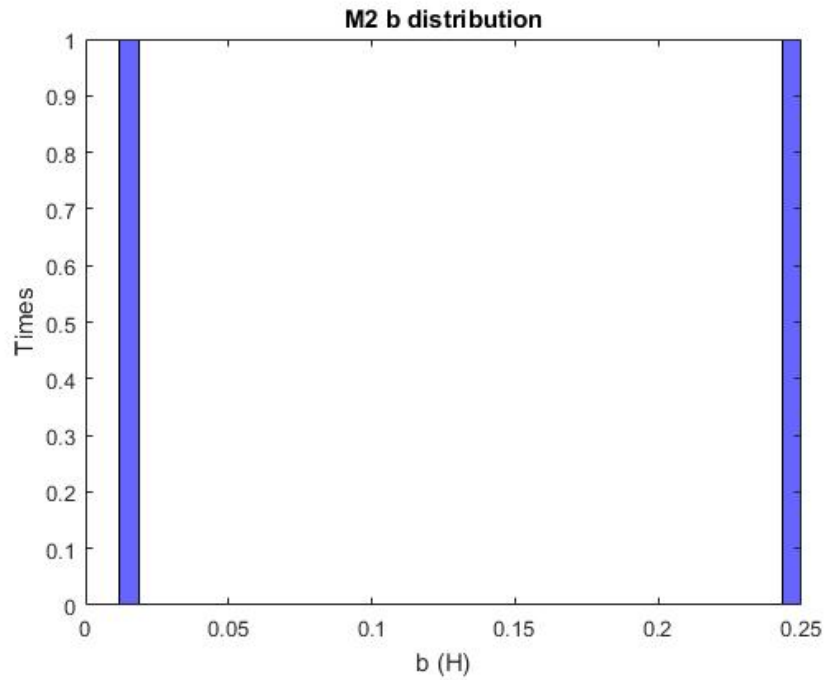


Figure 281: M2 web hole's pattern length distribution of W1 web corrosion pattern for beams with a diaphragm - MassDOT

The data gathered from the inspection reports is very small for the research team to extract valid conclusions.

12.2.3. Pattern W2

12.2.3.1. Web Corrosion

The W2 corrosion pattern was observed in total only 47 times. The parameters for the corrosion patterns can be found with corresponding diagrams in Section 1.5 *Corrosion Patterns* of this report.

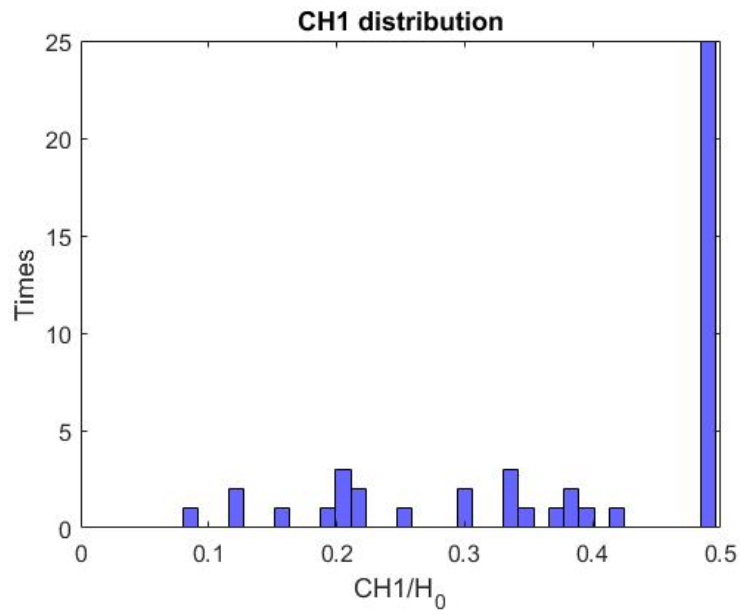


Figure 282. CH1 distribution of W2 pattern for beams with a diaphragm - MassDOT

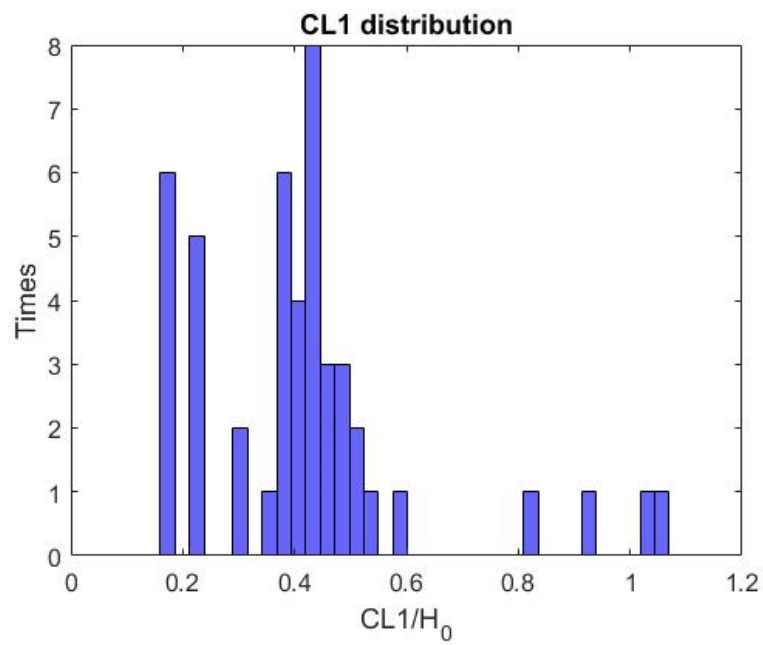


Figure 283: CL1 distribution of W2 pattern for beams with a diaphragm - MassDOT

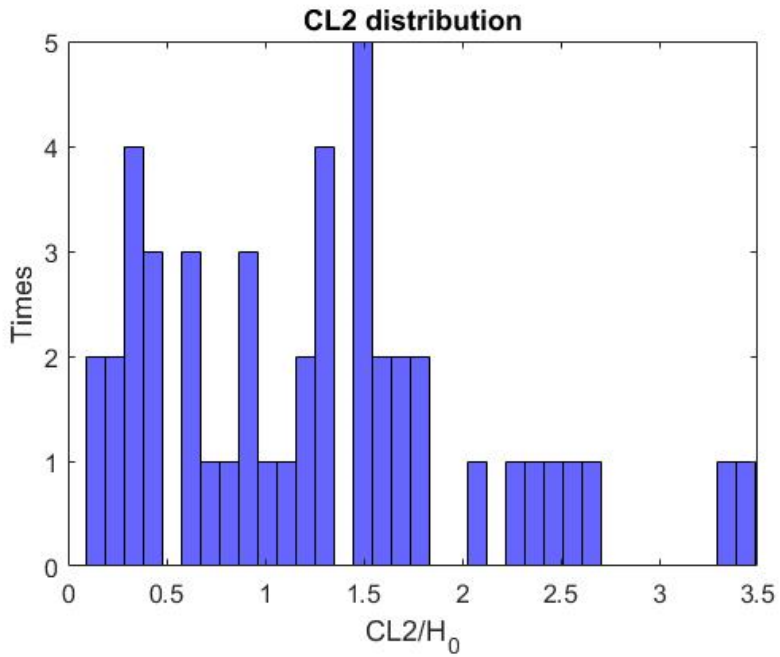


Figure 284: CL2 distribution of W2 pattern for beams with a diaphragm - MassDOT

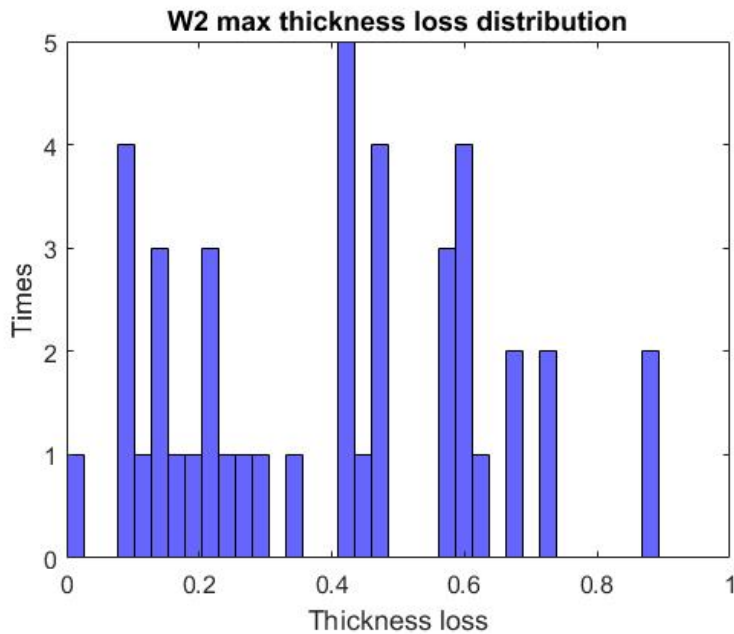


Figure 285: Web thickness loss distribution of W2 pattern for beams with a diaphragm - MassDOT

From the above figure, our team stated:

$$0 < CH_1 \leq 0.5H_0$$

$$0 < CL_1 \leq 0.6H_0$$

$$0 < CL_2 \leq 1.8H_0$$

$\frac{t_{loss}}{t_{web}}$ takes values of {0.2,0.4,0.6,0.8}

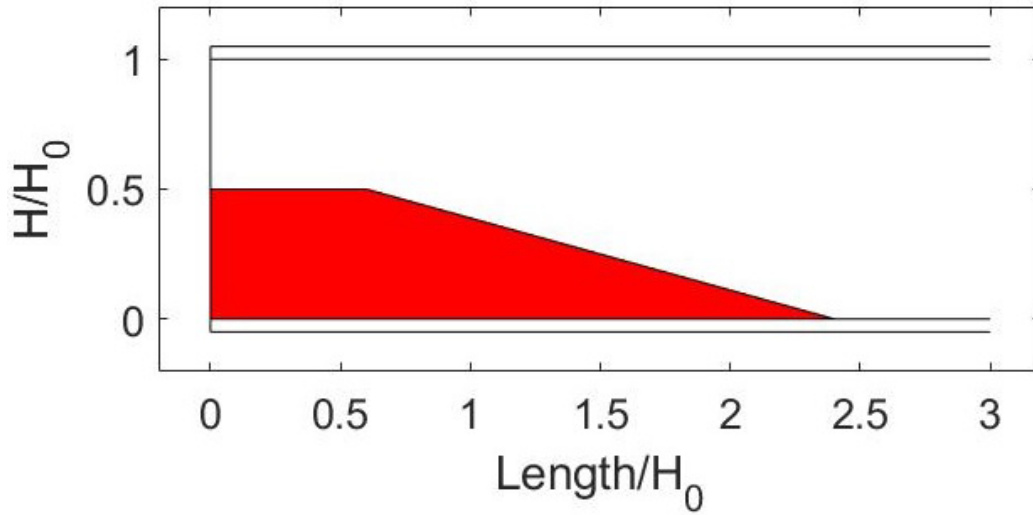


Figure 286: Extreme W2 web corrosion pattern for beams with a diaphragm - MassDOT

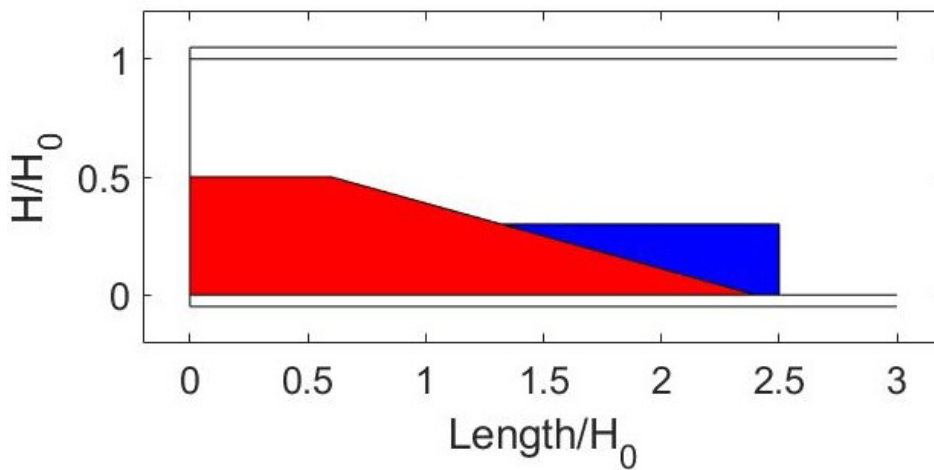


Figure 287: W2 extreme web corrosion scenario (with red color) projected over W1 CASE B extreme web corrosion scenario (with blue color) - MassDOT

The W1 corrosion pattern can be considered as a case of W2 with CL2 equal to zero here.

12.2.3.2. Flange Corrosion

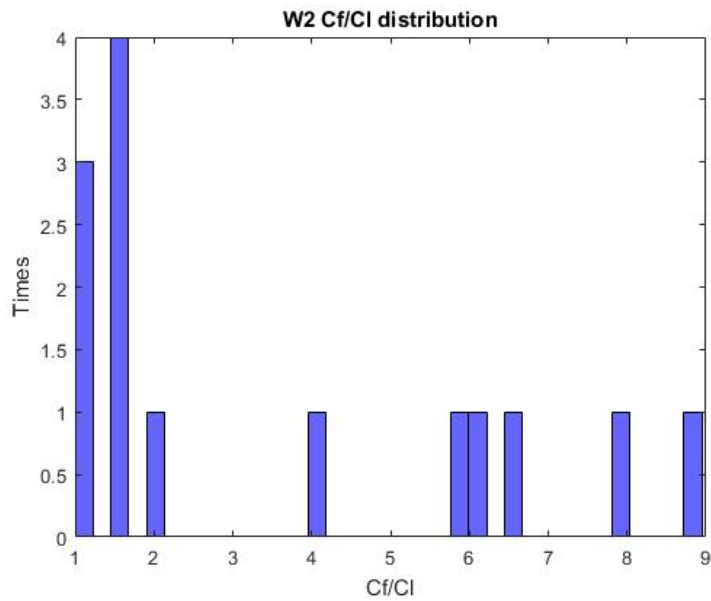


Figure 288: Ratio of flange to web corrosion length distribution of W2 web corrosion pattern corrosion for beams with a diaphragm - MassDOT

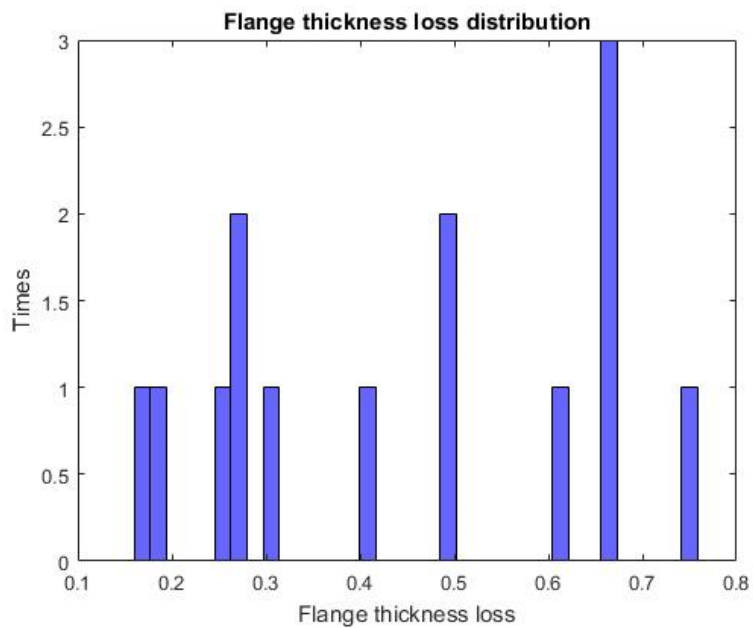


Figure 289: Max flange loss thickness distribution of W2 web corrosion pattern for beams without a diaphragm - MassDOT

12.2.3.3. Holes

Table 83: Holes for beams with a diaphragm – MassDOT

	Number	No hole	M1	M2	M3	M4	M12	M13	M24
W1	214	190	11	4	5	2	2	0	0

W2	47	41	1	4	0	0	1	0	0
W3	160	112	23	5	6	2	7	4	1
W4	16	13	1	2	0	0	0	0	0
W5	9	9	0	0	0	0	0	0	0
W6	0	0	0	0	0	0	0	0	0

According to the table above, the W2 corrosion pattern is combined once with the M1 hole corrosion pattern and 4 times with the M2 hole corrosion pattern. As it was already mentioned W2 and W1 will be combined and used as one pattern. Thus, for the M1 hole corrosion pattern our team checked if the dimensions of the unique hole belong in the range of the W1 pattern and M1 pattern combination. The unique hole with $a=0.089H_0$ and $b=0.31H_0$ satisfies the limits of Figure 100.

For M2 hole corrosion pattern, the sample for the W1 pattern was very small, so the team was not able to extract conclusions. This led our team to process the M2 hole corrosion pattern for both W1 and W2 together:

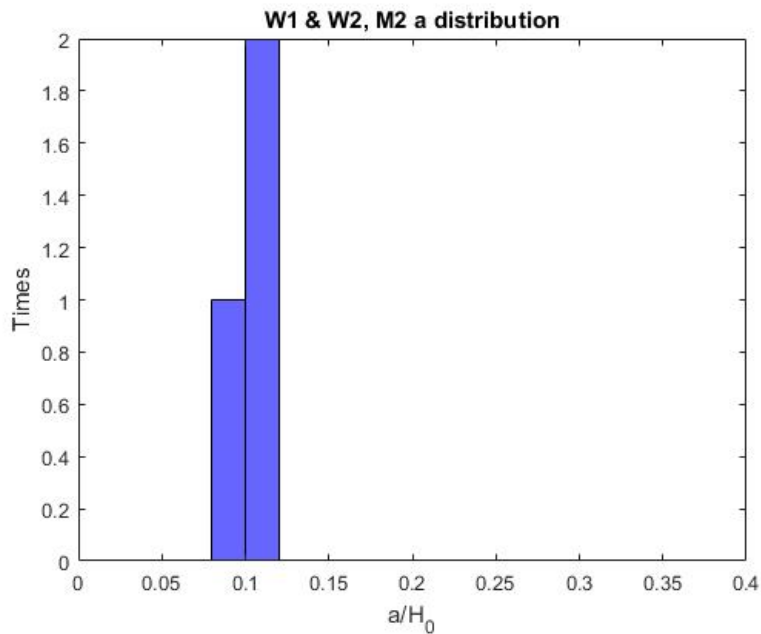


Figure 290: M2 web hole's pattern height distribution of W1 and W2 web corrosion patterns for beams with a diaphragm - MassDOT

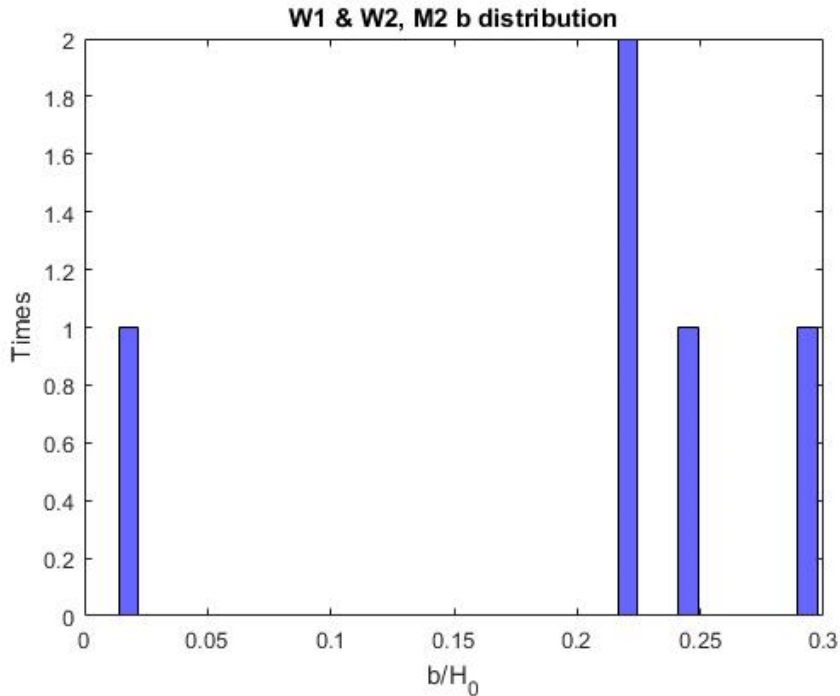


Figure 291: M2 web hole's pattern length distribution of W1 and W2 web corrosion patterns for beams with a diaphragm - MassDOT

Following this grouping, our team still found the sample to be very small (3 values for M2a, and 5 for M2b). We then assumed that M2 holes present thin and long 100% material loss areas underneath the diaphragm:

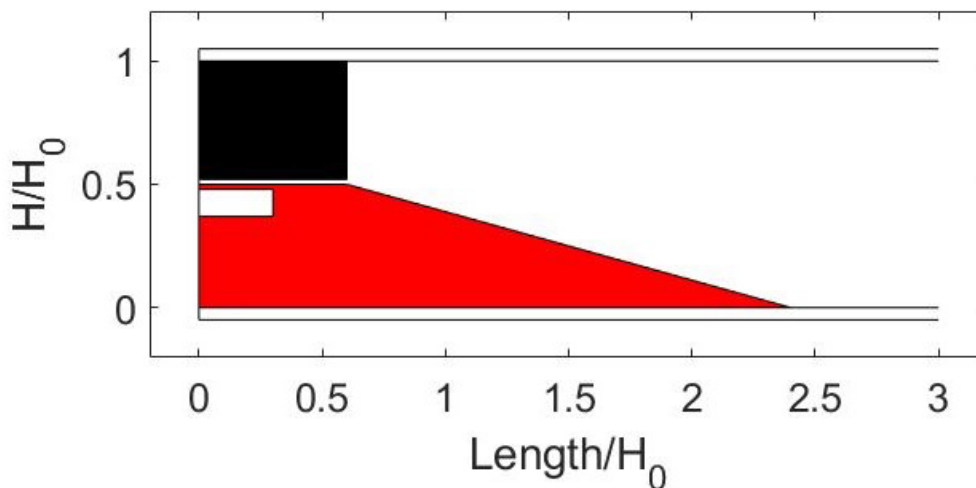


Figure 292: M2 hole pattern projected on the extreme W2 web corrosion pattern. With black color is illustrated the diaphragm that could be found with these patterns. The parameters are $a \leq 0.11$, and $b \leq 0.3$ - MassDOT

12.2.4. Pattern W3

12.2.4.1. Web Corrosion

The data analysis started with the CH2 distribution. The parameters for the corrosion patterns can be found with corresponding diagrams in Section 1.5 *Corrosion Patterns* of this report.

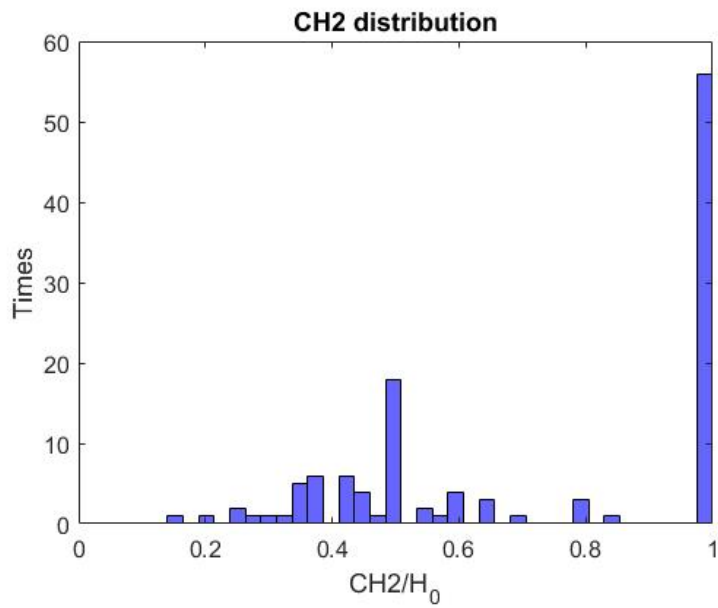


Figure 293. CH2 distribution of W3 web corrosion pattern for beams with a diaphragm - MassDOT

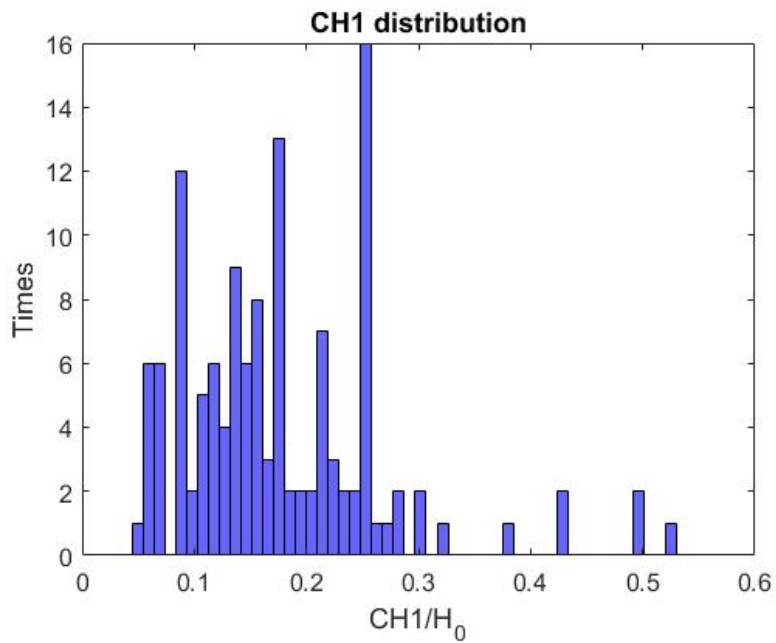


Figure 294: CH1 distribution of W3 web corrosion pattern for beams with a diaphragm - MassDOT

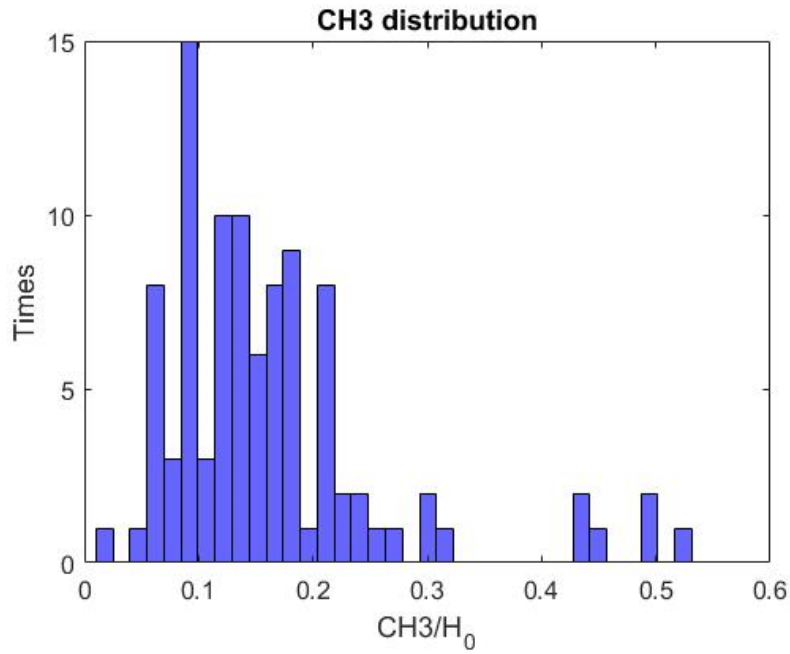


Figure 295: CH3 distribution of W3 web corrosion pattern for beams with a diaphragm - MassDOT

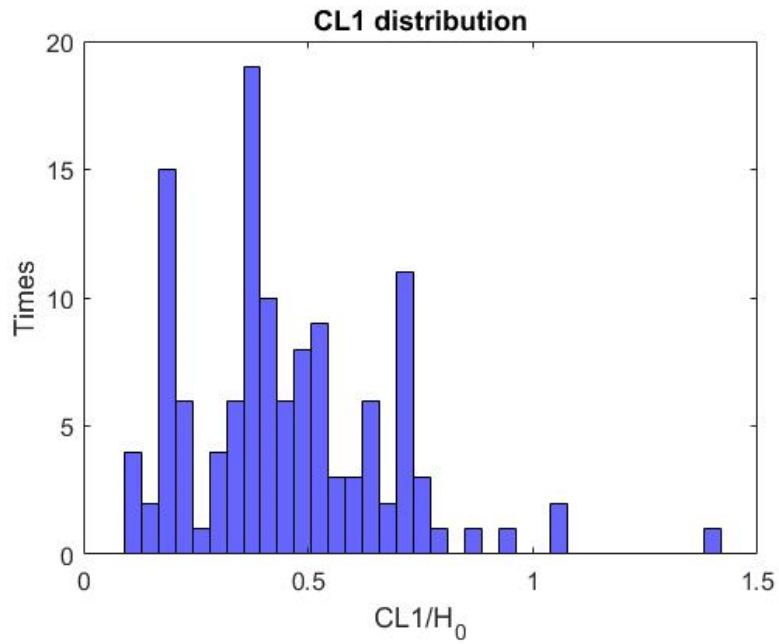


Figure 296: CL1 distribution of W3 web corrosion pattern for beams with a diaphragm - MassDOT

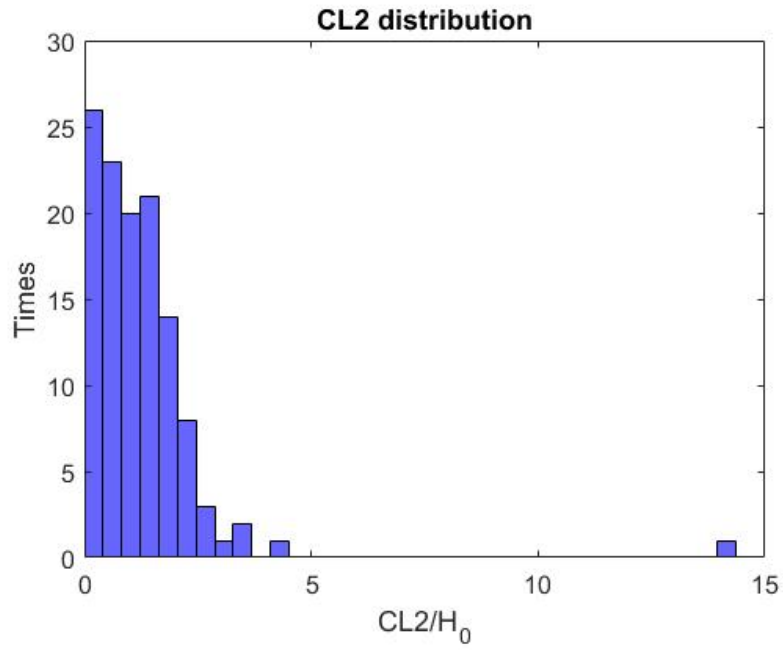


Figure 297: CL2 distribution of W3 web corrosion pattern for beams with a diaphragm - MassDOT

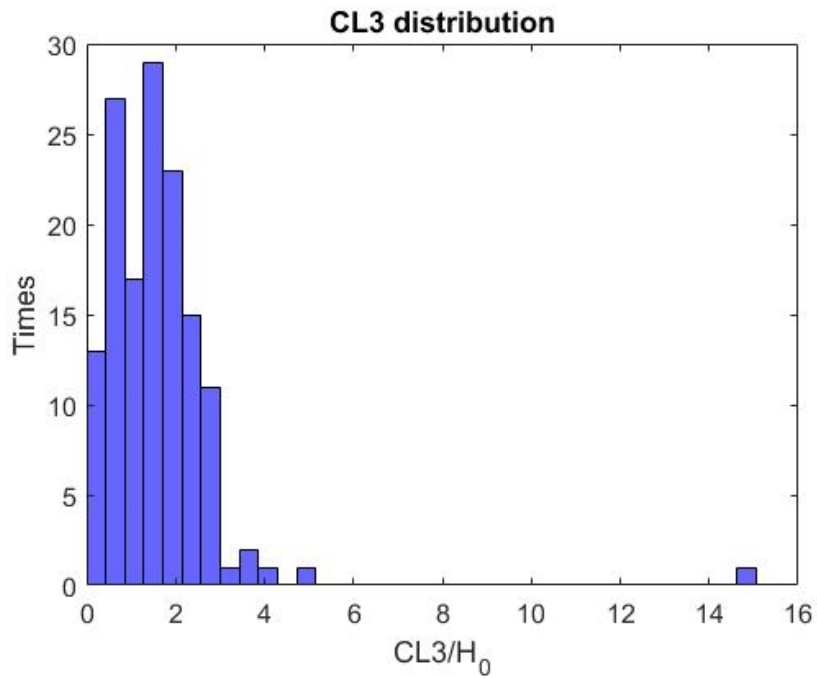


Figure 298: CL3 distribution of W3 web corrosion pattern for beams with a diaphragm - MassDOT

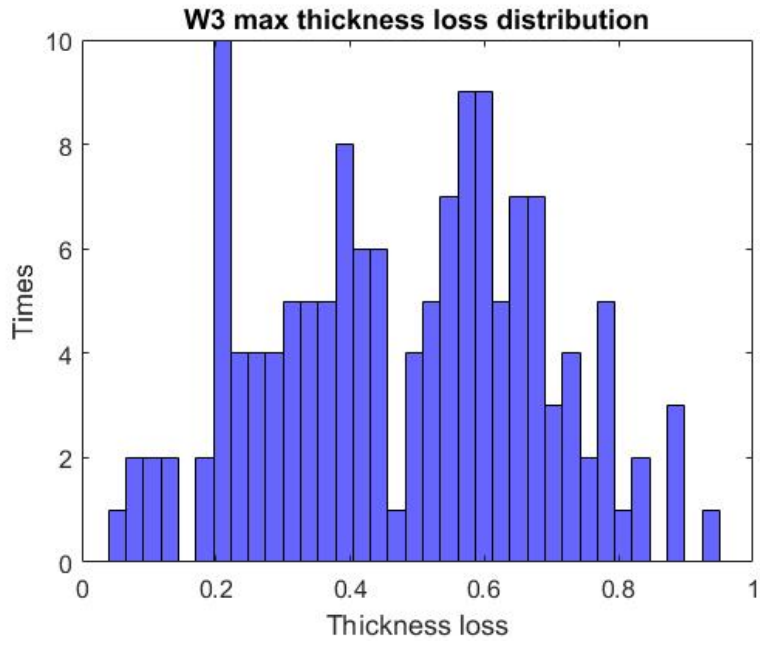


Figure 299: Ma web thickness loss distribution of W3 web corrosion pattern for beams with a diaphragm - MassDOT

From the CH2 histogram, two main trends are noticed, either a) full height corrosion, or b) corrosion up to 50% of H_0 .

$$CH_2 = H_0 \text{ or } 0 < CH_2 \leq 0.5H_0$$

For full height corrosion:

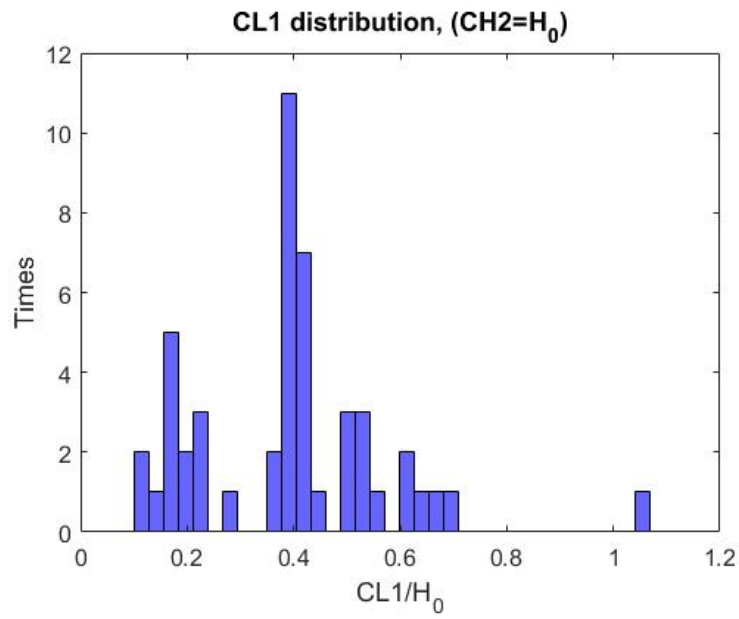


Figure 300: CL1 distribution of W3 web corrosion pattern with full height corrosion for beams with a diaphragm - MassDOT

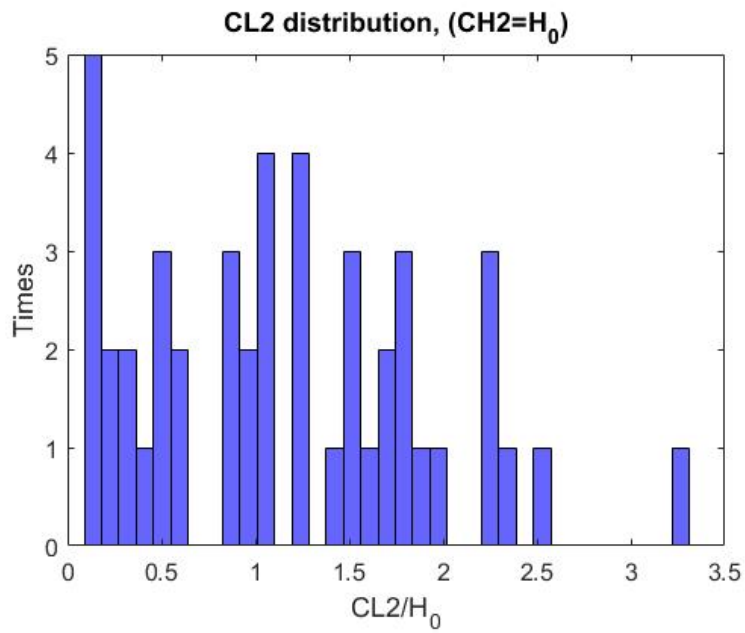


Figure 301: CL2 distribution of W3 web corrosion pattern with full height corrosion for beams with a diaphragm - MassDOT

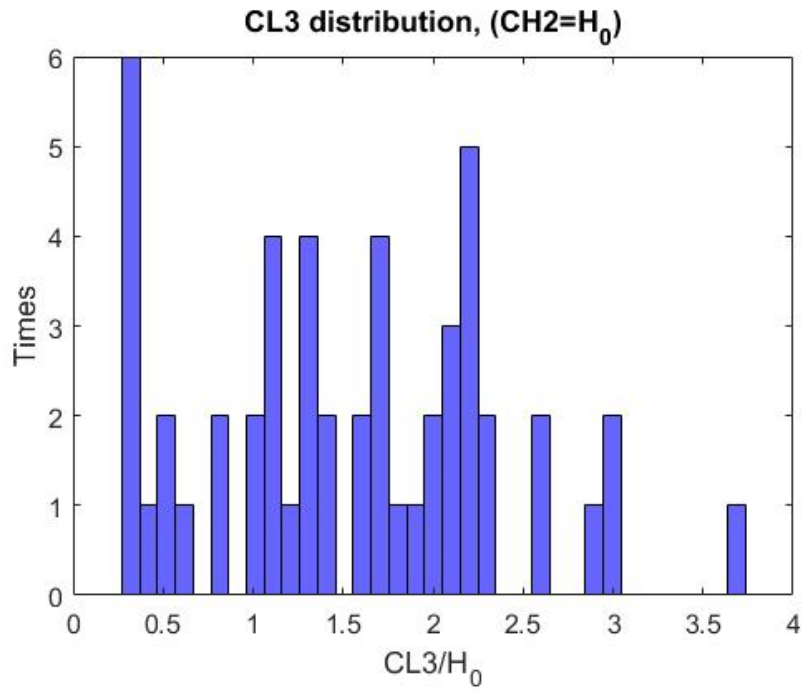


Figure 302: CL3 distribution of W3 web corrosion pattern with full height corrosion for beams with a diaphragm - MassDOT

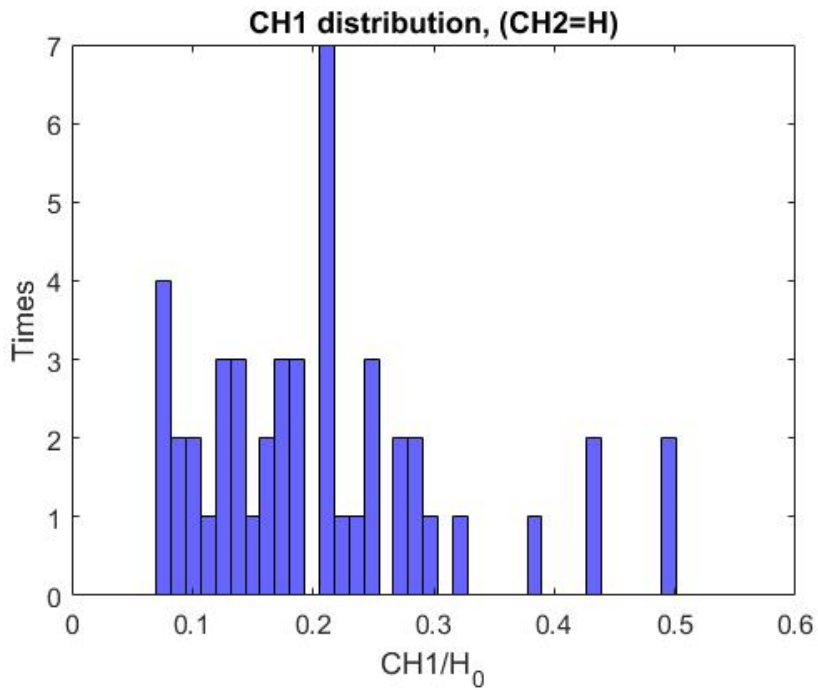


Figure 303: CH1 distribution of W3 web corrosion pattern with full height corrosion for beams with a diaphragm - MassDOT

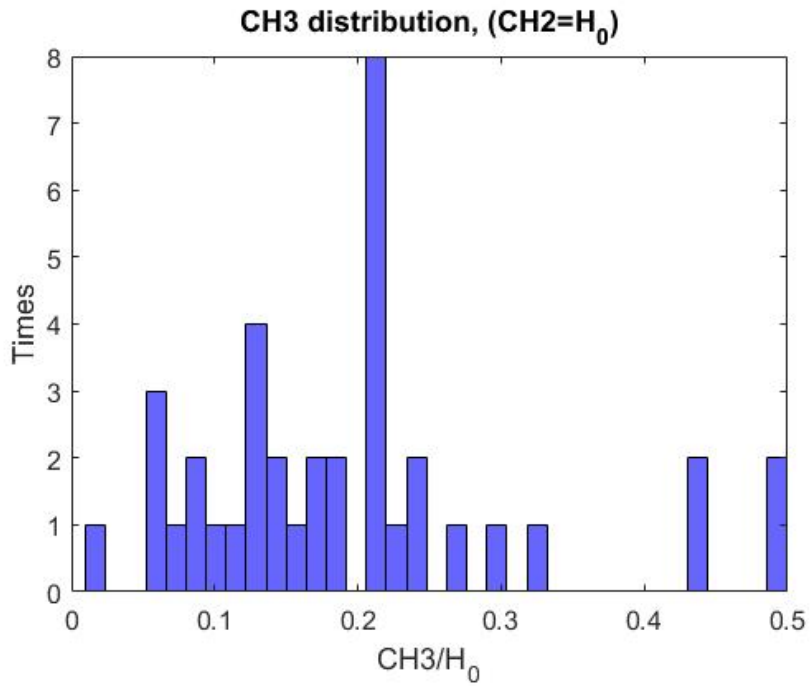


Figure 304: CH3 distribution of W3 web corrosion pattern with full height corrosion for beams with a diaphragm - MassDOT

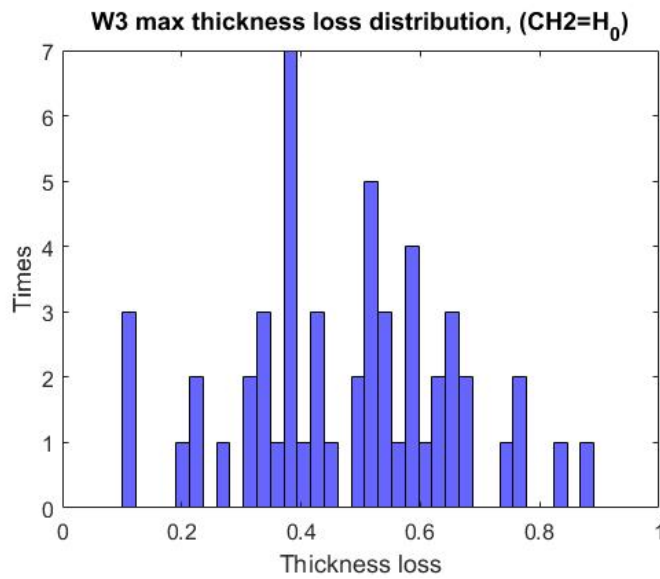


Figure 305: Max web thickness loss distribution of W3 web corrosion pattern with full height corrosion for beams with a diaphragm - MassDOT

From the CL3 histogram, two main trends were noticed:

$$0.25H_0 < CL_3 \leq 0.6H_0 \text{ and } 0.6H_0 < CL_3 \leq 2.25H_0$$

For full height corrosion and $0.25H_0 < CL_3 \leq 0.6H_0$

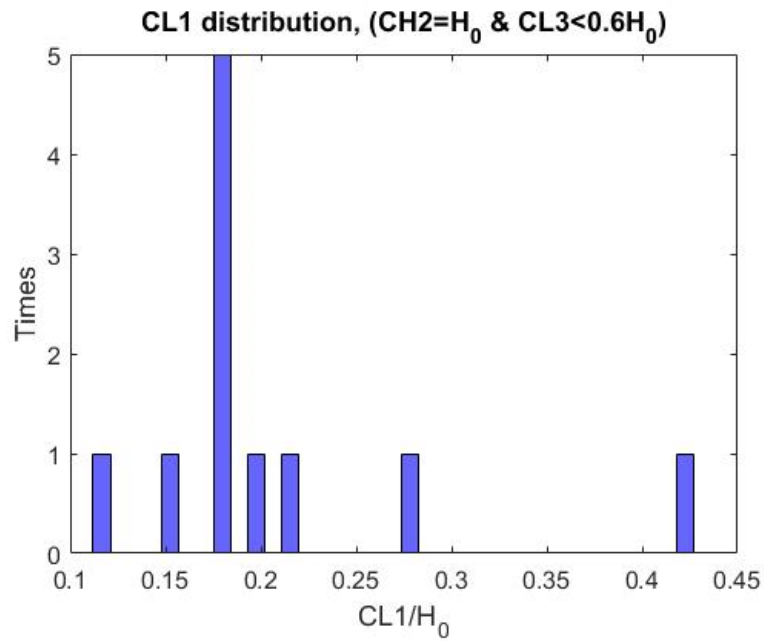


Figure 306: CL1 distribution of W3 web corrosion pattern with full height corrosion and deteriorated length up to 60% of H_0 for beams with a diaphragm - MassDOT

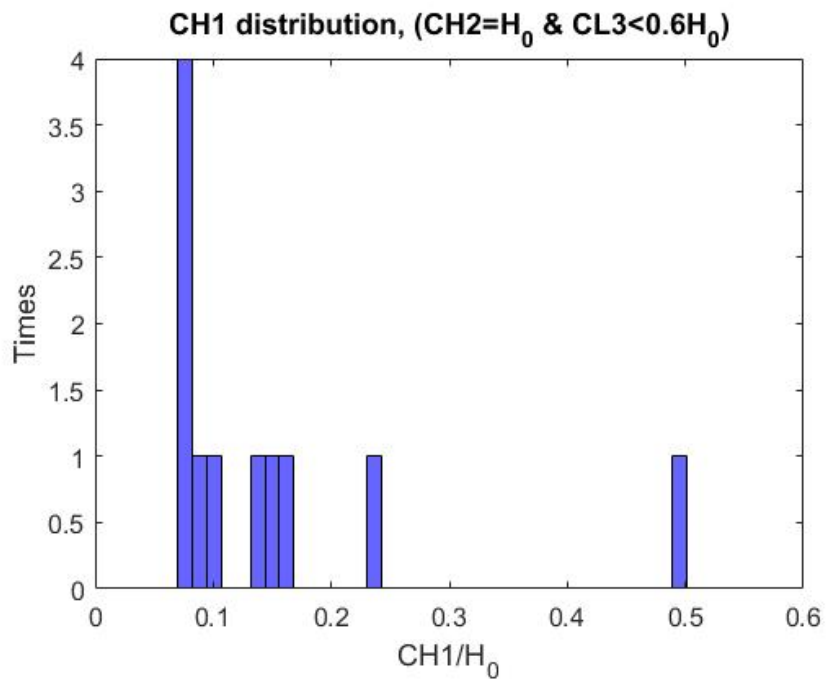


Figure 307: CH1 distribution of W3 web corrosion pattern with full height corrosion and deteriorated length up to 60% of H_0 for beams with a diaphragm - MassDOT

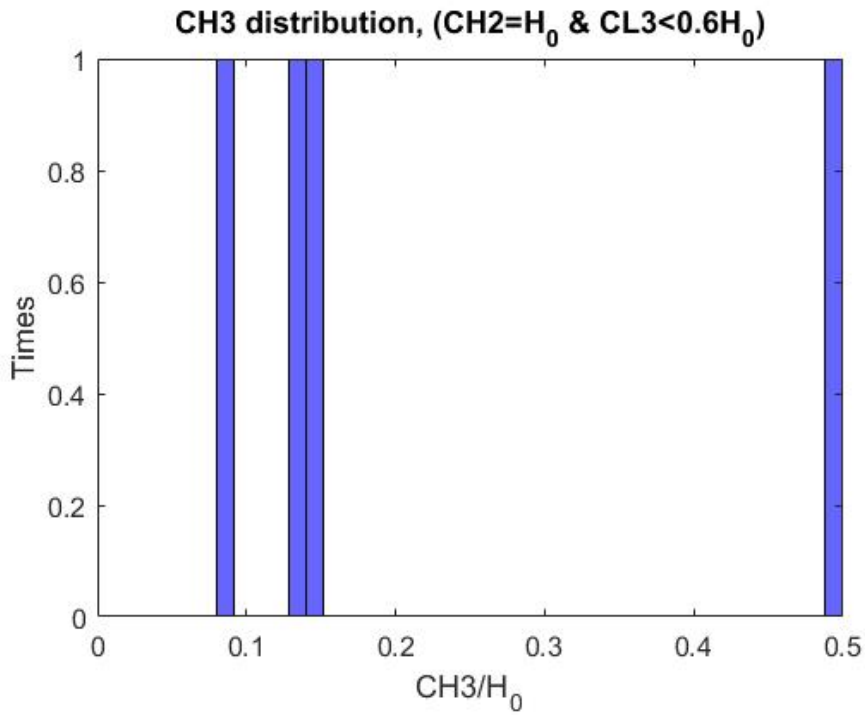


Figure 308: CH3 distribution of W3 web corrosion pattern with full height corrosion and deteriorated length up to 60% of H₀ for beams with diaphragm a - MassDOT

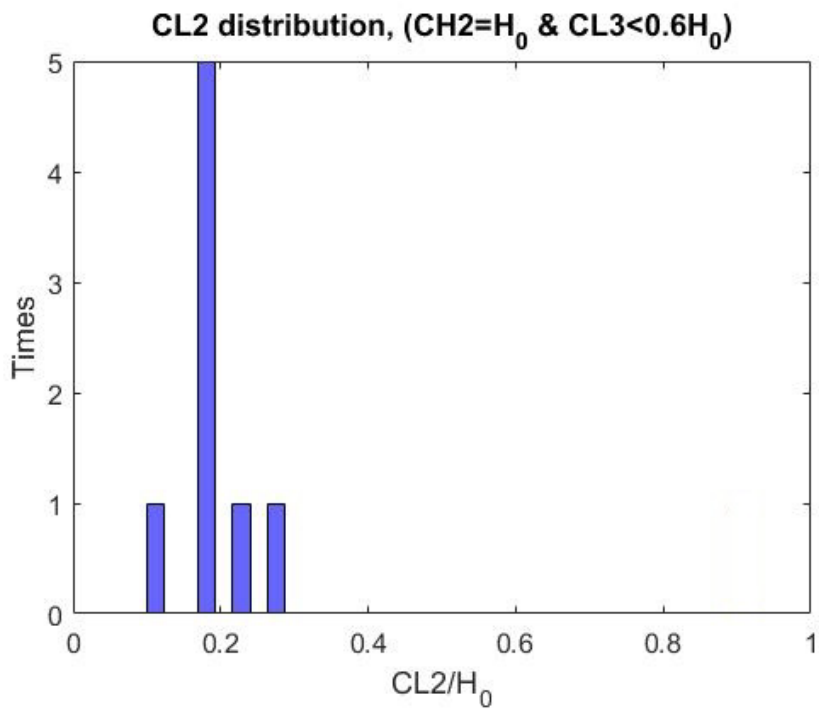


Figure 309: CL2 distribution of W3 web corrosion pattern with full height corrosion and deteriorated length up to 60% of H₀ for beams with a diaphragm - MassDOT

W3 max thickness loss distribution, ($CH2=H_0$ & $CL3<0.6H_0$)

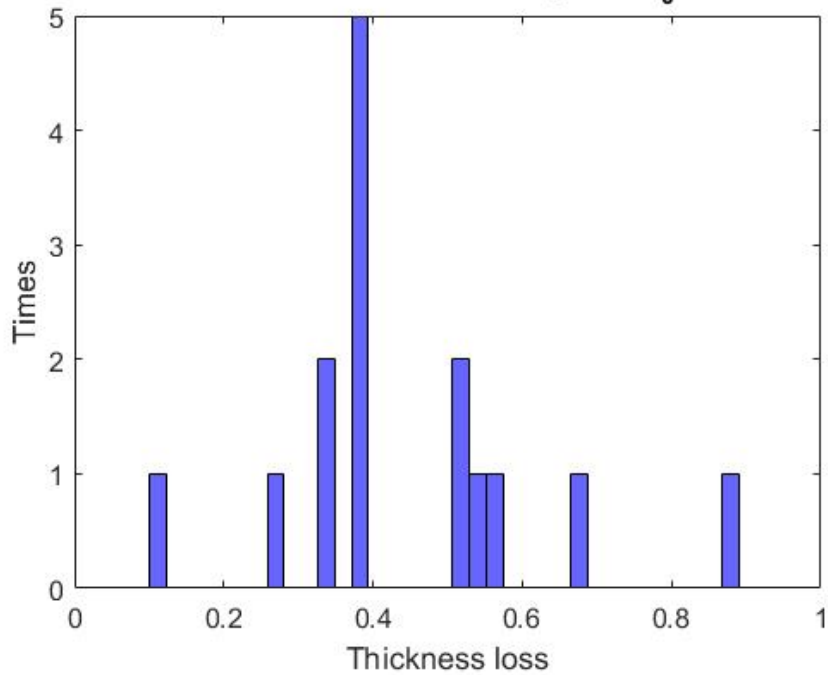


Figure 310: Max web thickness loss distribution, of W3 web corrosion pattern, with full height corrosion and deteriorated length up to 60% of H_0 for beams with a diaphragm - MassDOT

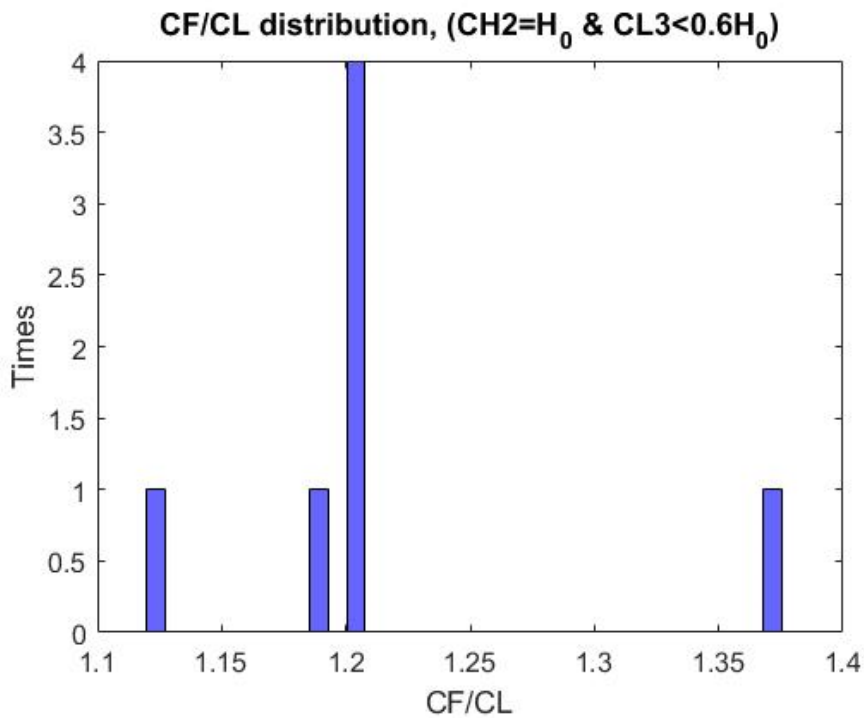


Figure 311: Ratio of flange to web corrosion length distribution, of W3 web corrosion pattern, with full height corrosion and deteriorated length up to 60% of H_0 for beams with a diaphragm - MassDOT

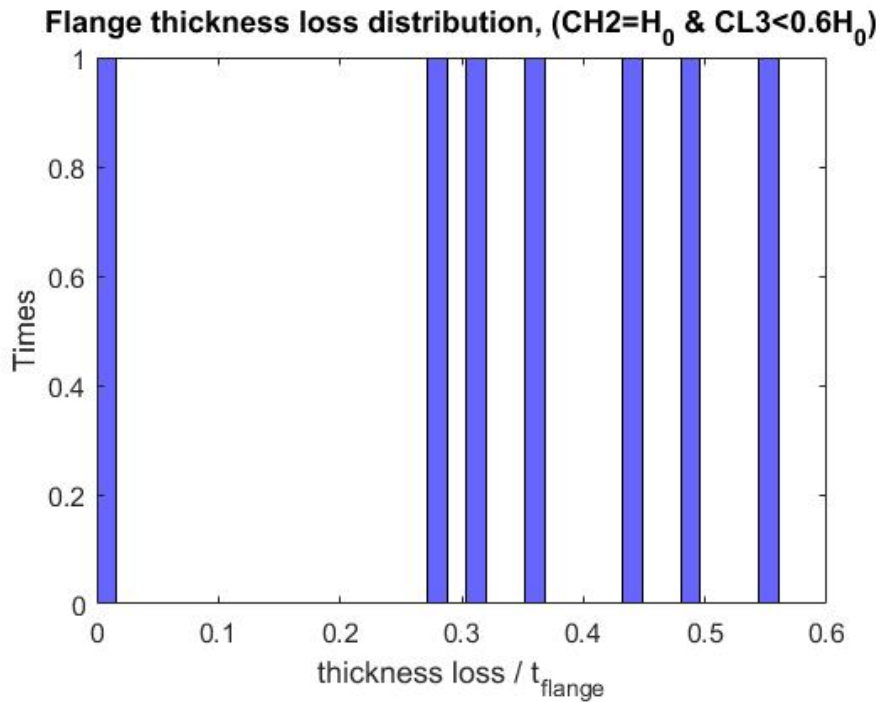


Figure 312: Max flange loss thickness distribution, for beams with W3 web corrosion pattern, with full height corrosion, deteriorated length up to 60% of H₀ and with a diaphragm - MassDOT

$$0.25H_0 < CL_3 \leq 0.6H_0$$

$$0.1H_0 < CL_1 \leq 0.2H_0$$

$$0.06H_0 < CH_1 = CH_3 \leq 0.16H_0$$

$$\frac{t_{loss}}{t_{web}} \text{ takes values of } \{0.4, 0.6\}$$

$$\frac{c_f}{c_l} = 1.2 \text{ and}$$

$$\frac{t_{loss}}{t_{flange}} \text{ takes values of } \{0.3, 0.6\}$$

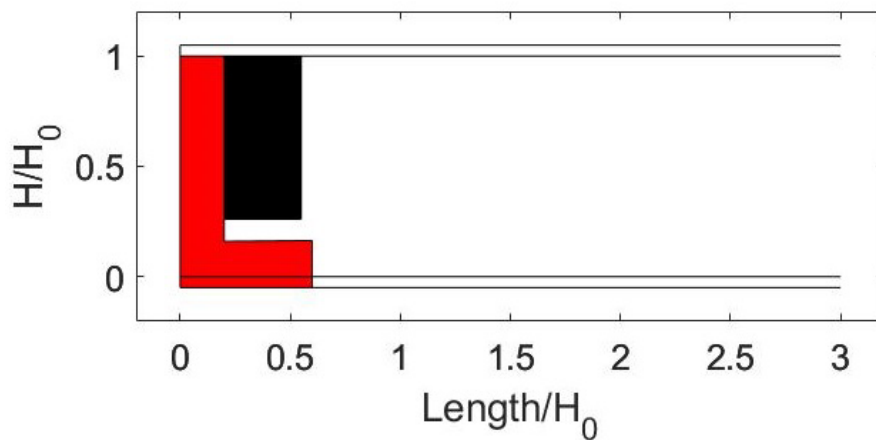


Figure 313: First extreme flange and W3 web corrosion scenario for beams with a diaphragm. - MassDOT

For full height corrosion and $CL3 \leq 2.3$

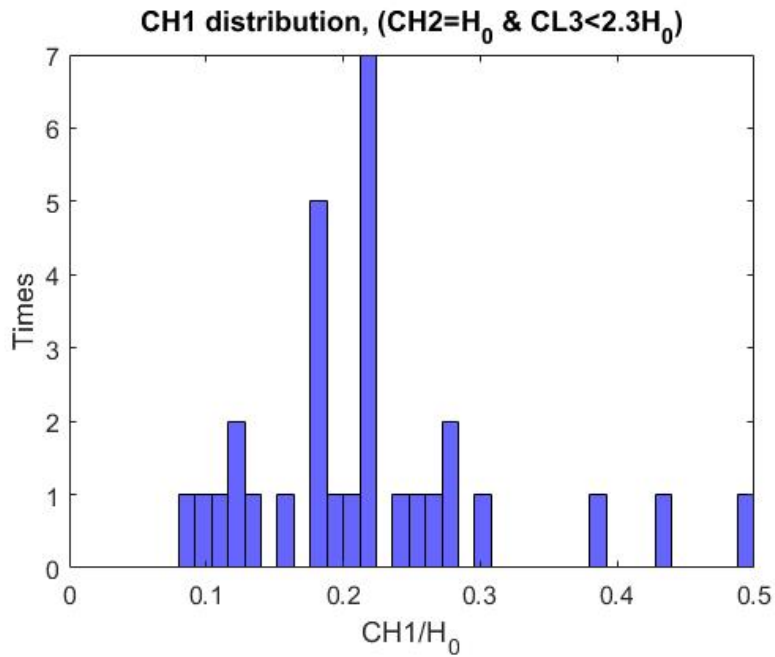


Figure 314: CH1 distribution of W3 web corrosion pattern, with full height corrosion and deteriorated length up to 230% of H_0 , for beams with a diaphragm - MassDOT

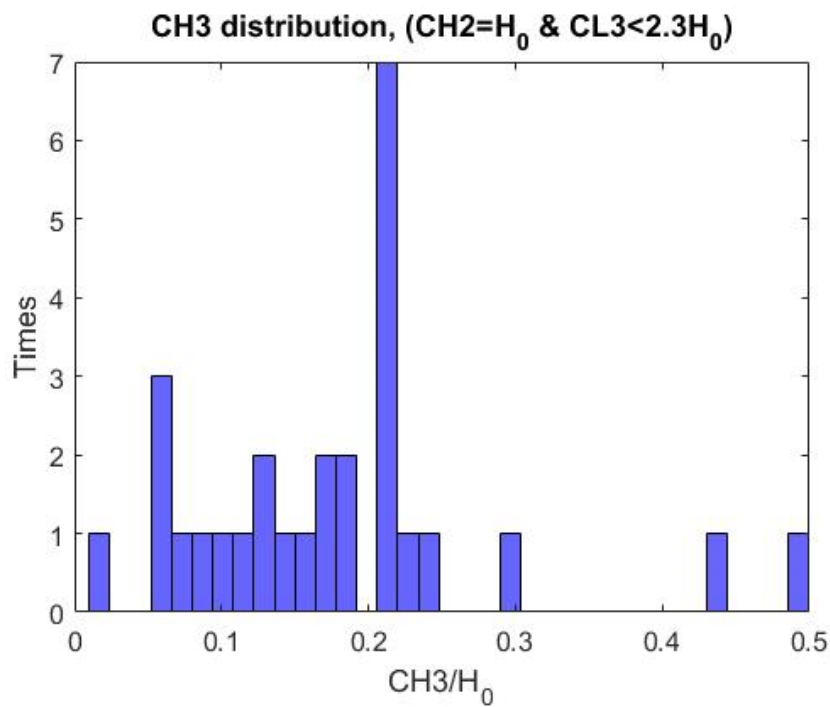


Figure 315: CH3 distribution of W3 web corrosion pattern, with full height corrosion and deteriorated length up to 230% of H_0 , for beams with a diaphragm - MassDOT

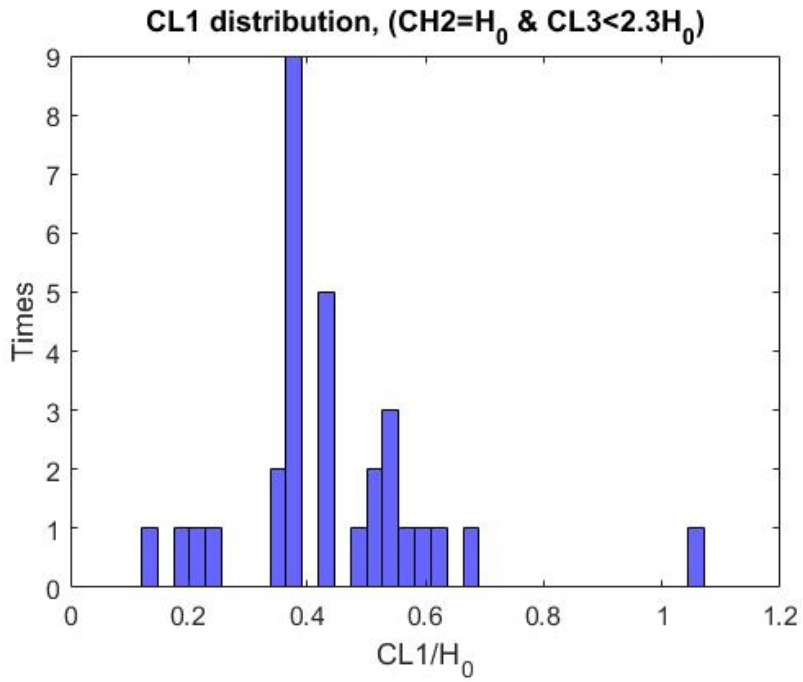


Figure 316: CL1 distribution of W3 web corrosion pattern, with full height corrosion and deteriorated length up to 230% of H_0 , for beams with a diaphragm - MassDOT

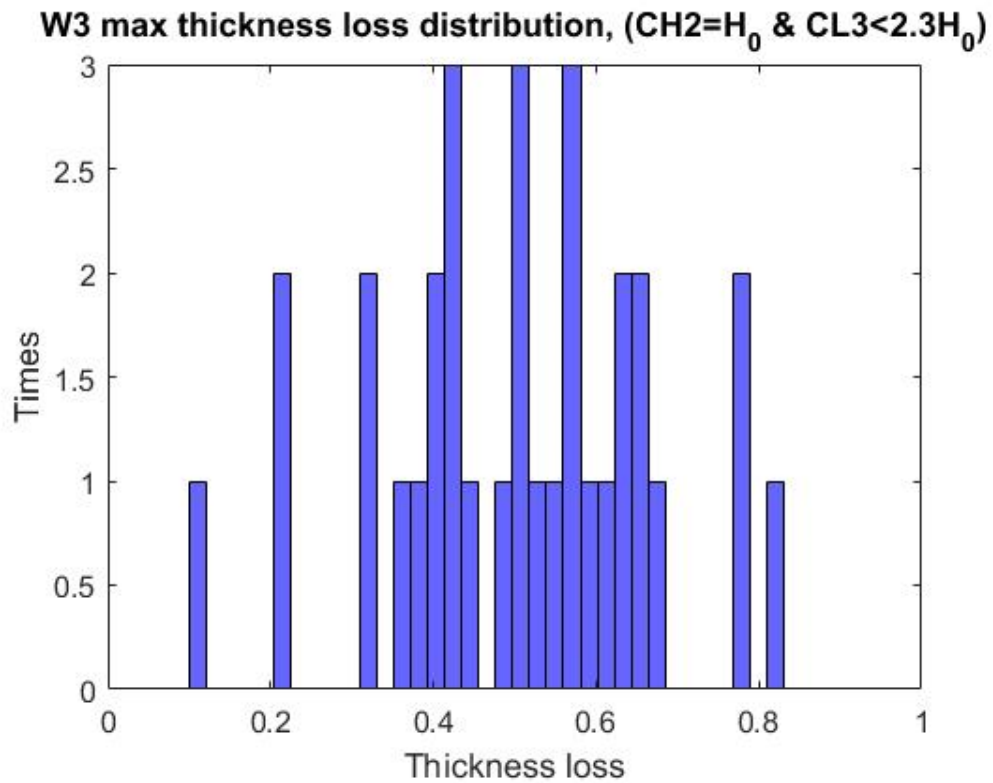


Figure 317: Max web thickness loss distribution, of W3 web corrosion pattern, with full height corrosion and deteriorated length up to 230% of H_0 , for beams with a diaphragm - MassDOT

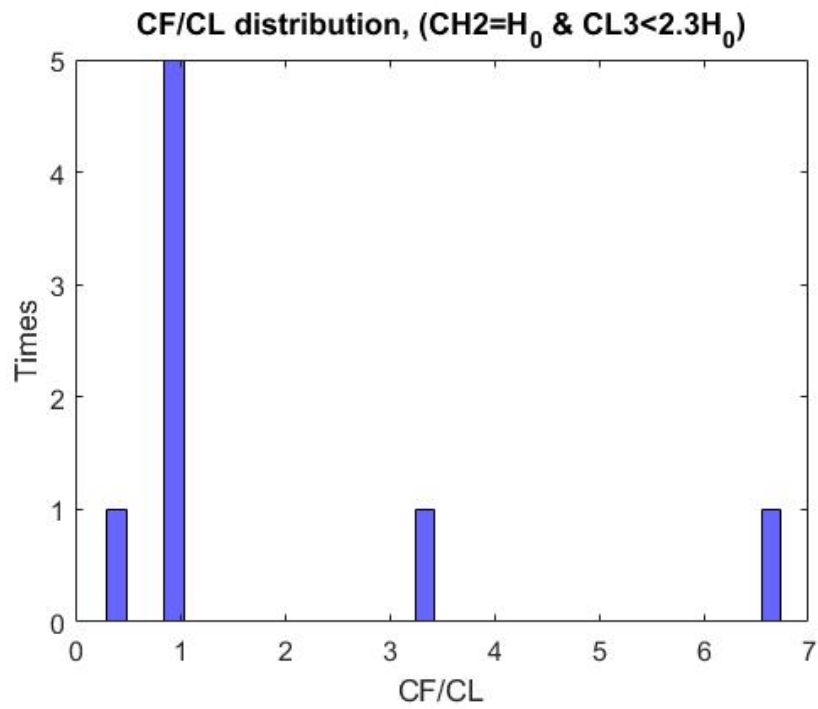


Figure 318: Ratio of flange to web corrosion length distribution, of W3 web corrosion pattern, with full height corrosion and deteriorated length up to 230% of H_0 for beams with a diaphragm - MassDOT

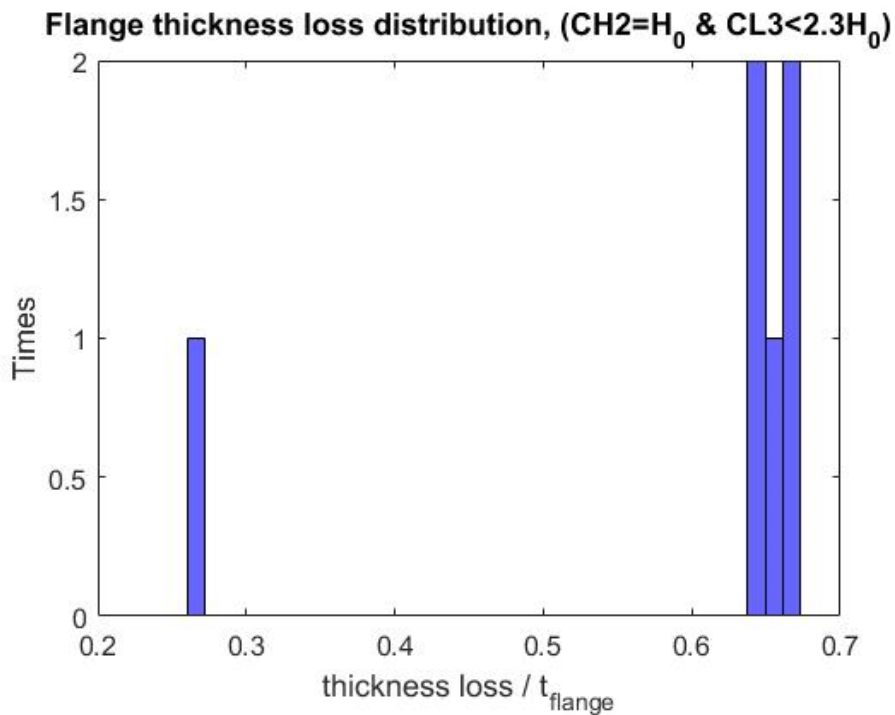


Figure 319: Max flange loss thickness distribution, for beams with W3 web corrosion pattern, with full height corrosion, deteriorated length up to 230% of H_0 and with a diaphragm - MassDOT

$$0.6H_0 < CL_3 \leq 2.3H_0$$

$$0.2H_0 < CL_1 \leq 0.6H_0$$

$$0.05H_0 < CH_1 = CH_3 \leq 0.30H_0$$

$\frac{t_{loss}}{t_{web}}$ takes the values of {0.4,0.6,0.8}

$$\frac{c_f}{c_l} = 1 \text{ and}$$

$\frac{t_{loss}}{t_{flange}}$ takes the value of {0.65}

Below depicts the second extreme corrosion scenario for the flange and W3 corrosion pattern combination.

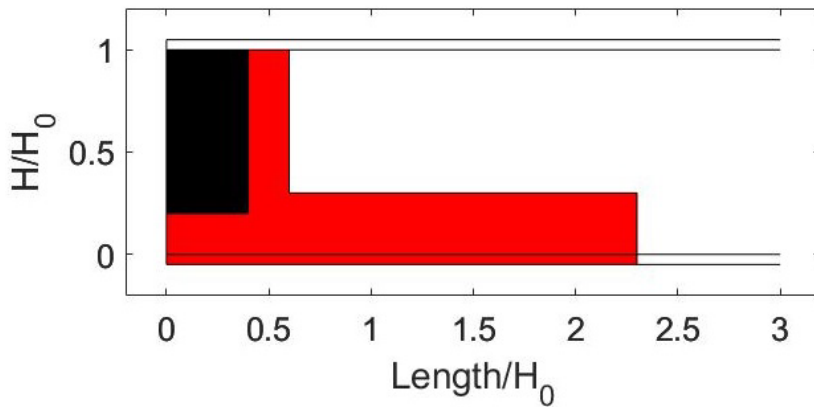


Figure 320: Second extreme flange and W3 web corrosion scenario for beams with a diaphragm - MassDOT

For height $\leq 0.5H_0$

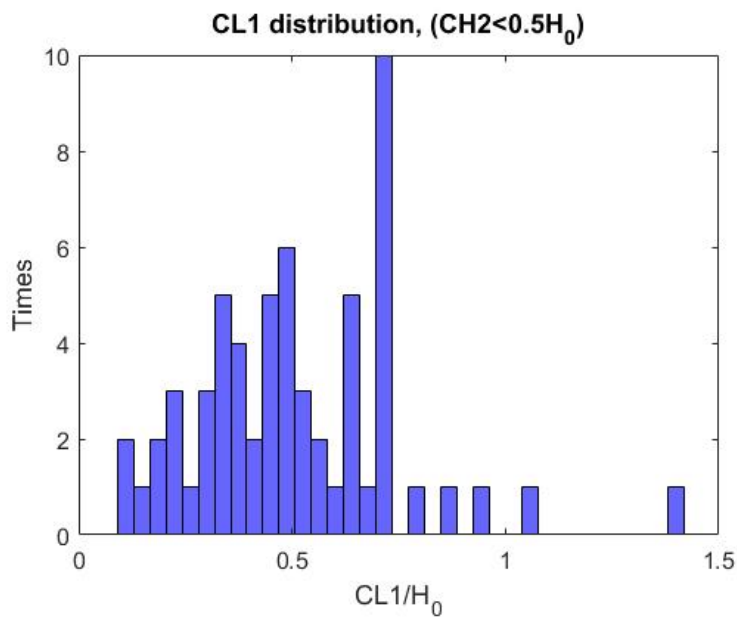


Figure 321: CL1 distribution of W3 web corrosion pattern, with corrosion height up to 50% of H_0 , for beams with a diaphragm - MassDOT

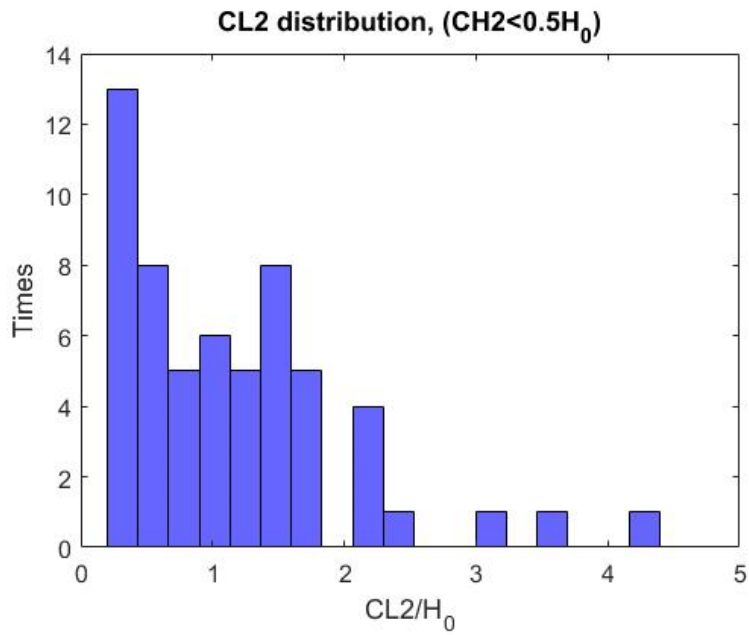


Figure 322: CL2 distribution of W3 web corrosion pattern, with corrosion height up to 50% of H_0 , for beams with a diaphragm - MassDOT

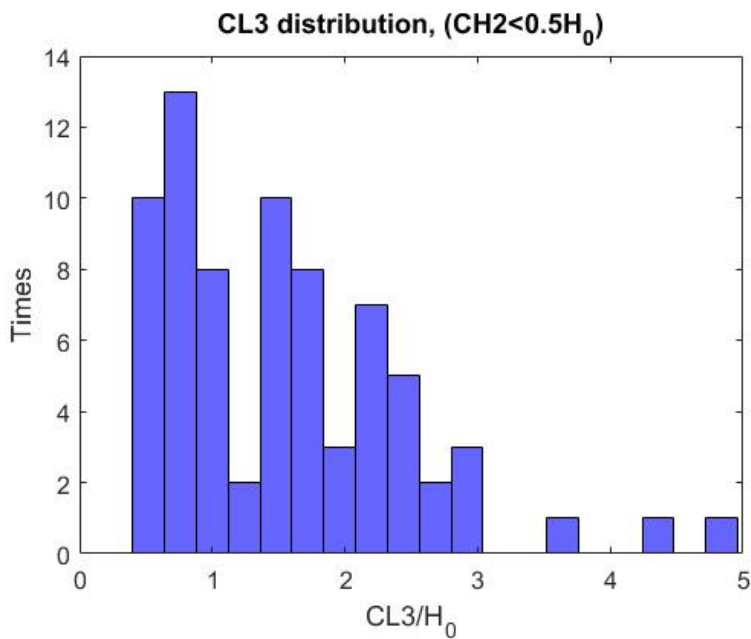


Figure 323: CL3 distribution of W3 web corrosion pattern, with corrosion height up to 50% of H_0 , for beams with a diaphragm - MassDOT

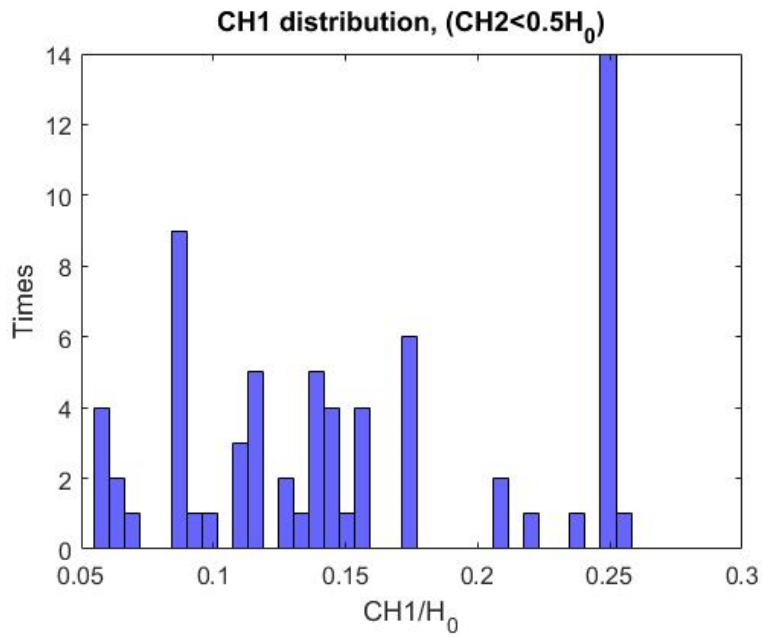


Figure 324: CH1 distribution of W3 web corrosion pattern, with corrosion height up to 50% of H₀, for beams with a diaphragm - MassDOT

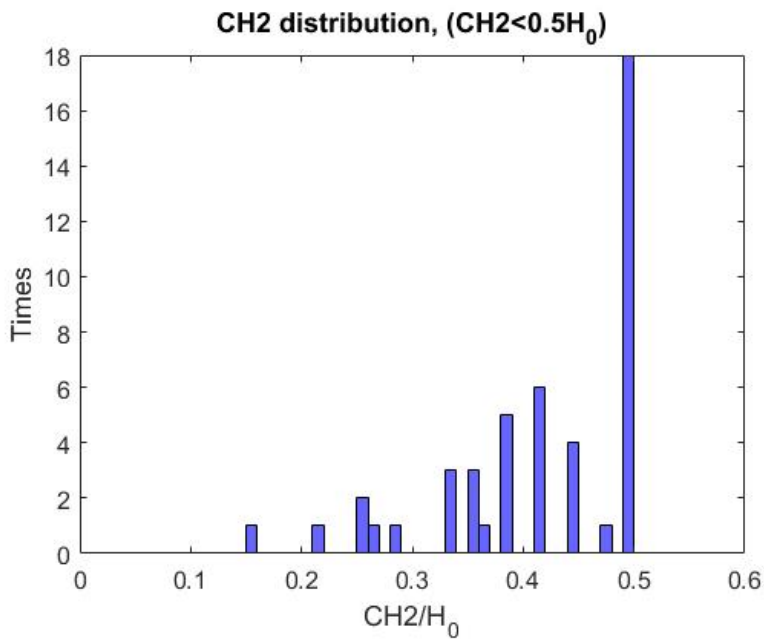


Figure 325: CH2 distribution of W3 web corrosion pattern, with corrosion height up to 50% of H₀, for beams with a diaphragm - MassDOT

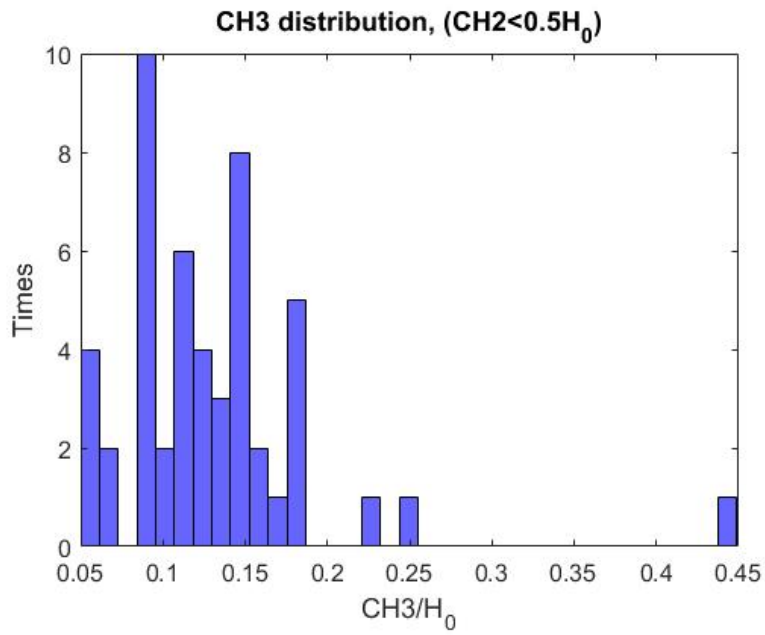


Figure 326: CH3 distribution of W3 web corrosion pattern, with corrosion height up to 50% of H_0 , for beams with a diaphragm - MassDOT

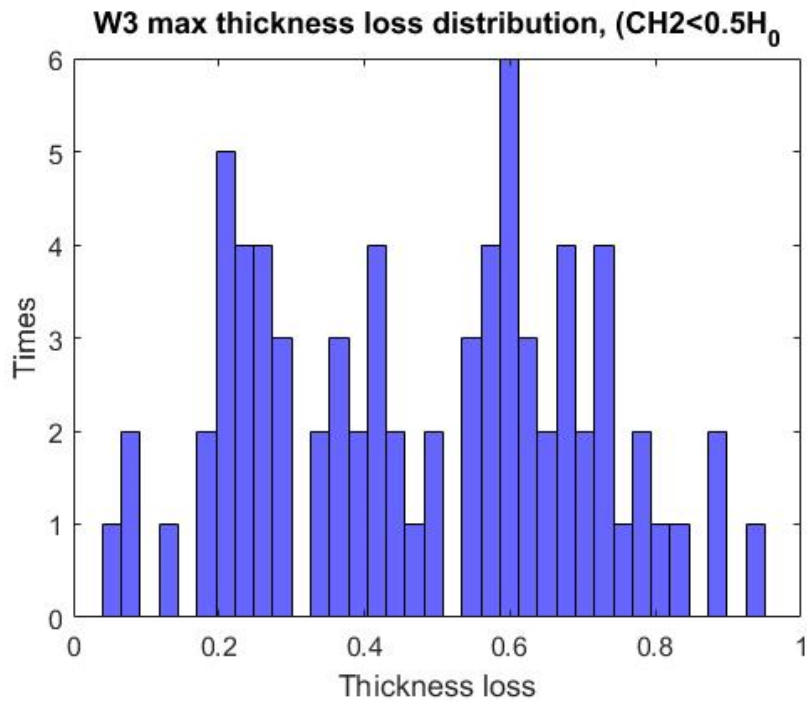


Figure 327: Max web thickness loss distribution of W3 web corrosion pattern, with corrosion height up to 50% of H_0 , for beams with a diaphragm - MassDOT

12.2.4.2. Flange Corrosion

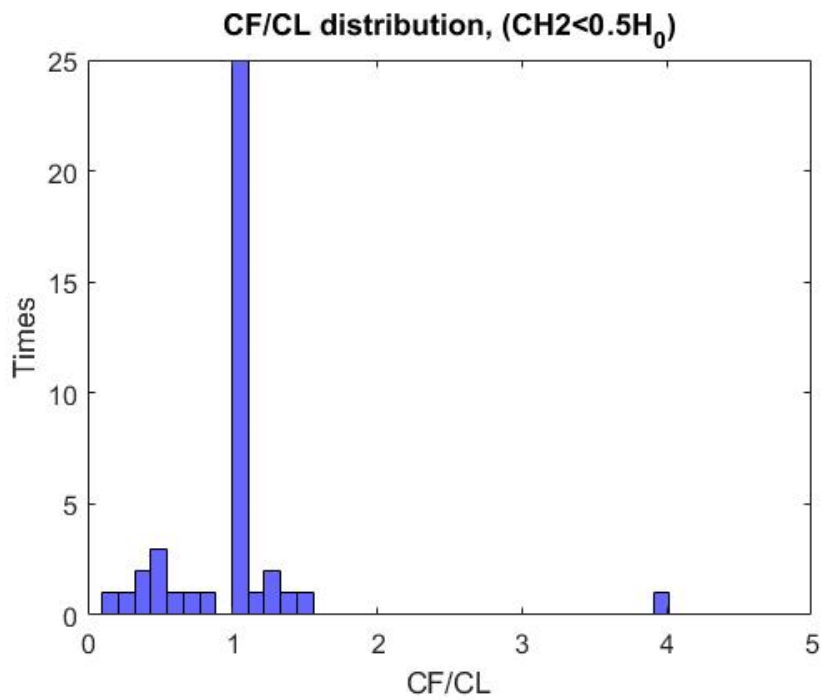


Figure 328: Ratio of flange to web corrosion length distribution, of W3 web corrosion pattern, with corrosion height up to 50% of H_0 , for beams with a diaphragm - MassDOT

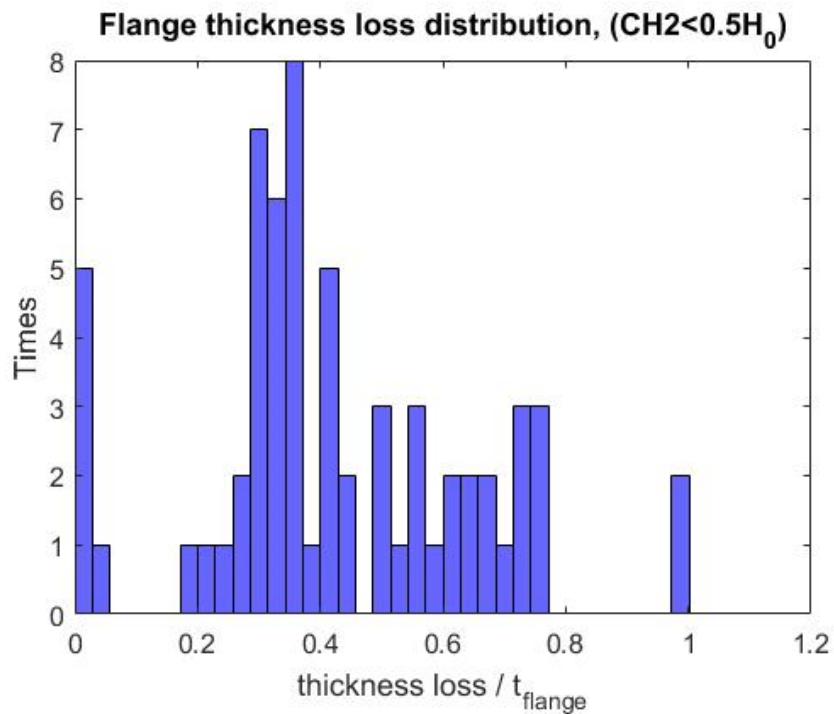


Figure 329: Max flange loss thickness distribution, for beams with W3 web corrosion pattern, with corrosion height up to 50% of H_0 , for beams with a diaphragm - MassDOT

$$0.5H_0 < CL_3 \leq 3H_0$$

$$0.1H_0 < CL_1 \leq 0.75H_0$$

$$0.05H_0 < CH_1 \leq 0.25H_0$$

$$0.05H_0 < CH_3 \leq 0.18H_0$$

$\frac{t_{loss}}{t_{web}}$ takes the values of {0.4,0.6,0.8}

$$\frac{c_f}{c_l} = 1 \text{ and}$$

$\frac{t_{loss}}{t_{flange}}$ takes the values of {0.3,0.6,0.8}

Below depicts the third extreme corrosion scenario for the flange and W3 corrosion pattern combination.

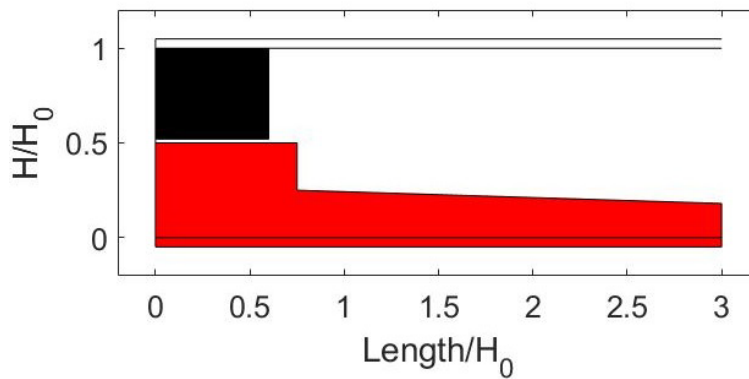


Figure 330: Third extreme flange and W3 web corrosion scenario for beams with a diaphragm - MassDOT

12.2.4.3. Holes

Below, the histogram describes the distribution of holes dimensions for the M1 hole corrosion pattern.

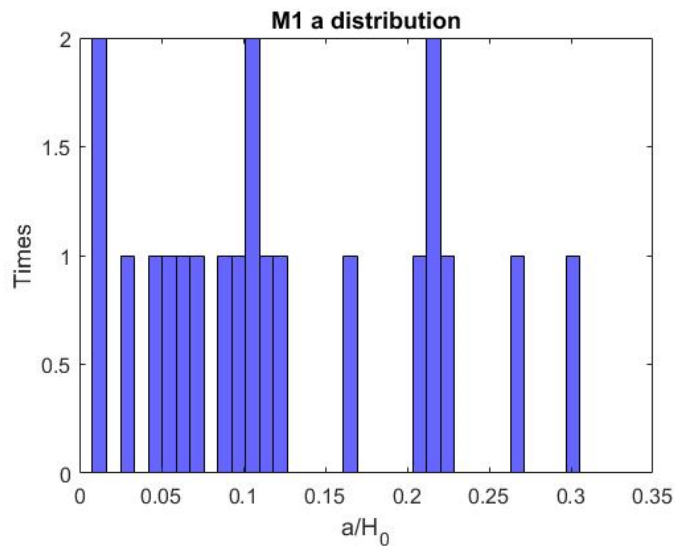


Figure 331: M1 web hole's pattern height distribution of W3 web corrosion pattern for beams with a diaphragm - MassDOT

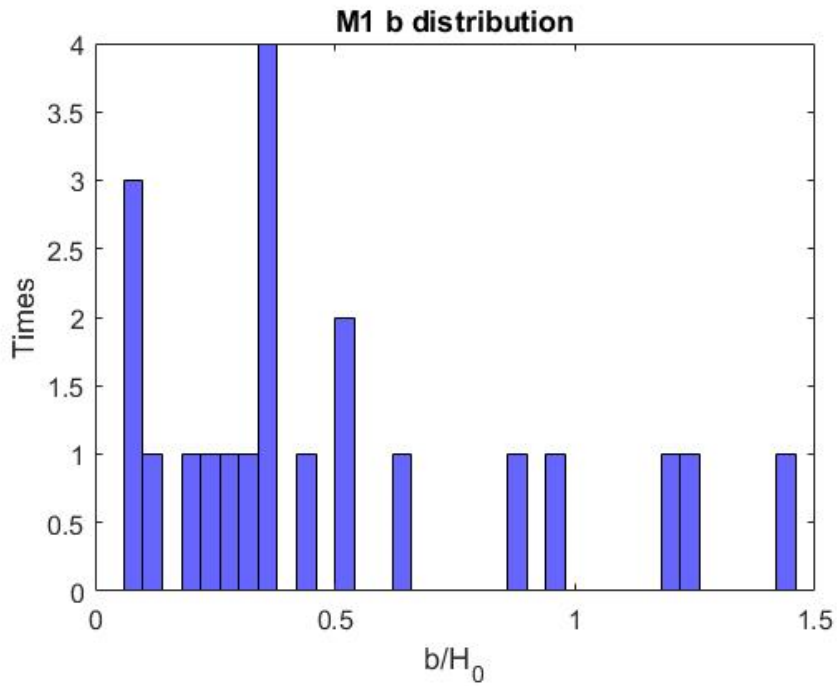


Figure 332: M1 web hole's pattern length distribution of W3 web corrosion pattern for beams with a diaphragm - MassDOT

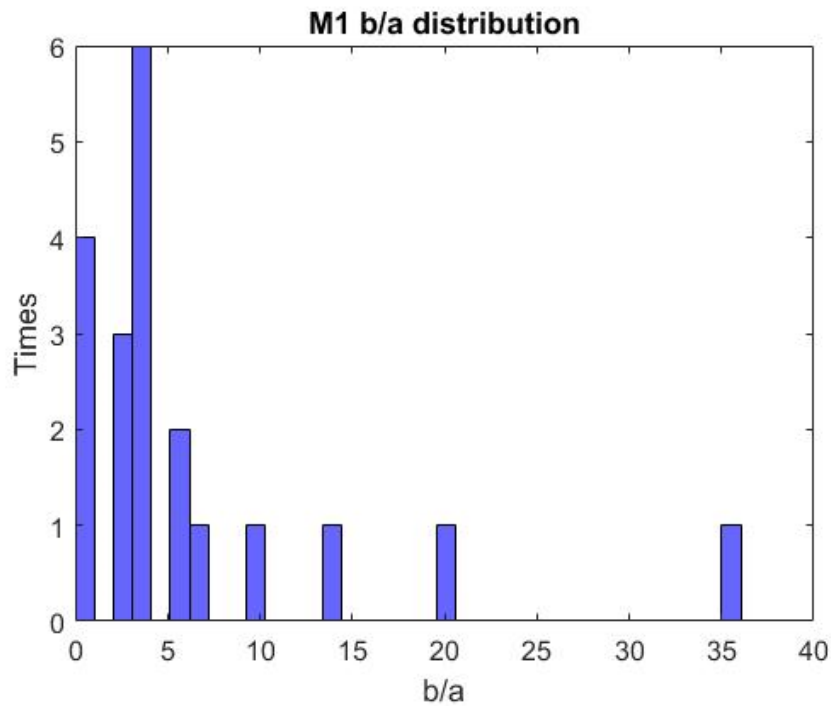


Figure 333: M1 web hole's ratio length to height distribution of W3 web corrosion pattern for beams with a diaphragm - MassDOT

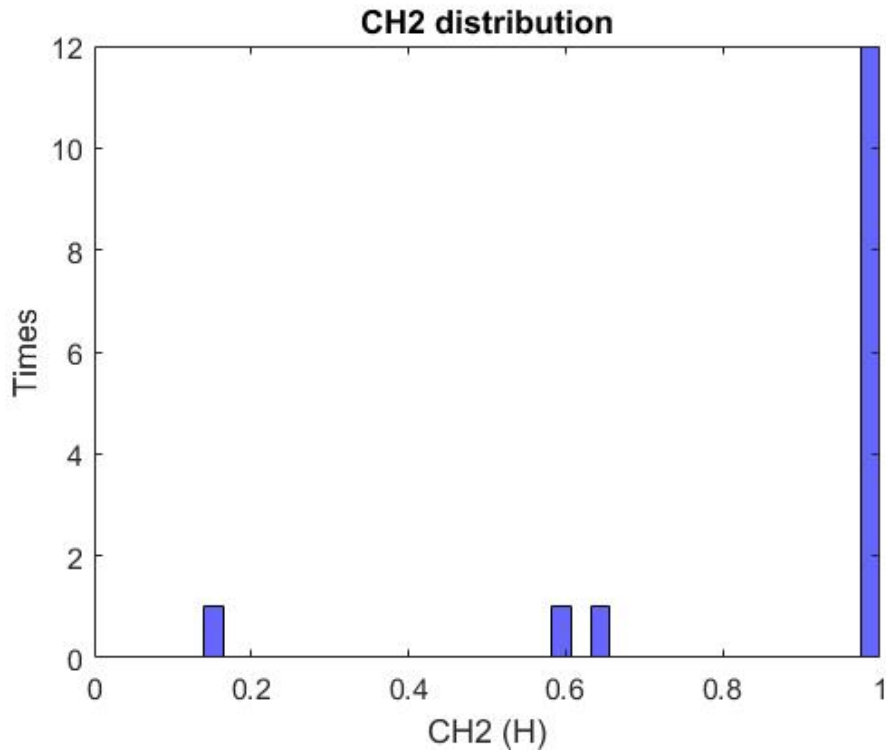


Figure 334: Max corrosion height distribution of W3 pattern with M1 hole, for beams with a diaphragm - MassDOT

From the figure above, it was noticed that holes appear mainly at the full height of the corroded web. The holes observed seem to be mainly thin and long across the web. From Figure 333, most of the cases have ratio of hole's length to height up to 6. From Figure 332, the hole length is up to 50% of H_0 . Thus, for the extreme corrosion hole scenario, the hole's height is considered as 0.083.

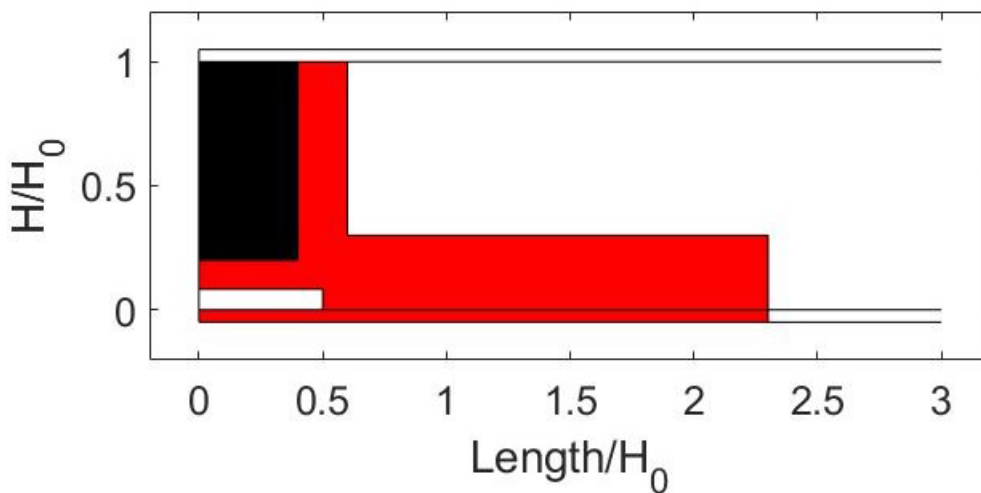


Figure 335: M1 hole pattern projected on the second extreme W3 web corrosion pattern scenario. With black color is illustrated the diaphragm that could be found with these patterns - MassDOT

12.2.5. Pattern W4

The parameters for the corrosion patterns can be found with corresponding diagrams in Section 1.5 *Corrosion Patterns* of this report.

12.2.5.1. Web Corrosion

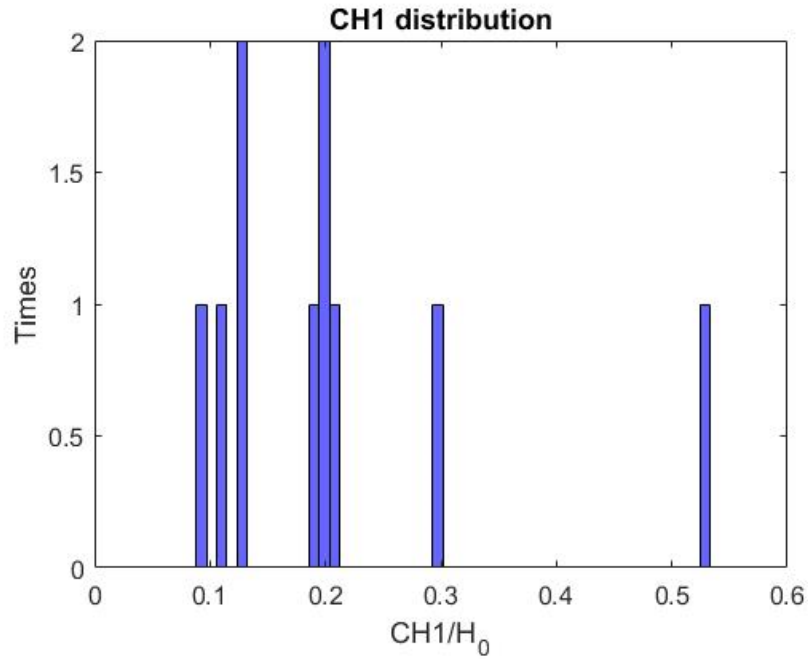


Figure 336: CH1 distribution of W4 web corrosion pattern for beams with a diaphragm - MassDOT

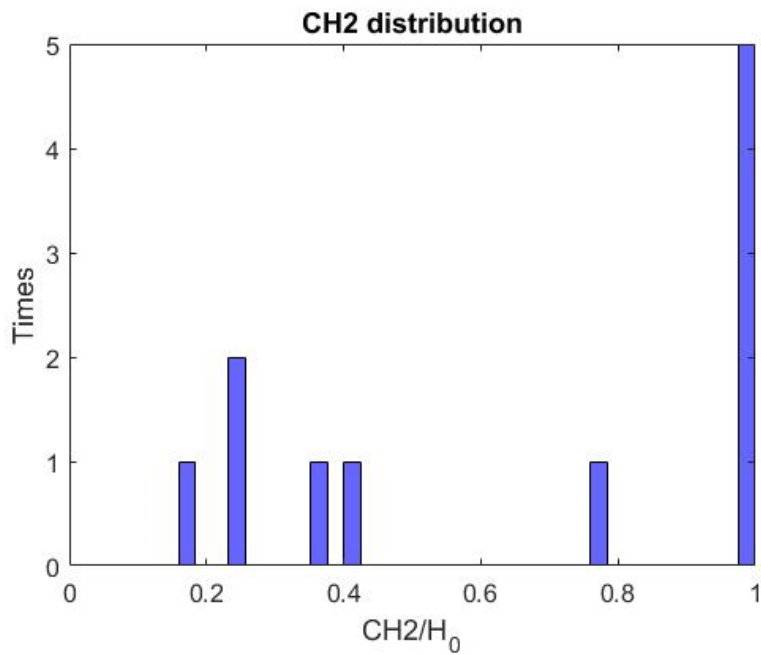


Figure 337: CH2 distribution of W4 web corrosion pattern for beams with a diaphragm - MassDOT

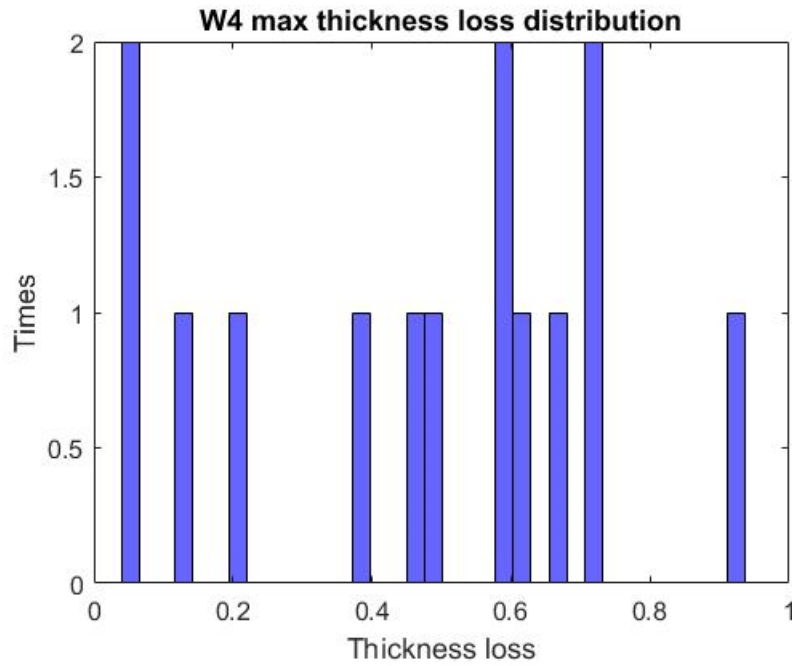


Figure 338: Max web thickness loss distribution of W4 web corrosion pattern for beams with a diaphragm - MassDOT

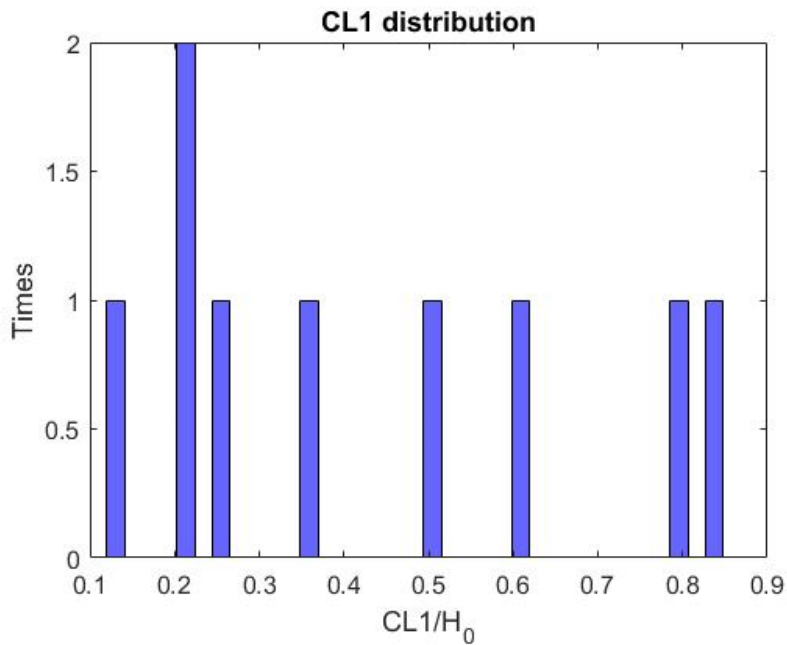


Figure 339: CL1 distribution of W4 web corrosion pattern for beams with a diaphragm - MassDOT

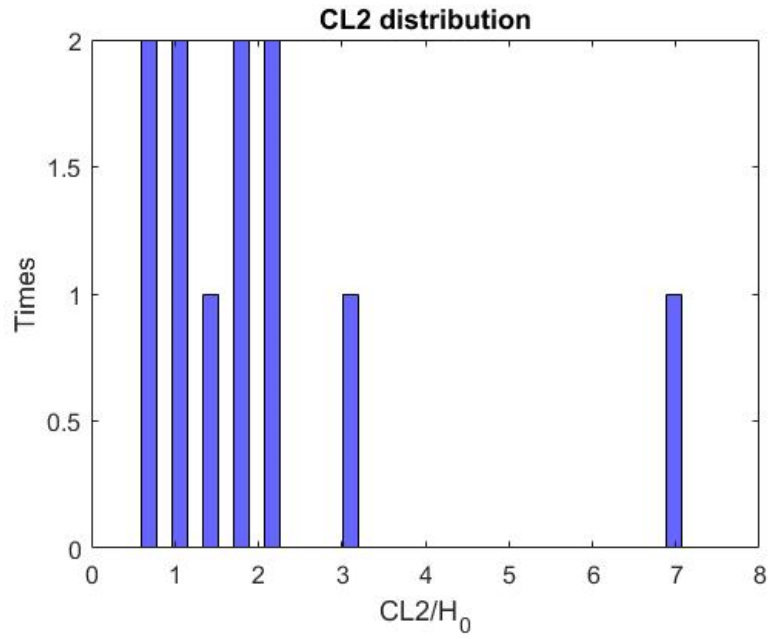


Figure 340: CL2 distribution of W4 web corrosion pattern for beams with a diaphragm - MassDOT

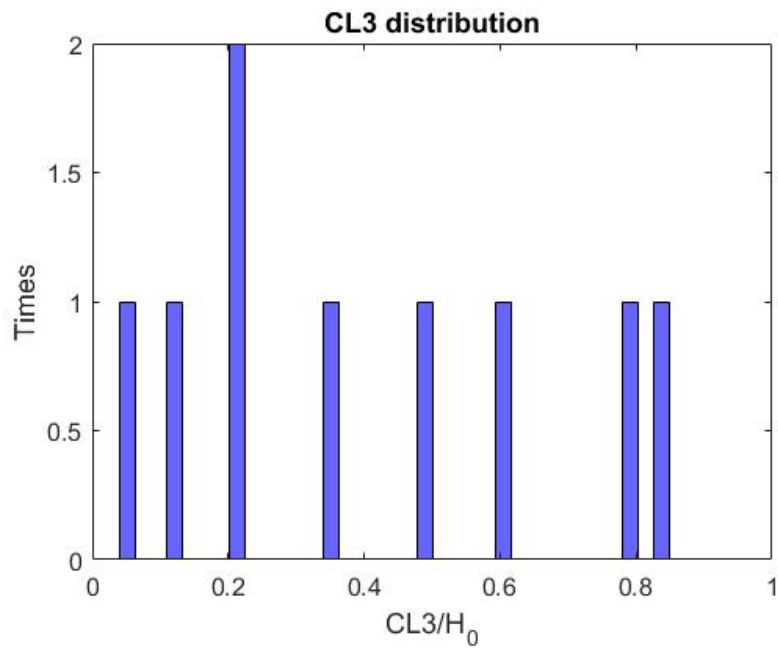


Figure 341: CL3 distribution of W4 web corrosion pattern for beams with a diaphragm - MassDOT

Like in W3 patterns there are observed two trends a) full height corrosion and b) up to 40%H₀. For full height corrosion:

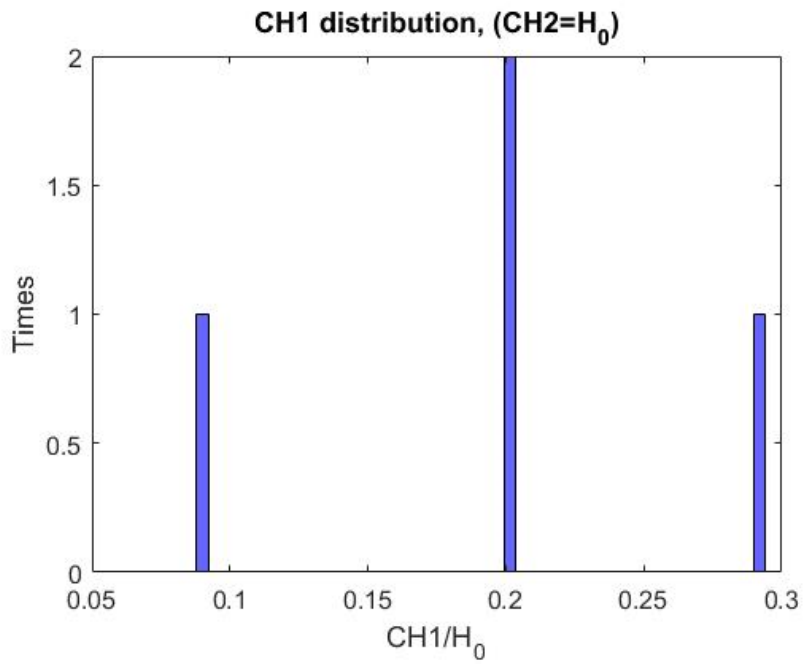


Figure 342: CH1 distribution of W4 web corrosion pattern with full height corrosion for beams with a diaphragm - MassDOT

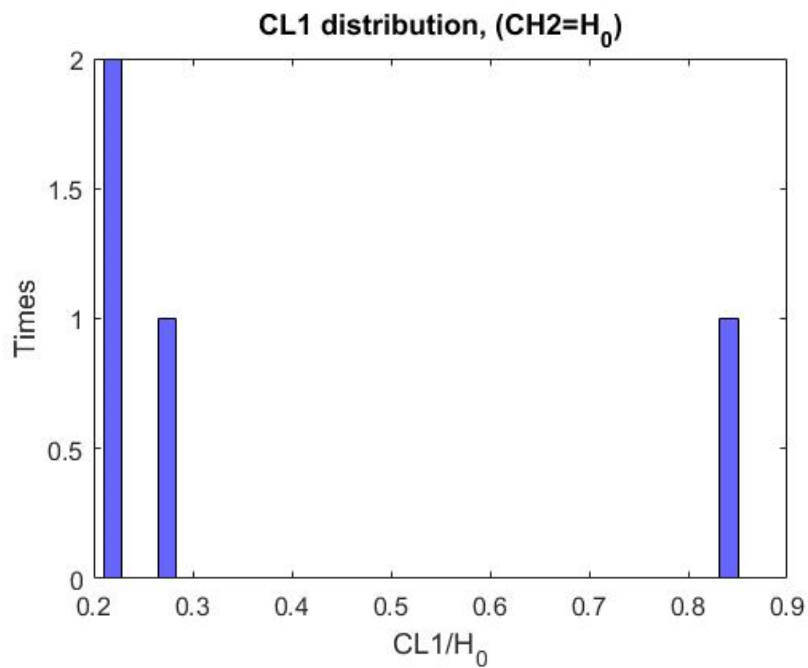


Figure 343: CL1 distribution of W4 web corrosion pattern with full height corrosion for beams with a diaphragm - MassDOT

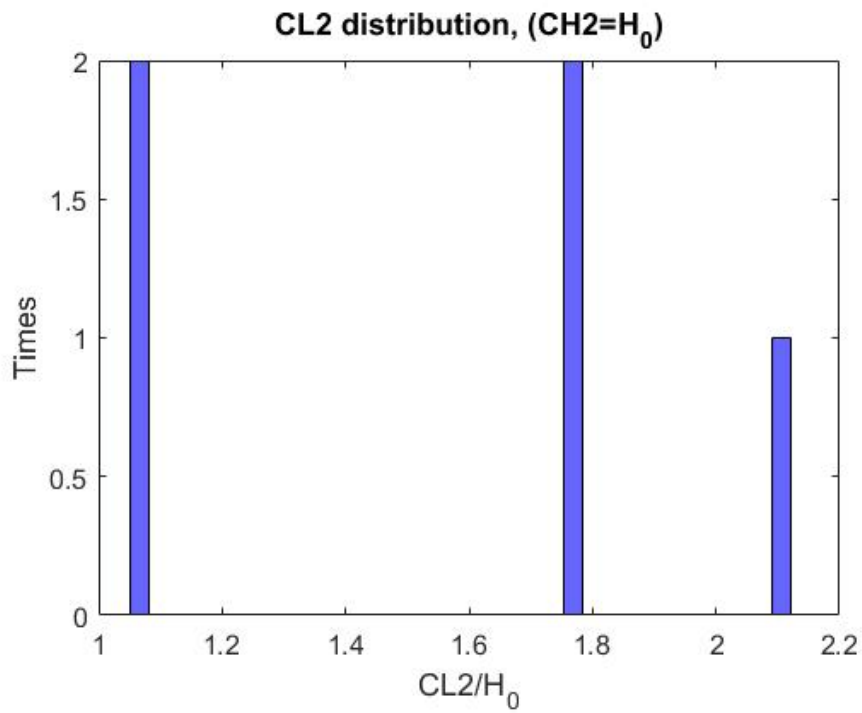


Figure 344: CL2 distribution of W4 web corrosion pattern with full height corrosion for beams with a diaphragm - MassDOT

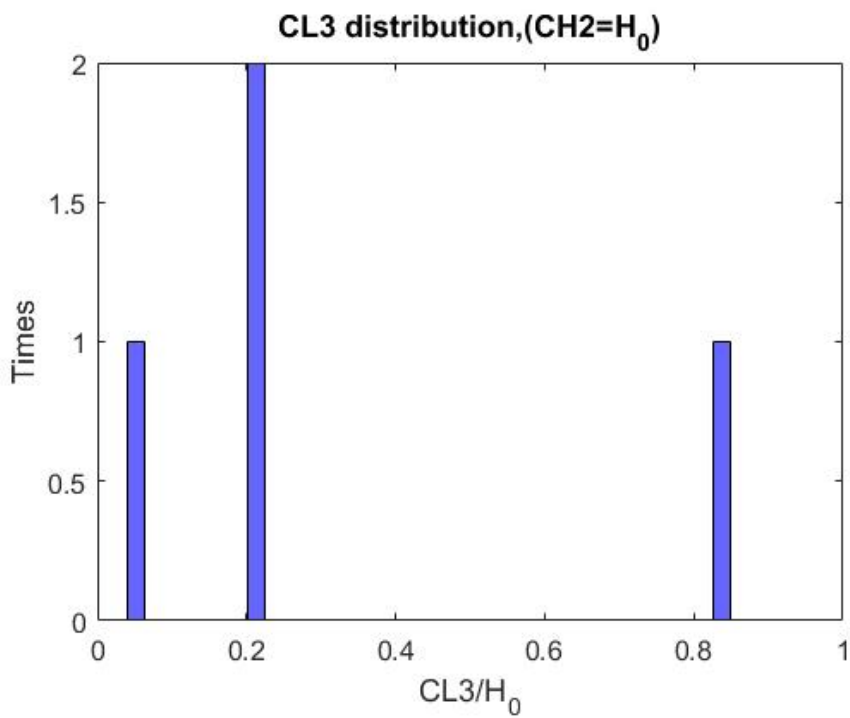


Figure 345: CL3 distribution of W4 web corrosion pattern with full height corrosion for beams with a diaphragm - MassDOT

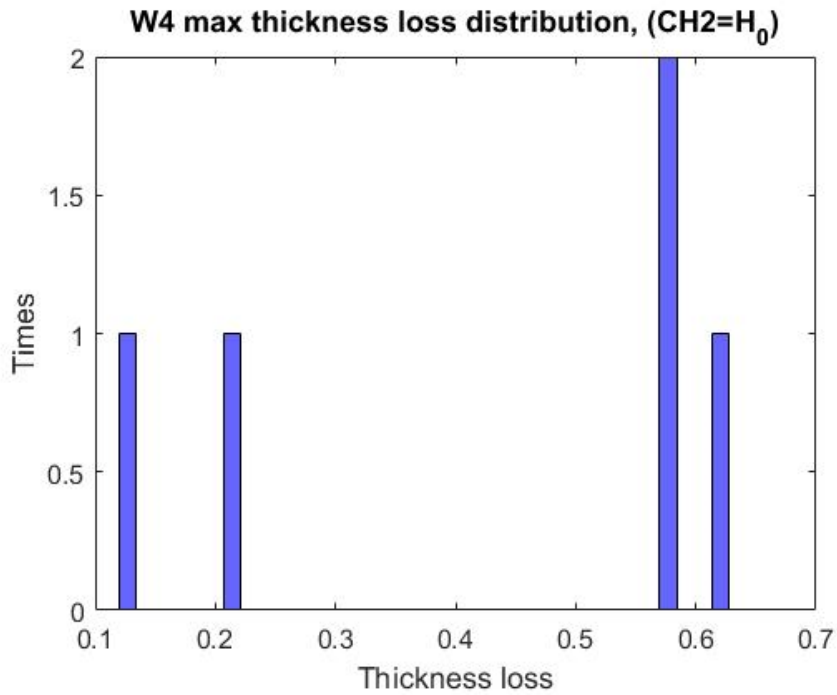


Figure 346: Max web thickness loss distribution of W4 web corrosion pattern with full height corrosion for beams with a diaphragm - MassDOT

Given that the sample of data is small:

$$0.2H_0 < CL_1 < 0.8H_0$$

$$1H_0 \leq CL_2 \leq 2.1H_0$$

$$0.2H_0 < CL_3 < 0.8H_0$$

$$0.1H_0 < CH_1 \leq 0.3H_0$$

$\frac{t_{loss}}{t_{web}}$ takes values of {0.1,0.2,0.6}

the extreme scenario:

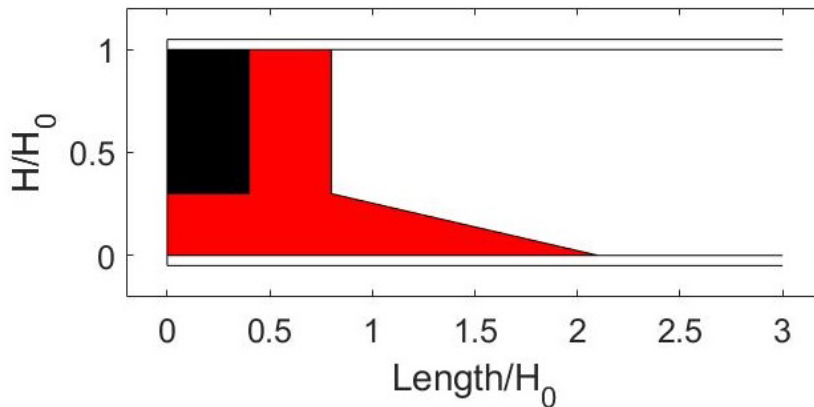


Figure 347: First extreme W4 web corrosion scenario for beams with a diaphragm - MassDOT

Even when considering the small sample, the W4 corrosion pattern with full height corrosion seems to follow the corresponding W3 corrosion pattern.

For $CH_2 \leq 0.4H_0$

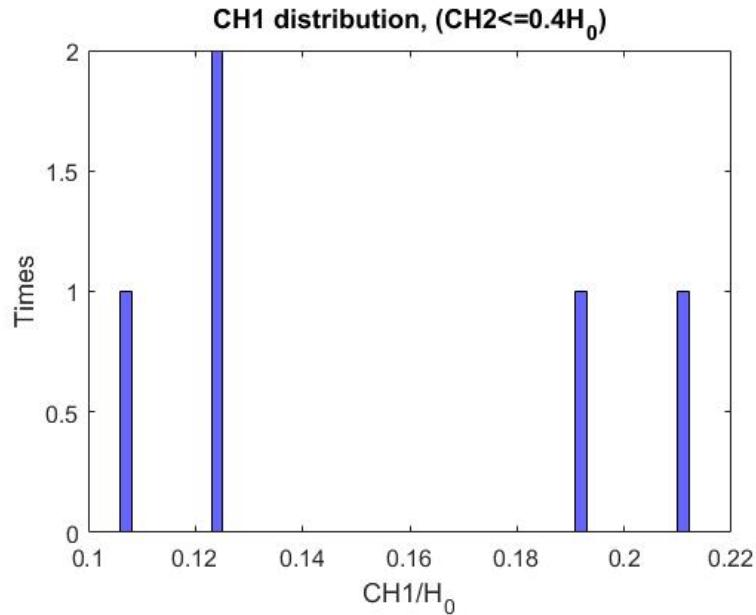


Figure 348: CH1 distribution of W4 web corrosion pattern, with corrosion height up to 40% of H_0 , for beams with a diaphragm - MassDOT

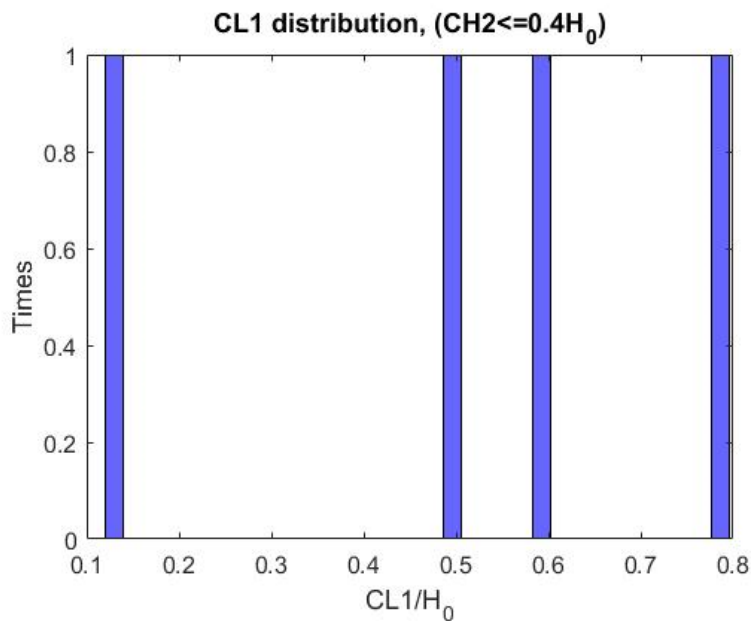


Figure 349: CL1 distribution of W4 web corrosion pattern, with corrosion height up to 40% of H_0 , for beams with a diaphragm - MassDOT

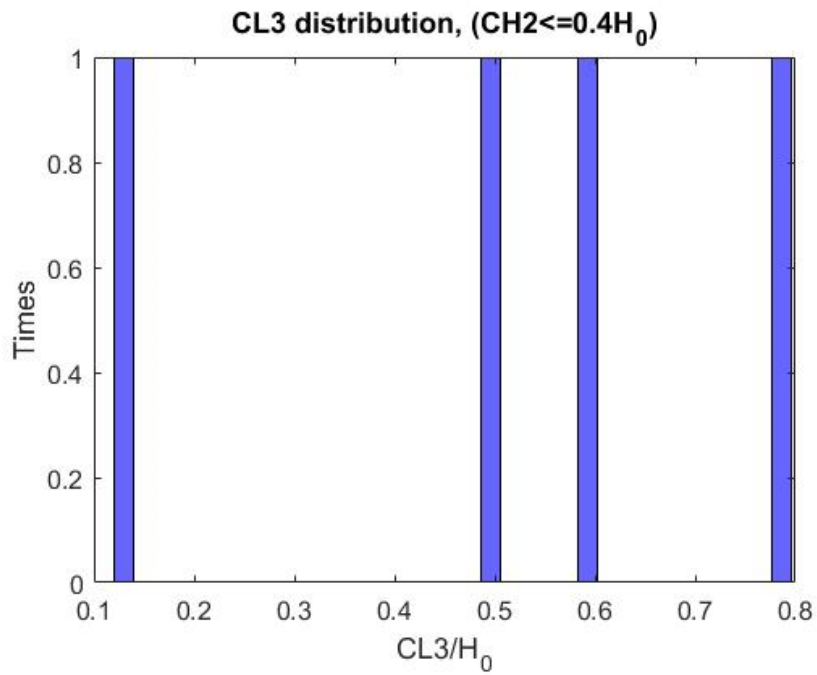


Figure 350: CL3 distribution of W4 web corrosion pattern, with corrosion height up to 40% of H₀, for beams with a diaphragm - MassDOT

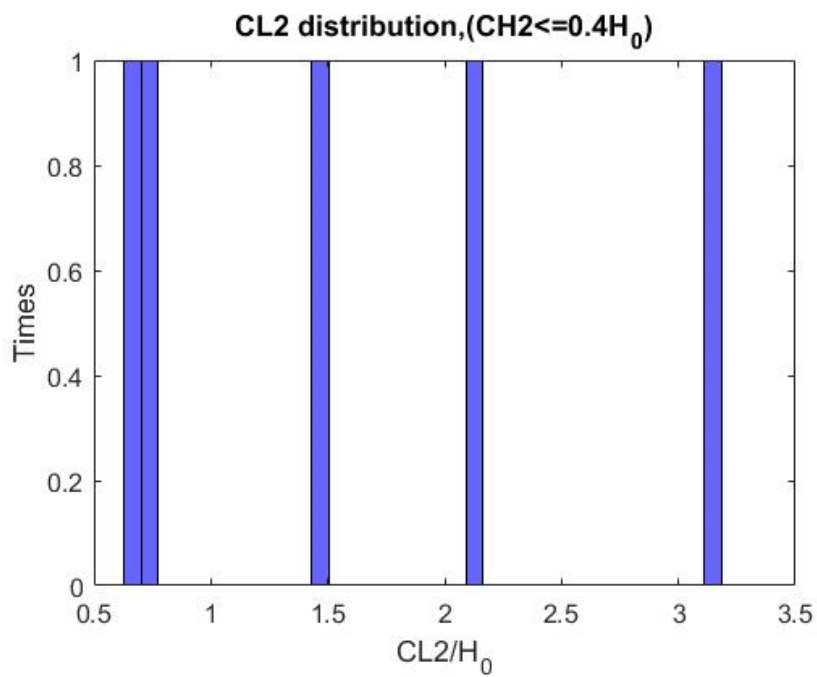


Figure 351: CL2 distribution of W4 web corrosion pattern, with corrosion height up to 40% of H₀, for beams with a diaphragm - MassDOT

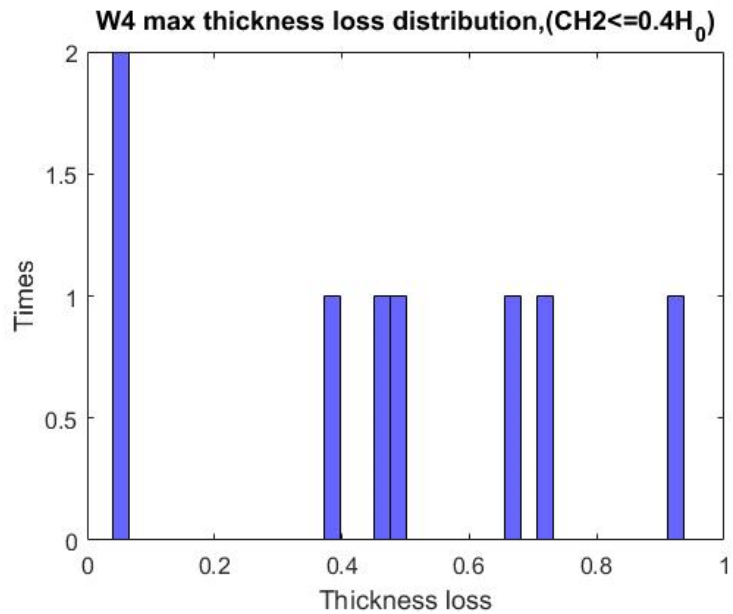


Figure 352: Max web thickness loss distribution of W4 web corrosion pattern, with corrosion height up to 40% of H_0 , for beams with a diaphragm - MassDOT

$$0.1H_0 < CL_1 \leq 0.8H_0$$

$$0.6H_0 < CL_2 \leq 3.1H_0$$

$$0.1H_0 < CL_3 \leq 0.8H_0$$

$$0.1H_0 < CH_1 \leq 0.2H_0$$

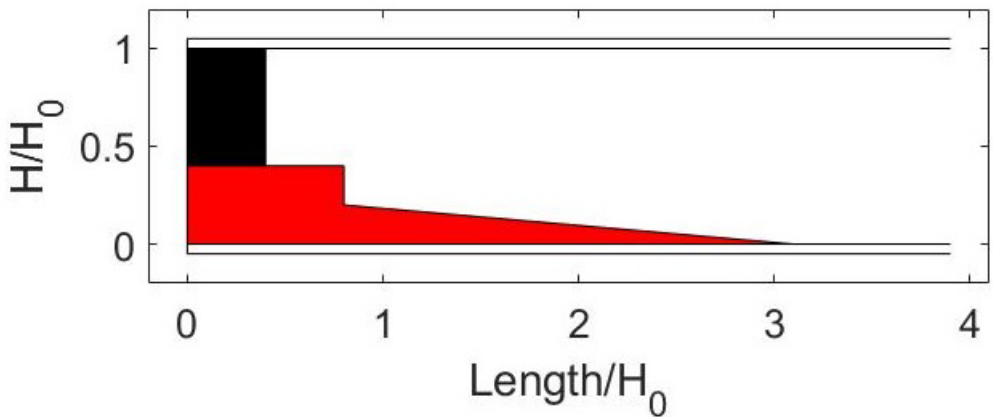


Figure 353: Second extreme W4 web corrosion scenario for beams with a diaphragm - MassDOT

Upon inspection, the W3 corrosion pattern seems to follow the corresponding W4 corrosion pattern.

12.2.5.2. Holes

The M1 corrosion hole pattern is found only once, and it presents itself as pit hole (0.0044*0.0044). The M2 hole corrosion pattern is combined with the W3 M2 pattern combination.

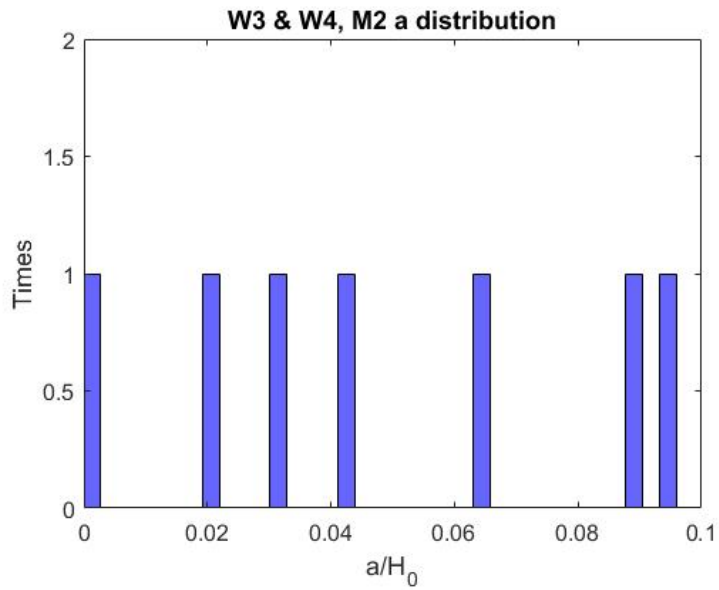


Figure 354: M2 web hole's pattern height distribution of W3 and W4 web corrosion pattern for beams with a diaphragm - MassDOT

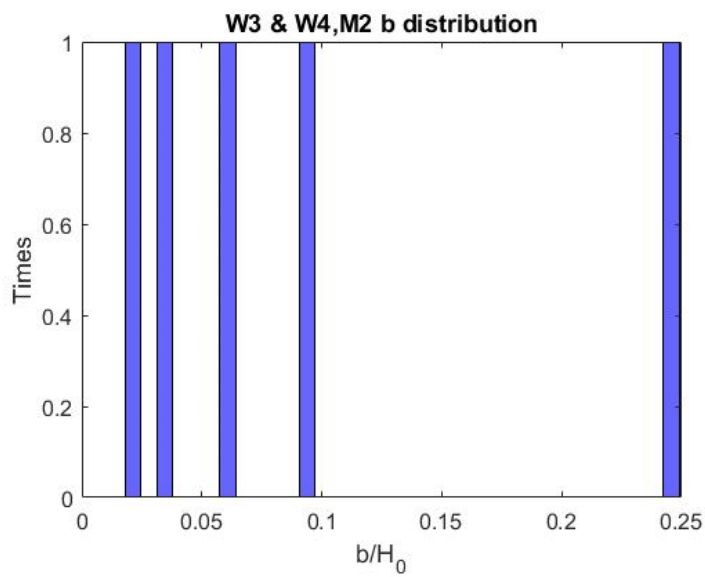


Figure 355: M2 web hole's pattern length distribution of W3 and W4 web corrosion pattern for beams with a diaphragm - MassDOT

The worst-case scenario for the M2 hole corrosion pattern was projected on an extreme W4 corrosion pattern with the following parameters: $a=0.1$ $b=0.25$

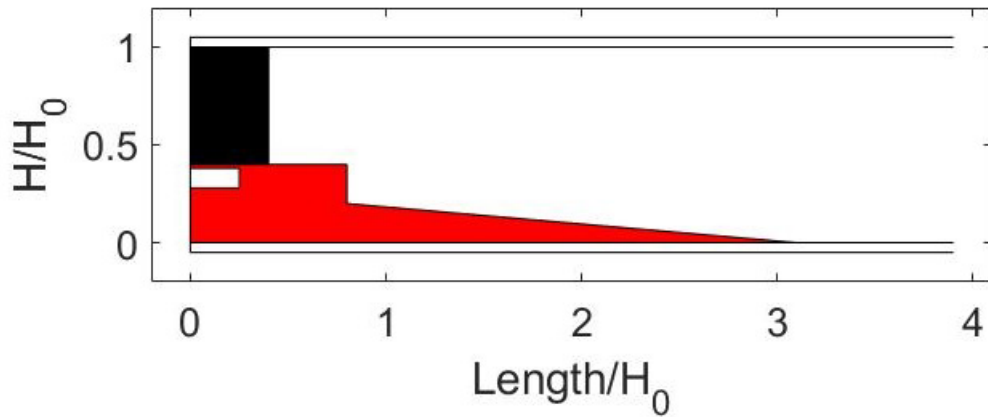


Figure 356: Extreme M2 hole pattern scenario projected on second extreme W4 web corrosion scenario for beams with a diaphragm - MassDOT

12.2.6. Pattern W5

The parameters for the corrosion patterns can be found with corresponding diagrams in Section 1.5 *Corrosion Patterns* of this report.

12.2.6.1. Web Corrosion

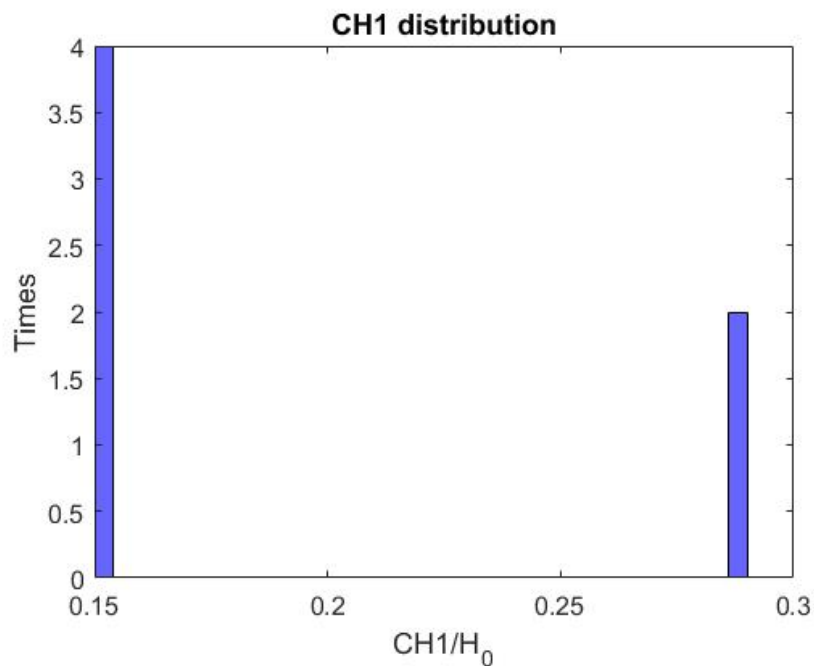


Figure 357. CH1 distribution of W5 web corrosion pattern for beams with a diaphragm - MassDOT

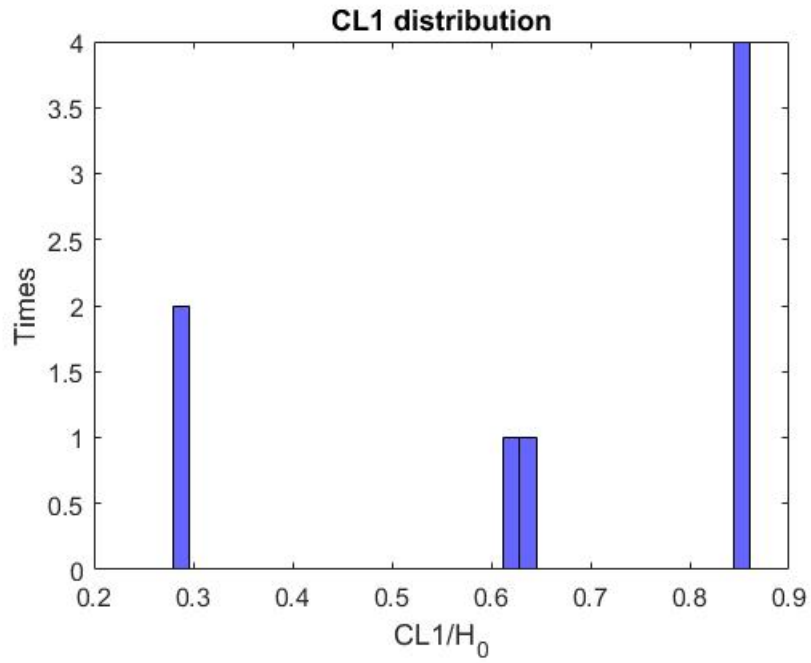


Figure 358: CL1 distribution of W4 web corrosion pattern for beams with a diaphragm - MassDOT

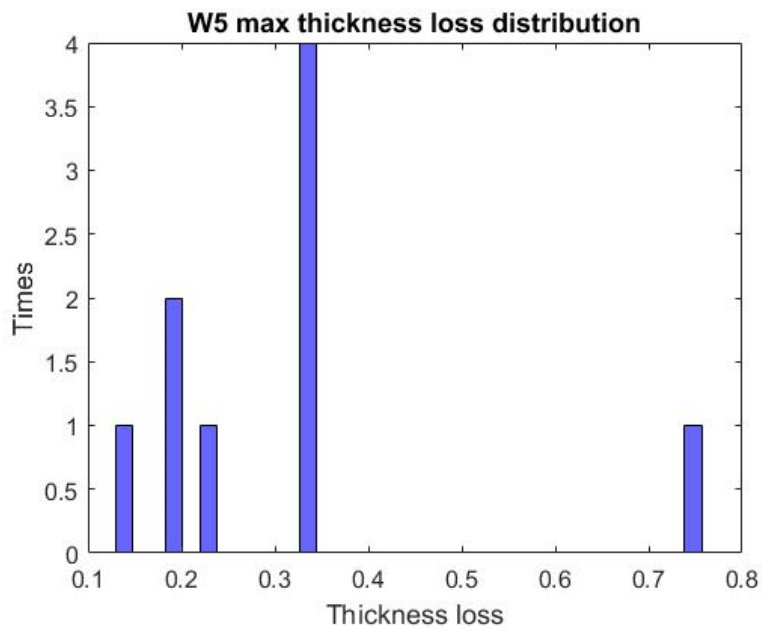


Figure 359: Max web thickness loss distribution of W5 web corrosion pattern for beams with a diaphragm - MassDOT

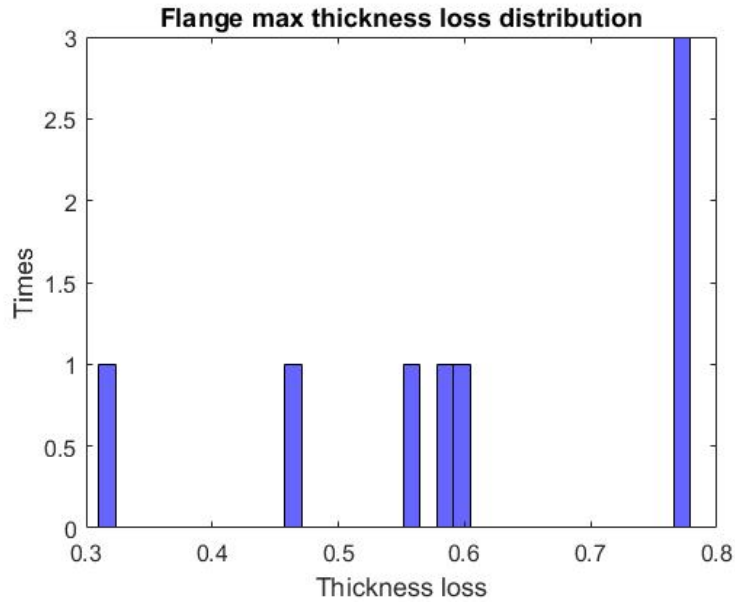


Figure 360: Max flange thickness loss of beams with W5 web corrosion pattern for beams with a diaphragm - MassDOT

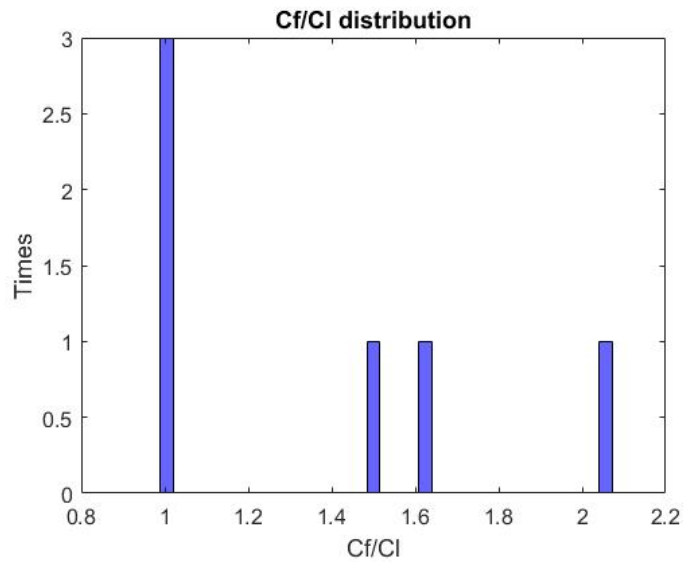


Figure 361: Ratio of flange to web corrosion length distribution, of W5 web corrosion pattern for beams with a diaphragm - MassDOT

$$0.3H_0 \leq CL_1 \leq 0.85H_0$$

$$0.15H_0 < CH_1 \leq 0.30H_0$$

$$\frac{t_{loss}}{t_{web}} \text{ takes the value of } \{0.35\}$$

$$\frac{t_{loss}}{t_{flange}} \text{ takes the values of } \{0.3, 0.6, 0.8\} \text{ with } \frac{C_f}{C_l} \text{ taking the values of } \{1, 1.6\}$$

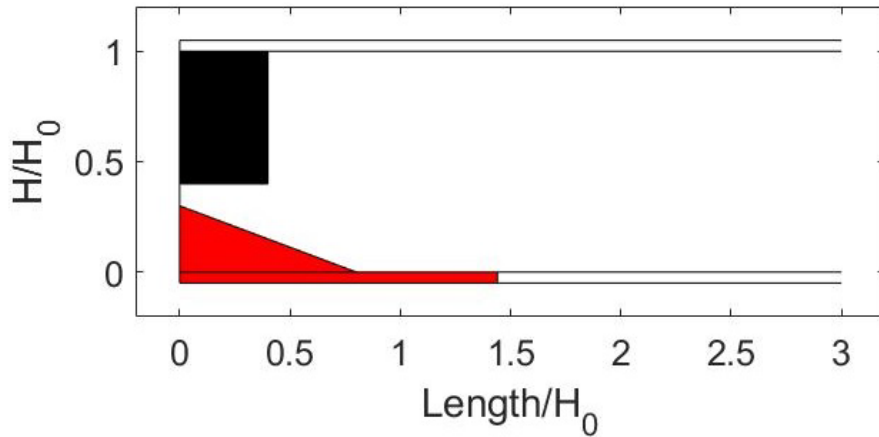


Figure 362: Extreme W5 web corrosion scenario for beams with a diaphragm - MassDOT

12.3. Rhode Island

12.3.1. Introduction

As discussed in the previous sections, the data was divided into two groups: (i) beams without diaphragm and (ii) beams with diaphragm. Additionally, due to significantly differences in the amount of data provided by each state, the results are also divided into groupings by state. Therefore, in this section only beam ends with diaphragms from Rhode Island are considered.

Figure 363 depicts the frequency of corrosion patterns for beam ends with a diaphragm system from Rhode Island. This also means that the graph denotes the total amount of times each pattern appears in the reports.

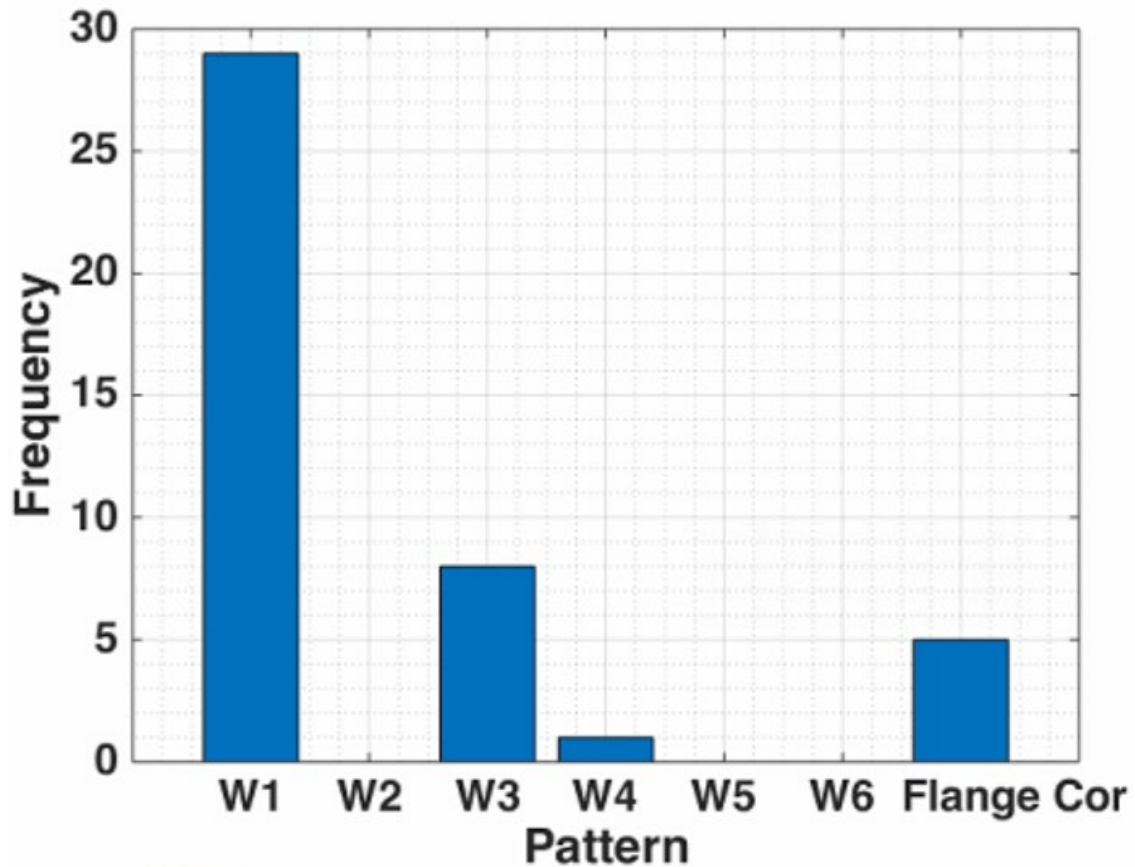


Figure 363: Web corrosion patterns distribution for beams ends with a diaphragm – RIDOT

It is imperative to note that the parameters defined for each corrosion pattern (CH1, CH2, CH3, CL1, CL2, CL3) have been normalized by the web height, H0, defined as $H_0 = H - 2t_f$.

12.3.2. Pattern W1

12.3.2.1. Web corrosion

Similar to the beams without a diaphragm system, the study of trends in the data began with the analysis for the distribution of the total height of corrosion. The parameters for the corrosion patterns can be found with corresponding diagrams in Section 1.5 *Corrosion Patterns* of this report. This resulted in the data presented in Figure 364, which depicts the histogram of CH1 combined with pattern W1. This was obtained from the bridge inspection reports provided by RIDOT.

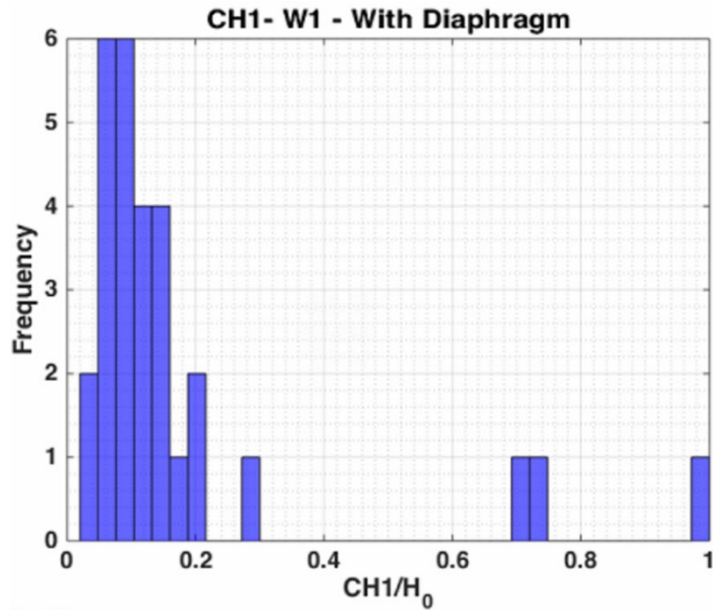


Figure 364: CH1 distribution for beams with diaphragm and W1 corrosion pattern – RIDOT

Figure 364 clearly depicts that $0 < CH_1 \leq 0.2H_0$. With the goal of understanding the relationship between the other parameters of corrosion and the corrosion height, our team had to analyze the behavior of the other parameters given that $CH_1 < 0.2H_0$. Figure 365 and Figure 366 depict the length of corrosion and the web thickness loss for this case.

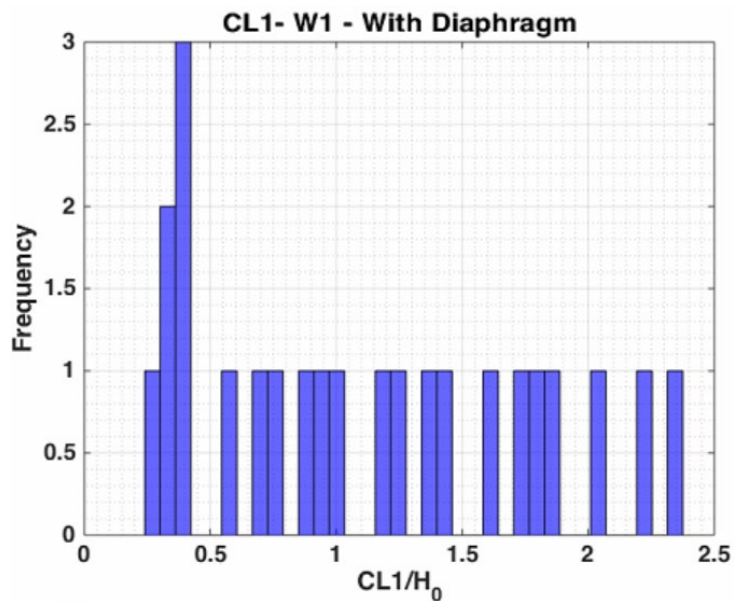


Figure 365: CL1 distribution for beams with diaphragm and W1 corrosion pattern – RIDOT

Although no clear trend is observed from Figure 365, the graph lead our team to state that the length can span $0.25H_0$ up to $2.5H_0$. That is, $0.25H_0 \leq CL_1 \leq 2.5H_0$.

Figure 366 depicts the distribution of web thickness loss given that $CH1 < 0.2H_0$.

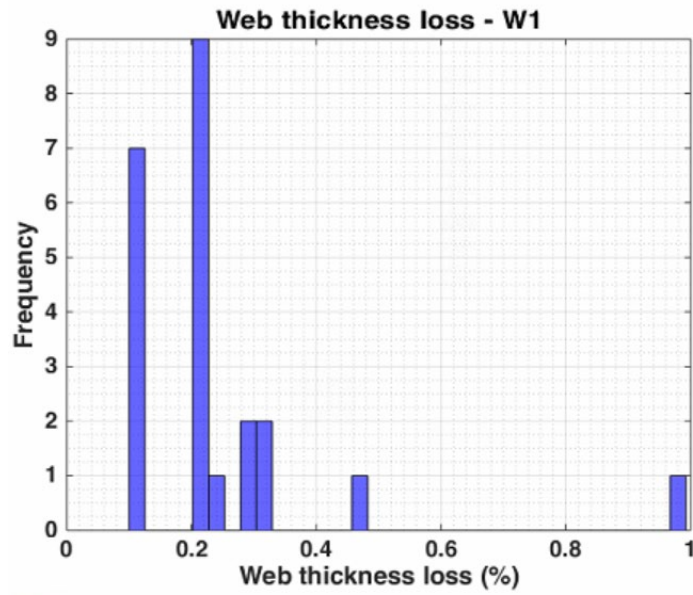


Figure 366: Web thickness loss distribution for beams with diaphragm and W1 corrosion pattern – RIDOT

From Figure 366, our team assumed that most of the beams have web thickness loss found in the following interval:

$$0.1 \leq \frac{t_{loss}}{t_{web}} \leq 0.3$$

Therefore, it is possible to define an extreme case of corrosion for beam ends with a diaphragm system, as depicted in Figure 367.

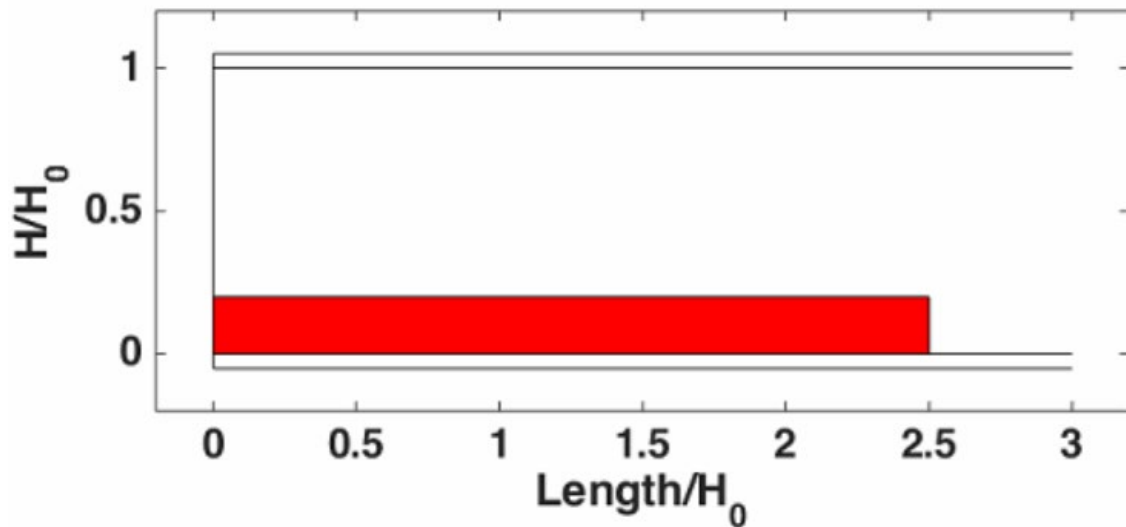


Figure 367: Extreme corrosion case of W1 pattern for beams with a diaphragm – RIDOT

Figure 368 describes the comparison between the extreme corrosion case pattern for the W1 corrosion pattern of beam ends with and without a diaphragm system.

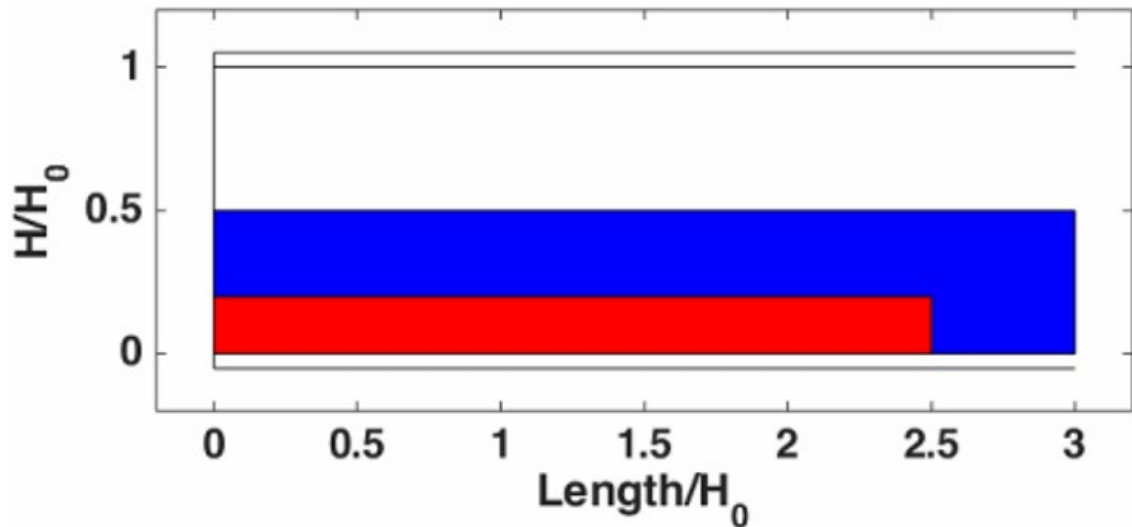


Figure 368: Comparison between extreme corrosion scenarios. Blue represents the extreme scenario for beams without diaphragm, whereas the region in red depicts extreme corrosion scenario for beams with a diaphragm – RIDOT

12.3.2.2. Flange corrosion

Only three cases of flange corrosion were recorded combined with W1 corrosion pattern for beam ends with a diaphragm system. As the amount of data was not sufficient for the research team to draw conclusions, Figure 369, Figure 370, Figure 371 depict only the statistics the research team was able to record from the bridge inspection reports.

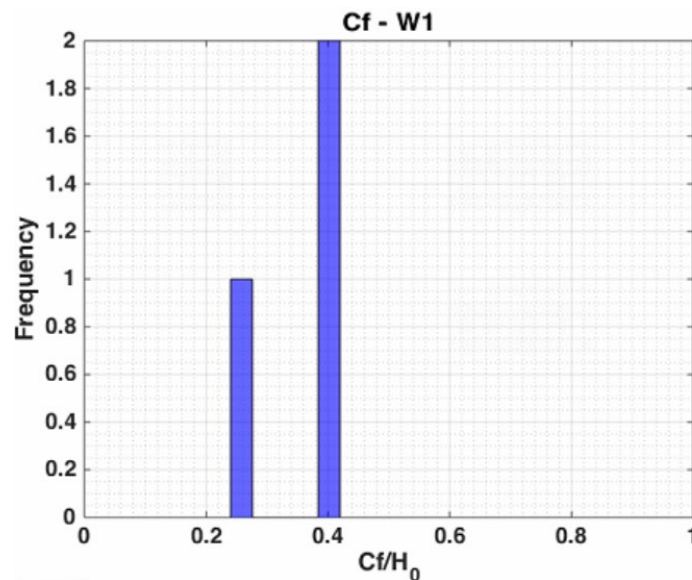


Figure 369: Flange corrosion length for beam ends with diaphragm for W1 pattern – RIDOT

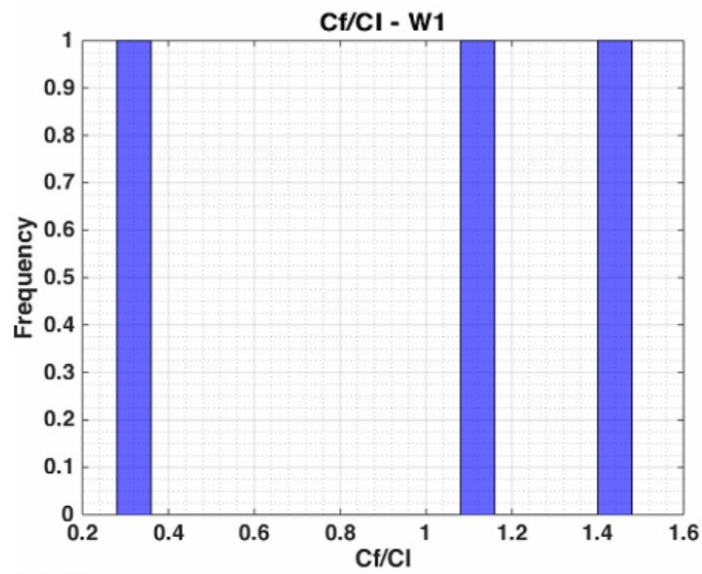


Figure 370: Ratio between flange corrosion length and web corrosion length for W1 pattern – RIDOT

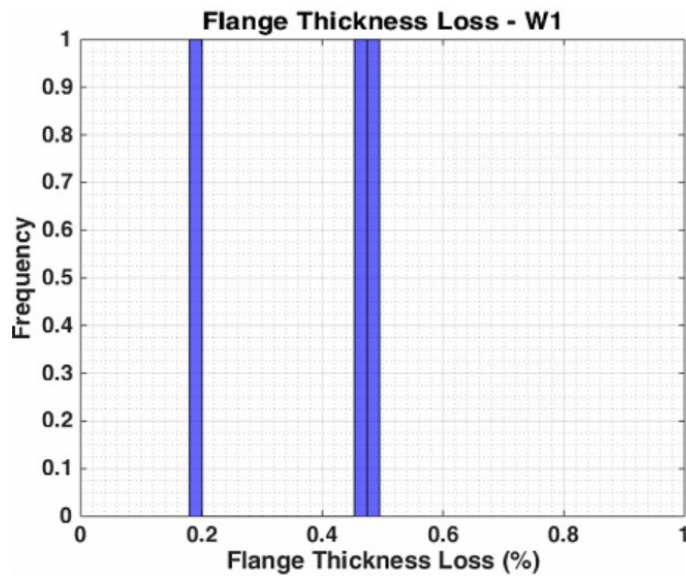


Figure 371: Flange thickness loss distribution for W1 pattern – RIDOT

12.3.2.3. Holes

Table 81 shows the occurrence of corrosion patterns and holes recorded from the bridge inspection reports provided by RIDOT.

Table 84: Holes and patterns for beams ends with diaphragm from RIDOT

	Number	No Hole	M1	M2	M3	M4	M1 and M2	M1 and M3	M2 and M4
W1	29	27	2	0	1	0	0	0	0
W2	0	0	0	0	0	0	0	0	0
W3	8	7	0	0	0	1	0	0	0
W4	1	1	0	0	0	0	0	0	0
W5	0	0	0	0	0	0	0	0	0
W6	0	0	0	0	0	0	0	0	0

As shown in Table 81, just three holes were recorded combined with the W1 corrosion pattern. Due to the small amount of available data, it was not possible to detect any trends. For this reason, Figure 372 and Figure 373 depict the dimensions of the M1 corrosion holes. Figure 374 and Figure 375 depict the dimensions of the M3 corrosion hole.

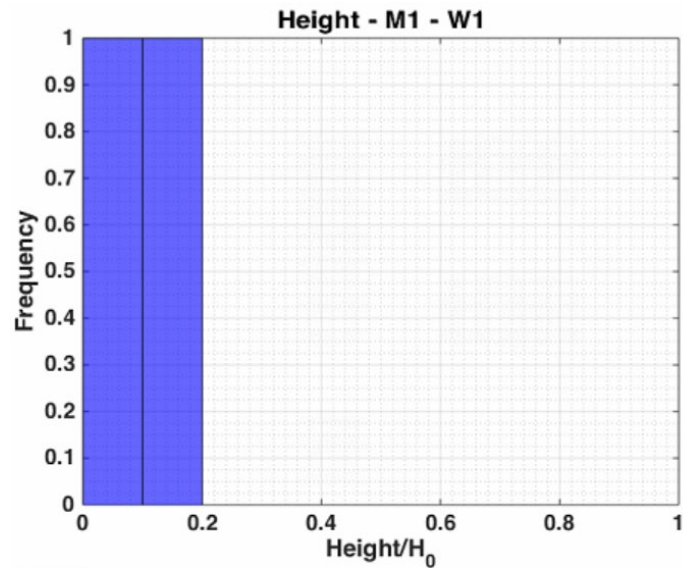


Figure 372: Height of M1 holes combined with W1 pattern – RIDOT

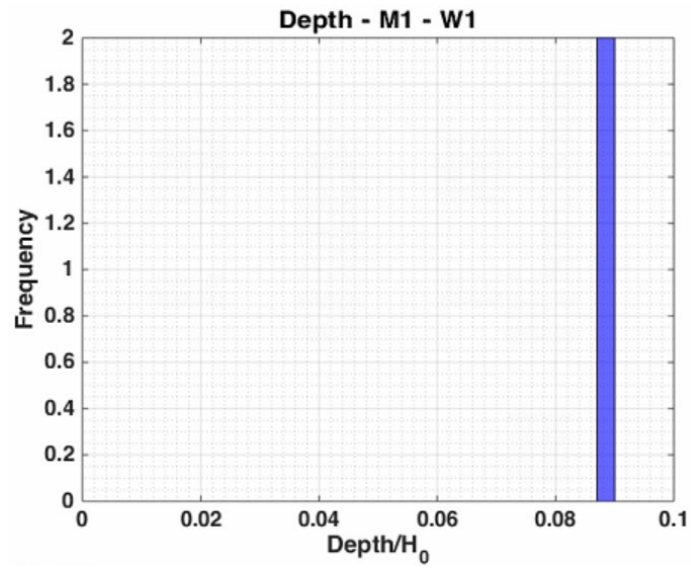


Figure 373: Depth of M1 holes combined with W1 pattern – RIDOT

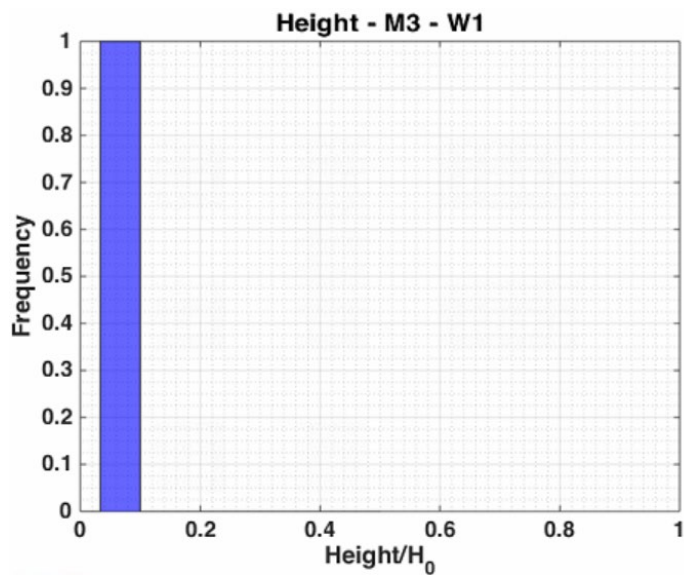


Figure 374: Height of M3 holes combined with W1 pattern – RIDOT

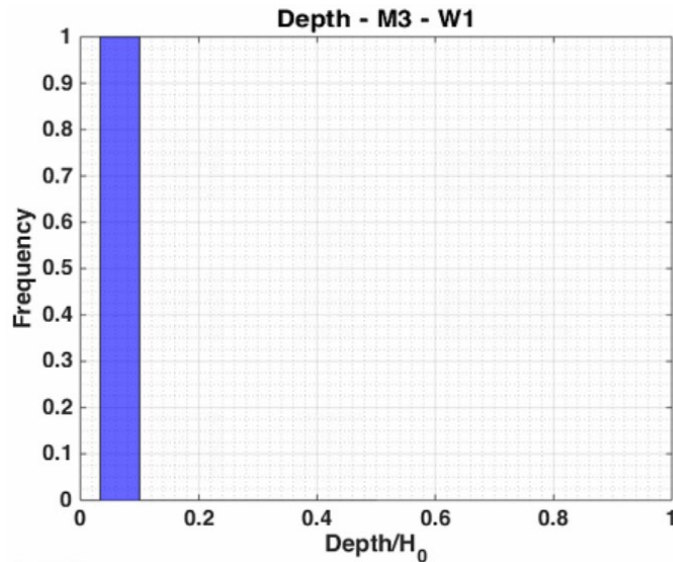


Figure 375: Depth of M3 holes combined with W1 pattern – RIDOT

12.3.3. Pattern W3

12.3.3.1. Web corrosion

Only eight cases of the W3 corrosion pattern were recorded by the research team. The parameters for the corrosion patterns can be found with corresponding diagrams in Section 1.5 *Corrosion Patterns* of this report. Similar to the other cases, the study began by analyzing the distribution of the total height of corrosion, depicted in Figure 376.

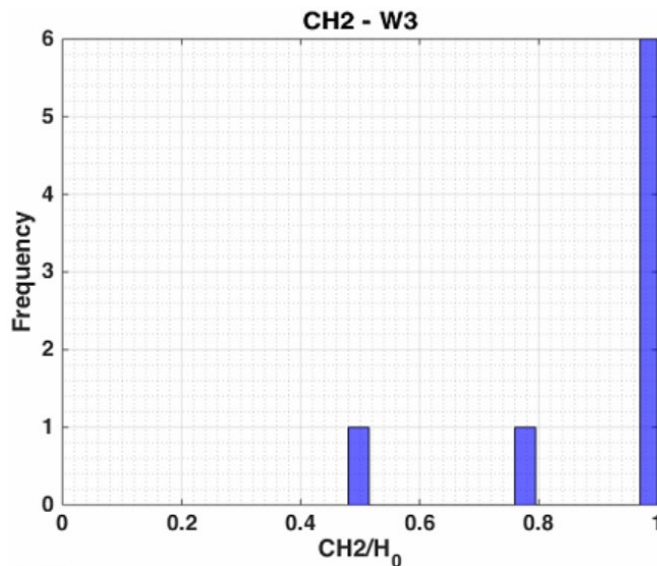


Figure 376: CH2 distribution for W3 pattern – RIDOT

Although Figure 376 clearly depicts that most of the beam ends have the height fully corroded, it was not possible to detect other major trends. The reason for that can be found in Figure 377, Figure 378, Figure 379, Figure 380 and Figure 381. These figures depict scatter among the histograms of the corrosion shape parameters. This limited our team in being able to detect trends in the corrosion data.

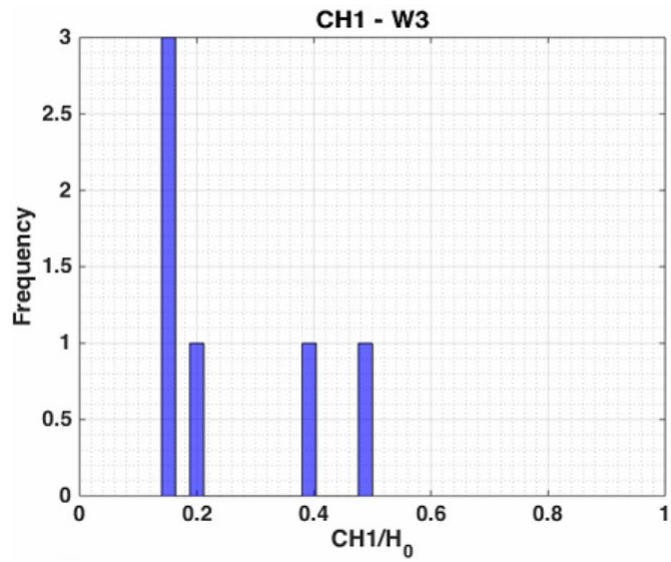


Figure 377: CH1 distribution for W3 pattern – RIDOT

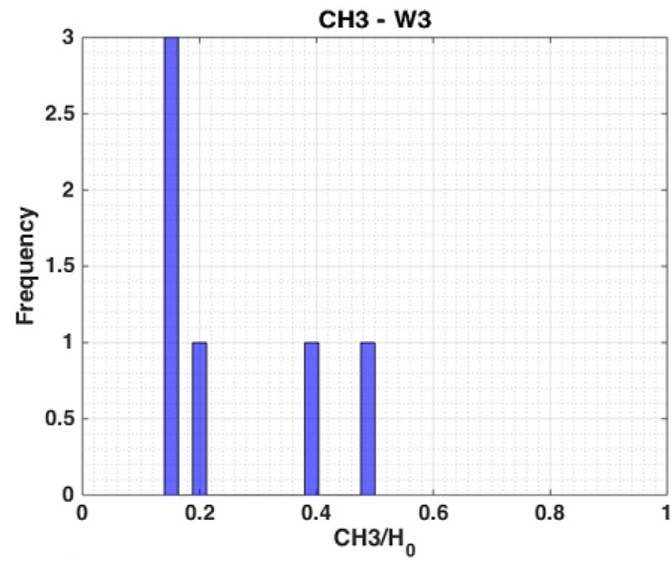


Figure 378: CH3 distribution for W3 pattern – RIDOT

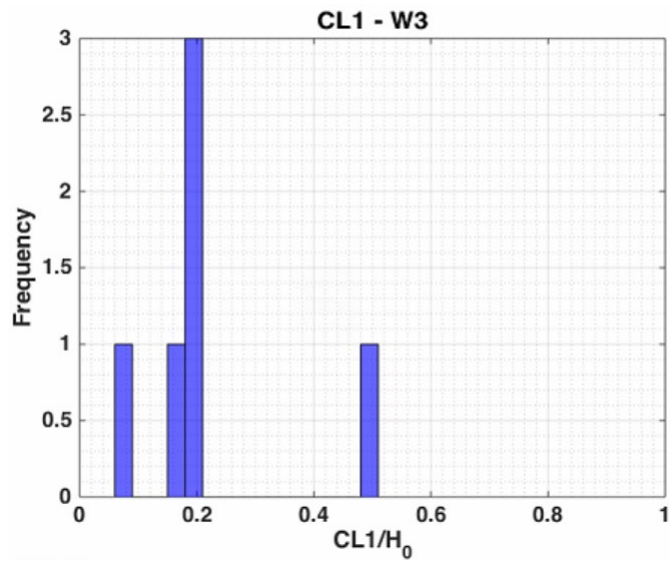


Figure 379: CL1 distribution for W3 pattern – RIDOT

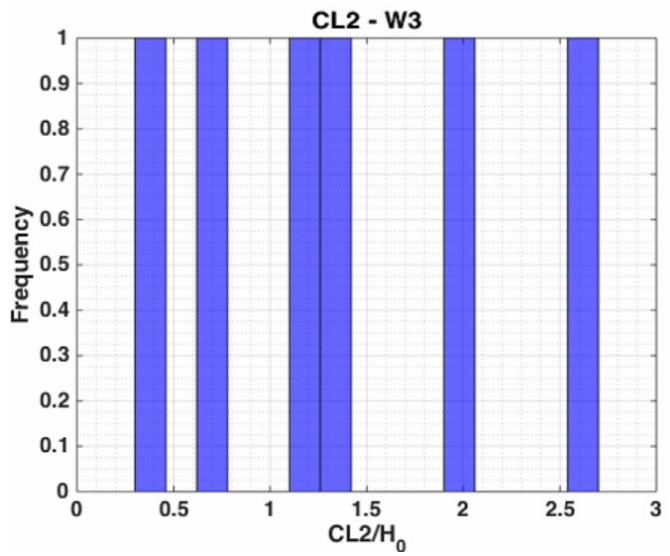


Figure 380: CL2 distribution for W3 pattern – RIDOT

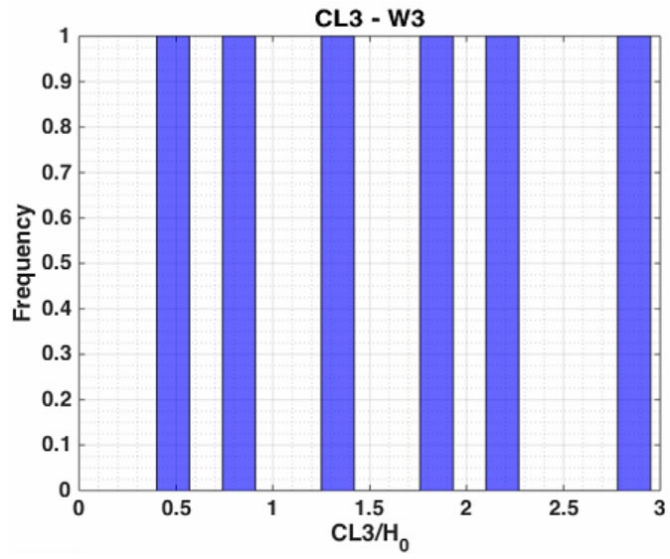


Figure 381: CL3 distribution for W3 pattern – RIDOT

Figure 382 depicts the web thickness loss for beams whose $CH_2=1H_0$.

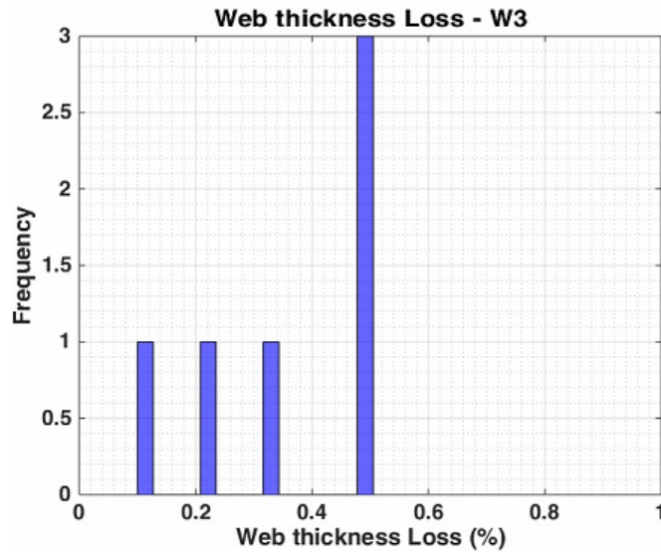


Figure 382: Web thickness loss distribution for W3 pattern – RIDOT

12.3.3.2. Flange corrosion

The research team was able to record information regarding the combination of flange corrosion and the W3 corrosion pattern for two cases. This meant that, due to the small amount of data available, the research team was not able to detect any trend in the data. Figure 383, Figure 384 and Figure 385 depict the statistics the research team was able to obtain from the compiled data.

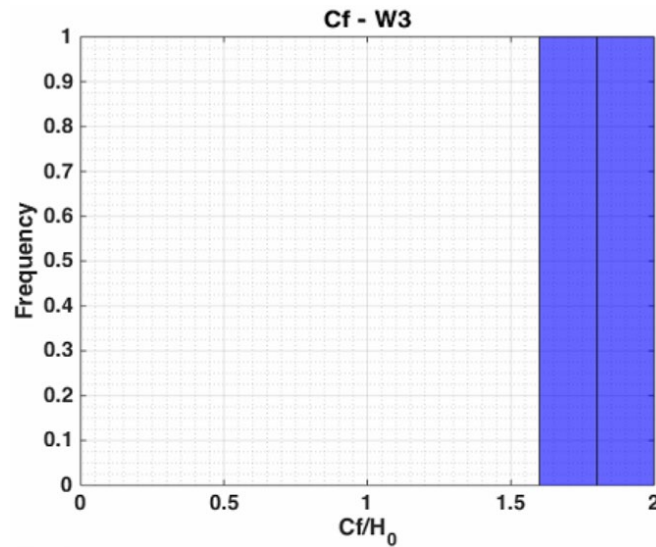


Figure 383: Flange corrosion length for W3 pattern – RIDOT

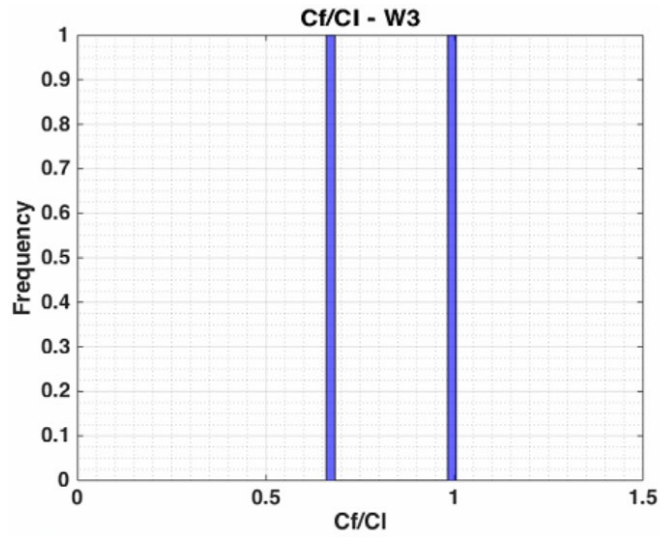


Figure 384: Ratio between flange corrosion length and web corrosion length for W3 pattern – RIDOT

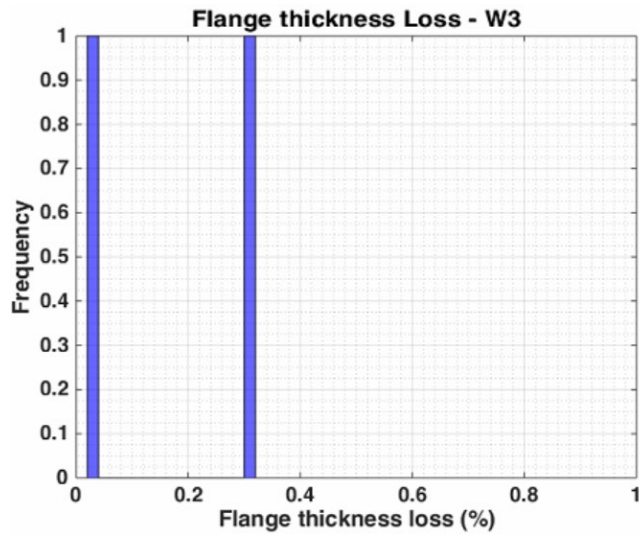


Figure 385: Flange thickness loss distribution for W3 pattern – RIDOT

12.3.3.3. Holes

Only a single hole was recorded combined with the W3 corrosion pattern, as shown in Table 56. This one hole does not constitute enough data for depicting trends. For this reason, the research team was not able to draw any conclusion. Finally, Table 57 shows the dimensions of the M4 corrosion hole normalized by H0.

Table 85: Dimensions of M4 hole combined with W3 pattern – RIDOT

Hole topology	Length	Deep	Distance from the end of the beam
M4	6%	3%	42%

13. References

1. “Bridges.” *ASCE's 2017 Infrastructure Report Card*, American Society of Civil Engineers, 2020, www.infrastructurereportcard.org/cat-item/bridges/. Accessed May 5, 2021.
2. Sugimoto, I., Kobayashi, Y., Ichikawa, A. (2006). Durability evaluation based on buckling characteristics of corroded steel deck girders. *QR of RTPI*, 47(3).
3. Roberts, T.M. (1981). Slender plate girders subjected to edge loading. *Proceedings of the Institution of Civil Engineers Part B*, 71:805-819.
4. Johansson, B., Lagerqvist, O. (1995). Resistance of plate edges to concentrated forces. *Journal of Constructional Steel Research*, 32:69-105.
5. Roberts, T.M., Shahabian, F. (2001). Ultimate resistance of slender web panels to combined bending shear and patch loading. *Journal of Constructional Steel Research*, 57:779-790.
6. Chacón, R., Mirambell, E., Real, E. (2009). Influence of designer-assumed initial conditions on the numerical modelling of steel plate girders subjected to patch loading, *Thin-Walled Structures*, 47: 391-402.
7. Hajdin, N., Markovic, N. (2012). Failure mechanism for longitudinally stiffed I girders subjected to patch loading. *Archive of Applied Mechanics*, 82:1377-1391.
8. Salkar, R., Salkar, A., Davids W. (2015). Crippling of webs with partial-depth stiffeners under patch loading. *Engineering Journal*, 221-231.
9. Kayser, J.R., Nowak, A.S. (1989). Capacity loss due to corrosion in steel-girder bridges. *Journal of Structural Engineering*, 115(6):1525-1537.
10. van de Lindt, J.W., Pei, S. (2006). Buckling reliability of deteriorating steel beam ends. *Electronic Journal of Structural Engineering*, 6.
11. Liu, C., Miyashita, T., Nagai, M. (2011). Analytical study on shear capacity of steel I-girders with local corrosion nearby supports. *Procedia Engineering*, 14:2276-2284.
12. Ahn, J.H., Kainuma, S., Kim, I.T. (2013). Shear failure behaviors of a web panel with local corrosion depending on web boundary conditions. *Thin-Walled Structures*, 73:302-317.
13. Ahn, J.H., Kainuma, S., Yasuo, F., Takehiro, I. (2013). Repair method and residual bearing strength evaluation of a locally corroded plate girder at support. *Engineering Failure Analysis*, 33:398-418.
14. Ahn, J.H., Kim, I.T., Kainuma, S., Lee, M.J. (2013). Residual shear strength of steel plate girder due to web local corrosion. *Journal of Constructional Steel Research*, 89:198-212.
15. Kim, I.T., Lee, M.J., Ahn, J.H., Kainuma, S. (2013). Experimental evaluation of shear buckling behaviors and strength of locally corroded web. *Journal of Constructional Steel Research*, 83:75-89.
16. Usukura, M., Yamaguchi, T., Suzuki, Y., Mitsugi, Y. (2013). Strength evaluation for a corroded damaged steel girder end considering its collapse mechanism. *Proceedings of the 13th East Asia-Pacific Conference on Structural Engineering and Construction (EASEC)*, Sapporo, Japan.
17. Yamaguchi, T., Akagi, T. (2013). Degradation of load-carrying capacity of steel I-girders and due to corrosion. *Proceedings of the 13th East Asia-Pacific Conference on Structural Engineering and Construction (EASEC)*, Sapporo, Japan.

18. Khurram, N., Sasaki, E., Katsuchi, H., Yamada, H. (2014). Experimental and numerical evaluation of bearing capacity of steel plate girder affected by end panel corrosion. *International Journal of Steel Structures*, 14(3):659-676.
19. Gheitasi, A., Harris, D. (2015). Redundancy and operational safety of composite stringer bridges with deteriorated girders. *Journal of Performance of Constructed Facilities*.
20. Miyashita, T., Nagai, M., Wakabayashi, D., Hidekuma, Y., Kobayashi, A., Okuyama, Y., Koide, N., Horimoto, W. (2015). Repair method for corroded steel girder ends using CFRP sheet. *IABSE-JSCE Joint Conference on Advances in Bridge Engineering-III*, Dhaka, Bangladesh.
21. Ogami, H., Fujii, K., Yamada, T., Iwasaki H. (2015). Renovation of corroded girder end in plate girder bridge with resin and rebars. *Implementing Innovative Ideas in Structural Engineering and Project Management*.
22. Zmetra, K.M., McMullen, K.F., Zaghi, A.E., Wille, K. (2017). Experimental study of UHPC repair for corrosion-damaged steel girder ends. *Journal of Bridge Engineering*, 22(8).
23. McGovern, J. B., Randall, E.A. Connecticut Department of Transportation: Bridge Inspection Manual, 2001, https://portal.ct.gov/-/media/DOT/documents/dpublications/inspection_manual_2019-11-15rev.pdf. Accessed March 15, 2021.
24. FHWA, U. (1995). Recording and coding guide for the structure inventory and appraisal of the nation's bridges. *Recording and coding guide for the structure inventory and appraisal of the nation's bridges*. US Department of Transportation, Bridge Management Branch, FHWA, Washington, DC.
25. NHDOT Bridge Inspection Manual, 2017, <https://www.nh.gov/dot/org/projectdevelopment/bridgedesign/documents/NHDOTBridgeInspectionManual.pdf>. Accessed March 30, 2021
26. RIDOT Bridge Inspection Manual, 2013, http://www.dot.ri.gov/documents/doingbusiness/RIDOT_Bridge_Inspection_Manual.pdf. Accessed March 30, 2021
27. VTrans Inspection Manual, 1997, http://vtransmaps.vermont.gov/Maps/Publications/Maps/Inventory/BC_inspection/VTransInspectionManual.pdf. Accessed March 30, 2021
28. Tzortzinis, Georgios, et al. Massachusetts Department of Transportation Office of Transportation Planning, 2019, *Development of Load Rating Procedures for Deteriorated Steel Beam Ends*, www.mass.gov/files/documents/2019/11/13/BeamEndsFinalReportOct_2019.pdf. Accessed May 7, 2021.
29. Georgios Tzortzinis, Chengbo Ai, Sergio F. Breña, Simos Gerasimidis, Using 3D laser scanning for estimating the capacity of corroded steel bridge girders: Experiments, computations and analytical solutions, *Engineering Structures*, Volume 265, 2022, 114407, ISSN 0141-0296, <https://doi.org/10.1016/j.engstruct.2022.114407>.
30. *AASHTO LRFD Bridge Design Specifications*. (2017a). American Association of State Highway and Transportation Officials.
31. MaineDOT. (2015). *MaineDOT Load Rating Guide*.
32. Casas, J. R., Frangopol, D. M., Turmo, J., Tzortzinis, G., Ai, C., Breña, S., & Gerasimidis, S. (2022). From point clouds to capacity assessment of corroded steel bridges. In *Bridge safety, maintenance, management, life-cycle, resilience and Sustainability Proceedings of the eleventh international conference on*

- bridge maintenance, Safety and Management (IABMAS 2022), Barcelona, Spain, July 11-15, 2022* (pp. 863–870). essay, CRC Press, Taylor & Francis Group.
33. Gerasimidis, S., Breña, S., & Tzortzinis, G. (2021). (tech.). *Improved Load Rating Procedures for Deteriorated Steel Beam Ends with Deteriorated Stiffeners* (Final Report September 2021 [May 2019-September 2021]). Massachusetts Department of Transportation.
 34. Tzortzinis, G., Breña, S. F., & Gerasimidis, S. (2022). Experimental testing, computational analysis and analytical formulation for the remaining capacity assessment of bridge plate girders with naturally corroded ends. *Engineering Structures*, 252, 113488. <https://doi.org/10.1016/j.engstruct.2021.113488>
 35. Tzortzinis, Georgios, Ai, C., Breña, S. F., & Gerasimidis, S. (2022). Using 3D laser scanning for estimating the capacity of corroded steel bridge girders: Experiments, computations and Analytical Solutions. *Engineering Structures*, 265, 114407. <https://doi.org/10.1016/j.engstruct.2022.114407>
 36. Tzortzinis, Georgios, Gerasimidis, S., Breña, S., & Knickle, B. (2019). *Development of Load Rating Procedures for Deteriorated Steel Beam Ends*.
 37. Tzortzinis, Georgios, Knickle, B. T., Bardow, A., Breña, S. F., & Gerasimidis, S. (2021a). Strength evaluation of deteriorated girder ends. I: Experimental study on naturally corroded I-beams. *Thin-Walled Structures*, 159, 107220. <https://doi.org/10.1016/j.tws.2020.107220>
 38. Tzortzinis, Georgios, Knickle, B. T., Bardow, A., Breña, S. F., & Gerasimidis, S. (2021b). Strength evaluation of deteriorated girder ends. II: Numerical study on corroded I-beams. *Thin-Walled Structures*, 159, 107216. <https://doi.org/10.1016/j.tws.2020.107216>
 39. Tzortzinis, Georgios, Knickle, B., Gerasimidis, S., Bardow, A., & Breña, S. (n.d.). Development of an analytical framework for strength assessment of corroded steel bridges. In *AISC Global Assets NSBA*.
 40. Tzortzinis, Georgios, Pryor, G., Yadav, K., Gerasimidis, S., & Breña, S. (n.d.). (tech.). *Development of Comprehensive Inspection Protocols for Deteriorated Steel Beam Ends*. Massachusetts. Dept. of Transportation. Office of Transportation Planning.
 41. Tzortzinis, Georgios, "A Comprehensive Protocol for Inspection and Assessment of Aging Steel Bridges: Experiments, Computations and 3D Laser Scanning of Field Corroded Girders" (2021). Doctoral Dissertations. 2377. <https://doi.org/10.7275/24216050>
https://scholarworks.umass.edu/dissertations_2/2377
 42. Tzortzinis, G., Knickle, B., Gerasimidis, S., Bardow, A., & Brena, S. (2019, April). Experiments and computations on steel bridge corroded beam ends. In *Proceedings of the Annual Stability Conference, Structural Stability Research Council, St. Louis, Missouri*.
 43. Tzortzinis, G., Breña, S. F., & Gerasimidis, S. (2021). *Improved Load Rating Procedures for Deteriorated Steel Beam Ends with Deteriorated Stiffeners*. MassDOT Research Rep, 21-024.
 44. Tzortzinis, G., Knickle, B., Gerasimidis, S., Bardow, A., & Brena, S. (2019). Identification of most common shapes and locations for beam end corrosion of steel girder bridges. TRB, Washington DC, USA.
 45. Tzortzinis, Georgios, Filippatos, A., Wittig, J., Gude, M., Provost, A., Ai, C., & Gerasimidis, S. (Under Review). *Structural Integrity of Aging Steel Bridges by 3D Laser Scanning and Convolutional Neural Networks*.

46. USDOT FHWA. (2023). Home - LTBP InfoBridge.
<https://infobridge.fhwa.dot.gov/>
47. MassDOT. (2023). *MassDOT Bridge Manual*. (Under Review)
48. MassDOT. (2015). *MassDOT Bridge Inspection Handbook*.
49. SIMULIA, Providence, RI, *Abaqus user's manual* (2014).
50. GE Inspection Technologies PocketMIKE, Lewistown, PA, *Operating Manual* (2004).
51. CloudCompare, *Cloud Compare Version 2.6. 1 User Manual* (2019).
52. Artec 3D. "Artec Leo User Guide." *About Artec Leo - Artec Leo Documentation*, 2021, http://docs.artec-group.com/leo/1.7/?_ga=2.197646886.865482500.1682180005-1047251027.1682180005.
53. Riegl, *Riegl VZ-200 brochure* (2020).
54. Kanakamedala, D., Seo, J., Varma, A. H., Connor, R. J., & Tarasova, A. (2023). Shear and bearing capacity of corroded steel beam bridges and the effects on load rating (Joint Transportation Research Program Publication No. FHWA/IN/JTRP-2023/11). West Lafayette, IN: Purdue University.
<https://doi.org/10.5703/1288284317634>
55. Tarasova, A., Kanakamedala, D., Varma, A. H., Seo, J., & Connor, R. J. (2023). Assessment of Innovative Repair Methods for Corroded Steel Girder Bridges Using the House of Quality Matrix. *Transportation Research Record*, 0(0).
<https://doi.org/10.1177/03611981231175893>
56. CTDOT. (2018). *CTDOT Bridge Load Rating Manual*.
57. Javier, E. M. (2021). *Methods for Evaluation of the Remaining Strength in Steel Bridge Beams with Section Losses due to Corrosion Damage* (Doctoral dissertation, Virginia Tech).
58. Javier III, E. M., Hebdon, M. H., & Provines, J. T. (2021). *Methods for Evaluation of the Remaining Shear Capacity in Steel Bridge Beams With Section Losses Attributable to Corrosion Damage* (No. FHWA/VTRC 22-R4). Virginia Transportation Research Council (VTRC).